

Social interactions and regulatory pathways influencing
Bacillus subtilis biofilm formation and motility

Dissertation

To Fulfill the
Requirements for the Degree of
„Doctor of Philosophy“ (PhD)

Submitted to the
**Council of the Faculty of Biological
Sciences**
of the
Friedrich Schiller University Jena

by M. Sc. Theresa Hölscher

born on 15.04.1990 in Alsfeld, Germany

Reviewers:

- 1) Prof. Dr. Ákos T. Kovács, Technical University of Denmark, Lyngby, Denmark
/ Friedrich-Schiller-University Jena, Germany
- 2) Prof. Dr. Kirsten Küsel, Friedrich-Schiller-University Jena, Germany
- 3) Prof. Dr. Jan-Willem Veening, University of Lausanne, Switzerland

Date of the Dissertation defense: 26.09.2018

Table of contents

Overview of manuscripts	1
Summary	7
Zusammenfassung	8
Introduction	9
1. Sociomicrobiology.....	9
1.1 Social interactions – competition.....	10
1.2 Social interactions – cooperation.....	12
2. Sociomicrobiology of <i>Bacillus subtilis</i>	16
2.1 Competition of <i>B. subtilis</i>	16
2.2 Cooperation of <i>B. subtilis</i>	18
3. Regulation of <i>B. subtilis</i> swimming motility, biofilm formation and sliding motility.....	20
3.1 Regulation of <i>B. subtilis</i> swimming motility and flagellar assembly.....	20
3.2 <i>B. subtilis</i> biofilm formation and regulation of multicellular behavior.....	23
3.3 Regulation of <i>B. subtilis</i> sliding motility.....	26
Aim and outline of the dissertation	28
Chapter 1: Impaired competence in flagellar mutants of <i>Bacillus subtilis</i> is connected to the regulatory network governed by DegU.....	31
Chapter 2: Motility, chemotaxis and aerotaxis contribute to competitiveness during bacterial pellicle biofilm development.....	43
Chapter 3: Hampered motility promotes the evolution of wrinkly phenotype in <i>Bacillus subtilis</i>	59
Chapter 4: Laboratory evolution of microbial interactions in bacterial biofilms.....	81
Chapter 5: De novo evolved interference competition promotes the spread of biofilm defectors.....	91
Chapter 6: Sliding on the surface: bacterial spreading without an active motor.....	105
Chapter 7: A duo of potassium-responsive histidine kinases govern the multicellular destiny of <i>Bacillus subtilis</i>	117
Chapter 8: Presence of calcium lowers the expansion of <i>Bacillus subtilis</i> colony biofilms.....	135
Chapter 9: Monitoring spatial segregation in surface colonizing microbial populations.....	151
Chapter 10: Differential shareability of goods explains social exploitation during sliding.....	163

General Discussion	189
1. Motility as social behavior.....	189
2. Phenotypic heterogeneity and bet-hedging.....	190
3. The flexible strategy of <i>B. subtilis</i>	192
4. Experimental evolution as a tool to investigate microbial social interactions.....	193
5. The purpose of sliding motility.....	196
6. Sliding as byproduct or distinct process?.....	197
7. Public goods and the maintenance of cooperation during sliding.....	198
8. Cooperative interactions in nature.....	199
Concluding remarks	202
References	203
Supporting information	215
Supporting information for Chapter 1	215
Supporting information for Chapter 2	219
Supporting information for Chapter 3	227
Supporting information for Chapter 5	233
Supporting information for Chapter 7	247
Supporting information for Chapter 8	260
Supporting information for Chapter 9	263
Supporting information for Chapter 10	266
Acknowledgements	275
Curriculum Vitae	277
Declaration of Independent Assignment	279

Overview of Manuscripts

This cumulative dissertation comprises the following published and unpublished manuscripts.

Author abbreviations:

Ákos T. Kovács (ATK), Alexa Price-Whelan (APW), Anandaroopan Sundaram (AS), Anna Dragoš (AD), Anne Richter (AR), Anne-Kathrin Dietel (AKD), Balázs Bálint (BBal), Benjamin Bartels (BBar), Cecilia Leñini (CL), Christian Kost (CK), Darío Vileta (DV), Eisha Mhatre (EM), Franziska Brockhaus (FB), Gergely Maóti (GM), Gert Bange (GB), Jordi van Gestel (JvG), Jörg Bossert (JB), Lars E. P. Dietrich (LEPD), Maritta Kunert (MK), Marivic Martin (MMa), Martin Westermann (MWa), Mike Mühlstädt (MMü), Oscar P. Kuipers (OPK), Patrick Pausch (PP), Paula de Oña (PdO), Ramses Gallegos-Monterrosa (RGM), Roberto Grau (RGG), Roberto Kolter (RK), Theresa Hölscher (TH), Tim Sehrt (TSe), Tina Schiklang (TSi), Vaughn S. Cooper (VSC), Verónica Donato (VD), Wilhelm Boland (WB), Yu-Cheng Lin (YCL)

- **Impaired competence in flagellar mutants of *Bacillus subtilis* is connected to the regulatory network governed by DegU.**

Authors: Theresa Hölscher, Tina Schiklang, Anna Dragoš, Anne-Kathrin Dietel, Christian Kost, Ákos T. Kovács

Publication in: Environmental Microbiology Reports (2018), 10(1):23-32,
doi:10.1111/1758-2229.12601.

Presented as: Chapter 1.

Conceived the project	AD (35%), TH (35%), ATK (30%)
Designed the experiments	TH (70%), ATK (30%)
Constructed bacterial strains	TH (10%), TSi (90%)
Performed the experiments	TH (15%), TSi (80%), AD (5%)
Assisted with equipment and analysis	AKD (50%), CK (50%)
Analysed experimental data	TH (50%), TSi (50%)
Wrote the manuscript	TH (90%), ATK (10%)

- **Motility, chemotaxis and aerotaxis contribute to competitiveness during bacterial pellicle biofilm development.**

Authors: Theresa Hölscher, Benjamin Bartels, Yu-Cheng Lin, Ramses Gallegos-Monterrosa, Alexa Price-Whelan, Roberto Kolter, Lars E. P. Dietrich, Ákos T. Kovács

Publication in: Journal of Molecular Biology (2015), 427(23):3695-3708,
doi:10.1016/j.jmb.2015.06.014.

Presented as: Chapter 2.

Conceived the project	ATK (100%)
Designed the experiments	TH (10%), BBar (25%), YCL (10%), RK (5%), LEPD (10%), ATK (40%)
Constructed bacterial strains	BB (60%), YCL (30%), RGM (10%)
Performed the experiments	TH (20%), BBar (50%), YCL (30%)
Analysed experimental data	TH (30%), BBar (40%), YCL (30%)
Wrote the manuscript	TH (60%), APW (15%), LEPD (10%), ATK (15%)

- **Hampered motility promotes the evolution of wrinkly phenotype in *Bacillus subtilis*.**

Authors: Anne Richter, Theresa Hölscher, Patrick Pausch, Tim Sehrt, Franziska Brockhaus, Gert Bange, Ákos T. Kovács

This manuscript was submitted to Molecular Microbiology for publication.

Presented as: Chapter 3.

Conceived the project	ATK (100%)
Designed the experiments	ATK (50%), AR (20%), PP (10%), GB (20%)
Constructed bacterial strains	AR (20%), PP (20%), TSe (20%), FB (40%)
Performed the experiments	AR (50%), TH (5%), TSe (10%), FB (10%), PP (20%), ATK (5%)
Analysed experimental data	AR (50%), PP (30%), GB (10%), ATK (10%)
Wrote the manuscript	TH (50%), ATK (50%)

- **Laboratory evolution of microbial interactions in bacterial biofilms.**

Authors: Marivic Martin, Theresa Hölscher, Anna Dragoš, Vaughn S. Cooper, Ákos T. Kovács

Publication in: Journal of Bacteriology (2016), 198(19):2564-2571, doi: 1128/JB.01018-15 (Mini-Review).

Presented as: Chapter 4.

Conceived the paper	ATK (100%)
Wrote the manuscript	MMA (25%), TH (25%), AD (20%), VSC (10%), ATK (20%)

- ***De novo* evolved interference competition promotes the spread of biofilm defectors.**

Authors: Marivic Martin, Anna Dragoš, Theresa Hölscher, Gergely Maóti, Balázs Bálint, Martin Westermann, Ákos T. Kovács

Publication in: Nature Communications (2017), 8:15127, doi: 10.1038/ncomms15127.

Presented as: Chapter 5.

Conceived the project	ATK (100%)
Designed the experiments	MMA (25%), AD (25%), TH (25%), ATK (25%)
Constructed bacterial strains	MMA (40%), AD (30%), TH (30%)
Performed the experiments	MMA (40%), AD (30%), TH (30%)
Analysed experimental data	MMA (30%), AD (30%), TH (30%), BBal (10%)
Performed genome resequencing	GM (50%), BBal (50%)
Performed electron microscopy	MWa (100%)
Wrote the manuscript	MMA (20%), AD (40%), TH (20%), ATK (20%)

- **Sliding on the surface: bacterial spreading without an active motor.**

Authors: Theresa Hölscher, Ákos T. Kovács

Publication in: Environmental Microbiology (2017), 19(7):2537-2545, doi: 10.1111/1462-2920.13741 (Mini-Review).

Presented as: Chapter 6.

Conceived the paper	TH (50%), ATK (50%)
Wrote the manuscript	TH (90%), ATK (10%)

- **A duo of potassium-responsive histidine kinases govern the multicellular destiny of *Bacillus subtilis*.**

Authors: Roberto Grau, Paula de Oña, Maritta Kunert , Cecilia Leñini, Ramses Gallegos-Monterrosa, Eisha Mhatre, Darío Vileta, Verónica Donato, Theresa Hölscher, Wilhelm Boland, Oscar P. Kuipers, Ákos T. Kovács

Publication in: mBio (2015), 6(4):e00581-15, doi: 1128/mBio.00581-15.

Presented as: Chapter 7.

Conceived the project	RGG (50%), ATK (50%)
Designed the experiments	RGG (50%), ATK (50%)
Constructed bacterial strains	RGG (50%), RGM (10%), EM (10%), TH (10%), ATK (20%)
Performed the experiments	RGG (30%), PdO (10%), CL (10%), DV (10%), TH (10%), VD (10%), ATK (20%)
Analysed experimental data	RGG (60%), ATK (40%)
Performed chemical analysis	MK (100%)
Analysed chemical data	MK (80%), WB (20%)
Contributed materials and reagents	OPK (60%), WB (40%)
Wrote the manuscript	RGG (60%), ATK (40%)

- **Presence of calcium lowers the expansion of *Bacillus subtilis* colony biofilms.**

Authors: Eisha Mhatre, Anandaroopan Sundaram, Theresa Hölscher, Mike Mühlstädt, Jörg Bossert, Ákos T. Kovács

Publication in: Microorganisms (2017), 5(10):7, doi: 3390/microorganisms5010007.

Presented as: Chapter 8.

Conceived the project	EM (50%), ATK (50%)
Designed the experiments	EM (60%), AS (20%), ATK (20%)
Constructed bacterial strains	AS (80%), TH (20%)
Performed the experiments	EM (20%), AS (60%), TH (20%)
Analysed experimental data	EM (40%), AS (40%), TH (10%), ATK (10%)
Assisted surface tension measurements	MMü (80%), JB (20%)
Wrote the manuscript	EM (80%), ATK (20%)

- **Monitoring spatial segregation in surface colonizing microbial populations.**

Authors: Theresa Hölscher, Anna Dragoš, Ramses Gallegos-Monterrosa, Marivic Martin, Eisha Mhatre, Anne Richter, Ákos T. Kovács

Publication in: Journal of Visualized Experiments (2016), 116: e54752, doi: 3791/54752.

Presented as: Chapter 9.

Conceived the project	ATK (100%)
Designed the experiments	TH (80%), ATK (20%)
Performed the experiments	TH (100%)
Analysed experimental data	TH (100%)
Contributed method, analysis tool	AD (20%), RGM (20%), MMa (20%), EM (20%), AR (20%)
Wrote the manuscript	TH (40%), ATK (60%)

- **Differential shareability of goods explains social exploitation during sliding.**

Authors: Theresa Hölscher, Jordi van Gestel, Ákos T. Kovács

This manuscript is in preparation for future submission for publication.

Presented as: Chapter 10.

Conceived the project	ATK (100%)
Designed the experiments	TH (70%), ATK (30%)
Constructed bacterial strains	TH (100%)
Performed the experiments	TH (100%)
Analysed experimental data	TH (100%)
Performed simulation	JvG (100%)
Wrote the manuscript	TH (90%), ATK (10%)

Summary

Microorganisms contribute immensely to shaping our environment and lives. Understanding them, especially their complex interactions with the biotic and abiotic environment, is an important goal of the microbiological research field. Recent work has revealed that social theory can also be applied to microorganisms. Various examples, particularly of bacteria and yeast, have established how they engage in social interactions with other microbes, resulting in the development of the novel research field of Sociomicrobiology. Social interactions of microbes do not only comprise competitive interactions involving competition over resources for the own benefit, but also cooperative interactions where a cell or population provides help for another. Both can occur within one species as well as interspecifically.

In this dissertation, intraspecific social interactions of the Gram-positive model organism *Bacillus subtilis* were investigated. The focus of this work lies on the social behavior of biofilm formation and motility, with an emphasis on flagellum-mediated swimming and collective sliding motility. Interactions of strains capable of and lacking these behaviors were analyzed with the help of molecular biology techniques, fluorescence microscopy and experimental evolution setups. Further, the connection of different social phenotypes through the regulatory networks controlling them, were explored. The investigated social behaviors were demonstrated to be additionally linked through their functions in different lifestyles of *B. subtilis*.

In particular, regulatory connections of motility and competence for DNA uptake as well as motility and biofilm formation were exposed. The importance of the influence of swimming motility and chemotaxis on competitiveness during pellicle biofilm development of *B. subtilis* was determined and matrix overproducers that evolved predominantly during pellicle formation of non-motile strains were examined. A matrix non-producer developed better incorporation abilities into a wild type pellicle during a long-term experiment, which was found to be coupled to the evolution of a phage-mediated interference competition. Moreover, the transition from collective sliding motility to the sessile biofilm state was shown to be governed by the regulator Spo0A and sliding was revealed as a possibility of expansion for mature colony biofilms in the absence of calcium ions. Finally, secreted sliding facilitating substances were demonstrated to differ in their availability to neighboring cells and, consequently, their exploitability by non-producers.

Zusammenfassung

Mikroorganismen tragen immens zur Gestaltung unserer Umwelt und unseres Lebens bei. Sie zu verstehen, besonders ihre komplexen Interaktionen mit der biotischen und abiotischen Umwelt, ist ein wichtiges Ziel des mikrobiologischen Forschungsgebiets. Neueste Untersuchungen haben ergeben, dass Sozialtheorie auch auf Mikroorganismen angewendet werden kann. Verschiedene Beispiele, besonders von Bakterien und Hefen, haben gezeigt, wie sie soziale Interaktionen mit anderen Mikroben eingehen, was in der Entwicklung des neuen Forschungsfeldes der Soziomikrobiologie resultierte. Soziale Interaktionen von Mikroben beinhalten nicht nur wettbewerbsorientierte Interaktionen mit Wettbewerb um Ressourcen zum eigenen Vorteil, sondern auch kooperative Interaktionen, bei denen eine Zelle oder Population Hilfe für eine andere bereitstellt. Beide Formen können innerhalb einer Spezies oder interspezifisch auftreten.

In dieser Dissertation wurden intraspezifische soziale Interaktionen des grampositiven Modellorganismus *Bacillus subtilis* untersucht. Der Fokus dieser Arbeit lag auf dem sozialen Verhalten der Biofilmbildung und Bewegung mit Schwerpunkt auf Flagellum-vermitteltem Schwimmen und kollektiver Fortbewegung mittels *sliding*. Interaktionen von Stämmen mit und ohne Befähigung zu diesem Verhalten wurden mit Hilfe von molekularbiologischen Methoden, Fluoreszenzmikroskopie und experimenteller Evolution analysiert. Weiterhin wurde die Verbindung von unterschiedlichen sozialen Phänotypen durch die regulatorischen Netzwerke, die diese kontrollieren, erforscht. Es wurde demonstriert, dass die untersuchten sozialen Verhaltensweisen zusätzlich durch ihre Funktion in verschiedenen Lebensstilen von *B. subtilis* verbunden sind.

Insbesondere wurden die regulatorische Verbindung von Bewegung und Kompetenz zur DNA Aufnahme, sowie Bewegung und Biofilmbildung aufgedeckt. Die Bedeutsamkeit des Einflusses der Schwimmbewegung und Chemotaxis auf die Wettbewerbsfähigkeit während der Entwicklung eines *pellicle* Biofilms von *B. subtilis* wurde festgestellt und Matrix-Überproduzenten, die hauptsächlich während der *pellicle* Bildung von unbeweglichen Stämmen entstanden, wurden untersucht. Zusätzlich entwickelte ein Nicht-Produzent der Biofilmmatrix die Fähigkeit zur besseren Eingliederung in *pellicles* des Wildtyps, was mit der Evolution eines Phagen-vermittelten Interferenzwettbewerbs gekoppelt war. Weiterhin wurde gezeigt, dass der Übergang von kollektivem *sliding* zum sessilen Biofilm von dem Regulator Spo0A gesteuert wird und dass *sliding* eine Möglichkeit zur Expansion von ausgereiften Koloniebiofilmen in Abwesenheit von Calciumionen darstellt. Schließlich wurde bewiesen, wie sich sekretierte, *sliding* unterstützende Substanzen in ihrer Verfügbarkeit für Nachbarzellen und daher in ihrer Ausbeutbarkeit durch Nicht-Produzenten unterscheiden.

Introduction

Microorganisms represent the smallest form of life on earth, yet without them the evolution of other multicellular life forms would not have been possible. They are involved in an abundance of environmental processes as well as nutrient cycles, and are playing a crucial role in balancing and sustaining life on earth¹. Additionally, all higher organisms are associated in some way or another with microbial populations affecting them and their surroundings. Due to their vast impact on the environment, animals and human beings, microbiology is a most important field of research. Lately, it has been recognized that a common lifestyle among microbes, especially bacteria, is the formation of communities enclosed in an extracellular matrix, the so called biofilm². This shifted research focus towards interactions between bacteria, especially in these agglomerations. Moreover, researchers began to apply social theory to bacteria, finding that they also engage in social behavior. As a result of their large population size, possible genetic manipulation and short generation time, bacteria are employed more and more to analyze social behavior in general, test social theories and find answers to problems such as the evolution of cooperation³⁻⁶.

1. Sociomicrobiology

Microorganisms engage in a variety of interactions with their biotic environment, not only members of their own species but also other microorganisms and higher organisms such as plants. The recently developed field of sociomicrobiology investigates the social interactions among microbes and their behavior in microbial groups or communities. The term sociomicrobiology was first introduced by Parsek and Greenberg⁷ as researchers became increasingly interested in social behavior in microorganisms. Especially the collective bacterial activities of biofilm formation (also see below) and quorum sensing received attention with regard to cooperation of several cell types and species⁸. Research in this direction also increased due to better understanding of the natural lifestyle of bacterial communities which is often in contrast to shaken clonal cultures in liquid medium employed in many laboratory settings so far^{2,9}. This resulted in the development of a new field of research that combines social evolution theory and microbiology. Exploring social interactions of microbes is not only important because we can gain a better understanding of the behavior of microbial populations, but it also allows the development of applications improving human everyday life, such as new approaches to treat diseases or the optimization of microbial communities used in waste water treatment plants^{10,11}.

To date, numerous different social phenotypes have been recognized and explored in microbes. Their social interactions are commonly classified in four different categories

depending on their effect for recipient and donor in terms of fitness (see Fig. 1;⁴): A positive effect for the actor (with the benefit of the social behavior outweighing the costs) as well as the recipient is defined as mutual benefit, whereas behavior with a positive effect for only the actor is referred to as selfishness. If the interaction is beneficial for the recipient but comes with a cost for the actor that is higher than the benefit, it is altruistic, but is defined as spite if it has only negative consequences for both. Therefore, interactions leading to a benefit of the recipient (mutual benefit and altruism) are cooperative whereas interactions with a negative effect on the recipient (selfishness and spite) can be classified as competition.

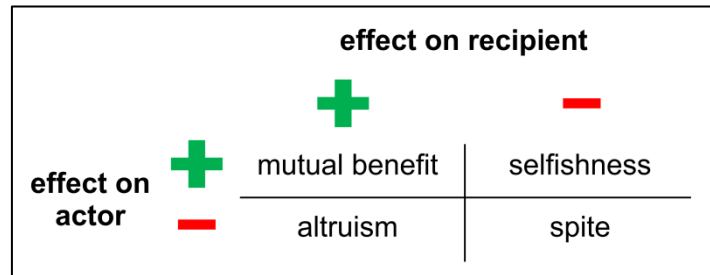


Figure 1. Social interaction classifications. Modified after West *et al.*, 2006⁴.

1.1 Social interactions - competition

Competition is probably the more explicable and prevalent type of interaction (e.g. ^{12,13}). Most habitats are populated with microorganisms, which inevitably leads to conflicts over resources if several species or cells have the same needs. The conditions, under which competition can occur, require therefore an intersection of used resources that mainly comprise nutrients and metabolic niches as well as space. Thereby, the resources have to be limiting to promote competition as a distinct selective pressure is required, occurring in environments with rare nutrients or high cell density. Consequently, environmental factors like habitat heterogeneity, disturbance rate, nutrient availability, abundance and complexity or species diversity have a large influence on the outcome of competitive interactions and possible coexistence of microorganisms. In general, competitive interactions can either be passive, meaning the competitors decrease the resource by using it up (exploitative competition) or the competitors can actively inhibit or harm each other (interference competition) (see Fig. 2). Passive competition is usually classified as selfish since the uptake of e.g. the limiting nutrient source is benefiting the actor, but has a negative effect on the recipient as less of the nutrients are available. One example of passive competition is the investment in a high growth rate that facilitates maximal uptake and usage of nutrients leading to an advantage of the competitor in a well-mixed environment¹⁴. In other cases, motility can be employed to reach a favorable environment ahead of competitors and supports the often competitive initial colonization. The role of motility was demonstrated for

example during root colonization of *Pseudomonas fluorescens*, where less or non-motile strains were largely excluded from the root population^{15,16}.

An important and widespread example for an active competition mechanism is the production of antimicrobial substances targeting cells of other species or distant relatives of the same species. Although spiteful behavior does not seem to be common in nature, production of antimicrobials belongs in this category as along with the inflicted damage on the recipient, it is accompanied by the metabolic burden of production for the actor. However, for this classification I disregard the theory of signaling as another purpose of antimicrobial substances in sub-inhibitory concentrations. Another straightforward example of contact dependent active competition is the type VI secretion system of several Gram-negative bacteria like *Pseudomonas aeruginosa* or *Vibrio cholerae* that actively injects toxins into specific target cells^{17,18}.

Competition often results in specialization and adaptation to specific niches facilitated by specific mutations as it allows coexistence of strains or organisms. Culturing the Gram-negative bacterium *P. fluorescens* in the spatially heterogeneous environment of a medium containing tube resulted in diversification into three coexisting variants that inhabited three different niches (bottom, medium and air-liquid interface)¹⁹. The emergence and properties of the three variants is reviewed in more detail in Chapter 4 of this thesis. One of the *P. fluorescens* variants that evolved during the above mentioned experiment showed a colony biofilm phenotype with a highly wrinkled structure which was connected to overproduction of a polysaccharide²⁰. This phenotype readily emerges also in various other bacterial species such as *Burkholderia cenocepacia*²¹, *Pseudomonas aeruginosa*²² and *Bacillus subtilis*²³ during adaptation to heterogenous environments. It seems to be directly or indirectly related to overproduction of the biofilm matrix that often leads to a fitness advantage of these variants in their specific niche^{19,20,24}. In contrast, if a formerly spatially structured environment is disturbed causing higher homogeneity, one competitor might gain dominance over otherwise stable phenotypes due to the lack of suitable niches.

However, the definition of a competitive behavior also depends on the context it is described in. A well analyzed example is represented by siderophore production of pseudomonads. These Gram-negative bacteria produce amongst others pyoverdine, a molecule that is secreted into the environment and able to chelate iron there²⁵. Successful iron acquisition is crucial for survival in many habitats, making siderophore production advantageous for nutrient acquisition and therefore a competitive trait^{26,27}. On the other hand, siderophore production is cooperative for cells of the same species and population since they are secreted and can be used by neighbors as well as by the producer^{28,29}.

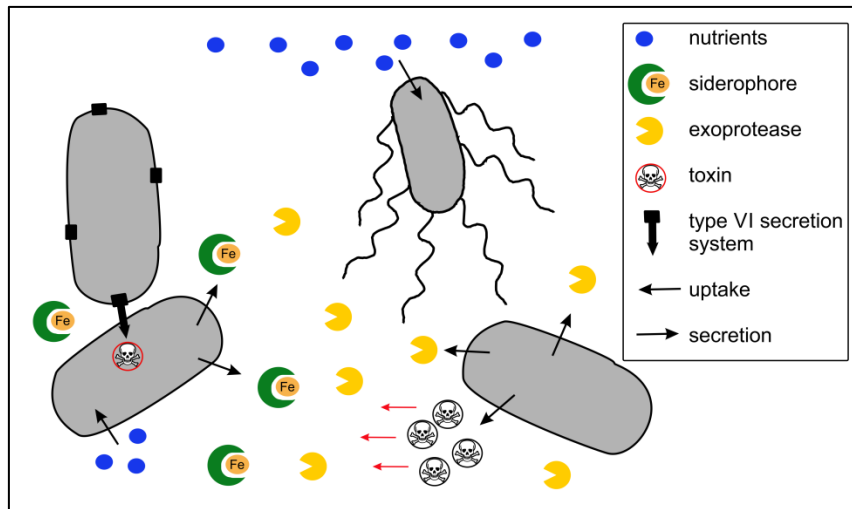


Figure 2. Examples of competitive strategies. Illustration shows passive and active competition mechanisms, such as nutrient uptake and consumption, movement towards nutrient sources, secretion of siderophores and exoproteases, toxin production as well as attack via a type VI secretion system.

1.2 Social interactions - cooperation

Probably the largest topic of interest in sociomicrobiology is the field of cooperation, where researchers strive to explain the existence of microbial phenotypes engaging in behaviors that benefit one or more cells other than the actor. Here, I use this broad definition of cooperation as increasing the fitness of a recipient^{4,30}, although sometimes the fitness cost for the actor is implemented as well. The focus lies mainly on the question how cooperation could evolve and how it is maintained despite the common principle of “survival of the fittest” described by Charles Darwin³¹. Although we observe cooperative behaviors in nature, they can theoretically be exploited by individuals who neglect to pay the costs of engaging in the cooperative behavior but gain the benefits. This leads to a competitive advantage of these so called “cheaters” who could take over and possibly collapse the population³². As evolutionary stability and success is defined by the amount of offspring or genes passed to the next generation, such exploitation would diminish the offspring of cooperators and finally result in extinction of the cooperative behavior. In social theory, this problem is referred to as “tragedy of the commons”. It was explained on the example of herdsmen that add sheep to a common pasture for their own gain, which is larger for the individual herdsman than the general loss due to overgrazing^{4,33}. Therefore, despite the benefit of long-term cooperation (no overgrazing), selfish behavior with smaller short-term benefits that is employed by individuals (profit of more sheep) destabilizes cooperation.

Cooperation can take form in various types of behavior like for example altruistic sacrifice, metabolic cross-feeding or public good production^{3,5} (see Fig. 3). Among the first recognized forms of cooperation is the altruistic behavior of *Myxococcus xanthus*. During starvation this Gram-negative myxobacterium forms spores on elevated multicellular fruiting bodies thereby

sacrificing the vegetative cells forming the support structures³⁴. In contrast, during bidirectional metabolic cross-feeding, two strains or genotypes benefit by feeding on the secreted byproducts of each other or through the connection by intercellular nanotubes^{35,36}. This form of cooperation is debated since it is claimed to be only an incidental result of selfish behavior, but fits into the broad definition of cooperation benefitting a recipient⁴. Additionally, the recently developed Black Queen hypothesis argues that metabolic dependencies can evolve based on the inherent leakiness of many cellular functions (and therefore the production of commonly available extracellular products) and a higher fitness due to the loss of unnecessary genes^{37,38}. This selfish usage of another cells' byproducts could lead to genome reduction due to cost efficiency resulting in metabolic dependency. Then, the dependency has to be maintained to survive which allows the development of costly cooperative behaviors³⁷⁻³⁹.

Another common form of cooperation is the production of so called public goods, substances that are usually costly to produce and excreted into the environment for the profit of the producer as well as neighboring cells (mutual benefit, e.g. ⁵). Public goods are widespread in nature and range from digestive enzymes^{40,41} and siderophores^{42,43} over toxins targeting competitors to structural components of the biofilm matrix^{44,45} and surfactants facilitating collective motility^{16,46}. Many of these behaviors are controlled by quorum sensing, a mechanism for bacteria to assess the density of their population by small diffusible molecules followed by a gene regulatory response at a certain density threshold^{47,48}. Quorum sensing already represents a possibility to stabilize cooperation since it ensures the expression of the cooperative behavior only when enough cells are present in the population^{49,50}. Thus, this kind of facultative cooperation facilitates a higher advantage of the potentially costly cooperative behavior due to the presence of enough recipients and protects the cells at least to some degree from exploitation⁵¹. Facultative cooperation can also be regulated by the nutrient level like in swarming of *P. aeruginosa* where rhamnolipids necessary for this collective motility are only produced at a certain carbon/nitrogen ratio thereby keeping the costs at a minimum⁵².

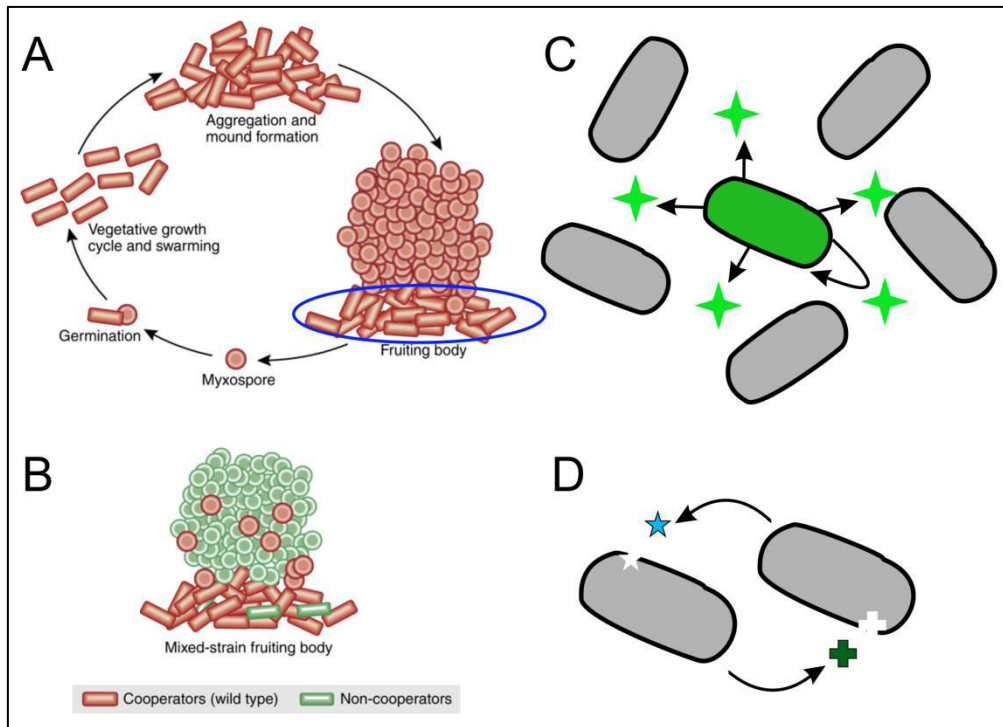


Figure 3. Examples of cooperation. (A) Altruism of *M. xanthus*: Sacrifice of the vegetative cells (blue circle) in favour of spores during fruiting body formation (from Xavier, 2011⁶). (B) Invasion of cheaters in *M. xanthus* fruiting body (from Xavier, 2011⁶). (C) Cooperation through production of public goods. (D) Bidirectional metabolic cross-feeding.

The maintenance of cooperation during evolution is only possible, if the cooperative behavior can be directed towards the cooperators rather than towards non-contributive individuals. Such an effect can be reached via the mechanism of kin selection, especially useful to explain altruistic behaviors^{5,53}: If the cooperative behavior is predominantly directed towards close relatives, the costly trait persists since those relatives carry the same or very similar genes (e.g. ^{54,29}). This theory was formulated in Hamilton's rule that predicts a stable cooperation if relatedness or the benefit of the cooperative behavior is high^{55,56}. The most intuitive example for this would be clonal populations which are of course less common in nature than in the laboratory, but can nevertheless exist if few cells colonize new habitat patches.

A more direct mechanism of kin selection is kin discrimination where cells recognize their kin or non-kin by means of certain features providing them with the possibility to direct the cooperative behavior towards or away from them. Consequently, cells can either cooperate with their kin or withhold cooperation from non-kin. This difference can be illustrated by two examples. *Proteus mirabilis* swarming cell populations recognize their kin with the same genes, so called *ids* genes, and include them in the swarm, but kill non-kin via toxin secretion⁵⁷. On the other hand, swarms of *B. subtilis* attack all other cells – only kin survive because they have the matching immunity system⁵⁸ (see also below).

Another key condition in the stabilization of cooperation is limited dispersal or proximity of cells and/or public goods and therefore spatial structure of a microbial population⁵⁹. In homogenous environments with high dispersal such as laboratory liquid shaken cultures, the public goods or related cells would diffuse or move away, rendering the cooperative behavior ineffective. However, if the cooperator is surrounded by its offspring i.e. other cooperators that stay in its vicinity or diffusion of the public goods is limited and they are thus concentrated locally, cooperation is much more stable^{49,60–62} (see Fig. 4). This is the case for example in biofilms, where the cells are encased in an extracellular matrix that reduces the diffusion of public goods and confines the cells to a defined area^{63,64}. This way, spatial structure can allow the exclusion of “cheaters” since they are less likely to interact with cooperators and exploit the cooperative behavior^{63,65}. Moreover, there is evidence that cooperators can organize themselves into spatially distinct groups or patches, excluding cheaters^{66,67}. A recent study suggests in addition, that the spatial clustering of cheaters relative to the cooperator structure also has to be considered for the cooperation stabilizing effect of spatial structure⁶⁸. Similar to biofilms, positive assortment can structure the population of expanding colonies on a surface. Due to genetic drift, an expanding colony composed of initially well mixed cells forms sectors the consisting of the same genotype⁶⁹. Consequently, it is possible that sectors are composed entirely of cooperators facilitating maintenance of cooperation^{59,70,71} (also see below and Chapter 9, 10) which was shown for example for expanding populations of yeast⁷². Additionally, resource availability was shown to have an influence on the spatial segregation and sector formation⁷³.

Although, as described above, there are many examples where cheaters are excluded from cooperator populations or areas, both types can also co-exist^{74–76}. MacLean *et al.* revealed that under certain conditions, the presence of “cheaters” can even lead to a maximized population fitness⁷⁷. However, the outcome is often dependent on the environmental conditions and on the scale, that is examined. Likewise, the relation between cooperation and competition is not always easy to untangle: competition for e.g. nutrients might still play a role in populations of cooperators whereas cooperation of one species can also be stabilized by interspecific competition⁷⁸.

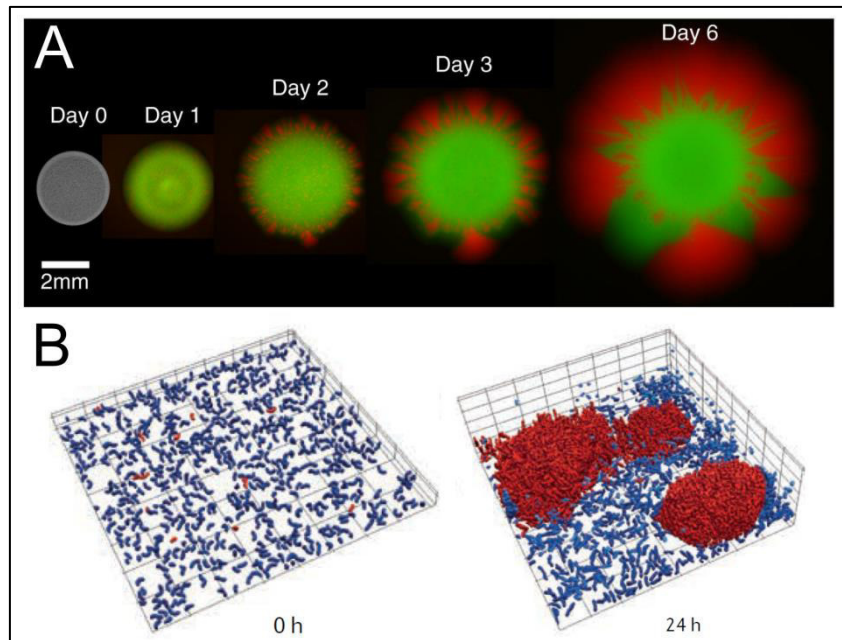


Figure 4. Spatial structure promotes cooperation. (A) Spatial expansion of cooperators (red) and cheaters (green) of *Saccharomyces cerevisiae* (adapted from van Dyken *et al.*, 2013⁷²). (B) During *V. cholerae* submerged biofilm formation matrix secreting cells (co-operators, red) dominate over non-secretors (blue) (adapted from Nadell *et al.*, 2016⁶⁴).

2. Sociomicrobiology of *Bacillus subtilis*

In this work, the bacterium *Bacillus subtilis* was employed to analyze social interactions in relation to the development of biofilms as well as collective movement. *B. subtilis* is a Gram-positive model organism that is commonly present in soil and assumed to be ubiquitous in nature⁷⁹. It is employed to investigate various processes such as cell differentiation and population heterogeneity (e.g. ⁸⁰), gene regulation^{1,81}, natural competence⁸², endospore formation^{1,83} and biofilm formation^{84–87}. As *B. subtilis* is present in densely populated habitats such as the soil, it constantly encounters other organisms. Consequently, *B. subtilis* engages in inter- as well as intra-species social interactions, including both competition and cooperation, examples of which are described below.

2.1 Competition of *B. subtilis*

Besides the common passive competition for nutrient sources through production of secreted digestive enzymes such as for example the starch degrading alpha-amylase^{88,89}, *B. subtilis* employs a number of active mechanisms to gain an advantage over competitors. An important secreted substance produced under various conditions and several developmental stages of *B. subtilis* is the cyclic lipopeptide surfactin. Surfactin is an amphiphilic molecule and exhibits strong biosurfactant properties⁹⁰, reducing the surface tension of water. In

addition, surfactin is also an unspecific antimicrobial: It can target the cellular membrane, resulting in a disturbance of the lipid bilayer integrity, leakage of cytoplasmic content and eventually cell death^{91,92}. The antimicrobial features of surfactin make it a useful weapon for *B. subtilis* in interspecific competition, contributing for example to the inhibition of *Staphylococcus aureus* growth in co-cultures⁹³. Besides surfactin, *Bacillus* species are able to produce other lipopeptides, various iturins that exhibit amongst others anti-inflammatory, anti-tumor and anti-fungal activities⁹⁴, as well as other antimicrobial natural products such as bacillaene that enhance competitiveness in soil⁹⁵.

Biofilm formation is another competitive strategy of *B. subtilis*. Biofilms are three-dimensional aggregates of cells that reside in a self-produced matrix composed of different substances (extracellular polysaccharides, proteins, and DNA amongst others)^{2,96-98}. They can confer protection against for example environmental disturbances or antimicrobials⁹⁹⁻¹⁰² and thus provide a competitive advantage. Additionally, some toxic molecules can be integrated into the biofilm matrix and thereby rendered harmless¹⁰³. On the other hand, also the inhibition of the competitors' biofilm formation can confer a benefit due to increased vulnerability (see below). Likewise, the existence of any kind of motile behavior can facilitate the initial establishment in a new habitat where it is often crucial to be faster than any competitors (see Chapter 2, also Chapter 8). In *B. subtilis*, the bistable expression of motility related genes allows the rapid adaptation to conditions where motility provides a competitive advantage without the potentially crucial delay of flagellar synthesis (see below)¹⁰⁴. On the other hand, *B. subtilis* can employ motility to escape a competitive environment and probable cell death¹⁰⁵. The interspecies interaction between *B. subtilis* and *Bacillus simplex* is an example of how different competitive mechanisms can work together: During biofilm formation of *B. subtilis* in the vicinity of a *B. simplex* colony, surfactin and two toxins are produced that target *B. simplex* at concentrations which are inert for *B. subtilis*¹⁰⁶. Additionally, *B. subtilis* cells engulf the *B. simplex* colony in a flagellum-dependent manner, leading to the elimination of *B. simplex*¹⁰⁶. The toxins involved in killing *B. simplex* have been reported to also facilitate a cannibalistic behavior i.e. intraspecific competition of *B. subtilis*. Under starvation conditions, *B. subtilis* enters the developmental program of sporulation that is irreversible after a certain stage⁸³ but subject of a bet-hedging strategy¹⁰⁷. However, sporulation can be delayed by killing some siblings and feeding off the thereby liberated nutrients (cannibalism). The killing is mediated by the extracellular toxins SkfA and SdpC that are produced by a subpopulation of cells along with immunity mechanisms, thus eliminating the non-producers^{108,109}. Moreover, competition between cells of the same species and even with the same ancestor can develop during evolution of niche specialists in a biofilm. Dragoš *et al.* showed that an evolved *B. subtilis* variant that does not contribute to matrix production, is able to reside in a biofilm with the matrix-producers and exploit them¹¹⁰.

Members of the genus *Bacillus* also developed the ability to interfere with quorum sensing signals from Gram-negative bacteria²⁶. *N*-acyl homoserine lactones, so called AHLs, are

employed by various Gram-negative bacteria to assess population density and regulate different phenotypes via quorum sensing. Researchers discovered that *Bacillus* species isolated from soil produce an AHL lactonase able to disintegrate the AHL quorum sensing signal, thus inhibiting their quorum dependent behavior^{111,112}. This was demonstrated for biofilm formation of *V. cholerae* which is controlled in response to quorum sensing and accumulation of the AHL signal^{113,114}. Presence of the AHL lactonase resulted in reduced biofilm formation of *V. cholerae*¹¹¹ possibly providing a competitive advantage at least in the colonization of free space.

2.2 Cooperation of *B. subtilis*

In addition to many competitive traits, *B. subtilis* employs various cooperative mechanisms, especially intraspecific ones. As mentioned above, biofilm formation is a possible competitive strategy in a challenge of different bacterial species, but viewed with focus on a population or intraspecific interactions it can also be a cooperative behavior. *B. subtilis* biofilm formation is achieved by the cooperative production of structural matrix components by subpopulations of cells that differentiate into distinct cell types^{115,116}. Biofilms can exhibit different forms, but the in *B. subtilis* commonly studied ones are pellicles swimming on top of the medium, in medium submerged biofilms and colony biofilms on agar surfaces (see Fig. 5).

Some matrix components are assumed to be public goods since they are excreted and commonly available^{71,117} like for example proteases^{115,118} or the protein component TasA and exopolysaccharides, where it has been shown that non-producers can complement each other in pellicle biofilms¹¹⁷ (see also Chapter 5). Besides, van Gestel *et al.* demonstrated that exopolysaccharide production is a cooperative trait that although it can be exploited by non-producers in mixed conditions, it is protected in a spatially well structured environment with positive assortment⁷¹. Cooperative growth of *B. subtilis* by amylase secretion was also shown to generate patches of cells (i.e. spatial structure) that could survive with lower starting cell densities than well-mixed populations⁶⁷. Further, submerged biofilms of *B. subtilis* were found to be coordinated in their growth behavior, displaying coupled metabolic oscillations of growth and growth arrest mediated by electric signaling^{119,120}. This would generate competition for nutrients but *B. subtilis* resolves this conflict between cooperation and competition by switching to alternate growth cycles at low nutrient supply – if one biofilm grows, the other halts¹²⁰.

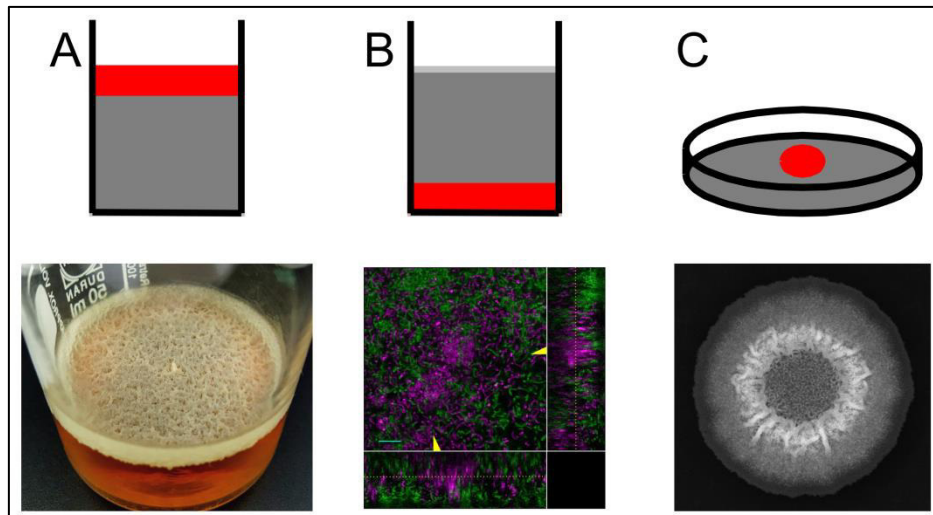


Figure 5. *B. subtilis* biofilm formation. The images depict three types of biofilms formed by *B. subtilis*: (A) Pellicle at the air-liquid interface, (B) a submerged biofilm at the surface-liquid interface and (C) a colony biofilm at the surface-air interface. The upper part represents the simplified schematic of the photo (A) or microscopic image (B, C) in the lower section. Images A and B were obtained by Marivic Martin and Eisha Mhatre, respectively.

Moreover, cooperation in *B. subtilis* occurs in two collective types of movement, swarming and sliding. Swarming is a flagellum-mediated multicellular motility that allows rapid translocation over surfaces and additionally requires the quorum sensing controlled secretion of surfactin by a subpopulation of cells^{46,121–123}. Thus, a sufficiently high cell density for the secretion of the public good surfactin is guaranteed so that it effectively facilitates swarming. During analyses of swarms of soil isolates it was discovered that *B. subtilis* is able to discriminate between kin and non-kin at a high level. Strains with up to 99.8 % identity of housekeeping genes formed distinct boundaries between swarms, avoiding cooperation, whereas closely related strains merged¹²⁴. This discrimination based upon non-kin exclusion rather than kin recognition, was less strict in the interaction with more distant species like *Bacillus cereus* and the antagonistic interaction seemed to correlate with a possible public good exploitation^{58,125}. Therefore, *B. subtilis* probably cooperates only with closely related strains and with other species that do not represent a threat due to public good exploitation.

Similar to swarming, surfactin supports a second type of surface translocation, called sliding, where the collective movement of cells is powered by cell division (passive)^{121,123,126} (see also Chapter 6). In *B. subtilis*, sliding also requires the secretion of exopolysaccharides and the bacterial hydrophobin BsIA¹²⁷ (see also Chapter 7). In addition to secretion of potential public goods (see Chapter 10), division of labor between exopolysaccharide producing cells and surfactin producers was demonstrated to be crucial for the structure of dendritic sliding colonies of *B. subtilis*¹²⁷.

As many other bacteria, *B. subtilis* has been studied at single cell level in the past and so called domesticated strains like *B. subtilis* 168 were mainly used for research^{128,129}. These domesticated strains exhibit changes in many characteristics compared to wild strains that

were developed through long use in the laboratory or X-ray and UV treatments^{129,130}. Therefore, the domesticated strains possess several mutations¹²⁸ or lack entire plasmids leading for example to better transformability¹³¹. Notably, some of the cooperative behaviors exhibited by wild strains like NCIB3610 are lost or diminished in domesticated strains. Thus, most domesticated strains lack the ability to swarm and form reduced biofilms in comparison to wild strains^{132,133}, although there are striking differences between subgroups of the same strain and some domesticated strains are still biofilm proficient¹³⁴. A somehow special case is represented by the strain *B. subtilis* natto, which was not domesticated in the laboratory but used for a long time to produce the Japanese fermented soybean dish natto^{135,136}. Many variants of this strain lost their ability to swim and swarm possibly due to producing high amounts of the polymer poly- γ -glutamate^{137,138} but are able to slide over surfaces (see Chapter 7).

3. Regulation of *B. subtilis* swimming motility, biofilm formation and sliding motility

3.1 Regulation of *B. subtilis* swimming motility and flagellar assembly

As many other bacteria, *B. subtilis* is capable of swimming motility in a liquid environment and possesses several peritrichously arranged flagella per cell¹³⁹. The bacterial flagellum is a molecular machine composed of many subunits and proteins which require tight regulation and well-timed gene expression. The flagellum can be dissected into the filament, the hook and the basal body with attached stator units^{140,141} (see Fig. 6). The basal body attaches the flagellum to the cytoplasmic membrane with a rod extending into the peptidoglycan layer and provides structural functions such as facilitating secretion of hook and filament proteins or torque generation for rotation of the flagellum¹⁴². It is the first part of the flagellum to be assembled, starting with the secretion apparatus which resembles a type III secretion system. Besides the secretion apparatus, the basal body is composed of a central rod, the surrounding basal ring consisting of the protein FliF¹⁴³ with the rotor structure composed of FliG located below. Together with the motor and stator (MotA and MotB), the rotor is responsible for torque generation and rotation of the flagellum^{142,144,145}. Attached to the rotor, protein rings of FliM and FliY regulate the directional switch of flagellar rotation^{142,146,147}. The hook determines the angle of rotation of the flagellum and connects the filament with the basal body. It is secreted through the rod and assembled from units of the protein FlgE^{148,149}. After a change in substrate specificity, the Hag monomer (or flagellin) is secreted, forming the tightly packed helical filament as last part in the construction of the flagellum^{142,150,151}.

FliM and FliY additionally mediate the connection to the chemotaxis system of *B. subtilis* through their interaction with the chemotaxis response regulator CheY (e.g. ¹⁵²). If CheY is phosphorylated by the main chemotaxis kinase CheA in response to a chemoeffector binding

to its receptor, it can bind to FliM, causing a directional switch to anticlockwise rotation and therefore a forward motion of the cell. FliY is able to de-phosphorylate CheY thus supporting adaptation and reset of the chemotaxis system (¹⁵³ amongst other adaptation systems, see also¹⁵⁴). Additional modulation and adaptation of the *B. subtilis* chemotaxis system is ensured by the methylation circuit consisting of CheR and CheB since chemoreceptor methylation inhibits the phosphorylation of CheA. This is assisted by CheD which indirectly facilitates methylation. Further, in a negative feedback loop, CheV potentially hinders CheA kinase activity, when it is phosphorylated by CheA¹⁵².

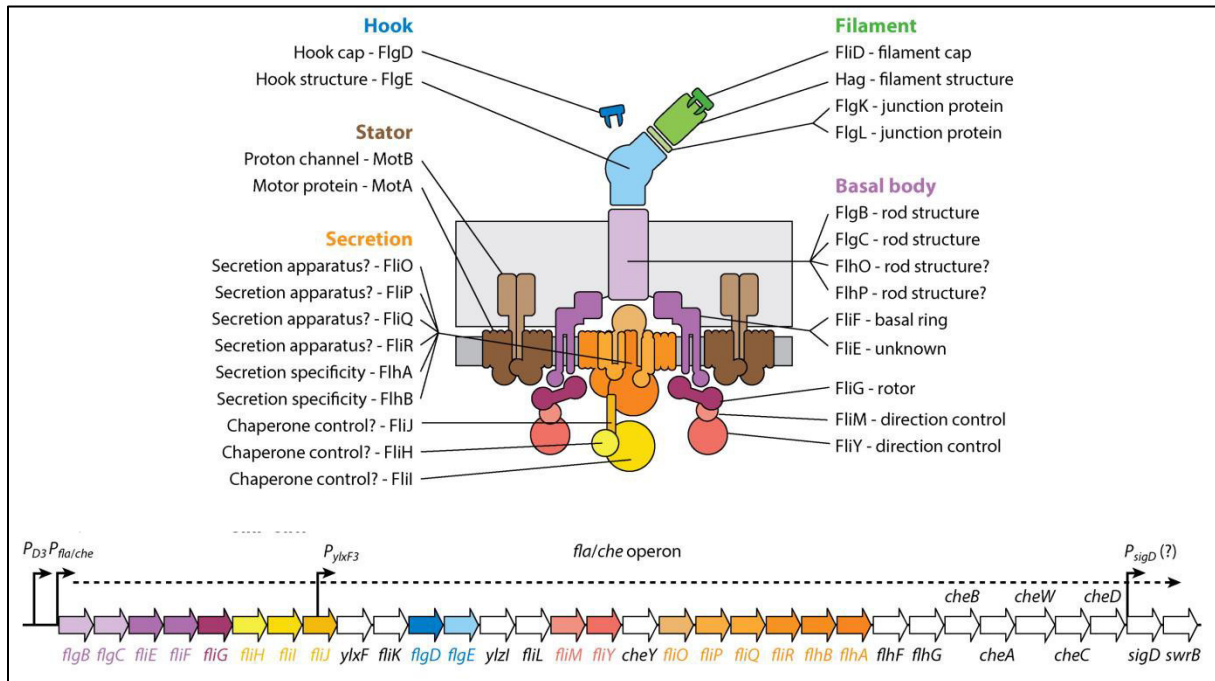


Figure 6. *B. subtilis* flagellum and main flagellar genes. The upper part of the image depicts the flagellum with color coded structural parts. The same color code is used for the main flagellar genes which are encoded in the *fla/che* operon depicted below. Arrows represent promoters (adapted from Mukherjee and Kearns, 2014¹⁴²).

The flagellar proteins of *B. subtilis* are encoded mainly by genes of the *fla/che* operon (see Fig. 6) and some additional smaller gene clusters¹⁰⁴. These genes are organized in a hierarchical manner: the *fla/che* operon contains basal body and hook genes and is transcribed first¹⁵⁵. At the end of the *fla/che* operon, the gene for the alternative sigma factor σ^D is located, controlling the transcription of secondary flagellar genes like for example *hag*, encoding the flagellar filament protein^{156,157}.

Expression of the *fla/che* operon is governed by different regulators. An important global regulator of *B. subtilis* that is also involved in flagellar motility is DegU (e.g. ¹⁵⁸). In its phosphorylated form, DegU~P can bind one promoter of the *fla/che* operon and thus inhibit expression of flagellar genes¹⁵⁹. Additionally, DegU~P can bind to the promoter region of *flgM*, a gene encoding an anti-sigma factor antagonizing σ^D , and activate its transcription¹⁶⁰ so that late flagellar genes are not expressed and the flagellar assembly cannot be completed. On the other hand, in the presence of the regulator SwrA which seems to interact

with DegU~P, the latter is converted to an activator of the *fla/che* operon, also resulting in higher levels of σ^D ^{161–163}.

Moreover, σ^D was demonstrated to play an important role during bistable expression of flagellar genes. In a planktonic culture of growing *B. subtilis* cells, two phenotypes can be observed: cells exist either as motile single cells or as non-motile chains^{104,142,163}. One explanation for this phenomenon is bistability, the cells have either a sufficient level of σ^D to promote assembly of functional flagella or the level is below the threshold and late flagellar genes are not expressed^{81,155}. To those belongs not only *hag*, but also genes encoding autolysins responsible for cell separation after division, so that a low level of σ^D results in chaining¹⁶⁴. In this scenario, the threshold of σ^D is reached due to noise in the transcription of the *fla/che* operon and the position of its gene: it was shown that the transcription of the long operon lessens at the end and as σ^D is located towards the end, its amount in the cell can vary^{81,155,165}.

A partly conflicting mechanism involves an epigenetic switch created by the regulators SinR and SlrR that also controls whether cells are motile or form chains^{81,116,166} (see Fig. 7). In motile cells, the level of the regulator SinR is high, which represses genes encoding components of the biofilm extracellular matrix that is also associated with cell chaining^{166–169}. Additionally, SinR represses the expression of the *slrR* regulatory gene, so that the level of the SlrR regulator is low¹⁷⁰. However, in the presence of SinR-antagonist SinI, *slrR* is de-repressed, SlrR can be produced and binds SinR. This SlrR-SinR complex represses motility and autolysin genes, turning motility off and the complex formation prevents SinR from repressing matrix genes leading to cell chaining¹⁶⁶. Both mechanisms certainly exist in *B. subtilis* cells, but until now it is not clear which one controls the transition between motile cells and chains or whether they somehow act jointly. However, it has been suggested that the epigenetic switch can occur stochastically in a planktonic population or in a determined way at the onset of biofilm formation (see below)^{166,171}.

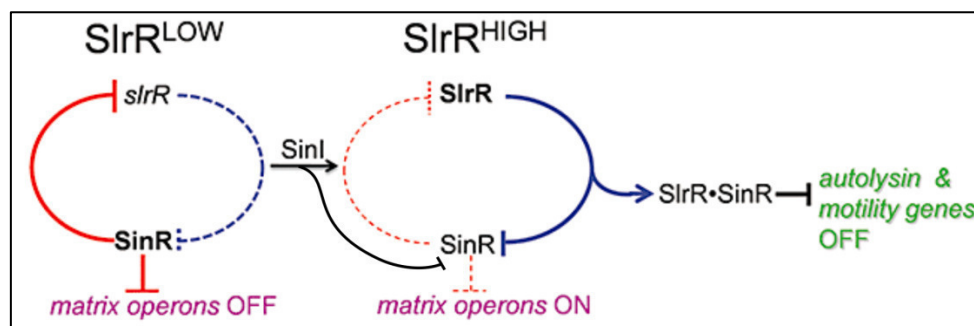


Figure 7. SinR-SlrR switch. The double-negative feedback loop between SlrR and SinR results in SlrR high and low states and ensures controlled expression of matrix or motility genes. T-bars represent inhibition (adapted from Chai *et al.*, 2010¹⁷²).

3.2 *B. subtilis* biofilm formation and regulation of multicellular behavior

As sessile communities enclosed in an extracellular matrix, the requirement of motility in a biofilm is low and most cells are non-motile. Therefore, the start of biofilm formation is characterized by a general transition from motile to sessile cells, although both planktonic populations and biofilms of *B. subtilis* exhibit phenotypic heterogeneity and contain subpopulations of distinctly differentiated cells^{84,116}. Thus, motility and biofilm formation are generally believed to be opposite and mutually exclusive developmental states which is reflected in their regulation. Biofilm formation is a complex process involving many regulatory elements, which is why the most important regulators and connections are mentioned in this section.

B. subtilis biofilm formation can be initiated by mainly two mechanisms that potentially occur in parallel (overview in Fig. 8). First, *B. subtilis* can integrate various environmental signals and respond to certain conditions with the onset of biofilm formation. Several membrane bound and cytoplasmic histidine kinases (KinA, KinB, KinC, KinD and KinE) are responsible for the integration of these signals which trigger autophosphorylation of the kinase¹⁷³. The phosphoryl group is then transferred to the master regulator of biofilm formation and sporulation, Spo0A, via a phosphorelay involving the phosphotransferases Spo0F and Spo0B^{116,173–175}. Spo0A is crucial for biofilm formation and its phosphorylated form activates transcription of many biofilm genes. It activates transcription of *sinI*, leading to production of SinI and the de-repression of matrix genes (see above)¹⁷⁶ and represses the gene encoding the regulator AbrB which is a repressor of biofilm matrix genes in the absence of Spo0A~P^{177,178}.

The matrix of *B. subtilis* consists of three major components that were demonstrated to be essential for characteristic biofilm formation. The first is the exopolysaccharide component already mentioned above which is produced by enzymes encoded by the *epsA-O* operon and is secreted into the environment^{45,116,179}. One of its structural components comprises for example poly-*N*-acetyl glucosamine but the final exopolysaccharide structure has not been revealed^{180,181}. The second main component is the protein TasA which forms fibres and is anchored to the cell via a second protein TapA. Both are encoded in the *tapA-sipW-tasA* operon which, like the *eps* operon, is repressed by AbrB and SinR^{116,117,167,168,182–185}. If both former components are missing, *B. subtilis* fails to form a biofilm⁴⁵ (see also Chapter 5). Defects of biofilm formation in different mutants like for example $\Delta sinI$ can be rescued by suppressor mutations in *sinR* that lead to an elevated production of the biofilm matrix¹⁶⁸. Thirdly, the protein BslA which is also secreted, forms a hydrophobic outer layer on the colony or pellicle biofilm surface and contributes to architectural complexity as well as protection of the biofilm^{186–190}.

At the onset of biofilm formation, various triggers can activate the kinases ranging from glycerol and Mn²⁺^{191,192} over plant polysaccharides^{193,194} to impaired oxidative

phosphorylation¹⁹⁵. These signals are partly specifically sensed by one kinase but there is also a certain overlap between them and the kinase contribution varies depending on the conditions^{116,196}. Moreover, the kinases seem to be organized in a spatio-temporal manner: while KinA and KinB are more active in the older parts of a colony biofilm possibly being more involved in sporulation, KinC and KinD control the young peripheral zone being rather involved in colony biofilm formation^{196,197}. One particular trigger of biofilm formation, the leakage of potassium ions sensed by KinC, is caused by self-produced surfactin and therefore dependent on the cell density since surfactin production is regulated by quorum sensing^{198,199}. This activation proved to be an example of paracrine signalling as a subpopulation senses the quorum sensing signal and responds with surfactin production. This subpopulation cannot sense the surfactin signal, but another subpopulation is triggered and starts to produce the biofilm matrix²⁰⁰. However, biofilm formation through potassium leakage can also be triggered by other natural products such as the fungicide nystatin¹⁹⁸.

A second mechanism by which the transition from motile to biofilm forming cells can be promoted is the mechanosensory property of the flagellum. The inhibition of flagellar rotation, e.g. upon surface contact, activates the DegS-DegU two component system, resulting in elevated levels of the phosphorylated form of the DegU regulator²⁰¹. In turn, DegU~P stimulates transcription of biofilm related target genes^{202–204} and especially activates indirectly the production of the protein BslA which is part of the matrix and crucial for the hydrophobic properties of the *B. subtilis* biofilm^{177,189,202,205}. DegU also functions in the connection between motility and biofilm formation by the activation of poly- γ -glutamate production which was shown to be elevated in cells with a defective flagellar motor¹³⁷. Additionally, flagellar rotation is inhibited in matrix producing cells during *B. subtilis* biofilm formation, since one protein involved in exopolysaccharide production, EpsE, has a second function and acts as a flagellar clutch^{201,203}. It interacts with the rotor protein FliG, causing the uncoupling of power source and flagellar rotation apparatus²⁰⁷. Thus, the flagellar clutch is a rapid mechanism that can act without the delay occurring while inhibiting transcription of flagellar genes²⁰⁸.

Once phosphorylated, Spo0A initiates transcription of biofilm genes but in a heterogeneous manner: only a subpopulation becomes matrix producers due to the bistability of Spo0A activation and its connection to SinI and SinR (see above)²⁰⁹. The reason for this bistability was first assumed to be the positive autoregulatory loop that acts on *spo0A* and modulation of the phosphorelay by external phosphatases^{210,211}. More recent studies however implicate that a stochastic activity of gene transcription of the phosphorelay elements and posttranslational modifications suffice to generate heterogeneous levels of Spo0A in the population²¹². The phosphorelay was identified as a noise generator and since its phosphate flux seems to be the limiting element for Spo0A activation, heterogeneity in the latter is the consequence^{213,214}. Therefore, the level of phosphorylated Spo0A as a regulator for a lot of processes, is involved in the control of phenotypic heterogeneity in *B. subtilis* (also see below).

Spo0A was initially discovered as the master regulator for sporulation in *B. subtilis* and the process of biofilm formation was found to be tightly connected to endospore production. At intermediate concentrations of Spo0A~P, matrix genes are expressed whereas a high level of Spo0A~P leads to entry into the sporulation pathway. Both types of differentiated cells exist in a biofilm but spores develop from matrix producers due to their regulation by Spo0A²¹⁵⁻²¹⁷ with KinD potentially acting as a checkpoint in response to sensing the extracellular matrix²¹⁸. Moreover, a spatio-temporal organization of the subpopulations was demonstrated by Vlamakis *et al.* for colony biofilms, showing that sporulating cells are localized at the top whereas matrix producers exist throughout the biofilm²¹⁷.

Apart from surfactin- or matrix producers and sporulating cells, the *B. subtilis* biofilm retains a subpopulation of motile cells in which Spo0A is in the off state and that reside mainly in the bottom part of a biofilm colony or possibly in water channels formed by the matrix^{217,219}. Thus, the level of Spo0A~P determines the fate of the cell and governs differentiation: with maturation of the biofilm cells transition from motile over matrix producing to sporulating cells.

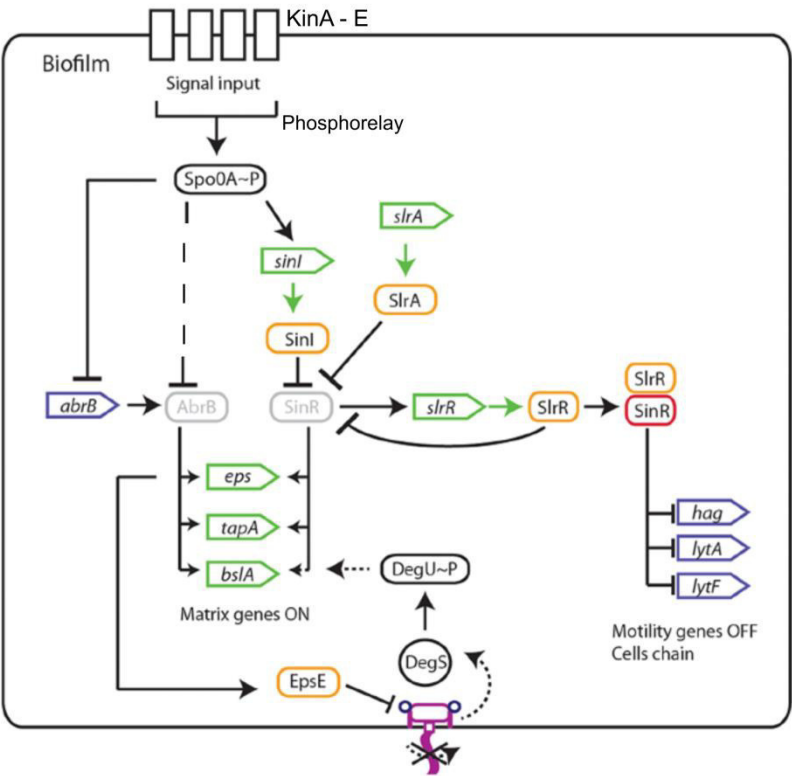


Figure 8. Simplified overview of the gene regulation during biofilm formation. T-bars represent repression, arrows represent activation, grey areas indicate inactivity, rounded rectangles represent proteins, open arrow boxes represent genes and the pink structure represents the flagellum (modified from Cairns *et al.*, 2014⁸⁴).

3.3 Regulation of *B. subtilis* sliding motility

In this section, sliding of *B. subtilis* is described only briefly, as detailed information can be found in published papers, included in this thesis as Chapters 6 and 7, as well as Chapter 10.

Besides biofilm formation and sporulation, Spo0A also controls sliding, a collective and passive type of surface motility powered by the expansive force of dividing cells^{123,220} (see Chapter 6). Sliding of *B. subtilis* was first observed during experiments on *B. subtilis* colonization of plant roots¹²⁶ and was shown to be dependent on sufficient amounts of several macro- and micronutrients but especially potassium and a high affinity potassium transporter were essential for sliding^{126,221,222}. Potassium seems to activate sliding via the histidine kinase KinB (see Chapter 7) that is also involved in biofilm formation. The phenotype of the sliding colony is controlled by potassium as well: In an environment with higher potassium concentrations, sliding is planar whereas dendrites appear at lower (but still sufficient) potassium levels^{126,222}. In addition to KinB, KinC was also shown to be important for triggering sliding motility. Both kinases activate Spo0A through the already described phosphorelay leading to the expression of matrix genes, especially the *epsA-O* operon which was demonstrated to be vital for sliding motility¹²⁷. In addition to exopolysaccharides, the hydrophobin protein BslA and surfactin were also revealed to be required for sliding motility and aid the translocation across the surface through their hydrophobic and lubricant properties^{126,127,221} (see Chapter 7).

Similar to biofilms, sliding colonies seem to be highly organized in a spatio-temporal manner. Van Gestel *et al.* uncovered that matrix and surfactin producers are spatially segregated in the sliding colony. Matrix producers form tightly packed bundles of cell chains that are surrounded by surfactin producing cells¹²⁷. In addition, these bundles formed larger loops at the edge of the colony, termed van Gogh bundles, that were hypothesized to support migration of dendritic sliding¹²⁷. The development of the sliding colony is characterized by a first phase with many surfactin producers followed by a second phase with an increase in matrix producers¹²⁷. Moreover, the two kinases KinB and KinC seem to have organized roles in controlling sliding. While KinB is assumed to be more active in the young peripheral parts of the sliding colony, KinC probably regulates sliding in the inner and older regions (see Chapter 7).

In general, sliding is assumed to be an intermediate state between planktonic or single cells and biofilm formation. Its regulatory control by the biofilm master regulator Spo0A and biofilm involved kinases suggest that sliding precedes biofilm formation and a gradual transition occurs depending on the level of phosphorylated Spo0A¹⁹⁷ (see Fig. 9).

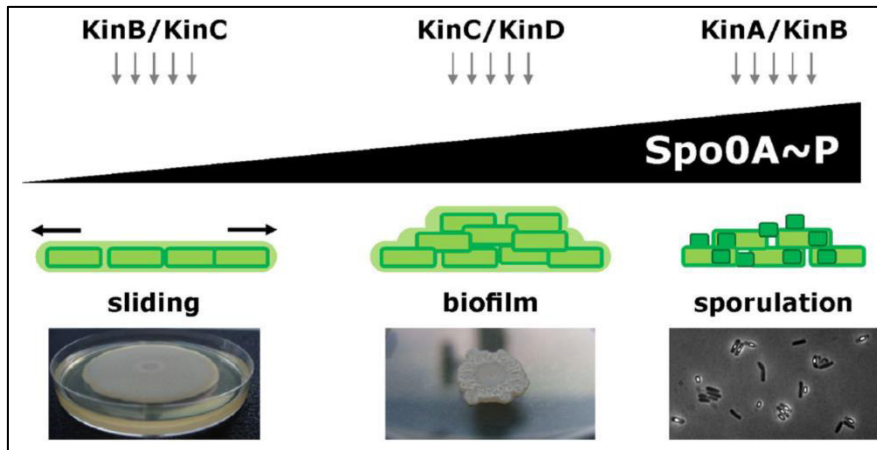


Figure 9. Level of Spo0A~P controls differentiation of *B. subtilis*. Low amounts of Spo0A~P activate sliding mainly through KinB and KinC, biofilm formation is activated by medium amounts of Spo0A~P (mainly KinC, KinD) and at high levels of Spo0A~P the cells sporulate (mainly KinA, KinB) (adapted from Kovács, 2015¹⁹⁷).

Aim and outline of the dissertation

This cumulative dissertation aims to analyze the social interactions of the bacterium *Bacillus subtilis* with focus on the cooperative behaviors of biofilm formation and motility, especially the collective sliding, including the regulatory processes controlling them. It comprises ten Chapters of published and one unpublished manuscript which are framed by an introduction and general discussion.

The introduction provides background information for the Chapters and outlines the concepts of sociomicrobiology with representative examples. It introduces the Gram-positive model organism *B. subtilis* and gives an overview over biofilm formation and motility as well as the regulation apparatus governing those processes.

In the first part, Chapter 1 investigated the regulatory connection of flagellar motility and competence and the involvement of the global regulator DegU which also influences biofilm formation. The objective of the following Chapter 2 was to examine the role of flagellar motility during pellicle biofilm formation as well as the influence of chemotaxis, specifically aerotaxis, and their contribution to competitiveness of *B. subtilis* and *P. aeruginosa*. In Chapter 3, biofilm matrix overproducers with a wrinkly phenotype that evolved predominantly in strains lacking functional flagella during pellicle formation were studied and found to contain mutations in the regulator SinR.

Experimental evolution in the laboratory can help to understand adaptive evolutionary processes and the development of social interactions over time. Chapter 4 serves as more detailed introduction to the technique of laboratory evolution with emphasis on biofilms as spatially structured environment and demonstrates its usefulness by means of two main example studies. Subsequently, in Chapter 5 we conducted our own evolution experiment with *B. subtilis* regarding the possibility of exploitation of matrix production by evolved defectors during biofilm formation and the underlying evolutionary changes.

Chapter 6 aimed to give an overview of sliding motility in various bacteria, the different compounds facilitating it and, if possible, its regulatory basis in the respective organism. This provided the basis for the following Chapters concerning sliding motility. Chapter 7 determined the genetic requirements of sliding motility and identified regulators involved in controlling it, complementing previous studies. Furthermore, sliding was analyzed in relation to colony biofilm expansion in Chapter 8, which was hindered by calcium ions through surfactin inhibition.

In the video based article of Chapter 9 the usefulness of fluorescent markers, advanced microscopic techniques and image analysis tools for the investigation of social interactions in

spatially structured populations was explained and emphasized. This was complemented by the following Chapter 10 which applied those techniques to analyze the shareability of the three main sliding facilitating compounds and the social interactions of engineered producer and non-producer strains during sliding motility.


In the last section of the general discussion, I discuss the major conclusions of the thesis Chapters, the relevance of the findings for microbial life of *B. subtilis* in nature and their implications for social interactions of *B. subtilis* with its biotic environment.

Chapter 1

Impaired competence in flagellar mutants of *Bacillus subtilis* is connected to the regulatory network governed by DegU

Published in: Environmental Microbiology Reports (2018)

Impaired competence in flagellar mutants of *Bacillus subtilis* is connected to the regulatory network governed by DegU

Theresa Hölscher,^{1†} Tina Schiklang,^{1†}
Anna Dragoš,¹ Anne-Kathrin Dietel,^{2,3}
Christian Kost^{2,3} and Ákos T. Kovács ^{1,4*}

¹Terrestrial Biofilms Group, Institute of Microbiology,
Friedrich Schiller University Jena, Jena, Germany.

²Experimental Ecology and Evolution Group,
Department of Bioorganic Chemistry, Max Planck
Institute for Chemical Ecology, Jena, Germany.

³Department of Ecology, School of Biology/Chemistry,
University of Osnabrück, Osnabrück, Germany.

⁴Bacterial Interactions and Evolution Group,
Department of Biotechnology and Biomedicine,
Technical University of Denmark, Kgs Lyngby, Denmark.

Summary

The competent state is a developmentally distinct phase, in which bacteria are able to take up and integrate exogenous DNA into their genome. *Bacillus subtilis* is one of the naturally competent bacterial species and the domesticated laboratory strain 168 is easily transformable. In this study, we report a reduced transformation frequency of *B. subtilis* mutants lacking functional and structural flagellar components. This includes *hag*, the gene encoding the flagellin protein forming the filament of the flagellum. We confirm that the observed decrease of the transformation frequency is due to reduced expression of competence genes, particularly of the main competence regulator gene *comK*. The impaired competence is due to an increase in the phosphorylated form of the response regulator DegU, which is involved in regulation of both flagellar motility and competence. Altogether, our study identified a close link between motility and natural competence in *B. subtilis* suggesting that hindrance in motility has great impact on differentiation of this bacterium not restricted only to the transition towards sessile growth stage.

Received 26 September, 2017; revised 1 November, 2017; accepted 1 November, 2017. *For correspondence. E-mail atkovacs@dtu.dk; Tel. +45 45 252527; Fax +45 45 884922.

[†]Contributed equally.

Introduction

When facing stressful environmental conditions, bacteria can respond with a variety of post-exponential modifications including secretion of degradative enzymes, sporulation or genetic competence. *Bacillus subtilis* is one of the bacterial species that are able to take up free DNA from the environment and incorporate it into its own genome, a phenomenon referred to as natural competence (Dubnau, 1991). To import extracellular DNA into *B. subtilis* cells, a pseudopilus formed by proteins encoded by the *comG* operon facilitates binding to the receptor protein ComEA, which is located in the bacterial cell membrane (Inamine and Dubnau, 1995; Chen *et al.*, 2005). As only single stranded DNA is imported, the membrane-associated nuclease NucA catalyzes cleavage of the DNA after successful binding (Provedvi *et al.*, 2001). Subsequent transport of the DNA through a membrane channel formed by the protein ComEC is mediated by the ATPase ComFA that probably requires the transmembrane proton motive force (Maier *et al.*, 2004).

To take up DNA, cells have to be in a developmental state, in which a specific set of genes and regulators are expressed (Dubnau, 1991; Berka *et al.*, 2002). Regulation of the whole apparatus required for competence development is complex. Briefly, entry into the competence state occurs in a bistable manner during the early stationary phase, where a minority of cells produces high level of the competence master regulator ComK above a certain threshold that is required to switch on competence development, the so called 'K-state' (van Sinderen *et al.*, 1995; Maamar and Dubnau, 2005; Smits *et al.*, 2005; Dubnau and Losick, 2006). It was demonstrated that noise in the expression of *comK* determines the competent subpopulation and allows a dynamic stress response regarding competence development (Maamar *et al.*, 2007; Mugler *et al.*, 2016). Eventually, ComK activates the expression of late competence operons encoding the DNA-binding and -uptake machinery as well as genes, whose products are responsible for DNA integration (Berka *et al.*, 2002; Ogura *et al.*, 2002; Hamoen *et al.*, 2003). Increase of the ComK level is linked to a quorum sensing-mediated accumulation of

the small ComS protein, which interferes with ComK degradation during the exponential phase (Turgay *et al.*, 1998). ComK is able to bind the *comK* promoter, triggering its own transcription, thus creating an auto-stimulatory loop (van Sinderen and Venema, 1994). This binding is further stabilized by the non-phosphorylated form of the regulator DegU to increase the level of ComK above the threshold sufficient for competence development (Hamoen *et al.*, 2000).

However, DegU is not only crucial for competence initiation, but also involved in the regulation of many other processes including protease production, biofilm development, and, particularly, flagellar motility (Murray *et al.*, 2009; Mukherjee and Kearns, 2014). The main components of the hook and basal body of the flagellum are encoded by the large *fla/che* operon. Transcription of this operon is activated by a complex formed by the regulator SwrA and phosphorylated DegU (DegU~P), which binds to one of the *fla/che* promoters (Mordini *et al.*, 2013; Mukherjee and Kearns, 2014). Amongst other genes, the operon contains the gene encoding the sigma factor σ^D that activates transcription of motility genes outside the *fla/che* operon like the *hag* gene (encoding flagellin), *motA* and *motB* (encoding flagellar stator proteins), as well as transcription of *lytF*, which is necessary for separation of motile cells after cell division (Serizawa *et al.*, 2004; Chen *et al.*, 2009). The level of σ^D and its position in the *fla/che* operon determines the cell fate, i.e. subpopulations of motile single cells or non-motile chains (Cozy and Kearns, 2010). The function of DegU~P changes in the absence of SwrA. In this case, DegU~P seems to inhibit motility via the same promoter of the *fla/che* operon (Amati *et al.*, 2004). Additionally, DegU~P can activate the anti-sigma factor FlgM by binding to its promoter region in the absence of SwrA (Hsueh *et al.*, 2011) allowing FlgM to antagonize σ^D (Caramori *et al.*, 1996). Consequently, DegU~P indirectly suppresses transcription of σ^D -dependent genes (Hsueh *et al.*, 2011). It was suggested that a completion of flagellum assembly can be sensed by the DegSU two component system: FlgM, which is activated by DegU~P, causes inhibition of σ^D -dependent genes, when the assembly of the flagellum is impeded (Cozy and Kearns, 2010; Hsueh *et al.*, 2011).

In addition to its role on modulating the expression of flagellum-related genes in *B. subtilis*, the phosphorylation and therefore the activity of DegU, has been shown to be influenced by a mechanical signal transmitted by the flagellum (Cairns *et al.*, 2013). Inhibition of flagellar rotation by the flagellar clutch or by tethering the flagella results in an increased DegU~P level in the cell.

In this study, we report a correlation between motility function and competence development, which in

B. subtilis is connected by the multifunctional response regulator DegU. We show that mutants lacking a functional flagellum such as Δhag , $\Delta motA$ and $\Delta flgE$ exhibited a reduced transformation frequency. This was due to a decrease in competence gene expression, particularly reduced levels of the competence master regulator ComK, which can be reverted by overexpressing *comK* in the *hag*-mutant. Finally, we suggest that the reduced transformation frequency was likely due to an imbalance in the phosphorylation level of DegU.

Results

Lack of active flagella impairs competence for DNA uptake in B. subtilis

While genetically modifying various *B. subtilis* strains, a striking difference in transformation frequency was observed between the wild type and a non-motile mutant lacking the gene encoding flagellin, *hag*. To explore this phenomenon, we tested the transformability of wild type (strain 168) and *hag*-mutant in competence medium (see section "Experimental Procedures"), where the *hag*-mutant showed a more than 100-fold reduced transformation frequency relative to the wild type (Fig. 1A and B): while the transformation frequency of the wild type ranged between 3×10^{-5} and 5×10^{-5} , that of the *hag*-mutant was reduced to values below 3×10^{-7} . Similarly, the undomesticated *B. subtilis* strains DK1042 (transformable derivative of NCIB 3610) and PS216 showed reduced transformation efficiency when the *hag* gene of these strains was disrupted (Fig. S1). To investigate whether this difference in transformation frequency between the two strains resulted from a lower growth rate of the *hag*-mutant, the growth behaviour of wild type and *hag*-mutant grown in competence medium was evaluated over time. As depicted in Fig. 1B, the *hag*-mutant showed a clear growth advantage and reached a higher OD compared to the wild type (unpaired two-sample *t*-test with Welch Correction: $P = 0.001$, $n = 5$), thus supporting our previous observations (Hölscher *et al.*, 2015). Further, it was tested whether the addition of DNA at different time points would increase the transformation frequency of the *hag*-mutant. However, the mutant showed a consistently low transformation frequency over the course of several hours, indicating that a shifted timing of the initiation of the competence state is unlikely to be the reason for the observed decrease in transformation frequency (Fig. 1C). To test whether this phenomenon is restricted to the *hag*-mutant or connected to the lack of an active motility apparatus in general, mutants lacking other functional flagellum-related genes were investigated. The transformation frequencies of mutants lacking the gene encoding one of the flagellar motor units, *motA*

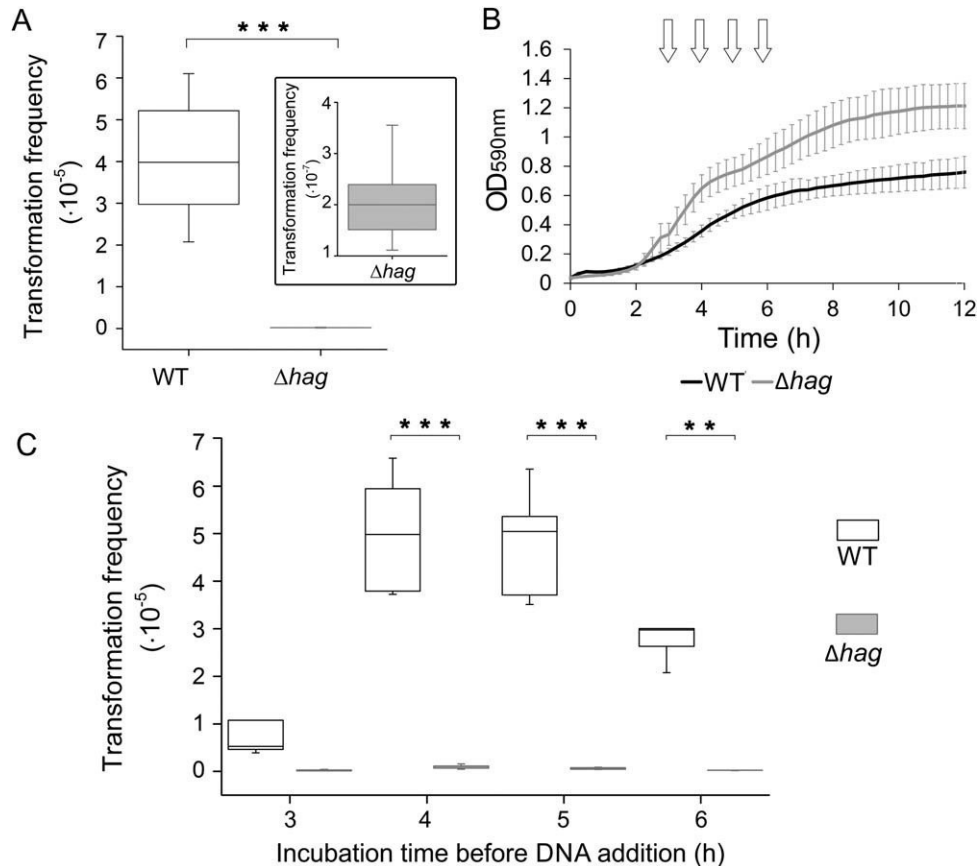


Fig. 1. Transformation frequency is reduced in a mutant lacking flagellin protein.

A. Transformation frequency of *B. subtilis* wild type and *hag*-mutant after 6 h incubation in competence medium (unpaired two-sample *t*-test with Welch Correction: $P = 3.1 \times 10^{-5}$, $n = 9$). The inset shows a zoom-in of the *hag*-mutant data.

B. Growth dynamics of wild type and *hag*-mutant during 12 h incubation in competence medium. Standard deviations for the measurements are depicted in light grey (unpaired two-sample *t*-test with Welch Correction: $P = 0.001$, $n = 5$).

Arrows indicate the time points of DNA addition to investigate the transformation frequency over time, which is shown as box-and-whisker plot in (C). The line in the boxes represents the median and the box indicates the 25th to 75th percentile. Asterisks indicate statistically significant differences between wild type and *hag*-mutant (unpaired two-sample *t*-test with Welch Correction for WT – Δ *hag*, $P = 0.125$ for 3 h, $P < 0.01$ for 4 h, 5 h, 6 h; $n = 6$).

and the gene encoding the hook protein, *flgE*, were decreased in both cases compared to the wild type (Fig. 2; unpaired two-sample *t*-test with Welch Correction: $P = 0.01$ for WT – Δ *motA*, $P = 0.039$ for WT – Δ *flgE*, $n = 9$ for both). Although the wild type transformation frequency was slightly different, the transformation frequencies of both Δ *motA* and Δ *flgE* were around 10-times lower than that of the wild type (Fig. 2). In contrast, a *cheA*-mutant lacking the main chemotaxis sensor kinase showed a similar transformation frequency than the wild type (Fig. S2; unpaired two-sample *t*-test with Welch Correction: $P = 0.232$, $n = 3$), suggesting that the presence of an active flagellum, but not directed motility *per se* is required for full competence development. In sum, these results demonstrate that the observed impaired competence is linked to a loss of flagellar function.

Lack of competence in flagellar mutants is due to the reduced expression of competence genes

To determine if the detected diminished transformation frequency of flagellar mutants was due to altered competence gene expression, the fluorescent reporter P_{comG} -*gfp* was introduced into these strains. This reporter allows the detection of cells expressing the *comG* operon-encoding genes required for pseudopilus formation and DNA uptake. In addition, this reporter provides a proxy on the activity of the ComK protein, the master regulator of competence. Qualitative microscopy analyses of cultures harbouring the reporter, and which were grown in competence medium for 5 h, showed indeed a decreased number of fluorescent (i.e. *comG* expressing) cells in the *hag*-mutant compared to the wild type, whereas a control strain lacking *comK* showed no fluorescence (Fig. 3A). For quantitative determination of

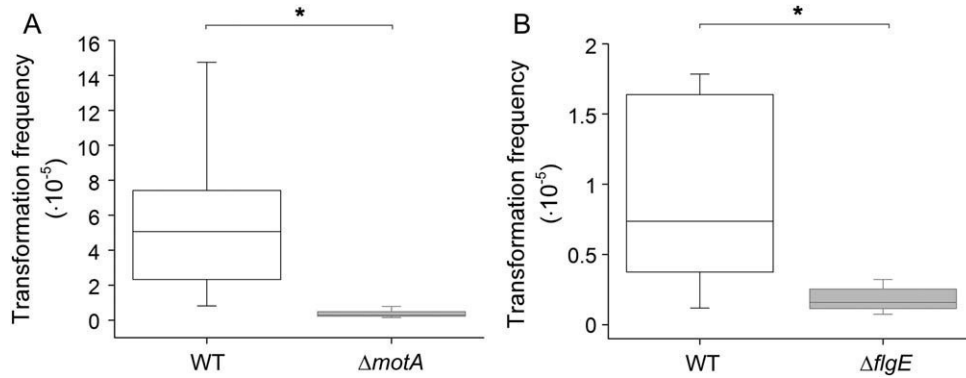


Fig. 2. Mutants impaired in flagellar function exhibit lower transformation frequencies.

Deletion of the gene encoding a flagellar stator (*motA*; A) or the gene encoding the hook protein (*flgE*; B) results in significantly lower transformation frequency of the respective strain compared to the wild type after incubation in competence medium for 6 h. The line in the boxes represents the median, the box indicates 25th to 75th percentile. Asterisks indicate statistically significant differences (unpaired two-sample *t*-test with Welch Correction: $P = 0.01$ for $\Delta motA$; $P = 0.039$ for $\Delta flgE$; $n = 9$ for all).

competence gene expression within the population, flow cytometric measurements were performed that revealed 24.7% of fluorescent cells in wild type cultures (mean value), but only 4.6% of fluorescent cells for the *hag*-mutant (Fig. 3B and C; unpaired two-sample *t*-test with Welch Correction: $P = 0.004$, $n = 3$), thus confirming the microscopy results. Similarly, the *motA* and *flgE* mutants were analysed microscopically as well as by using flow

cytometry. Both methods revealed fewer cells activated transcription of competence genes in these mutants compared to the wild type (Fig. 4; unpaired two-sample *t*-test with Welch Correction: $P = 0.017$ for WT – $\Delta motA$, $P = 1.3 \times 10^{-9}$ for WT – $\Delta flgE$, $n = 3$ for both; mean percentage of fluorescent cells: 16.7% for wild type, 4.5% for $\Delta motA$, 4.2% for $\Delta flgE$). Flow cytometry measurements at different time points during growth in

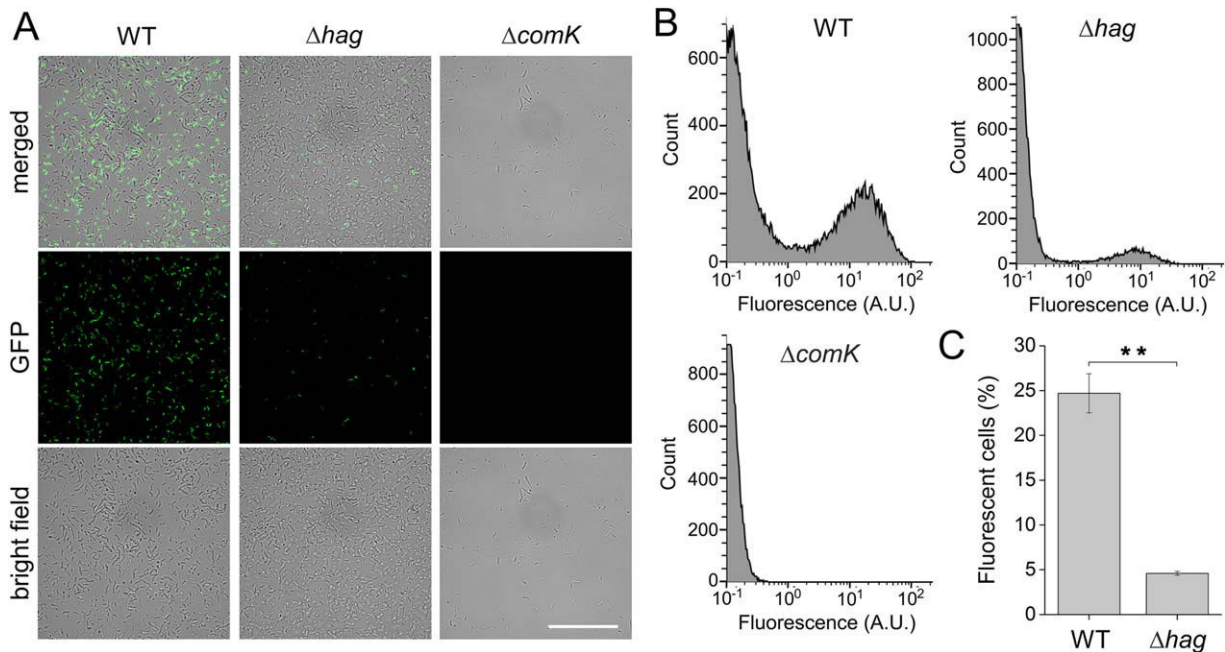


Fig. 3. Fewer cells of the *hag*-mutant express competence genes compared to the wild type.

A. Representative microscopy images of strains harbouring the P_{comG} -*gfp* reporter in wild type, Δhag or $\Delta comK$ genetic background. Images were recorded after incubation in competence medium for 5 h. The scale bar represents 50 μm .

B. Histograms of flow cytometric measurements showing the cell count and the fluorescence in arbitrary units for wild type, Δhag and $\Delta comK$ including background fluorescence. Representative images are shown for each strain.

C. Percentage of fluorescent cells determined from the data in (B) for wild type and *hag*-mutant by isolating the fluorescent population with fluorescence intensities above 3 A.U. Asterisks indicate significant differences (unpaired two-sample *t*-test with Welch Correction: $P = 0.036$, $n = 3$).

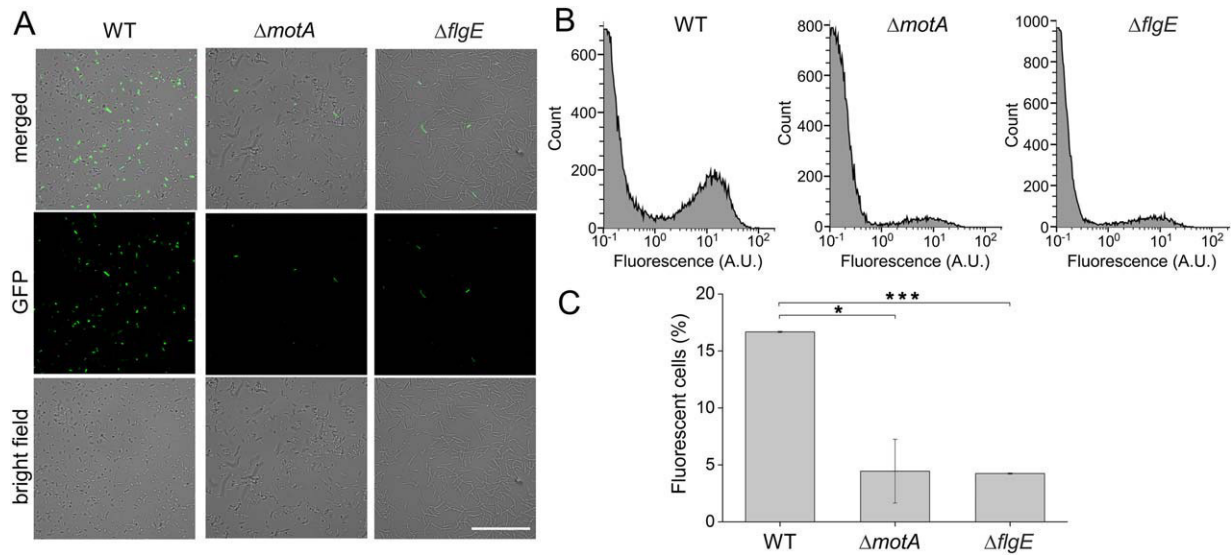


Fig. 4. Competence gene expression is reduced in mutants lacking a functional flagellum.

A. Representative microscopy images of strains harbouring the P_{comG} -*gfp* reporter in wild type, $\Delta motA$ or $\Delta flgE$ genetic background. Images were recorded after 5 h incubation in competence medium. The scale bar represents 50 μ m.

B. Histograms of flow cytometric measurements showing the cell count and the fluorescence in arbitrary units for wild type, $\Delta motA$ or $\Delta flgE$. Representative images are shown for each strain.

C. Percentage of fluorescent cells determined from the data in (B) by isolating the fluorescent population with fluorescence intensities above 3 A.U. showing a significant difference (asterisks) between wild type and $\Delta motA$ ($P = 0.017$) as well as wild type and $\Delta flgE$ ($P < 0.001$) with $n = 3$ for both (unpaired two-sample *t*-test with Welch Correction).

competence medium confirmed a similarly reduced fraction of competent cells in the *hag*-mutant compared to the wild type strain (Fig. S3).

Reduced competence in *hag*-mutant can be rescued by overexpression of *comK*

The reduced competence gene expression in the tested flagellar mutants suggested a regulatory link between flagellar motility and competence. To investigate if regulatory elements upstream of *comK* were responsible for our observations and if a bypass of those could therefore rescue transformation frequency in the flagellar mutant, we examined a strain with an additional copy of *comK* under the control of a xylose-inducible promoter (P_{xyf} -*comK*). Indeed, in combination with P_{xyf} -*comK*, the transformation level of the *hag*-mutant increased back to a level that was statistically indistinguishable from wild type levels (mean transformation frequency of 5.3×10^{-6} for the wild type and 8.5×10^{-6} for Δhag P_{xyf} -*comK*; Kruskal-Wallis test: $P = 0.453$, $n = 9$, Fig. 5A). Despite this observed increase in the *hag* strain upon *comK* overexpression, the wild type strain, which contained an inducible copy of *comK* showed a higher transformation frequency (Fig. 5A, Kruskal-Wallis test: $P = 3.4 \times 10^{-4}$ for WT – WT P_{xyf} -*comK*, $P = 3.4 \times 10^{-4}$ for WT P_{xyf} -*comK* – Δhag P_{xyf} -*comK*, $n = 9$ for both), which was probably due to higher levels of *comK*

transcription at the native locus as previously observed (Hahn *et al.*, 1996).

Reduced competence in flagellar mutants is likely connected to unbalanced *DegU* phosphorylation

As the above results suggested that regulatory elements in response to impaired flagellar motility are responsible for the decreased *comK* expression, we investigated *DegU* as a likely candidate causing the reduced competence in flagellar mutants. As non-phosphorylated *DegU* was implicated to be required for *comK* transcription (Dahl *et al.*, 1992; Hamoen *et al.*, 2000), two variants of *degU* were tested: *degU32*, which harbours a mutation resulting in an extended half-life and thus higher stability of the phosphorylated form of the *DegU* protein (*DegU*~P), and *degU146*, which cannot be phosphorylated (Dahl *et al.*, 1991; 1992; Kunst *et al.*, 1994). Both variants were tested in wild type as well as the Δhag background to observe differences in transformability compared to the wild type strain. The results of this experiment indicated that the transformation frequency of the *degU32* strain was slightly decreased (Fig. 5B), which is consistent with previous publications, suggesting that non-phosphorylated *DegU* is required for priming *comK* transcription. The observed difference, however, was only marginally significant in our experimental setup (Fig. 5B; Kruskal-Wallis test: $P = 0.078$, $n = 6$). Surprisingly, when combined with the Δhag

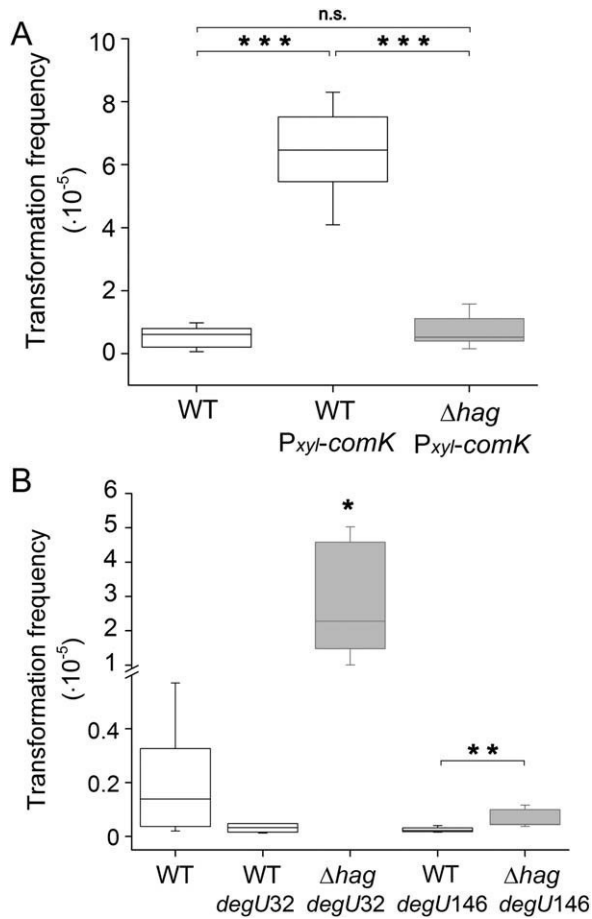


Fig. 5. Synthetically induced *comK* and *degU146* increase competence of Δ *hag*.

A. Transformation frequencies of wild type compared to strains harbouring a xylose-inducible copy of *comK* (*P_{xyl}-comK*) with wild type or Δ *hag* genetic background (Kruskal-Wallis test for WT – WT *P_{xyl}-comK*: $P = 3.4 \times 10^{-4}$; for WT *P_{xyl}-comK* – Δ *hag* *P_{xyl}-comK*: $P = 3.4 \times 10^{-4}$, $n = 9$ for both).

B. Transformation frequencies of WT compared to strains harbouring either a phosphorylated DegU variant (*degU32*) or a non-phosphorylatable DegU variant (*degU146*) in wild type or Δ *hag* background. Strain Δ *hag* *degU32* is significantly different from all other strains (Kruskal-Wallis test: $P < 0.05$ for all, $n = 6$). The line in the boxes represents the median, the box indicates 25th to 75th percentile. Asterisks indicate statistically significant differences (Kruskal-Wallis test: $P = 0.007$, $n = 6$).

mutation, the transformability of *degU32* increased significantly far above wild type levels, despite presumably possessing low levels of non-phosphorylated DegU to induce the ComK auto-stimulatory loop (Fig. 5B; Kruskal-Wallis test: $P = 0.004$, $n = 6$). Furthermore, we observed a tendency towards a reduced albeit non-significant transformation frequency in the *degU146* strain compared to the wild type (Fig. 5B; Kruskal-Wallis test: $P > 0.05$, $n = 6$). This result was similar to the one observed for *degU32*, although no negative impact on transformability was expected in strain *degU146* due to

the abolished phosphorylation of DegU. Interestingly, the *degU146* strain combined with the Δ *hag* mutation exhibited transformation frequencies at the same level than the wild type strain (Fig. 5B; Kruskal-Wallis test: $P > 0.05$, $n = 6$) that was significantly higher than the transformation frequency of the single *degU146* mutant (Fig. 5B; Kruskal-Wallis test, $P = 0.007$, $n = 6$). These results suggest that altering the phosphorylation state of DegU in flagellar mutants can revert the negative impact on competence, which was caused by a lack of motility.

Increased viscosity enhances competence in *B. subtilis*

A recent study showed that restricting the flagellar rotation by viscous medium results in induction of flagellar gene transcription and activation of the DegSU two-component system in *Paenibacillus* sp. NAIST15-1 (Kobayashi *et al.*, 2017). Accordingly, we tested whether an increased viscosity of the medium changes the transformability in *B. subtilis*. Indeed, the average transformation frequency of the wild type strain was threefold higher in a medium of increased viscosity. The corresponding statistical test, however, indicated only a trend towards a statistically significant difference (Fig. 6; unpaired two-sample *t*-test: $P = 0.095$, $n = 4$).

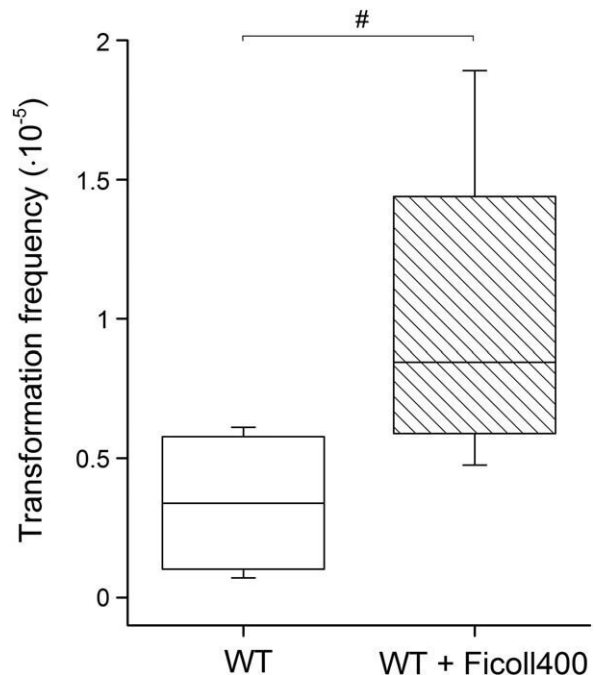


Fig. 6. Competence is improved in viscous medium. Transformation frequency of the wild type strain grown in normal competence medium and in medium with increased viscosity. The line in the boxes represents the median, the box indicates 25th to 75th percentile, # indicates marginally significant differences (unpaired two-sample *t*-test: $P = 0.095$, $n = 4$).

Discussion

Many cellular processes in *B. subtilis* are tightly connected through their underlying regulatory networks. Examples include motility and biofilm formation or biofilm formation and sporulation (e.g. Vlamakis *et al.*, 2013; Marlow *et al.*, 2014; Hölscher *et al.*, 2015). Here, we report an additional connection between flagellar motility and competence development. We could show that mutants with impaired flagellar function have defects in competence development. Such mutants displayed a considerably lower transformation frequency and expression of late competence genes, suggesting that it is due to an altered expression of the competence master regulator gene *comK*. The rescue experiment with an inducible *comK* confirmed that indeed competence could be rescued in the Δhag strain, since Δhag P_{xyr}-*comK* exhibited a wild type transformation level.

In a recently published study, similar effects were observed even though different methods have been used: Diethmaier and colleagues found that the expression of *comK* is lower in deletion mutants of the *fla/che* operon, *hag* and the second stator gene *motB* (Diethmaier *et al.*, 2017). While in their study the expression of *comK* was primarily monitored using a *comK* promoter fusion, our experiments predominantly assayed transformation frequency. Both studies, however, report a negative effect of the deletion of flagellar components on competence development. The extent to which wild type and mutant differ in competence development is in the same order of magnitude between the studies: for example Diethmaier *et al.* observe a 10-fold reduced number of *comG* expressing-cells in Δhag (Diethmaier *et al.*, 2017), whereas our flow cytometry experiments showed a slightly lower, fivefold reduction. Additionally, by investigating the transformation frequency in a *cheA* mutant, we could also show that the chemotactic response does not seem to have an influence on competence development.

Investigating modified variants of the response regulator DegU, we found that the transformation frequency of the *hag*-mutant could be restored to wild type level when the mutant carried a non-phosphorylatable DegU variant (*degU146*). This result suggests that a high level of DegU~P in the flagellar mutants was the reason for the decreased expression of the competence genes and *comK*, which could be counteracted by introducing a non-phosphorylatable variant of DegU. By additionally investigating a strain harbouring a *degU-yfp* fusion, Diethmaier *et al.* also suggested an increased level of DegU~P to be present in the *hag*-mutant (Diethmaier *et al.*, 2017), which is consistent with our conclusions. In addition, the authors detected a reduced expression of *comK* in a strain with the *degU32* variant, which

produces a form of DegU~P with higher stability (Diethmaier *et al.*, 2017). Comparable results were obtained by Msadek *et al.*, who found that high levels of DegU~P inhibit competence (Msadek *et al.*, 1990). We observed a similar, although weak statistical trend towards a reduced transformation frequency in *degU32* strain. Miras and Dubnau (2016) have recently highlighted that differences in the DegU phosphorylation pathway among diverse *B. subtilis* isolates were likely responsible for variance in DNA transformation efficiency among certain domesticated and undomesticated strains. Moreover, slight differences in competence induction levels could also be affected by strain-specific characteristics. For example, *B. subtilis* 168 strains derived from different laboratories can exhibit striking variations in biofilm robustness (Gallegos-Monterrosa *et al.*, 2016). As suggested by Diethmaier and colleagues, the reduced transformation frequency in *degU32* might be caused by the high DegU~P levels of this strain. However, the *degU32* strain exhibits a non-motile phenotype and in the undomesticated strains DegU32 is not able to interact with SwrA at the P_A promoter of the *fla/che* operon (*swrA* is inactive in domesticated strains), leading to repression of P_A (*fla/che*) (Amati *et al.*, 2004; Mordini *et al.*, 2013). Due to low or no expression of the basic flagellar genes, this phenotype could mimic the situation observed in the flagellar mutants. In addition, we observed an increased transformation frequency when the *hag* gene was deleted from the *degU32* background. This is in contrast to the model assuming that increased levels of phosphorylated DegU in the cells lowers competence. Therefore, it is possible that yet unidentified factors are also involved in connecting motility and competence development that might be independent of DegU~P. At this point however, we cannot provide a reasonable explanation for the increased transformation frequency of Δhag *degU32*.

Interestingly, induction of competence state has negative impact on motility in *B. subtilis*. ComK negatively controls *hag* gene expression by stimulating the transcription of *comFA-C* operon and the downstream located anti-sigma factor coding gene, *flgM* (Liu and Zuber, 1998). This feedback loop presents another intriguing connection between these two cellular processes.

Diethmaier *et al.* (2017) proposed that increased DegU~P and lower *comK* expression in the flagellar mutants and in a strain with straight flagella was caused by a lower viscous load. In line with this report, we also observed that higher viscosity in the medium resulted in an increased transformation frequency. Nevertheless, a possible role of the DegSU two-component system in sensing incomplete assembly of flagella and dysfunction as suggested previously (Hsueh *et al.*, 2011; Cairns

et al., 2013) could also explain the increased DegU~P levels in the flagellar mutants.

Together, our results identify a connection between two major physiological processes, providing another example of the complexity of intracellular regulatory networks and the vast amount of tasks a single regulator can cover.

Experimental procedures

Strains and cultivating conditions

The strains used in this study and their mutant derivatives are listed in Table S1. Mutants constructed in this study were obtained by natural transformation of a *B. subtilis* recipient strain with genomic DNA from a donor strain. Strain TB831 was created by transformation of strain 168 P_{xyr}comK with genomic DNA of strain GP902 (J. Stülke lab collection). To obtain strains TB926 and TB925, genomic DNA of strain 168 P_{comG}-gfp was used to transform strain TB710 and TB689 respectively. Strain TB928 was obtained by transforming strain 168 P_{xyr}comK with genomic DNA of GP901 (J. Stülke lab collection). To create strain TB935 and TB936, strain 168 was transformed with genomic DNA obtained from strain QB4371 (Kunst *et al.*, 1994) and QB4458 (Dahl *et al.*, 1991) respectively. Their derivatives harbouring also a mutation of *hag* (TB923 and TB924) were created by transformation with genomic DNA, which was obtained from GP901. In-frame deletions of *motA*, *flgE* and *cheA* were created using plasmids pEC1, pDP306 and pDP338, respectively, as previously described (Courtney *et al.*, 2012; Chan *et al.*, 2014; Calvo and Kearns, 2015). Strains were verified by fluorescence microscopy (P_{comG}-gfp reporter), PCR (*hag*-mutants) or sequencing (*degU* variants), using the oligonucleotides listed in Table S2. For experiments with strains harbouring the inducible construct P_{xyr}comK, 1% of xylose (final concentration) was added for induction (see van den Esker *et al.*, 2017). To increase medium viscosity, 10% Ficoll400 (Carl Roth) was added to the medium before culture inoculation and the mix was vortexed vigorously for ca. 20 s.

Transformation frequency assay

To assess the transformation frequency of different strains, a modified version of the transformation protocol from Konkol *et al.* (2013) was used. One millilitre of each culture grown in 3 ml Lysogeny broth (LB) medium (LB-Lennox, Carl Roth; 10 g l⁻¹ tryptone, 5 g l⁻¹ yeast extract and 5 g l⁻¹ NaCl) for 16 h was centrifuged for 2 min at 11 000 × g. The pellet was washed twice in de-ionized water and was re-suspended in 100 µl de-ionized water. The re-suspended culture was diluted (1:80) in complete competence medium (MC: 1.8 ml de-ionized

water, 6.7 µl 1 M MgSO₄, 50 µl 0.2% L-Tryptophan, 200 µl 10xMC; per 100 ml 10xMC: 14.036 g K₂HPO₄ [×3H₂O], 5239 g KH₂PO₄, 20 g glucose, 10 ml 300 mM tri-sodium citrate, 1 ml 83.97 mM ammonium iron (III) citrate, 1 g casein hydrolysate, 2 g potassium glutamate [H₂O]) and incubated at 37°C, 225 r.p.m. For experiments with strains harbouring P_{xyr}comK, 10xMC with fructose instead of glucose was used. After 6 h incubation time, 5 µl DNA with an antibiotic marker (PY79 *safA*::Tet gDNA, 60 ng µl⁻¹) was added to 500 µl culture. Any alteration in incubation time before addition of the DNA is indicated in the results section. Each culture was incubated for 30 min, then 500 µl fresh LB medium was added and the culture was incubated for another 1 h under the conditions mentioned above. Serial dilutions of cultures supplemented with DNA were prepared and plated on LB medium supplemented with 1.5% agar to determine the number of colony-forming units (cfu). Additionally, 50 and 100 µl undiluted cultures supplemented with gDNA as well as controls were plated on tetracycline (Tet) containing LB-agar plates (10 µg ml⁻¹ Tet) to determine the number of transformant colonies. The transformation frequency was calculated by dividing the number of transformants per ml by cfu per ml.

Growth curve experiments

To examine growth properties, cultures were inoculated in LB medium from frozen glycerol stocks and incubated for ca. 16 h at 37°C shaking at 225 r.p.m. Cultures were diluted 1:100 in 200 µl fresh completed MC medium (see above) and the OD_{590 nm} was recorded for 16 h using a TECAN Infinite F200 PRO microplate reader. The cultures were incubated with orbital shaking with a duration of 800 s and an amplitude of 3 mm at 37°C and the OD₅₉₀ was measured every 15 min.

Fluorescence microscopy

Strains were investigated using a confocal laser scanning microscope (LSM 780, Carl Zeiss) equipped with an argon laser and a Plan-Apochromat/1.4 Oil DIC M27 63× objective. Cultures were grown prior microscopy for 5 h (if not indicated otherwise) in competence medium under the same conditions as described above (see section “Transformation Frequency Assay”). Excitation of the fluorescent reporter (GFP) was performed at 488 nm and the emitted fluorescence was recorded at 493–598 nm. For image visualisation, Zen 2012 software (Carl Zeiss) was used, brightness and contrast were adjusted equally in all images.

Flow cytometry

Flow cytometric measurements were performed using a Partec CyFlow® Space (Sysmex Partec GmbH,

Germany), which was equipped with a solid-state laser for excitation of green/yellow fluorescent proteins at 488 nm. Single cells were detected in forward and side-ward scatter channels as well as in one fluorescent channel. A minimum of 40 000 cells were analysed for the experiments. To define the background fluorescence signal, non-labelled *B. subtilis* cultures were analysed as control. Cultures used for measurements were grown for 5 h (if not indicated otherwise) in competence medium under the same conditions as described above (see section "Transformation Frequency Assay"). For evaluation of the data, the FlowJo® software (FlowJo LLC, Ashland, KY, USA) was used and a gate was set at three fluorescence units for all samples to isolate the fluorescent population and determine the percentage of fluorescent cells.

Statistics

Statistical analyses were performed using OriginPro 2016 (V93E, OriginLab Northampton, MA, USA). Unpaired two-sample *t*-test with Welch Correction or a Kruskal-Wallis test was used to test for significant differences.

Acknowledgements

We thank Daniel Kearns for providing plasmids, Anne Richter for constructing the in-frame deletion mutants, and Tadeja Marin for initial observations. We thank Wiep Klaas Smits for his comment on our bioRxiv submission. This project was funded by grant KO4741/3-1 from the German Research Foundation (DFG). T.H. and A.D. were supported by International Max Planck Research School and Alexander von Humboldt foundation fellowships respectively. CK was supported by the Volkswagen Foundation (I/85 290) as well as the German Research Foundation (SFB 944/2–2016, KO 3909/2-1). Á.T.K. was supported by a Startup fund from the Technical University of Denmark.

References

Amati, G., Bisicchia, P., and Galizzi, A. (2004) DegU-P represses expression of the motility *fla-che* operon in *Bacillus subtilis*. *J Bacteriol* **186**: 6003–6014.

Berka, R.M., Hahn, J., Albano, M., Draskovic, I., Persuh, M., and Cui, X. (2002) Microarray analysis of the *Bacillus subtilis* K-state: genome-wide expression changes dependent on ComK. *Mol Microbiol* **43**: 1331–1345.

Cairns, L.S., Marlow, V.L., Bissett, E., Ostrowski, A., and Stanley-Wall, N.R. (2013) A mechanical signal transmitted by the flagellum controls signalling in *Bacillus subtilis*. *Mol Microbiol* **90**: 6–21.

Calvo, R.A., and Kearns, D.B. (2015) FlgM is secreted by the flagellar export apparatus in *Bacillus subtilis*. *J Bacteriol* **197**: 81–91.

Caramori, T., Barilla, D., Nessi, C., Sacchi, L., and Galizzi, A. (1996) Role of FlgM in sigma(D)-dependent gene expression in *Bacillus subtilis*. *J Bacteriol* **178**: 3113–3118.

Chan, J.M., Guttenplan, S.B., and Kearns, D.B. (2014) Defects in the flagellar motor increase synthesis of poly- γ -glutamate in *Bacillus subtilis*. *J Bacteriol* **196**: 740–753.

Chen, I., Christie, P.J., and Dubnau, D. (2005) The ins and outs of DNA transfer in bacteria. *Science* **310**: 1456–1460.

Chen, R., Guttenplan, S.B., Blair, K.M., and Kearns, D.B. (2009) Role of the σ D-dependent autolysins in *Bacillus subtilis* population heterogeneity. *J Bacteriol* **191**: 5775–5784.

Courtney, C.R., Cozy, L.M., and Kearns, D.B. (2012) Molecular characterization of the flagellar hook in *Bacillus subtilis*. *J Bacteriol* **194**: 4619–4629.

Cozy, L.M., and Kearns, D.B. (2010) Gene position in a long operon governs motility development in *Bacillus subtilis*. *Mol Microbiol* **76**: 273–285.

Dahl, M.K., Msadek, T., Kunst, F., and Rapoport, G. (1991) Mutational analysis of the *Bacillus subtilis* DegU regulator and its phosphorylation by the DegS protein kinase. *J Bacteriol* **173**: 2539–2547.

Dahl, M.K., Msadek, T., Kunst, F., and Rapoport, G. (1992) The phosphorylation state of the DegU response regulator acts as a molecular switch allowing either degradative enzyme synthesis or expression of genetic competence in *Bacillus subtilis*. *J Biol Chem* **267**: 14509–14514.

Diethmaier, C., Chawla, R., Canzoneri, A., Kearns, D.B., Lele, P.P., and Dubnau, D. (2017) Viscous drag on the flagellum activates *Bacillus subtilis* entry into the K-state. *Mol Microbiol* **106**: 367–380.

Dubnau, D. (1991) Genetic competence in *Bacillus subtilis*. *Microbiol Rev* **55**: 395–424.

Dubnau, D., and Losick, R. (2006) Bistability in bacteria. *Mol Microbiol* **61**: 564–572.

van den Esker, M.H., Kovács, Á.T., and Kuipers, O.P. (2017) YsbA and LytST are essential for pyruvate utilization in *Bacillus subtilis*. *Environ Microbiol* **19**: 83–94.

Gallegos-Monterrosa, R., Mhatre, E., and Kovács, Á.T. (2016) Specific *Bacillus subtilis* 168 variants form biofilms on nutrient-rich medium. *Microbiology* **162**: 1922–1932.

Hahn, J., Luttinger, A., and Dubnau, D. (1996) Regulatory inputs for the synthesis of ComK, the competence transcription factor of *Bacillus subtilis*. *Mol Microbiol* **21**: 763–775.

Hamoen, L.W., Van, Werkhoven, A.F., Venema, G., and Dubnau, D. (2000) The pleiotropic response regulator DegU functions as a priming protein in competence development in *Bacillus subtilis*. *Proc Natl Acad Sci U S A* **97**: 9246–9251.

Hamoen, L.W., Venema, G., and Kuipers, O.P. (2003) Controlling competence in *Bacillus subtilis*: shared use of regulators. *Microbiology* **149**: 9–17.

Hölscher, T., Bartels, B., Lin, Y.-C., Gallegos-Monterrosa, R., Price-Whelan, A., Kolter, R. *et al*, (2015) Motility, chemotaxis and aerotaxis contribute to competitiveness during bacterial pellicle biofilm development. *J Mol Biol* **427**: 3695–3708.

Hsueh, Y.H., Cozy, L.M., Sham, L.T., Calvo, R.A., Gutu, A.D., Winkler, M.E., and Kearns, D.B. (2011) DegU-phosphate activates expression of the anti-sigma factor FlgM in *Bacillus subtilis*. *Mol Microbiol* **81**: 1092–1108.

Inamine, G.S., and Dubnau, D. (1995) ComEA, a *Bacillus subtilis* integral membrane protein required for genetic

- transformation, is needed for both DNA binding and transport. *J Bacteriol* **177**: 3045–3051.
- Kobayashi, K., Kanesaki, Y., and Yoshikawa, H. (2017) Surface sensing for flagellar gene expression on solid media in *Paenibacillus* sp. NAIST15-1. *Appl Environ Microbiol* **83**: e00585-17.
- Konkol, M.A., Blair, K.M., and Kearns, D.B. (2013) Plasmid-encoded comI inhibits competence in the ancestral 3610 strain of *Bacillus subtilis*. *J Bacteriol* **195**: 4085–4093.
- Kunst, F., Msadek, T., Bignon, J., and Rapoport, G. (1994) The DegS/DegU and ComP/ComA two-component systems are part of a network controlling degradative enzyme synthesis and competence in *Bacillus subtilis*. *Res Microbiol* **145**: 393–402.
- Liu, J., and Zuber, P. (1998) A molecular switch controlling competence and motility: competence regulatory factors ComS, MecA, and ComK control sigmaD-dependent gene expression in *Bacillus subtilis*. *J Bacteriol* **180**: 4243–4251.
- Maamar, H., and Dubnau, D. (2005) Bistability in the *Bacillus subtilis* K-state (competence) system requires a positive feedback loop. *Mol Microbiol* **56**: 615–624.
- Maamar, H., Raj, A., and Dubnau, D. (2007) Noise in gene expression determines. *Science* **317**: 526–529.
- Maier, B., Chen, I., Dubnau, D., and Sheetz, M.P. (2004) DNA transport into *Bacillus subtilis* requires proton motive force to generate large molecular forces. *Nat Struct Mol Biol* **11**: 643–649.
- Marlow, V.L., Porter, M., Hopley, L., Kiley, T.B., Swedlow, J.R., Davidson, F.A., and Stanley-Wall, N.R. (2014) Phosphorylated DegU manipulates cell fate differentiation in the *Bacillus subtilis* biofilm. *J Bacteriol* **196**: 16–27.
- Miras, M., and Dubnau, D. (2016) A DegU-P and DegQ-dependent regulatory pathway for the K-state in *Bacillus subtilis*. *Front Microbiol* **7**: 1–14.
- Mordini, S., Osera, C., Marini, S., Scavone, F., Bellazzi, R., Galizzi, A., and Calvio, C. (2013) The role of SwrA, DegU and PD3 in *flaI* expression in *B. subtilis*. *PLoS One* **8**: e85065.
- Msadek, T., Kunst, F., Henner, D., Klier, A., Rapoport, G., and Dedonder, R. (1990) Signal transduction pathway controlling synthesis of a class of degradative enzymes in *Bacillus subtilis*: expression of the regulatory genes and analysis of mutations in *degS* and *degU*. *J Bacteriol* **172**: 824–834.
- Mugler, A., Kittisopikul, M., Hayden, L., Liu, J., Wiggins, C.H., Süel, G.M., Walczak, A.M., and Maslov, S. (2016) Noise expands the response range of the *Bacillus subtilis* competence circuit. *PLoS Comput Biol* **12**: 1–21.
- Mukherjee, S., and Kearns, D.B. (2014) The structure and regulation of flagella in *Bacillus subtilis*. *Annu Rev Genet* **48**: 319–340.
- Murray, E.J., Kiley, T.B., and Stanley-Wall, N.R. (2009) A pivotal role for the response regulator DegU in controlling multicellular behaviour. *Microbiology* **155**: 1–8.
- Ogura, M., Yamaguchi, H., Kobayashi, K., Ogasawara, N., Fujita, Y., and Tanaka, T. (2002) Whole-genome analysis of genes regulated by the *Bacillus subtilis* competence transcription factor ComK. *J Appl Microbiol* **184**: 2344–2351.
- Provedvi, R., Chen, I., and Dubnau, D. (2001) NucA is required for DNA cleavage during transformation of *Bacillus subtilis*. *Mol Microbiol* **40**: 634–644.
- Serizawa, M., Yamamoto, H., Yamaguchi, H., Fujita, Y., Kobayashi, K., Ogasawara, N., and Sekiguchi, J. (2004) Systematic analysis of SigD-regulated genes in *Bacillus subtilis* by DNA microarray and Northern blotting analyses. *Gene* **329**: 125–136.
- van Sinderen, D., and Venema, G. (1994) ComK acts as an autoregulatory control switch in the signal transduction route to competence in *Bacillus subtilis*. *J Bacteriol* **176**: 5762–5770.
- van Sinderen, D., Luttinger, A., Kong, L., Dubnau, D., Venema, G., and Hamoen, L. (1995) *comK* encodes the competence transcription factor, the key regulatory protein for competence development in *Bacillus subtilis*. *Mol Microbiol* **15**: 455–462.
- Smits, W.K., Eschevins, C.C., Susanna, K.A., Bron, S., Kuipers, O.P., and Hamoen, L.W. (2005) Stripping *Bacillus*: ComK auto-stimulation is responsible for the bistable response in competence development. *Mol Microbiol* **56**: 604–614.
- Turgay, K., Hahn, J., Burghoorn, J., and Dubnau, D. (1998) Competence in *Bacillus subtilis* is controlled by regulated proteolysis of a transcription factor. *EMBO J* **17**: 6730–6738.
- Vlamakis, H., Chai, Y., Beaugregard, P., Losick, R., and Kolter, R. (2013) Sticking together: building a biofilm the *Bacillus subtilis* way. *Nat Rev Microbiol* **11**: 157–168.

Supporting Information

Additional Supporting Information may be found in the online version of this article at the publisher's web-site:

Fig. S1. Reduced competence in different *B. subtilis* strains. Transformation frequency of *B. subtilis* wild-type and *hag*-mutant of strains PS216 and 3610 after incubation in competence medium for 6 h ($n = 3$). Error bars represent the standard deviation.

Fig. S2. Chemotactic response is not connected to competence. Transformation frequency of *B. subtilis* wild-type and *cheA*-mutant, encoding the main sensor kinase of the chemotaxis system, after incubation in competence medium for 6 h (unpaired two-sample t-test with Welch Correction: $P = 0.232$, $n = 3$). Error bars represent the standard deviation.

Fig. S3. Fewer cells express competence genes in the *hag*-mutant over time. Percentage of fluorescent (i.e. competence gene expressing) cells determined from flow cytometric measurements of wild-type and *hag*-mutant harboring P_{comG} -*gfp* after 3 h, 4 h and 5 h incubation in competence medium (unpaired two-sample t-test with Welch Correction: $P < 0.05$, $n = 3$). A gate at fluorescence intensities above 3 A.U. was used to isolate the fluorescent population. Error bars represent the standard deviation.

Table S1. Strains used in this study. Antibiotics are abbreviated as follows: Kanamycin – Kan, Chloramphenicol – Chl, Tetracyclin – Tet.

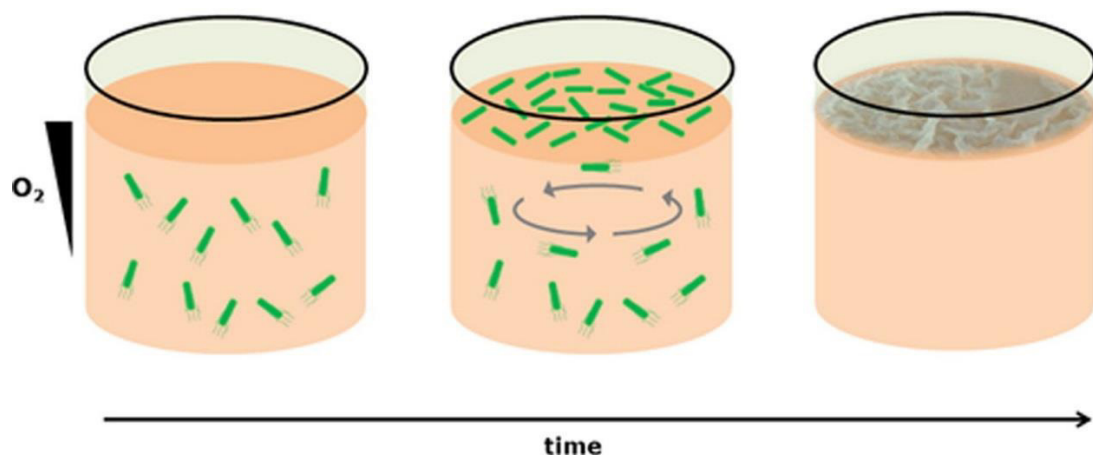
Table S2. Oligonucleotides used in this study

Chapter 2

Motility, chemotaxis and aerotaxis contribute to competitiveness during bacterial pellicle biofilm development

Published in: Journal of Molecular Biology (2015)

Graphical abstract:





Motility, Chemotaxis and Aerotaxis Contribute to Competitiveness during Bacterial Pellicle Biofilm Development

Theresa Hölscher^{1,†}, Benjamin Bartels^{1,†}, Yu-Cheng Lin^{2,†},
Ramses Gallegos-Monterrosa¹, Alexa Price-Whelan², Roberto Kolter³,
Lars E.P. Dietrich² and Ákos T. Kovács¹

¹ - *Terrestrial Biofilms Group, Institute of Microbiology, Friedrich Schiller University Jena, D-07743 Jena, Germany*

² - *Department of Biological Sciences, Columbia University, New York, NY 10027, USA*

³ - *Department of Microbiology and Immunobiology, Harvard Medical School, Boston, MA 02115, USA*

Correspondence to Ákos T. Kovács: *Institute of Microbiology, Friedrich Schiller University Jena, Neugasse 23, D-07743 Jena, Germany. akos-tibor.kovacs@uni-jena.de*

<http://dx.doi.org/10.1016/j.jmb.2015.06.014>

Edited by I. B. Holland

Abstract

Biofilm formation is a complex process involving various signaling pathways and changes in gene expression. Many of the sensory mechanisms and regulatory cascades involved have been defined for biofilms formed by diverse organisms attached to solid surfaces. By comparison, our knowledge on the basic mechanisms underlying the formation of biofilms at air–liquid interfaces, that is, pellicles, is much less complete. In particular, the roles of flagella have been studied in multiple solid-surface biofilm models but remain largely undefined for pellicles. In this work, we characterize the contributions of flagellum-based motility, chemotaxis and oxygen sensing to pellicle formation in the Gram-positive *Bacillus subtilis*. We confirm that flagellum-based motility is involved in, but is not absolutely essential for, *B. subtilis* pellicle formation. Further, we show that flagellum-based motility, chemotaxis and oxygen sensing are important for successful competition during *B. subtilis* pellicle formation. We report that flagellum-based motility similarly contributes to pellicle formation and fitness in competition assays in the Gram-negative *Pseudomonas aeruginosa*. Time-lapse imaging of static liquid cultures demonstrates that, in both *B. subtilis* and *P. aeruginosa*, a turbulent flow forms in the tube and a zone of clearing appears below the air–liquid interface just before the formation of the pellicle but only in strains that have flagella.

© 2015 Elsevier Ltd. All rights reserved.

Introduction

Research over the last several decades has shown that natural bacterial communities exist mainly as biofilms, cellular aggregates encased in self-produced matrices that often form on surfaces [1–3]. The term for a biofilm can depend on the type of interface at which it is found: colonies form on solid surfaces in air, submerged or flow cell biofilms form on solid surfaces in liquid and pellicle biofilms form on liquid in air [4]. Pellicle formation has been described for various Gram-negative and Gram-positive bacteria [5–11] and proceeds through several stages. In early stages, a thin layer of cells appears at the air–liquid interface. This layer

originates either from cells attached to the wall of the vessel that spread over the liquid or from cell clusters in the middle of the medium surface that spread outward [6,12]. In later stages, three-dimensional structures can develop as the pellicle grows and thickens, resulting in the formation of wrinkles [4,5,13].

The exact mechanisms underpinning the initial stages of pellicle formation (i.e., how cells reach the interface) are not well characterized. The production of an extracellular matrix is essential for pellicle formation in all species examined, while most cells of the biofilm are non-motile [6,14]. Different types of motility, Brownian motion or buoyancy could all influence whether or not cells

are close to the air–liquid interface during the initiation stage [12]. As cells in a biofilm are sessile, biofilm formation and motility are considered opposing mechanisms [15]. This is supported by the fact that, in many investigated organisms, genes required for biofilm formation and flagellar motility are inversely regulated, often with c-di-GMP being involved [15–18]. However, many bacteria show defects in pellicle formation when genes involved in flagellum synthesis are mutated and the ability to form a pellicle is completely abolished in some species [7,9,12,19,20].

The air–liquid interface represents a favorable environment especially for aerobic microorganisms, since access to oxygen in high concentrations and nutrients from the medium are provided. The presence of oxygen as an electron acceptor in the atmospheric phase is important for pellicle formation in bacteria such as *Escherichia coli* and *Shewanella oneidensis*, which do not form pellicles under anaerobic conditions when alternative electron acceptors are provided in the medium [10,19]. Further, the movement toward oxygen, that is, positive aerotaxis, is proposed to control movement of the cells toward the air–liquid interface in *S. oneidensis* [7] and regulates biofilm formation on abiotic surfaces in *Ralstonia solanacearum* [21]. Oxygen has been shown to be a crucial factor for survival and growth of coexisting strains of *Brevibacillus* sp. and *Pseudoxanthomonas* sp. at the air–liquid interface [22]. In *Pseudomonas aeruginosa*, decreased availability of oxygen in the atmosphere has been shown to be detrimental to pellicle integrity, and provision of an alternative electron acceptor in the medium promoted growth in the liquid phase below the pellicle [23].

Bacillus subtilis is a highly tractable Gram-positive model for biofilm formation. The regulation of *B. subtilis* pellicle formation and morphogenesis has been well characterized in undomesticated strains [5,12,16,24–26], but the roles of flagellar motility and aerotaxis in this process have not been fully elucidated. Domesticated, laboratory strains of *B. subtilis* have mostly reduced biofilm forming ability [27]. Using the undomesticated strain ATCC 6051, Kobayashi showed that flagellum-deficient mutants exhibit a delay in pellicle formation [12]. However, this effect was not observed in the minimal medium MSgg, which is generally used to investigate both colony biofilms and pellicles of *B. subtilis* wild isolates. Based on these results, it was concluded that flagella may rather play an indirect regulatory role in pellicle formation [12]. It has been hypothesized that *B. subtilis* cells migrate to the air–liquid interface due to aerotaxis [5] but this has not been demonstrated experimentally. Further, lack of flagellar motility did not alter colony biofilm spreading on agar medium as demonstrated by Seminara *et al.* [28]. *B. subtilis* can also colonize a semisolid surface

via multicellular movements [29]. While hyperflagellated cells move in rafts [30], flagellum-less isolates of *B. subtilis* are able to slide in a surfactin-dependent manner [31]. Notably, the flagellum serves as a transmitter of mechanical signals during surface attachment (i.e., initiation of biofilm formation) to activate gene expression in *B. subtilis* via the DegS/DegU two-component system [32]. Throughout this paper, we will refer to the movement based on individual cell as motility.

Motility also plays an important role in *P. aeruginosa* biofilms as the structures of flow cell biofilms are altered when motility and its switch-off during biofilm formation is not tightly controlled [9,15,33–35]. For example, evolved hyperswarmers are out-competed by the less motile ancestral strain in surface-attached biofilms indicating a trade-off between biofilm formation and flagellar motility [36]. In *P. aeruginosa*, flagella and pili contribute to specific types of motility (swimming/swarming and twitching, respectively) [37]. It was also investigated whether flagella and pili are involved in the formation of pellicles of *P. aeruginosa* PAO1. Yamamoto *et al.* observed that a flagellum-deficient mutant fails to produce a normally structured pellicle and pellicle formation is delayed. On the contrary, pili-deficient mutants and mutants deficient in both pili and flagella formed proper pellicles [9].

In this work, we characterized the roles of flagellum-dependent motility, chemotaxis and oxygen sensing in pellicle development of *B. subtilis*. We found that, although flagellar motility was not strictly required for pellicle formation, it conferred a competitive advantage over non-motile mutants in static competition assays. Mutants defective in flagellar motility, chemotaxis or oxygen sensing were also at a disadvantage when competed against the parent strain under these conditions. *P. aeruginosa* PA14 mutants lacking flagella showed a partial defect in pellicle formation and a disadvantage in competition assays. We reasoned that flagella might facilitate localization near the surface and thereby contribute to increased turbidity near the air–liquid interface in static cultures. Time-lapse imaging revealed formation of an intriguing transparent zone near the air–liquid interface in wild-type *B. subtilis* and *P. aeruginosa* static cultures during the time preceding pellicle formation. Non-flagellated mutants showed more culture turbidity in this region.

Results

Flagellar motility is required for wild-type pellicle maturation dynamics in *B. subtilis*

To investigate the role and costs of flagellar motility during pellicle formation, the

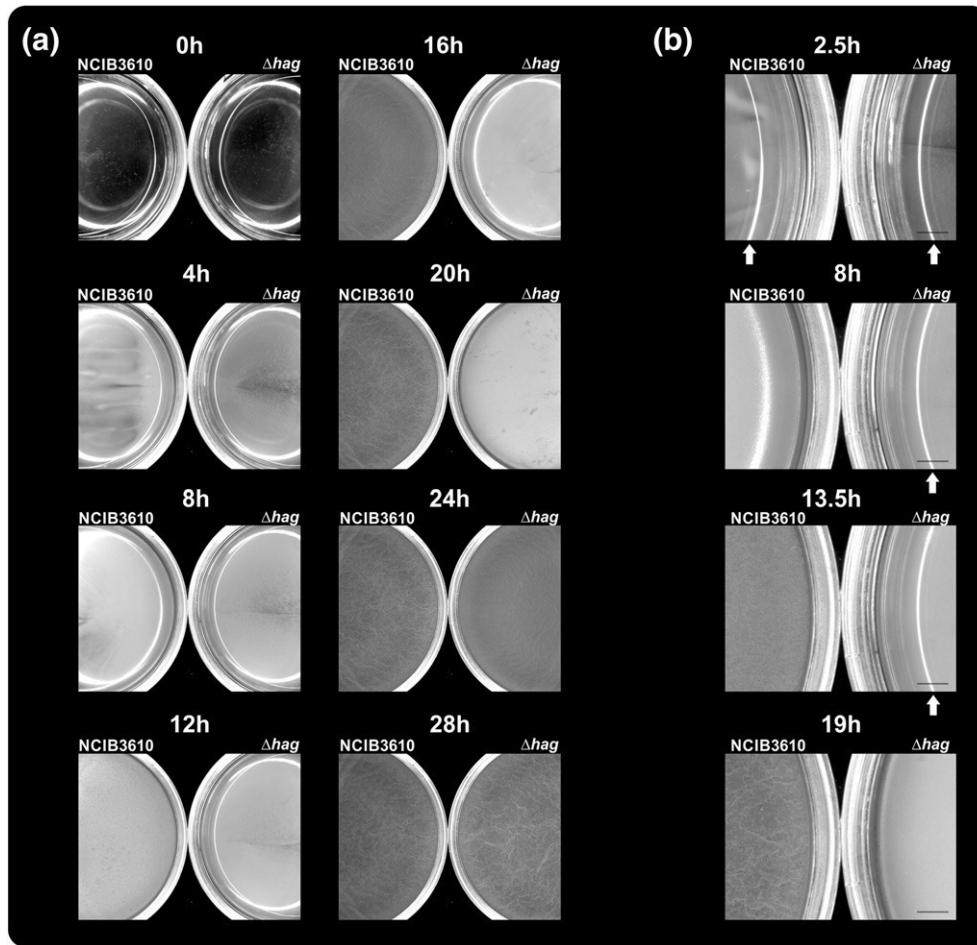


Fig. 1. (a) Pellicle formation of *B. subtilis* wild type (left petri dish) and its Δhag derivative (right petri dish) is shown in 35-mm-diameter petri dishes containing MSgg medium. (b) Magnified section of the petri dishes at selected time point mentioned in the text. Scale bar indicates 2 mm. Arrows point to the reflected light on the medium surface before a thin layer of pellicle is formed. The time points are presented from Video S1.

flagellin-deficient and therefore immotile mutant Δhag of *B. subtilis* strain NCIB3610 was used. First, pellicle formation of Δhag and the wild type was compared in the biofilm-promoting medium MSgg to test whether the previously described delay of the Δhag mutant in rich medium would also be present in this minimal medium. As shown in Fig. 1a and Video S1, planktonic growth of both strains could be noticed at the same time (i.e., cultures became turbid). Subsequently, the wild type formed a thick layer of pellicle after 8 h of incubation (observable as reduced light reflectivity of the medium surface on Fig. 1b) and wrinkled after 19 h. The Δhag mutant exhibited delayed pellicle formation, with initiation at 15 h after inoculation and wrinkle formation after 25 h. The wild-type-like appearance of the Δhag mutant pellicle demonstrated that pellicle formation and morphogenesis *per se* was not impeded by lack of flagella. Further, when the wild type and the Δhag mutant were inoculated at high starting cell densities

(~OD₆₀₀ of 1.0), no delay in pellicle formation was observed (data not shown). The delay of the Δhag mutant was not due to disadvantages in growth as the Δhag mutant reached higher OD (optical density) values and therefore showed enhanced growth in shaken cultures when compared to the wild type (Fig. S1). The latter result suggests that the production of flagellin is accompanied by energetic costs for the wild type. The same growth advantage was observed for mutants lacking components of the flagellum indicating that both flagellum production and flagellar activity are costly for the cell (Fig. S1).

The Δhag mutant is outcompeted by wild-type cells during pellicle formation

To assay whether the cost of flagellin production influences the competitiveness of the *B. subtilis* wild-type strain, we performed a competition with the Δhag mutant under pellicle promoting and

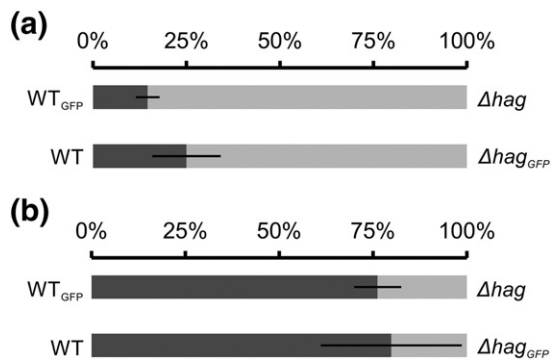


Fig. 2. Relative abundance of *B. subtilis* wild type (dark gray) and Δhag (light gray) strains in competition experiments performed under shaken (a) ($n = 3$, Student's t test $p < 0.05$) or static (b) ($n = 6$, Student's t test $p < 0.01$) conditions. Under planktonic conditions (a), the cultures reached stationary phase (20 h of incubation) and grew for about 5.8 generations. Bars represent percentages of strains in the pellicles. Error bars indicate standard deviation.

non-promoting conditions. The wild type and the Δhag mutant were inoculated together in MSgg medium in a 1:1 ratio and incubated under static (pellicle promoting) or shaking (pellicle non-promoting) conditions. One of the strains was labeled with constitutively expressed GFP (green fluorescent protein) and the final ratio of the two strains was determined by CFU (colony-forming units) counting. The experiment was repeated with a switched label

to exclude any effects caused by the production of GFP (NCIB3610 versus Δhag_{GFP} and NCIB3610_{GFP} versus Δhag). Under shaken, well-aerated conditions, the wild type was outcompeted by the Δhag mutant indicating that the cost of flagellin production leads to disadvantages for the wild type under this condition (Fig. 2a). However, under pellicle promoting conditions, the Δhag mutant was strongly outcompeted by the wild type (Fig. 2b). This finding indicates that flagellar motility is important in the competition for the favorable niche at the air-liquid interface.

To verify the results, we repeated the pellicle competition experiment with strains labeled with different constitutively produced fluorescent markers for green and red fluorescence (GFP and mKATE2, respectively). The fluorescent strains were followed in competition experiments (Video S2) and fluorescence intensities were measured after 3 days and normalized against the fluorescence intensities of control competitions (see Materials and Methods for normalization details). The fluorescent signals in the pellicles were analyzed by both fluorescence microscopy and a microplate fluorometer. In pellicles, the Δhag mutant was outcompeted by the wild type regardless of the fluorescent label as determined by quantitative fluorescence intensity measurements (Fig. 3a) and stereomicroscopy (Fig. 3b).

To investigate whether other strains with defects in flagellar motility would show disadvantages in pellicle competitions with the wild type, we engineered mutants with deletions in *motA* (encoding

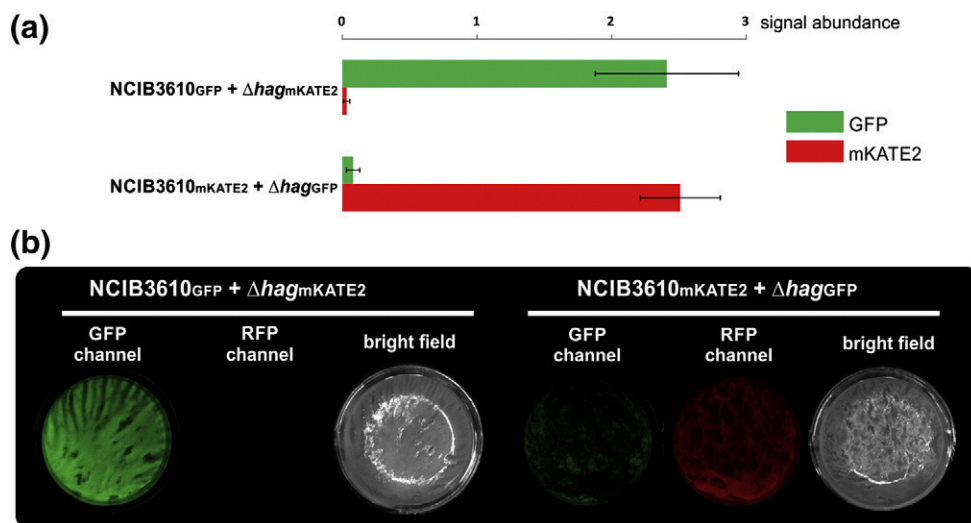


Fig. 3. Competition of GFP- or mKATE2-labeled wild type and Δhag strains of *B. subtilis* strains during pellicle formation. Relative fluorescence level (arbitrary units) quantified in a plate reader (a) ($n = 4$, Student's t test $p < 0.001$) or visualized using a stereomicroscope (b). Error bars indicate standard deviation. Certain wells (16 mm diameter) of a 24-well plate are shown in the green- or red-fluorescence channels (false-colored green and red) together with its bright-light images.

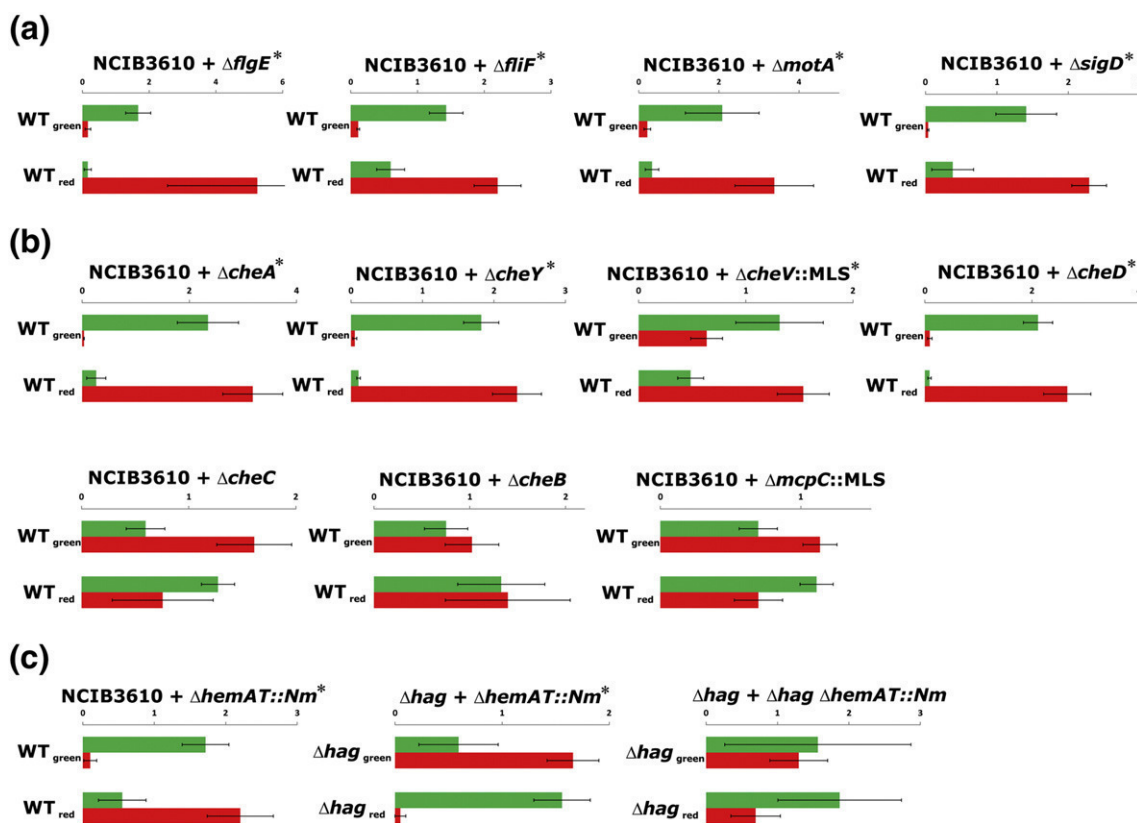


Fig. 4. Competition of GFP- or mKATE2-labeled *B. subtilis* strains during pellicle formation. Mutants are categorized by the locus' involvement in (a) flagellum biosynthesis and regulation, (b) chemotaxis or (c) aerotaxis. Relative fluorescence levels (arbitrary units are shown on the axis) were quantified in a fluorescence plate reader and are shown with bar charts ($n = 4$). Green and red bars indicate relative GFP and mKATE2 levels, respectively. In each graph, the upper bars represent the mix of NCIB3610_{GFP} and mutant_{mKATE2} strains (WT_{green}), while the down bars represent the mix of NCIB3610_{mKATE2} and mutant_{GFP} strains (WT_{red}). Error bars indicate standard deviation. Significant differences (Student's t test $p < 0.05$; see Materials and Methods) are indicated with a star next to the strains used for competitions.

part of the motor complex), *fliF* (encoding the cell wall anchor), *flgE* (encoding the hook protein) and *sigD* (encoding the sigma factor regulating flagella, motility, chemotaxis and autolysis) and added the fluorescent tag constructs described above. Mutants defective in swimming motility—namely $\Delta motA$, $\Delta fliF$, $\Delta flgE$ and $\Delta sigD$ —were outcompeted by the wild type in 1:1 pellicle competitions (Fig. 4a, Fig. S2 and Table S1). A disadvantage was observed regardless of whether the mutants lacked a specific flagellar component or exhibited reduced gene expression of the whole apparatus (i.e., in the $\Delta sigD$ strain). Importantly, all mutant strains formed pellicle structures comparable to those of the wild type when grown as monocultures (Fig. S2).

Chemotaxis and oxygen sensing contribute to *B. subtilis* competitiveness in pellicles

As chemotaxis and oxygen sensing have been proposed to play roles in the initial stages of pellicle

formation in various bacterial species, we tested a collection of *B. subtilis* NCIB3610 mutants defective in chemotaxis for their competitiveness against the wild type in pellicles. In *B. subtilis*, most of the chemotaxis genes are located in the same operon as the genes encoding flagellar proteins, namely, the *fla/che* operon. The chemotaxis machinery includes a two-component system that consists of the receptor-coupled kinase CheA and the response regulator CheY. Phosphorylated CheY binds to a flagellar motor component leading to counterclockwise rotation of the flagellum and therefore swimming. Additional proteins (e.g., CheV, CheR-CheB and CheC-CheD circuits) are involved in adaptation, the process by which the signaling state of the chemotaxis pathway is reset to a background concentration [38]. The mutants tested were $\Delta mcpC$ (receptor involved in amino acid chemotaxis), $\Delta cheA$ (receptor-coupled kinase), $\Delta cheB$ (involved in methylation of receptors), $\Delta cheC$ and $\Delta cheD$ (both regulating CheA autophosphorylation),

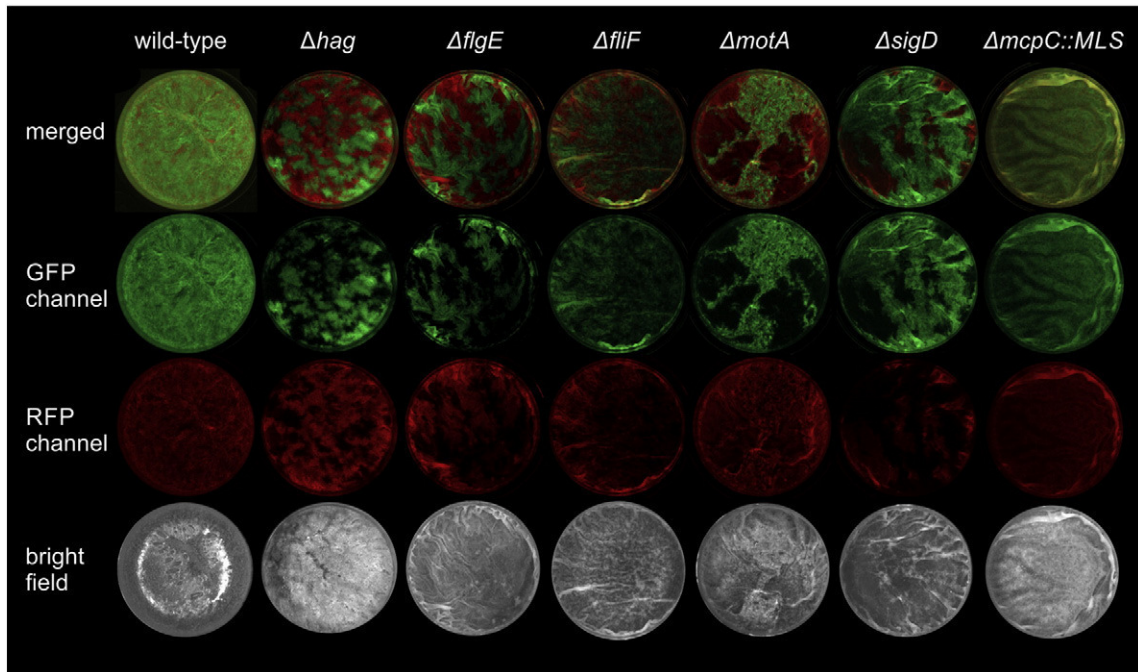


Fig. 5. Stereomicroscopy images of *B. subtilis* wild type or mutant strains competed against its genetically identical but differently labeled derivative. Wells (16 mm diameter) of a 24-well plate are shown in the green- or red-fluorescence channels (false-colored green and red) together with merged and bright-light images. Representative examples for each strain are shown.

$\Delta cheV$ (link between receptors and CheA) and $\Delta cheY$ (response regulator) [30,39]. All mutants that retained some form of (albeit reduced) chemotaxis, that is, $\Delta mcpC$, $\Delta cheC$ and $\Delta cheB$, were able to successfully compete with the wild type as demonstrated by high intensities of the corresponding fluorescence (Fig. 4b and Table S1). In contrast, chemotaxis-null strains ($\Delta cheV$, $\Delta cheY$ and $\Delta cheA$) were outcompeted by the wild type (Fig. 4b, Fig. S2 and Table S1) suggesting that the ability to sense attractants or repellents provides benefits for colonization of the air-liquid interface.

Aerotaxis is a special form of chemotaxis in which oxygen functions as the attractant or repellent. In pellicle formation of aerobic bacteria, oxygen has been suggested to be an important factor mediating active movement toward the surface of the medium, where the highest oxygen concentrations are present [6]. A strain with a knockout of the *hemAT* gene, encoding the *B. subtilis* oxygen sensor protein [40], was constructed and competed against the wild type. As can be seen in Fig. 4c and Fig. S2, the $\Delta hemAT$ mutant was outcompeted by the wild type. Further, the $\Delta hemAT$ mutant was competed against the Δhag mutant to investigate which mutation leads to greater disadvantage. Here, the Δhag mutant was outcompeted by the $\Delta hemAT$ mutant showing that immobility is more harmful than lack of oxygen sensing for the individual cells during pellicle

co-colonization. However, during the competition of a $\Delta hemAT \Delta hag$ double mutant with the Δhag mutant, both were present in a more or less equal ratio in the pellicle. This finding indicates that ability to sense oxygen is not providing an advantage when the bacteria are not able to actively swim. These results suggest that oxygen sensing provides an advantage during competition for the air-liquid interface.

Pellicle intermixing depends on motility, but not on chemotaxis

In the competition experiments described above, strains were differentiated by their constitutive expression of the fluorescent protein GFP or mKATE2. Control experiments included genetically identical strains that were only distinguished by their labeling (e.g., WT_{GFP} versus WT_{mKATE2} or Δhag_{GFP} versus Δhag_{mKATE2}). Using stereomicroscopy, we observed that the differentially labeled but otherwise wild-type strains mixed well during pellicle formation (Fig. 5, first column), similar to mutants lacking certain chemotaxis- or aerotaxis-related genes, for example, $\Delta mcpC::MLS$ (Fig. 5, last column). However, strains that lacked functional flagella (Δhag , $\Delta motA$, $\Delta fliF$, $\Delta flgE$ and $\Delta sigD$ strains) showed increased spatial assortment, that is, green- and red-fluorescent patches of individual strains. These

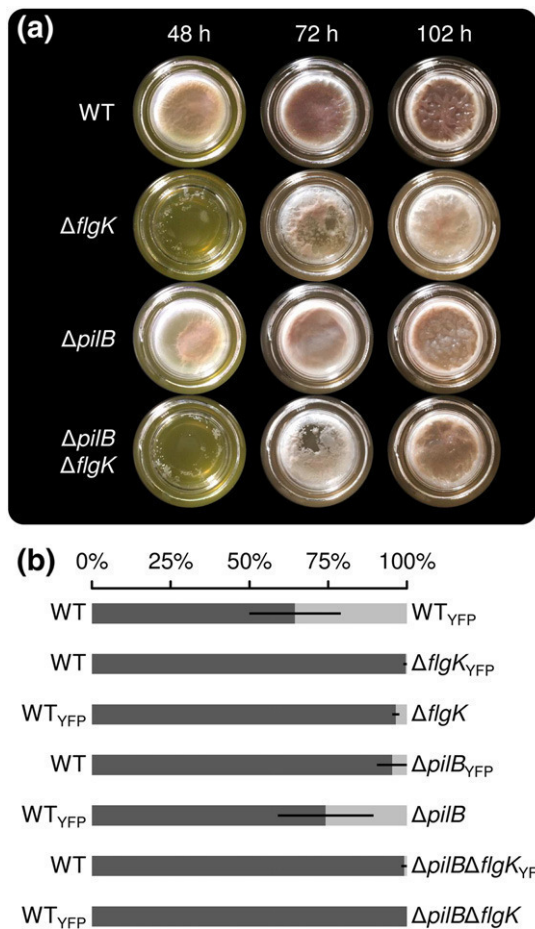


Fig. 6. Pellicle formation of *P. aeruginosa* wild type and mutant strains in borosilicate scintillation vials (28 mm diameter) containing LB medium (a). Relative abundance of *P. aeruginosa* wild type (dark gray) and mutant (light gray) strains in competition experiments performed under static conditions (b) (WT versus WT_{GFP}: $n = 6$; others: $n = 3$). Bars represent percentages of strains indicated on the side of the bar. Error bars indicate standard deviation.

results suggest not only that active flagellar motility is important for *B. subtilis* to reach the air–medium interface but also that flagellar motility could be required for mixing of cells during the initiation of the pellicle.

***P. aeruginosa* pellicle formation is also influenced by motility**

To evaluate the broader relevance of our observations, we next examined the role of motility in pellicle development of the Gram-negative biofilm model organism *P. aeruginosa*. Pellicle formation of *P. aeruginosa* PAO1 was previously shown to require flagellar motility [9]. However, this work suggested that cells lacking both flagella and pili

form pellicles that are comparable to the wild-type strain. Here, we tested the importance of the flagellum and the type IV pilus for pellicle development in *P. aeruginosa* PA14. Pellicles of strains lacking the genes *flgK* (flagellar hook-associated protein), *pilB* (type IV pilus motor protein) or both ($\Delta pilB \Delta flgK$) were investigated. The $\Delta flgK$ mutation prevents swimming and swarming, while $\Delta pilB$ prevents twitching in *P. aeruginosa* PA14 [36,41]. Mutants lacking the *flgK* gene showed delayed pellicle development when compared to the wild type, while the $\Delta pilB$ mutant showed pellicle development that was similar to that of the wild type (Fig. 6a). Interestingly, pellicle formation is not abolished in the mutants, as after 102 h, a robust pellicle comparable with that of the wild type was observed. Patchy structures of the pellicles were observed in early pellicle formation stages of the $\Delta flgK$ and $\Delta pilB \Delta flgK$ mutants (Fig. 6a, after 48 h and 72 h) similar to a previous description [9] but were not detected in later stages of pellicle development.

Additionally, competition experiments similar to those conducted with *B. subtilis* were performed with *P. aeruginosa* PA14. The $\Delta pilB$, $\Delta flgK$ and $\Delta pilB \Delta flgK$ mutants were competed against the wild type in pellicles with initial ratios of 1:1. To distinguish the competing strains, we fluorescently labeled one with YFP. A fluorescence label swap indicated a slight reduction in fitness for labeled strains. In these experiments, all motility mutants were outcompeted by the wild type (Fig. 6b). While the $\Delta flgK$ and the $\Delta pilB \Delta flgK$ mutant were strongly outcompeted (<4% and <1% of the pellicle, respectively), the $\Delta pilB$ mutant showed a less severe disadvantage (5–26% of the pellicle) when grown together with the wild type. These results demonstrate that, in *P. aeruginosa*, motility is not required for pellicle formation but provides a benefit against a non-motile strain during the colonization of the air–liquid interface.

Pellicle formation is preceded by population mixing and the appearance of a cleared zone

The involvement of motility in the formation of pellicles by diverse bacteria led us to hypothesize that it enables cells to counteract sedimentation and stay at the surface. Cells with impaired motility might therefore be expected to sink, leading to decreased culture turbidity. To evaluate this, we recorded the side view of static liquid cultures over several days. We were surprised to find that a zone of clearing appeared specifically in strains capable of flagellum-dependent motility, while flagellum-null mutants showed homogenous turbidity over time (Fig. 7 and Videos S3–S6). The clear zone was visible relatively early after inoculation and eventually disappeared

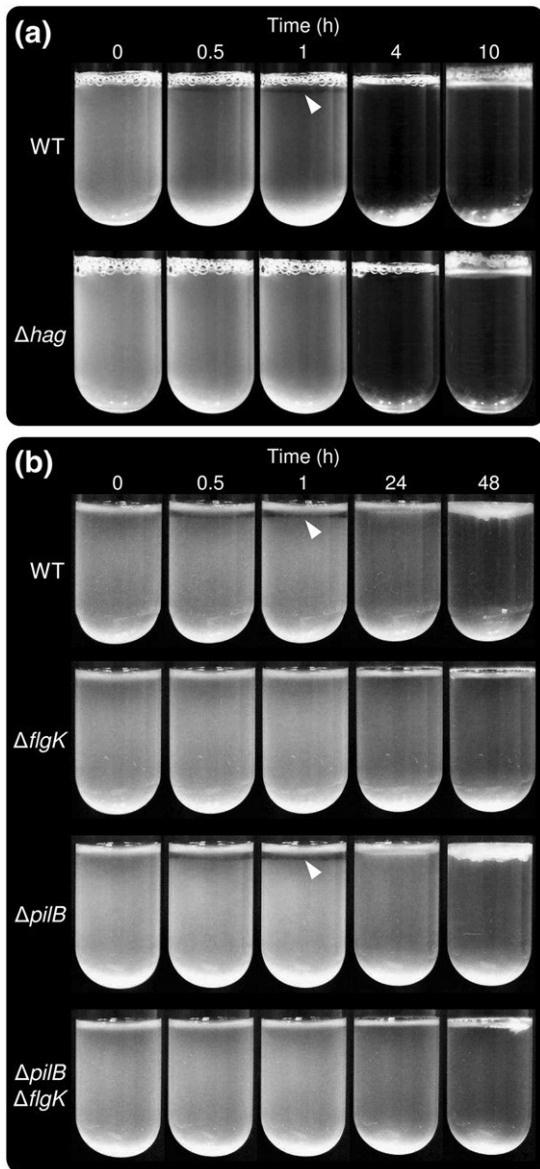


Fig. 7. Pellicle formation of *B. subtilis* wild type and its Δhag derivative in MSgg medium, shown from the side (a). Pellicle formation of *P. aeruginosa* wild type and $\Delta flgK$, $\Delta pilB$ and $\Delta flgK \Delta pilB$ strains in LB medium, shown from the side (b). Selected time points are presented from Videos S3 and S5.

when the pellicle started to thicken. The fact that the transparent zone appears in strains exhibiting earlier pellicle formation suggests that cells in this zone abruptly exit and swim toward the surface of the liquid to access more oxygen. However, the fact that the *B. subtilis* $\Delta hemAT$ static cultures inoculated at high cell density exhibit clear zones similar to those formed by the wild type (Video S7) suggests that

oxygen is not the signal that stimulates exit from the region just below the pellicle. Alternative potential explanations are that a gradient of another nutrient attracts cells away from this zone or that a waste product/chemorepellent accumulates in the region due to the high cell density of the pellicle immediately above. Emergence of the zone of clearing coincided with the appearance of a turbulent flow in the lower portion of the culture tube, both at high cell density and at low cell density (Videos S3–S6). This flagellum-dependent turbulent flow is particularly intriguing as it could serve to facilitate the mixing of oxygen into the medium and represent a population-level strategy for resource acquisition. Our time-lapse observation of *B. subtilis* and *P. aeruginosa* pellicle development indicates that motility plays a central role in defining population dynamics and conferring a growth advantage in this model biofilm system.

Discussion

This study examined the contributions of motility to fitness during bacterial pellicle biofilm development of *B. subtilis* and *P. aeruginosa*, as well as the relevance of oxygen availability to the behavior of *B. subtilis* static cultures. We observed that, in both organisms, pellicle formation was delayed in motility-deficient mutants. Despite this delay, the mutant strains exhibited wild-type morphology demonstrating that motility is not essential for robust pellicle formation. We hypothesize that, in the non-motile strains, pellicle formation is delayed because of a lack of directed movement toward the air–liquid interface. The cell number may increase mainly by division of the few cells that reached the air–liquid interface by passive, non-directional Brownian motion, slowing down the process of pellicle formation. This is supported by the fact that, at high initial cell density, the delay of the *B. subtilis* Δhag and *P. aeruginosa* $\Delta flgK$ mutants was abolished. Further, we observed that motility-deficient strains of *B. subtilis* and *P. aeruginosa* were outcompeted in pellicle competition experiments with their respective wild-type counterparts. This result can also be explained by our hypothesis that the motility-deficient cells make it to the liquid surface only by chance and therefore only inefficiently contribute to formation of a mixed pellicle. On the contrary, the wild-type cells can move toward the air–liquid interface in a directed manner at initial stages of pellicle formation; these cells are therefore present in the pellicle in higher abundance. These results suggest that it is important for successful competition with other strains to reach the air–liquid interface efficiently. We conclude that motility contributes to successful competition for residence at the air–liquid interface although it is not essential for pellicle

formation *per se*. It is also important to note that motility is a costly trait, which was shown for *B. subtilis* in competition experiments performed under conditions that do not promote pellicle formation (Fig. 2a).

Most probably, cells perceive the location of the air–liquid interface by the sensing of an attractant, which is then translated into directed movement by the chemotaxis system [38]. *B. subtilis* mutants lacking core components of the chemotaxis machinery were also outcompeted by wild-type cells during pellicle development. This suggests that sensing of certain signals is important for successful pellicle co-colonization. In these chemotaxis mutant strains, even if the cells are able to move and sense an attractant, they lack the translation of signals into directed movement. Thus the cells move around randomly and only the cells that are located at the air–liquid interface by chance can participate in pellicle formation. In *B. subtilis*, we identified oxygen as a putative trigger for active movement toward the air–liquid interface since the $\Delta hemAT$ mutant, which is not able to sense oxygen [40], was outcompeted by the wild type in static co-cultures. Thus, it was able to move but lacked information regarding the direction of the most favorable conditions in its surroundings, resulting again in random distribution in the liquid. Yamamoto *et al.* showed that, in *P. aeruginosa* PAO1, pellicle formation was reduced under oxygen-depleted conditions [23], suggesting that aerotaxis might be important for localization to the air–liquid interface in this organism as well. In *S. oneidensis*, aerotaxis was also found to be important since, without oxygen, pellicle initiation was abolished [7]. Further, pellicle maturation of *S. oneidensis* was blocked under anoxic conditions in cultures where pellicle formation was allowed to be initiated in the presence of oxygen. Similarly, *E. coli* does not form biofilms at the air–liquid interface under anoxic conditions [10]. These findings indicate that oxygen and aerotaxis might be generally important for locating the air–liquid interface and proper initiation of pellicle formation in diverse bacterial species. Armitano *et al.* also concluded that chemotaxis and a functional flagellum are essential for pellicle formation in *S. oneidensis* since the respective mutants did not form a pellicle [7]. However, the pellicle formation ability was investigated after only 20 h; it is therefore possible that pellicle formation is just delayed in both mutants. Nevertheless, their results show that, in diverse bacteria, functional flagella and the chemotaxis system are important for normal progress of at least the initial stages of pellicle formation.

Interestingly, flagellar motility, but not chemotaxis, also influences population intermixing in *B. subtilis* pellicles. Spatial segregation has been shown to facilitate the stabilization of cooperative traits in *B. subtilis* colony biofilms [42] and also influences interaction in microbial populations [43]. Non-motile strains show increased spatial segregation. This

elevated assortment could be due to reduced flagellar motility within a newly formed and still dynamic layer of pellicle or, alternatively, it could be caused by a dissimilar surface colonization mechanism of the motile and non-motile strains. Kobayashi previously proposed a model in which *B. subtilis* cell clusters float to the surface of a biofilm-promoting, nutrient-rich medium during pellicle formation [12]. While our experiments highlight the importance of an active signal-driven motility, non-motile strains might colonize the air–medium interface via clusters of cells that expand to form a convergent layer. This could then be observed as spatially segregated clusters of cells initiated by two strains with distinct fluorescent labels, as we present here. We hypothesize that the two putative mechanisms, single-cell and cluster-based pellicle initiation, might coexist in the wild-type strain or depend on the culturing conditions.

We further observed a zone of clearing below the initial pellicle layer in wild-type *B. subtilis*, wild-type *P. aeruginosa* and the *P. aeruginosa* $\Delta pilB$ mutant but not in *B. subtilis* or *P. aeruginosa* flagellum-deficient mutants. The formation of this zone may be triggered by the higher abundance of oxygen close to the air–liquid interface. However, time-lapse experiments of the $\Delta hemAT$ *B. subtilis* strain initiated with high cell densities showed the presence of the clearing zone suggesting that, under such conditions, sensing of oxygen plays no significant role. In contrast, the *B. subtilis* Δhag strain was not delayed in pellicle formation when a high initial cell density was used. As the clearing occurs in the Gram-positive *B. subtilis* and the Gram-negative *P. aeruginosa*, we speculate that the occurrence of this clear zone may be a general property of pellicle-forming, facultative aerobes. The mechanism underlying the formation of the clear zone remains to be investigated.

Materials and methods

Bacterial strains, plasmids and materials

All strains used in this study are listed in Table 1. The *B. subtilis* strains are derivatives of the wild isolate NCIB3610 (referred to as the wild type) otherwise indicated. The *P. aeruginosa* strains are derivatives of strain PA14 (referred to as the wild type) and were created as described below. *B. subtilis* fluorescently labeled strains were created by phage transduction. *E. coli* MC1061 and UQ950 strains were used for cloning.

Growth conditions, biofilm conditions and competition experiments

B. subtilis overnight cultures were grown aerobically in 3 mL Lenox broth (Carl-Roth GmbH, Karlsruhe, Germany) medium at 37 °C, shaking at 225 rpm. For routine liquid cultures of *P. aeruginosa* PA14, the cells were grown in

Table 1. Strains and plasmids used in this study

Strains/plasmids	Characteristics	Source or reference
<i>B. subtilis</i>		
NCIB3610	prototroph	[5]
168hyGFP	168 amyE::Phyperspank-GFP (Cm ^R)	[42]
168hymKATE2	168 amyE::Phyperspank-mKATE2 (Cm ^R)	[42]
DS1677	NCIB3610 Δ hag	[50]
TB201	DS1677 transduced with Phy-mKATE2	This study
TB185	DS1677 transduced with Phy-GFP	This study
DS4681	NCIB3610 Δ flgE	[51]
TB203	DS4681 transduced with Phy-mKATE2	This study
TB187	DS4681 transduced with Phy-GFP	This study
DS7080	NCIB3610 Δ flfF	[52]
TB208	DS7080 transduced with Phy-mKATE2	This study
TB192	DS7080 transduced with Phy-GFP	This study
DS7498	NCIB3610 Δ motA	[52]
TB210	DS7498 transduced with Phy-mKATE2	This study
TB193	DS7498 transduced with Phy-GFP	This study
DS6420	NCIB3610 Δ sigD	[53]
TB204	DS6420 transduced with Phy-mKATE2	This study
TB188	DS6420 transduced with Phy-GFP	This study
DS6887	NCIB3610 Δ cheA	[39]
TB213	DS6887 transduced with Phy-mKATE2	This study
TB197	DS6887 transduced with Phy-GFP	This study
DS7306	NCIB3610 Δ cheB	[39]
TB209	DS7306 transduced with Phy-mKATE2	This study
TB194	DS7306 transduced with Phy-GFP	This study
DS6867	NCIB3610 Δ cheC	[39]
TB205	DS6867 transduced with Phy-mKATE2	This study
TB189	DS6867 transduced with Phy-GFP	This study
DS6868	NCIB3610 Δ cheD	[39]
TB206	DS6868 transduced with Phy-mKATE2	This study
TB190	DS6868 transduced with Phy-GFP	This study
DS70	NCIB3610 Δ cheV::MLS	[30]
TB199	DS70 transduced with Phy-mKATE2	This study
TB183	DS70 transduced with Phy-GFP	This study
DS6870	NCIB3610 Δ cheY	[39]
TB207	DS6870 transduced with Phy-mKATE2	This study
TB191	DS6870 transduced with Phy-GFP	This study
DS180	NCIB3610 Δ mcpC::MLS	[30]
TB200	DS180 transduced with Phy-mKATE2	This study
TB184	DS180 transduced with Phy-GFP	This study
TB239	168 Δ hemAT::Nm	This study
TB241	3610 transduced with hemAT::Nm	This study
TB243	TB241 transduced with Phy-mKATE2	This study
TB244	TB241 transduced with Phy-GFP	This study
TB242	DS1677 transduced with hemAT::Nm	This study
TB245	TB242 transduced with Phy-mKATE2	This study
TB246	TB242 transduced with Phy-GFP	This study
<i>P. aeruginosa</i>		
PA14	Clinical isolate UCBPP-PA14	[54]
LD592	PA14 with chromosomally integrated constitutive eYFP	[55]
LD371	PA14 Δ flgK	This study
LD2221	PA14 Δ flgK (LD371) with chromosomally integrated constitutive eYFP	This study
LD369	PA14 Δ pilB	This study
LD2222	PA14 Δ pilB (LD369) with chromosomally integrated constitutive eYFP	This study
LD384	PA14 Δ pilB Δ flgK	This study
LD2151	PA14 Δ pilB Δ flgK (LD384) with chromosomally integrated constitutive eYFP	This study
<i>E. coli</i>		
MC1061	host for cloning; araD139, Δ (ara, leu)7694, Δ lacX74, galU ⁻ , galK ⁻ , hsr ⁻ , hsm ⁻ , strA	[56]
UQ950	DH5 α λ (pir) host for cloning; F ⁻ (argF-lac)169 ϕ 80dlacZ58(Δ M15) glnV44(AS) rfbD1 gyrA96(Nal ^r) recA1 endA1 spoT1 thi-1 hsdR17 deoR λ pir ⁺	D. Lies
BW29427	donor strain for conjugation; thrB1004 pro thi rpsL hsdS lacZ Δ M15RP4-1360 Δ (araBAD)567 Δ dapA1341::[erm pir(wt)]	B. Wanner
β -2155	donor strain for conjugation; thrB1004 pro thi strA hsdS lacZ Δ M15 Δ dapA::erm (Erm ^r) pir::RP4 [::kan (Km ^r) from SM10]	[57]

Table 1 (continued)

Strains/plasmids	Characteristics	Source or reference
<i>Saccharomyces cerevisiae</i> InvSc1	MA α /MAT α <i>leu2/leu2 trp1-289/trp1-289 ura3-52/ura3-52 his3-Δ1/his3-Δ1</i>	[48]
<i>Plasmids</i>		
pBEST501	PrepU-neo, Amp ^R	[58]
pBluescript SK+	cloning vector, Amp ^R	Stratagene
pTB120	Nm ^R cassette cloned into pBluescript SK+	This study
pTB235	Nm ^R cassette with upstream and downstream regions of <i>B. subtilis hemAT</i>	This study
pMQ30	Yeast-based allelic-exchange vector; <i>sacB^R CEN/ARSH URA3⁺ Gen^f</i>	[48]
pLD348	<i>flgK</i> deletion fragments cloned into pMQ30	This study
pLD349	<i>pilB</i> deletion fragments cloned into pMQ30	This study
pAKN69	Mini-Tn7 derived fluorescent labeling vector; mini-Tn7(Gm)P _{A1/04/03} :: <i>eyfp</i>	[49]
pUX-BF13	R6K replicon-based helper plasmid providing the Tn7 transposition function <i>in trans</i> ; Amp ^r	[59]

For phage transduction, strains 168hyGFP, 168hymKATE2 and TB239 were used as donor.

2 mL lysogeny broth [44] in tubes that are 12 mm x 100 mm at 37 °C with shaking at 250 rpm. Growth conditions for pellicles are described below.

Construction of *B. subtilis* strains

GFP- and mKATE-labeled *B. subtilis* strains and Δ *hemAT* mutants in *B. subtilis* NCIB3610 were obtained via phage transduction. Constructs were then transferred to selected NCIB3610 derivatives using SPP1-mediated generalized phage transduction [45]. For the construction of the Δ *hemAT* mutant, first, a PCR fragment containing a neomycin resistance cassette was amplified with primer pair oRGM2 and oRGM7 (see primer sequences in Table 2) from pBEST501 and cloned into the SmaI site of pBluescriptSK+ to create pTB120. Upstream and downstream regions of *hemAT* gene were PCR amplified with primer pairs oTB78-oTB79 and oTB80-oTB81 and

were sequentially cloned into the XhoI-PstI and BamHI-SacI sites of pTB120, respectively, resulting in pTB235. Plasmid pTB235 was confirmed through sequencing. The *Eam11011* linearized pTB235 was transformed into *B. subtilis* 168 with natural competence [46] and transformants were selected on LB agar medium with 5 μ g/mL kanamycin. Deletion in the *hemAT* gene was confirmed by PCR with primer pair oTB82-oTB83 and by sequencing.

Construction of *P. aeruginosa* strains

Construction of deletion and complementation plasmids

Unmarked deletions were generated for the genes *flgK* (PA14_50360) and *pilB* (PA14_58750) in wild-type PA14 as previously described [47]. Deletion plasmids were generated using yeast gap repair cloning. Flanking regions (~1 kb in length) for *flgK* and *pilB* were generated using primers listed in Table 2. The flanking regions and the

Table 2. Primers used in this study

Primers	Sequence (5' to 3')
<i>For B. subtilis constructs</i>	
oRGM2	TACCGTTCGTATAATGTATGCTATACGAAGTTATAGATCAATTTGATAATTAATAATAC
oRGM7	TACCGTTCGTATAGCATACATTATACGAAGTTATTAGAGCTTGGGTTACAGGCATGG
oTB78	GATCCTCGAGAAGCCGGCACGCCATTAAG
oTB79	TTATCGGCCAAGGAAAC
oTB80	GATCGGATCCAAACCGGTCTGCCATACG
oTB81	CACGGAGCTCATGGGAATGGCCGTACATC
oTB82	GGCCGAATTTATGAAGAGAC
oTB83	AAGATCCGCATTGCTTATGG
<i>For P. aeruginosa constructs</i>	
Δ <i>flgK</i> 5' flank-1	GGAATTGTGAGCGGATAACAATTTACACAGGAAACAGCTAGGTGATGAAGTCGCTGGTC
Δ <i>flgK</i> 5' flank-2	ACTGACCCATGTCCGACCTACCAACCTGATCCAGTTCCAG
Δ <i>flgK</i> 3' flank-1	CTGGAACCTGGATCAGGTTGGTAGGTCCGGACATGGGTCAGT
Δ <i>flgK</i> 3' flank-2	CCAGGCAAATTTCTGTTTTATCAGACCGCTTCTGCGTTCTGATCACCAGCAGTACCAGGACA
Δ <i>pilB</i> 5' flank-1	GGAATTGTGAGCGGATAACAATTTACACAGGAAACAGCTTGGCATCCTCTCTGCTATTTTC
Δ <i>pilB</i> 5' flank-2	GCAGATCGTTGAAGCCTTCTGCCTTTTCATCGAGAAGTTCA
Δ <i>pilB</i> 3' flank-1	TGAACCTTCTCGATGAAAAGGCAGAAGGCTTCAACGATCTGC
Δ <i>pilB</i> 3' flank-2	CCAGGCAAATTTCTGTTTTATCAGACCGCTTCTGCGTTCTGATGCTGGACACGTCTTGTGTTGA

linearized allelic-replacement vector pMQ30 were assembled by gap repair cloning using the yeast strain InvSc1 [48]. The resulting deletion plasmid was transformed into *E. coli* BW29427 and mobilized into PA14 using biparental conjugation. PA14 single recombinants were selected on LB agar containing 100 µg/mL gentamicin. Potential *flgK* or *pilB* deletion mutants were generated by selecting for double recombinants that grew in the presence of 10% sucrose. These candidates were further analyzed by PCR to detect the desired deletion.

Constitutive eYFP expressing strains

The construct containing the *eyfp* gene under a constitutive promoter was genomically inserted through a Tn7 transposon-based system [49]. The *eyfp*-containing plasmid pAKN69 was mobilized into PA14 via triparental conjugation, which involves (1) donor strain *E. coli* BW29427 harboring pAKN69, (2) donor strain *E. coli* β-2155 harboring the helper plasmid pJX-BF13 and (3) the recipient PA14 strains. YFP-tagged PA14 clones were selected on LB agar containing 100 µg/mL gentamicin.

Biofilm growth and pellicle competition experiments in *B. subtilis*

For pellicle formation of *B. subtilis*, 20 µL of overnight culture was mixed with 2 mL of biofilm promoting minimal medium MSgg [5] in a well (16 mm diameter) of a 24-well plate. The culture was statically incubated at 30 °C for 3 days. For pellicle competition experiments with CFU determination, each competitor was inoculated to a final OD of 0.05 in 2 mL MSgg in a well of a 24-well plate and incubated statically at 30 °C. After incubation, the pellicles were harvested, disrupted by sonication (2 × 12 pulses of 1 s with 30% amplitude; Ultrasonic Processor VCX-130, Zinsser Analytics, Frankfurt am Main, Germany) and plated on LB and chloramphenicol containing (5 µg/mL) agar plates in dilutions. The CFU count was recorded and the relative percentage of each competitor in the pellicle was calculated based on their antibiotic resistance. For competition experiments under shaking conditions, each competitor was inoculated to a final OD of 0.05 in 5 mL MSgg in a 100-mL bottle and incubated at 30 °C and 225 rpm shaking for 20 h. The cultures reached the stationary phase and grew for about 5.8 generations. Afterwards, the CFU count was determined as previously described for the pellicle competition (see above). A two-sided Student's *t* test was performed.

For fluorescence competition experiments, 10 µL of overnight cultures of each competitor was mixed with 2 mL MSgg in a well of a 24-well plate and incubated as described above. The fluorescence intensity was measured using an infinite F200PRO plate reader (TECAN Group Ltd., Männedorf, Switzerland). Fluorescence intensities of mutant strains against wild-type competitions ("assay competitions") measured with the plate reader were normalized against the fluorescence intensities of competitions of wild type_{GFP} against wild type_{mKATE2} ("wild-type control competition") or mutant_{GFP} against mutant_{mKATE2} ("mutant control competition"). Wild-type signals were normalized based on the "wild type against wild type" control competition. Analogously, signals of

mutant fluorescence were normalized, resulting in percentage numbers. Each competition was performed in four replicates, if not stated otherwise. A two-sided Student's *t* test was applied to check whether obtained fluorescence intensity measurements were statistically significantly different (significance level $\alpha = 0.05$; number of replicates $n = 4$; degrees of freedom $f = 3$; critical value $c = 3.182$). Results were deemed significantly different if the calculated *t* value was outside of the critical interval $-c \leq t \leq c$.

Biofilm growth and pellicle competition experiments in *P. aeruginosa*

Overnight cultures were diluted 100×, subcultured for ~2.5 h to OD₅₀₀ of 0.5–0.7 and then diluted to OD₅₀₀ of 0.5. For the pellicle morphology assay, 230 µL of the exponential-phase culture (OD₅₀₀ of 0.5) was diluted in 23 mL of LB in a borosilicate scintillation vial (9718G12; Thomas Scientific) and grown at 37 °C for 2 days to form pellicles. For competition assays, cells were mixed at 500 µL:500 µL, and 50 µL of each mix was then diluted in 5 mL of LB in a borosilicate tube (18 mm × 150 mm) and incubated without shaking at 37 °C for 2 days. For CFU counts of samples from competition experiments, each pellicle was transferred to 1 mL of 1% tryptone in a bead beating tube containing 0.5 g of zirconium beads (1.4 mm; OPS Diagnostics). Pellicles were homogenized at 400 rpm for 5 min at 4 °C. We plated 10⁻⁷ of the total amount of cells from each pellicle on 1% tryptone agar medium for CFU counting. YFP-tagged strains were identified using a Typhoon FLA 7000 scanner (GE Healthcare).

Fluorescence microscopy

Bright-field, green- and red-fluorescence images of the pellicles were taken with an Axio Zoom V16 stereomicroscope (Carl Zeiss, Jena, Germany) at a magnification of 3.5× equipped with a Zeiss CL 9000 LED light source, HE eGFP filter set (excitation at 470/40 nm and emission at 525/50 nm), HE mRFP filter set (excitation at 572/25 nm and emission at 629/62 nm) and an AxioCam MRm monochrome camera (Carl Zeiss). The exposure times were set to 0.1 s, 0.85 s and 3 s for bright field, green fluorescence and red fluorescence, respectively. ImageJ (National Institute of Health, Bethesda, MD, USA) was used for background subtraction and channel merging. For time-lapse experiments, cultures in 35-mm-diameter Falcon petri dishes (VWR, Darmstadt, Germany) were incubated in INUL-MS2-F1 incubators (Tokai Hit, Shizuoka, Japan) at 30 °C and images were recorded every 30 min.

Time-lapse experiments (side view)

For *P. aeruginosa* time-lapse videos, the growth conditions were the same as those described for competition experiments, starting at OD (500 nm) of 0.005 or 2.0 at 37 °C. For *B. subtilis*, pellicles were grown in MSgg medium, starting at OD = 0.005 or 1.2 at 30 °C. Images were recorded every minute using an iPod touch (Apple) or a customized recording system (Logitech HD Webcam C525) under LED illumination. Image acquisition and lighting were synchronized with LabVIEW (National Instruments).

Supplementary data to this article can be found online at <http://dx.doi.org/10.1016/j.jmb.2015.06.014>.

Acknowledgements

We thank Daniel Kearns for sharing *B. subtilis* strains and his comments. T.H. and R.G.-M. are supported by International Max Planck Research School and Consejo Nacional de Ciencia y Tecnología-German Academic Exchange Service CONA-CyT-DAAD, respectively. Work in the laboratory of A.T.K. is supported by a Marie Curie Career Integration Grant (PheHetBacBiofilm), Grant KO4741/2-1 from the Deutsche Forschungsgemeinschaft within the framework of the Deutsche Forschungsgemeinschaft Priority Program SPP1617 and a Jena School for Microbial Communication start-up fund. The Dietrich laboratory is supported by grant R01-AI103369 from National Institute of Allergy and Infectious Diseases/National Institutes of Health.

Received 21 May 2015;

Received in revised form 10 June 2015;

Accepted 20 June 2015

Available online 26 June 2015

Keywords:

Bacillus subtilis;
Pseudomonas aeruginosa;
biofilm;
pellicle development;
motility

†T.H., B.B. and Y.-C.L. contributed equally to this work.

References

- [1] R. Kolter, E.P. Greenberg, Microbial sciences: the superficial life of microbes, *Nature* 441 (2006) 300–302.
- [2] J.W. Costerton, Z. Lewandowski, D.E. Caldwell, D.R. Korber, H.M. Lappin-Scott, Microbial biofilms, *Annu. Rev. Microbiol.* 49 (1995) 711–745.
- [3] D. Lopez, H. Vlamakis, R. Kolter, Biofilms, *Cold Spring Harbor Perspect. Biol.* 2 (2010) a000398.
- [4] K.P. Lemon, A.M. Earl, H.C. Vlamakis, C. Aguilar, R. Kolter, Biofilm development with an emphasis on *Bacillus subtilis*, *Curr. Top. Microbiol. Immunol.* 322 (2008) 1–16.
- [5] S.S. Branda, J.E. Gonzalez-Pastor, S. Ben-Yehuda, R. Losick, R. Kolter, Fruiting body formation by *Bacillus subtilis*, *Proc. Natl. Acad. Sci. U. S. A.* 98 (2001) 11621–11626.
- [6] J. Armitano, V. Méjean, C. Jourlin-Castelli, Gram-negative bacteria can also form pellicles, *Environ. Microbiol. Rep.* 6 (2014) 534–544.
- [7] J. Armitano, V. Méjean, C. Jourlin-Castelli, Aerotaxis governs floating biofilm formation in *Shewanella oneidensis*, *Environ. Microbiol.* 15 (2013) 3108–3118.
- [8] Y. Nait Chabane, S. Marti, C. Rihouey, S. Alexandre, J. Hardouin, O. Lesouhaitier, et al., Characterisation of pellicles formed by *Acinetobacter baumannii* at the air–liquid interface, *PLoS One* 9 (2014) e111660.
- [9] K. Yamamoto, H. Arai, M. Ishii, Y. Igarashi, Involvement of flagella-driven motility and pili in *Pseudomonas aeruginosa* colonization at the air–liquid interface, *Microbes Environ.* 27 (2012) 320–323.
- [10] M. Colon-Gonzalez, M.M. Mendez-Ortiz, J. Membrillo-Hernandez, Anaerobic growth does not support biofilm formation in *Escherichia coli* K-12, *Res. Microbiol.* 155 (2004) 514–521.
- [11] P.B. Rainey, M. Travisano, Adaptive radiation in a heterogeneous environment, *Nature* 394 (1998) 69–72.
- [12] K. Kobayashi, *Bacillus subtilis* pellicle formation proceeds through genetically defined morphological changes, *J. Bacteriol.* 189 (2007) 4920–4931.
- [13] G. O’Toole, H.B. Kaplan, R. Kolter, Biofilm formation as microbial development, *Annu. Rev. Microbiol.* 54 (2000) 49–79.
- [14] T. Abee, Á.T. Kovács, O.P. Kuipers, S. van der Veen, Biofilm formation and dispersal in Gram-positive bacteria, *Curr. Opin. Biotechnol.* 22 (2011) 172–179.
- [15] S.B. Guttenplan, D.B. Kearns, Regulation of flagellar motility during biofilm formation, *FEMS Microbiol. Rev.* 37 (2013) 849–871.
- [16] H. Vlamakis, Y. Chai, P. Beauregard, R. Losick, R. Kolter, Sticking together: building a biofilm the *Bacillus subtilis* way, *Nat. Rev. Microbiol.* 11 (2013) 157–168.
- [17] S.B. Guttenplan, K.M. Blair, D.B. Kearns, The EpsE flagellar clutch is bifunctional and synergizes with EPS biosynthesis to promote *Bacillus subtilis* biofilm formation, *PLoS Genet.* 6 (2010) e1001243.
- [18] O.E. Petrova, K.E. Cherny, K. Sauer, The *Pseudomonas aeruginosa* diguanylate cyclase GcbA, a homolog of *P. fluorescens* GcbA, promotes initial attachment to surfaces, but not biofilm formation, via regulation of motility, *J. Bacteriol.* 196 (2014) 2827–2841.
- [19] Y. Liang, H. Gao, J. Chen, Y. Dong, L. Wu, Z. He, et al., Pellicle formation in *Shewanella oneidensis*, *BMC Microbiol.* 10 (2010) 291.
- [20] K.P. Lemon, D.E. Higgins, R. Kolter, Flagellar motility is critical for *Listeria monocytogenes* biofilm formation, *J. Bacteriol.* 189 (2007) 4418–4424.
- [21] J. Yao, C. Allen, The plant pathogen *Ralstonia solanacearum* needs aerotaxis for normal biofilm formation and interactions with its tomato host, *J. Bacteriol.* 189 (2007) 6415–6424.
- [22] K. Yamamoto, S. Haruta, S. Kato, M. Ishii, Y. Igarashi, Determinative factors of competitive advantage between aerobic bacteria for niches at the air–liquid interface, *Microbes Environ.* 25 (2010) 317–320.
- [23] K. Yamamoto, H. Arai, M. Ishii, Y. Igarashi, Trade-off between oxygen and iron acquisition in bacterial cells at the air–liquid interface, *FEMS Microbiol. Ecol.* 77 (2011) 83–94.
- [24] K. Kobayashi, SlrR/SlrA controls the initiation of biofilm formation in *Bacillus subtilis*, *Mol. Microbiol.* 69 (2008) 1399–1410.
- [25] D.B. Kearns, F. Chu, S.S. Branda, R. Kolter, R. Losick, A master regulator for biofilm formation by *Bacillus subtilis*, *Mol. Microbiol.* 55 (2005) 739–749.
- [26] E. Mhatre, R.G. Monterrosa, Á.T. Kovács, From environmental signals to regulators: modulation of biofilm development in Gram-positive bacteria, *J. Basic Microbiol.* 54 (2014) 616–632.
- [27] A.L. McLoon, S.B. Guttenplan, D.B. Kearns, R. Kolter, R. Losick, Tracing the domestication of a biofilm-forming bacterium, *J. Bacteriol.* 193 (2011) 2027–2034.

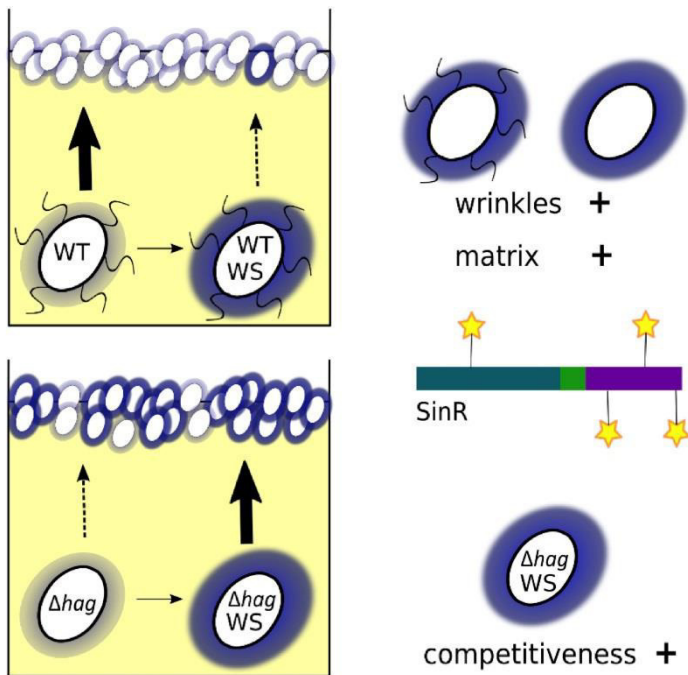
- [28] A. Seminara, T.E. Angelini, J.N. Wilking, H. Vlamakis, S. Ebrahim, R. Kolter, et al., Osmotic spreading of *Bacillus subtilis* biofilms driven by an extracellular matrix, *Proc. Natl. Acad. Sci. U. S. A.* 109 (2012) 1116–1121.
- [29] D.B. Kearns, A field guide to bacterial swarming motility, *Nat. Rev. Microbiol.* 8 (2010) 634–644.
- [30] D.B. Kearns, R. Losick, Swarming motility in undomesticated *Bacillus subtilis*, *Mol. Microbiol.* 49 (2003) 581–590.
- [31] R.F. Kinsinger, M.C. Shirk, R. Fall, Rapid surface motility in *Bacillus subtilis* is dependent on extracellular surfactin and potassium ion, *J. Bacteriol.* 185 (2003) 5627–5631.
- [32] L.S. Cairns, V.L. Marlow, E. Bissett, A. Ostrowski, N.R. Stanley-Wall, A mechanical signal transmitted by the flagellum controls signalling in *Bacillus subtilis*, *Mol. Microbiol.* 90 (2013) 6–21.
- [33] M. Whiteley, M.G. Banger, R.E. Bumgarner, M.R. Parsek, G.M. Teitzel, S. Lory, et al., Gene expression in *Pseudomonas aeruginosa* biofilms, *Nature* 413 (2001) 860–864.
- [34] M. Klausen, A. Heydorn, P. Ragas, L. Lambertsen, A. Aes-Jorgensen, S. Molin, et al., Biofilm formation by *Pseudomonas aeruginosa* wild type, flagella and type IV pili mutants, *Mol. Microbiol.* 48 (2003) 1511–1524.
- [35] G.A. O'Toole, R. Kolter, Flagellar and twitching motility are necessary for *Pseudomonas aeruginosa* biofilm development, *Mol. Microbiol.* 30 (1998) 295–304.
- [36] D. van Ditmarsch, K.E. Boyle, H. Sakhtah, J.E. Oyler, C.D. Nadell, E. Deziel, et al., Convergent evolution of hyperswarming leads to impaired biofilm formation in pathogenic bacteria, *Cell Rep.* 4 (2013) 697–708.
- [37] T. Köhler, L.K. Curty, F. Barja, C. van Delden, J.C. Pechere, Swarming of *Pseudomonas aeruginosa* is dependent on cell-to-cell signaling and requires flagella and pili, *J. Bacteriol.* 182 (2000) 5990–5996.
- [38] S.L. Porter, G.H. Wadhams, J.P. Armitage, Signal processing in complex chemotaxis pathways, *Nat. Rev. Microbiol.* 9 (2011) 153–165.
- [39] R.A. Calvo, D.B. Kearns, FlgM is secreted by the flagellar export apparatus in *Bacillus subtilis*, *J. Bacteriol.* 197 (2015) 81–91.
- [40] S. Hou, R.W. Larsen, D. Boudko, C.W. Riley, E. Karatan, M. Zimmer, et al., Myoglobin-like aerotaxis transducers in Archaea and Bacteria, *Nature* 403 (2000) 540–544.
- [41] S.L. Kuchma, N.J. Delalez, L.M. Filkins, E.A. Snavely, J.P. Armitage, G.A. O'Toole, Cyclic di-GMP-mediated repression of swarming motility by *Pseudomonas aeruginosa* PA14 requires the MotAB stator, *J. Bacteriol.* 197 (2015) 420–430.
- [42] J. van Gestel, F.J. Weissing, O.P. Kuipers, Á.T. Kovács, Density of founder cells affects spatial pattern formation and cooperation in *Bacillus subtilis* biofilms, *ISME J.* 8 (2014) 2069–2079.
- [43] Á.T. Kovács, Impact of spatial distribution on the development of mutualism in microbes, *Front. Microbiol.* 5 (2014) 649.
- [44] G. Bertani, Lysogeny at mid-twentieth century: P1, P2, and other experimental systems, *J. Bacteriol.* 186 (2004) 595–600.
- [45] R.E. Yasbin, F.E. Young, Transduction in *Bacillus subtilis* by bacteriophage SPP1, *J. Virol.* 14 (1974) 1343–1348.
- [46] C. Anagnostopoulos, J. Spizizen, Requirements for transformation in *Bacillus subtilis*, *J. Bacteriol.* 81 (1961) 741–746.
- [47] L.E. Dietrich, C. Okegbe, A. Price-Whelan, H. Sakhtah, R.C. Hunter, D.K. Newman, Bacterial community morphogenesis is intimately linked to the intracellular redox state, *J. Bacteriol.* 195 (2013) 1371–1380.
- [48] R.M. Shanks, N.C. Caiazza, S.M. Hinsa, C.M. Toutain, G.A. O'Toole, *Saccharomyces cerevisiae*-based molecular tool kit for manipulation of genes from Gram-negative bacteria, *Appl. Environ. Microbiol.* 72 (2006) 5027–5036.
- [49] L. Lambertsen, C. Sternberg, S. Molin, Mini-Tn7 transposons for site-specific tagging of bacteria with fluorescent proteins, *Environ. Microbiol.* 6 (2004) 726–732.
- [50] K.M. Blair, L. Turner, J.T. Winkelman, H.C. Berg, D.B. Kearns, A molecular clutch disables flagella in the *Bacillus subtilis* biofilm, *Science* 320 (2008) 1636–1638.
- [51] C.R. Courtney, L.M. Cozy, D.B. Kearns, Molecular characterization of the flagellar hook in *Bacillus subtilis*, *J. Bacteriol.* 194 (2012) 4619–4629.
- [52] J.M. Chan, S.B. Guttenplan, D.B. Kearns, Defects in the flagellar motor increase synthesis of poly-gamma-glutamate in *Bacillus subtilis*, *J. Bacteriol.* 196 (2014) 740–753.
- [53] L.M. Cozy, A.M. Phillips, R.A. Calvo, A.R. Bate, Y.H. Hsueh, R. Bonneau, et al., SirA/SinR/SirR inhibits motility gene expression upstream of a hypersensitive and hysteretic switch at the level of sigma(D) in *Bacillus subtilis*, *Mol. Microbiol.* 83 (2012) 1210–1228.
- [54] L.G. Rahme, E.J. Stevens, S.F. Wolfort, J. Shao, R.G. Tompkins, F.M. Ausubel, Common virulence factors for bacterial pathogenicity in plants and animals, *Science* 268 (1995) 1899–1902.
- [55] I. Ramos, L.E. Dietrich, A. Price-Whelan, D.K. Newman, Phenazines affect biofilm formation by *Pseudomonas aeruginosa* in similar ways at various scales, *Res. Microbiol.* 161 (2010) 187–191.
- [56] M.J. Casadaban, S.N. Cohen, Analysis of gene control signals by DNA fusion and cloning in *Escherichia coli*, *J. Mol. Biol.* 138 (1980) 179–207.
- [57] C. Dehio, M. Meyer, Maintenance of broad-host-range incompatibility group P and group Q plasmids and transposition of Tn5 in *Bartonella henselae* following conjugal plasmid transfer from *Escherichia coli*, *J. Bacteriol.* 179 (1997) 538–540.
- [58] M. Itaya, K. Kondo, T. Tanaka, A neomycin resistance gene cassette selectable in a single copy state in the *Bacillus subtilis* chromosome, *Nucleic Acids Res.* 17 (1989) 4410.
- [59] Y. Bao, D.P. Lies, H. Fu, G.P. Roberts, An improved Tn7-based system for the single-copy insertion of cloned genes into chromosomes of Gram-negative bacteria, *Gene* 109 (1991) 167–168.

Chapter 3

Hampered motility promotes the evolution of wrinkly phenotype in *Bacillus subtilis*

Submitted for publication to: Molecular Microbiology (2018)

Graphical abstract:



Abbreviated Summary

During biofilm establishment at the air-liquid interface, *Bacillus subtilis* evolves matrix overproducers with a wrinkly colony phenotype (WS). This is caused by mutations in the regulator SinR which alter its dimerization and DNA interaction properties. The matrix overproducers appear mostly in a non-motile mutant where they possess a competitive advantage for biofilm formation, which is not present in the wild type background.

Hampered motility promotes the evolution of wrinkly phenotype in *Bacillus subtilis*

Anne Richter^{1,2,#}, Theresa Hölscher^{2,#}, Patrick Pausch³, Tim Sehrt², Franziska Brockhaus^{2,†}, Gert Bange³, Ákos T. Kovács^{1,2,*}

¹ Bacterial Interactions and Evolution Group, Department of Biotechnology and Biomedicine, Technical University of Denmark, Lyngby, Denmark

² Terrestrial Biofilms Group, Institute of Microbiology, Friedrich Schiller University Jena, Jena, Germany

³ LOEWE Center for Synthetic Microbiology, Department of Chemistry, Philipps University Marburg, 35043 Marburg, Germany

*For correspondence. E-mail atkovacs@dtu.dk

Authors contributed equally

†This paper is dedicated to the memory of Franziska Brockhaus, who died during preparation of this manuscript.

Running title: evolution of wrinkly *B. subtilis*

Keywords: *Bacillus subtilis*, biofilm, pellicle, wrinkly colony, evolution

Summary

Selection for a certain trait in microbes depends on the genetic background of the strain and the selection pressure of the environmental conditions acting on the cells. In contrast to the sessile state in the biofilm, various bacterial cells employ flagellum-dependent motility under planktonic conditions suggesting that the two phenotypes are mutually exclusive. However, flagellum dependent motility facilitates the prompt establishment of floating biofilms on the air-medium interface, called pellicles. Previously, pellicles of *B. subtilis* were shown to be preferably established by motile cells, causing a reduced fitness of non-motile derivatives in the presence of the wild type strain. Here, we show that lack of fully assembled flagella promotes the evolution of matrix overproducers that can be distinguished by the characteristic wrinkled colony morphotype. The wrinkly phenotype is associated with amino acid substitutions in the master repressor of biofilm-related genes, SinR. By analyzing one of the mutations, we show that it alters the tetramerization and DNA binding properties of SinR, allowing an increased expression of the operon responsible for exopolysaccharide production. Finally, we demonstrate that the wrinkly phenotype is advantageous when cells lack flagella, but not in the wild type background.

Introduction

Trait loss can have detrimental or beneficial consequences on the fitness of individuals. Eventually, loss in certain phenotypic attributes can have both negative and positive impact depending on the environmental conditions. However, impairment of certain paths might allow the evolution of new traits to compensate for the fitness loss. Such a trait loss and evolution can be easily detected in microbes that are able to promptly adapt to the selection pressure of their environment. Due to their rapid reproduction and pheno- or genotypic adaptation, evolution can be recognized even within few days. For example, *Pseudomonas fluorescens* rapidly adapts to static conditions and produces a microcosm at the air-medium interface, established by cellulose polymer overproducing derivatives (Rainey and Rainey, 2003). These matrix overproducers, distinguished by their typical wrinkled colony morphotype in the laboratory can emerge in numerous bacterial species (Hansen *et al.*, 2007; Poltak and Cooper, 2011; Flynn *et al.*, 2016). The evolution of these wrinkly morphotypes in *Pseudomonas* is governed by the altered bis-(3'-5')-cyclic dimeric guanosine monophosphate (c-di-GMP) levels in the cells (Goymer *et al.*, 2006; Traverse *et al.*, 2013). It is suggested that the complexity and flexibility of the regulatory system around c-di-GMP facilitates adaptation to new environments (Lind *et al.*, 2015). Interestingly, elimination of the major c-di-GMP modulating components revealed several other mutational pathways allowing the appearance of wrinkly morphotypes. In addition, the appearance and fixation of newly evolved genotypes is facilitated by the spatial structure present in biofilms (Martin *et al.*, 2016).

Various biofilm types are established by *Bacillus subtilis* under laboratory conditions, including pellicles at the air-medium interface (Branda *et al.*, 2001; Gallegos-Monterrosa *et al.*, 2016; Mhatre *et al.*, 2016). *B. subtilis* cells inhabiting the biofilms are sessile and produce a matrix consisting of exopolysaccharides (EPS), protein fibers (TasA) and hydrophobin protein (BslA) (Branda *et al.*, 2004; Romero *et al.*, 2010; Kobayashi and Iwano, 2012; Hopley *et al.*, 2013). Complex regulatory pathways ensure the mutually exclusive expressions of genes related to biofilm matrix production and motility (Chai, Kolter, *et al.*, 2010; Chai, Norman, *et al.*, 2010). In addition to its role as the major repressor of biofilm formation, SinR also affects the expression of genes related to motility and cell separation collectively with other regulatory proteins (Chai, Norman, *et al.*, 2010). Therefore, SinR has a central role in coordinating the exclusive expression of genes responsible for motile and sessile states.

While flagellum-dependent motility is not essential for the establishment of pellicles in *B. subtilis*, it facilitates the rapid formation of new biofilms (Hölscher *et al.*, 2015). Therefore, strains lacking motility are delayed in pellicle formation and are outcompeted by cells possessing the functional motility apparatus and exhibiting aerotaxis (Hölscher *et al.*, 2015).

Rapid appearance of distinct *B. subtilis* morphotypes has been previously described in a 2-month-long batch culture experiment under static and shaken conditions (Leiman *et al.*, 2014). Under both conditions, versatile morphotypes evolved including derivatives with reduced matrix production and lineages with enhanced matrix expression. In the latter case, mutation in the *sinR* gene was identified by candidate-gene approach. Interestingly, mutations in *sinR* rapidly emerge in colonies of *B. subtilis* lacking SinI, an antagonist of SinR function (Kearns *et al.*, 2005). Additionally, emergence of *sinR* mutants solves the problem of toxic galactose metabolites accumulation in the *galE* mutant, where elevated EPS production functions as a shunt for the toxic molecule (Chai *et al.*, 2012). Therefore, the adaptation pathway through *sinR* mutations appears to be a general dénouement for numerous adaptation processes in *B. subtilis* biofilms.

Here, we study how the lack of functionally assembled flagella influences the evolution of wrinkly morphotypes in *B. subtilis* and demonstrate that matrix-overproduction caused by non-synonymous mutations in SinR primarily aids non-motile cells.

Results and Discussion

Evolution of wrinkly morphotypes in pellicles of *B. subtilis*

Lack of motility delays the establishment of *B. subtilis* pellicles (Hölscher *et al.*, 2015). During the previous study, when various biofilm competition experiments were performed using non-motile *B. subtilis* strains and colony-forming units (CFU) were assayed on LB plates, the appearance of a distinct colony phenotype was noticeable. The wrinkles and size of the observed colonies were clearly increased compared to their ancestors used for the study (Fig. 1a). Interestingly, these wrinkled spreader colonies (hereafter called WS morphotypes) were mostly apparent for the strain lacking the gene coding for the flagellin protein (i.e. *hag*). Therefore, a series of mutant strains used in our previous study (Hölscher *et al.*, 2015) was examined for the frequency of wrinkled derivatives during pellicle formation. Strains lacking various parts of the flagellum (flagellin (*hag*), hook (*flgE*), or basal body (*fliF*)), having disrupted regulation of motility (*sigD* mutant) or harboring a non-active flagellum (*motA* mutant) contained an increased amount of WS colonies during pellicle formation compared to the wild type (Fig. 1b).

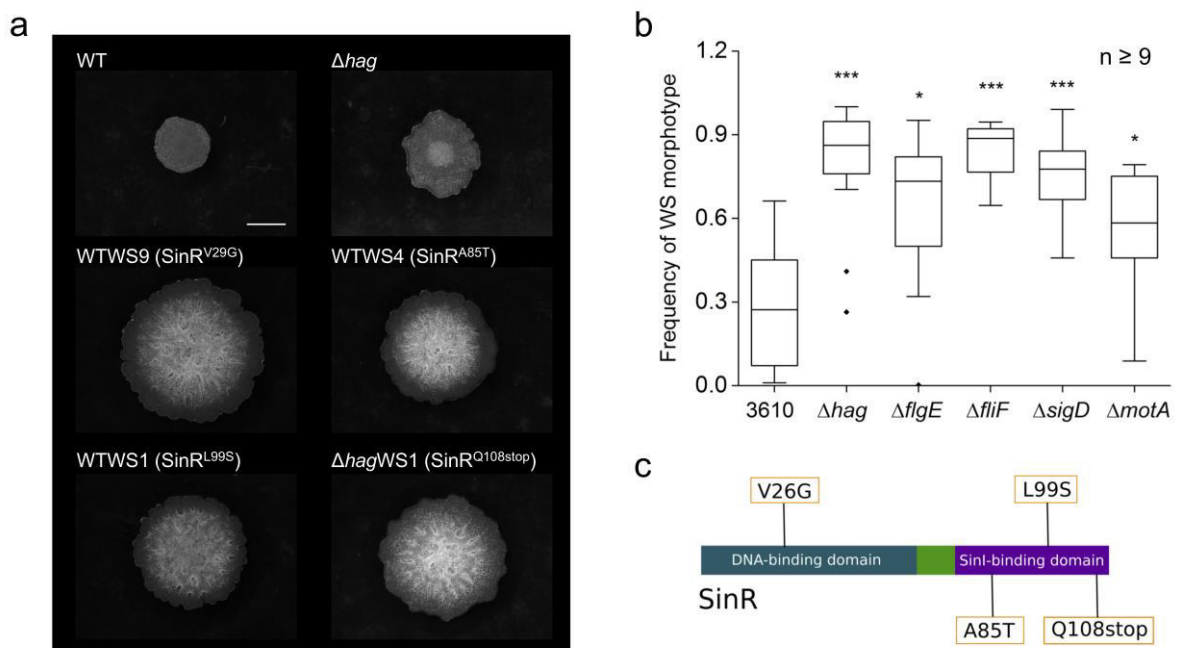


Figure 1. WS morphotypes exhibit elevated wrinkle formation and appear especially in non-motile mutant.

(a) Microscopy images of WS morphotypes isolated from WT and Δhag strains. Representative images for the phenotype of each detected mutation, indicated in parentheses, are displayed. The scale bar represents 2 mm. (b) Frequency of WS morphotypes in various derivatives of *B. subtilis*. Boxes represent quartile 1-3, the line represents the median and whiskers indicate the upper and lower inner fence and dots represent outliers. Asterisks indicate significant differences (two sample Student's t test assuming unequal variances: P values: Δhag , $8.27 \cdot 10^{-6}$; $\Delta flgE$, 0.013; $\Delta fliF$, $1.23 \cdot 10^{-7}$; $\Delta sigD$, $2.21 \cdot 10^{-5}$, $\Delta motA$, 0.0125; $n \geq 9$). (c) Schematic representation of the SinR protein with domains and location of the detected mutations depicted.

WS morphotypes harbor non-synonymous mutations in *sinR*

After isolation of ten WS morphotypes each from cultures of wild type and flagellin-lacking mutant (WTWS1-10 and Δhag WS1-10, respectively), we analyzed the *sinR* gene encoding a major regulator of *B. subtilis* motility and biofilm formation, since wrinkle formation is among other factors associated with matrix production (Branda *et al.*, 2004; Asally *et al.*, 2012). Sequencing revealed several non-synonymous substitutions resulting in SinR variants with the following changes in amino acid composition: V26→G, A85→T, L99→S and Q108→stop. V26G was located in the DNA-binding domain of SinR, whereas the other three mutations were found in the SinI-binding domain (Fig. 1c). All isolated morphotypes contained one of those mutations and exhibited a phenotype with increased wrinkles (Fig. 1a). Therefore, one of these mutations was sufficient to induce increased wrinkle formation in *B. subtilis*. While we cannot exclude the possibility of additional mutations present in the WS morphotypes that also contributes to the observed phenotypes, it is unlikely due to the relatively short time span of the experiments. In our further experiments, we investigated strains representative for one of the detected mutations.

WS morphotypes exhibit increased expression of matrix genes

As SinR is responsible for repression of the biofilm matrix genes, we examined their expression using strains containing the P_{tapA} -*yfp* reporter, which is an indicator for the expression of the matrix operon *tapA-sipW-tasA*. Matrix gene expression of different WS morphotypes, a *sinR* mutant, as well as the ancestral strains of the wild type and *hag* mutant was qualitatively analyzed using fluorescence microscopy (Fig. 2a). While P_{tapA} -*yfp* expression was scarcely present in the wild type and *hag* mutant, it notably increased in the *sinR* mutant as well as in the WS morphotypes, whose cells occurred also primarily in chains. Mutation in *sinR* increases chain formation in planktonic cultures of *B. subtilis* as observed before (Kearns *et al.*, 2005). Interestingly, the wild type and *hag* mutant showed detectable, although heterogeneous matrix gene expression in small clusters appearing after prolonged incubation, but they represented only a minor portion of the culture (Fig. S1). In comparison, the matrix gene expression of the *sinR* mutant and the WS morphotypes seemed to be very homogeneous (Fig. 2a). These results were confirmed by a quantitative analysis of the P_{tapA} -*yfp* expression of the same strains over the course of 24 h (Fig. 2b). Here, the difference in expression level between *sinR* deletion mutant and the WS morphotypes became apparent, indicating that the mutations of the *sinR* variants did not abrogate the function of SinR completely.

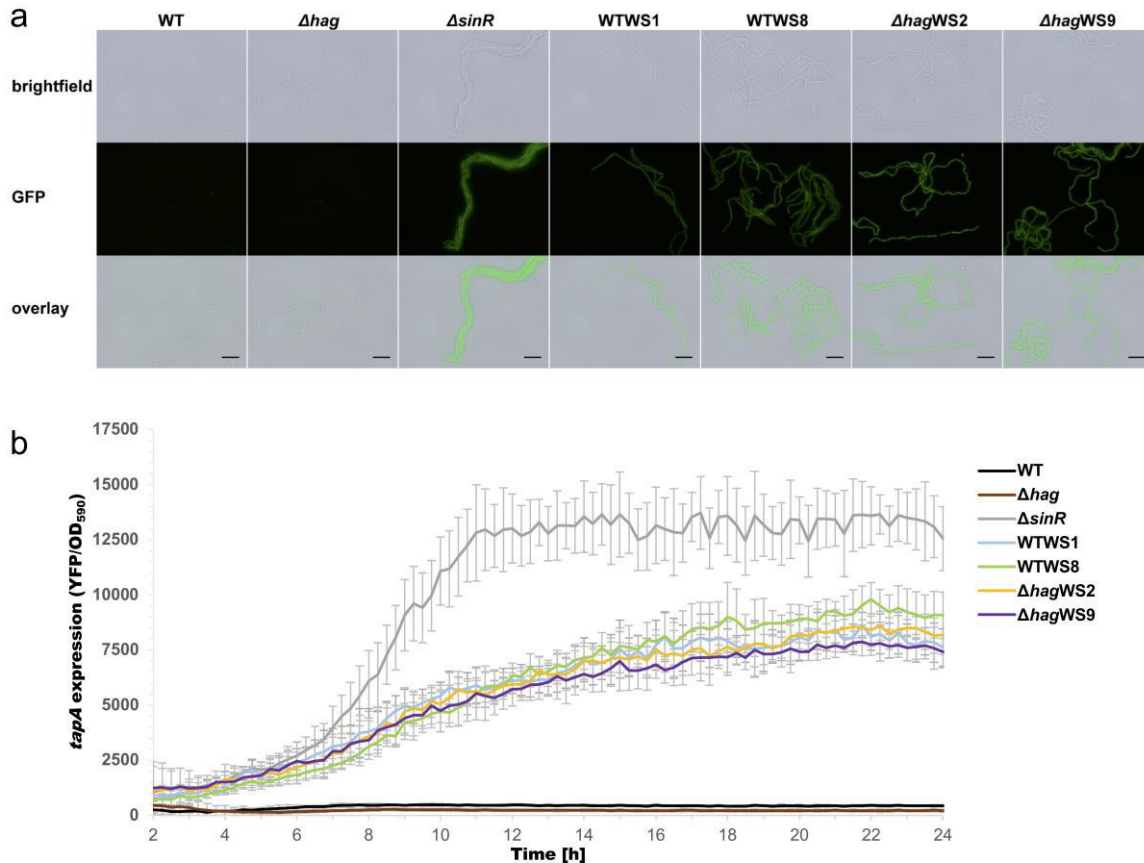


Figure 2. Increased matrix gene expression of WS morphotypes. (a) Representative confocal microscopy images of strains with P_{tapA} -yfp reporter (false colored green) indicating matrix gene expression. Wild type, Δhag and $\Delta sinR$ were compared to representative WS morphotypes of each wild type and Δhag background harboring the mutations V26G (WTWS9 and $\Delta hagWS9$) and L99S (WTWS1 and $\Delta hagWS2$). The scale bar represents 10 μm . (b) OD normalized expression of P_{tapA} -yfp of strains from (a) over time. Error bars represent the standard deviation.

SinR-L99S differs from wildtype in its interaction with SinI and the SinR operator

Due to the increased matrix gene expression, we hypothesized that the mutated SinR variants exhibit altered interaction properties with SinI or DNA. To test this hypothesis, the interaction of the SinR-L99S variant and SinI was investigated and compared to the interaction with the wild-type SinR. Variants SinR-V26G and SinR-A85T were not tested due to insolubility after overexpression under the conditions described in the Experimental Procedures section. To quantify the interaction between SinI and SinR or the SinR-L99S variant, we performed isothermal titration calorimetry (ITC), where SinR was titrated with SinI. In these experiments, a truncated version of SinI was used, a synthetic peptide consisting of amino acids 9-39 (encoded by $sinI^{9-39}$). However, this short version was able to induce cell chaining when overexpressed in *B. subtilis* cells, similar to an overexpression of the full *sinI* (Fig. 3). Therefore, the short SinI version was sufficient to bind *in vivo* to SinR leading to a de-repression of the matrix genes and, thus formation of chains.

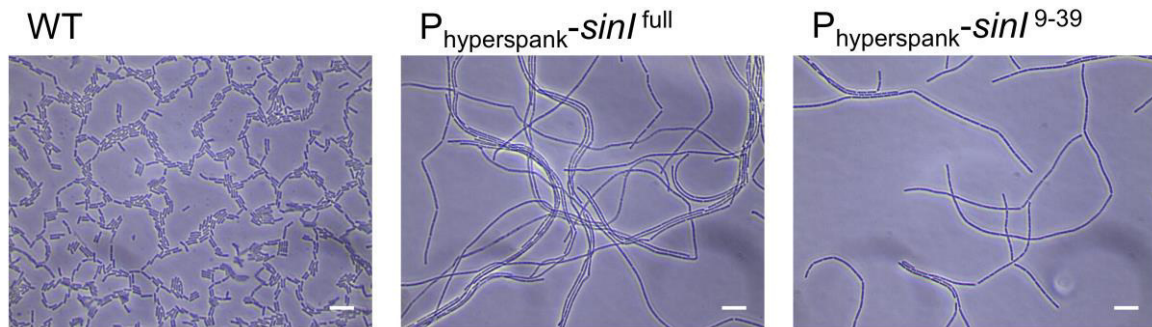


Figure 3. Truncated SinI supports cell chaining. Microscopy images of wild type and two *B. subtilis* strains harboring a *sinI* overexpression construct of the full gene (*sinI*^{full}) or a truncated version (*sinI*⁹⁻³⁹). The scale bar represents 10 μm .

We observed tight binding of SinI to SinR with an apparent dissociation constant (K_D) of approximately 7 nM and a stoichiometry of $N = 1.2 \pm 0.02$ assuming a one-site binding model (Fig. 4a). This data are in good agreement with the previously reported K_D of below 10 nM for the SinR/SinI interaction (Newman *et al.*, 2013). When we titrated the SinR L99S variant with the SinI peptide, we observed two distinct binding events (Fig. 4a). Applying a two-sites binding model, K_D s of approximately 162 nM and 571 nM for the binding sites 1 and 2, respectively, were determined (Fig. 4a). These data suggest that binding of SinI to the SinR-L99S is weaker than for the wildtype and occurs in two different binding events. However, the summed stoichiometry of binding event 1 ($N_1 = 0.898 \pm 0.358$) and 2 ($N_2 = 0.448 \pm 0.382$) of $N \approx 1.35$ suggests to us that no additional binding site is present. Interpreting our findings in the context of the SinI/SinR crystal structure delivers a plausible explanation for the bi-phasic binding of SinI to the SinR-L99S variant: In brief, SinR homo-dimerization with SinR and hetero-dimerization with SinI is mainly facilitated via the two C-terminal α -helices of SinR and is characterized by a hydrophobic core at the interface surrounded by polar interactions (Fig. 4c). Exchange of leucine to serine at position 99 at the border of the hydrophobic core creates a polar environment that should disturb the interaction with the unpolar interaction interface of SinI. This might also be the reason why we observed a two-phased binding event of the SinI peptide to SinR-L99S. It might well be that the SinI/SinR-L99S interaction occurs in a sequential manner and is first established by the N-terminal α -helix of SinI, before the C-terminal α -helix interlocks at the opposed site at the altered dimer interface. Closer inspection of the thermodynamic parameters revealed that SinI binding to wildtype SinR is entropy driven, as suggested by the positive ΔS of 24.7 cal mol⁻¹ deg⁻¹ and negative ΔH of -3752 \pm 135.6 cal mol⁻¹ and might therefore be largely established by hydrophobic interactions. In contrast, binding of SinI to the SinR-L99S variant occurs in two steps with binding event 1 being characterized by a positive ΔS of 17.9 cal mol⁻¹ deg⁻¹ and a negative ΔH of -3928 \pm 1450 cal mol⁻¹ indicative of an interaction that is mainly established via hydrophobic interaction. However, binding event 2 is characterized by

a negative ΔS of $-22.9 \text{ cal mol}^{-1} \text{ deg}^{-1}$ and a negative ΔH of $-1.524\text{E}4 \pm 1.24\text{E}4 \text{ cal mol}^{-1}$. Hence, the mechanism of binding event 2 seems enthalpic and entropic, and might involve expulsion of structured H_2O molecules from the binding site. This observation supports the model in which SinI association to SinR-L99S occurs in two steps with the second binding step being affected by an impaired hydrophilic interface caused by the polar serine in position 99.

Next, we reasoned that the presence of serine at position 99 might affect the formation and stability of the SinR tetramer. We therefore analyzed the oligomeric properties of SinR and SinR-L99S by analytical size exclusion chromatography (SEC), revealing that wildtype SinR and SinR-L99S both occur almost exclusively as tetramers (Fig. S2a). However, the L99S mutation might affect tetramer stability. Therefore, we assayed the tetramer dissociation properties of the wildtype and SinR-L99S by ITC. To do so, wild-type or mutant SinR protein was titrated into buffer. Strikingly, while the wild-type SinR did not dissociate, the L99S variant showed reproducibly detectable reduction in tetramer stability upon rapid dilution (Fig. 4b). It might well be that this subtle defect has significant consequences at the functional level, i.e. the interaction of SinR with the DNA operator sequence. However, analytical SEC of reconstituted SinR/IR-DNA and SinR-L99S/IR-DNA complexes revealed that interaction of SinR or SinR-L99S with the IR-DNA SinR operator occurs in the tetrameric state (Fig. S2b). Taken together, these findings agree well with the binding model proposed by Newman and co-workers (Newman *et al.*, 2013).

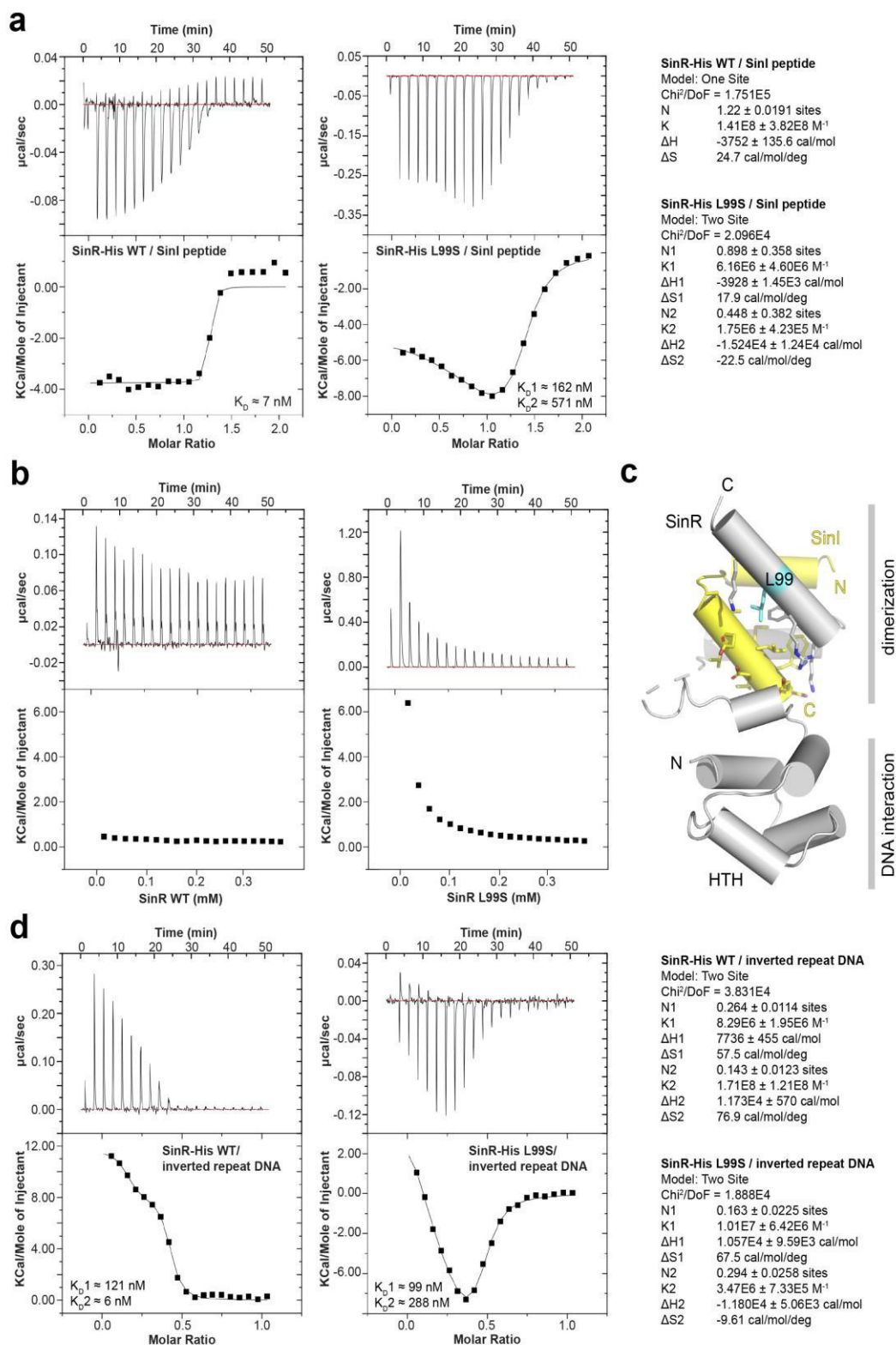


Figure 4. SinR-L99S differs in its interaction with SinI and DNA. (a) ITC measurements of the interaction between the SinI peptide and SinR (left thermogram) and SinR-L99S (right thermogram). Derived thermodynamic parameters are shown on the right site. (b) ITC complex dissociation experiments of SinR (left thermogram) and SinR-L99S (right thermogram). (c) Cartoon representation of the *B. subtilis* SinR/SinI complex crystal structure (PDB-ID: 1B0N; Newman et al. 2013). SinR is colored in grey and SinI is colored in yellow. Leucine 99 (cyan) and the surrounding SinR/SinI interface region is shown in stick representation. N and C indicate N-termini and C-termini, respectively. (d) ITC measurements of the interaction between the inverted repeat DNA and SinR (left thermogram) and SinR-L99S (right thermogram). Derived thermodynamic parameters are shown on the right site.

SinR-L99S shows impaired interaction with the SinR operator

Having demonstrated that SinR-L99S interacts as tetramers with the IR-DNA SinR operator, we wondered whether the interaction of SinR-L99S with IR-DNA differs from wildtype SinR in respect to the binding affinity. We performed ITC on SinR, respectively SinR-L99S, in the sample cell and titrated the IR-DNA into the cell. ITC revealed that interaction of SinR with the IR-DNA occurs in a bi-phasic manner. We therefore applied a two-sites binding model to the data, revealing that the two binding events are characterized by K_D s of approximately 121 nM and 6 nM for the binding sites 1 and 2, respectively (Fig. 4d). Our study confirms previous experiments stating the high-affinity interaction of SinR with IR-DNA (Newman *et al.*, 2013). The summed stoichiometry of binding event 1 ($N1 = 0.264 \pm 0.0114$) and 2 ($N2 = 0.143 \pm 0.0123$) of $N \approx 0.41$ further suggests to us that one IR-DNA fragment is able to interact with two SinR proteins, which is in good agreement with the crystal structure of SinR in complex with the IR-DNA SinR operator (Fig. S3) (Newman *et al.*, 2013). As shown above by analytical size exclusion chromatography, interaction of the IR-DNA occurs at the tetramer, likely in a 4:2 stoichiometry (SinR:IR-DNA). It is therefore unclear if the two observed binding events represent cooperative binding events at the same IR-DNA fragment or cooperative binding events at the opposed sites of the tetramer, relayed via the dimerization domain of SinR.

Strikingly, ITC titration of the L99S variant SinR protein with the IR-DNA fragment revealed that the interaction was impaired, as suggested by the K_D s of approximately 99 nM for site 1 and 288 nM for site 2 (Fig. 4d). Interestingly, while binding event 1 is comparable to the wildtype interaction for binding site 1 in the affinity and thermodynamic parameters $\Delta S1$ and $\Delta H1$, the thermodynamic parameters for binding event 2 changed from a $\Delta S2$ of 76.9 cal mol⁻¹ deg⁻¹ and a $\Delta H2$ of 1.173E4 +/- 570 cal mol⁻¹ for the wildtype interaction to a $\Delta S2$ of -9.61 cal mol⁻¹ deg⁻¹ and a $\Delta H2$ of -1.18E4 +/- 5.06E3 cal mol⁻¹ for the SinR-L99S/SinI interaction. In summary, the interaction of SinR with the IR-DNA is changed by serine in position 99 at the SinR dimerization interface in that it seems to alter not only the affinity for the IR-DNA at the DNA binding site in the second binding step, but also the mechanism by which the interaction is established. Hence, the interaction of wild-type SinR with the IR-DNA is characterized by positive cooperativity, while the SinR-L99S/IR-DNA interaction is impaired and displays features of negative cooperativity. This might result in de-repression of SinR target operons in case of the SinR-L99S variant and is in good agreement with the observed phenotype.

WS morphotype in Δhag background is advantageous during pellicle establishment

Next, we were interested in whether the WS morphotypes success during colonization of the air-liquid interface is altered, since they appeared frequently under these conditions. To test this, we competed the WS morphotype SinR^{L99S} (WTWS1 and Δhag WS2) against their respective ancestral strains (i.e. wild type or *hag* mutant) under conditions allowing pellicle formation and detected the strains using constitutively expressed fluorescence reporters. Figure 5a shows that both wild type and WS morphotype were equally successful in colonization of the air-liquid interface, which was comparable to the controls with competitions of the same strain. In contrast, the competition between the *hag* mutant and its derived WS morphotype revealed that the Δhag WS morphotype was able to outcompete the *hag* mutant during pellicle establishment (Fig. 5a). Interestingly, in each competition with the WS morphotype, the structure of the pellicle displayed a higher spatial segregation of cells than the wild type control competition that was visible as patches of red or green fluorescent regions. In the Δhag background, this effect can be explained by the inability to mix due to lack of flagella (comparable with the Δhag control competition as described previously by (Hölscher *et al.*, 2015)). However, in the WTWS morphotypes, this assortment could be due to a reduced motility that accompanies the increased matrix production. Additionally, the high amount of produced matrix might add to the adhesiveness of the cells, so that they clump together after cell division. The semi-quantitative analysis of the signal abundance for these competition experiments confirmed the superior surface colonization of the WS morphotypes compared to the ancestor in the Δhag but not the wild type background (Fig. 5b). In addition, the Δhag WS morphotype was able to establish a thin pellicle at the air-liquid interface faster than the *hag* mutant when compared as single strain cultures (Video S1).

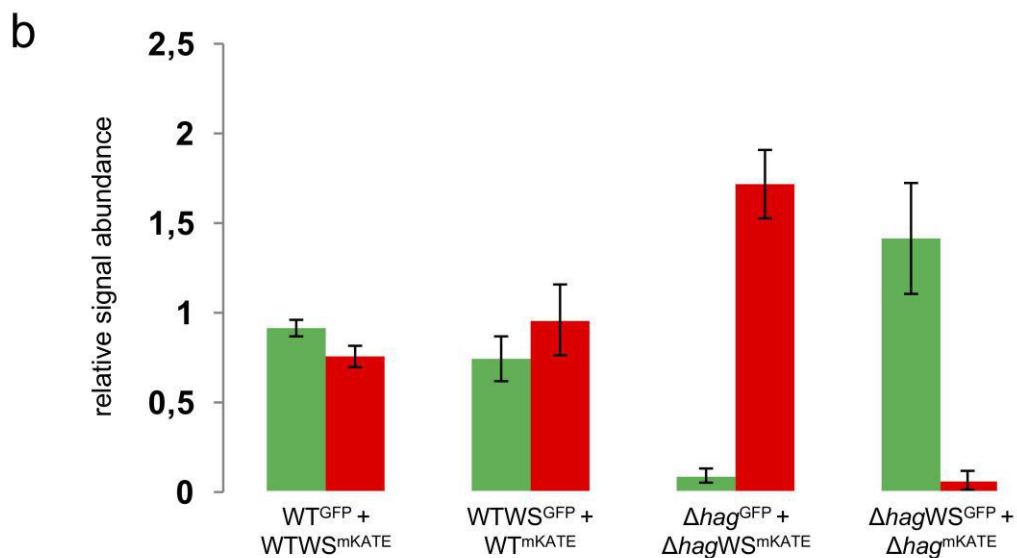
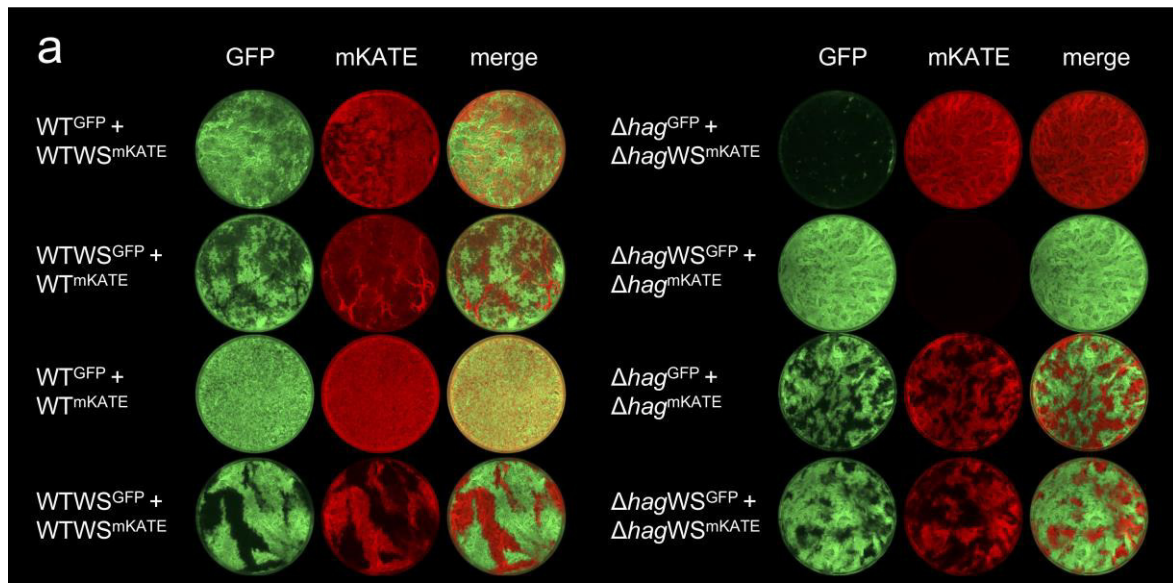


Figure 5. WS morphotypes outcompete ancestor in Δhag but not wild type background. (a) Microscopy images of competitions between green (GFP) and red (mKATE) fluorescently labelled wild type (left) or *hag* mutant (right) and derived WS morphotypes (SinR^{L99S}). False colored images of wells of a 24-well plate (diameter: 16 mm) are displayed. Control competitions with swapped fluorescent reporters (2nd row) and between otherwise identical strains (3rd and 4th row) were performed for each. (b) Semi-quantitative analysis of relative signal abundance for competitions of ancestor and WS morphotype from (a) (two sample Student's t test assuming unequal variances: WT^{GFP} + WTWS^{mKATE} P = 0.005; WTWS^{GFP} + WT^{mKATE} P = 0.134; Δhag ^{GFP} + Δhag WS^{mKATE} P = $2.8 \cdot 10^{-4}$; Δhag WS^{GFP} + Δhag ^{mKATE} P = 0.0027; n = 4). Error bars represent the standard deviation.

Selection pressure, not mutation rate is responsible for WS morphotype appearance

To investigate if an increased mutability of the *hag* mutant compared to the wild type is responsible for the primary occurrence of WS morphotypes in this strain, we determined the frequency of streptomycin-resistant mutants in both strains. Since the frequency of mutants in wild type and Δhag with respective mean values of $8,05 \cdot 10^{-6}$ (standard deviation: $5,01 \cdot 10^{-6}$) and $8,26 \cdot 10^{-6}$ (standard deviation: $2,35 \cdot 10^{-6}$) were comparable, we could exclude the mutation rate as reason for the frequent appearance of WS morphotypes. Because of the advantage of the WS morphotype in surface colonization in the Δhag background, we

conclude that there the selection pressure was high enough to result in mutations aiding the establishment of a pellicle at the air-liquid interface. This was probably caused by decreasing oxygen levels towards the bottom of the vessel as well as the limited number of cells that reach the liquid surface due to the lack of swimming motility, which is present in the wild type. Besides or because of an increased adhesiveness, the elevated matrix production of the WS morphotypes possibly results in a higher buoyancy, which counterbalances the lack of swimming and facilitates the fast surface colonization as indicated by video S1. Therefore, an increased selection pressure was likely responsible for the primary occurrence of WS morphotypes in the *hag* mutant. Although suppressor mutants of *sinR* were found under different conditions in the laboratory (Chai *et al.*, 2012; Leiman *et al.*, 2014), in nature, the observed mutations in SinR probably appear less frequent since most environmental isolates of *B. subtilis* are motile. Therefore, we hypothesize that the prerequisites for a selection of WS morphotypes in environmental setting is not significant in contrast to laboratory conditions.

Conclusions

Bacteria possess the ability to adapt to a huge variety of environments and conditions, with often impressive solutions to their challenges. To overcome their disadvantage of slow surface colonization in small numbers during pellicle establishment, non-motile *B. subtilis* strains develop suppressor mutations in *sinR*, encoding an important regulator and part of the intricate regulatory network governing biofilm formation in *B. subtilis*. These mutations alter its DNA- and protein-binding properties, leading to increased production of the biofilm matrix. In turn, matrix overproduction allows a faster surface colonization than the ancestor, successfully outcompeting it. Therefore, *B. subtilis* provides an interesting example of bacterial adaptability and resourcefulness in conditions with a specific selective pressure as well as it might explain their success on earth.

Experimental Procedures

Media composition and culturing conditions

All the strains used in this study are listed in Table S1. For cloning, mutant generation and colony morphology experiments, strains were cultivated in Lysogeny Broth medium (LB-Lennox, Carl Roth, Germany; 10 g l⁻¹ tryptone, 5 g l⁻¹ yeast extract and 5 g l⁻¹ NaCl) supplemented with 1.5 % Bacto agar if required. To select for wrinkly phenotypes in pellicles, strains were pre-grown in LB medium overnight and diluted 1:100 in MSgg medium (5 mM potassium phosphates buffer (pH 7), 100 mM MOPS, 2 mM MgCl₂, 700 μM CaCl₂, 100 μM MnCl₂, 50 μM FeCl₃, 1 μM ZnCl₂, 2 μM thiamine, 0.5 % glycerol, 0.5 % glutamate (Branda *et al.*, 2001)). When 2 ml culture was incubated in a 24-well plate under static conditions at 30 °C, pellicles were formed at the air-medium interface after 72 h. If appropriate, the following antibiotics were used: Kanamycin (Km, 5 μg ml⁻¹), Lincomycin + Erythromycin (MLS, 12.5 μg ml⁻¹ + 1 μg ml⁻¹, respectively), Chloramphenicol (Cm, 5 μg ml⁻¹), Spectinomycin (Spec, 100 μg ml⁻¹) and Ampicillin (Amp, 100 μg ml⁻¹).

Isolation of WS strains and genetic analysis of the *sinIR* locus

Wild type or various mutant strains of *B. subtilis* were grown in MSgg medium under static conditions and adequate dilutions were spread on LB agar plates to obtain single colonies. Colonies with wrinkly phenotypes were counted. Selected colonies were cultivated in LB medium, genomic DNA was extracted using EURex Bacterial & Yeast Genomic DNA Kit (Roboklon GmbH, Berlin, Germany), the *sinIR* locus was PCR amplified using primers oTB98 and oTB99 (see Table S2 for oligonucleotide sequences), and PCR products were sequenced (GATC GmbH, Cologne, Germany).

Constructions of plasmids and strains

B. subtilis strains (using DK1042 based strains that is naturally competent version of NCIB3610 (Konkol *et al.*, 2013)) were obtained via natural competence transformation using genomic or plasmid DNA (Kunst and Rapoport, 1995). Strains with constitutively expressing green- or red-fluorescent reporters were obtained by transforming genomic DNA from 168hyGFP or 168hymKATE, respectively (van Gestel *et al.*, 2014). Biofilm specific reporter strains were created using genomic DNA from DL821 harboring a P_{tapA}-*yfp* reporter construct (López *et al.*, 2009). To overexpress the *sinI* and *sinI*^{Δ39} genes, the full and the truncated genes were obtained using oligonucleotides oTB124-oTB125 and oTB126-oTB127 (Table S2), respectively, digested with *Hind*III and *Sph*I enzymes, and cloned into the corresponding sites of pDR111 (kind gift from David Rudner), resulting in pTB695 and pTB696, respectively. The obtained plasmids were verified using sequencing and introduced into *B. subtilis* DK1042 using natural competence (Kunst and Rapoport, 1995). Transformants were

selected on LB plates with appropriate antibiotics. When appropriate, successful transformation was validated using the fluorescence reporter activity of the strains or amylase-negative phenotype on 1 % starch agar plates.

To overexpress the *sinR*, the wild type gene was amplified by PCR from *B. subtilis* 168 genomic DNA (sequence identical in NCIB 3610) using SinR_NcoI_F and SinR_H6_BamHI_R primers (Table S2), harboring a C-terminal hexa-histidine tag. The fragment was digested with *NcoI* and *BamHI* restriction enzymes and cloned into a pET24d vector for overexpression in *E. coli*. Mutagenesis of SinR was performed in a two-step PCR mutagenesis with the respective mutagenesis primer pairs (Table S2) and subsequent cloning as described above.

Microscopy analysis of competition experiments and *sinI* overexpression

For competition experiments, pre-grown GFP and mKATE labeled strains were mixed at equal optical density and diluted 1:100 in MSgg medium. After 72 h of growth, the fluorescence intensity was measured using an infinite F200PRO plate reader (TECAN Group Ltd, Männedorf, Switzerland). Bright field, green- and red-fluorescence images of the pellicles were taken with an Axio Zoom V16 stereomicroscope (Carl Zeiss, Jena, Germany) at 3.5x magnification equipped with a Zeiss CL 9000 LED light source, HE eGFP filter set (excitation at 470/40 nm and emission at 525/50 nm), HE mRFP filter set (excitation at 572/25 nm and emission at 629/62 nm), and an AxioCam MRm monochrome camera (Carl Zeiss, Jena, Germany). The exposure times were set to 0.01 s, 1 s and 3 s for bright field, green- and red-fluorescence, respectively. ImageJ (National Institute of Health, Bethesda, MD, USA) was used for background subtraction and channel merging.

For *sinI* overexpression, strains TB697 or TB698 were pre-grown in LB medium overnight, diluted 1:100 in fresh LB medium, and incubated in the absence or presence of 0.1 mM IPTG for 4 h. Samples were added to microscopy slides containing a thin layer of 1 % agarose, glass coverslips were placed on the samples and the cells were visualized using MOTIC BA310E phase contrast microscope equipped with a 100x/1.25 PHASE EC-H objective and a MOTICAM 3 camera (VWR, Darmstadt, Germany).

Reporter assays

To monitor biofilm coupled gene expression, wild type and selected wrinkly isolates harboring the P_{tapA} -*yfp* reporter construct were pre-grown on LB agar plates. One colony was inoculated in 3 ml liquid LB medium and incubated for 5 h at 37 °C and 225 rpm, diluted to DO_{600} of 0.1 in LB medium, and 200 μ l aliquots of the cultures were inoculated into a 96-well plate. The samples were incubated for 24 h at 30 °C with continuous shaking among measurements, and optical density and fluorescence was recorded every 15 minutes.

For single-cell level fluorescence microscopy, one colony from overnight grown plate was inoculated in 3 ml liquid LB and incubated for 5 h at 37 °C and 225 rpm. 5 µl of culture was spotted on a microscope slide coated with 0.8 % agarose, covered with a cover slip and examined under the fluorescence microscope (Olympus Bx51; 100× oil objective). Images were captured using bright light (exposure time 15 ms) and fluorescence light using the GFP filter (exposure time 500 ms).

Fluctuation assay

To determine the mutation rate, a fluctuation assay was performed with wild type and *hag* mutant as described in (Martin *et al.*, 2017), except for the use of MSgg medium (n = 48).

Expression and protein purification

Constructs, pET24sinR^{WT} and their mutagenized variants were transformed into *E. coli* BL21(DE3) for overexpression. Proteins were overexpressed in 1 l LB autoinduction media (1.8% w/v lactose) shaking at 30 °C overnight. Cells were harvested the next morning and resuspended in 20 ml buffer A (20 mM HEPES/NaOH pH 8.0, 500 mM NaCl, 40 mM imidazole). Cells were lysed two times with a M-110L Microfluidizer (Microfluidics) and centrifuged at 20,000 r.p.m. for 20 min at 4 °C to remove cell debris. The supernatant was applied onto a 1 ml HisTrap HP column (GE Healthcare) for Ni-NTA affinity chromatography. The column was washed with 15 column volumes of buffer A and proteins were eluted with 5 ml buffer B (20 mM HEPES/NaOH, pH 8.0, 500 mM NaCl, 500 mM imidazole). Proteins were concentrated to 1 ml and further purified by size-exclusion chromatography using a HiLoad 26/60 Superdex 200 gel-filtration column in buffer C (20 mM HEPES/NaOH, 500 mM NaCl).

Isothermal titration calorimetry

ITC experiments were performed on a MicroCal ITC 200 instrument (GE Healthcare). The SinI⁹⁻³⁹ peptide (SinI protein from amino acid 9 to 39) was synthesized with a free amine at the N-terminus and free acid group at the C-terminus (peptides&elephants GmbH, Potsdam, Germany). The peptide was dissolved in an appropriate volume of buffer C, which was used for the purification of SinR^{WT} and SinR^{L99S}. Concentrations were determined by measuring the A₂₈₀ using a NanoDrop Lite spectrophotometer (Thermo Scientific). For the ITC SinR/SinI interaction experiment, 200 µl of SinR^{WT} or SinR^{L99S} (25 µM) was added to the sample cell and 250 µM SinI⁹⁻³⁹ peptide solution were titrated in at 25 °C for a total of 20 injections, each separated by 150 s, consisting of 0.2 µl SinI⁹⁻³⁹ peptide for the initial injection and 2 µl for the following 19 injections. For the SinR dissociation ITC experiment, 200 µl of buffer C was added to the sample cell and 2 mM SinR^{WT} or SinR^{L99S} were titrated in at 25 °C for a total of 20 injections, each separated by 150 s, consisting of 0.2 µl SinI⁹⁻³⁹ peptide for the initial

injection and 2 μ l for the following 19 injections. For the ITC SinR-inverted repeat DNA interaction experiment, 200 μ l of SinR^{WT} or SinR^{L99S} (30 μ M) was added to the sample cell and 150 μ M inverted repeat DNA was titrated in at 25 °C for a total of 20 injections, each separated by 150 s, consisting of 0.2 μ l SinI⁹⁻³⁹ peptide for the initial injection and 2 μ l for the following 19 injections. The inverted repeat primers were prior to the experiment dissolved in buffer C and annealed by heating to 95 °C for 5 min and a subsequent controlled cooling down to 10 °C for 1 h, using a PCR cycler. ITC data were processed using the Origin ITC software (OriginLab) and thermodynamic parameters were obtained by fitting the data to a one set of sites binding model or a two sets of sites binding model, depending on the data.

Acknowledgements

This project was founded by a grant KO4741/3-1 from the Deutsche Forschungsgemeinschaft (DFG) to Á.T.K. T.H. was supported by International Max Planck Research School for Chemical Ecology (IMPRS-CE). Work in the laboratory of Á.T.K. is supported by a startup grant from the Technical University of Denmark and partly by the Danish National Research Foundation (DNRF137) for the Center for Microbial Secondary Metabolites. P.P. thanks the International Max-Planck-Research School for Environmental, Cellular and Molecular Microbiology (IMPRS-Mic) for financial support. G.B. acknowledges support from the Collaborative Research Initiative CRC-TRR 174 of DFG for financial support.

Author Contributions

ÁTK design of the study; AR, TH, TS, FB, PP, ÁTK conducted experiments; AR, PP, GB, ÁTK interpreted the data; TH and ÁTK wrote the manuscript; AR, PP, GB corrected the manuscript

Conflict of interest. None declared

References

- Asally, M., Kittisopikul, M., Rue, P., Du, Y., Hu, Z., Cagatay, T., *et al.* (2012) Localized cell death focuses mechanical forces during 3D patterning in a biofilm. *Proc Natl Acad Sci* **109**: 18891–18896.
- Branda, S.S., González-Pastor, J.E., Ben-Yehuda, S., Losick, R., and Kolter, R. (2001) Fruiting body formation by *Bacillus subtilis*. *Proc Natl Acad Sci U S A* **98**: 11621–11626.
- Branda, S.S., González-Pastor, J.E., Dervyn, E., Ehrlich, S.D., Losick, R., and Kolter, R. (2004) Genes involved in formation of structured multicellular communities by *Bacillus subtilis*. *J Bacteriol* **186**: 3970–3979.
- Chai, Y., Beauregard, P.B., Vlamakis, H., Losick, R., and Kolter, R. (2012) Galactose metabolism plays a crucial role in biofilm formation by *Bacillus subtilis*. *MBio* **3**: e00184-12.
- Chai, Y., Kolter, R., and Losick, R. (2010) Reversal of an epigenetic switch governing cell chaining in *Bacillus subtilis* by protein instability. *Mol Microbiol* **78**: 218–229.
- Chai, Y., Norman, T., Kolter, R., and Losick, R. (2010) An epigenetic switch governing daughter cell separation in *Bacillus subtilis*. *Genes Dev* **24**: 754–765.
- Flynn, K.M., Dowell, G., Johnson, T.M., Koestler, B.J., Waters, C.M., and Cooper, V.S. (2016) Evolution of ecological diversity in biofilms of *Pseudomonas aeruginosa* by altered cyclic diguanylate signaling. *J Bacteriol* **198**: 2608–2618.
- Gallegos-Monterrosa, R., Mhatre, E., and Kovács, Á.T. (2016) Specific *Bacillus subtilis* 168 variants form biofilms on nutrient-rich medium. *Microbiology* **162**: 1922–1932.
- Gestel, J. van, Weissing, F.J., Kuipers, O.P., and Kovács, Á.T. (2014) Density of founder cells affects spatial pattern formation and cooperation in *Bacillus subtilis* biofilms. *ISME J* **8**: 2069–2079.
- Goymer, P., Kahn, S.G., Malone, J.G., Gehrig, S.M., Spiers, A.J., and Rainey, P.B. (2006) Adaptive divergence in experimental populations of *Pseudomonas fluorescens*. II. Role of the GGDEF regulator WspR in evolution and development of the wrinkly spreader phenotype. *Genetics* **173**: 515–526.
- Hansen, S.K., Rainey, P.B., Haagenen, J.A.J., and Molin, S. (2007) Evolution of species interactions in a biofilm community. *Nature* **445**: 533–536.
- Hobley, L., Ostrowski, A., Rao, F. V., Bromley, K.M., Porter, M., Prescott, A.R., *et al.* (2013) BslA is a self-assembling bacterial hydrophobin that coats the *Bacillus subtilis* biofilm. *Proc Natl Acad Sci* **110**: 13600–13605.
- Hölscher, T., Bartels, B., Lin, Y.-C., Gallegos-Monterrosa, R., Price-Whelan, A., Kolter, R., *et al.* (2015) Motility, chemotaxis and aerotaxis contribute to competitiveness during bacterial pellicle biofilm development. *J Mol Biol* **427**: 3695–3708.
- Kearns, D.B., Chu, F., Branda, S.S., Kolter, R., and Losick, R. (2005) A master regulator for biofilm formation by *Bacillus subtilis*. *Mol Microbiol* **55**: 739–749.

- Kobayashi, K., and Iwano, M. (2012) BslA(YuaB) forms a hydrophobic layer on the surface of *Bacillus subtilis* biofilms. *Mol Microbiol* **85**: 51–66.
- Konkol, M.A., Blair, K.M., and Kearns, D.B. (2013) Plasmid-encoded comI inhibits competence in the ancestral 3610 strain of *Bacillus subtilis*. *J Bacteriol* **195**: 4085–4093.
- Kunst, F., and Rapoport, G. (1995) Salt stress is an environmental signal affecting degradative enzyme synthesis in *Bacillus subtilis*. *J Bacteriol* **177**: 2403–2407.
- Leiman, S.A., Arboleda, L.C., Spina, J.S., and McLoon, A.L. (2014) SinR is a mutational target for fine-tuning biofilm formation in laboratory-evolved strains of *Bacillus subtilis*. *BMC Microbiol* **14**: 301.
- Lind, P.A., Farr, A.D., and Rainey, P.B. (2015) Experimental evolution reveals hidden diversity in evolutionary pathways. *Elife* **2015**: e07074.
- López, D., Vlamakis, H., Losick, R., and Kolter, R. (2009) Paracrine signaling in a bacterium. *Genes Dev* **23**: 1631–1638.
- Martin, M., Dragoš, A., Hölscher, T., Maróti, G., Bálint, B., Westermann, M., and Kovács, Á.T. (2017) *De novo* evolved interference competition promotes the spread of biofilm defectors. *Nat Commun* **8**: 15127.
- Martin, M., Hölscher, T., Dragoš, A., Cooper, V.S., and Kovács, Á.T. (2016) Laboratory evolution of microbial interactions in bacterial biofilms. *J Bacteriol* **198**: 2564–2571.
- Mhatre, E., Troszok, A., Gallegos-Monterrosa, R., Lindstädt, S., Hölscher, T., Kuipers, O.P., and Kovács, Á.T. (2016) The impact of manganese on biofilm development of *Bacillus subtilis*. *Microbiology* **162**: 1468–1478.
- Newman, J.A., Rodrigues, C., and Lewis, R.J. (2013) Molecular basis of the activity of SinR Protein, the master regulator of biofilm formation in *Bacillus subtilis*. *J Biol Chem* **288**: 10766–10778.
- Poltak, S.R., and Cooper, V.S. (2011) Ecological succession in long-term experimentally evolved biofilms produces synergistic communities. *ISME J* **5**: 369–378.
- Rainey, P.B., and Rainey, K. (2003) Evolution of cooperation and conflict in experimental bacterial populations. *Nature* **425**: 72–74.
- Romero, D., Aguilar, C., Losick, R., and Kolter, R. (2010) Amyloid fibers provide structural integrity to *Bacillus subtilis* biofilms. *Proc Natl Acad Sci* **107**: 2230–2234.
- Traverse, C.C., Mayo-Smith, L.M., Poltak, S.R., and Cooper, V.S. (2013) Tangled bank of experimentally evolved *Burkholderia* biofilms reflects selection during chronic infections. *Proc Natl Acad Sci* **110**: E250–E259.

Chapter 4

Laboratory evolution of microbial interactions in bacterial biofilms

Published in: Journal of Bacteriology (2016)

Laboratory Evolution of Microbial Interactions in Bacterial Biofilms

Marivic Martin,^a Theresa Hölscher,^a Anna Dragoš,^a  Vaughn S. Cooper,^b  Ákos T. Kovács^a

Terrestrial Biofilms Group, Institute of Microbiology, Friedrich Schiller University Jena, Jena, Germany^a; Department of Microbiology and Molecular Genetics, University of Pittsburgh, Pittsburgh, Pennsylvania, USA^b

Microbial adaptation is conspicuous in essentially every environment, but the mechanisms of adaptive evolution are poorly understood. Studying evolution in the laboratory under controlled conditions can be a tractable approach, particularly when new, discernible phenotypes evolve rapidly. This is especially the case in the spatially structured environments of biofilms, which promote the occurrence and stability of new, heritable phenotypes. Further, diversity in biofilms can give rise to nascent social interactions among coexisting mutants and enable the study of the emerging field of sociomicrobiology. Here, we review findings from laboratory evolution experiments with either *Pseudomonas fluorescens* or *Burkholderia cenocepacia* in spatially structured environments that promote biofilm formation. In both systems, ecotypes with overlapping niches evolve and produce competitive or facilitative interactions that lead to novel community attributes, demonstrating the parallelism of adaptive processes captured in the lab.

Since the pioneering discoveries of Robert Koch, most bacteria generally have been studied in planktonic cultures, wherein cells grow dispersed from one another. Recently, the spatially structured environments (definitions of terminology are given in Table 1) of tightly packed bacterial biofilms have been recognized as more appropriate models to study microbial growth and interactions (1), because microbes may live more frequently in biofilms on inanimate or host surfaces (2) and the physiology of biofilm cells differs from that of planktonic cultures (3). The regulation of biofilm formation, persistence, and dispersal has been investigated at the molecular level for many years now, but much more remains to be discovered, particularly related to how biofilm cells interact when attached to one another (4, 5). The increasing interest in biofilm models has revealed the complexity of microbial social interactions (6). Since microbes, to some extent, share the structural components of biofilms (e.g., exopolysaccharides), the process of biofilm construction can be viewed as a form of cooperation, at least within a single lineage of cells (7–9). In addition, biofilm itself provides a structured environment that promotes other types of resource exchange among clonemates or metabolically interdependent strains (10–12). However, biofilm formation may also be triggered as a competitive or defensive response against other strains or species (13). In addition, the structured environment of biofilms creates gradients of nutrients that potentiate the competition for limiting resources, resulting in exploitative competition between cohabiting species (14).

Despite the increasing knowledge of the ecology (13, 15, 16), genetics (17–19), or physical mechanisms (20, 21) of biofilm development and the mechanisms that stabilize cooperation during biofilm formation (7, 9, 10, 22), we still know little about the long-term evolutionary dynamics within biofilm communities. It is unclear how social interactions shape biofilm evolution and how evolution in structured environments shift the balance between competition and mutualism. Long-term serial transfer experiments provide a key approach to fill this gap. Experimental evolution allows studying adaptation under controlled conditions and identification of the evolutionary forces and ecological processes that shape microbial cultures (23, 24). Today, the genomic changes of experimentally evolved bacteria can be easily explored

using next-generation sequencing methods (25) that allow understanding of the molecular basis of evolutionary adaptation.

Here, by reviewing a set of experimental evolution studies, we demonstrate that biofilms are both good models to study the origins of social interactions and to examine how these interactions are shaped in time and space. We focus on the form and strength of interactions between microbial species, ecotypes, or early differentiated lineages cohabiting structured environments of biofilms. Based on the existing literature, we describe how such interactions influence the evolution of microbial communities. Importantly, evolutionary changes in microbial communities may be driven by a set of abiotic factors (e.g., fluctuations in the environment) or biotic components other than microbes (e.g., plant, animal, and human host or symbiont), which are not discussed in the paper. The study of evolutionary dynamics within biofilms and the origin of microbial interactions are significant for several reasons (26). First, biotic interactions among neighbors generate major selective forces that drive the development of many important traits of microbes, such as antibiotic resistance (27). Second, understanding how biofilms evolve can aid in predicting of evolutionary outcomes. Third, tracking molecular evolution in biofilms helps to unravel new regulatory pathways related to biofilm formation, persistence, or dispersal. Here, we present how recent advances in experimental evolution of biofilm systems fulfill this potential.

LABORATORY EVOLUTION OF COOPERATION AND INTERFERENCE IN STRUCTURED ENVIRONMENTS

A pioneering long-term evolution experiment with *Escherichia coli* started in 1988 by Richard Lenski provided direct evidence

Accepted manuscript posted online 4 April 2016

Citation Martin M, Hölscher T, Dragoš A, Cooper VS, Kovács ÁT. 2016. Laboratory evolution of microbial interactions in bacterial biofilms. *J Bacteriol* 198:2564–2571. doi:10.1128/JB.01018-15.

Editor: G. A. O'Toole, Geisel School of Medicine at Dartmouth

Address correspondence to Ákos T. Kovács, akos-tibor.kovacs@uni-jena.de.

M.M., T.H., and A.D. contributed equally to this article.

Copyright © 2016, American Society for Microbiology. All Rights Reserved.

TABLE 1 Description of terms originating from ecology or evolutionary biology that are used in the text^a

Term	Definition	Reference(s)
Competition	Negative interaction among organisms resulting from overlapping resource requirements or chemical warfare, which leads to reduced fitness of the interacting individuals	
Antagonism (parasitism, predation)	Interaction between two organisms in which one profits at the expense of the other (in terms of fitness); the behavior is a derived strategy	
Synergistic interaction/facilitation	Interaction that leads to an increased fitness of the interacting individuals relative to monocultures	35, 66, 72
Productivity	Increase in biomass or cell numbers over time that reflects the efficiency with which a given organism converts energy into biomass	
Niche complementation	When species inhabit functionally complementary niches or environments resulting in reduced competition	71, 73
Generalist	An ecotype that can tolerate a broad range of conditions (e.g., food sources, temperature stress, etc.)	69
Specialist	An ecotype that can tolerate a rather narrow range of conditions (e.g., food sources, temperature stress, etc.)	69
Ecotype	Organism that pursues a certain ecological strategy and differs in some fitness-relevant traits from other organisms	68
Morphotype	Different colony morphology	35, 69
Spatial structure/structured conditions	Environment with low degree of mixing	
Biotic interactions	Any ecological interactions that occurs between two living organisms; in contrast, interactions are termed abiotic when they involve nonliving elements, e.g., sunlight, temp, pH, etc.	
Social interactions	Interaction/behaviors in which the performance of two individuals influences each other's fitness positively or negatively; here, the definition of social interactions refers to microbes	74
Sociality	The ability and extent of a group or an individual to engage in social interactions	
Sociomicrobiology	Research field in which social interactions of microorganisms are investigated	
Cooperation	Costly behavior of one individual that increases the fitness of another individual and which has evolved for this purpose	74, 75
Public goods	Secreted compounds which are freely available for each member of the population, i.e., "public." These substances benefit the population or community yet do not have to be costly to produce	74

^a The definitions explain the context of their usage in the text.

that microbes can be evolved in the lab and their phenotypic and genotypic changes can be tracked over time (28). Lenski's experiment is still in progress, reaching 64,000 generations in January 2016, and many similar studies have been performed by other researchers on different microbial species (not only bacteria but also yeasts, phages, or protists) covering basic scientific questions (29, 30) or even in directly applicative projects (31). While planktonic cultures offer a simple setup to study the evolution of bacteria (23, 28, 31, 32), several studies have shown that the selective pressures in unstructured conditions differ from those in biofilms (33–36). For example, homogeneous, well-mixed environments may select against "social" genotypes that secrete costly metabolites, so-called "public goods," and rather favor fast-reproducing selfish individuals (37). This is not surprising since mixing decreases the likelihood for such metabolites to be retained in the vicinity of the secretor and does not guarantee that the secretions will benefit its closest relatives or offspring cells (38), one of the core preconditions required for the evolution of sociality (39). Recent reports have shown that the situation differs dramatically in biofilms, where the secretors have the primary access to the substances produced, allowing the public good producers to easily outnumber the nonproducers (12, 22, 40, 41). It is therefore expected that structured environments would select for "social" adaptation strategies of microbes.

Experimental evolution studies provide evidence for the prediction that evolution in structured environments can favor ad-

aptations to sociality (34, 35, 42–44). For example, Koch and colleagues demonstrated how the emergence of a strain with an increased level of cell-cell communication can eventually lead to evolution of antibiotic resistance to vancomycin, a last-resort antibiotic (27). Briefly, methicillin-resistant *Staphylococcus aureus* grown in a colony biofilm diversifies sequentially into mutants in which the first clones (named W) are selected due to increased cell-cell signaling, which triggered more surfactin and toxic bacteriocin secretion. Next, bacteriocin-resistant mutants that are also resistant to intermediate levels of vancomycin evolved in response to this new environment (27). Although overall diversification of *S. aureus* was driven by competition, the success of the W variant was due to an increased level of cooperation via the Agr quorum-sensing system that in addition triggered increased levels of bacteriocin secretion (27). This dynamic of evolved resistance depends on the structured environment that promotes both efficient cell-cell communication and intimate interactions between the strains. Bacteriocin producers trigger the appearance of a resistant variant in their vicinity due to local increased exposure to the toxic compound. Another study demonstrated that spontaneous mutants of *Pseudomonas fluorescens* with increased polysaccharide secretions (i.e., mucoid isolates) are able to use these secretions to position themselves on the oxygen-rich surface of the colony and dominate the population (45). The emergence of such mucoid isolates is not observed when the spatial structure of the colony is manually disturbed during development. Therefore,

spatial assortment not only promotes stability of cooperation in biofilms (22, 40) but also supports the evolution of novel public good producers that results in increased biofilm matrix production (34, 45). Spatial structure can also promote diversification into strong and weak secretors as shown in *Pseudomonas aeruginosa* colonies, where repetitive reinoculation of *P. aeruginosa* from the edge or the middle of colony biofilms resulted in clones with reduced or diversified matrix production levels, respectively (34). Structured environments can also support stable coexistence of cooperative and noncooperative strains, thereby promoting diversity within species (46).

In fact, environmental spatial structure is probably the major factor promoting diversity in the microbial world (47). Although spatial structure limits the number of possible interactions with nonrelatives and therefore promotes the evolution of public good production, it also facilitates intimate local interactions between neighboring species. Based on cocultivation studies of various natural isolates, interaction with nonrelatives seems to be dominated by competition (48, 49). Coevolution experiments document how such competition between two closely interacting species can progress into more exploitative interaction (50, 51). For example, an experimental community of *Pseudomonas putida* and *Acinetobacter* sp. was evolved and shown to produce an intimate and specialized association that results in more stable and more productive community than the ancestors. In the ancestral community, *P. putida* was dependent on *Acinetobacter* for benzoate that manifested in an exploitative interaction between the two strains (50). During coevolution, *P. putida* increased its stickiness due to mutations in a gene related to lipopolysaccharide synthesis. This enabled a more intimate relationship between the two species and more efficient exploitation of *Acinetobacter* by *P. putida*. Although coevolution resulted in a more exploitative interaction that was detrimental for one of the partners, the overall productivity of the community was doubled (50).

A similar pattern was recently observed by Kim and colleagues (52) where clonal populations of *P. fluorescens* rapidly diversified into morphotypes M (mucoid) and D (dry and wrinkly). The two morphotypes spread collectively faster than either of them in monoculture, which the authors describe as “division of labor.” Microscopy analyses revealed that D dominates the spreading bulk of the colony sitting at the top of M. The authors proposed that the role of M is to reduce the tension of the solid surface, while D aids M by pushing it outward. Although D constitutes only 90% of the spreading colony and its interaction with M is exploitative, the performance of the whole community is improved as in the case of *P. putida* and *Acinetobacter*. Importantly, in contrast to the preassembled community of *P. putida* and *Acinetobacter*, the exploitative (and at the same time group beneficial) relationship between D and M evolved *de novo* from a monoclonal ancestor (52). In another study, new colony structures observed on agar medium were found to be indicative of altered biofilm formation or adaptation to a particular biofilm niche requirement (53). Studies on *P. fluorescens* microcosms revealed that certain morphotypes (e.g., the wrinkly morphotype) can be selected only under static conditions but not in shaking cultures (36). Similarly, the diversification of the Gram-positive *Bacillus subtilis* is also highly dependent on the condition used in experimental evolution (33). Namely, colony types with intermediate biofilm robustness dominated under static conditions, whereas those of marginal biofilm robustness (very high or very low) were much less

common than shaking cultures (33). This result again highlights the impact of spatial structure on the outcome of laboratory evolution experiments.

EXPERIMENTALLY EVOLVED BIOFILMS OF *P. FLUORESCENS* AND *BURKHOLDERIA CENOCEPACIA*: MODELS OF BIOFILM DIVERSIFICATION

Below, we describe in greater detail studies of the laboratory evolution of *P. fluorescens* and *B. cenocepacia* in spatially structured biofilm environments, in which a mixture of ecological generalists and specialists evolve and coexist. The first project began in 1998 when Rainey and Travisano reported rapid diversification of *P. fluorescens* into 3 different colony types, preferentially inhabiting different niches of static liquid medium (surface, bottom, and the medium) (36). The story of *B. cenocepacia* began 13 years later, when the field of experimental evolution was already more advanced (e.g., the Lenski’s evolution experiment had exceeded 50,000 generations). In 2011, Poltak and Cooper tracked the evolution of a *B. cenocepacia* community in a carefully designed microcosm equipped with floating beads that can be repeatedly colonized and decolonized by the evolving community. These two projects resulted in more than 30 research papers that vastly improved our understanding of ecological and molecular dynamics of adaptation in biofilms, making the two pioneering studies (35, 36) milestones in the field of experimental evolution. In the following sections, we examine each experimental design and findings separately, focusing mainly on the social interactions within the evolving microcosms.

EVOLUTION OF COOPERATION AND EXPLOITATION WITHIN AND BETWEEN ECOTYPES IN *P. FLUORESCENS* STATIC MICROCOSM

When *P. fluorescens* natural isolate SBW25 is incubated in unshaken glass vials (“static microcosms”) in nutrient-rich medium, this strain rapidly diversifies into three main phenotypically and genotypically different variants (36). Each of these variants is specialized for a certain niche in the spatially structured microcosm and forms phenotypically distinct colonies when grown on agar plates (Fig. 1A). The ancestral smooth morphotype (S) grows predominantly in the liquid column of the microcosm, whereas the fuzzy spreader (F) forms aggregates at the bottom of the tube. The third colony variant is called the wrinkly spreader (W) and occupies the air-liquid interface where it forms a robust pellicle or biofilm (36, 44).

The diversification of the ancestral strain is greatly influenced by the oxygen gradient that is created by the ancestor itself shortly after inoculation of the microcosm (54). Close to the air-liquid interface, the oxygen level is high but decreases rapidly with increasing depth. This spatially heterogeneous environment therefore selects for specialist mutants that prevail under different levels of oxygen availability (54). Without such spatial heterogeneity, no morphologically different variants evolved, and this heterogeneous environment was also essential for maintenance of diversity (36). The W variant in particular is very successful in the spatially structured microcosm since it rapidly accounts for 30 to 50% of the whole population (36, 54) and achieves higher fitness than the S morphotype (53). This advantage and the rise of the W variant depends on its ability to access the elevated oxygen levels in the upper zone of the microcosm by forming a floating pellicle, while other variants grow slower in low-oxygen conditions (54).

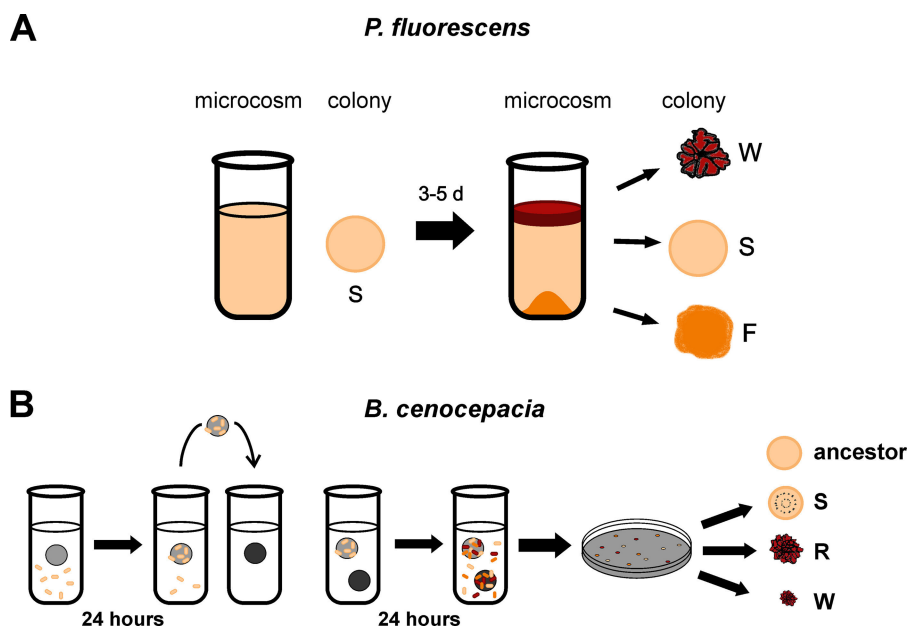


FIG 1 Experimental setup of biofilm evolution in the *P. fluorescens* microcosm (A) and the *B. cenocepacia* bead selection method (B). Biofilm populations in both setups reveal successive adaptive diversification into three ecotypes, namely, smooth or studded (S), fuzzy (F) or ruffled spreader (R), and wrinkly spreader (W). Note that the evolved smooth variant of *B. cenocepacia* is distinct from the ancestor exhibiting enhanced biofilm formation.

To form biofilms at the air-liquid interface, W mutants adapt by producing more cellulose polymers (53) that constitute the biofilm matrix and provide the robustness and structure necessary for a floating mat. It is important to note that in producing this cellulose pellicle, W mutants inherently become more cooperative by producing a public good, but similarly to other biofilm-based cooperative traits (22, 55), it is costly for the individuals to produce (53). Intriguingly, Rainey and Rainey (43) showed that non-cooperators that were evolved in the presence of cooperators could invade biofilms formed by cooperating cells. These noncooperators showed an S-like morphology with no aggregation properties and their invasion caused biofilm collapse. Brockhurst et al. (42) also showed that the frequency of cooperators was higher when more resources were provided for the microcosm since relatively less energy was invested toward public good production. However, even under such conditions, competition might occur within the biofilm among different W variants.

Most studies addressing microbial cooperation describe non-cooperators as “cheaters” or “free-loaders” and focus solely on their social exploitation. Yet, a study of Hammerschmidt et al. (56) used *P. fluorescens* to show that noncooperating cells carrying the S phenotype can function as colonists of new habitats. They reported that although S cells cause premature collapse of the biofilm mat formed by the W, they can also found a new microcosm where they diversify again and form W biofilms. Therefore, the relationship between W and S resembles the one between a vegetative cell and a spore, where only the latter can survive harsh conditions and give rise to new population, often at the cost of vegetative cells (57). The noncooperating S cells, therefore, could serve as new founders (germ line), allowing the reestablishment of the biofilm collective in another potential environment. This simple life cycle facilitated the maintenance of cooperative collectives. In addition, rapid switching between phenotypes (W and S variants) can be also interpreted as a bet-hedging mechanism that

benefits simple organisms, like bacteria in fluctuating environments (58).

Genome sequencing of the *P. fluorescens* W variant revealed mutations in the diguanylate cyclases (DGCs) WspR, AwsR, and MwsR that catalyze the synthesis of cyclic diguanylate monophosphate (c-di-GMP) from GTP (59, 60). Initially, the impact of the *wsp* operon was understood only in the evolution of the W variant (53, 59, 61), while the influences of mutations in *aws* and *mws* genes were revealed only after additional evolutionary experiments (60). Specifically, when the static microcosm of *P. fluorescens* was allowed to adapt in a *wsp*-deficient background (using $\Delta wspABCDEFR$ as the ancestor), the *aws*-dependent circuit was discovered, resulting in a similar W variant. The third alternative circuit (*mws*), leading to the evolution of W, was discovered after evolution of *P. fluorescens* that carried both $\Delta wspABCDEFR$ and $\Delta awsXRO$ alleles (60). These mutations in all three loci are mainly responsible for the increased c-di-GMP level that manifests in elevated cellulose production by the W variant (60, 62). Specifically, increased c-di-GMP is responsible for the activation of a membrane-bound enzyme complex responsible for cellulose synthesis that is encoded by the *wss* operon (53).

Initially, a screen of the W variant transposon library for loss of the wrinkly colony morphology supported the fact that the genes of this operon (*wssA-wssJ* and *wspR*) are crucial for the W variant (53). The operon encodes the DGC WspR and several proteins exhibiting similarity to known cellulose biosynthesis components and chemotaxis systems (53). Mutations in two genes of this operon, *wspE* and *wspF*, were also shown to be responsible for WS variant appearance. WspE represents a histidine kinase that activates WspR by phosphorylation, suggesting that certain mutations in WspE might lead to WspR overactivation (44, 60). WspF is thought to be involved in modulation of WspR activity, indicating that a mutation in the *wspF* gene might have effects similar to those in WspE (61). Later analysis of *wsp*-independent circuits

revealed the role of the *aws* locus in W variant formation. The authors discovered deletions in *awsX*, a negative regulator of diguanylate cyclase AwsR. They proposed that this new W variant resulted from overproduction of the acetylated cellulose through the *wss* pathway due to lack of AwsR regulation and increased synthesis of c-di-GMP (60). Another *wsp*- and *aws*-independent circuit resulting in the W phenotype was also related to increased activity of another diguanylate cyclase MwsR, which, in contrast to AwsR, was not caused by mutations in an extragenic negative regulator but by mutations in the *mwsR* gene itself (60). These experiments demonstrate that several pathways can lead to increased production of c-di-GMP and therefore elevated expression of the *wss* cellulose operon in certain members of the population that in turn increases overall fitness.

LONG-TERM EXPERIMENTAL EVOLUTION OF A COMPLETE BIOFILM LIFE CYCLE USING *B. CENOCEPACIA*

Evolution during the full life cycle of a biofilm, from attachment and maturation to dispersal, can be experimentally studied using a simple bead selection method (Fig. 1B) (35). Here, bacteria growing in a test tube must attach to a plastic bead to be transferred to a new tube with fresh medium each day. The new tube also contains a new bead; thus, a new biofilm must form on an uninhabited surface on a daily basis. Because tubes are incubated on a roller drum, established biofilms are continually subjected to shear forces that select for attachment, planktonic growth, and reattachment. Importantly, this cycle enables easy archiving of the evolving populations as well as precise reconstitution to study the ecological and evolutionary forces prevailing at that time (35), which renders the model especially suitable for long-term experimental evolution (LTEE). Additionally, LTEE can be paired with contemporary sequencing methods to identify the mutational mechanisms, enabling adaptation in the laboratory (25, 63, 64).

Adaptation under these conditions with minimal galactose growth medium has been studied for the opportunistic respiratory pathogen *B. cenocepacia*, but such an approach can be also applied for microbes in natural settings or during host infections (65). However, modifications of the bead-based experimental evolution setup, such as changes in the number of beads or in nutrient concentration, may allow the detailed study of social interactions (35), the degree of facilitation or competition among cells in the biofilm (66), and the predicted colonization and dispersal-dependent fitness (67).

With this novel approach, the biofilm population of *B. cenocepacia* revealed sequential adaptive diversification into three classes of heritable colony morphologies distinctive from that of the ancestor (35), similar to the diversification of *P. fluorescens* during biofilm establishment. The *B. cenocepacia* morphotypes were classified as studded or smooth (S), ruffled spreader (R), and wrinkly spreader (W) (35). Morphologically, the *B. cenocepacia* variants are similar to the experimentally evolved *P. fluorescens* colony types (36). As in *P. fluorescens*, these different *B. cenocepacia* morphotypes inhabit different niches in the test tube (35) and were therefore characterized as separate ecotypes (35, 68). The W variant, possessing strong adhesion to the bead and tube walls in monoculture, is an early colonist of the plastic bead. As the R frequency increases, the W variant declines in frequency. S cells, on the other hand, escalate steadily throughout the growth phase, suggesting that the early evolved S variant adheres to the later-evolved R and W variants, which are better surface colonizers. As S variants re-

main the dominant type in the community, their proportion decreases slightly prior to transfer as the frequencies of R and W variants escalate from their low initial occurrence (35).

Intriguingly, the three coevolved ecotypes in such biofilm community reach higher productivity than each one of them in monoculture or their expected productivity in the mix. This increased productivity is attributed to the prevailing facilitative effect of niche complementarity (35, 66), in which the ecotypes inhabit different spatial regions of the biofilm. Further synergy among these morphotypes was revealed in a cross-feeding assay demonstrating that the specialists (R and W variants) profit from metabolic by-products of other communal members but not from their own metabolites. This suggests the evolution of a resilient symbiotic food web wherein the generalist S variant achieves high biomass by superior growth but attaches preferentially to the biofilm produced by R and W cells, which in turn profit from secreted metabolites (35). Nonetheless, only the late S variant increased its productivity in the mix culture relative to that in its monoculture, while total productivities of R and W in the mix were reduced compared to those of their monocultures, although the per capita production of R and W increased (66). This indicates that although the competition in the late community was lessened both by facilitative effects (66) and via cross-feeding between R and W (35), it still affected the system.

The sequencing of evolved *B. cenocepacia* clones and populations revealed that the observed colony morphologies are the result of different mutations (69) that affect the regulation of the “stick-or-swim” decision (66, 67, 69). Surprisingly, biofilm specialists (R and W variants) recurrently evolved from generalist types (S variant) by adaptive mutations in the *wsp* locus homologous to the one first described in *P. fluorescens* (69). Sequencing of both population samples and clones revealed complex dynamics driving the evolution of the three ecotypes. Initially, cells that best attached to the plastic beads achieved high frequencies by way of mutations in genes related to the biofilm lifestyle regulator c-di-GMP. These mutations produced distinct colony morphologies and excluded the ancestor genotype. The independent occurrence of these adaptive changes in parallel populations suggests that changes in c-di-GMP production are sufficient for the adaptive niche partitioning because they generate ecotypes with different tendencies to attach or disperse (69). Subsequent mutations related to central metabolism and polysaccharide biosynthesis influenced the proliferation of the S variant and enhanced its competition against earlier mutants. Surprisingly, new *wsp* mutations evolving from S haplotypes gave rise to new R and W mutants, which invaded these more specialized biofilm niches. Interestingly, competition among ecotypes for limiting iron led to the remodelling of the entire community, as both S and W lineages independently acquired mutations in the promoter sequence of bacterioferritin and excluded all cells lacking either of these mutations (69).

A focused analysis on mutations evolved in replicate population B1 (one out of six independently evolving biofilm populations) determined the molecular basis of ecological differentiation of S, R, and W (69). In addition to the *wsp* mutations discussed above, at least eight independent mutations in the gene *yciR* (also known as *rpfR*) were discovered (69, 70). YciR harbors a PAS sensor domain that binds the quorum-sensing molecule *cis*-2-dodecenoic acid (BDSF) (70) as well as a diguanylate cyclase (GGDEF) and a phosphodiesterase (EAL) domain. YciR has been found in many bacterial species to function as a phosphodiesterase

that is responsible for degradation of c-di-GMP and the attenuation of biofilm development (66). A single mutation in *yciR* carried by the R ecotype resulted in its increased biofilm formation. Moreover, ecotype S carried a deletion of *yciR* along with 94 other neighboring genes (69). The different phenotypes of the *yciR* mutants imply that altering different domains can produce different ecological strategies that coordinate quorum sensing of BDSF with c-di-GMP metabolism and hence the stick-or-swim cell decision.

Meanwhile, analogous to the *P. fluorescens* system, the genetic causes of the wrinkly phenotype in *B. cenocepacia* are single missense mutations in either *wspA* or *wspE*, the products of which are involved in the biofilm signal transduction cascade related to c-di-GMP synthesis (71). Although the cognate diguanylate cyclase or phosphodiesterase in this bacterium is not yet known, subsequent evolution studies using W mutants as ancestors revealed a new two-component regulator (Bcen2424_1436) that could relate to the c-di-GMP response and explain this phenotype more generally. Further, growth of W mutants in planktonic culture generated strong selection to regain planktonic fitness, often favoring loss-of-function mutations in Wsp (67). Such mutations could limit subsequent evolution of the wrinkly biofilm in fluctuating environments (67).

CONCLUDING REMARKS

These laboratory experimental systems used spatially structured environments to demonstrate how microbial communities can evolve from clonal ancestors and generate complex ecological interactions. In both experimental setups (*P. fluorescens* static microcosms and *B. cenocepacia* biofilms on suspended beads), the spatially heterogeneous environment facilitated the evolution of distinct ecotypes. These systems allow for the study of adaptive diversification in real time and provide direct insights into evolutionary processes that used to be limited to theoretical models, like the positive feedback between niche construction and natural selection. Intriguingly, the diversified communities can be shaped by the range of social and ecological interactions, including antagonism (i.e., social exploitation of the W by S variants observed in *P. fluorescens*), niche complementation, or even synergistic interactions via cross-feeding as observed in *B. cenocepacia*. Finally, the interactions that arose between the ecotypes of the evolved community became a new factor determining biofilm productivity that could not be observed with an isogenic ancestor community. Importantly, parallel evolution experiments performed under unstructured conditions (planktonic cultures) in both species did not show diversification patterns similar to those of the structured environments in the biofilms (Fig. 2) (35, 36). In addition to the basic understanding of evolutionary processes, these studies provide insight into how microbes adapt at the molecular level. In both systems, wrinkly phenotypes emerged from mutations related to *wsp* genes, two-component transcriptional regulators, and polysaccharide production-associated genes. Understanding how opportunistic pathogens (e.g., *Burkholderia*) or beneficial root colonizers (e.g., *P. fluorescens*) undergo adaptive diversification in biofilms could illuminate the ecological forces that drive adaptation during chronic infections or plant biocontrol.

In the future, an experimental evolution approach using constructed microbial interactions might also provide a better understanding of the forces that govern assembly of natural mixed-species biofilms as well as how best to engineer stable, synthetic microbial ecosystems. More broadly, laboratory evolution of bio-

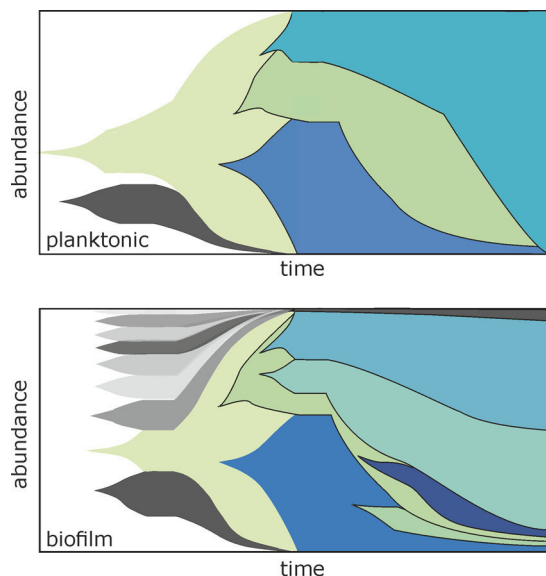


FIG 2 The population genetic dynamics of experimentally evolved bacterial populations differs between planktonic and biofilm cultures. Planktonic adaptation is frequently explained by few beneficial mutations that evolve sequentially on a haplotype that fixes and purges diversity. In contrast, biofilm adaptation involves the rise of multiple contending mutations in a spatially structured environment that preserves genetic diversity. This structure can also facilitate the evolution of ecological interactions that maintain diversity.

film populations can be an important asset in our understanding of ecoevolutionary dynamics within more complex communities of multicellular organisms that are less amenable to manipulation.

ACKNOWLEDGMENT

We thank Christian Kost for his valuable comments on the ecoevolutionary terms.

FUNDING INFORMATION

This work, including the efforts of Ákos T. Kovács, was funded by Marie Curie Career Integration Grant (PheHetBacBiofilm). This work, including the efforts of Vaughn S. Cooper, was funded by National Aeronautics and Space Administration (NASA) Astrobiology Institute (CAN-7 NNA15BB04A). This work, including the efforts of Theresa Hölscher, was funded by International Max Planck Research School. This work, including the efforts of Vaughn S. Cooper, was funded by HHS | National Institutes of Health (NIH) (R01GM110444). This work, including the efforts of Ákos T. Kovács, was funded by Deutsche Forschungsgemeinschaft (DFG) (KO4741/3-1). This work, including the efforts of Anna Dragoš, was funded by Alexander von Humboldt-Stiftung (Humboldt Foundation) (POL 1158809 STP-2).

This work, including the efforts of Ákos T. Kovács and Marivic Martin, was funded by Deutsche Forschungsgemeinschaft (DFG) (KO4741/2-1) within the priority program SPP1617. The funders had no role in study design, data collection and interpretation, or the decision to submit the work for publication.

REFERENCES

1. Stewart PS, Franklin MJ. 2008. Physiological heterogeneity in biofilms. *Nat Rev Microbiol* 6:199–210. <http://dx.doi.org/10.1038/nrmicro1838>.
2. Kolter R, Greenberg EP. 2006. Microbial sciences: the superficial life of microbes. *Nature* 441:300–302. <http://dx.doi.org/10.1038/441300a>.
3. Mikkelsen H, Duck Z, Lilley KS, Welch M. 2007. Interrelationships between colonies, biofilms, and planktonic cells of *Pseudomonas aeruginosa*. *J Bacteriol* 189:2411–2416. <http://dx.doi.org/10.1128/JB.01687-06>.

4. Davies D. 2003. Understanding biofilm resistance to antibacterial agents. *Nat Rev Drug Discov* 2:114–122. <http://dx.doi.org/10.1038/nrd1008>.
5. McDougald D, Rice SA, Barraud N, Steinberg PD, Kjelleberg S. 2012. Should we stay or should we go: mechanisms and ecological consequences for biofilm dispersal. *Nat Rev Microbiol* 10:39–50. <http://dx.doi.org/10.1038/nrmicro2695>.
6. Parsek MR, Greenberg EP. 2005. Sociomicrobiology: the connections between quorum sensing and biofilms. *Trends Microbiol* 13:27–33. <http://dx.doi.org/10.1016/j.tim.2004.11.007>.
7. Boyle KE, Heilmann S, van Ditmarsch D, Xavier JB. 2013. Exploiting social evolution in biofilms. *Curr Opin Microbiol* 16:207–212. <http://dx.doi.org/10.1016/j.mib.2013.01.003>.
8. Nadell CD, Xavier JB, Foster KR. 2009. The sociobiology of biofilms. *FEMS Microbiol Rev* 33:206–224. <http://dx.doi.org/10.1111/j.1574-6976.2008.00150.x>.
9. Xavier JB, Foster KR. 2007. Cooperation and conflict in microbial biofilms. *Proc Natl Acad Sci U S A* 104:876–881. <http://dx.doi.org/10.1073/pnas.0607651104>.
10. Kovács ÁT. 2014. Impact of spatial distribution on the development of mutualism in microbes. *Front Microbiol* 5:649. <http://dx.doi.org/10.3389/fmicb.2014.00649>.
11. Mitri S, Xavier JB, Foster KR. 2011. Social evolution in multispecies biofilms. *Proc Natl Acad Sci U S A* 108(Suppl 2):10839–10846. <http://dx.doi.org/10.1073/pnas.1100292108>.
12. Pande S, Kaftan F, Lang S, Svatos A, Germerodt S, Kost C. 2016. Privatization of cooperative benefits stabilizes mutualistic cross-feeding interactions in spatially structured environments. *ISME J* 10:1413–1423. <http://dx.doi.org/10.1038/ismej.2015.212>.
13. Oliveira NM, Martinez-García E, Xavier J, Durham WM, Kolter R, Kim W, Foster KR. 2015. Biofilm formation as a response to ecological competition. *PLoS Biol* 13:e1002191. <http://dx.doi.org/10.1371/journal.pbio.1002191>.
14. Yamamoto K, Haruta S, Kato S, Ishii M, Igarashi Y. 2010. Determinative factors of competitive advantage between aerobic bacteria for niches at the air-liquid interface. *Microbes Environ* 25:317–320. <http://dx.doi.org/10.1264/jisme2.ME10147>.
15. Davey ME, O'Toole GA. 2000. Microbial biofilms: from ecology to molecular genetics. *Microbiol Mol Biol Rev* 64:847–867. <http://dx.doi.org/10.1128/MMBR.64.4.847-867.2000>.
16. Donlan RM. 2002. Biofilms: microbial life on surfaces. *Emerg Infect Dis* 8:881–890. <http://dx.doi.org/10.3201/eid0809.020063>.
17. Fazli M, Almlad H, Rybtke ML, Givskov M, Eberl L, Tolker-Nielsen T. 2014. Regulation of biofilm formation in *Pseudomonas* and *Burkholderia* species. *Environ Microbiol* 16:1961–1981. <http://dx.doi.org/10.1111/1462-2920.12448>.
18. Teschler JK, Zamorano-Sanchez D, Utada AS, Warner CJ, Wong GC, Lington RG, Yildiz FH. 2015. Living in the matrix: assembly and control of *Vibrio cholerae* biofilms. *Nat Rev Microbiol* 13:255–268. <http://dx.doi.org/10.1038/nrmicro3433>.
19. Vlamakis H, Chai Y, Beauregard P, Losick R, Kolter R. 2013. Sticking together: building a biofilm the *Bacillus subtilis* way. *Nat Rev Microbiol* 11:157–168. <http://dx.doi.org/10.1038/nrmicro2960>.
20. Asally M, Kittisopikul M, Rue P, Du Y, Hu Z, Cagatay T, Robinson AB, Lu H, Garcia-Ojalvo J, Suel GM. 2012. Localized cell death focuses mechanical forces during 3D patterning in a biofilm. *Proc Natl Acad Sci U S A* 109:18891–18896. <http://dx.doi.org/10.1073/pnas.1212429109>.
21. Stewart PS. 2014. Biophysics of biofilm infection. *Pathog Dis* 70:212–218. <http://dx.doi.org/10.1111/2049-632X.12118>.
22. van Gestel J, Weissing FJ, Kuipers OP, Kovács ÁT. 2014. Density of founder cells affects spatial pattern formation and cooperation in *Bacillus subtilis* biofilms. *ISME J* 8:2069–2079. <http://dx.doi.org/10.1038/ismej.2014.52>.
23. Barrick JE, Lenski RE. 2013. Genome dynamics during experimental evolution. *Nat Rev Genet* 14:827–839. <http://dx.doi.org/10.1038/nrg3564>.
24. Elena SF, Lenski RE. 2003. Evolution experiments with microorganisms: the dynamics and genetic bases of adaptation. *Nat Rev Genet* 4:457–469. <http://dx.doi.org/10.1038/nrg1088>.
25. Brockhurst MA, Colegrave N, Rozen DE. 2011. Next-generation sequencing as a tool to study microbial evolution. *Mol Ecol* 20:972–980. <http://dx.doi.org/10.1111/j.1365-294X.2010.04835.x>.
26. Steenackers HP, Parijs I, Foster KR, Vanderleyden J. 2016. Experimental evolution in biofilm populations. *FEMS Microbiol Rev* 40:373–397. <http://dx.doi.org/10.1093/femsre/fuw002>.
27. Koch G, Yepes A, Forstner KU, Wermser C, Stengel ST, Modamio J, Ohlsen K, Foster KR, Lopez D. 2014. Evolution of resistance to a last-resort antibiotic in *Staphylococcus aureus* via bacterial competition. *Cell* 158:1060–1071. <http://dx.doi.org/10.1016/j.cell.2014.06.046>.
28. Lenski RE, Rose MR, Simpson SC, Tadler SC. 1991. Long-term experimental evolution in *Escherichia coli*. I. Adaptation and divergence during 2,000 generations. *Am Nat* 138:1315–1341.
29. Meyer JR, Dobias DT, Weitz JS, Barrick JE, Quick RT, Lenski RE. 2012. Repeatability and contingency in the evolution of a key innovation in phage lambda. *Science* 335:428–432. <http://dx.doi.org/10.1126/science.1214449>.
30. terHorst CP. 2011. Experimental evolution of protozoan traits in response to interspecific competition. *J Evol Biol* 24:36–46. <http://dx.doi.org/10.1111/j.1420-9101.2010.02140.x>.
31. Blaby IK, Lyons BJ, Wroclawska-Hughes E, Phillips GC, Pyle TP, Chamberlin SG, Benner SA, Lyons TJ, Crecy-Lagard V, Crecy E. 2012. Experimental evolution of a facultative thermophile from a mesophilic ancestor. *Appl Environ Microbiol* 78:144–155. <http://dx.doi.org/10.1128/AEM.05773-11>.
32. Barrick JE, Yu DS, Yoon SH, Jeong H, Oh TK, Schneider D, Lenski RE, Kim JF. 2009. Genome evolution and adaptation in a long-term experiment with *Escherichia coli*. *Nature* 461:1243–1247. <http://dx.doi.org/10.1038/nature08480>.
33. Leiman SA, Arboleda LC, Spina JS, McLoon AL. 2014. SinR is a mutational target for fine-tuning biofilm formation in laboratory-evolved strains of *Bacillus subtilis*. *BMC Microbiol* 14:301. <http://dx.doi.org/10.1186/s12866-014-0301-8>.
34. Madsen JS, Lin YC, Squyres GR, Price-Whelan A, de Santiago Torio A, Song A, Cornell WC, Sorensen SJ, Xavier JB, Dietrich LE. 2015. Facultative control of matrix production optimizes competitive fitness in *Pseudomonas aeruginosa* PA14 biofilm models. *Appl Environ Microbiol* 81:8414–8426. <http://dx.doi.org/10.1128/AEM.02628-15>.
35. Paltak SR, Cooper VS. 2011. Ecological succession in long-term experimentally evolved biofilms produces synergistic communities. *ISME J* 5:369–378. <http://dx.doi.org/10.1038/ismej.2010.136>.
36. Rainey PB, Travisano M. 1998. Adaptive radiation in a heterogeneous environment. *Nature* 394:69–72. <http://dx.doi.org/10.1038/27900>.
37. Ghoul M, Griffin AS, West SA. 2014. Toward an evolutionary definition of cheating. *Evolution* 68:318–331. <http://dx.doi.org/10.1111/evo.12266>.
38. Wakano JY, Nowak MA, Hauert C. 2009. Spatial dynamics of ecological public goods. *Proc Natl Acad Sci U S A* 106:7910–7914. <http://dx.doi.org/10.1073/pnas.0812644106>.
39. Hamilton WD. 1964. The genetical evolution of social behaviour. II. *J Theor Biol* 7:17–52. [http://dx.doi.org/10.1016/0022-5193\(64\)90039-6](http://dx.doi.org/10.1016/0022-5193(64)90039-6).
40. Drescher K, Nadell CD, Stone HA, Wingreen NS, Bassler BL. 2014. Solutions to the public goods dilemma in bacterial biofilms. *Curr Biol* 24:50–55. <http://dx.doi.org/10.1016/j.cub.2013.10.030>.
41. Van Dyken JD, Müller MJ, Mack KM, Desai MM. 2013. Spatial population expansion promotes the evolution of cooperation in an experimental Prisoner's Dilemma. *Curr Biol* 23:919–923. <http://dx.doi.org/10.1016/j.cub.2013.04.026>.
42. Brockhurst MA, Buckling A, Racey D, Gardner A. 2008. Resource supply and the evolution of public-goods cooperation in bacteria. *BMC Biol* 6:20. <http://dx.doi.org/10.1186/1741-7007-6-20>.
43. Rainey PB, Rainey K. 2003. Evolution of cooperation and conflict in experimental bacterial populations. *Nature* 425:72–74. <http://dx.doi.org/10.1038/nature01906>.
44. Spiers AJ. 2014. A mechanistic explanation linking adaptive mutation, niche change, and fitness advantage for the wrinkly spreader. *Int J Evol Biol* 2014:675432. <http://dx.doi.org/10.1155/2014/675432>.
45. Kim W, Racimo F, Schluter J, Levy SB, Foster KR. 2014. Importance of positioning for microbial evolution. *Proc Natl Acad Sci U S A* 111:E1639–E1647. <http://dx.doi.org/10.1073/pnas.1323632111>.
46. Hol FJ, Galajda P, Nagy K, Woolthuis RG, Dekker C, Keymer JE. 2013. Spatial structure facilitates cooperation in a social dilemma: empirical evidence from a bacterial community. *PLoS One* 8:e77042. <http://dx.doi.org/10.1371/journal.pone.0077042>.
47. Kassen R. 2002. The experimental evolution of specialists, generalists, and the maintenance of diversity. *J Evol Biol* 15:173–190. <http://dx.doi.org/10.1046/j.1420-9101.2002.00377.x>.
48. Abrudan MI, Smakman F, Grimbergen AJ, Westhoff S, Miller EL, van

- Wezel GP, Rozen DE. 2015. Socially mediated induction and suppression of antibiosis during bacterial coexistence. *Proc Natl Acad Sci U S A* 112: 11054–11059. <http://dx.doi.org/10.1073/pnas.1504076112>.
49. Foster KR, Bell T. 2012. Competition, not cooperation, dominates interactions among culturably microbial species. *Curr Biol* 22:1845–1850. <http://dx.doi.org/10.1016/j.cub.2012.08.005>.
 50. Hansen SK, Rainey PB, Haagensen JA, Molin S. 2007. Evolution of species interactions in a biofilm community. *Nature* 445:533–536. <http://dx.doi.org/10.1038/nature05514>.
 51. Kim HJ, Boedicker JQ, Choi JW, Ismagilov RF. 2008. Defined spatial structure stabilizes a synthetic multispecies bacterial community. *Proc Natl Acad Sci U S A* 105:18188–18193. <http://dx.doi.org/10.1073/pnas.0807935105>.
 52. Kim W, Levy SB, Foster KR. 2016. Rapid radiation in bacteria leads to a division of labour. *Nat Commun* 7:10508. <http://dx.doi.org/10.1038/ncomms10508>.
 53. Spiers AJ, Kahn SG, Bohannon J, Travisano M, Rainey PB. 2002. Adaptive divergence in experimental populations of *Pseudomonas fluorescens*. I. Genetic and phenotypic bases of wrinkly spreader fitness. *Genetics* 161:33–46.
 54. Koza A, Moshynets O, Otten W, Spiers AJ. 2011. Environmental modification and niche construction: developing O₂ gradients drive the evolution of the Wrinkly Spreader. *ISME J* 5:665–673. <http://dx.doi.org/10.1038/ismej.2010.156>.
 55. Nadell CD, Bassler BL. 2011. A fitness trade-off between local competition and dispersal in *Vibrio cholerae* biofilms. *Proc Natl Acad Sci U S A* 108:14181–14185. <http://dx.doi.org/10.1073/pnas.1111147108>.
 56. Hammerschmidt K, Rose CJ, Kerr B, Rainey PB. 2014. Life cycles, fitness decoupling and the evolution of multicellularity. *Nature* 515:75–79. <http://dx.doi.org/10.1038/nature13884>.
 57. Strassmann JE, Zhu Y, Queller DC. 2000. Altruism and social cheating in the social amoeba *Dictyostelium discoideum*. *Nature* 408:965–967. <http://dx.doi.org/10.1038/35050087>.
 58. Beaumont HJ, Gallie J, Kost C, Ferguson GC, Rainey PB. 2009. Experimental evolution of bet hedging. *Nature* 462:90–93. <http://dx.doi.org/10.1038/nature08504>.
 59. Goymier P, Kahn SG, Malone JG, Gehrig SM, Spiers AJ, Rainey PB. 2006. Adaptive divergence in experimental populations of *Pseudomonas fluorescens*. II. Role of the GGDEF regulator WspR in evolution and development of the wrinkly spreader phenotype. *Genetics* 173:515–526.
 60. McDonald MJ, Gehrig SM, Meintjes PL, Zhang XX, Rainey PB. 2009. Adaptive divergence in experimental populations of *Pseudomonas fluorescens*. IV. Genetic constraints guide evolutionary trajectories in a parallel adaptive radiation. *Genetics* 183:1041–1053.
 61. Bantinaki E, Kassen R, Knight CG, Robinson Z, Spiers AJ, Rainey PB. 2007. Adaptive divergence in experimental populations of *Pseudomonas fluorescens*. III. Mutational origins of wrinkly spreader diversity. *Genetics* 176:441–453.
 62. Malone JG, Williams R, Christen M, Jenal U, Spiers AJ, Rainey PB. 2007. The structure-function relationship of WspR, a *Pseudomonas fluorescens* response regulator with a GGDEF output domain. *Microbiology* 153:980–994. <http://dx.doi.org/10.1099/mic.0.2006/002824-0>.
 63. Adams J, Rosenzweig F. 2014. Experimental microbial evolution: history and conceptual underpinnings. *Genomics* 104:393–398. <http://dx.doi.org/10.1016/j.ygeno.2014.10.004>.
 64. Lang GI, Desai MM. 2014. The spectrum of adaptive mutations in experimental evolution. *Genomics* 104:412–416. <http://dx.doi.org/10.1016/j.ygeno.2014.09.011>.
 65. Andersen SB, Marvig RL, Molin S, Krogh Johansen H, Griffin AS. 2015. Long-term social dynamics drive loss of function in pathogenic bacteria. *Proc Natl Acad Sci U S A* 112:10756–10761. <http://dx.doi.org/10.1073/pnas.1508324112>.
 66. Ellis CN, Traverse CC, Mayo-Smith L, Buskirk SW, Cooper VS. 2015. Character displacement and the evolution of niche complementarity in a model biofilm community. *Evolution* 69:283–293. <http://dx.doi.org/10.1111/evo.12581>.
 67. O'Rourke D, FitzGerald CE, Traverse CC, Cooper VS. 2015. There and back again: consequences of biofilm specialization under selection for dispersal. *Front Genet* 6:18. <http://dx.doi.org/10.3389/fgene.2015.00018>.
 68. Cohan FM. 2001. Bacterial species and speciation. *Syst Biol* 50:513–524. <http://dx.doi.org/10.1080/10635150118398>.
 69. Traverse CC, Mayo-Smith LM, Poltak SR, Cooper VS. 2013. Tangled bank of experimentally evolved *Burkholderia* biofilms reflects selection during chronic infections. *Proc Natl Acad Sci U S A* 110:E250–259. <http://dx.doi.org/10.1073/pnas.1207025110>.
 70. Deng Y, Schmid N, Wang C, Wang J, Pessi G, Wu D, Lee J, Aguilar C, Ahrens CH, Chang C, Song H, Eberl L, Zhang LH. 2012. Cis-2-dodecenoic acid receptor RpfR links quorum-sensing signal perception with regulation of virulence through cyclic dimeric guanosine monophosphate turnover. *Proc Natl Acad Sci U S A* 109:15479–15484. <http://dx.doi.org/10.1073/pnas.1205037109>.
 71. Cooper VS, Staples RK, Traverse CC, Ellis CN. 2014. Parallel evolution of small colony variants in *Burkholderia cenocepacia* biofilms. *Genomics* 104:447–452. <http://dx.doi.org/10.1016/j.ygeno.2014.09.007>.
 72. Day T, Young KA. 2004. Competitive and facilitative evolutionary diversification. *Bioscience* 54:101–109. [http://dx.doi.org/10.1641/0006-3568\(2004\)054\[0101:CAFED\]2.0.CO;2](http://dx.doi.org/10.1641/0006-3568(2004)054[0101:CAFED]2.0.CO;2).
 73. Cordero OX, Polz MF. 2014. Explaining microbial genomic diversity in light of evolutionary ecology. *Nat Rev Microbiol* 12:263–273. <http://dx.doi.org/10.1038/nrmicro3218>.
 74. West SA, Griffin AS, Gardner A, Diggle SP. 2006. Social evolution theory for microorganisms. *Nat Rev Microbiol* 4:597–607. <http://dx.doi.org/10.1038/nrmicro1461>.
 75. Crespi BJ. 2001. The evolution of social behavior in microorganisms. *Trends Ecol Evol* 16:178–183. [http://dx.doi.org/10.1016/S0169-5347\(01\)02115-2](http://dx.doi.org/10.1016/S0169-5347(01)02115-2).

Chapter 5

De novo evolved interference competition promotes the spread of biofilm defectors

Published in: Nature Communications (2017)

ARTICLE

Received 5 Oct 2016 | Accepted 2 Mar 2017 | Published 2 May 2017

DOI: 10.1038/ncomms15127

OPEN

De novo evolved interference competition promotes the spread of biofilm defectors

Marivic Martin^{1,*}, Anna Dragoš^{1,*}, Theresa Hölscher^{1,*}, Gergely Maróti², Balázs Bálint³, Martin Westermann⁴
& Ákos T. Kovács¹

Biofilms are social entities where bacteria live in tightly packed agglomerations, surrounded by self-secreted exopolymers. Since production of exopolymers is costly and potentially exploitable by non-producers, mechanisms that prevent invasion of non-producing mutants are hypothesized. Here we study long-term dynamics and evolution in *Bacillus subtilis* biofilm populations consisting of wild-type (WT) matrix producers and mutant non-producers. We show that non-producers initially fail to incorporate into biofilms formed by the WT cells, resulting in 100-fold lower final frequency compared to the WT. However, this is modulated in a long-term scenario, as non-producers evolve the ability to better incorporate into biofilms, thereby slightly decreasing the productivity of the whole population. Detailed molecular analysis reveals that the unexpected shift in the initially stable biofilm is coupled with newly evolved phage-mediated interference competition. Our work therefore demonstrates how collective behaviour can be disrupted as a result of rapid adaptation through mobile genetic elements.

¹Terrestrial Biofilms Group, Institute of Microbiology, Friedrich Schiller University Jena, Jena 07743, Germany. ²Institute of Biochemistry, Biological Research Centre, Hungarian Academy of Sciences, Szeged 6726, Hungary. ³Seqomics Biotechnology Ltd., Mórahalom 6782, Hungary. ⁴Electron Microscopy Center, Jena University Hospital, Jena 07743, Germany. * These authors contributed equally to this work. Correspondence and requests for materials should be addressed to Á.T.K. (email: atkovacs@dtu.dk).

Biofilms, consisting of densely packed single- or multi-species communities embedded in self-produced slimy polymers, represent the most common microbial life form^{1–3}. Several recent studies have shown that the spatial structure of biofilms has a major impact on competition and cooperation among microbes and drives evolutionary changes within microbial communities (reviewed in refs 4,5). One particularly well-studied example used static cultures of *Pseudomonas fluorescens*, where an oxygen gradient led to the emergence of a new wrinkly (W) phenotype that secretes polysaccharides and forms a biofilm at the air–liquid interface^{6,7}. Interestingly, biofilms formed by W undergo a premature collapse caused by the incorporation of another phenotype into the biofilm without sharing the metabolic costs of exopolymer production⁸. This scenario of biofilm collapse reflects the phenomenon known as ‘tragedy of the commons’, which happens due to invasion by non-cooperators and depletion of an overly-exploited resource (in this case the exopolymer)⁹.

How often the ‘tragedy of the commons’ happens in other biofilm communities remains an open question in sociomicrobiology. Several studies suggest that exopolymer production cannot easily be exploited by non-producing defectors^{10,11}. Such robustness of cooperation-based biofilm formation is often explained by limited sharing of matrix components^{10–12}, the low costs of polymer production¹¹, the spatial assortment of cells in biofilms¹³ or even the intrinsic nature of certain matrix components that are exclusively shared between mother and daughter cells¹⁴. Although the key principles of certain non-producer exclusion mechanisms are becoming clear, competition experiments involving producers and non-producers are usually conducted over short timescales^{11–14}, leaving a window of opportunity for unexpected evolutionary scenarios¹⁵. Data from various bacterial models suggest that defectors can leave a fingerprint on the evolution of social strains and promote the evolution of novel cheating-suppression mechanisms¹⁶. These can be linked to lowering the cost of cooperation by the wild-type (WT) cells¹⁷. Selection can also work to the advantage of the non-producers, which can evolve better exploitation skills^{15,17}. In extreme cases, cooperators can be *de novo* selected from the population of cheats¹⁸. In general, long-term scenarios in socially heterogeneous populations of microbes are still very difficult to predict.

In this manuscript, we study the long-term social dynamics of co-cultures comprising matrix producer and non-producer strains using the widespread soil bacterium *Bacillus subtilis*. *B. subtilis* forms thick, robust structures at the air–liquid interface (pellicle) facilitated by two crucial secreted compounds: an exopolysaccharide, Eps (encoded by *epsA–O*), and a protein component, TasA (encoded by *tapA–sipW–tasA*). In a standing culture, driven by oxygen limitation, matrix-producing strains form pellicles¹⁹. Strains lacking either one or both matrix components cannot form robust biofilms at the air–liquid interface and they barely colonize the liquid surface²⁰. Moreover, strains producing only one of the components are able to complement each other and form a WT-like pellicle²⁰. This strongly suggests that both matrix components secreted by producers are freely shared with non-producers and could therefore be exploited by non-producing mutants.

Here we show that on a short timescale, *B. subtilis* matrix non-producers have a tremendous disadvantage in co-culture with the WT. We further demonstrate how unexpected adaptive events involving mobile genetic elements can shift the social dynamics in the population and reduce biofilm formation.

Results

Biofilm non-producers are outcompeted from mixed pellicles.

A positive result in a complementation assay of *B. subtilis* Δeps and $\Delta tasA$ biofilm mutants suggests that both key biofilm components, Eps and TasA, can be shared (Fig. 1a)²⁰. We therefore predicted that the double mutant $\Delta eps\text{--}\Delta tasA$, which cannot form a pellicle in monoculture²⁰, would still be able to incorporate into the pellicle when co-cultured with the WT. To test our hypothesis, we mixed WT and $\Delta eps\text{--}\Delta tasA$ strains in a 1:1 ratio and allowed the pellicle to form (see Methods). The final ratio of the WT to the $\Delta eps\text{--}\Delta tasA$ strain was assessed by two alternative methods: antibiotic marker based colony forming unit (c.f.u.) counts (Fig. 1a) and fluorescence microscopy (here, GFP and mKATE2 producing WT and $\Delta eps\text{--}\Delta tasA$ mutants were used, respectively, or we used the same strains with swapped fluorescent markers; Fig. 1b,c). Surprisingly both c.f.u. assay and microscopy indicated a dramatic advantage of the WT over

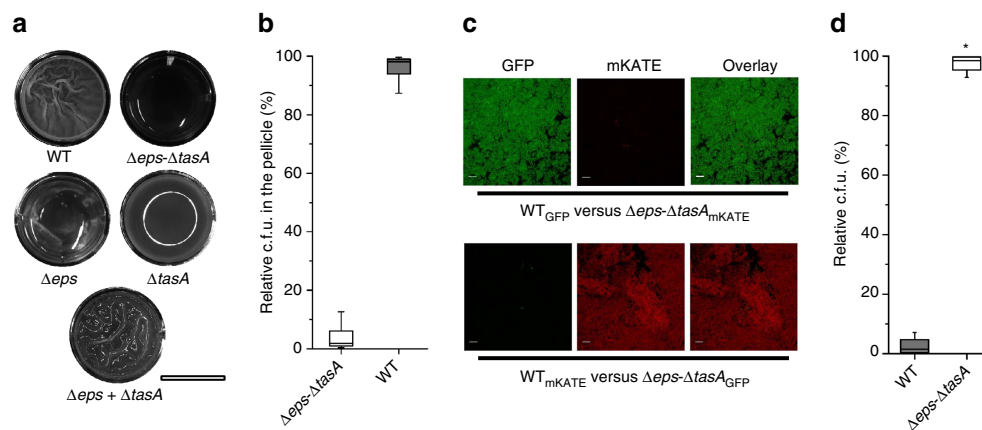


Figure 1 | Matrix non-producer strain does not incorporate into the wild-type pellicle. (a) Pellicle biofilms of wild-type (WT) *Bacillus subtilis* 168 and its mutant derivatives were recorded using an Axio Zoom microscope equipped with a black and white camera. Scale bar, 1 cm. The reflection of the light source can be observed in the $\Delta tasA$ culture. (b) Pellicle competition assay between $\Delta eps\text{--}\Delta tasA$ and WT ($n = 25$). (c) Confocal microscopy images of pellicle biofilm from culture initially consisting of a 1:1 ratio of WT and $\Delta eps\text{--}\Delta tasA$ (upper) and cells with swapped fluorescence protein labels (lower). Scale bars, 10 μm. (d) Planktonic culture competition assay between $\Delta eps\text{--}\Delta tasA$ and WT ($n = 25$). Boxes represent Q1–Q3, lines represent the median, and bars span from max to min. The experiments were independently repeated at least three times. * indicates that the relative c.f.u. is significantly higher than the relative c.f.u. of $\Delta eps\text{--}\Delta tasA$ ancestor in the pellicle (in panel b).

$\Delta eps-\Delta tasA$; the latter was almost completely outcompeted from the pellicle formed by the WT (Fig. 1a–c).

The incorporation success of $\Delta eps-\Delta tasA$ into the pellicle was positively dependent on its initial frequency (Pearson's correlation coefficient $r=0.74$; Supplementary Fig. 1A). Specifically, the mutant showed increased pellicle incorporation, up to $23 \pm 1.9\%$, which also correlated with decline in total c.f.u. of the pellicle, but only when its initial proportion was $>50\%$, while at initial frequencies $<50\%$, the pellicle incorporation ranged from 0.11 to 5% (Supplementary Fig. 1A).

To understand if the availability of nutrients influenced the ability of non-producers to incorporate into the pellicle, the competition assay was repeated using a medium in which the broth and other components were doubled ($4 \times$ SG, see Methods). It was observed that the $\Delta eps-\Delta tasA$ strain could incorporate better in richer medium (Supplementary Fig. 1B). Using $2 \times$ SG, the incorporation ability of the $\Delta eps-\Delta tasA$ strain was 2% (mean; $n=5$; s.d. = 1.37), while in $4 \times$ SG medium pellicle incorporation increased to 6.72% (mean; $n=5$; s.d. = 3.40). Importantly, the starting ratios in these competition assays were identical (46.72% $\Delta eps-\Delta tasA$; mean; $n=5$; s.d. = 14.4), therefore, the possibility of the initial frequency influencing these results could be excluded.

Finally, to ensure that the above result was caused by a mechanism that is specific to biofilm conditions and not simply caused by a growth defect of the $\Delta eps-\Delta tasA$ strain, WT versus $\Delta eps-\Delta tasA$ competition experiments were also performed in planktonic cultures where oxygen distribution is more homogeneous and no fitness benefits from biofilm formation are to be expected^{11,13,21}. In planktonic culture, $\Delta eps-\Delta tasA$ had a strong fitness advantage over the WT (Fig. 1d) that is likely due to the release of the mutant from the metabolic costs of Eps and TasA production¹³, as also indicated by its higher growth rate in planktonic culture conditions (Supplementary Fig. 1C). We therefore concluded that a specific mechanism prevents incorporation of the $\Delta eps-\Delta tasA$ mutant into *B. subtilis* pellicles.

The ratio of non-producers increases during co-evolution. For the investigation of long-term dynamics in *B. subtilis* WT and $\Delta eps-\Delta tasA$ mutant co-culture over time, a serial transfer experiment was conducted in conditions promoting pellicle formation (see Methods). During the evolution experiment, two transfer methods were applied: in transfer method A, the disrupted biofilm suspension was used directly for the inoculation of fresh medium; in transfer method B the disrupted biofilm suspension was heat-treated, thereby selecting only spores for the inoculation (for detailed description see Methods). Method B was chosen to select for individuals that successfully went through the entire biofilm life cycle.

The ratio of WT to the $\Delta eps-\Delta tasA$ mutant was monitored by selective plating of frozen stocks prepared at different timepoints from the experiment, from the 2nd up to the final (10th) transfer. Despite the initial incorporation failure of $\Delta eps-\Delta tasA$ into the pellicle (Fig. 1a–c), its representation in certain populations of transfer method B was observed to increase dramatically over longer timescales. Remarkably, in parallel populations where transfer method B was applied (that is, selection for spores), the fraction of the $\Delta eps-\Delta tasA$ mutant was considerably higher after the 10th transfer than at the start of the experimental evolution in all but two replicates (Fig. 2b). Importantly, with several exceptions (in replicates 2 that remained relatively stable WT: $\Delta eps-\Delta tasA$ ratio over time and replicate 4 that showed an outlying outburst of $\Delta eps-\Delta tasA$ at passage 8), the percentage of the $\Delta eps-\Delta tasA$ mutant was increased in each successive passage of these populations (Fig. 2b). The values rose to $>30\%$ in

general and to a maximum of around 80% after the 10th transfer of replicate 5. Also, in one out of five parallel populations that were transferred by method A, the fraction of $\Delta eps-\Delta tasA$ was slightly higher after the 10th transfer compared to that at the beginning of the evolution experiment (Fig. 2a).

Non-producers evolve to better incorporate into the pellicle. To further investigate the evolutionary phenomena involved in improved performance of $\Delta eps-\Delta tasA$ in the evolved biofilm population, single clones of both the WT and $\Delta eps-\Delta tasA$ mutant were isolated from three randomly chosen populations after the 10th transfer where an increase of $\Delta eps-\Delta tasA$ in the pellicle was observed (replicates 3, 4 and 5 from transfer method B) (Fig. 2b). All evolved populations and single clones that were further analysed (or genetically modified) in this study are listed in Supplementary Table 2. For clarity, we refer to evolved matrix producers (WT strains) as eMP and to the evolved matrix non-producers ($\Delta eps-\Delta tasA$) as eNMP.

First, to understand which of the co-cultured strains evolved to facilitate better incorporation of the mutant into the pellicle, a series of pellicle competition assays were performed. Competition assays revealed that all but one tested eNMP strains from populations B410m and B510m, and one isolate from population B310m, could increase their fraction within the pellicles as compared to their ancestor when co-cultured with the ancestor WT (Fig. 3a,b). This result was confirmed by both c.f.u. assay (Fig. 3a) and fluorescence microscopy (Fig. 3b). Moreover, the ancestor $\Delta eps-\Delta tasA$ performed even worse when co-cultured with the eMP strains compared to its performance against the WT ancestor (Fig. 3). Therefore, the eMPs completely suppressed the ancestral $\Delta eps-\Delta tasA$.

The performance of three selected eMP and eNMP representatives (one from each evolved population) against the WT ancestor was additionally determined by calculating the selection rate coefficient. All eMPs showed a positive selection rate and their relative c.f.u. in the pellicle was significantly higher than 50% (Supplementary Fig. 3). However, the ancestor $\Delta eps-\Delta tasA$ and eNMPs had negative selection rates, which indicates poor performance during competition with the ancestor WT. Nevertheless, the ancestor $\Delta eps-\Delta tasA$ strain showed the poorest performance (selection rate value of -3.36) and all the eNMPs, B310mA, B410mB and B510mC, revealed improved performance compared to the ancestor mutant strain, with selection rate values of -2.59 , -1.14 and -2.25 , respectively.

Finally, the eNMPs were challenged with the eMPs selected from the corresponding populations (that is, B310mA versus B310wtA or B410mB versus B410wtB). We noticed that the eNMPs from population B310m exhibited a slight decrease in pellicle incorporation compared to their pellicle incorporation when in competition with the ancestor WT (Fig. 3). Overall the eMPs performed better at suppressing the eNMPs as compared to the WT ancestor, however, certain eNMPs from populations B410m and B510m still displayed significantly improved incorporation whether competing against the evolved or ancestor WT (Fig. 3). On the basis of these competition assays, we conclude that evolutionary changes in the $\Delta eps-\Delta tasA$ mutant, rather than the WT, resulted in the improved performance of the non-producers in mixed pellicles.

It was further revealed that the incorporation success of the eNMPs did not depend on their initial frequency. Competition assays with different starting ratios of the WT ancestor to each of the eNMPs (B310mA, B410mB and B510mC) revealed that the eNMPs exhibited higher levels of pellicle incorporation regardless of their starting frequency (Supplementary Fig. 1D–F). B310mA, B410mB and B510mC showed an average pellicle incorporation percentage of

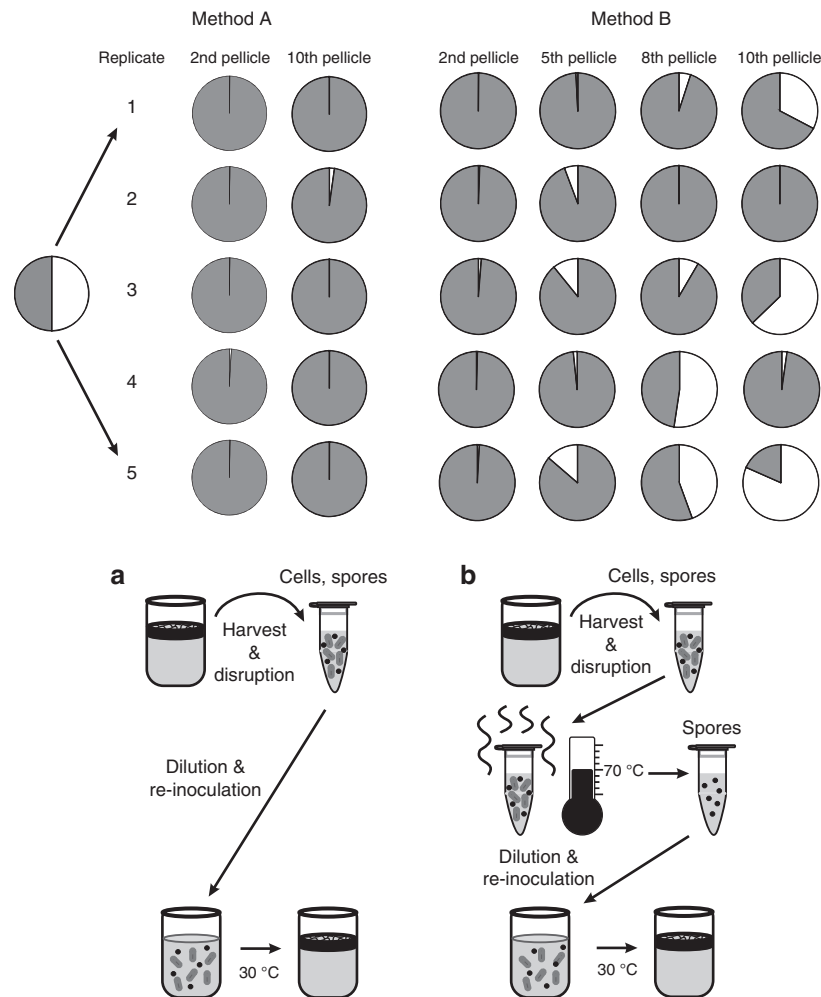


Figure 2 | Fraction of WT and $\Delta eps-\Delta tasA$ strains changes during pellicle serial transfer. In transfer method (a), the pellicle was harvested, disrupted (see Methods) and the suspension of spores and cells was directly used for inoculation of new medium. After harvest and disruption, the cells in transfer method (b) were heat-treated at 70 °C for 15 min to eliminate all vegetative cells. The resulting spore suspension was used to inoculate new medium and was incubated for 2–3 days to allow for pellicle formation. For transfer method (b), the gradual change of wild-type (grey) and $\Delta eps-\Delta tasA$ (white) ratio during the evolution experiment is also presented. The ratio was followed during evolution experiments using the disrupted pellicle suspension directly. In addition, the ratio was redetermined from frozen glycerol stocks for the second, eighth and tenth pellicles.

9.13% (Pearson's correlation coefficient $r=0.17$), 18% ($r=0.22$) and 27% ($r=0.16$), respectively (Supplementary Fig. 1D–F).

Further experiments also revealed that, in contrast to the ancestor mutant (Supplementary Fig. 1B), the incorporation percentage of the eNMP B310mA was not affected by doubling the concentration of resources in the medium (Supplementary Fig. 1B); the incorporation of the evolved B310mA was $9.54\% \pm 3.04\%$ in $2 \times$ SG medium and $9.88\% \pm 2.04\%$ in $4 \times$ SG. These results suggest that the incorporation efficiency of the eNMPs might be driven by a different mechanism from that in the ancestor $\Delta eps-\Delta tasA$.

Incorporation of eNMPs decreases biofilm productivity. A productivity assay was performed to understand the effect of increased incorporation of the eNMPs on the biofilm productivity and to compare the productivity of the eMPs relative to the ancestor WT. Productivity was measured by weighing the whole biomass of the pellicle and is represented as relative productivity compared with the ancestor WT (that is, ancestor WT productivity = 1).

As expected, the productivity of the mixed pellicle consisting of the WT ancestor and mutant ancestor was very similar to the productivity of the WT ancestor grown alone, indicating that the presence of the ancestor $\Delta eps-\Delta tasA$ did not affect the biofilm productivity (Fig. 4). This result agrees with our results showing that ancestor $\Delta eps-\Delta tasA$ was almost completely outcompeted from the pellicle (Fig. 1a–c). In contrast, the productivity of pellicles containing both the ancestor WT and the eNMPs was lower than the productivity of the monoculture WT (productivity values < 1), indicating that the population was negatively affected overall when eNMPs were present (Fig. 4). Interestingly, the eMPs in monocultures (B310wtA, B410wtB and B510wtC) had higher productivity than the WT ancestor (Fig. 4; Supplementary Fig. 4A). Finally, we examined the productivities of the evolved pairs with common evolutionary histories (B310wtA + B310mA; B410wtB + B410mB; and B510wtC + B510mC). For all three pairs, the productivity of the mixed pellicles was lower than the productivity of the ancestor WT; however, these differences were statistically significant only for the pairs B410wtB + B410mB and B510wtC + B510mC (Fig. 4). Nevertheless, in all combinations, the eNMP + eMP productivities were significantly lower than the corresponding eMP productivity, indicating reproducible

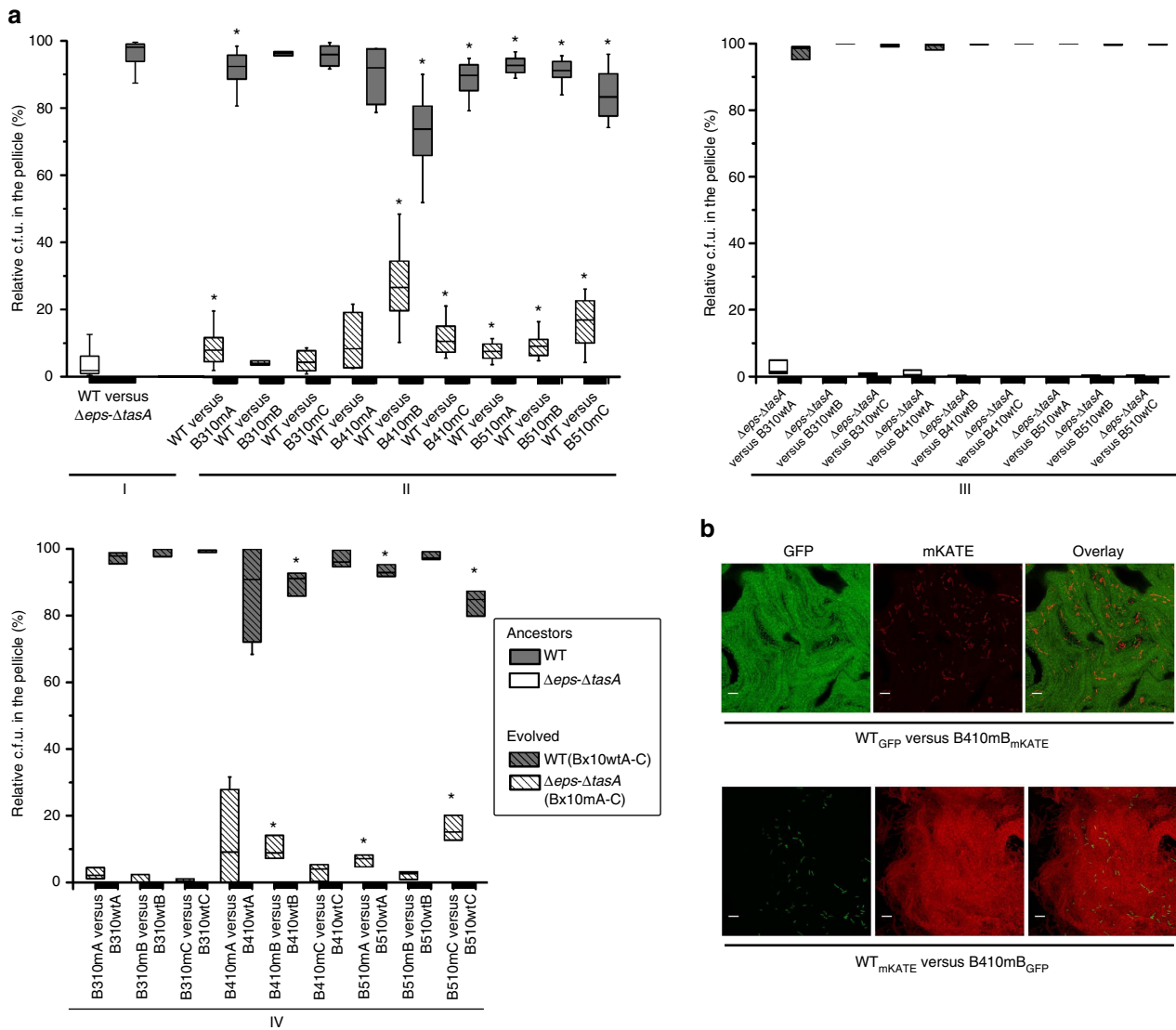


Figure 3 | Pellicle competition assay. (a) WT ancestor and $\Delta eps-\Delta tasA$ mutant ancestor (I); and WT ancestor and eNMP strains 310mA, 310mB, 310mC, 410mA, 410mB, 410mC and 510mA, 510mB, 510mC (II). On a separate panel (above right): pellicle competition assay between WT ancestor and $\Delta eps-\Delta tasA$ mutant ancestor, eMP strains (three isolates per population, as in a) and $\Delta eps-\Delta tasA$ mutant ancestor (III). On a panel below: pellicle competition assay between WT ancestor and $\Delta eps-\Delta tasA$ mutant ancestor, eMP strains and eNMP strains sharing evolutionary history (IV). Boxes represent Q1-Q3, lines represent the median, and bars span from max to min. Each competition assay was replicated in parallel with the ancestor WT versus $\Delta eps-\Delta tasA$ combination at least twice. * in sections II and IV indicate that the relative c.f.u. are significantly different from the relative c.f.u. of WT versus $\Delta eps-\Delta tasA$ ancestor competition. (b) Confocal microscopy images of pellicle biofilms (left) including swapped fluorescence marker proteins (right). Scale bars, 10 μ m.

negative effects of the eNMPs on the productivity of the entire evolved population (Fig. 4). In addition, the pellicles formed by the populations from sequential evolutionary timepoints showed overall decreases in productivity in evolutionary time (Supplementary Fig. 4B), presumably caused by the increasing frequency of eNMPs in pellicles (Fig. 2b).

These results show that although matrix producers evolved a higher productivity, higher incorporation of the coevolved matrix non-producers into the pellicle eventually decreased the overall population productivity.

eMPs and eNMPs contain multiple SNPs in prophage elements. To understand the genetic basis of the observed evolutionary dynamics, the genomes of three eMP and three eNMP populations separated from the 10th transfer of method B cultures (replicates 3, 4 and 5), where the frequency of non-producers was observed to increase during evolution (either gradually or periodically), were subjected to high-

throughput sequencing (Supplementary Table 2). The genomes of corresponding three single isolates of eMPs (B310wtA, B410wtB and B510wtC) and three eNMPs (B310mA, B410mB and B510mC) from those populations were also sequenced. In addition, the genomes of the WT ancestor and the $\Delta eps-\Delta tasA$ ancestor were resequenced to screen for any single SNPs that emerged before the evolution experiment during standard stock preparation and laboratory procedures. The sequencing of six populations (eMPs B310wt, B410wt and B510wt and eNMPs B310m, B410m and B510m) and six single isolates (B310wtA, B410wtB, B510wtC, B310mA, B410mB and B510mC) revealed multiple single-nucleotide polymorphisms (SNPs) exclusively accumulated in three distinct sites on the chromosome compared to the ancestors: two prophage-like regions previously described as prophage-like element 5 and prophage-like element 6 (ref. 22), and the SP β prophage region (Supplementary Data 1; Fig. 5a,b). In population B310 there were 617 SNPs, while in populations B410 and B510 the number of SNPs exceeded 1000. More than

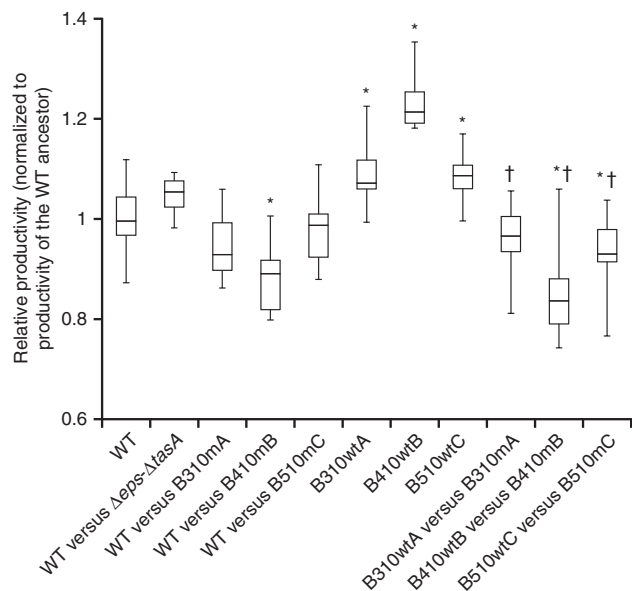


Figure 4 | Productivity assay based on biofilm biomass. Productivity of Δ eps- Δ tasA ancestor and eNMPs B310mA, B410mB and B510mC, respectively, in co-cultures with WT ancestor, monocultures of eMPs B310wtA, B410wtB and B510wtC, and co-cultures of eNMPs with corresponding eMPs compared to the WT ancestor ($n = 10$; t -Student; two-tail $P < 0.05$). Boxes represent Q1-Q3, lines represent the median, and bars span from max to min. Each WT versus co-culture/eMP comparison was replicated at least twice. *—productivities significantly different from the WT ancestor. †—productivities significantly lower from the corresponding eMP cultures.

50% of SNPs detected in single isolates overlapped with SNPs found in the corresponding populations (Supplementary Data 1; Fig. 6a,b).

Further analysis of the sequenced genomes revealed that there was also a large parallel mutational overlap between the evolutionarily unrelated populations and single isolates (regardless of WT or Δ eps- Δ tasA background; Supplementary Data 1; Fig. 6a,b). For visual representation of this overlap we produced a windowed-average identity score for the alignment of the entire 134 kbp SP β region of the evolved strains/populations to the ancestral SP β (Supplementary Fig. 5A). A global analysis of SNPs from all six single isolates showed that the majority of SNPs represented synonymous substitutions (58%), 17% were non-synonymous but evolutionarily conserved (that is, similar; Blosum62 matrix score ≥ 1), 9% were evolutionarily non-conserved and non-synonymous (Blosum62 matrix score ≤ 0), and the remaining 16% of the substitutions were located in non-coding regions (Supplementary Fig. 5B). We also compared the distributions of SNPs in the eMPs and eNMPs by analysing the functions of affected genes. We observed that eMPs accumulated more SNPs than the corresponding eNMPs, especially in genes related to the toxin production and secretion (Supplementary Data 1; Supplementary Fig. 5D,E). However, most of the affected genes belonged to the unknown function category.

More detailed analyses of the sequencing data on the evolved strains suggested duplications of certain genome fragments and genome rearrangements compared to the ancestors. Duplications were indicated by the increased sequencing coverage within the SNP-containing regions (Supplementary Fig. 6A) and the striking pattern of SNP frequencies (Supplementary Data 1; Supplementary Fig. 6B), which was confirmed by PCR and Sanger sequencing of the particularly highly-mutated SP β fragment (2,178,034–2,179,407) from the genomic DNA of B310mA and

B310wtA (Supplementary Fig. 6C). Interestingly, the PCR product obtained from B310mA gave a clear chromatogram with all SNPs present, whereas B310wtA showed a heterogeneous chromatogram with double peaks in the positions of SNPs, one peak coming from an ancestor-like base and the other from the evolved-like base (Supplementary Fig. 6C). In addition, the SP β fragments could still be amplified by PCR even after deletion of the original SP β region from the chromosomes of B410mB and B510mC (Supplementary Fig. 6D–F). The identification of genome rearrangements was made after *de novo* assembly of sequencing reads into contigs (Fig. 6c). All of the predicted rearrangements involved sequences belonging to prophage-like elements 5 and 6 and various SP β fragments, and included the exact regions where multiple SNPs accumulated (Fig. 6c). The presence of two randomly selected rearrangements (contig type 1 and type 4) was confirmed by PCR to occur exclusively in the evolved strains; it did not occur in the ancestor WT or ancestor Δ eps- Δ tasA (Supplementary Fig. 6G). Altogether, we conclude that the emergence of multiple SNPs in all evolved strains (both eMPs and eNMPs) was linked to duplications and rearrangements within prophage elements in the *B. subtilis* genome. It is important to note that the mutation frequencies of the ancestor and the evolved strains were similar, as confirmed using fluctuation assays (Supplementary Fig. 5C). The obtained mutation frequencies were comparable to previously reported data for other *B. subtilis* strains²³, suggesting that the ancestor strains used here were not hypermutators. Moreover, when the same ancestor strain was evolved for ~ 350 generations in emulsion droplets, 60 SNPs and short deletions were identified (Eisha Mhatre and Á.T. Kovács, unpublished data).

Hybrid SP β prophage shows lytic activity towards the ancestors.

Rearrangements involving SP β prophage regions have previously been described as a result of the hybridization of SP β with another *B. subtilis* phage, phi3T (ref. 24). A hybrid form of SP β can undergo spontaneous excision from the chromosome to form a pseudodolysogen, or it can enter a lytic cycle leading to active phage-particle release²⁴. To verify whether the eMPs and eNMPs in the present study spontaneously released phage particles into the medium, phages were precipitated from the supernatants of cultures of selected evolved strains and of the WT ancestor (as a negative control) and visualized by transmission electron microscopy.

No phage particles could be detected in the precipitate obtained from the WT ancestor, which was in line with previous findings²⁵. When the WT ancestor was grown in the presence of the prophage-inducing agent mitomycin C, PBSX-like phage particles were detected in its supernatant, which again reproduced previous results²⁶ (Supplementary Fig. 7A). However, even in the absence of mitomycin C, the evolved strains B410mB and B410wtB released two types of phage particles—PBSX-like particles with a small head and a rigid tail (assignment based on ref. 26), and SP β -like particles with a big head and a longer, flexible tail (assignment based on an image provided by Vladimir Lazarevic, Hôpitaux Universitaires de Genève, Switzerland, personal communication; Fig. 7a; Supplementary Fig. 7A). The addition of mitomycin C to B410mB and B410wtB cultures resulted in a dramatic increase in the number of SP β -like phage particles in the culture supernatants (Supplementary Fig. 7A). SP β -like particles could not be detected in the supernatant of B310mA^{SP β -} cultures, but were still present in B410mB^{SP β -} cultures, which corresponded well with the results of molecular analysis, which indicated successful deletion of SP β from strain B310mA^{SP β -} but not from B410mB^{SP β -} (Supplementary Figs 6D–F and 7A).

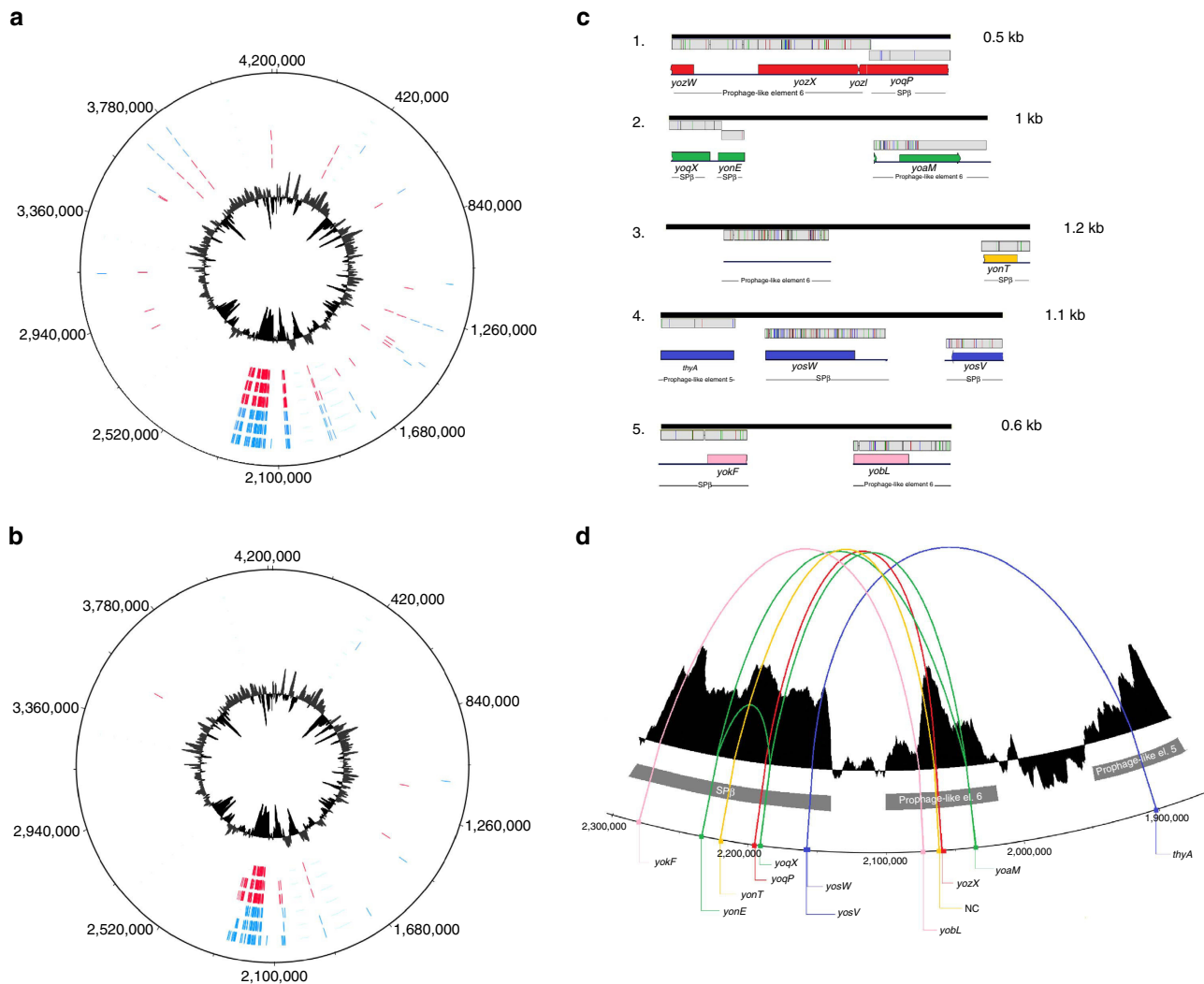


Figure 5 | Multiple SNPs and genome rearrangements are detected in the evolved strains. Genome wide distribution of SNP loci across the evolved *B. subtilis* populations (a) and single isolates (b) generated using the DNAPlotter tool⁵⁶. (a) SNPs from six populations are presented on separate tracks; starting from the outside and moving towards the inside: B310wt, B410wt, B510wt (all shown in blue), B310m, B410m, and B510m (all shown in red). (b) SNPs in six isolates are presented on separate tracks; starting from the outside and moving towards the inside: B310wtA, B410wtB, B510wtC (all shown in blue), B310mA, B410mB, and B510mC (all shown in red). Internal black circles represent GC profiles. (c) Genome rearrangements predicted for the evolved strains based on bioinformatics analysis of the sequencing data. Black lines represent *de novo* assembled contigs with their sizes indicated on the right, grey boxes show aligned fragments of the reference genome (GenBank accession number AL009126), and stripes show SNP positions. Visualization was performed using Geneious software⁵⁷. Corresponding genes (or non-coding regions) in the reference *B. subtilis* genome are shown below the alignment with different coloration used for each type of rearrangement. (d) DNA plotter graphical representation of predicted genome rearrangements (zoom view on the SP β and prophage-like element 6 and 5 regions). The black histogram represents the GC profile, where three clusters of low-GC content directly correspond to SP β , prophage-like element 6 and prophage-like element 5. Distantly located genes that participated in rearrangements and became neighbours in the evolved strains are connected by arched lines (different colour used for each rearrangement) and are additionally marked with dots of the same colour. The coloration used for each rearrangement type corresponds to that in c.

Next, the lytic activity of the SP β particles released by the evolved strains was tested against the ancestor strains. A series of plaque assays were performed where each strain served both as a supernatant donor and as potential prey. Neither of the ancestor strains (WT or Δ *eps*- Δ *tasA*) showed lytic activity when serving as the supernatant donor, but they were both susceptible to the lytic activity of almost all supernatants of the evolved strains (Fig. 6b, Supplementary Fig. 7B). Strain B310mA^{SP β -} performed exactly the same as the ancestors, showing no lytic activity but displaying susceptibility to all supernatants, including that of B310mA (from which it was derived; Fig. 6b; Supplementary Fig. 7B). Despite the fact that all evolved strains showed lytic activity and immunity, they could be differentiated into strong (for example, B410mB) and moderate levels (for example,

B510wtC) (Fig. 6b; Supplementary Fig. 7B). The lytic activity of the supernatants of all evolved populations was assessed, including all five populations from transfer method A and all five populations from transfer method B (Fig. 2). Strong lytic activity towards the ancestor WT strain was found exclusively in populations that showed an increased incorporation of non-producers into the pellicle following the evolution experiment, specifically population 2 from transfer method A, and populations 1, 3, 4 and 5 from transfer method B (Supplementary Fig. 7C). Further, populations that did not show increased incorporation of non-producers and lacked lytic activity towards the ancestor strains did not contain multiple SNPs within the SP β regions, as confirmed by Sanger sequencing of the 2,178,034–2,179,407 genomic fragment.

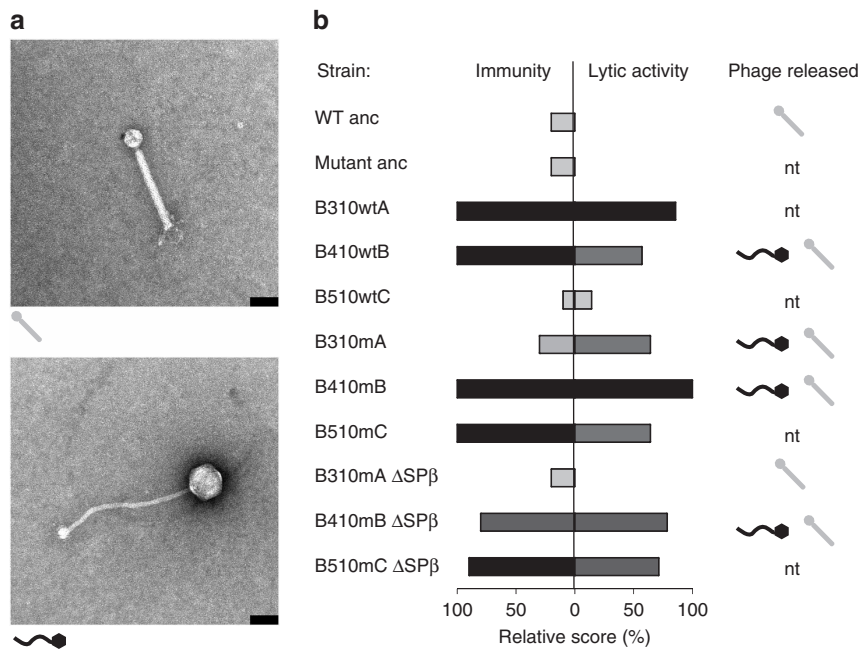


Figure 6 | Lytic phage activity appears in the evolved strains. (a) Electron micrographs of phage particles purified from *B. subtilis* supernatants. Upper image shows PBSX-like phage particle released by the ancestor WT only in the presence of mitomycin C, and by all evolved strains in the absence of mitomycin C. The lower image shows SPβ-like phage particle spontaneously released by all evolved strains tested, but not by the ancestor WT or by B310mA^{SPβ}. Scale bars, 70 nm. (b) Results of plaque assays performed with the ancestor WT, ancestor $\Delta eps-\Delta tasA$ and all the evolved strains, where each strain served both as a supernatant donor and as a potential host. Each strain was given 1 immunity point when resistant to a given supernatant (excluding its own supernatant), and a number of lytic activity points when showing lytic activity towards a given host (excluding itself), depending on the strength of lytic activity. Specifically, the number of points was equal to a maximal log dilution factor where lytic activity was still present (for example, a lytic activity that can still be detected in a conditioned medium diluted to 10^{-3} but not 10^{-4} is denoted with 3 points). Obtained immunity and lytic activity scores were then divided by the maximum value of each and are presented as relative percentages. Darkness of the bars is proportional to immunity/lytic activity scores values. High immunity/lytic activity scores correlated with presence of SPβ-like particles (black in the right-hand column) isolated from the culture medium of those strains. 'nt' indicates media were not tested by transmission electron microscopy. The experiment was independently replicated four times.

Spontaneous phage release by the evolved strains and their lytic activity towards the ancestors suggested that higher incorporation of the eNMPs into pellicles may be the result of newly evolved interference competition. We therefore examined whether the ancestor mutant could acquire the evolved-like phenotype with higher incorporation pellicle properties through a single-phage transduction step. For the infection assay, a 1:1 mixture of the WT and $\Delta eps-\Delta tasA$ ancestors was introduced into standard $2 \times$ SG medium supplemented with phage precipitate obtained from B410mB where the presence of SPβ-like phage particles was detected. After a single growth cycle, three colonies of the WT and three colonies of $\Delta eps-\Delta tasA$ were isolated and their acquired lytic activity towards the ancestor strains was assessed. Finally, pellicle competition assays were performed using the WT ancestor and the three $\Delta eps-\Delta tasA$ strains isolated from the infected population (ImA, ImB and ImC). As expected, the phage-infected strains behaved similarly to the evolved mutants, showing >4-fold (in the case of ImA) and >2.5-fold (ImB and ImC) increased incorporation rates into the pellicle compared with the ancestor mutant (Fig. 7).

Phage release facilitates higher pellicle inclusion of eNMPs. Finally, we asked whether the presence of an identical active phage variant in both producers and non-producers is sufficient to explain the higher incorporation of the eNMPs into pellicles. This was first tested by assaying the infected mutants (ImA, ImB and ImC) with the infected WT strains (Supplementary Fig. 8). No increased pellicle incorporation of the mutants was observed, indicating that higher incorporation of the mutants cannot be explained by a general increase of phage activity in the entire

population (Supplementary Fig. 8), but is due instead to subtle differences within phage elements of evolved non-producers and producers.

This was further confirmed by a fitness assay that involved $\Delta eps-\Delta tasA$ and WT strains with an isogenic evolved background. Isogenic evolved WT and mutant strains were obtained simply by introducing the $\Delta eps-\Delta tasA$ deletions into eMPs. Genome resequencing confirmed that the obtained $\Delta eps-\Delta tasA$ strains still contained the genetic background of corresponding eMPs (Supplementary Data 1). When the eMPs B310wtA, B410wtB and B510wtC were competed against their direct derivatives B310wtA $\Delta eps-\Delta tasA$, B410wtB $\Delta eps-\Delta tasA$, and B510wtC $\Delta eps-\Delta tasA$, respectively, a very low pellicle incorporation percentage of the mutants was observed, which was comparable to the performance of the ancestor $\Delta eps-\Delta tasA$ against the ancestor WT (Supplementary Fig. 8). As expected, competition assays with the WT ancestor revealed that the transformants had comparable incorporation probabilities to the eNMPs (Fig. 7). These results indicated that although producers and non-producers showed very similar general adaptation patterns involving major changes in mobile genetic elements, some of these changes were specific to the evolved non-producers, resulting in their improved incorporation into pellicles, most likely through an advantage in interference competition.

Discussion

Stability of cooperative interactions can determine the performance of microbes in most medically and biotechnologically relevant situations^{27–32}. In recent years, understanding of microbial group behaviours and the mechanisms that prevent

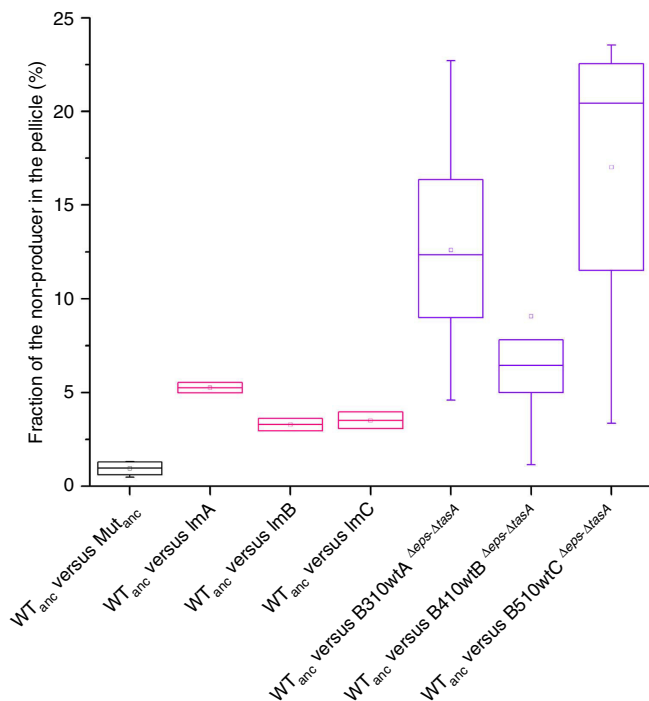


Figure 7 | Evolved mutants and ancestor mutants hosting the evolved phage have increased incorporations into the pellicle. Competition assay between the WT ancestor and $\Delta eps-\Delta tasA$ ancestor (control) ($n = 7$); between the WT ancestor and three single colonies obtained after transduction of the $\Delta eps-\Delta tasA$ ancestor with phage particles released by eNMP B410mB ($n = 2$); and between the WT ancestor and eMPs (B310wtA, B410wtB, and B510wtC) with deleted *eps* and *tasA* ($n = 10$; $n = 10$; $n = 7$, respectively). Boxes represent Q1–Q3, lines represent the median, and bars span from max to min. Each competition assay in parallel with the ancestor WT versus $\Delta eps-\Delta tasA$ was replicated at least twice.

spreading of non-cooperative mutants has become one of the key aims of sociomicrobiology. Long timescale evolutionary experiments have already demonstrated the evolutionary plasticity of social interactions in various bacterial models^{18,33,34}. Here we describe a scenario where a biofilm matrix non-producer that is initially eliminated from the population increases its performance over longer timescales and evolves the ability to better incorporate into the biofilm. The evolution of improved invasion of biofilms by non-producers was previously observed by Zhang *et al.*¹⁵. They excluded the possibility of general adaptation being responsible for the changed social dynamics in biofilms since the evolved producer did not increase its performance towards the ancestor producer. In the present work, an increased selection coefficient and improved productivity of the evolved WT could be observed in monocultures; the same, unfortunately, could not be tested for the evolved mutants because of their inability to form pellicles in monocultures. We therefore hypothesize that the evolved increased-biofilm-incorporation-ability of the mutant was a side effect of extremely fast general adaptation of both producer and non-producers driven by mobile genetic elements. Interestingly, the improved incorporation of the non-producers into biofilms was not reproduced when both WT and non-producer strains had identical evolved genetic backgrounds (that of the evolved WT strains). This means that although the general adaptation pattern in the entire population was very similar, the non-producers are evolutionarily ahead of the producers and carry certain specific changes that allow their improved performance in

incorporation into biofilms formed by the evolved WT strains. We believe those specific differences are hidden within prophage elements of the evolved strains, and they could be revealed by *de novo* sequencing in the future.

In the ancestral population, the matrix non-producers ($\Delta eps-\Delta tasA$, which do not secrete two key matrix components Eps and TasA) can hardly incorporate into pellicle biofilms formed by the WT. This result was rather unexpected for two reasons: first, previous work demonstrated that both Eps and TasA are shared with non-producing strains²⁰, and, second, the production of at least one of those compounds (Eps) was proven to be costly and exploitable¹³. Although we did not study the competition mechanism in detail, a positive correlation between fitness, initial $\Delta eps-\Delta tasA$ frequency and resource availability suggests that in the ancestral population the growth of $\Delta eps-\Delta tasA$ is not only limited by the lack of oxygen, but also by carbon resources. We speculate that this is caused by a delay in surface co-colonization of $\Delta eps-\Delta tasA$, because the producer can partially privatize the matrix components. Since the WT is released from oxygen-limitation first, it can quickly deplete the remaining carbon resources, preventing further growth of the mutant. This model, however, awaits further studies.

The pellicle incorporation mechanism of evolved $\Delta eps-\Delta tasA$ does not depend on resource concentration or on the initial frequency of the mutant in the co-culture. It is likely that new antagonistic interactions involving infection and lysis of the ancestor WT by the evolved mutant delay surface colonization by the WT, giving the mutant a prolonged window of opportunity for co-colonization. A similar mechanism could play a role in the competition between the evolved mutant and the evolved WT, since the evolved WT strains spontaneously release phages into the medium and show a delay in pellicle formation.

How did the new lytic properties evolve? We believe that multiple rearrangements in the genomes of the evolved strains, combined with series of SNPs in regions that were rearranged, resulted in new lytic properties of the normally inactive domesticated SP β prophage. Since this scenario was more likely to occur on sporulation treatment (that is, treatment method B), we suspect that the multiple heat-treatments involved in this treatment might have promoted phage activation³⁵ or even rearrangements of phage elements in the genome³⁶. The accumulation of multiple SNPs and rearrangements resembles the previously reported evolutionary response of the *Streptococcus thermophilus* phage to the host's CRISPR system³⁷, however, no CRISPR/Cas has yet been identified in *B. subtilis*. Alternatively, rapid diversification within prophage regions combined with lytic induction may be a universal adaptive pattern of bacteria to a biofilm lifestyle, as it was previously also observed during experimental evolution of *Pseudomonas aeruginosa* biofilms³⁸. Our work also demonstrates how such newly evolved phage warfare shifts social dynamics in the bacterial population in favour of biofilm non-producers. The dynamics of host-phage interactions is long studied in various experimental systems³⁹. It was previously observed that lytic phages can shift the balance in competitive interactions by reducing the frequency of a winning partner⁴⁰, or impair biofilm formation ability as a trade-off for phage immunity⁴¹. We hypothesize that in the case of the *B. subtilis* pellicles, the disadvantage of matrix producers could originate from the degeneration of toxin/secretion-related genes in the evolved wild-types that in turn became less efficient competitors than the evolved mutants.

The improved fitness of the evolved WT strain in monoculture could be a direct result of the evolved spontaneous phage release. Normally, the excision of the SP β prophage from the *B. subtilis* chromosome takes place before sporulation and allows reconstitution of the *spsM* gene involved in spore polysaccharide

biosynthesis⁴². Sanchez-Vizueté *et al.*⁴³ demonstrated that removal of SP β from the chromosome permanently restores *spsM*, resulting in increased biofilm thickness. We presume that frequent spontaneous excision of SP β , or even pseudolysogeny (as demonstrated in ref. 24) in the evolved WT strains, could positively contribute to the biofilm productivity through *spsM* reconstitution. Excision of prophage from the host chromosome was recently linked to improved biofilm formation by *Shewanella oneidensis* facing cold stress⁴⁴. Such a phage excision benefited the host through gene inactivation rather than reconstitution (as observed in ref. 43). Similar genetic switches triggered by prophage excision were also described in several other species (reviewed in ref. 45).

The *B. subtilis* SP β prophage carries a bacteriocin-immunity system⁴⁶, several putative toxin-antitoxin systems⁴⁷ and cell wall hydrolases⁴⁸. Several SP β segments of >250 nucleotides exhibit >90% identity with *B. subtilis* chromosomal regions²⁵ promoting recombination events, especially in naturally competent strains. Not surprisingly, recent reports strongly indicate a key role of phage elements in rapid evolution of kin recognition mechanisms and antagonistic interactions between closely related, sympatric *B. subtilis* strains^{49,50}. Accumulation of SNPs in the SP β region was also observed in the evolution experiments of Overkamp *et al.*⁵¹, where *B. subtilis* was kept in zero-growth conditions for 42 days. Among hundreds of SNPs discovered by Overkamp *et al.*⁵¹, 80% overlapped with the SNPs reported in this study. In addition, most of the SNPs detected were synonymous and evolutionarily conserved, suggesting selection against loss of function. Recent reports show that even non-synonymous mutations can positively contribute to fitness^{52,53}. This again suggests that mutations or rearrangements within phage elements can be a very important evolutionary force in *B. subtilis*, with a major impact on social interactions. Recently, the profound impact of prophages on the evolution of a pathogenic bacterium was experimentally demonstrated in *P. aeruginosa* biofilms⁵⁴, where the presence of phages resulted in strong selection against phage recognition elements (type IV pilus), at the same time enhancing parallel evolution⁵⁴. Similar selective pressure could emerge after fast evolution of active SP β variants in *B. subtilis* biofilms, resulting in striking parallelism in evolved populations of both WT and Δ *eps*- Δ *tasA* bacteria.

Our work demonstrates how social dynamics in an initially very robust biofilm can be shifted by unexpected evolutionary events. We show that an adaptive genotype that is quickly tailored by mobile genetic elements can easily spread through horizontal gene transfer. The same adaptive path, although beneficial for the producer, became maladaptive in a mixed population where producers coexisted with non-producers.

Methods

Strains and cultivation conditions. Supplementary Table 1 describes strains used in this study and construction of their mutant derivatives. Strain *B. subtilis* 168 hymKATE P_{yapA} -yfp was obtained by transforming the laboratory strain, *B. subtilis* 168, with genomic DNA from DL821 and selecting for MLS resistance. Subsequently, the created strain was transformed with genomic DNA from 168 hymKate and selecting on chloramphenicol resistance and for the loss of amylase activity. The Δ *eps* and Δ *tasA* strains were obtained by transforming the 168 strains with genomic DNA isolated from DL1032 and specifically selecting for tetracycline or kanamycin resistance, respectively. The double mutant Δ *eps*- Δ *tasA* was obtained by transforming 168 Δ *eps* with genomic DNA from DL1032 and selecting on the kanamycin marker. The Δ *eps*- Δ *tasA* hyGFP and Δ *eps*- Δ *tasA* hymKate strains were obtained by transforming the Δ *eps*- Δ *tasA* strain with genomic DNA obtained from 168 hyGFP and 168 hymKate, respectively. Deletion of *epsA-O* and *tasA* genes were confirmed with PCR using oligos described in Supplementary Table 3. Strains were maintained in LB medium (Lennox broth; Carl Roth, Germany), while 2 \times SG medium was used for biofilm induction⁵⁵.

Experimental evolution and competition assays. Experimental evolution was performed using co-cultures of fluorescently labelled but otherwise WT and

Δ *eps*- Δ *tasA* strains grown in 2 ml 2 \times SG medium statically in a 24-well plate at 30 °C for 2–3 days. For transfer method A, the mature pellicles were harvested, mildly disrupted, and reinoculated after 100 \times dilution. For transfer method B, the pellicles were additionally heat-treated after disruption and diluted \times 20 during reinoculation. The sporulation frequency in the conditions applied in the evolution experiment was about 20% (Supplementary Fig. 2). To maintain similar selection bottlenecks in the two transfer methods, a fivefold lower dilution factor was used in transfer method B.

After the 2nd, 8th and 10th pellicle transfers, frozen stocks were preserved. Evolved populations or single isolates were isolated by selecting with appropriate antibiotics. Competition experiments were performed by mixing certain ratios of 100-fold diluted LB-pregrown cultures which were then incubated in static pellicle forming conditions for 3 days or in agitated planktonic cultures for 16 h. The numbers of c.f.u. of the inocula and the final cultures were determined on LB-agar plates containing selective antibiotics, incubated overnight at 37 °C. Prior the c.f.u. assays, pellicles were sonicated according to a protocol optimized in our laboratory (2 cycles each containing 12 \times 1 s pulses at 20% amplitude with 1 s pause between the pulses), that ensured efficient disruption of biofilm clumps (as verified by microscopy) and therefore accurate total cell counts in the pellicles.

Microscopy. Bright field images of whole pellicles were obtained with an Axio Zoom V16 stereomicroscope (Carl Zeiss, Jena, Germany) equipped with a Zeiss CL 9000 LED light source and an AxioCam MRm monochrome camera (Carl Zeiss). The pellicles were also analysed using a confocal laser scanning microscope (LSM 780 equipped with an argon laser, Carl Zeiss) and Plan-Apochromat/1.4 Oil DIC M27 \times 63 objective. Fluorescent reporter excitation was performed with the argon laser at 488 nm and the emitted fluorescence was recorded at 484–536 nm and 567–654 nm for GFP and mKate, respectively. To generate pellicle images, Z-stack series with 1 μ m steps were acquired. Zen 2012 Software (Carl Zeiss) was used for both stereomicroscopy and CLSM image visualization.

Productivity assay. For productivity assays, pellicles were inoculated into 4 ml of 2 \times SG medium placed in 35 mm-diameter Petri dishes and incubated for 3 days at 30 °C. Next, the medium fraction was removed, and pellicles were dried at 55 °C for 3 h. The dry biomass was determined on an analytical balance.

Fluctuation assay. To determine the mutation rate, single colonies were picked from LB-agar medium and cultivated for 18 h in LB broth at 37 °C. After 100-times dilution in 2 \times SG medium, cultures ($n = 10$ for each strain) were subsequently cultivated for 18 h with vigorous shaking, and dilution series were plated on LB-agar medium to assay the frequency of streptomycin (50 μ g ml⁻¹) resistant c.f.u. after 18–24 h at 37 °C.

Genome resequencing and genome analysis. Genomic DNA of selected populations or isolated strains was isolated using the EUREX Bacterial and Yeast Genomic DNA Kit from cultures grown for 18 h. For the evolved population, single-end fragment reads were sequenced using a Life Technologies SOLiD 5500xl sequencer. Base-calling was carried out with the software provided by the supplier. All other downstream analysis steps were done in CLC Genomics Workbench Tool 7.0.4. Reads were length-filtered, keeping only ≥ 50 nucleotide long fragments. Mapping used only those reads that displayed $\geq 80\%$ similarity to the reference genome (GenBank accession number AL009126) over $\geq 60\%$ of the read length (meaning an alignment of ≥ 30 nucleotides having ≥ 24 identical matches). Non-specific reads were randomly placed to one of their possible genomic locations. Quality-based SNP and small in/del variant calling was carried out requiring $\geq 10 \times$ read coverage with $\geq 20\%$ variant frequency. Only variants suggested by good quality bases ($Q \geq 20$) were taken into account. Furthermore, mutations had to be supported by evidence from both DNA strands.

For single isolate strains, paired-end fragment reads (2 \times 250 nucleotides) were generated using an Illumina MiSeq sequencer. Primary data analysis (base-calling) was carried out with MiSeq Reporter software (Illumina). All further analysis steps were done in CLC Genomics Workbench Tool 8.0.2. Reads were quality-trimmed using an error probability of 0.05 (Q13) as the threshold. Reads that displayed $\geq 80\%$ similarity to the reference genome (GenBank accession number AL009126) over $\geq 80\%$ of their read lengths were used in mapping. Non-specific reads were randomly placed to one of their possible genomic locations. Quality-based SNP and small In/Del variant calling was carried out requiring $\geq 40 \times$ read coverage with $\geq 20\%$ variant frequency. Only variants supported by good quality bases ($Q \geq 20$) were taken into account and only if they were supported by evidence from both DNA strands. Selected genomic regions were validated by Sanger sequencing (GATC Biotech, Konstanz, Germany) using oligos listed in Supplementary Table 3.

Transmission electron microscopy analysis. Selected bacterial strains were grown overnight in LB medium at 37 °C with shaking at 200 r.p.m. In the case of mitomycin-C-treated cultures, mitomycin C was added in late exponential phase to a final concentration of 0.5 μ g ml⁻¹. Culture supernatants were collected, mixed at a 1:4 ratio with PEG-8000 solution (PEG-8000 20%, 2 M NaCl), incubated on ice for at least 90 min and finally centrifuged (20 min, 7,600 r.p.m.) to obtain

precipitate. The pellet was resuspended in 10% of the original supernatant volume in TBS solution (50 mM Tris-HCl, 150 mM NaCl, pH 7), incubated on ice for 90 min and centrifuged (20 min, 7600 r.p.m.). Supernatant was carefully transferred to clean Eppendorf tubes. Purified samples (100 μ l) were adsorbed onto duplicate 400 mesh carbon-coated Cu grids (Quantifoil, Großlobichau, Germany) for 2 min. Before use, the carbon grids were hydrophilized by 30 s of electric glow discharging. The grids were washed twice in distilled water and stained for 30 s with 1% uranyl acetate. Virus morphologies were examined using a Zeiss CEM 902A transmission electron microscope (Carl Zeiss AG, Oberkochen, Germany). At least 20 images were taken per sample at different magnifications using a 1k FastScan CCD-Camera (camera and software from TVIPS, Munich, Germany).

Statistical analyses. Statistical differences between two experimental groups were identified using two-tailed Student's *t*-tests assuming equal variance. Variances in the two main types of datasets (c.f.u. counts in competition assays and weight of biomass) were similar across different samples. One data point with a value greater than the mean plus 3 times the s.d. was removed from the dataset of $n > 10$ as an outlier. Normal distributions within the two main data types (biomass and c.f.u.) were confirmed by Kolmogorov-Smirnov ($P > 0.05$). No statistical methods were used to predetermine sample size and the experiments were not randomized.

Data availability. The genome resequencing data are available in Supplementary Data 1. The authors declare that all other relevant data supporting the findings of the study are available within the article and its Supplementary Information files, or from the corresponding author upon request.

References

- Costerton, J. W., Lewandowski, Z., Caldwell, D. E., Korber, D. R. & Lappin-Scott, H. M. Microbial biofilms. *Annu. Rev. Microbiol.* **49**, 711–745 (1995).
- Hall-Stoodley, L., Costerton, J. W. & Stoodley, P. Bacterial biofilms: from the natural environment to infectious diseases. *Nat. Rev. Microbiol.* **2**, 95–108 (2004).
- Röder, H. L., Sørensen, S. J. & Burmølle, M. Studying bacterial multispecies biofilms: where to start? *Trends Microbiol.* **24**, 503–513 (2016).
- Martin, M., Hölscher, T., Dragos, A., Cooper, V. S. & Kovács, Á. T. Laboratory evolution of microbial interactions in bacterial biofilms. *J. Bacteriol.* **198**, 2564–2571 (2016).
- Steenackers, H. P., Parijs, I., Foster, K. R. & Vanderleyden, J. Experimental evolution in biofilm populations. *FEMS Microbiol. Rev.* **40**, 373–397 (2016).
- Rainey, P. B. & Travisano, M. Adaptive radiation in a heterogeneous environment. *Nature* **394**, 69–72 (1998).
- Udall, Y. C., Deeni, Y., Hapca, S. M., Raikes, D. & Spiers, A. J. The evolution of biofilm-forming Wrinkly Spreaders in static microcosms and drip-fed columns selects for subtle differences in wrinkleability and fitness. *FEMS. Microbiol. Ecol.* **91**, fiv057 (2015).
- Hammerschmidt, K., Rose, C. J., Kerr, B. & Rainey, P. B. Life cycles, fitness decoupling and the evolution of multicellularity. *Nature* **515**, 75–79 (2014).
- Hardin, G. The tragedy of the commons. The population problem has no technical solution; it requires a fundamental extension in morality. *Science* **162**, 1243–1248 (1968).
- Xavier, J. B. & Foster, K. R. Cooperation and conflict in microbial biofilms. *Proc. Natl Acad. Sci. USA* **104**, 876–881 (2007).
- Irie, Y. *et al.* The *Pseudomonas aeruginosa* PSL polysaccharide is a social but non-cheatable trait in biofilms. Preprint at *bioRxiv* <http://dx.doi.org/10.1101/049783> (2016).
- Srinandan, C. S., Elango, M., Gnanadhas, D. P. & Chakravorty, D. Infiltration of matrix-non-producers weakens the *Salmonella* biofilm and impairs its antimicrobial tolerance and pathogenicity. *Front. Microbiol.* **6**, 1468 (2015).
- van Gestel, J., Weissing, F. J., Kuipers, O. P. & Kovács, Á. T. Density of founder cells affects spatial pattern formation and cooperation in *Bacillus subtilis* biofilms. *ISME J.* **8**, 2069–2079 (2014).
- Nadell, C. D., Drescher, K., Wingreen, N. S. & Bassler, B. L. Extracellular matrix structure governs invasion resistance in bacterial biofilms. *ISME J.* **9**, 1700–1709 (2015).
- Zhang, Q. G., Buckling, A., Ellis, R. J. & Godfray, H. C. Coevolution between cooperators and cheats in a microbial system. *Evolution* **63**, 2248–2256 (2009).
- Manhes, P. & Velicer, G. J. Experimental evolution of selfish policing in social bacteria. *Proc. Natl Acad. Sci. USA* **108**, 8357–8362 (2011).
- Kümmerli, R. *et al.* Co-evolutionary dynamics between public good producers and cheats in the bacterium *Pseudomonas aeruginosa*. *J. Evol. Biol.* **28**, 2264–2274 (2015).
- Fiegna, F., Yu, Y. T., Kadam, S. V. & Velicer, G. J. Evolution of an obligate social cheater to a superior cooperator. *Nature* **441**, 310–314 (2006).
- Hölscher, T. *et al.* Motility, chemotaxis and aerotaxis contribute to competitiveness during bacterial pellicle biofilm development. *J. Mol. Biol.* **427**, 3695–3708 (2015).
- Branda, S. S., Chu, F., Kearns, D. B., Losick, R. & Kolter, R. A major protein component of the *Bacillus subtilis* biofilm matrix. *Mol. Microbiol.* **59**, 1229–1238 (2006).
- Madsen, J. S. *et al.* Facultative control of matrix production optimizes competitive fitness in *Pseudomonas aeruginosa* PA14 biofilm models. *Appl. Environ. Microbiol.* **81**, 8414–8426 (2015).
- Kunst, F. *et al.* The complete genome sequence of the gram-positive bacterium *Bacillus subtilis*. *Nature* **390**, 249–256 (1997).
- Viret, J. F. & Alonso, J. C. A new mutator strain of *Bacillus subtilis*. *Mol. Gen. Genet.* **208**, 353–356 (1987).
- Spancake, G. A., Hemphill, H. E. & Fink, P. S. Genome organization of SPbeta c2 bacteriophage carrying the *thyp3* gene. *J. Bacteriol.* **157**, 428–434 (1984).
- Lazarevic, V. *et al.* Nucleotide sequence of the *Bacillus subtilis* temperate bacteriophage SPβc2. *Microbiology* **145**, 1055–1067 (1999).
- Okamoto, K. *et al.* Properties of the defective phage of *Bacillus subtilis*. *J. Mol. Biol.* **34**, 413–428 (1968).
- Inglis, R. F., Gardner, A., Cornelis, P. & Buckling, A. Spite and virulence in the bacterium *Pseudomonas aeruginosa*. *Proc. Natl Acad. Sci. USA* **106**, 5703–5707 (2009).
- Itoh, T. *et al.* Cooperative degradation of chitin by extracellular and cell surface-expressed chitinases from *Paenibacillus* sp. strain FPU-7. *Appl. Environ. Microbiol.* **79**, 7482–7490 (2013).
- Katsuyama, C. *et al.* Complementary cooperation between two syntrophic bacteria in pesticide degradation. *J. Theor. Biol.* **256**, 644–654 (2009).
- Li, Y. H. & Tian, X. Quorum sensing and bacterial social interactions in biofilms. *Sensors (Basel)* **12**, 2519–2538 (2012).
- Pollitt, E. J., West, S. A., Cruz, S. A., Burton-Chellew, M. N. & Diggle, S. P. Cooperation, quorum sensing, and evolution of virulence in *Staphylococcus aureus*. *Infect. Immun.* **82**, 1045–1051 (2014).
- Raymond, B., West, S. A., Griffin, A. S. & Bonsall, M. B. The dynamics of cooperative bacterial virulence in the field. *Science* **337**, 85–88 (2012).
- Andersen, S. B., Marvig, R. L., Molin, S., Krogh Johansen, H. & Griffin, A. S. Long-term social dynamics drive loss of function in pathogenic bacteria. *Proc. Natl Acad. Sci. USA* **112**, 10756–10761 (2015).
- Velicer, G. J., Kroos, L. & Lenski, R. E. Loss of social behaviors by *Myxococcus xanthus* during evolution in an unstructured habitat. *Proc. Natl Acad. Sci. USA* **95**, 12376–12380 (1998).
- Siegel, E. C. & Marmor, J. Temperature-sensitive induction of bacteriophage in *Bacillus subtilis* 168. *J. Virol.* **4**, 610–618 (1969).
- Kawamura, F., Saito, H. & Ikeda, Y. A method for construction of specialized transducing phage rho 11 of *Bacillus subtilis*. *Gene* **5**, 87–91 (1979).
- Paez-Espino, D. *et al.* CRISPR immunity drives rapid phage genome evolution in *Streptococcus thermophilus*. *MBio* **6**, e00262-15 (2015).
- McElroy, K. E. *et al.* Strain-specific parallel evolution drives short-term diversification during *Pseudomonas aeruginosa* biofilm formation. *Proc. Natl Acad. Sci. USA* **111**, E1419–E1427 (2014).
- Lenski, R. E. & Levin, B. R. Constraints on the coevolution of bacteria and virulent phage: a model, some experiments, and predictions for natural communities. *Am. Nat.* **125**, 585–602 (1985).
- Brockhurst, M. A., Fenton, A., Roulston, B. & Rainey, P. B. The impact of phages on interspecific competition in experimental populations of bacteria. *BMC. Ecol.* **6**, 19 (2006).
- Brockhurst, M. A., Buckling, A. & Rainey, P. B. The effect of a bacteriophage on diversification of the opportunistic bacterial pathogen, *Pseudomonas aeruginosa*. *Proc. Biol. Sci.* **272**, 1385–1391 (2005).
- Abe, K. *et al.* Developmentally-regulated excision of the SPbeta prophage reconstitutes a gene required for spore envelope maturation in *Bacillus subtilis*. *PLoS Genet.* **10**, e1004636 (2014).
- Sanchez-Vizueta, P. *et al.* Identification of *ypqP* as a new *Bacillus subtilis* biofilm determinant that mediates the protection of *Staphylococcus aureus* against antimicrobial agents in mixed-species communities. *Appl. Environ. Microbiol.* **81**, 109–118 (2015).
- Zeng, G. *et al.* Cold adaptation regulated by cryptic prophage excision in *Shewanella oneidensis*. *ISME J.* **10**, 2787–2800 (2016).
- Feiner, R. *et al.* A new perspective on lysogeny: prophages as active regulatory switches of bacteria. *Nat. Rev. Microbiol.* **13**, 641–650 (2015).
- Dubois, J. Y. *et al.* Immunity to the bacteriocin sublancin 168 is determined by the SunI (YofF) protein of *Bacillus subtilis*. *Antimicrob. Agents Chemother.* **53**, 651–661 (2009).
- Jahn, N., Preis, H., Wiedemann, C. & Brantl, S. BsrG/SR4 from *Bacillus subtilis* – the first temperature-dependent type I toxin-antitoxin system. *Mol. Microbiol.* **83**, 579–598 (2012).
- Sudiarta, I. P., Fukushima, T. & Sekiguchi, J. *Bacillus subtilis* CWpF of the SPβ prophage has two novel peptidoglycan hydrolase domains, muramidase and cross-linkage digesting D-endopeptidase. *J. Biol. Chem.* **285**, 41232–41243 (2010).
- Lyons, N. A., Kraigher, B., Stefanic, P., Mandic-Mulec, I. & Kolter, R. A combinatorial Kin discrimination system in *Bacillus subtilis*. *Curr. Biol.* **26**, 733–742 (2016).

50. Stefanic, P., Kraigher, B., Lyons, N. A., Kolter, R. & Mandic-Mulec, I. Kin discrimination between sympatric *Bacillus subtilis* isolates. *Proc. Natl Acad. Sci. USA* **112**, 14042–14047 (2015).
51. Overkamp, W. *et al.* Physiological and cell morphology adaptation of *Bacillus subtilis* at near-zero specific growth rates: a transcriptome analysis. *Environ. Microbiol.* **17**, 346–363 (2015).
52. Agashe, D. *et al.* Large-effect beneficial synonymous mutations mediate rapid and parallel adaptation in a bacterium. *Mol. Biol. Evol.* **33**, 1542–1553 (2016).
53. Bailey, S. F., Hinz, A. & Kassen, R. Adaptive synonymous mutations in an experimentally evolved *Pseudomonas fluorescens* population. *Nat. Commun.* **5**, 4076 (2014).
54. Davies, E. V. *et al.* Temperate phages both mediate and drive adaptive evolution in pathogen biofilms. *Proc. Natl Acad. Sci. USA* **113**, 8266–8271 (2016).
55. Kobayashi, K. *Bacillus subtilis* pellicle formation proceeds through genetically defined morphological changes. *J. Bacteriol.* **189**, 4920–4931 (2007).
56. Carver, T., Thomson, N., Bleasby, A., Berriman, M. & Parkhill, J. DNAPlotter: circular and linear interactive genome visualization. *Bioinformatics* **25**, 119–120 (2009).
57. Kearse, M. *et al.* Geneious Basic: an integrated and extendable desktop software platform for the organization and analysis of sequence data. *Bioinformatics* **28**, 1647–1649 (2012).

Acknowledgements

We are grateful to Christian Kost and Michael Brockhurst for helpful discussions. *B. subtilis* strain SPmini was kindly provided by Prof Tsutomu Sato (Research Center of Micro-Nano Technology, Hosei University). This work was funded by grant KO4741/2-1 from the Deutsche Forschungsgemeinschaft (DFG) within the priority program SPP1617 and a Startup Fund from Jena School for Microbial Communications (JSMC). MG was supported by GINOP-2.3.2-15-2016-00011 (EU Structural Funds). T.H. and A.D. were supported by International Max Planck Research School and Alexander von Humboldt foundation fellowships, respectively.

Author contributions

A.T.K. conceived the project; M.M., A.D., T.H., and A.T.K. designed the research; M.M., A.D. and T.H. performed the research; M.M., A.D. and T.H. analysed the data; M.W. performed the electron microscopy; G.M. and B.B. performed and analysed genome resequencing; and M.M., A.D., T.H., and A.T.K. wrote the paper.

Additional information

Supplementary Information accompanies this paper at <http://www.nature.com/naturecommunications>

Competing interests: The authors declare no competing financial interests.

Reprints and permission information is available online at <http://npg.nature.com/reprintsandpermissions/>

How to cite this article: Martin, M. *et al.* *De novo* evolved interference competition promotes the spread of biofilm defectors. *Nat. Commun.* **8**, 15127 doi: 10.1038/ncomms15127 (2017).

Publisher's note: Springer Nature remains neutral with regard to jurisdictional claims in published maps and institutional affiliations.



This work is licensed under a Creative Commons Attribution 4.0 International License. The images or other third party material in this article are included in the article's Creative Commons license, unless indicated otherwise in the credit line; if the material is not included under the Creative Commons license, users will need to obtain permission from the license holder to reproduce the material. To view a copy of this license, visit <http://creativecommons.org/licenses/by/4.0/>

© The Author(s) 2017

Chapter 6

Sliding on the surface: bacterial spreading without an active motor

Published in: Environmental Microbiology (2017)

Minireview

Sliding on the surface: bacterial spreading without an active motor

Theresa Hölscher and Ákos T. Kovács *†*Terrestrial Biofilms Group, Institute of Microbiology, Friedrich Schiller University Jena, Jena, Germany.*

Summary

Bacteria are able to translocate over surfaces using different types of active and passive motility mechanisms. Sliding is one of the passive types of movement since it is powered by the pushing force of dividing cells and additional factors facilitating the expansion over surfaces. In this review, we describe the sliding proficient bacteria that were previously investigated in details highlighting the sliding facilitating compounds and the regulation of sliding motility. Besides surfactants that reduce the friction between cells and substratum, other compounds including exopolysaccharides, hydrophobic proteins, or glycopeptidolipids were discovered to promote sliding. Therefore, we present the sliding bacteria in three groups depending on the additional compound required for sliding. Despite recent accomplishments in sliding research there are still many open questions about the mechanisms underlying sliding motility and its regulation in diverse bacterial species.

Introduction

Most natural habitats of bacteria include abiotic or biotic surfaces like soil particles, the root mantle or even algal clusters in the ocean. Bacteria have therefore developed different mechanisms to move over such substrates, ranging from active appendage-mediated motility to

passive spreading. The first landmark classification of bacterial movement types was conducted by Henrichsen in 1972. He examined the movement of over 30 bacterial species on agar plates and classified them into the distinct types of swarming, swimming, gliding, twitching, sliding and darting, although the latter is not used anymore (Henrichsen, 1972). A major reason why his paper is still cited today despite novel findings regarding the underlying mechanisms is the precise definition he provided for each type of movement. These definitions are still practical even though additional criteria were discovered since. Before Henrichsen's article, many of the movement types were just described as swarming or spreading and it was often not distinguished between the different surface colonization modes that exploit an active motor. In addition to the multicellular flagellum-driven swarming, these include type IV pilus-dependent twitching and focal adhesion complex supported gliding (Kearns, 2010). Further, swarming-based collective motility might be facilitated by additional secreted proteins, promoting wandering colony formation during surface colonization (Kobayashi *et al.*, 2016). Contrary to surface colonization that requires active appendages, sliding is defined as a passive bacterial translocation created by expansive forces accelerated by surfactants that reduce surface tension (Henrichsen, 1972; Kearns, 2010). The original definition of sliding also incorporated colony growth (Henrichsen, 1972). However, it was recently recognized that bacterial sliding necessitates more constituents than previously assumed. In this review, we present an overview of the various components required for expansion and describe bacteria in which sliding was investigated in more detail to divide them in three groups according to the so far characterized sliding facilitating machinery (Fig. 1). We are aware that new discoveries of sliding mechanisms could possibly require regrouping of the below discussed bacteria or result in a system with additional groups. Some of the spreading mechanisms characterized as sliding might even have an underlying active part that is not known yet, as suggested before (Shrout, 2015). However, we provide a first attempt of classifying the sliding proficient

Received 2 February, 2017; revised: 20 March, 2017; accepted 23 March, 2017. *For correspondence. E-mail atkovacs@dtu.dk; Tel. (+45) 4525 2600; Fax (+45) 4588 4922 †Department of Biotechnology and Biomedicine, Technical University of Denmark, Denmark.

bacteria since the current knowledge of different sliding mechanisms is still very limited and does therefore not allow a more sophisticated system.

In the first group, we describe bacteria that require only the pushing force of cell division and a secreted surfactant (considering state-of-the-art research). Bacterial sliding that involves additional secreted components like exopolysaccharides is illustrated in group II. Finally, group III is composed of bacteria that necessitate growth and another component, but no surfactant. In this review we focus on the bacterial species in which the sliding mechanism was investigated more extensively. Henrichsen (1972) depicted also other species capable of sliding, however, to our knowledge the sliding behaviour of those bacteria was not examined beyond that article or like in case of *Flavobacterium sp.* and *Acinetobacter calcoaceticus* surface spreading was correctly identified as gliding and twitching respectively (Henrichsen, 1984; Shrivastava and Berg, 2015; Shrout, 2015). In the following sections we will describe the sliding behaviour of different bacteria assigned to the above mentioned groups and elaborate about the so far known requirements and regulatory pathways involved.

Growth and surfactant dependent sliding (group I)

The opportunistic pathogen *Pseudomonas aeruginosa* belongs to group I since until now, rhamnolipid biosurfactants were the only secreted components found to be important for sliding (Fig. 2). Murray and colleagues discovered the sliding ability of *P. aeruginosa* when a *fliC pilA* double mutant, designed to be a negative control that can neither swarm nor twitch, was also spreading on semisolid agar plates (Murray and Kazmierczak, 2008). This type of movement was identified as sliding since swimming, swarming and twitching was not possible due to a lack of flagellin ($\Delta fliC$) and type IV pili ($\Delta pilA$). The requirement of rhamnolipids was confirmed by using a mutant lacking the gene responsible for the production of the rhamnolipid precursor that showed severely decreased sliding (Murray and Kazmierczak, 2008). The regulatory components important for sliding in *P. aeruginosa* overlap with the regulation of swarming and biofilm formation. The regulators identified were the two component system GacA/GacS (see the overview of regulatory pathways related to sliding in Table 1) that regulates swarming motility for which rhamnolipid production is also necessary. GacA/GacS is proposed to indirectly influence the expression of exopolysaccharide genes during biofilm formation. A random transposon mutagenesis experiment of the *fliC pilA* double mutant resulted in mutants with increased sliding behaviour and tendril formation that harboured transposon insertions in *gacA* and *gacS*. As tests with these hyper-sliders (*fliC*

pilA gacA triple mutant) showed no difference in rhamnolipid production and the lack of flagella and pili was confirmed, the response regulator GacA seems to target additional yet unknown genes responsible for the hyper-sliding phenotype (Murray and Kazmierczak, 2008). The transposon mutagenesis also revealed another regulator, RetS to be involved in sliding. The role of RetS during sliding was not investigated further, however, rhamnolipid production in the *fliC pilA retS* triple mutant was not reduced (Murray and Kazmierczak, 2008). The third type of regulatory pathway discovered to play a role in sliding included cyclic di-GMP. The SadC and BifA enzymes are responsible for cyclic di-GMP synthesis and degradation respectively. Similar to swarming, overexpression of *sadC* inhibited sliding whereas overexpression of *bifA* resulted in increased sliding (Kuchma *et al.*, 2007; Merritt *et al.*, 2007; Murray and Kazmierczak, 2008). In conclusion, it is possible that additional factors under control of the revealed regulators are also involved in sliding but not identified yet.

Another organism from the same genus, *Pseudomonas syringae* pv. tomato DC3000 is also capable of sliding over semi-solid surfaces with the help of a surfactant. *P. syringae* uses another lipopeptide, syringafactin to reduce the surface tension and thereby facilitate passive movement. While investigating the regulation of motility in *P. syringae*, Nogales *et al.* discovered that a *fleQ* mutant lacking the proposed master regulator of motility can spread over semi-solid agar in a distinct pattern despite lacking flagella (Nogales *et al.*, 2015). This spreading was proposed to be sliding motility based on its flagellum-independency. Further, the essentiality of syringafactin was demonstrated using a double mutant (lacking the first gene of the operon encoding enzymes for syringafactin production, *syfA* next to *fleQ*) that was unable to spread. Interestingly, the *fliC* mutant lacking only flagellin was unable to spread in comparison to the *fleQ* mutant which was explained by the difference in syringafactin production level: the authors discovered that the amount of syringafactin is 40% higher in the *fleQ* mutant compared with *fliC* mutant and wild-type (Nogales *et al.*, 2015). RNA-seq experiments revealed that the expression of the *syf* operon and of *syfR*, the transcriptional regulator presumably activating the *syf* operon, is upregulated in the *fleQ* mutant. These results suggest a negative regulation of *syfR* and therefore also of the *syf* operon by FleQ. Additionally, in plant experiments the *fleQ syfA* double mutant showed diminished disease symptoms suggesting that sliding contributes to *P. syringae* colonization of the leaf surface, a habitat where flagella-dependent movement might not be optimal (Nogales *et al.*, 2015).

Similarly, a *fleQ* mutant of the plant-growth promoting bacterium *Pseudomonas fluorescens* SBW25 was also

Table 1. Known sensing and regulatory components and their targets for several bacteria described in this review.

Organism	Known sensing and regulatory components	Target genes/operons
<i>P. aeruginosa</i>	GacA/GacS two component system RetS cyclic di-GMP	<i>rhlAB</i> ?
<i>P. syringae</i> pv tomato DC3000	FleQ-dependent inhibition	<i>syfR</i> operon
<i>S. marcescens</i>	ExpR	EPSII
<i>B.s subtilis</i>	KinB/C dependent Spo0A phosphorylation	<i>epsA-O</i>
<i>S. enterica</i> serovar Typhimurium	PhoP/PhoQ two component system	<i>pagM</i>

discovered to exhibit sliding motility on semi-solid medium with the same colony morphology. Here, the sliding facilitating compound was identified to be the surfactant viscosin (Alsohim *et al.*, 2014).

Likewise, *Serratia marcescens* is one of the organisms where sliding was found to be dependent on the pushing force of cell division and a secreted surfactant without other sliding facilitating compounds being revealed so far. This ubiquitous gram-negative enteric bacterium was shown to translocate over agar surfaces in the passive manner characteristic for sliding under conditions that do not allow flagellum dependent movement (i.e. high agar concentration)(Matsuyama *et al.*, 1992). Matsuyama and colleagues discovered that the movement of *S. marcescens* is dependent on the lipopeptide surfactant Serrawettin since mutants unable to produce it were not able to spread across the surface (Matsuyama *et al.*, 1992). Further, they showed that non-flagellated mutants could also spread over plates with a low agar concentration usually used to observe flagellum-dependent movement (Matsuyama *et al.*, 1995). Spreading was abolished when the strain was defective for Serrawettin production but was restored with exogenously supplied Serrawettin. Notably, not only Serrawettin promoted spreading but also several surfactants of other bacterial species were able to complement Serrawettin defective *S. marcescens* strains (Matsuyama *et al.*, 1995). This suggests a purely functional role of lowering the surface tension to promote movement. As surface colonization was not dependent on flagella or chemotaxis components, the authors suggested a passive type of spreading which is fitting to the definition of sliding.

The gram-negative pneumonia-causing bacterium *Legionella pneumophila* also belongs to the group of bacteria that slide over surfaces with the help of a surfactant. *L. pneumophila* can spread over semi-solid agar plates in a 'lobed, wavelike pattern' as well as many other *Legionella* species (Stewart *et al.*, 2009). This behaviour was the first observation of surface translocation in *L. pneumophila* and was evident in the wild-type as well as in single and double mutants lacking the genes for flagellin (*flaA* mutant) and the type IV pilus (*pilE* mutant).

These results excluded the contribution of flagella and pili to the observed surface spreading mechanism that was therefore identified as sliding. Additionally, a translucent film was detected for all spreading *Legionella* species including the mentioned *L. pneumophila* mutants advancing well in front of the cells. Extracts of spreading plates with the film showed drop collapse and friction reduction characteristics indicating the presence of a surfactant molecule that presumably facilitates sliding (Stewart *et al.*, 2009). However, the composition of this film was not analysed in detail.

Because of the evolutionary relation of the type IV pilus and the type II secretion system (TIIS), mutants lacking different components of the TIIS were also tested for their sliding ability. Interestingly, all TIIS mutants were defective in sliding and did not show the characteristic film (Stewart *et al.*, 2009). However, when spotted on the film of the wild-type, sliding was restored suggesting that the TIIS mutants lack the secreted surfactant of *L. pneumophila*. There are several possible links between the TIIS and surfactant secretion: (i) the surfactant is secreted via the TIIS, (ii) the surfactant is modified by an enzyme secreted by the TIIS, and (iii) a regulatory network involved in surfactant production is influenced by the TIIS (Stewart *et al.*, 2009). Although the sliding-facilitating surfactant has not been identified yet in this species, it was shown in a subsequent study that *L. pneumophila* excretes a surfactant that exhibits antimicrobial activity towards other *Legionella* species and its production depends on lipid metabolism and the outer membrane protein TolC (Stewart *et al.*, 2011).

Exopolysaccharide facilitated sliding (group II)

Sliding motility of *Bacillus subtilis*, a gram-positive soil-dwelling bacterium, depends on a surfactant as well as exopolysaccharides, therefore it is presented in group II. This type of surface motility of *B. subtilis* was discovered while examining rhizosphere derived strains that exhibited a distinct dendritic growth pattern in a flagellum-independent manner (Kinsinger *et al.*, 2003; Fall *et al.*, 2006). If sufficient amounts of potassium ions were supplied in the medium, initial dendritic growth was followed by planar spreading (Kinsinger *et al.*, 2003). This transition

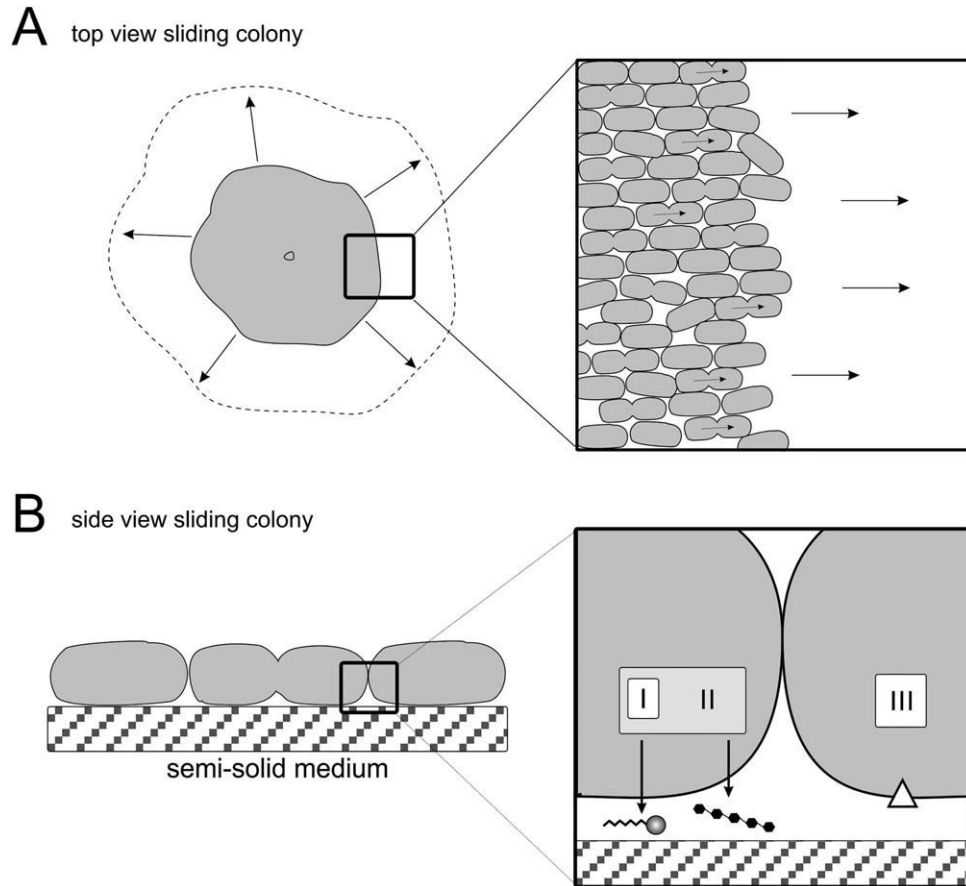


Fig. 1. Mechanism of sliding motility.

(A) Top view of an expanding sliding colony (left). On the right, a magnification of the marked region on the edge of the colony is depicted showing the expansion powered by the pushing force of dividing cells (arrows).

(B) Side view of a monolayer of cells at the edge of a sliding colony (left). The magnification highlights that sliding is promoted by a secreted surfactant (Group I, left), by a surfactant and exopolysaccharides (Group II, middle) or by an additional compound in the absence of surfactant (Group III, right).

to planar growth was also shown to be dependent on sufficient levels of other macro- and micronutrients suggesting a model where tendrils sliding occurs at low nutrient concentrations and converts to planar sliding at higher nutrient concentrations (Fall *et al.*, 2006). The potassium seemed to stimulate the production of surfactin, a cyclic lipopeptide surfactant which was shown to be necessary for *B. subtilis* sliding (Kinsinger *et al.*, 2003; Kinsinger *et al.*, 2005). Isolation of strains with reduced or diminished sliding using directed and random mutant screens led to the identification of additional genes connected to surfactin biosynthesis, growth or potassium transport, emphasizing the requirement of a surfactant and the pushing force of growing cells (Kinsinger *et al.*, 2005).

The requirement of exopolysaccharides (EPS) for *B. subtilis* sliding was recently demonstrated by two independent studies via mutant analysis and microarray experiments. Mutant strains lacking either the complete or part of the *epsA-O* operon whose products are

responsible for exopolysaccharide biosynthesis were not able to slide, showing that EPS is essential for sliding (Grau *et al.*, 2015; van Gestel *et al.*, 2015). Interestingly, the same *eps* gene cluster is also critical for *B. subtilis* biofilm formation (Vlamakis *et al.*, 2013).

The study by Grau *et al.* (2015) focussed on identifying the regulatory network governing sliding motility. Spo0A, a master regulator of various cellular processes in *B. subtilis* such as biofilm formation, sporulation, and cannibalism was found to be also the key modulator of sliding motility (Grau *et al.*, 2015). In addition to EPS, the microarray approach highlighted the differential expression of the *bslA* gene that encodes a bacterial hydrophobin protein. Mutant analysis proved that BslA is as indispensable for sliding as EPS production and surfactin secretion. The level of phosphorylated, and therefore transcriptionally active Spo0A in *B. subtilis* is modulated by soluble and membrane bound histidine kinases via a phosphorelay. Detailed analysis demonstrated that two of these kinases,


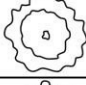





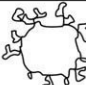

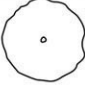

Group	Bacterium	Sliding facilitating component	Sliding morphology
I	<i>Serratia marcescens</i>	lipopeptide surfactant serrawettin	
	<i>Pseudomonas aeruginosa</i>	rhamnolipid biosurfactant	
	<i>Pseudomonas syringae</i> pv. tomato DC3000	lipopeptide surfactant syringafactin	
	<i>Pseudomonas fluorescens</i> SBW25	lipopeptide surfactant viscosin	
	<i>Legionella pneumophila</i>	unidentified surfactant	
II	<i>Bacillus subtilis</i>	surfactin, exopolysaccharides, protein BslA	 
	<i>Sinorhizobium meliloti</i>	siderophore rhizobactin, exopolysaccharide EPSII	
III	<i>Salmonella enterica</i> serovar Typhimurium	protein PagM	
	<i>Mycobacterium smegmatis</i>	acetylated glycopeptidolipids	 

Fig. 2. Bacteria discussed in this review are depicted that are capable of sliding.

The group species are categorized, the compound(s) that facilitate sliding, and the morphology of the individual sliding colonies are indicated.

KinB and KinC are required for sliding (Grau *et al.*, 2015), while KinB is possibly active on the edge of the sliding colony, KinC is rather active in the interior. Further, the level of phosphorylated Spo0A sufficient to activate sliding motility is lower than for triggering biofilm formation and sporulation suggesting that sliding occurs before biofilm formation (Grau *et al.*, 2015). Therefore, the fine modulation of active Spo0A-level allows the precise expression of genes leading to the distinct developmental pathways in *B. subtilis* (Kovács, 2016). In addition, the domain of the KinB kinase that resembles the selectivity sequence of the pore loop domain of eukaryotic potassium channels was demonstrated to be essential for sliding in response to the presence of potassium ions whose importance was also shown before (see above).

In the study of Grau *et al.* (2015), sliding was investigated mainly on rich medium with possibly higher potassium concentrations resulting in planar sliding colonies (Grau *et al.*, 2015). In contrast, van Gestel and colleagues used a minimal medium with low potassium

levels promoting sliding in a dendritic form (Fall *et al.*, 2006; van Gestel *et al.*, 2015). In this later study, the focus was brought on the differentiation of cells during sliding and how it affects migration. Additionally to EPS and the already known surfactin the authors identified also another component of the *B. subtilis* biofilm matrix, the protein TasA to be necessary for sliding (van Gestel *et al.*, 2015). While *tasA* was found to be unnecessary for sliding by Grau *et al.*, the differences could originate from different sliding modes. When mixed, different mutants of these components (surfactin, EPS, TasA) were able to at least partially complement each other for sliding, occasionally even performing better than the wild-type demonstrating the advantage of division of labour (van Gestel *et al.*, 2015). Using reporter strains, the temporal expression of genes involved in surfactin and matrix production was examined revealing a peak of surfactin producing cells at the early stage of dendrite formation followed by an increase of matrix producers. These cell types showed a distinct spatial arrangement

during the outgrowth of the dendrites. The matrix producers were located in bundles formed by chains of cells (so called 'van Gogh bundles') whereas the surfactin producers surrounded these bundles in a less coordinated form. When mutant strains were mixed to complement the sliding behaviour, the bundles contained only matrix producers, thereby demonstrating the requirement of the matrix producing cell type for bundle formation. The formation of bundles promoted the appearance of larger loops at the rim of the sliding expansion as demonstrated by time lapse experiments. These loops were suggested to facilitate migration in agreement with modelling experiments on the importance of loop formation on spreading (van Gestel *et al.*, 2015).

In summary, two hypotheses were proposed on the importance of EPS during sliding: van Gestel and colleagues demonstrated its requirement for bundle formation which in turn allows expansion, whereas Grau *et al.* proposed that EPS promotes spreading by generating osmotic pressure as shown for biofilms (Seminara *et al.*, 2012; Grau *et al.*, 2015). However, both hypotheses might actually be valid since two slightly different forms of sliding (dendritic and planar) were investigated in these studies. Importantly, both studies highlight the alternative functions of the extracellular matrix that in addition to be essential for biofilm development, also necessary for other processes, including surface spreading via sliding (Dragoš and Kovács, 2017).

In *Sinorhizobium meliloti*, sliding was also reported to facilitate surface movement of this gram-negative soil-dwelling bacterium. During investigations of discrepancies about the requirement of the quorum-sensing transcriptional regulator ExpR for swarming, it was discovered that *S. meliloti* strains harbouring a functional ExpR could spread over semisolid medium in a way atypical for swarming whereas mutants lacking ExpR were not able to spread (Nogales *et al.*, 2012). As strains lacking the flagellum behaved similarly, the surface movement was suggested to be sliding. As ExpR is among others responsible for the regulation of exopolysaccharide production in *S. meliloti*, a mutant unable to produce EPSII (galactoglucan) was investigated and found to be deficient in sliding (Nogales *et al.*, 2012). Similar to *B. subtilis*, EPSII could generate an osmotic pressure gradient which drives surface spreading in *S. meliloti* (Seminara *et al.*, 2012). Additionally, the authors claimed to have identified another type of movement that is independent of ExpR and flagella since an *expR* mutant without flagella was still able to colonize a semisolid minimal medium (Nogales *et al.*, 2012). This spreading was found to be dependent on siderophore rhizobactin production since mutation in the corresponding gene abolished spreading. It seems plausible that rhizobactin can act as a wetting agent and thereby

contribute to facilitate spreading (Nogales *et al.*, 2012). We hypothesize that this second type of movement could be also considered as sliding and while both rhizobactin and EPSII could promote surface colonization, secretion of either components is sufficient for spreading. When ExpR is intact EPSII can be produced and rhizobactin is not necessarily required but when ExpR and therefore also EPSII are missing and the iron concentration is low, rhizobactin can be produced and rescue sliding by acting as a wetting agent.

In addition to the laboratory conditions, the importance of sliding for *S. meliloti* in a natural habitat was demonstrated. *S. meliloti* is one of the bacteria known as rhizobia which can form a symbiotic interaction with legume plants where they fix nitrogen and provide it to the plant in exchange for nutrients. After recognition and entry into the root hair, *S. meliloti* invades the apoplast of the root hair via so called infection threads (e.g. Gage and Margolin, 2000). Fournier and colleagues found that *S. meliloti* forms clusters in these threads that move forward and become longer over time (Fournier *et al.*, 2008). This observation led them to conclude that sliding might facilitate infection thread colonization, additionally supported by the fact that rhizobia in the infection thread lack flagella (Gage and Margolin, 2000; Fournier *et al.*, 2008). This study represents one of the few examples where sliding was analysed in a natural setting and shows that there are indeed conditions under which it might be useful for a bacterium to slide.

Surfactant independent sliding (group III)

Bacteria belonging under the last category similarly require the pressure of growing cells for sliding but rather depend on an additional factor and not surfactant. For sliding of *Salmonella enterica* serovar Typhimurium under low Mg^{2+} conditions, the protein PagM was identified by mutant analysis (Park *et al.*, 2015). This protein seems to facilitate spreading through a surface protein (i.e. by being a surface protein itself or being connected to a so far unidentified one) since the sliding ability of a *pagM* mutant could be complemented in the presence of a strain with an intact *pagM* gene while proteinase treatment abolished this sliding. PagM is regulated by the PhoP/PhoQ system which is induced under low Mg^{2+} conditions (Park *et al.*, 2015). Interestingly, this protein can be identified uniquely in *S. enterica* which suggests a form of sliding that is slightly different from the above described mechanisms.

Another distinct sliding-facilitating mechanism was described for *Mycobacterium smegmatis*. As this gram-positive bacterium belongs to the generally non-flagellated genus of *Mycobacteria*, it was long believed to be impaired in any kind of translocation. Yet, it was

discovered that after several days of incubation, *M. smegmatis* is able to spread over the surface of semisolid plates (Martínez *et al.*, 1999). Interestingly, the spreading morphology was dependent on whether the medium was solidified using agar-agar or agarose, resulting in thin finger-like structures or a circular spreading front respectively. Using the circular spreading as a model, electron microscopic analysis revealed a distinct organization of cells in pseudo-filaments that were connected at distinct positions of the cells and not only at the poles. Further, it was confirmed that the spreading is accompanied by growth and almost no re-arrangement of the cells was observed in the spreading zone, indicating sliding (Martínez *et al.*, 1999). An investigation of different *M. smegmatis* colony variants uncovered the impaired sliding of a rough variant compared with the rather smooth wild-type. This led to the hypothesis that glycopeptidolipids (GPLs), molecules that are part of the outer layer of some mycobacterial

capsules, are connected to sliding since previous studies showed a correlation of a rough phenotype with a reduced amount of GPLs. Lipid extracts were analysed and showed a GPL characteristic pattern for the wild-type which was absent in the rough variant indicating that indeed GPL are facilitating *M. smegmatis* spreading (Martínez *et al.*, 1999). In a subsequent study, a transposon mutagenesis resulted in several mutants that lost the ability to slide (Recht *et al.*, 2000). All of them showed rough colony morphology and no GPLs could be detected in thin layer chromatography analyses. Almost all of the transposon insertions were located in the *mpe* gene encoding a non-ribosomal peptide synthetase involved in GPL biosynthesis thus providing a direct evidence for the importance of GPLs for sliding motility (Recht *et al.*, 2000). Only one additional mutant exhibiting a similar phenotype was identified to contain a transposon insertion in a gene coding for a putative membrane transporter (*tmtpC*) that could possibly be

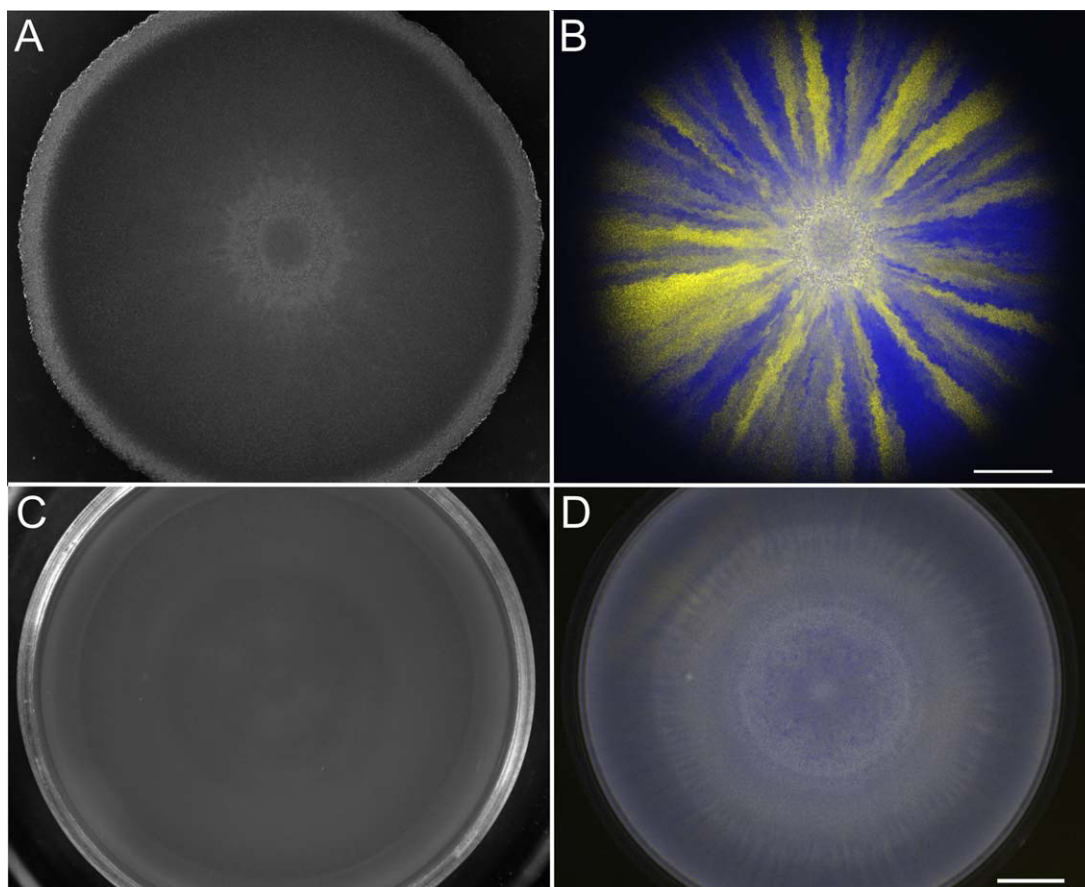


Fig. 3. Dissimilar spatial segregation levels can be appreciated in sliding and swarming colonies of *B. subtilis*.

To initiate sliding, two strains of *B. subtilis* *hag* mutant with different fluorescent markers were used. Similarly, the two *B. subtilis* strains that were used as inoculum for swarming possessed different fluorescent markers in the wild-type genetic background. Bright field images of sliding (A) and swarming (C) colonies. Overlay of the two fluorescent images with false colours (B, D). The semi-solid agar plates were incubated for 24h and 10h at 37°C for sliding and swarming, respectively, based on the methodology as described in Hölscher *et al.*, (2016). The scale bars correspond to 5 mm. [Color figure can be viewed at wileyonlinelibrary.com]

involved in carrying the GPLs across the cytoplasmic membrane. A defect in this type of sliding could not be fully complemented by surfactants like Serrawettin, purified GPLs or the presence of a sliding-proficient strains demonstrating the importance of cell envelope bound GPLs (Recht *et al.*, 2000).

Additionally, GPLs seem to be important for biofilm formation since the GPL deficient rough variants were not able to form biofilms attached to a plastic surface (Recht *et al.*, 2000). An additional screen of a transposon mutant library for impaired biofilm formation revealed a mutant with an intermediate phenotype in which sliding and biofilm formation were both diminished but not completely abolished (Recht and Kolter, 2001). In this mutant, a transposon was inserted in the *atf1* gene that encodes a putative acetyl transferase and is located in a GPL biosynthesis gene cluster. An analysis of the GPLs suggested that the product of *atf1* is responsible for acetylation of the GPLs. Based on these studies the following model was proposed: GPLs in the outermost layer of the *M. smegmatis* cell envelope increase the cell surface hydrophobicity therefore facilitating sliding and biofilm formation. Without or with non-acetylated GPLs, the cell surface is more hydrophilic leading to abolished or reduced sliding and biofilm formation respectively (Recht and Kolter, 2001).

Concluding remarks

In summary, a number of bacteria have been identified that are capable of passively migrating over surfaces, considered to be sliding. We described here three groups according to the sliding mechanism and necessary components. Notably, it is possible that some of the organisms e.g. from Group I belong actually to Group II, but the additional components contributing to sliding motility are yet to be discovered.

In addition, social interactions during sliding can be compared with swarming and biofilm formation. For example, spatial segregation can be dissimilar (Fig. 3), which might have an ultimately different impact on the adaptation and evolution of bacteria (Hölscher *et al.*, 2016; Martin *et al.*, 2016).

Many regulators and components important during sliding are also necessary for other processes like surfactants for swarming and exopolysaccharides for biofilm formation. Thus, it is possible that sliding motility represents an intermediate stage between different developmental processes under conditions that favours neither one nor the other and it might be an innovative way to exploit components evolved for other processes. In conclusion, it is very likely that so far we have only seen the tip of the iceberg and many other organisms are able to slide over surfaces.

Acknowledgements

This work was funded by grant KO4741/3-1 from the Deutsche Forschungsgemeinschaft (DFG). Further, the laboratory of Á.T.K. was supported by a Marie Skłodowska Curie career integration grant (PheHetBacBiofilm) and grant KO4741/2-1 from DFG. T.H. was supported by International Max Planck Research School.

Conflict of Interest

The authors declare no conflict of interest.

References

- Alsohim, A.S., Taylor, T.B., Barrett, G.A., Gallie, J., Zhang, X.X., Altamirano-Junqueira, A.E., *et al.* (2014) The bio-surfactant viscosin produced by *Pseudomonas fluorescens* SBW25 aids spreading motility and plant growth promotion. *Environ Microbiol* **16**: 2267–2281.
- Dragoš, A., and Kovács, Á.T. (2017) The peculiar functions of the bacterial extracellular matrix. *Trends Microbiol* **25**: 257–266.
- Fall, R., Kearns, D.B., and Nguyen, T. (2006) A defined medium to investigate sliding motility in a *Bacillus subtilis* flagella-less mutant. *BMC Microbiol* **6**: 31.
- Fournier, J., Timmers, A.C., Sieberer, B.J., Jauneau, A., Chabaud, M., and Barker, D.G. (2008) Mechanism of infection thread elongation in root hairs of *Medicago truncatula* and dynamic interplay with associated rhizobial colonization. *Plant Physiol* **148**: 1985–1995.
- Gage, D.J., and Margolin, W. (2000) Hanging by a thread: invasion of legume plants by rhizobia. *Curr Opin Microbiol* **3**: 613–617.
- Grau, R.R., de Ona, P., Kunert, M., Lenini, C., Gallegos-Monterrosa, R., Mhatre, E., *et al.* (2015) A Duo of Potassium-Responsive Histidine Kinases Govern the Multicellular Destiny of *Bacillus subtilis*. *MBio* **6**: e00581.
- Henrichsen, J. (1972) Bacterial surface translocation: a survey and a classification. *Bacteriol Rev* **36**: 478–503.
- Henrichsen, J. (1984) Not gliding but twitching motility of *Acinetobacter calcoaceticus*. *J Clin Pathol* **37**: 102–103.
- Hölscher, T., Dragoš, A., Gallegos-Monterrosa, R., Martin, M., Mhatre, E., Richter, A., and Kovács, Á.T. (2016) Monitoring Spatial Segregation in Surface Colonizing Microbial Populations. *J Vis Exp* **116**: e54752.
- Kearns, D.B. (2010) A field guide to bacterial swarming motility. *Nat Rev Microbiol* **8**: 634–644.
- Kinsinger, R.F., Shirk, M.C., and Fall, R. (2003) Rapid surface motility in *Bacillus subtilis* is dependent on extracellular surfactin and potassium ion. *J Bacteriol* **185**: 5627–5631.
- Kinsinger, R.F., Kearns, D.B., Hale, M., and Fall, R. (2005) Genetic requirements for potassium ion-dependent colony spreading in *Bacillus subtilis*. *J Bacteriol* **187**: 8462–8469.
- Kobayashi, K., Kanesaki, Y., and Yoshikawa, H. (2016) Genetic analysis of collective motility of *Paenibacillus* sp. NAIST15-1. *PLoS Genet* **12**: e1006387.
- Kovács, Á.T. (2016) Bacterial differentiation via gradual activation of global regulators. *Curr Genet* **62**: 125–128.

- Kuchma, S.L., Brothers, K.M., Merritt, J.H., Liberati, N.T., Ausubel, F.M., and O'toole, G.A. (2007) BifA, a cyclic-Di-GMP phosphodiesterase, inversely regulates biofilm formation and swarming motility by *Pseudomonas aeruginosa* PA14. *J Bacteriol* **189**: 8165–8178.
- Martin, M., Hölscher, T., Dragoš, A., Cooper, V.S., and Kovács, Á.T. (2016) Laboratory Evolution of Microbial Interactions in Bacterial Biofilms. *J Bacteriol* **198**: 2564–2571.
- Martínez, A., Torello, S., and Kolter, R. (1999) Sliding motility in mycobacteria. *J Bacteriol* **181**: 7331–7338.
- Matsuyama, T., Bhasin, A., and Harshey, R.M. (1995) Mutational analysis of flagellum-independent surface spreading of *Serratia marcescens* 274 on a low-agar medium. *J Bacteriol* **177**: 987–991.
- Matsuyama, T., Kaneda, K., Nakagawa, Y., Isa, K., Hara-Hotta, H., and Yano, I. (1992) A novel extracellular cyclic lipopeptide which promotes flagellum-dependent and -independent spreading growth of *Serratia marcescens*. *J Bacteriol* **174**: 1769–1776.
- Merritt, J.H., Brothers, K.M., Kuchma, S.L., and O'toole, G.A. (2007) SadC reciprocally influences biofilm formation and swarming motility via modulation of exopolysaccharide production and flagellar function. *J Bacteriol* **189**: 8154–8164.
- Murray, T.S., and Kazmierczak, B.I. (2008) *Pseudomonas aeruginosa* exhibits sliding motility in the absence of type IV pili and flagella. *J Bacteriol* **190**: 2700–2708.
- Nogales, J., Bernabéu-Roda, L., Cuéllar, V., and Soto, M.J. (2012) ExpR is not required for swarming but promotes sliding in *Sinorhizobium meliloti*. *J Bacteriol* **194**: 2027–2035.
- Nogales, J., Vargas, P., Farias, G.A., Olmedilla, A., Sanjuan, J., and Gallegos, M.T. (2015) FleQ coordinates flagellum-dependent and -independent motilities in *Pseudomonas syringae* pv. tomato DC3000. *Appl Environ Microbiol* **81**: 7533–7545.
- Park, S.Y., Pontes, M.H., and Groisman, E.A. (2015) Flagella-independent surface motility in *Salmonella enterica* serovar Typhimurium. *Proc Natl Acad Sci U S A* **112**: 1850–1855.
- Recht, J., and Kolter, R. (2001) Glycopeptidolipid acetylation affects sliding motility and biofilm formation in *Mycobacterium smegmatis*. *J Bacteriol* **183**: 5718–5724.
- Recht, J., Martínez, A., Torello, S., and Kolter, R. (2000) Genetic analysis of sliding motility in *Mycobacterium smegmatis*. *J Bacteriol* **182**: 4348–4351.
- Seminara, A., Angelini, T.E., Wilking, J.N., Vlamakis, H., Ebrahim, S., Kolter, R., et al. (2012) Osmotic spreading of *Bacillus subtilis* biofilms driven by an extracellular matrix. *Proc Natl Acad Sci U S A* **109**: 1116–1121.
- Shrivastava, A., and Berg, H.C. (2015) Towards a model for *Flavobacterium* gliding. *Curr Opin Microbiol* **28**: 93–97.
- Shrout, J.D. (2015) A fantastic voyage for sliding bacteria. *Trends Microbiol* **23**: 244–246.
- Stewart, C.R., Rossier, O., and Cianciotto, N.P. (2009) Surface translocation by *Legionella pneumophila*: a form of sliding motility that is dependent upon type II protein secretion. *J Bacteriol* **191**: 1537–1546.
- Stewart, C.R., Burnside, D.M., and Cianciotto, N.P. (2011) The surfactant of *Legionella pneumophila* is secreted in a TolC-dependent manner and is antagonistic toward other *Legionella* species. *J Bacteriol* **193**: 5971–5984.
- van Gestel, J., Vlamakis, H., and Kolter, R. (2015) From cell differentiation to cell collectives: *Bacillus subtilis* uses division of labor to migrate. *PLoS Biol* **13**: e1002141.
- Vlamakis, H., Chai, Y., Beauregard, P., Losick, R., and Kolter, R. (2013) Sticking together: building a biofilm the *Bacillus subtilis* way. *Nat Rev Microbiol* **11**: 157–168.

Chapter 7

A duo of potassium-responsive histidine kinases govern the multicellular destiny of *Bacillus subtilis*

Published in: mBio (2015)

A Duo of Potassium-Responsive Histidine Kinases Govern the Multicellular Destiny of *Bacillus subtilis*

Roberto R. Grau,^a Paula de Oña,^a Maritta Kunert,^c Cecilia Leñini,^a Ramses Gallegos-Monterrosa,^b Eisha Mhatre,^b Darío Vileta,^a Verónica Donato,^a Theresa Hölscher,^b Wilhelm Boland,^c Oscar P. Kuipers,^d Ákos T. Kovács^b

Departamento de Microbiología, Facultad de Ciencias Bioquímicas y Farmacéuticas (FCByF), Universidad Nacional de Rosario (UNR)—CONICET, Argentina^a; Terrestrial Biofilms Group, Institute of Microbiology, Friedrich Schiller University of Jena, Jena, Germany^b; Department of Bioorganic Chemistry, Max Planck Institute for Chemical Ecology, Jena, Germany^c; Molecular Genetics, Groningen Biomolecular Sciences and Biotechnology Institute, University of Groningen, Groningen, The Netherlands^d

ABSTRACT Multicellular biofilm formation and surface motility are bacterial behaviors considered mutually exclusive. However, the basic decision to move over or stay attached to a surface is poorly understood. Here, we discover that in *Bacillus subtilis*, the key root biofilm-controlling transcription factor Spo0A~P_i (phosphorylated Spo0A) governs the flagellum-independent mechanism of social sliding motility. A Spo0A-deficient strain was totally unable to slide and colonize plant roots, evidencing the important role that sliding might play in natural settings. Microarray experiments plus subsequent genetic characterization showed that the machineries of sliding and biofilm formation share the same main components (i.e., surfactin, the hydrophobin BslA, exopolysaccharide, and *de novo*-formed fatty acids). Sliding proficiency was transduced by the Spo0A-phosphorelay histidine kinases KinB and KinC. We discovered that potassium, a previously known inhibitor of KinC-dependent biofilm formation, is the specific sliding-activating signal through a thus-far-unnoticed cytosolic domain of KinB, which resembles the selectivity filter sequence of potassium channels. The differential expression of the Spo0A~P_i reporter *abrB* gene and the different levels of the constitutively active form of Spo0A, Sad67, in $\Delta spo0A$ cells grown in optimized media that simultaneously stimulate motile and sessile behaviors uncover the spatiotemporal response of KinB and KinC to potassium and the gradual increase in Spo0A~P_i that orchestrates the sequential activation of sliding, followed by sessile biofilm formation and finally sporulation in the same population. Overall, these results provide insights into how multicellular behaviors formerly believed to be antagonistic are coordinately activated in benefit of the bacterium and its interaction with the host.

IMPORTANCE Alternation between motile and sessile behaviors is central to bacterial adaptation, survival, and colonization. However, how is the collective decision to move over or stay attached to a surface controlled? Here, we use the model plant-beneficial bacterium *Bacillus subtilis* to answer this question. Remarkably, we discover that sessile biofilm formation and social sliding motility share the same structural components and the Spo0A regulatory network via sensor kinases, KinB and KinC. Potassium, an inhibitor of KinC-dependent biofilm formation, triggers sliding via a potassium-perceiving cytosolic domain of KinB that resembles the selectivity filter of potassium channels. The spatiotemporal response of these kinases to variable potassium levels and the gradual increase in Spo0A~P_i levels that orchestrates the activation of sliding before biofilm formation shed light on how multicellular behaviors formerly believed to be antagonistic work together to benefit the population fitness.

Received 15 April 2015 Accepted 1 June 2015 Published 7 July 2015

Citation Grau RR, de Oña P, Kunert M, Leñini C, Gallegos-Monterrosa R, Mhatre E, Vileta D, Donato V, Hölscher T, Boland W, Kuipers OP, Kovács ÁT. 2015. A duo of potassium-responsive histidine kinases govern the multicellular destiny of *Bacillus subtilis*. mBio 6(4):e00581-15. doi:10.1128/mBio.00581-15.

Editor Roberto Kolter, Harvard Medical School

Copyright © 2015 Grau et al. This is an open-access article distributed under the terms of the Creative Commons Attribution-Noncommercial-ShareAlike 3.0 Unported license, which permits unrestricted noncommercial use, distribution, and reproduction in any medium, provided the original author and source are credited.

Address correspondence to Roberto R. Grau, robertograu@fulbrightmail.org, or Ákos T. Kovács, akos-tibor.kovacs@uni-jena.de.

How do bacteria move from one location to another in natural niches? Most bacteria are able to swim in aquatic environments powered by rotating flagella, whereas a range of different mechanisms have evolved that facilitate surface spreading (1–4). While swimming is considered to be an individual behavior, cells are able to migrate together and cooperatively during surface translocation (1, 3, 4). Surface movement can depend on the presence of flagella (i.e., swarming), the extension and retraction of type IV pili (i.e., twitching motility), the involvement of focal adhesion complexes (i.e., gliding), or “passive” surface translocation (i.e., sliding). Although the mechanisms of swarming, twitching, and gliding motilities have been extensively studied in most bac-

teria with appendages, the information about the mechanism of sliding, its regulation, and its importance is sparse. Since its original definition, more than 4 decades ago, the concept of sliding as a passive surface translocation driven by expansive forces in the growing colony has not varied much (2, 3). However, sliding motility represents a heavily exploited mechanism that different pathogens of global importance (i.e., *Bacillus anthracis*, *Salmonella enterica*, *Staphylococcus aureus*, *Legionella pneumophila*, and mycobacteria) use for spreading (3, 5, 6).

Bacillus subtilis is a Gram-positive endospore-forming bacterium that has been extensively studied due to its diverse differentiation processes (7–11). Different *B. subtilis* strains swarm on

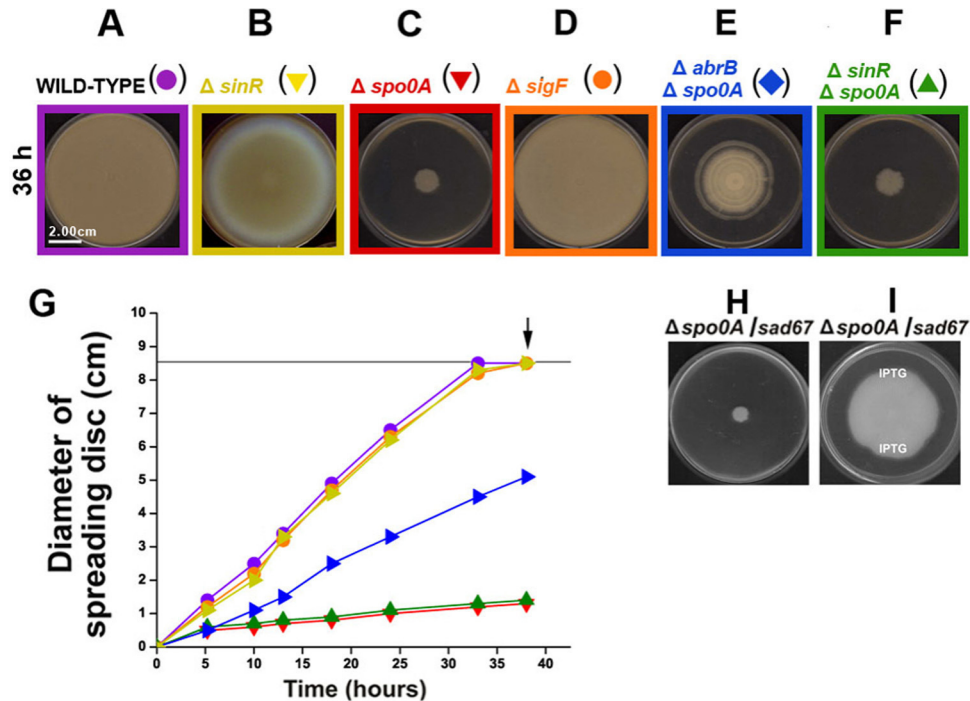


FIG 1 Revealing the genetic regulation of sliding motility in *B. subtilis*. (A to G) Sliding phenotype (A to F) and kinetic characterization (G) of different *B. subtilis* natto strains (see Table S1 in the supplemental material) affected in the expression of key regulators of gene expression. *B. subtilis* cells were cultured and inoculated on LB-0.7% agar plates as indicated in Materials and Methods. The arrows in panel G indicate the developmental times when the photographs shown in panels A to F were taken. Strain references for the symbols in panel G correspond to the reference colors shown in panels A to F. The horizontal black line at 8.5 cm shows the maximal size of motility related to the size of the agar plate used. Each value is the average from three replicates. (H and I) Active Spo0A (Sad67) triggers sliding motility in the *B. subtilis* natto strain. In the absence of IPTG supplementation, Spo0A-deficient but Sad67-positive cells are not motile on soft agar plates (H), but in the presence of IPTG, these cells recover full sliding proficiency (I). Solid IPTG, one or two grains, was poured on top of the solidified LB-0.7% agar (at the points indicated in panel I) in order to allow the dissolution of IPTG in the medium and the formation of a continuous gradient of the inducer.

semisolid agar plates (4, 12) or form architecturally complex biofilms with vein-like structures and apical tips (fruiting bodies) that project the formed spores into the air (7, 13–15). In addition, wild and undomesticated *B. subtilis* isolates (7, 16) have beneficial growth-promoting effects on plants and animals (17, 18) as well as probiotic effects in humans (19–21). If biofilm formation and an active surface motility are antagonistic but important attributes of a bacterium, how then is the collective decision to move over or stay attached to a surface taken and controlled? In this work, we use the model organism *B. subtilis* to investigate the genetic mechanism and regulatory network of sliding for surface colonization and their relationship with another prominent cooperative surface behavior, i.e., biofilm formation.

RESULTS AND DISCUSSION

The master regulator of sporulation and multicellular biofilm formation, Spo0A, controls sliding motility in *B. subtilis*. If bacteria use sliding in a cooperative manner to move across surfaces without the necessity for flagella or any other appendages, how does it take place and what are the regulatory networks that induce and control it? To solve this puzzle, we used two wild (undomesticated) *B. subtilis* strains of different genetic lineages, the Marburg-related strain NCIB3610, able to swarm and slide (7, 12, 22), and the human-probiotic natto-related strain RG4365 (16, 21), which only slides (see Fig. S1 in the supplemental material). It is known that the global transcription factor SinR is essential for the swimming and swarming motilities in *B. subtilis* (23). While,

as expected, the inactivation of *sinR* in the NCIB3610 strain yields a completely defective swarming phenotype (24), the inactivation of *sinR* in the RG4365 *B. subtilis* natto strain yields an almost unaffected sliding-proficient phenotype (Fig. 1A, B, and G). If SinR is not required to slide, is there any other transcription factor that contributes to the regulatory network of sliding? In *B. subtilis*, other multicellular and developmental programs (biofilm formation, fruiting body formation, and sporulation) are governed by the master transcription factor Spo0A of the phosphorelay signaling pathway (7, 25). Taking into account the dispensability of SinR activity for sliding proficiency, we wondered if this was also the case for Spo0A in sliding. Although swarming of an NCIB3610-isogenic *spo0A*-deletion strain was not affected (see below), a *spo0A*-deletion RG4365-derived strain was completely unable to slide on the agar surface (Fig. 1C and G). This result suggested that the master regulator of sporulation and biofilm formation, the protein Spo0A, would also be a key regulator of social sliding. The inactivation of *spoIIAC* (*sigF*), the distal gene of the tricistronic *spoIIA* operon, coding for the first compartment-specific sporulation sigma transcription factor (σ^F), did not affect the sliding phenotype of wild-type RG4365 cells (Fig. 1D and G) and suggested the independency of sliding from the sporulation program in *B. subtilis*. It is known that the absence of Spo0A activity results in an increase of the activities of the transcription factors SinR and AbrB (26) that could be responsible for the absence of sliding ability in the *spo0A* natto strain. If this were the case, the regulatory proteins SinR and/or AbrB could be an inhib-

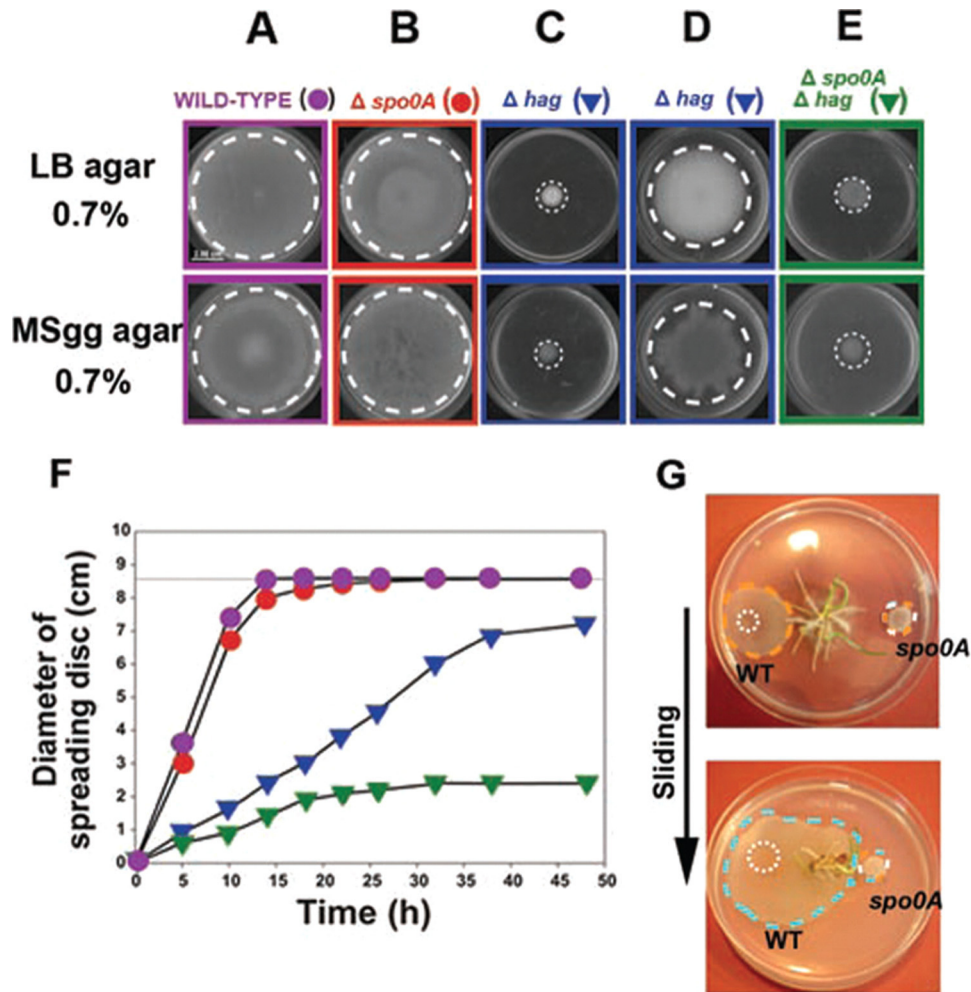


FIG 2 The key regulator of multicellular behavior, Spo0A, controls sliding motility in *B. subtilis*. (A and B) Spo0A activity is fully dispensable for the swarming proficiency of NCIB3610 cells. (C and D) Inactivation of flagellar synthesis (*hag* mutation) impairs swarming motility in NCIB3610 cells (C), but after a longer incubation (24 h or more), sliding proficiency is turned on in Hag-deficient cells (D). (E) Spo0A activity is essential for surface translocation ability of Hag-deficient cells. Photos shown in panels A to C and panels D and E correspond to the sliding migration of the indicated strains after 15 h and 40 h of incubation, respectively. (F) Kinetics of swarming and sliding motilities in Spo0A- and Hag-positive or -deficient NCIB3610 cells. (G) Important role of Spo0A and sliding proficiency for plant root colonization. As indicated in the supplemental material, as soon as sanitized wheat seeds germinated on LB-diluted agar plates, 3.0 μ l of stationary-phase cultures of wild-type and *spo0A* mutant cells was inoculated at the points indicated by the white dotted circles in the top panel. After 24 h of incubation, the wild-type (WT) and *spo0A* cells formed rounded colonies of similar size and appearance that were confined to the point of inoculation (data not shown). After 3 days of bacterial inoculation, wild-type cells, but not the *spo0A* cells, efficiently slid on the agar surface (the boundaries of the sliding disc are denoted by the orange dashed circle in the top panel). After 5 days (bottom panel), the wild-type cells were able to colonize the root rhizosphere (blue dashed circle) while the *spo0A* cells remained immobilized. Representative images of several independent experiments are shown.

itor of sliding motility. As shown in Fig. 1E to G, the inactivation of *abrB* but not *sinR* was able to restore (although only partially) the sliding ability of Spo0A-deficient cells and suggested that AbrB was negatively controlling the expression of at least one gene whose product was necessary for sliding proficiency (see below). To confirm the essential role of Spo0A for the proficiency of social sliding in *B. subtilis*, we constructed an RG4365-derived strain that harbored, in addition to a deletion of the wild-type copy of *spo0A*, an isopropyl- β -D-thiogalactopyranoside (IPTG)-inducible form of Spo0A (Sad67) that is active in the absence of phosphorylation (phosphorelay independent) (27–29). As shown in Fig. 1H and I, the supplementation with IPTG restored the sliding ability of the *spo0A*-deletion but Sad67-carrying strain and confirmed the essential role of Spo0A for social sliding proficiency in *B. subtilis*.

How widespread is sliding motility and how conserved is the role of Spo0A in different *B. subtilis* isolates? Although flagellum production is essential for swarming motility in the Marburg-related strain NCIB3610 (12), it has been reported that NCIB3610-derived *hag* strains (unable to make flagella) are able to slide on solid surfaces after longer periods of incubation (24 h or more) (30). Therefore, we wanted to know if the essential role of Spo0A for sliding proficiency in the *B. subtilis* natto strain is also manifest in Marburg-derived cells. To this end, we analyzed the surface translocation ability of different NCIB3610-derived strains under two experimental conditions: incubation on soft Luria-Bertani (LB) medium as shown in previous work and the conditions previously used by other groups, i.e., soft minimal salts glycerol glutamate (MSgg) agar medium, to investigate the sliding

ability of Marburg cells (31). As shown in Fig. 2, the inactivation of *spo0A* in NCIB3610 cells did not affect their motility behavior (compare Fig. 2A and B). As expected, the interruption of flagellin synthesis in the NCIB3610 *hag*-derived strain RG4384 (see Table S1 in the supplemental material) blocked the surface translocation in both soft media as monitored at a developmental time of 20 h (Fig. 2C). However, after longer incubation, the NCIB3610 *hag* cells moved on the agar surface by a sliding mechanism as previously reported (Fig. 2D) (31). Remarkably, the inactivation of *spo0A* in the Marburg-derived *hag* strain (Δ *hag* Δ *spo0A* double mutant strain RG4385 [see Table S1]) completely abolished the ability of these flagellum-less and Spo0A-deficient NCIB3610-derived cells to translocate on the agar surface and confirmed the key role of Spo0A as the master regulator of social sliding motility in *B. subtilis* (Fig. 2E and F).

What might be the importance of bacterial sliding in nature? *B. subtilis* is a beneficial bacterium that improves plant and animal growth (17, 18) as well as possessing advantageous probiotic properties in humans (19, 21). One desired attribute of a host-colonizing bacterium is the ability to spread over and colonize a particular niche (i.e., the rhizosphere) and establish a long-lasting community (i.e., a biofilm) associated with the host (19, 32). Notably, as shown in Fig. 2G, Spo0A plays a key role in the ability of the plant growth-promoting rhizobacterium *B. subtilis* (33, 34) to activate social sliding and colonize the root rhizosphere.

Microarray analysis of *B. subtilis* cells under sliding conditions. Our initial analysis uncovered the novel roles of the transcription factors AbrB and Spo0A as a repressor and an activator of sliding, respectively. What other genes are important for sliding proficiency in *B. subtilis* and what is the role of AbrB and Spo0A in their expression? To answer these questions, we performed microarray experiments under different environmental conditions and in various genetic backgrounds. On the one hand, we compared the global gene expression of the *spo0A* mutant RG4370 with that of the wild-type natto strain RG4365 on LB plates with a 0.7% agar concentration, where, as was shown, the wild-type and the *spo0A* mutant strains were proficient and impaired in sliding, respectively (see Table S2A in the supplemental material). In a second type of experiment, we examined wild-type cells under sliding-restrictive conditions using LB plates with a 1.5% agar concentration and compared their transcriptome with the pattern of gene expression under sliding-permissive conditions on 0.7% agar plates (see Table S2B). These microarray analyses showed that 310 and 295 genes were significantly (P value, $<10^{-4}$) up- or downregulated in the *spo0A* mutant strain compared to the wild-type strain, respectively, while 72 and 100 genes were found to be up- and downregulated, respectively, at an increased agar concentration (see Table S2).

Interestingly, most of the genes belonging to the σ^D regulon, which is related to flagellum motility and chemotaxis, were activated in the *spo0A* mutant strain under sliding-permissive conditions. However, the *B. subtilis* natto strain lacks flagella under this and all tested genetic backgrounds (see Fig. S1E to G in the supplemental material and data not shown). It has been suggested that Marburg-related wild-type cells (i.e., NCIB3610) lack flagellum production for translocation on solid surfaces depending on extracellular surfactin and potassium ion (22). More recently, it was shown that synthesis of the exopolysaccharide (EPS) of the extracellular matrix is genetically coupled to the inhibition of

flagellum-mediated motility (23), and as we show below, EPS expression is increased under sliding-permissive conditions.

While mutation in *spo0A* resulted in differential expression of various genes under sliding-permissive conditions on LB medium, we did not find any sporulation-related gene in the wild-type strain to be differentially expressed under this experimental condition (sliding turned on [see Table S2A in the supplemental material]). One simple explanation for this observation is that under the condition used (i.e., rich LB medium and sliding-permissive conditions), sporulation is not activated in the wild-type strain and, therefore, mutation in *spo0A* has no effect on these genes in the wild-type strain during sliding. In contrast, we observed elevated expression of sporulation σ^G -dependent genes in wild-type cells grown under non-sliding-permissive conditions (higher agar concentration [see Table S2B in the supplemental material]). This induction of sporulation genes in samples from 1.5% agar plates is probably due to the fact that under this sliding-restrictive condition, *B. subtilis* cannot spread, nutrients around cells become limited, and sporulation is started similarly to the conditions during formation of complex colony biofilms (11, 35, 36).

Which other genes are expressed during active sliding? We found that in wild-type cells under sliding-permissive conditions (see Table S2B in the supplemental material) and in comparison to the *spo0A* mutant strain (see Table S2A), genes related to biofilm matrix production (*sipW*, *tasA*, and *eps* in the case of the *spo0A* mutant), biofilm surface layer (*bslA*), fatty acid synthesis (*fab*), and surfactin synthesis (*srfAC* in the case of the *spo0A* mutant) were upregulated.

Sliding but not swarming depends on the *bslA* and *eps* genes. The microarray experiments presented above showed that genes related to biofilm formation and biofilm surface layer are upregulated under the conditions when sliding is feasible and suggest that this gene repertoire could include novel and necessary components of the sliding machinery in *B. subtilis* (Fig. 3A). Therefore, mutations in *bslA*, *epsG*, or *tasA* genes were introduced into the wild-type *B. subtilis* natto strain RG4365. Mutations in *bslA* or *epsG* abolished sliding of the *B. subtilis* natto strain (Fig. 3B). On the other hand, mutation of the *tasA* gene did not alter the sliding properties of the *B. subtilis* natto strain. Are EPS production and BslA synthesis required for sliding proficiency? We examined the effect of the mutations of *bslA* and *epsG* in the *B. subtilis* NCIB3610 wild-type strain (proficient in swarming and sliding) and its *hag* derivative (proficient only in sliding). While swarming of *bslA* and *epsG* mutants in the NCIB3610 background was not altered (Fig. 3C), sliding properties of *hag bslA* and *hag epsG* double mutant strains were decreased similarly to the *bslA* and *epsG* single mutants of the *B. subtilis* natto strain (Fig. 3D). These experiments show that both the BslA protein and the EPS, which are essential components of the biofilm matrix in *B. subtilis*, are indispensable for sliding. The microarray analysis showed that *abrB* was downregulated under sliding-permissive conditions (see Table S2A in the supplemental material), which is in agreement with our experimental results that showed the partial restoration of sliding proficiency of the *spo0A* mutant strain when *abrB* was also deleted (Fig. 1E). Accordingly, AbrB is a repressor of *bslA* (37, 38), a gene that here was shown as required for full sliding proficiency (Fig. 3B).

In line with the experiments on the *B. subtilis* natto strain, swarming and sliding were not decreased after a mutation was

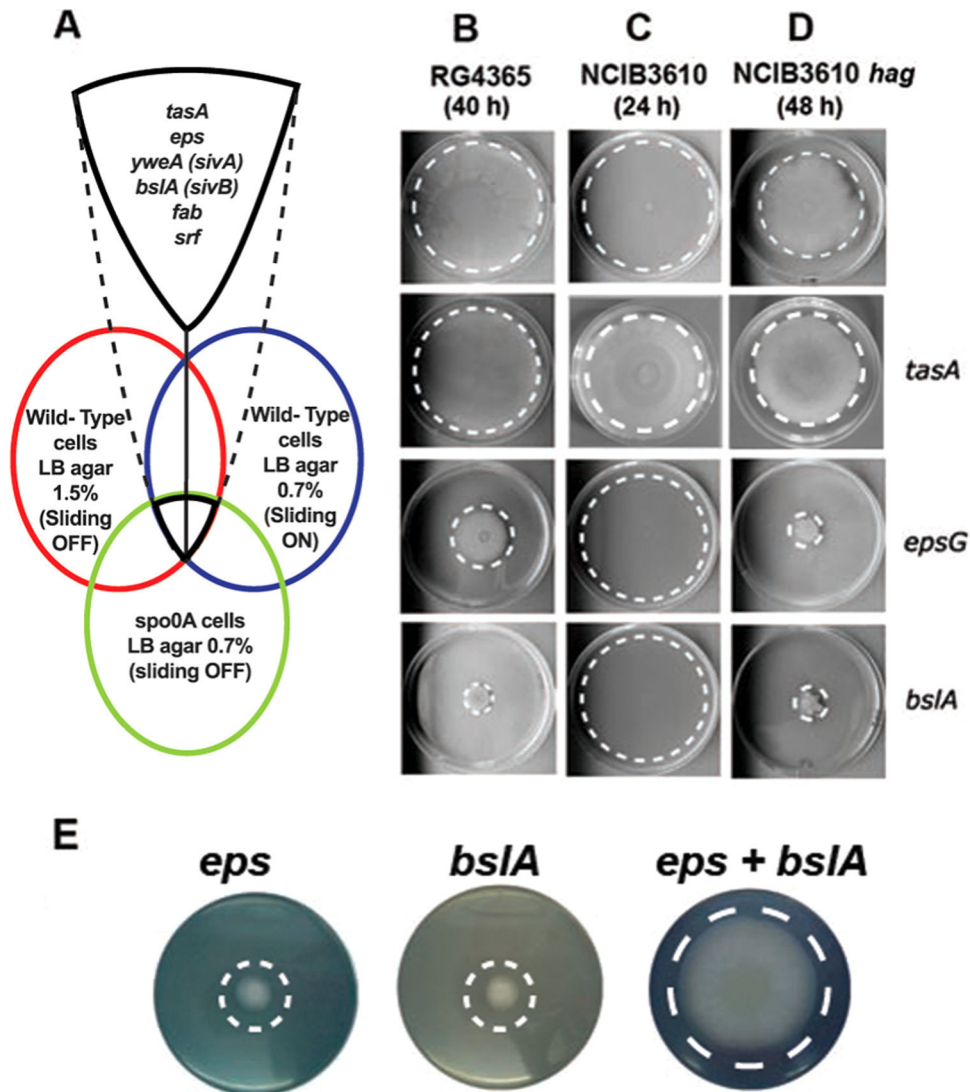


FIG 3 Sliding and swarming ability of mutant *B. subtilis* strains. (A) The cartoon highlights the *B. subtilis* genes with possible novel roles in sliding motility as suggested by the microarray experiments performed (see text for details). (B) Sliding properties of *B. subtilis* matto strain derivatives; from top to bottom, wild-type, *tasA*, *epsG*, and *bsIA* strains. (C) Swarming of *B. subtilis* NCIB3610 and its derivatives comparable to those in panel B. (D) Sliding of *B. subtilis* NCIB3610 *hag* strain and double mutant *hag tasA*, *hag epsG*, and *hag bsIA* strains. (E) Transcomplementation of sliding-deficient strains. Neither *bsIA* nor *eps* mutant cells are able to slide separately, but when they are poured together, sliding proficiency is restored.

introduced into the *tasA* gene of NCIB3610 or into *hag* strains, respectively (Fig. 3C and D), suggesting that the other essential component of the biofilm matrix, TasA, has no role in the ability of *B. subtilis* to slide. It is interesting that based on the microarray analysis, several genes encoding antimicrobial metabolites (i.e., bacilysin, bacillibactin, and plipastatin) were increased under sliding-permissive conditions (see Table S2 in the supplemental material). In this scenario, the known antimicrobial activity of TasA (39) might suggest a role of this protein in protection of sliding cells against predators instead of a crucial role of this protein in motility.

Understanding the role of the cellular components of the sliding machinery in *B. subtilis*. The array experiments showed that the operon related to surfactin production (*srf*) was induced under sliding-permissive conditions (see Table S2 in the supplemental material), a result that is in agreement with the essential

role of this surfactant in sliding proficiency (see Fig. S2A). Surfactin is a secreted lipopeptide molecule that in addition to its function in cell-cell communication, as a paracrine signal during multicellularity (10, 40), has been proposed to allow the spreading of multicellular colonies through the production of surfactant waves that decrease the surface tension of the surrounding space (41). In addition, the EPS overproduced during active sliding is also a component of the extracellular matrix that has been identified as a major force driving biofilm growth, due to the osmotic stress generated by its secretion in the extracellular space (42). Therefore, it is feasible that during sliding the secreted surfactin and EPS, by producing waves of surfactant and gradients of osmotic pressure in the intercellular space of the motile community, respectively, constitute two major forces driving the cooperative sliding of the cells sitting on the surface.

In addition, the overexpression of the KinA inhibitor SivA (dif-

ferential expression of *svaA* is indicated in Table S2A in the supplemental material) (Fig. 3A) (43) would ensure that sporulation is not triggered during active sliding and suggests that KinA is not the histidine kinase involved in the activation of Spo0A for sliding proficiency (see below).

What would be the role of BslA, the other major molecule overproduced during active sliding? It has been shown that BslA is a hydrophobin-like protein secreted to the extracellular space, where it forms surface layers at both the agar-cell and air-cell interfaces around the biofilm (44, 45). Because of its physiochemical properties, BslA behaves as an elastic and highly hydrophobic layer coating the biofilm (44–46). Here, we also confirm that BslA is a major contributor to the water repellence of sliding cells (see Fig. S2B and C in the supplemental material). Moreover, the deficiency in BslA synthesis allows the aqueous solution to pass through the cells immediately (see Fig. S2C). These results suggest that this hydrophobin-like protein could play a role during active sliding as a protector of sliding cells against surface wetting, as was proposed previously for biofilms (45, 47). In this scenario, we hypothesize that the sliding-deficient phenotype of *eps* and *bslA* cells could be circumvented when the two types of cells are present together under sliding-permissive conditions. Supporting this hypothesis, a previous study on *B. subtilis* biofilm formation also suggests that these components can be shared among strains producing one but not the other component (48). As shown in Fig. 3E, mixing *epsG* and *bslA* derivatives of the *B. subtilis* natto strain restores the sliding ability. Interestingly, during the time that our work was under review, van Gestel et al. showed that sliding of *B. subtilis* 3610 depends on the division of labor between matrix (EPS) and surfactin producer subpopulations (49). Analyzing a specific set of mutants, they could also show the complete deficiency in sliding of *srfa* and *eps* mutants. In contrast to our observation of the dispensability of TasA activity for sliding in *B. subtilis* natto and Hag-deficient NCIB3610 cells poured on LB soft medium, sliding of wild-type 3610 on MSggN agar medium was only partly impaired in colony expansion (49). This partially different observation of the TasA requirement for sliding may be due to the different media and growth conditions used for the experiments.

While the genes involved in fatty acid (FA) synthesis (i.e., *fabF*, *fabHBA*, *fabG*, etc.) were overexpressed in wild-type cells under sliding-permissive conditions, those genes involved in FA degradation (i.e., *fadR*, *fadA*, *fadE*, etc.) were downregulated at the same time (see Table S2 in the supplemental material). Is an active lipid synthesis, and therefore active membrane formation and remodeling, necessary to slide? In order to confirm the *in silico* results and test the formulated hypothesis, we proceeded to specifically block *de novo* FA synthesis in *B. subtilis* cells grown under swarming- and sliding-supportive conditions. To this end, we treated *B. subtilis* cells with the antibiotic cerulenin, which is a specific inhibitor of the FabF condensing enzyme (14), at sub-MICs (below $2 \mu\text{g} \cdot \text{ml}^{-1}$), which do not affect the vegetative growth of the NCIB3610 and RG4365 strains (50) (see Fig. S3A and B). Our results show that sub-MICs of cerulenin produce a dose-dependent impediment of sliding motility as well as swarming in *B. subtilis* (Fig. 4A; also see Fig. S3C and D). These results confirm the microarray data and suggest that an active *de novo* FA synthesis constitutes an overlooked requirement for surface (sliding and swarming) motility.

Surprisingly, the supplementation with exogenous FAs (nC_{16:0}

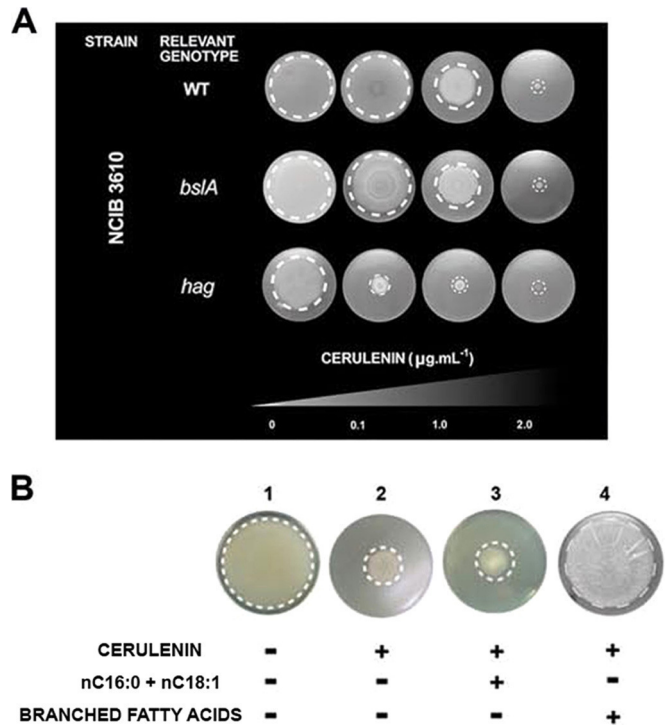


FIG 4 *De novo* branched fatty acid synthesis is required for swarming and sliding proficiencies in *B. subtilis*. (A) Dose-dependent inhibitory effect of sub-MICs of cerulenin on swarming and sliding proficiencies of NCIB3610-related wild-type and *bslA* and *hag* mutant strains, respectively. Sliding and swarming experiments were performed as indicated in the legend to Fig. 1 but with the inclusion of the indicated cerulenin concentration in the soft agar plates. (B) Exogenous branched FAs but not linear FAs (palmitic [nC_{16:0}] and oleic [nC_{18:1}] acids) restore the sliding proficiency of the *B. subtilis* natto strain in the absence of *de novo* FA synthesis.

and nC_{18:1}, palmitic and oleic acids, respectively) of LB soft agar plates containing cerulenin ($2 \mu\text{g} \cdot \text{ml}^{-1}$) did not bypass the inhibition of surface motility in *B. subtilis* but allowed the resumption of the planktonic growth of a similar cerulenin-treated culture incubated under shaking conditions (see Fig. S4A in the supplemental material). Why did the addition of nC_{16:0} and nC_{18:1} FAs not suppress the negative effect of cerulenin on sliding but allow the resumption of planktonic growth? To answer this question, we analyzed the FA profile in samples of wild-type cells grown under sliding-permissive conditions and liquid shaking culture (see Fig. S4B). *B. subtilis*, unlike *Escherichia coli*, synthesizes linear and branched (iso- and anteiso-) saturated fatty acids at 37°C to maintain an adequate membrane fluidity. We found that under active sliding there is a predominance of the synthesis of saturated FAs with lower melting points (anteiso-C_{15:0} and anteiso-C_{17:0}) and a decrease in the synthesis of the FAs with higher melting points (linear nC_{15:0} and nC_{16:0}). Overall, during active sliding, the percentage of linear FAs drops from 25.0 to 4.0% while the content of anteiso-FAs rises from 26.0 to 54.0%. Simultaneously, the global content of iso-FAs remains around 50.0%, independently of the growth conditions (see Fig. S4B). The notable increase in the synthesis of low-melting-point anteiso-FAs and the simultaneous decrease in the synthesis of linear FAs would allow the synthesis of membrane lipids with lower melting points and therefore the biogenesis of membranes with higher fluidity. We hypothesize that

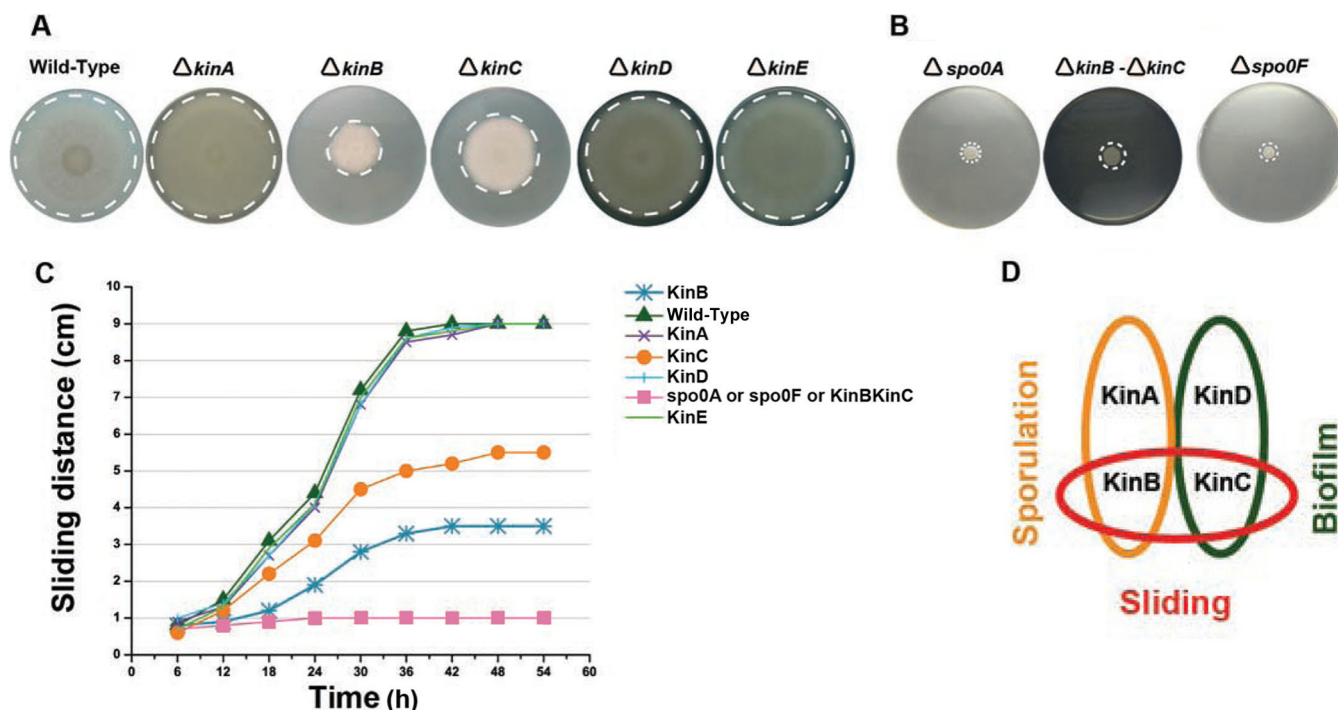


FIG 5 The phosphorelay sensor kinases KinB and KinC govern social sliding motility in *B. subtilis*. (A) Sliding phenotype of single *kin* mutant *B. subtilis* natto strains (see Table S1 in the supplemental material) after 40 h of incubation on soft LB agar plates at 37°C. (B) Complete sliding-deficient phenotype of *spo0A*, *spo0F*, and double *kinB kinC* mutant strains of the *B. subtilis* natto strain under conditions of incubation similar to those indicated for panel A. (C) Kinetics of sliding motility of different phosphorelay mutants over time. Note that the line with pink squares is common to the *spo0A*, *spo0F*, and *kinB kinC* mutant strains. (D) Sporulation, biofilm (at atmospheric oxygen level), and sliding motility are Spo0A-dependent developmental programs that *B. subtilis* preferentially regulates by duos of phosphorelay sensor kinases.

the synthesis of cellular membranes with a higher fluidity might facilitate the group translocation of *B. subtilis* cells on solid surfaces in the absence of the propelling force of the flagella (see Fig. S1B). In this scenario, the increase in membrane fluidity that might be required to slide could not be reached with the supply of linear FAs to cerulenin-treated cultures under sliding-permissive conditions. To test this idea, we supplemented *B. subtilis* cells incubated under sliding-permissive conditions in the presence of cerulenin with branched FAs. As predicted by the hypothesis, the sliding proficiency was fully restored when branched FAs were added as a supplement to the cells with an interrupted *de novo* FA synthesis (Fig. 4B).

The phosphorelay signaling system coordinates multiple multicellular behaviors in *B. subtilis*. Until now, two multicellular behaviors of *B. subtilis* have been known to be under the control of the phosphorelay signaling system: fruiting body formation (including spore formation) and biofilm development (7, 11, 51). As demonstrated in this work, sliding motility is a type of cooperative behavior under the novel control of Spo0A phosphorylated by inorganic phosphate (Spo0A~P_i) and therefore of the phosphorelay.

Which phosphorelay histidine kinase governs sliding motility? To solve this question, we constructed RG4365-isogenic phosphorelay-*kin* mutant strains to analyze their sliding behavior. As shown in Fig. 5A, the wild-type and the *kinA*, *kinD*, and *kinE* single mutant strains show similar and proficient patterns of sliding motility. On the other hand, mainly the *kinB* and, to a much lesser extent, the *kinC* single mutant strains display a partial im-

pairment in sliding. To confirm that KinB and KinC are sensor kinases involved in the control of sliding, we constructed a *kinB kinC* double mutant strain and compared its sliding phenotype with those of the *spo0A* mutant and the other phosphorelay-defective control strain, the *spo0F* single mutant, which are completely impaired in surface translocation. As shown in Fig. 5B, the *kinB kinC* double mutant strain displayed a complete impairment in sliding proficiency that was equivalent in magnitude to the sliding deficiency of the *spo0A* and *spo0F* mutant strains. In Fig. 5C, the sliding kinetics of the different phosphorelay mutant strains confirm that KinB and KinC are the two sensor kinases that govern sliding motility in *B. subtilis* and that KinB activity is more significant than KinC activity for the proficiency in that behavior. As expected, the transcomplementation (into the nonessential *amyE* locus) of the *kinB* and *kinC* mutant strains with a wild-type copy of *kinB* and *kinC*, respectively, restored full sliding proficiency (see Fig. S5 in the supplemental material).

Interestingly, the sliding-controlling KinC kinase (this work) has been proposed (along with KinD) to govern the onset of biofilm formation (10, 33–35, 52). Further, KinA and KinB have been suggested to alter biofilm development on certain media and at reduced oxygen levels (53). We confirm (data not shown) that in the RG4365 natto strain, as well as in the NCIB3610 strain (33, 34), both sensor kinases, KinC and KinD, govern the onset of biofilm development and extracellular matrix production in response to plant-derived polysaccharides that constitute one of the signals able to induce both kinases (33).

In toto, *B. subtilis* employs duos of phosphorelay histidine ki-

nases to control different multicellular behaviors. The histidine kinase duos KinA/KinB, KinC/KinD, and KinB/KinC govern the onset of sporulation and fruiting body formation (7, 8, 28, 54, 55), biofilm development under atmospheric oxygen pressure (10, 33–35, 51, 52), and social sliding (this work), respectively (Fig. 5D).

The sliding signal. What is the nature of the signal, acting on KinB and/or KinC, which is responsible for triggering sliding motility in *B. subtilis*? To answer this fundamental question, we had two premises. First, the sliding-inducing signal, responsible for the autophosphorylation of KinB and/or KinC, should not be strong enough to trigger KinB~P_i/KinC~P_i-dependent activation (phosphorylation) of Spo0A to the high levels of the regulator (Spo0A~P_i) needed for spore formation, because we did not observe induction of sporulation genes under conditions of active sliding (see Table S2 in the supplemental material). Second, the same signal that activates the autophosphorylation of KinB and/or KinC sensor kinases to make Spo0A~P_i and induce sliding motility would prevent initial KinB~P_i-dependent and/or KinC~P_i-dependent biofilm formation.

A recent report suggested that KinB is controlled by the respiratory apparatus via its second transmembrane segment (53). It is proposed that under conditions of reduced electron transport, KinB becomes active (formation of KinB~P_i) via a redox switch involving its second transmembrane segment with one or more cytochromes to induce biofilm formation and sporulation (53). We envision that under active sliding, in rich soft medium, the physiological conditions of the sliding cells would be different from the conditions of sessile cells forming a biofilm. Under conditions of biofilm formation, a crowded population of cells exists encased in the biofilm matrix with nutrients that become rapidly exhausted (11). Furthermore, if a reduced electron transport triggers KinB~P_i-dependent biofilm formation and sporulation, surface translocation (sliding) would not be activated at the same time since the two are antagonist responses (53). Therefore, we consider it unlikely that the status of the respiratory apparatus, sensed by the second transmembrane domain of KinB, could be the physiological condition triggering sliding.

Interestingly, it has been proved that intracellular potassium represents a negative signal for KinC (10, 52). Potassium is a major intracellular ion that impairs KinC activation through interaction with the cytoplasmic PAS-PAC sensor domain of the kinase (10). The intracellular potassium concentration decreases as *B. subtilis* cells reach the late logarithmic phase when newly synthesized surfactin, through its membrane pore formation activity, and the putative potassium channel YugO secrete the ion to the outside of the cell (10, 52). In this model, the surfactin/YugO-mediated intracellular drop in potassium concentration activates KinC. Curiously, in contrast to the round colonies formed on LB and LBY (LB medium supplemented with 4.0% yeast extract; see also reference 14) agar plates by the wild-type RG4365 strain and its isogenic *kinC* derivative, the *kinB* mutant strain forms colonies and biofilms with a tendril-shaped morphology that are very similar to the morphology of wild-type *B. subtilis* colonies grown on CM (casein digest-mannitol medium) plates, a solid medium with potassium deficiency (22) (Fig. 6A and B). Basically, low (micromolar) and high (millimolar) levels of potassium ions favor tendril-like and rounded colony formation, respectively (22). Due to the similar colony phenotypes of the *kinB* mutant and the wild-type strain grown on solid medium with low levels of potassium, we were motivated to investigate if potassium is involved in the reg-

ulation of KinB. Remarkably, as shown in Fig. 6C, we discovered a dose-dependent positive effect of potassium ions on sliding motility of the wild-type and *kinC* strains, which are proficient in *kinB* expression. This sliding stimulation was observed at potassium levels between 50 mM and 100 mM (data not shown) (with an optimal sliding-stimulatory concentration of 75 mM) that are comparable to the potassium concentrations that inhibited KinC from triggering biofilm formation (10, 52). In contrast, there was no effect of potassium supplementation on the sliding proficiency of the *kinB* mutant (Fig. 6C). These results strongly suggest that potassium represents a positive signal for KinB activation. A closer examination of the colony and biofilm phenotypes of the *kinB* mutant strain (Fig. 6A and B) seems to indicate that KinB might inhibit KinC from stimulating biofilm formation, and we are currently investigating this phenomenon.

It is known that the sensor histidine kinase KinB is, in addition to KinA, the main sporulation kinase of *B. subtilis* (54). Although a *kinB* mutant strain is proficient in sporulation (Spo⁺ phenotype), a double *kinA kinB* mutant strain is almost unable to sporulate (Spo⁰ phenotype) (54). Therefore, we were interested to investigate if the positive effect of potassium on KinB-dependent sliding proficiency was also valid for spore formation. As shown in Fig. 6D, potassium did not stimulate sporulation in either of the two KinB-proficient strains, i.e., wild-type (KinA⁺ KinB⁺) and *kinA* mutant (KinA⁻ KinB⁺), that were analyzed. Consequently, potassium constitutes a specific signal for sliding motility that precisely fulfills the two hypothesized premises to be ineffective in triggering sporulation (first premise, Fig. 6D) but, at the same time, strong enough to trigger sliding motility (second premise, Fig. 6C) (10, 52). In addition, the dual role of potassium ions (present at high intracellular levels at early times of growth) as activators and inhibitors of KinB and KinC activities, respectively, points to KinB as the phosphorelay kinase responsible for the start of the cooperative sliding movement (see below).

Does potassium represent a direct or an indirect signal to activate KinB? Searching for conserved domains and sequence motifs present in KinB that might be involved in the potassium response, we discovered a disregarded sequence (SLKTNGTG) residing on the ATP-binding region of KinB that is absent in the sequences of the other four phosphorelay sensor kinases (56) (Fig. 7A). This sequence possesses a significant homology to the highly conserved K⁺-filter (selectivity) sequence of the pore loop domain (P-domain) of potassium channels (T/S-x-x-T-x-G-x-G consensus sequence) (57, 58). Despite the many protein motifs and domains present in different types of potassium channels (58), the KinB K⁺-selectivity-like sequence (here called K* for simplicity) is the only common element related to K⁺ channels. While active KinB is a dimer (59), typical potassium channels are tetramers made up of predominantly identical subunits clustered to form the ion permeation pathway across the membrane (60–62). In addition to the absence of the pore motifs that surround the selectivity filter (Fig. 7B), KinB also lacks the different domains that have been described in different potassium channels (58, 60, 61). Furthermore, the K* resides in the cytosolic region of the kinase, while in all known (eukaryotic and prokaryotic) potassium channels the K⁺-filter resides in transmembrane domains. While these topological features exclude KinB as a potassium channel, they open the possibility that the kinase might sense the intracellular concentration of the ion throughout its cytosolic K*. Therefore, we tested if the K* plays a role or not in sliding motility. To this end,

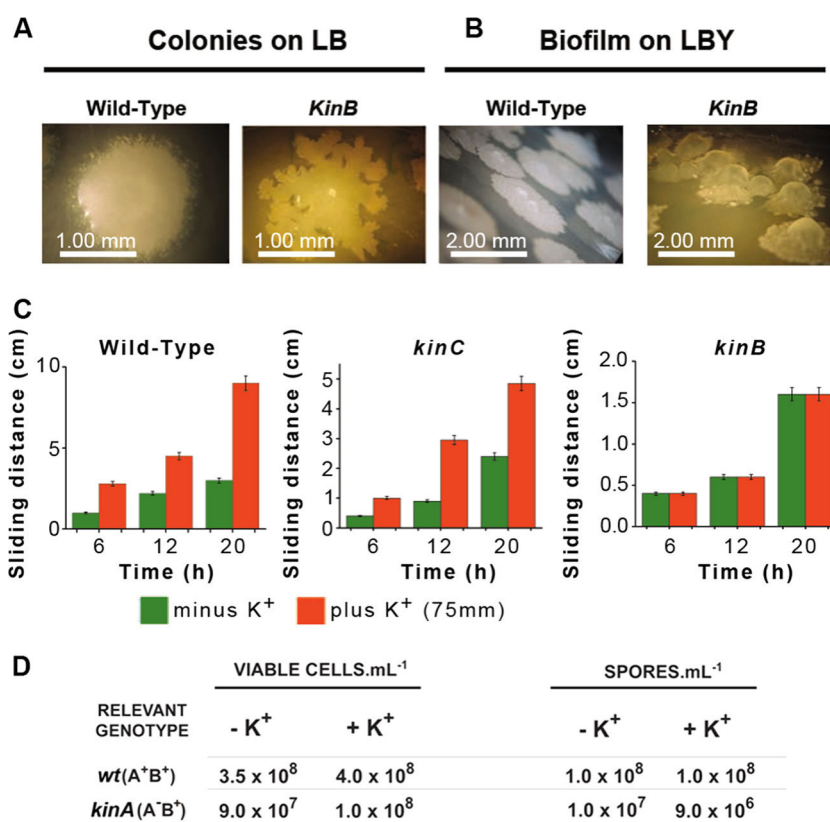


FIG 6 Potassium is the physiological signal that regulates sliding motility in *B. subtilis*. (A and B) Tendril-like morphology of RG4365-isogenic *kinB* colonies and biofilms (complex colonies) formed on LB (A) or LBY (B) medium. (C) Potassium stimulates sliding of KinB-positive (wild-type and *kinC* mutant strains) but not KinB-deficient (*kinB* strain) cells. (D) Potassium does not represent a signal for sporulation proficiency. Sporulation proficiencies of wild-type (*wt*) (*kinA*⁺ *kinB*⁺) and *kinA* mutant (*kinA* *kinB*⁺) strains in the presence and absence of added potassium ions (75 mM) are shown. Viable cells and spores were determined after 30 h of growth in SM as previously described (27). Results presented in panels C and D are representative of three experiments performed separately.

we constructed two types of *kinB* mutant strains harboring specific mutations in the K* (see Fig. S6 in the supplemental material). In one case, three out of the four conserved amino acids of the consensus K* were replaced by alanines (the fourth conserved amino acid, G, of the consensus sequence was not altered as it overlaps with a predicted ATPase motif of the kinase [Fig. 7A]) to give rise to the mutant KinB_{K*→A} (see Fig. S6). In the second constructed *kinB* mutant strain, 7 out of the 8 amino acids of the K* were deleted (mutant strain KinB_{ΔK*} [see Fig. S6]). One important consideration for both mutant strains before analysis of their roles in sliding is that they must be functional (i.e., promote spore formation). In this sense, the sliding-promoting activity of KinB should be separable from its biofilm/sporulation-promoting activities, a scenario that would explain why KinB-dependent sliding proficiency and KinB-dependent biofilm/spore formation are not simultaneously activated (see below).

Remarkably, while the complementation of a *kinA* *kinB* double mutant strain (originally Spo0 and deficient in sliding) with a wild-type copy of *kinB* restored sporulation and sliding proficiencies, both types of alterations in KinB (KinB_{K*→A} and KinB_{ΔK*}) were able to complement full sporulation proficiency but did not restore the KinB-driven sliding proficiency in that genetic (*kinA* *kinB*) background (Fig. 7B). Simultaneously, both constructed KinB mutants failed to restore sliding proficiency of *kinB* (Fig. 7C)

and *kinB* *kinC* (Fig. 7D) mutant strains and were also insensitive to the stimulation of sliding after potassium supplementation (Fig. 7E). These results confirm that the K⁺-selectivity-like sequence present in KinB (K*) plays an essential role in potassium sensing, leading to sliding proficiency that is located on a different part of the KinB protein than the electron transport-sensing transmembrane segment 2 responsible for triggering biofilm and spore formation (54).

Potassium constitutes the signal for the fine-tuned interconnection of social sliding and biofilm development. Potassium represents the most abundant ion in the cytoplasm (~200 mM in *E. coli* versus 7 mM content in LB medium) (58). Unlike most other intracellular cations, the high intracellular concentrations of potassium do not interfere significantly with vegetative growth. However, apart from the stimulatory effect of potassium on KinB (this work), it is known that potassium is a strong inhibitor of KinC activity (10, 52), but enigmatically, the activity of both histidine kinases (KinB and KinC) is required for full sliding proficiency (Fig. 5A and B). The simplest explanation for this apparent paradox is that KinB and KinC should work at different times of sliding development accompanying the drop in the intracellular concentration of potassium that happens during the transition from the log phase to the early stationary phase. We favor a scenario (i.e., in LB soft agar plates) in which, at the onset of sliding

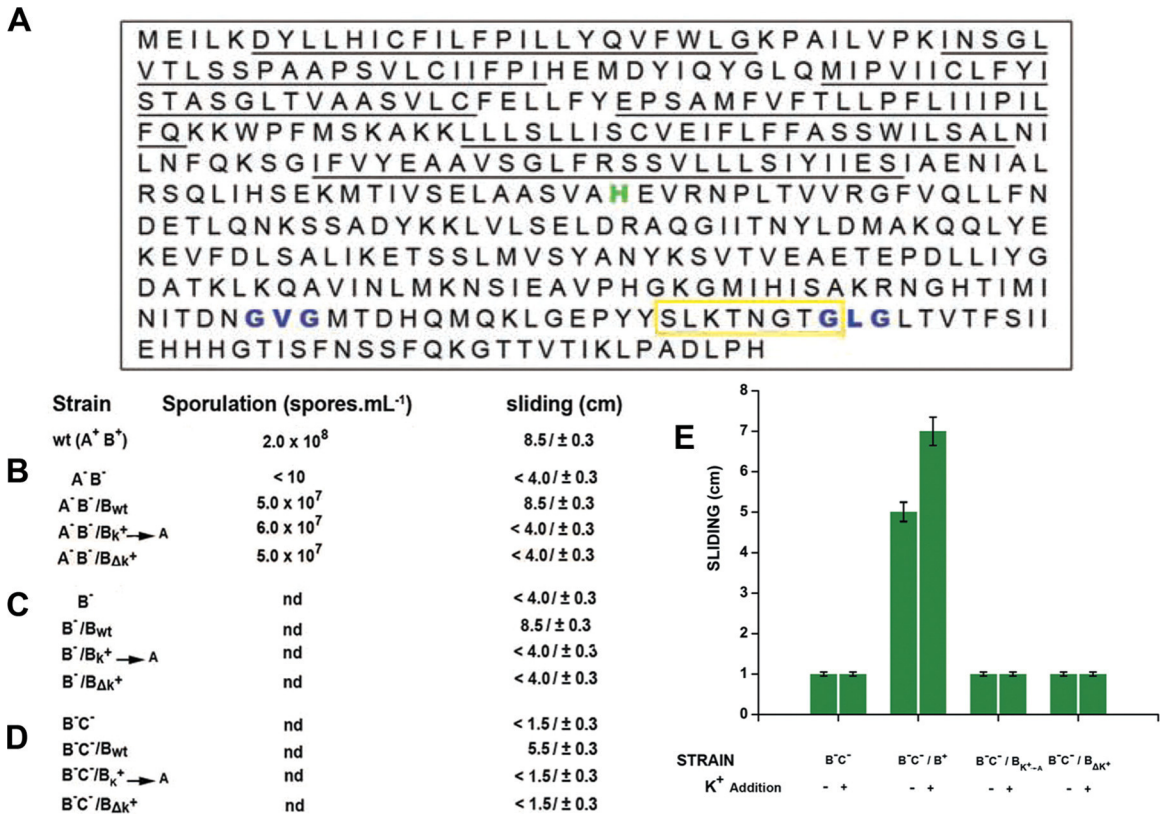


FIG 7 KinB harbors a cytosolic selectivity filter motif responsive to potassium ions that specifically allows sliding proficiency. (A) Amino acid sequence of KinB. The six continuous underlines indicate the six transmembrane domains of KinB. The histidine highlighted in green corresponds to the residue of autophosphorylation; the blue amino acid triplets represent the top and bottom sites of the ATP-binding domain of the kinase. The yellow box highlights the cytosolic sequence in KinB with homology to the potassium selectivity filter sequence present in potassium channels. (B to D) Sporulation and sliding proficiencies are separable KinB functions. KinB mutant strains affected in the integrity of the selective filter sequence were able to restore full sporulation proficiency of a Spo0 *kinA kinB* double mutant strain (A⁻B⁻ in panel B) but did not restore KinB-dependent sliding activity in that A⁻B⁻ background (B), either in *kinB* (B⁻) (C-) or in *kinB kinC* (B⁻C⁻) (D)-deficient mutant strains. B_{K⁺→A} and B_{ΔK⁺} indicate KinB proteins with Ala-exchanged and Ala-deletion K⁺-filter domains, respectively. (E) Mutation of the potassium selectivity sequence in KinB abolished the ability of *B. subtilis* to slide in response to potassium addition. Sliding and sporulation proficiencies were measured as indicated in Materials and Methods. Results presented in panels B to E are representative of four experiments performed separately after 40 h of incubation.

and at the edge of an active sliding colony (where the youngest cells would be present), the intracellular potassium concentration would be high because cells have plenty of nutrients and are in log phase. During this time, KinB (which is the first phosphorelay kinase to be expressed and therefore is present early on in the cell) (63) should be active (due to the potassium stimulus) in driving the synthesis of the sliding machinery while KinC activity would remain low because of its reduced expression at early times of growth and because of the presence of high levels of intracellular potassium (10, 52) (Fig. 8A, left image). As soon as sliding cells approach the late log phase on LB soft agar plates (probably at the inner, older portion of the sliding disc), surfactin and the potassium exporter YugO are expressed on the cellular membrane (10, 52). Therefore, the intracellular potassium concentration decreases, and KinB activity is downregulated and replaced by active KinC to maintain the appropriate levels of Spo0A~P_i required for the continued expression of genes needed for full sliding proficiency (i.e., *bslA*, *srf*, *eps*, and *fab*) and biofilm formation (see below) at the inner part of the sliding disc (Fig. 8A, right image). Supporting the view of this spatiotemporal regulation of the kinases, when wild-type (KinA- and KinB-positive) *B. subtilis* cells

are loaded on an optimized soft agar medium that in addition to sliding motility also allows biofilm formation (i.e., soft LBY agar) (14), it is possible to observe the formation of structures typical of a biofilm in the inner part of the sliding disc, while the outer borders remain flat (Fig. 8B, left image). This result strongly suggests that (under sliding-permissive conditions) KinC and KinB are active at the interior and at the edge of the sliding disc, respectively (Fig. 8A, right image). In agreement with this result, when *kinC* (KinB-positive and KinC-deficient) cells were incubated under similar conditions, the sliding disc, as expected, was smaller than the sliding disc formed by wild-type cells, and more importantly, no structure that resembles a biofilm was formed (Fig. 8B, middle image). Concordantly, a *kinB* strain (KinC-positive and KinB-deficient) formed typical biofilm wrinkle-like structures at the inside and outside regions of the slowly sliding cells (Fig. 8B, bottom right images). Overall, the former results (Fig. 6 to 8) suggest that potassium ions and KinB~P_i act earlier than KinC~P_i to activate the onset of sliding and confirm, once the potassium concentrations start to be different in distinct regions of the sliding disc, the spatiotemporal regulation of KinB and KinC (Fig. 8A). In addition, the KinC~P_i-dependent biofilm formation

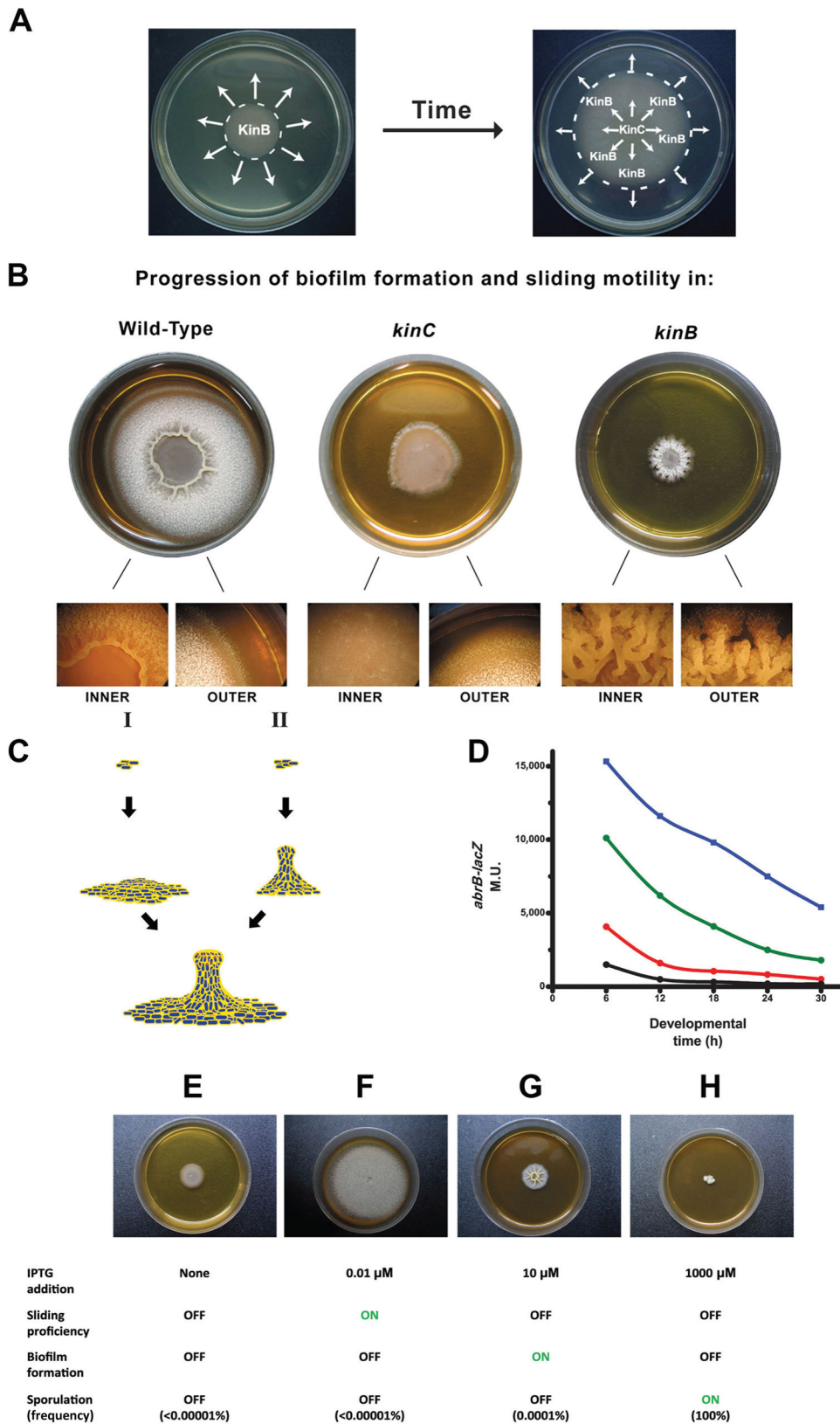


FIG 8 Spatiotemporal regulation of the sliding-inducing kinases. (A) At the onset of sliding, as soon as cells were poured on LBY-0.7% agar plates, KinB was the first-acting kinase while KinC remained inactive. This differential activity of KinB and KinC is due to the intracellular potassium input that activates and inhibits each kinase, respectively (left panel). As progression of sliding continues, there is a drop in the intracellular potassium concentration in the cells at the inner part of the sliding disc. Under this physiological condition, KinB and KinC become inactive and active inside the sliding disc, respectively, while KinB

(Continued)

observed at the interior (older) part of the sliding disc after incubation in a medium that allows biofilm and sliding (LB_Y soft agar plates) (left and middle images in Fig. 8B) suggests that the potassium-mediated activation of KinB to make Spo0A~P_i and start sliding motility (Fig. 6C and 7) is not only insufficient to induce KinB~P_i-dependent spore formation (Fig. 6D) but also insufficient to trigger the onset of KinB~P_i-dependent biofilm formation (middle image in Fig. 8B).

How can sliding and the sessile lifestyle of biofilm formation, which are social behaviors believed to be antagonistic to each other, be positively controlled by the same regulatory pathway (Spo0A~P_i), and why are the biofilm formation and sporulation pathways not activated upon increased KinB autophosphorylation during promotion of sliding motility? Fujita and Losick reported that a gradual increase in the levels and activity of Spo0A results in the expression of different sets of genes in *B. subtilis* (28). For instance, high levels of Spo0A~P_i stimulate sporulation (fruiting body formation) and low levels of Spo0A~P_i stimulate biofilm formation (64). Therefore, we hypothesize that sliding and biofilm formation developments require, as suggested by Chai et al. (64) for the cases of sporulation and biofilm formation, different levels of Spo0A~P_i to become active. Until now, it was clearly demonstrated that the sliding-permissive conditions used in this work (i.e., soft LB agar) and the potassium input that activates KinB (which at the same time inhibits KinC activity) (10) are adequate to support sliding (Fig. 1 and 6C) but insufficient to trigger sporulation (Fig. 6D) and biofilm formation (Fig. 8B, middle image, KinB⁺ KinC⁻ strain). Therefore, sliding motility in *B. subtilis* seems to be activated before biofilm formation and sporulation. But how is sliding and not the other developmental pathways triggered when KinB become active? In other words, which behavior needs lower levels of Spo0A~P_i to be triggered? We hypothesize two alternative progressions. In one scenario (Fig. 8C, model I), the surface-committed cells first slide and later on form the biofilm structures at the center. In the other situation (Fig. 8C, model II), the surface-attached cells first produce a sessile biofilm and cells at the edge of the biofilm engage in sliding later on. In both scenarios, the social behavior that is triggered first (sliding or biofilm formation) is the one that requires the smaller amount of Spo0A~P_i (28, 64). One approach to monitor the *in vivo* levels of Spo0A~P_i is to measure the expression of *abrB*, the most sensitive reporter of the Spo0A~P_i levels present in the cell (27, 28). Spo0A~P_i is a strong repressor of *abrB*, and very low levels of Spo0A~P_i (insufficient to trigger biofilm and sporulation) are sufficient to downregulate *abrB* (27, 28). Therefore, to obtain more

insight into the levels of Spo0A~P_i present during sliding and biofilm, we measured the levels of β -galactosidase (β -Gal) activity driven by the expression of an *abrB-lacZ* transcriptional fusion under conditions that favor sporulation (growth on sporulation medium [SM]-1.5% agar plates), sliding (growth on LB-0.7% agar plates), biofilm (growth on LB_Y-1.5% agar plates), or none of the abovementioned behaviors (growth on LB-1.5% agar plates). At different times, cells were removed from the petri dishes and the *abrB*-driven β -galactosidase activity was measured (Fig. 8D). As expected, the *abrB* expression was the lowest and highest (indicating the highest and smallest amounts of Spo0A~P_i, respectively) when the cells were grown on SM- and LB-1.5% agar plates, respectively (Fig. 8D). Interestingly, the levels of *abrB* expression under conditions of active sliding (growth on LB-0.7% agar plates) were significantly higher than the *abrB* levels observed under conditions of active biofilm formation (growth on LB_Y-1.5% agar plates). These results (Fig. 8D) suggest that the levels of Spo0A~P_i required to trigger sliding motility are lower than the levels of Spo0A~P_i needed to trigger biofilm formation, and therefore, the former behavior (sliding motility) would be triggered before biofilm formation when *B. subtilis* is attached and committed to a sessile differentiation (model I in Fig. 8C).

To confirm this interpretation, the $\Delta spo0A sad67$ strain (see Table S1 in the supplemental material) (27–29), where the synthesized active Spo0A (Sad67) level depends on the supplemental IPTG, was cultivated on LB_Y-0.7% agar plates supplemented with different amounts of IPTG. In this experiment, we hypothesized that the behavior (biofilm formation, sliding, or fruiting body formation-sporulation) expressed at the lowest IPTG concentration would reflect the multicellular *B. subtilis* response that requires the smallest amount of active Spo0A (Sad67) to be produced. As expected, in the absence of IPTG addition (Fig. 8E), *sad67* is not expressed and *B. subtilis* is unable to display (because Spo0A activity is completely absent in $\Delta spo0A$ cells) any of its different multicellular behaviors. As soon as the LB_Y-0.7% agar medium is supplemented with a small amount of IPTG (0.01 μ M), *B. subtilis* cells start to slide (Fig. 8F). When the IPTG concentration is increased to 10 μ M (and therefore more active Spo0A is produced in the surface-committed cells), *B. subtilis* triggers complex colony biofilm formation (Fig. 8G). At the largest amount of supplemental IPTG (1,000 μ M), the growth of *B. subtilis* is restricted (because high levels of active Spo0A inhibit vegetative division) (27–29) and *B. subtilis* directly induces the formation of fruiting bodies filled with spores (Fig. 8H). Overall, these results strongly suggest that the increase in the levels of active

Figure Legend Continued

remains active at the newest part (border) of the sliding community. (B) Wild-type *B. subtilis* RG4365 and its isogenic derivatives mutated in *kinC* or *kinB* were loaded on soft agar plates of LB_Y medium and incubated for 20 h at 37°C. Under these conditions of simultaneous stimulation of sliding and biofilm formation proficiencies, the formation of a structured biofilm in the inner part of the wild-type sliding disc is observed. In contrast, in the sliding disc of the *kinC* strain no biofilm structure is formed, suggesting that the biofilm observed in the inner part of the sliding disc of wild-type cells is a product of the KinC activity. In both cases (wild-type and *kinC* strains), the borders of the sliding discs are flat and unstructured. In the case of the *kinB* cells (right panel), KinC activity drives the formation of typical wrinkled structures, representative of a mature biofilm, inside and at the borders of the colony. (C) Two models for the temporal progression of multicellularity in *B. subtilis* as described in the text. (D) β -Galactosidase production from *P_{abrB}-lacZ* in *B. subtilis* cells grown on petri dishes filled with media that favor the expression of different social behaviors under the control of Spo0A~P_i: sliding motility (LB-0.7% agar; green line), biofilm formation (LB_Y-1.5% agar; red line), sporulation (SM-1.5% agar; black line), or none (LB-1.5% agar; blue line) (see text for details). Cells were taken from the petri dishes at the times indicated in the figure and assayed as described in the supplemental material. The results shown are representative of three independent experiments made in duplicate. M.U., Miller units. (E to H) Five microliters of an overnight culture of the natto strain RG4382 ($\Delta spo0A::Ery/P_{spac}-spo0A-sad67$ Cat) was inoculated on the middle of solidified LB_Y-0.7% agar medium prepared with different concentrations of IPTG as shown in the figure. After 20 h of incubation at 37°C, photographs were taken and the sporulation frequency (after elution of the cells from the petri dishes) was determined as described in Materials and Methods. The results are representative of seven independent experiments performed in triplicate.

Spo0A (Spo0A~P_i) (28, 64) allows the expression of the different behaviors of *B. subtilis* following a temporal sequence of social sliding motility, multicellular biofilm formation, and finally fruiting body formation (sporulation) (see Fig. S7).

Conclusions. *In toto*, we demonstrated how the model organism *B. subtilis* can cope with the basic, although fundamental, decision that it must take when it is attached and committed to a surface: to move or remain in place. We present a novel mechanistic model, containing a Spo0A command that explains the coordinated expression of the different behaviors of *B. subtilis*. In this model, the spatiotemporal regulation of KinB and KinC by potassium determines the Spo0A~P_i amount, which in turn orchestrates the onset and sequential progression of sliding motility, biofilm formation, and finally sporulation/fruiting body formation (Fig. 8; see also Fig. S7 in the supplemental material). Recent publications demonstrate the necessity of biofilm formation for the efficient colonization of the root surface and biocontrol properties of *B. subtilis* (33, 34). The common signal (potassium) and the common regulatory network under Spo0A control (the phosphorelay) (25) for sliding (this work), biofilm formation (this work and references 10 and 32 to 34), and sporulation-fruiting body formation (54) and our *in vitro* experiments (Fig. 2G) suggest that sliding might also contribute to the ability of the plant growth-promoting and biocontrol bacterium *B. subtilis* to reach the root surface and efficiently colonize the rhizosphere. Once again, *B. subtilis* offers an example of simplicity in how distinct prokaryotic social behaviors previously believed to be antagonistic and independent from each other, i.e., surface motility, biofilm formation, and sporulation, might work together to benefit the bacterium and the host.

MATERIALS AND METHODS

Strains and growth media. The three wild-type *B. subtilis* strains used in this study were the domesticated, laboratory reference strain JH642 and the two undomesticated and wild *B. subtilis* strains NCIB3610 and natto RG4365. These strains and their isogenic derivatives (see Table S1 in the supplemental material) were grown in Luria-Bertani (LB) and Schaeffer's sporulation medium (SM) as indicated previously (27). For experiments in biofilm formation, the biofilm-enhancer medium LBY was used (14). Cloning of *kinB* and *kinC* genes for complementation and site-directed mutagenesis is described below and in Table S3 in the supplemental material.

Spreading (swarming and sliding) experiments. For surface motility (swarming and sliding), LB plates fortified with 0.7% agar and dried for 1 h were inoculated with 1 μ l of 8×10^7 cells \cdot ml⁻¹ grown to mid-log phase at 37°C in LB broth. The inoculated petri dishes were then incubated at 37°C for 40 h. Each data point shown in the figures represents an average from 6 independent experiments. Data from one representative experiment are shown. Flagellum staining was performed as described previously (14).

DNA transformation and complementation experiments. Transformation of *B. subtilis*, to obtain isogenic derivatives of the parental strains, was carried out as previously described (27, 50). When appropriate, antibiotics were included at the following final concentrations: 1 μ g \cdot ml⁻¹ erythromycin (Ery), 5 μ g \cdot ml⁻¹ kanamycin (Kan), 5 μ g \cdot ml⁻¹ chloramphenicol (Cat), 75 μ g \cdot ml⁻¹ spectinomycin (Spc), and 2.5 μ g \cdot ml⁻¹ phleomycin (Pheo). Surfactin and cerulenin were obtained from Sigma-Aldrich. For those plates supplemented with IPTG in Fig. 11, one or two grains of IPTG was carefully added on top of the soft LB agar after solidification in order to allow IPTG diffusion and gradient formation.

β -Gal assays. The β -galactosidase (β -Gal) activity from liquid cultures was assayed as previously described (14, 27). In the case of the assays of β -Gal activity driven from colonies, cells were resuspended at a final

concentration of 3×10^9 CFU \cdot ml⁻¹ before measurement of the β -galactosidase activity (14, 27).

Transcriptome analysis. Cultures of the *B. subtilis* natto strain (RG4365) and its *spo0A* derivative (RG4370) were inoculated onto the middle of LB plates containing 0.7% or 1.5% agar. The bacterial biomass was removed from the plates with a spatula after 24 h of growth, and samples were stored at -80°C . At least three independent biological replicates were included. The pellets were immediately frozen in liquid nitrogen and stored at -80°C . RNA extraction was performed with the Macaloid/Roche protocol (37, 65) with two additional steps of phenol-chloroform washing. RNA concentration and purity were assessed using a NanoDrop ND-1000 spectrophotometer (Thermo Fisher Scientific). RNA samples were reverse transcribed into cDNA using the Superscript III reverse transcriptase kit (Invitrogen, Carlsbad, CA, USA) and labeled with Cy3 or Cy5 monoreactive dye (GE Healthcare Amersham, The Netherlands). Labeled and purified cDNA samples (NucleoSpin extract II; Biokè, Leiden, The Netherlands) were hybridized in Ambion Slidehyb #1 buffer (Ambion Europe Ltd.) at 48°C for 16 h. The arrays were constructed as described elsewhere (66). Briefly, specific oligonucleotides for all 4,107 open reading frames of *B. subtilis* 168 were spotted in duplicate onto aldehyde-coated slides (Cell Associates) and further handled using standard protocols for aldehyde slides. Slide spotting, slide treatment after spotting, and slide quality control determination were done as described previously (67). After hybridization, slides were washed for 5 min in 2 \times SSC (1 \times SSC is 0.15 M NaCl plus 0.015 M sodium citrate) with 0.5% SDS, washed 2 times for 5 min each in 1 \times SSC with 0.25% SDS, washed for 5 min in 1 \times SSC-0.1% SDS, dried by centrifugation (2 min, 2,000 rpm), and scanned in a GenePix 4200AL microarray scanner (Axon Instruments, CA, USA). Fluorescent signals were quantified using ArrayPro 4.5 (Media Cybernetics Inc., Silver Spring, MD) and further processed and normalized with MicroPrep (68). CyberT (69) was used to perform statistical analysis. Genes with a Bayes *P* value of $\leq 1.0 \times 10^{-4}$ were considered significantly affected.

Cloning of *kinB* and *kinC* genes and site-directed mutagenesis. The coding regions of *kinB* and *kinC* were amplified with oTB56-oTB57 and oTB61-oTB62 oligonucleotide pairs, respectively (oligonucleotide sequences are indicated in Table S3 in the supplemental material). The PCR products were digested with BamHI and EcoRI enzymes and cloned into the corresponding sites of pTB16. pTB16 is an *amyE* integration vector with a kanamycin resistance gene. pTB16 was created by amplifying the kanamycin resistance gene from pDG782 (70) with primers oDG1 and oDG2, restricting it with StuI and BamHI, and ligating it to the corresponding sites of PCR-amplified vector that was obtained with oX1 and oX2 on pX (71) plasmid as the template (see Table S3). Site-directed mutants of the *kinB* gene were obtained using an overlapping fragment PCR method (72), using polymerase X enzyme (Roboklon GmbH, Berlin, Germany). The 5' region of *kinB* was amplified with oTB56-oTB58 oligonucleotides, while the 3' region, containing mutations for 3 amino acid exchanges (S³⁸³A, T³⁸⁶A, and G³⁸⁸A) or a 7-amino-acid deletion (S³⁸³ to T³⁸⁹), was obtained with oTB59-oTB57 or oTB60-oTB57, respectively (see Table S3). The PCR fragments were used in a second round of PCR as a template accompanied with oTB56-oTB57 oligonucleotides, and fusion fragments were cloned in the same way as the wild-type *kinB* gene. The plasmid constructs obtained were sequenced before transformation into *B. subtilis* integrating into the *amyE* locus.

Fatty acid analysis. Approximately 20 mg of the sample was weighed in a screw-cap 4-ml glass vessel. For the transesterification, a methanol-hydrochloric acid solution was freshly prepared by adding 1 ml of acetyl chloride to 20 ml of methanol (73). Butylated hydroxytoluene (BHT; 3 μ g \cdot ml⁻¹) was added to prevent autoxidation of polyunsaturated fatty acids. Afterward, 1.5 ml of this solution was added to the sample. The solution was overlaid with nitrogen, and the vessel was tightly closed. After vortexing, the vessel was heated at 90°C for 1 h. Once cooled to room temperature, 1 ml of water and 1.5 ml of hexane were added for extraction of fatty acid methyl esters (FAMES). The tubes were vortexed and centri-

fused (6 min at 720 relative centrifugal force [RCF]). The hexane phase was isolated. The extraction procedure with hexane was repeated, and the combined organic solutions were dried over anhydrous Na₂SO₄ and concentrated to dryness under a gentle stream of nitrogen. The residue was redissolved in 0.2 ml (or 0.1 ml) of hexane (depending on the final concentration).

The Supelco 37-component FAME mix, the Supelco bacterial acid methyl ester mix, and the Supelco triglyceride mix (Supelco, Bellefonte, PA, USA) were used as reference standards to identify the FAMES.

An aliquot of the sample (1 μl) was analyzed on a Finnigan trace instrument (Thermo Fisher Scientific, Dreieich, Germany) equipped with a ZB5 column (15 m by 0.25 mm by 0.25 μm) with a 10-m Guardian end (Phenomenex, Aschaffenburg, Germany). Mass spectra were measured in electron impact (EI) mode at 70 eV. Helium at 1.5 ml · min⁻¹ served as the carrier gas. The gas chromatography (GC) injector (split ratio, 1:15), transfer line, and ion source were set at 250°C, 280°C, and 200°C, respectively. FAMES were eluted under programmed conditions from 50°C (2 min) followed by 10°C · min⁻¹ to 168°C, 1°C · min⁻¹ to 177°C, and 10°C · min⁻¹ to 320°C.

Preparation of branched fatty acid extract from *B. subtilis*. One hundred milliliters of a *B. subtilis* RG3465 culture was grown in LB broth at 37°C until the end of the vegetative phase (~6 h of growth); only saturated fatty acids, mainly branched fatty acids, are made at this temperature (74). Total membrane lipids (phospholipids [PLs] and glycolipids [GLs]) were extracted as previously described (74). Then, the PLs and GLs were hydrolyzed with cold diazomethane to obtain free fatty acids (FAs), which were completely dried and resuspended in 1 ml of ethanol (74). For the complementation experiments on cerulenin-treated *B. subtilis* cells, the free FAs were used at a 1:100 dilution rate.

Light microscopy and photography. The developed swarm and slide plates were visualized with a Stemi 2000 (Zeiss) stereomicroscope using a KL1500LCD (Zeiss) illumination system. A Power-Shot A80 (Canon) system was used to capture the photographs for swarm and slide images.

Plant root colonization experiments. Two sanitized wheat seeds were deposited on top of previously solidified 1/10-diluted LB in 0.7% agar plates and incubated in moisture chambers at 25°C with exposure to periods of 12 h of illumination. After 3 days of incubation, when wheat seeds started to germinate, 3.0 μl of stationary-phase cultures of wild-type and *spo0A* mutant cells was inoculated at the points indicated by the white dashed circles in Fig. 2. After 24 h of incubation and during the subsequent days, top-to-bottom pictures were taken to show the sliding and plant root colonization abilities of wild-type and *spo0A* *B. subtilis* cells.

Microarray data accession number. Microarray data have been deposited in the Gene Expression Omnibus database under accession no. GSE43840.

SUPPLEMENTAL MATERIAL

Supplemental material for this article may be found at <http://mbio.asm.org/lookup/suppl/doi:10.1128/mBio.00581-15/-DCSupplemental>.

- Figure S1, JPG file, 0.3 MB.
- Figure S2, JPG file, 1.2 MB.
- Figure S3, JPG file, 0.4 MB.
- Figure S4, JPG file, 0.4 MB.
- Figure S5, JPG file, 0.6 MB.
- Figure S6, JPG file, 0.7 MB.
- Figure S7, JPG file, 0.5 MB.
- Table S1, DOCX file, 0.03 MB.
- Table S2, DOCX file, 0.1 MB.
- Table S3, DOCX file, 0.01 MB.

ACKNOWLEDGMENTS

We thank N. R. Stanley Wall for the kind gift of strains NRS1502 and NRS2097 and J. Stülke for strain GP901. We thank Tamara Spalding, Adrian Rovetto, and Walter Ramirez for their assistance during the microarray experiments and genetic constructions. We also thank Rafael Carlucci for figure and caption design.

Work in the laboratory of R.R.G. is supported by CONICET (National Research Council of Argentina), ANCyT (National Agency of Science and Technology of Argentina), and the aid of the Pew Latin-American Program in Biological Sciences (Philadelphia, USA), the Fulbright Committee (Washington, DC, USA), and former Fundación Antorchas (Buenos Aires, Argentina). P.D.O./D.V. and C. L./V.D. are PhD fellows from ANCyT and CONICET, respectively. Work in the laboratory of A.T.K. is supported by a Marie Curie Career Integration Grant (PheHetBacBio-film), Grant KO4741/2-1 from the Deutsche Forschungsgemeinschaft (DFG) within the framework of the DFG Priority Programme SPP1617, a JSMC (Jena School for Microbial Communication) startup fund, and BacFoodNet COST Action FA1202. R.G.-M., E.M., and T.H. are funded by CONACyT-DAAD, JSMC, and IMPRS, respectively.

REFERENCES

1. Harshey RM. 2003. Bacterial motility on a surface: many ways to a common goal. *Annu Rev Microbiol* 57:249–273. <http://dx.doi.org/10.1146/annurev.micro.57.030502.091014>.
2. Henrichsen J. 1972. Bacterial surface translocation: a survey and a classification. *Bacteriol Rev* 36:478–503.
3. Jarrell KF, McBride MJ. 2008. The surprisingly diverse ways that prokaryotes move. *Nat Rev Microbiol* 6:466–476. <http://dx.doi.org/10.1038/nrmicro1900>.
4. Kearns DB. 2010. A field guide to bacterial swarming motility. *Nat Rev Microbiol* 8:634–644. <http://dx.doi.org/10.1038/nrmicro2405>.
5. Martínez A, Torello S, Kolter R. 1999. Sliding motility in mycobacteria. *J Bacteriol* 181:7331–7338.
6. Park SY, Pontes MH, Groisman EA. 2015. Flagella-independent surface motility in *Salmonella enterica* serovar Typhimurium. *Proc Natl Acad Sci U S A* 112:1850–1855. <http://dx.doi.org/10.1073/pnas.1422938112>.
7. Branda SS, González-Pastor JE, Ben-Yehuda S, Losick R, Kolter R. 2001. Fruiting body formation by *Bacillus subtilis*. *Proc Natl Acad Sci U S A* 98:11621–11626. <http://dx.doi.org/10.1073/pnas.191384198>.
8. Higgins D, Dworkin J. 2012. Recent progress in *Bacillus subtilis* sporulation. *FEMS Microbiol Rev* 36:131–148. <http://dx.doi.org/10.1111/j.1574-6976.2011.00310.x>.
9. Kovács AT, Smits WK, Mironczuk AM, Kuipers OP. 2009. Ubiquitous late competence genes in *Bacillus* species indicate the presence of functional DNA uptake machineries. *Environ Microbiol* 11:1911–1922. <http://dx.doi.org/10.1111/j.1462-2920.2009.01937.x>.
10. López D, Fischbach MA, Chu F, Losick R, Kolter R. 2009. Structurally diverse natural products that cause potassium leakage trigger multicellularity in *Bacillus subtilis*. *Proc Natl Acad Sci U S A* 106:280–285. <http://dx.doi.org/10.1073/pnas.0810940106>.
11. Vlamakis H, Chai Y, Beaugerard P, Losick R, Kolter R. 2013. Sticking together: building a biofilm the *Bacillus subtilis* way. *Nat Rev Microbiol* 11:157–168. <http://dx.doi.org/10.1038/nrmicro2960>.
12. Kearns DB, Losick R. 2003. Swarming motility in undomesticated *Bacillus subtilis*. *Mol Microbiol* 49:581–590. <http://dx.doi.org/10.1046/j.1365-2958.2003.03584.x>.
13. Abee T, Kovács AT, Kuipers OP, van der Veen S. 2011. Biofilm formation and dispersal in Gram-positive bacteria. *Curr Opin Biotechnol* 22:172–179. <http://dx.doi.org/10.1016/j.copbio.2010.10.016>.
14. Pedrido ME, Pedrido ME, de Oña P, Ramirez W, Leñini C, Goñi A, Grau R. 2013. Spo0A links de novo fatty acid synthesis to sporulation and biofilm development in *Bacillus subtilis*. *Mol Microbiol* 87:348–367. <http://dx.doi.org/10.1111/mmi.12102>.
15. Trejo M, Douarache C, Bailleux V, Poulard C, Mariot S, Regard C, Raspaud E. 2013. Elasticity and wrinkled morphology of *Bacillus subtilis* pellicles. *Proc Natl Acad Sci U S A* 110:2011–2016. <http://dx.doi.org/10.1073/pnas.1217178110>.
16. Lombardía E, Rovetto AJ, Arabolaza AL, Grau RR. 2006. A LuxS-dependent cell-to-cell language regulates social behavior and development in *Bacillus subtilis*. *J Bacteriol* 188:4442–4452. <http://dx.doi.org/10.1128/JB.00165-06>.
17. Bais HP, Fall R, Vivanco JM. 2004. Biocontrol of *Bacillus subtilis* against infection of Arabidopsis roots by *Pseudomonas syringae* is facilitated by biofilm formation and surfactin production. *Plant Physiol* 134:307–319. <http://dx.doi.org/10.1104/pp.103.028712>.
18. Emmert EA, Handelsman J. 1999. Biocontrol of plant disease: a (Gram-)

- positive perspective. *FEMS Microbiol Lett* 171:1–9. <http://dx.doi.org/10.1111/j.1574-6968.1999.tb13405.x>.
19. Cutting SM. 2011. *Bacillus* probiotics. *Food Microbiol* 28:214–220. <http://dx.doi.org/10.1016/j.fm.2010.03.007>.
 20. Senesi S, Ricca E, Henriques A, Cutting S. 2004. *Bacillus* spores as probiotic products for human use, p 131–141. In Ricca E, Henriques A, Cutting S (ed), *Bacterial spore formers: probiotics and emerging applications*. Taylor & Francis Group Ltd, New York, NY.
 21. VidyaLaxme B, Rovetto A, Grau R, Agrawal R. 2014. Synergistic effects of probiotic *Leuconostoc mesenteroides* and *Bacillus subtilis* in malted ragi (*Eleusine corocana*) food for antagonistic activity against *V. cholerae* and other beneficial properties. *J Food Sci Technol* 51:3072–3082. <http://dx.doi.org/10.1007/s13197-012-0834-5>.
 22. Kinsinger RF, Shirk MC, Fall R. 2003. Rapid surface motility in *Bacillus subtilis* is dependent on extracellular surfactin and potassium ion. *J Bacteriol* 185:5627–5631. <http://dx.doi.org/10.1128/JB.185.18.5627-5631.2003>.
 23. Blair KM, Turner L, Winkelman JT, Berg HC, Kearns DB. 2008. A molecular clutch disables flagella in the *Bacillus subtilis* biofilm. *Science* 320:1636–1638. <http://dx.doi.org/10.1126/science.1157877>.
 24. Kearns DB, Chu F, Branda SS, Kolter R, Losick R. 2005. A master regulator for biofilm formation by *Bacillus subtilis*. *Mol Microbiol* 55:739–749. <http://dx.doi.org/10.1111/j.1365-2958.2004.04440.x>.
 25. Burbulys D, Trach KA, Hoch JA. 1991. Initiation of sporulation in *B. subtilis* is controlled by a multicomponent phosphorelay. *Cell* 64:545–552. [http://dx.doi.org/10.1016/0092-8674\(91\)90238-T](http://dx.doi.org/10.1016/0092-8674(91)90238-T).
 26. Molle V, Fujita M, Jensen ST, Eichenberger P, González-Pastor JE, Liu JS, Losick R. 2003. The Spo0A regulon of *Bacillus subtilis*. *Mol Microbiol* 50:1683–1701. <http://dx.doi.org/10.1046/j.1365-2958.2003.03818.x>.
 27. Arabolaza AL, Nakamura A, Pedrido ME, Martelotto L, Orsaria L, Grau RR. 2003. Characterization of a novel inhibitory feedback of the anti-anti-sigma SpoIIAA on Spo0A activation during development in *Bacillus subtilis*. *Mol Microbiol* 47:1251–1263.
 28. Fujita M, Losick R. 2005. Evidence that entry into sporulation in *Bacillus subtilis* is governed by a gradual increase in the level and activity of the master regulator Spo0A. *Genes Dev* 19:2236–2244. <http://dx.doi.org/10.1101/gad.1335705>.
 29. Ireton K, Rudner DZ, Siranosian KJ, Grossman AD. 1993. Integration of multiple developmental signals in *Bacillus subtilis* through the Spo0A transcription factor. *Genes Dev* 7:283–294. <http://dx.doi.org/10.1101/gad.7.2.283>.
 30. Kinsinger RF, Kearns DB, Hale M, Fall R. 2005. Genetic requirements for potassium ion-dependent colony spreading in *Bacillus subtilis*. *J Bacteriol* 187:8462–8469. <http://dx.doi.org/10.1128/JB.187.24.8462-8469.2005>.
 31. Fall R, Kearns DB, Nguyen T. 2006. A defined medium to investigate sliding motility in a *Bacillus subtilis* flagella-less mutant. *BMC Microbiol* 6:31. <http://dx.doi.org/10.1186/1471-2180-6-31>.
 32. Rudrappa T, Bais HP. 2007. Arabidopsis thaliana root surface chemistry regulates in planta biofilm formation of *Bacillus subtilis*. *Plant Signal Behav* 2:349–350. <http://dx.doi.org/10.4161/psb.2.5.4117>.
 33. Beauregard PB, Chai Y, Vlamakis H, Losick R, Kolter R. 2013. *Bacillus subtilis* biofilm induction by plant polysaccharides. *Proc Natl Acad Sci U S A* 110:E1621–E1630. <http://dx.doi.org/10.1073/pnas.1218984110>.
 34. Chen Y, Cao S, Chai Y, Clardy J, Kolter R, Guo JH, Losick R. 2012. A *Bacillus subtilis* sensor kinase involved in triggering biofilm formation on the roots of tomato plants. *Mol Microbiol* 85:418–430. <http://dx.doi.org/10.1111/j.1365-2958.2012.08109.x>.
 35. Aguilar C, Vlamakis H, Guzman A, Losick R, Kolter R. 2010. KinD is a checkpoint protein linking spore formation to extracellular-matrix production in *Bacillus subtilis* biofilms. *mBio* 1(1):e00035-10. <http://dx.doi.org/10.1128/mBio.00035-10>.
 36. Vlamakis H, Aguilar C, Losick R, Kolter R. 2008. Control of cell fate by the formation of an architecturally complex bacterial community. *Genes Dev* 22:945–953. <http://dx.doi.org/10.1101/gad.1645008>.
 37. Kovács AT, Kuipers OP. 2011. Rok regulates *yuaB* expression during architecturally complex colony development of *Bacillus subtilis* 168. *J Bacteriol* 193:998–1002. <http://dx.doi.org/10.1128/JB.01170-10>.
 38. Verhamme DT, Murray EJ, Stanley-Wall NR. 2009. DegU and Spo0A jointly control transcription of two loci required for complex colony development by *Bacillus subtilis*. *J Bacteriol* 191:100–108. <http://dx.doi.org/10.1128/JB.01236-08>.
 39. Stöver AG, Driks A. 1999. Secretion, localization, and antibacterial activity of TasA, a *Bacillus subtilis* spore-associated protein. *J Bacteriol* 181:1664–1672.
 40. López D, Vlamakis H, Losick R, Kolter R. 2009. Paracrine signaling in a bacterium. *Genes Dev* 23:1631–1638. <http://dx.doi.org/10.1101/gad.1813709>.
 41. Angelini TE, Roper M, Kolter R, Weitz DA, Brenner MP. 2009. *Bacillus subtilis* spreads by surfing on waves of surfactant. *Proc Natl Acad Sci U S A* 106:18109–18113. <http://dx.doi.org/10.1073/pnas.0905890106>.
 42. Seminara A, Angelini TE, Wilking JN, Vlamakis H, Ebrahim S, Kolter R, Weitz DA, Brenner MP. 2012. Osmotic spreading of *Bacillus subtilis* biofilms driven by an extracellular matrix. *Proc Natl Acad Sci U S A* 109:1116–1121. <http://dx.doi.org/10.1073/pnas.1109261108>.
 43. Garti-Levi S, Eswara A, Smith Y, Fujita M, Ben-Yehuda S. 2013. Novel modulators controlling entry into sporulation in *Bacillus subtilis*. *J Bacteriol* 195:1475–1483. <http://dx.doi.org/10.1128/JB.02160-12>.
 44. Hobley L, Ostrowski A, Rao FV, Bromley KM, Porter M, Prescott AR, MacPhee CE, Van Aalten DM, Stanley-Wall NR. 2013. BslA is a self-assembling bacterial hydrophobin that coats the *Bacillus subtilis* biofilm. *Proc Natl Acad Sci U S A* 110:13600–13605. <http://dx.doi.org/10.1073/pnas.1306390110>.
 45. Kobayashi K, Iwano M. 2012. BslA (YuaB) forms a hydrophobic layer on the surface of *Bacillus subtilis* biofilms. *Mol Microbiol* 85:51–66. <http://dx.doi.org/10.1111/j.1365-2958.2012.08094.x>.
 46. Kovács AT, van Gestel J, Kuipers OP. 2012. The protective layer of biofilm: a repellent function for a new class of amphiphilic proteins. *Mol Microbiol* 85:8–11. <http://dx.doi.org/10.1111/j.1365-2958.2012.08101.x>.
 47. Epstein AK, Pokroy B, Seminara A, Aizenberg J. 2011. Bacterial biofilm shows persistent resistance to liquid wetting and gas penetration. *Proc Natl Acad Sci U S A* 108:995–1000. <http://dx.doi.org/10.1073/pnas.1011033108>.
 48. van Gestel J, Weissing FJ, Kuipers OP, Kovács AT. 2014. Density of founder cells affects spatial pattern formation and cooperation in *Bacillus subtilis* biofilms. *ISME J* 8:2069–2079. <http://dx.doi.org/10.1038/ismej.2014.52>.
 49. van Gestel J, Vlamakis H, Kolter R. 2015. From cell differentiation to cell collectives: *Bacillus subtilis* uses division of labor to migrate. *PLoS Biol* 13:e1002141. <http://dx.doi.org/10.1371/journal.pbio.1002141>.
 50. Gottig N, Pedrido ME, Méndez M, Lombardía E, Rovetto A, Philippe V, Orsaria L, Grau R. 2005. The *Bacillus subtilis* SinR and RapA developmental regulators are responsible for inhibition of spore development by alcohol. *J Bacteriol* 187:2662–2672. <http://dx.doi.org/10.1128/JB.187.8.2662-2672.2005>.
 51. Mhatre E, Monterrosa RG, Kovács AT. 2014. From environmental signals to regulators: modulation of biofilm development in Gram-positive bacteria. *J Basic Microbiol* 54:616–632. <http://dx.doi.org/10.1002/jobm.201400175>.
 52. Lundberg ME, Becker EC, Choe S. 2013. MstX and a putative potassium channel facilitate biofilm formation in *Bacillus subtilis*. *PLoS One* 8:e60993. <http://dx.doi.org/10.1371/journal.pone.0060993>.
 53. Kolodkin-Gal I, Elsholz AK, Muth C, Girguis PR, Kolter R, Losick R. 2013. Respiration control of multicellularity in *Bacillus subtilis* by a complex of the cytochrome chain with a membrane-embedded histidine kinase. *Genes Dev* 27:887–899. <http://dx.doi.org/10.1101/gad.215244.113>.
 54. Trach KA, Hoch JA. 1993. Multisensory activation of the phosphorelay initiating sporulation in *Bacillus subtilis*: identification and sequence of the protein kinase of the alternate pathway. *Mol Microbiol* 8:69–79. <http://dx.doi.org/10.1111/j.1365-2958.1993.tb01204.x>.
 55. Wang L, Grau R, Perego M, Hoch JA. 1997. A novel histidine kinase inhibitor regulating development in *Bacillus subtilis*. *Genes Dev* 11:2569–2579. <http://dx.doi.org/10.1101/gad.11.19.2569>.
 56. Szurmant H, Hoch JA. 2013. Statistical analyses of protein sequence alignments identify structures and mechanisms in signal activation of sensor histidine kinases. *Mol Microbiol* 87:707–712. <http://dx.doi.org/10.1111/mmi.12128>.
 57. Heginbotham L, Lu Z, Abramson T, MacKinnon R. 1994. Mutations in the K⁺ channel signature sequence. *Biophys J* 66:1061–1067. [http://dx.doi.org/10.1016/S0006-3495\(94\)80887-2](http://dx.doi.org/10.1016/S0006-3495(94)80887-2).
 58. Kuo MM, Haynes WJ, Loukin SH, Kung C, Saimi Y. 2005. Prokaryotic K⁺ channels: from crystal structures to diversity. *FEMS Microbiol Rev* 29:961–985. <http://dx.doi.org/10.1016/j.femsre.2005.03.003>.
 59. Fabret C, Feher VA, Hoch JA. 1999. Two-component signal transduction in *Bacillus subtilis*: how one organism sees its world. *J Bacteriol* 181:1975–1983.

60. Choe S. 2002. Potassium channel structures. *Nat Rev Neurosci* 3:115–121. <http://dx.doi.org/10.1038/nrn727>.
61. Derst C, Karschin A. 1998. Evolutionary link between prokaryotic and eukaryotic K⁺ channels. *J Exp Biol* 201:2791–2799.
62. Doyle DA, Morais Cabral J, Pfuetzner RA, Kuo A, Gulbis JM, Cohen SL, Chait BT, MacKinnon R. 1998. The structure of the potassium channel: molecular basis of K⁺ conduction and selectivity. *Science* 280:69–77. <http://dx.doi.org/10.1126/science.280.5360.69>.
63. Jiang M, Shao W, Perego M, Hoch JA. 2000. Multiple histidine kinases regulate entry into stationary phase and sporulation in *Bacillus subtilis*. *Mol Microbiol* 38:535–542. <http://dx.doi.org/10.1046/j.1365-2958.2000.02148.x>.
64. Chai Y, Chu F, Kolter R, Losick R. 2008. Bistability and biofilm formation in *Bacillus subtilis*. *Mol Microbiol* 67:254–263. <http://dx.doi.org/10.1111/j.1365-2958.2007.06040.x>.
65. van Hijum SA, de Jong A, Baerends RJ, Karsens HA, Kramer NE, Larsen R, den Hengst CD, Albers CJ, Kok J, Kuipers OP. 2005. A generally applicable validation scheme for the assessment of factors involved in reproducibility and quality of DNA-microarray data. *BMC Genomics* 6:77. <http://dx.doi.org/10.1186/1471-2164-6-77>.
66. van Hijum SA, de Jong A, Buist G, Kok J, Kuipers OP. 2003. UniFrag and GenomePrimer: selection of primers for genome-wide production of unique amplicons. *Bioinformatics* 19:1580–1582. <http://dx.doi.org/10.1093/bioinformatics/btg203>.
67. Kuipers OP, de Jong A, Baerends RJ, van Hijum SA, Zomer AL, Karsens HA, den Hengst CD, Kramer NE, Buist G, Kok J. 2002. Transcriptome analysis and related databases of *Lactococcus lactis*. *Antonie Van Leeuwenhoek* 82:113–122. <http://dx.doi.org/10.1023/A:1020691801251>.
68. van Hijum SA, Garcia de la Nava J, Trelles O, Kok J, Kuipers OP. 2003. MicroPreP: a cDNA microarray data pre-processing framework. *Appl Bioinformatics* 2:241–244.
69. Baldi P, Long AD. 2001. A Bayesian framework for the analysis of microarray expression data: regularized t-test and statistical inferences of gene changes. *Bioinformatics* 17:509–519. <http://dx.doi.org/10.1093/bioinformatics/17.6.509>.
70. Guérout-Fleury AM, Shazand K, Frandsen N, Stragier P. 1995. Antibiotic-resistance cassettes for *Bacillus subtilis*. *Gene* 167:335–336. [http://dx.doi.org/10.1016/0378-1119\(95\)00652-4](http://dx.doi.org/10.1016/0378-1119(95)00652-4).
71. Kim L, Mogk A, Schumann W. 1996. A xylose-inducible *Bacillus subtilis* integration vector and its application. *Gene* 181:71–76. [http://dx.doi.org/10.1016/S0378-1119\(96\)00466-0](http://dx.doi.org/10.1016/S0378-1119(96)00466-0).
72. Yang L, Ukil L, Osmani A, Nahm F, Davies J, De Souza CP, Dou X, Perez-Balaguer A, Osmani SA. 2004. Rapid production of gene replacement constructs and generation of a green fluorescent protein-tagged centromeric marker in *Aspergillus nidulans*. *Eukaryot Cell* 3:1359–1362. <http://dx.doi.org/10.1128/EC.3.5.1359-1362.2004>.
73. Rodríguez-Ruiz J, Belarbi E, Sánchez JLG, Alonso DL. 1998. Rapid simultaneous lipid extraction and transesterification for fatty acid analyses. *Biotechnol Tech* 12:689–691. <http://dx.doi.org/10.1023/A:1008812904017>.
74. Grau R, de Mendoza D. 1993. Regulation of the synthesis of unsaturated fatty acids by growth temperature in *Bacillus subtilis*. *Mol Microbiol* 8:535–542. <http://dx.doi.org/10.1111/j.1365-2958.1993.tb01598.x>.
75. Nishito Y, Osana Y, Hachiya T, Pependorf K, Toyoda A, Fujiyama A, Itaya M, Sakakibara Y. 2010. Whole genome assembly of a natto production strain *Bacillus subtilis* natto from very short read data. *BMC Genomics* 11:243. <http://dx.doi.org/10.1186/1471-2164-11-243>.
76. Mirel DB, Chamberlin MJ. 1989. The *Bacillus subtilis* flagellin gene (*hag*) is transcribed by the sigma 28 form of RNA polymerase. *J Bacteriol* 171:3095–3101.
77. Zhang Y, Miller RM. 1992. Enhanced octadecane dispersion and biodegradation by a *Pseudomonas* rhamnolipid surfactant (biosurfactant). *Appl Environ Microbiol* 58:3276–3282.
78. Goldstein SA, Colatsky TJ. 1996. Ion channels: too complex for rational drug design? *Neuron* 16:913–919. [http://dx.doi.org/10.1016/S0896-6273\(00\)80114-2](http://dx.doi.org/10.1016/S0896-6273(00)80114-2).
79. Johansson I, Blatt MR. 2006. Interactive domains between pore loops of the yeast K⁺ channel TOK1 associate with extracellular K⁺ sensitivity. *Biochem J* 393:645–655. <http://dx.doi.org/10.1042/BJ20051380>.

Chapter 8

Presence of calcium lowers the expansion of *Bacillus subtilis* colony biofilms

Published in: Microorganisms (2017)



Article

Presence of Calcium Lowers the Expansion of *Bacillus subtilis* Colony Biofilms

Eisha Mhatre ¹, Anandaroopan Sundaram ¹, Theresa Hölscher ¹, Mike Mühlstädt ², Jörg Bossert ² and Ákos T. Kovács ^{1,*}

¹ Terrestrial Biofilms Group, Institute of Microbiology, Friedrich Schiller University Jena, Jena 07743, Germany; eisha.r.mhatre@gmail.com (E.M.); sundar.sabitha@gmail.com (A.S.); thoelscher@ice.mpg.de (T.H.)

² Otto Schott Institute of Materials Research, Friedrich Schiller University Jena, Jena 07743, Germany; mike.muehlstaedt@uni-jena.de (M.M.); Joerg.Bossert@uni-jena.de (J.B.)

* Correspondence: akos-tibor.kovacs@uni-jena.de; Tel.: +49-3641-949980

Academic Editor: Rikke Louise Meyer

Received: 11 January 2017; Accepted: 8 February 2017; Published: 16 February 2017

Abstract: Robust colony formation by *Bacillus subtilis* is recognized as one of the sessile, multicellular lifestyles of this bacterium. Numerous pathways and genes are responsible for the architecturally complex colony structure development. Cells in the biofilm colony secrete extracellular polysaccharides (EPS) and protein components (TasA and the hydrophobin BslA) that hold them together and provide a protective hydrophobic shield. Cells also secrete surfactin with antimicrobial as well as surface tension reducing properties that aid cells to colonize the solid surface. Depending on the environmental conditions, these secreted components of the colony biofilm can also promote the flagellum-independent surface spreading of *B. subtilis*, called sliding. In this study, we emphasize the influence of Ca²⁺ in the medium on colony expansion of *B. subtilis*. Interestingly, the availability of Ca²⁺ has no major impact on the induction of complex colony morphology. However, in the absence of this divalent ion, peripheral cells of the colony expand radially at later stages of development, causing colony size to increase. We demonstrate that the secreted extracellular compounds, EPS, BslA, and surfactin facilitate colony expansion after biofilm maturation. We propose that Ca²⁺ hinders biofilm colony expansion by modifying the amphiphilic properties of surfactin.

Keywords: *Bacillus subtilis*; biofilm; calcium; surfactin; sliding; colony expansion

1. Introduction

Bacteria tend to form sessile, multicellular communities under environmental settings, known as biofilms. In these communities, cells embed themselves in secreted substances that facilitate adherence to surfaces as well as to neighbouring cells. The structures of architecturally complex colonies have been correlated to the general ability of bacteria to develop biofilms [1,2]. When establishing a biofilm, cells of the Gram-positive soil dwelling microbe *Bacillus subtilis* secrete extracellular polysaccharides (EPS), a matrix protein component (TasA), and a hydrophobin protein that assembles on the surface (BslA) [3–6]. In addition, antimicrobial compounds, including surfactin, are secreted that increase the competitiveness of *B. subtilis* against other microbes [7]. The biofilm matrix components carry out numerous functions in addition to the attachment and the colony structure complexity [8], such as protection from environmental attacks [9], colony spreading [10], or sliding [11,12]. Importantly, colonies lacking EPS and TasA production have reduced morphologies and appear smooth [3]. Cells devoid of BslA lose their hydrophobicity and are prone to water-soluble antimicrobials [4,5]. These above described components, EPS, BslA, and surfactin seem to collectively aid flagellum-independent surface spreading, a coordinated behaviour observed in bacteria [11–13].

The expression and synthesis of these secreted products that facilitate biofilm formation and surface spreading are tightly regulated at the level of transcription and affected by various histidine kinases and subsequent cytoplasmic response regulators [6,14,15]. The cytoplasmic and membrane bound histidine kinases (KinA, KinB, KinC, and KinD), in response to dynamic and challenging environmental cues, initiate the phosphorylation of Spo0A (Spo0A~P), the main regulator of various stationary stage processes, via a phosphorelay. The gradual increase in Spo0A~P level influences the cells' commitment towards certain differentiation processes. KinA and KinB activation results in a large pool of Spo0A~P, sufficient for the cells to undergo sporulation [16,17]. Moreover, KinC and KinD were described to respond to a plethora of signals to maintain a low amount of Spo0A~P that is sufficient to activate the expression of genes responsible for biofilm matrix production [6,15]. Recently, it was demonstrated that KinB and KinC collectively induce *B. subtilis* sliding in a spatiotemporal manner [11]. Apart from being a collective behaviour strategy, sliding is also studied in the context of cooperative strategies in bacteria. Heterogeneity in expression of genes required for the secreted components that aid sliding creates a division of labour between surfactin- and matrix-producing cells at the expanding front of the colony [12].

Examination of the factors and processes that influence colony growth and spreading properties in bacteria facilitate our understanding of bacterial population level behaviours. Here, we report that the presence of Ca^{2+} ions in the environment restricts colony expansion following colony biofilm development. The mature colony formation of *B. subtilis* under laboratory conditions requires three to four days after which the colonies are rugose, structurally complex, and display white chalky patterns attributed to sporulation [1,15]. After maturation of *B. subtilis* biofilms, cells in the middle grow slowly, are encapsulated and well protected, while the peripheral cells continue to grow in the direction of new nutrient sources [18]. Our experiments show that when the growth medium was lacking Ca^{2+} salts, biofilm colonies continue to expand in a way that resembles sliding. Considering that most media used to study biofilm colony structures contain Ca^{2+} salts, this phenomenon is seldom observed. Further, we propose that an interaction between Ca^{2+} and surfactin might be responsible for preventing the colony expansion in the presence of Ca^{2+} in the medium.

2. Materials and Methods

2.1. Bacterial Strains, Plasmids, and Media

B. subtilis DK1042 (naturally competent derivative of the undomesticated NCIB 3610) and its derived mutants were used in this study (Table 1). The strains were inoculated from glycerol cryo-stocks in LB medium (Lysogeny broth, 1% tryptone, 0.5% yeast extract, 0.5% NaCl) overnight before spotting them on the agar plates for complex colony formation. The media used for colony studies are 2×SG [19] and MSgg [1] with 1.5% or 0.7% agar concentration. The original recipes of 2×SG and MSgg contain $\text{Ca}(\text{NO}_3)_2$ and CaCl_2 , respectively. For generation of strains, genomic or plasmid DNA was transformed into DK1042 using natural competence [20] and the cells were selected on the LB agar with respective antibiotic concentrations. The antibiotic concentrations used were the same as stated previously [15].

For the construction of the P_{bslA} -*gfp* reporter plasmid (pTB670), the *bslA* promoter region was PCR amplified using primers oTH23 (5'-ACTGAATTCGGGAGCGGGAGGTTCAAGTG-3') and oTH24 (5'-GCAGCTAGCGCGTTTCATAACAAAATTCC-3') from *B. subtilis* 3610 genomic DNA, restricted with *EcoRI* and *NheI*, cloned into the corresponding sites of *prrmB*-GFP plasmid [21], and transformed into *Escherichia coli* MC1061.

To construct plasmid pTB497 harbouring a constitutively expressed *gfp* gene, the $P_{\text{hyperspank}}$ -*gfp* fragment was PCR amplified with primers oTH1 (5'-GCATCTAGAGTTGCTCGCGGGTAAATGTG-3') and oTH2 (5'-CGAGAATTCATCCAGAAGCCTTGCATATC-3') from plasmid phy-GFP [22], digested with *XbaI* and *EcoRI*, ligated into plasmid pWK-Sp [23], and transformed into *E. coli* MC1061. Resulting plasmids were verified by sequencing.

Table 1. Strains used in the study.

Strain	Genotype	Reference, Source, or Construction
DK1042	3610 <i>comI</i> ^{Q12I}	[20]
TB500	3610 <i>comI</i> ^{Q12I} <i>amyE</i> ::P _{hysperpank} - <i>gfp</i> (<i>spec</i> ^R)	pTB497 → DK1042
TB602	3610 <i>comI</i> ^{Q12I} Δ <i>tasA</i> :: <i>spec</i> ^R	TB163 [11] → DK1042
TB277	3610 <i>comI</i> ^{Q12I} Δ <i>srfAA</i> :: <i>Cm</i>	RG551 [11] → DK1042
TB530	3610 <i>comI</i> ^{Q12I} Δ <i>hag</i> :: <i>neo</i>	TB24 [11] → TB500
TB524	3610 <i>comI</i> ^{Q12I} Δ <i>epsA-O</i> :: <i>tet</i> ^R	DL1032 [24] → TB500
TB526	3610 <i>comI</i> ^{Q12I} Δ <i>bslA</i> :: <i>cm</i> ^R	NRS 2097 [25] → TB500
TB398	3610 <i>comI</i> ^{Q12I} Δ <i>kinA</i> :: <i>mls</i> ^R	JH12638 [11] → DK1042
TB399	3610 <i>comI</i> ^{Q12I} Δ <i>kinB</i> :: <i>tet</i> ^R	JH19980 [11] → DK1042
TB400	3610 <i>comI</i> ^{Q12I} Δ <i>kinC</i> :: <i>spec</i> ^R	BAL393 [11] → DK1042
TB401	3610 <i>comI</i> ^{Q12I} Δ <i>kinD</i> :: <i>cm</i> ^R	BAL691 [11] → DK1042
TB402	3610 <i>comI</i> ^{Q12I} Δ <i>kinE</i> :: <i>cm</i> ^R	BAL692 [11] → DK1042
TB672	3610 <i>comI</i> ^{Q12I} Δ <i>kinB</i> :: <i>tet</i> ^R Δ <i>kinC</i> :: <i>spec</i> ^R	TB400 → TB399
TB656	3610 <i>comI</i> ^{Q12I} Δ <i>kinC</i> :: <i>spec</i> ^R Δ <i>kinD</i> :: <i>cm</i> ^R	TB400 → TB401
TB671	3610 <i>comI</i> ^{Q12I} Δ <i>degU</i> :: <i>neo</i> ^R	Δ <i>degU</i> [26] → DK1042
TB51	3610 <i>comI</i> ^{Q12I} Δ <i>lcfA</i> :: <i>mls</i> ^R	MW2 [27] → DK1042
TB363	3610 <i>comI</i> ^{Q12I} <i>sacA</i> ::P _{epsA} - <i>gfp</i> (<i>neo</i> ^R)	[28]
TB373	3610 <i>comI</i> ^{Q12I} <i>sacA</i> ::P _{tapA} - <i>gfp</i> (<i>neo</i> ^R)	[28]
TB685	3610 <i>comI</i> ^{Q12I} <i>amyE</i> ::P _{bslA} - <i>gfp</i> (<i>cm</i> ^R)	pTB670 → DK1042
TB740	3610 <i>comI</i> ^{Q12I} P _{srfAA} - <i>gfp</i> (<i>spec</i> ^R)	BD4720 [29] → DK1042

2.2. Colony Biofilm Formation

For colony spotting, 2×SG or MSgg medium with 1.5% agar were poured and allowed to solidify with closed petri dish lid. Both media were prepared with or without the supplementation of 1 mM Ca(NO₃)₂. Once solidified, the plates were opened completely under sterile laminar airflow conditions, and dried for 20 min. Once dried, 2 µL of the overnight grown cultures were spotted on the plate (not more than two colonies per plate), and the lids were closed once the spotted culture dried. The plates were incubated at 30 °C for seven to eight days.

2.3. Swarming and Sliding

Swarming and sliding was assayed on LB or 2×SG medium solidified with 0.7% agar. The exact preparation of media and plates were previously described [30]. Plates were incubated at 37 °C and swarming diameter was recorded every hour between 3 and 7 h after inoculation, while sliding was documented after 24 and 48 h.

2.4. Imaging and Colony Size Measurements

The colonies grown on the 1.5% agar plates were imaged depending on the medium using an AxioZoom V16 microscope equipped with an AxioCam MRm monochrome camera (Carl Zeiss Microscopy GmbH, Jena, Germany). The colony diameters were also measured to quantitate the colony spread in the presence and absence of the supplemented Ca²⁺. Images were calibrated using Image J version 2.0.0-rc-15. Sliding and swarming disks were recorded using a Nikon D3300 camera (Düsseldorf, Germany) equipped with a Nikon AF-S DX Nikkor 18–55 mm objective.

2.5. Growth and Fluorescent Reporter Assays

Overnight cultures of *B. subtilis* strains were diluted 100-fold in 2×SG medium supplemented with different amounts of Ca(NO₃)₂; 200 µL aliquots of the culture were placed in the wells of a 96-well plate and incubated under shaken conditions at 30 °C. Growth and fluorescence intensity were recorded every 15 min using an infinite F200PRO plate reader (TECAN Group Ltd., Männedorf, Switzerland).

2.6. Surface Tension Measurements

Wild-type or mutant strains were grown overnight in 20 mL 2×SG medium in 50 mL bottles at 37 °C under well agitated conditions. The cells were removed by centrifugation and the culture supernatant was used. The surface tension was measured according to the Wilhelmy plate method using a tensiometer (DCAT 21, DataPhysics, Filderstadt, Germany) interfaced to a computer using the SCAT-33 software, at room temperature (25 °C) and atmosphere pressure. Briefly, 5–10 mL of the supernatant was added to the vessel. The Wilhelmy plate (platinum-iridium plate) used in this study has a wetted length of 40.20 mm. Before each measurement run, the Wilhelmy plate was rinsed with deionized water and subsequently flamed red-hot with a butylene burner. To detect the supernatant's surface the Wilhelmy plate was moved towards the supernatant's surface using a motor speed of 1 mm/s and a detection weight threshold of 8.00 mg. Afterwards, the Wilhelmy plate was immersed 3 mm into the supernatant. The measurement was performed at 5 Hz and stopped after attaining a standard deviation below 0.03 mN/m for 50 consecutive measuring points. To calculate the force from the equivalent mass value obtained by the microbalance, the local gravitational acceleration value (9.81485 m/s²) for the Otto-Schott-Institute of Materials Research (Jena, Germany), was used. Ten measurements were recorded for each sample, and the experiment was repeated for three biological samples and performed independently twice. The measurements on the various samples were also performed with increasing concentrations of Ca(NO₃)₂ to observe the alteration in liquid surface tension.

3. Results

3.1. Presence of Ca²⁺ Prevents Cells to Spread Out from Matured Biofilm Colonies

When previously examining the impact on Mn²⁺ on colony biofilm development of *B. subtilis* [15], we also tested whether the lack of other components in the medium 2×SG has an effect on the colony biofilm development of various *B. subtilis* strains. Interestingly, we observed that the colonies of *B. subtilis* DK1042 (the naturally competent derivative of the undomesticated NCIB 3610 that forms comparable colony biofilms to NCIB 3610) grown on 2×SG plates without the supplemented Ca(NO₃)₂ grew normally until day 3, after which the peripheral cells began to spread and the colony size kept on increasing (Figure 1A). Importantly, no difference in colony growth was observed until three days, and only minor difference was observed in structure. In this paper, we concentrate on the colony size, thus the expansion of the biofilm colonies that denotes the radial expansion of cells after biofilm colony maturation, thus the expansion observed after three days of cultivation. The 2×SG medium contains Ca(NO₃)₂ as one of its components. Hence, under normal conditions where all the medium components were supplemented, the colonies were rugose with concentric white chalky patterns around (Figure 1A and [15]). In contrast, when the medium lacked Ca(NO₃)₂, the cells at the colony periphery started to expand on the agar surface after three to four days of incubation. To test whether omitting Ca²⁺ or NO₃⁻ triggers the colony expansion at this later time point of colony development, other salts were tested in 2×SG medium. Neither NO₃⁻ nor other divalent cations restricted colony expansion similar to Ca²⁺ (Figure S1).

In addition, omitting Ca²⁺ in the biofilm inducing minimal medium, MSgg had a similar impact on the colony spreading (Figure 1B), although the colony biofilm structures differ in the two media. Quantitative measurement of the colony size on 2×SG and MSgg medium revealed that in the absence of Ca²⁺, biofilm colonies spread more and are significantly bigger in size than in the presence of Ca²⁺ (Figure 1C,D). Excluding Ca²⁺ had no major impact on pellicle development on 2×SG medium (Figure S2A).

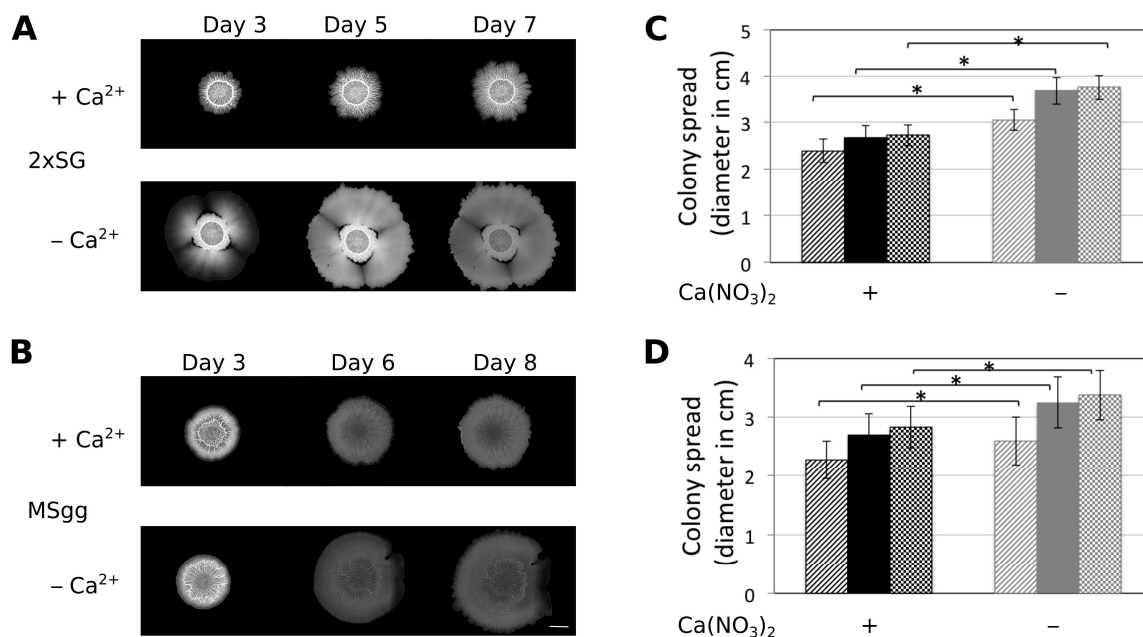


Figure 1. Presence of Ca^{2+} restricts colony expansion. Colonies of *B. subtilis* are shown in the presence and absence of Ca^{2+} on 2×SG (A) and MSgg (B) media at different days after inoculation. The scale bar at the lower right corner denotes 5 mm. The colony expansion diameters are presented on 2×SG (C) and MSgg (D) media after three or four (striped), five or six (filled), and seven or eight (checked) days, respectively, after inoculation in the presence (black bars) or absence (grey bars) of Ca^{2+} . The error bars indicate 95% confidence intervals. * denotes significant differences ($p < 0.05$) analysed with paired *t*-test.

3.2. Ca^{2+} Restricts Flagellum-Independent Expansion of Biofilm Colonies

The colony expansion (observed after the three days of biofilm development) in the absence of Ca^{2+} was also influenced by nutrient depletion, since cells showed no outgrowth when Ca^{2+} was omitted from 4×SG medium that consisted of twice as much nutrients as 2×SG, while colony expansion was observed when nutrients were reduced (Figure S2B). Dispersal has been described as the ultimate stage of the biofilm lifecycle following nutrient depletion and overcrowding of the sessile population [31]. Colony expansion might be an alternative mechanism to those observed during dispersal. Fleeing from the biofilm is generally facilitated by single cell motility or via small cluster of cells breaking off. As the presence of Ca^{2+} ions restricted the dispersal of complex biofilm colonies, we questioned whether flagellum-dependent motility is necessary for the observed surface spreading. Colony expansion of *B. subtilis* strains lacking the *hag* gene that encoded the flagellin protein was assayed in presence and absence of Ca^{2+} . The Δhag strain behaved similar to the *B. subtilis* wild type (WT) as lack of Ca^{2+} supplementation in the medium increased spreading (Figure 2). Interestingly, the spreading of Δhag was more uniform compared to the WT where expansion was observable from small sectors of the matured biofilm colonies (Figure 1).

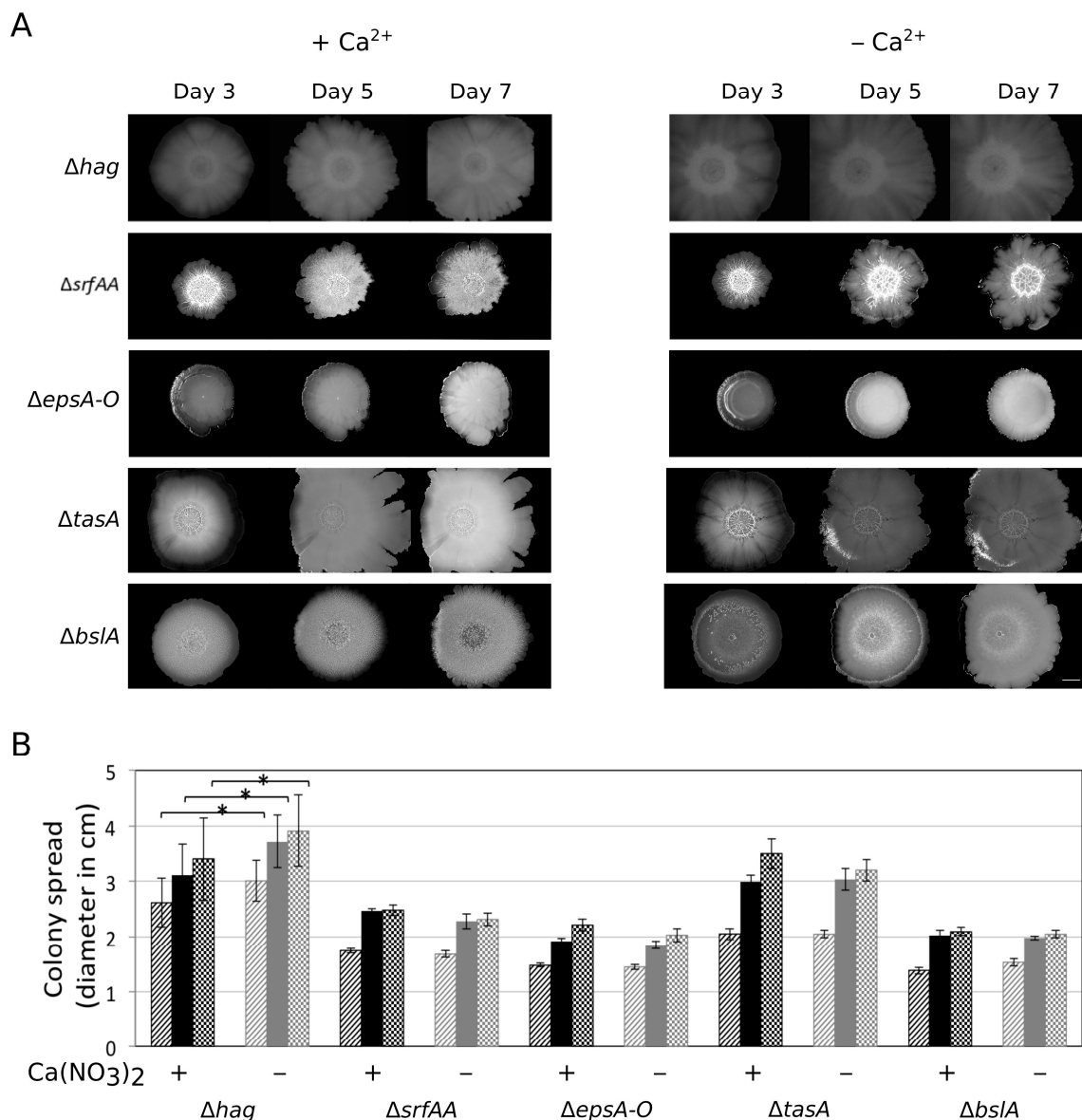


Figure 2. Colony expansion of various mutants of *B. subtilis*. **(A)** The colony images of Δhag , $\Delta srfAA$, $\Delta epsA-O$, $\Delta bslA$, and $\Delta tasA$ strains are shown three, five, and seven days after inoculation on $2\times SG$ medium in the presence or absence of Ca^{2+} . The scale bar indicates 5 mm. **(B)** The colony expansion diameters of the mutants presented in panel A are shown after three (striped), five (filled), and seven (checked) days. Black bars present data in the presence of Ca^{2+} , while grey bars indicate the absence of Ca^{2+} . The error bars indicate 95% confidence intervals. Data was analysed with paired t-test for significantly different samples ($* = p < 0.05$).

3.3. Importance of the Components Required for Sliding on Colony Expansion

Surface spreading of *B. subtilis* has been generally examined using semi-solid medium containing 0.5%–0.7% agar. Under these conditions, *B. subtilis* can colonize the agar medium surface using flagellum-dependent swarming or flagellum-independent sliding [11,12,32]. As flagellum-dependent motility was not required for colony expansion, we hypothesized that the observed spreading is similar to sliding that necessitates the collective secretion of EPS, TasA, BslA, and surfactin. Deletion of any of the genes essential for production of these components prevents colony expansion on $2\times SG$ medium without Ca^{2+} supplementation (Figure 2). Therefore, the sliding machinery facilitates the colony expansion after biofilm maturation. A similar trend was observed when the colony sizes of the mutant

strains were recorded on MSgg medium in the presence or absence of Ca^{2+} (Figure S3A). To examine if swarming or sliding are influenced by excess Ca^{2+} in the medium, surface colonization of wild-type and Δhag strains of *B. subtilis* exhibiting swarming and sliding, respectively, were assayed on both LB and 2×SG media containing 0.7% agar and different levels of $\text{Ca}(\text{NO}_3)_2$ (Figure 3). *B. subtilis* swarming diameter was diminished when 100 mM Ca^{2+} was supplemented in both media (Figure 3A,D), while it was somewhat reduced in the presence of 1 and 10 mM Ca^{2+} on 2×SG medium (Figure 3B,D). Moreover, the sliding disk of *B. subtilis* Δhag strain was decreased in the presence of 10 mM Ca^{2+} supplementation in both LB and 2×SG media (Figure 3C,E). These data suggested that Ca^{2+} targeted a component that was required for both swarming and sliding. Importantly, the increased $\text{Ca}(\text{NO}_3)_2$ concentration had no or minor impact on the growth rate of *B. subtilis* cultivated in liquid 2×SG medium (Figure 3F).

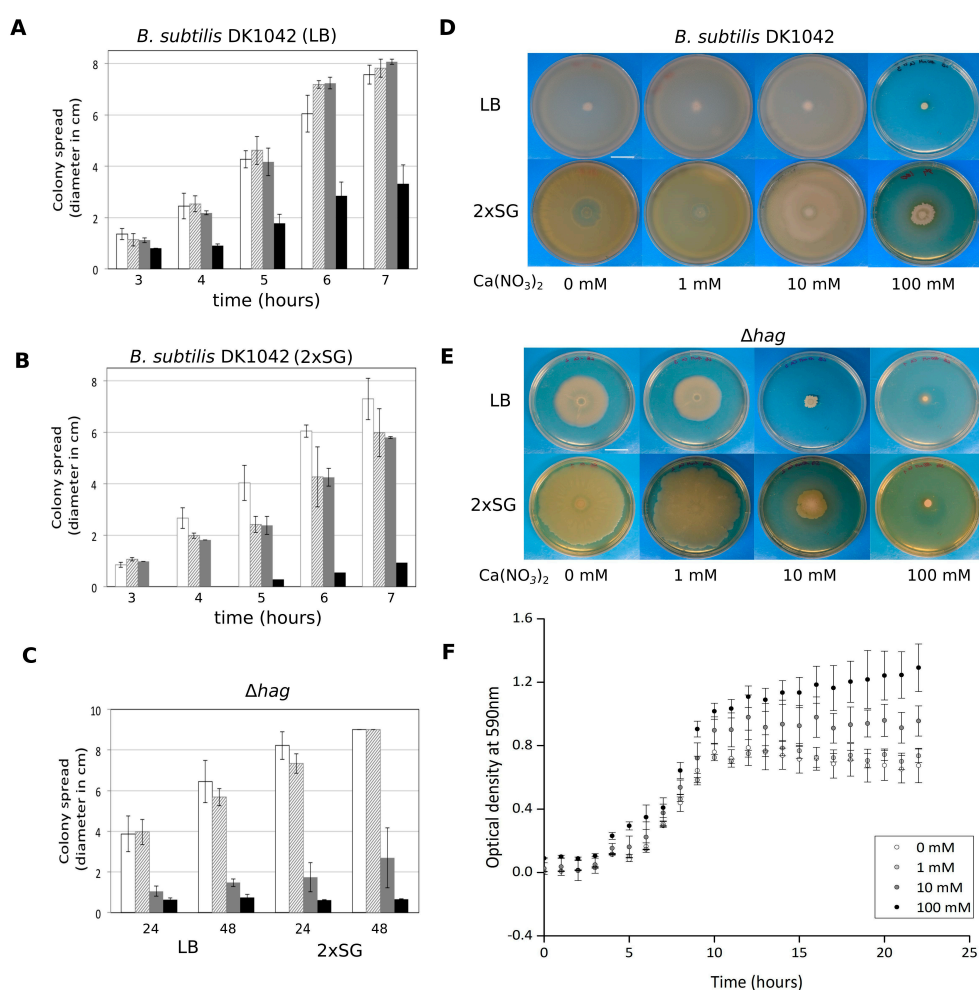


Figure 3. Impact of the presence of Ca^{2+} on swarming and sliding mediated surface colonization of *B. subtilis* DK1042 and Δhag strains, respectively, on Lysogeny broth (LB) and 2×SG medium. Swarming diameter of *B. subtilis* DK1042 strain after 3 to 7 h on LB (A) and 2×SG (B) media with 0.7% agar without (white bars) or with 1 (stripped bars), 10 (grey bars), 100 mM (black bars) Ca^{2+} supplemented. Sliding diameter of *B. subtilis* Δhag strain (C) after 24 and 48 h on LB (left) and 2×SG (right) media supplemented with various amount of $\text{Ca}(\text{NO}_3)_2$ (labelling similar to S4A). Swarming (D) and sliding (E) disk of wild type (WT) and Δhag strains, respectively, 24 h after inoculation on LB (above) and 2×SG (below) media with 0.7% agar in the absence or presence of various amounts of Ca^{2+} supplementation. Scale bars indicate 2 cm. Growth properties of *B. subtilis* DK1042 (F) in 2×SG medium supplemented with different amount $\text{Ca}(\text{NO}_3)_2$ from 1 mM to 100 mM.

A recent study demonstrated that calcium mineralization in *B. subtilis* colonies impacts biofilm rigidity and scaffolding. This study demonstrated the importance of *lcfA* in bio-mineralization in colonies [33,34]. Incidentally, LcfA is also involved in fatty acid degradation during surfactin production [27]. Nevertheless, mutation in *lcfA* gene did not prevent colony expansion in the absence of Ca^{2+} (Figure S3B).

3.4. Colony Expansion on Ca^{2+} Limited Medium Depends on KinB and KinC, the Major Sliding-Inducing Sensor Kinases

Since KinB and KinC were reported to activate sliding in *B. subtilis* [11], mutants lacking individual genes coding for the Kin histidine kinases were tested for the colony expansion abilities in the absence of Ca^{2+} . None of the single mutants was reduced for colony expansion spreading in Ca^{2+} -depleted medium (Figure 4 and Figure S3B). While both KinB and KinC are important for full activation of sliding in *B. subtilis*, only deletion of both kinases results in sliding-deficient phenotype [11]. Consistently, *B. subtilis* harbouring both *kinB* and *kinC* deletions lacked the ability to spread in the absence of Ca^{2+} (Figure 4). As the DegS-DegU two component system was previously described to indirectly activate *bslA* transcription [25,26,35], we tested a strain with a deletion of the *degU* gene for colony expansion. However, the *degU* mutant colony spreading was increased in the absence of Ca^{2+} supplementation (Figure S3B). One explanation for this result could be that although expression of the *bslA* gene is reduced in the *degU* mutant, expression of the *epsA-O* and the *tapA-sipW-tasA* operons is increased [36,37].

3.5. Ca^{2+} Does Not Impact the Expression of the EPS, *tasA*, and *srfA* Genes in Planktonic Cultures

The colony expansion in the absence of Ca^{2+} could be related to changes in the expression levels of the *srfAA*, *epsA-O*, *tasA*, or *bslA* genes. Therefore, the impact of Ca^{2+} supplementation in the 2×SG liquid medium was tested on strain harbouring P_{srfAA} -*yfp*, P_{epsA} -*gfp*, P_{tapA} -*gfp*, or P_{bslA} -*gfp* fusions. Following the reporter activity over time revealed that the gene expressions of *epsA-O*, and *tapA-sipW-tasA*, and *srfAA-AC* were unaffected, while *bslA* was barely decreased in liquid culture grown in the presence of supplemented Ca^{2+} (Figure 4C–F). Expressions from P_{epsA} -*gfp* and P_{tapA} -*gfp* were comparable in colonies in the presence or absence of supplemented Ca^{2+} (data not shown). Importantly, we cannot exclude the possibility that gene expression of *bslA* and *srfA* in matured colony biofilm is increased locally in the absence of Ca^{2+} , influencing the expression of genes responsible for colony expansion.

3.6. Influence of Ca^{2+} on the Amphiphilic Properties of Surfactin Molecules

Next, we addressed the question of how the presence of Ca^{2+} could disturb colony expansion independent of affecting expression of genes related to sliding. Previous studies demonstrated that divalent cations, including Ca^{2+} , form complexes with surfactin secreted by *B. subtilis* [38]. Thus, if the Ca^{2+} supplemented in the medium forms a complex with surfactin and alters its amphiphilic property (i.e., surface tension reduction), surfactin facilitated sliding properties might change. To demonstrate that Ca^{2+} can directly influence surfactin properties, surface tensions of spent media (overnight grown culture supernatants) from different strains were recorded in the presence of increasing amounts of Ca^{2+} by the Wilhelmy plate method using a DataPhysics tensiometer DCAT21 [39]. When culture supernatant contained surfactin (e.g., WT and *epsA-O* strain), the liquid surface tension was lower compared to the medium control and the supernatant of the $\Delta srfAA$ strain (Figure 5A).

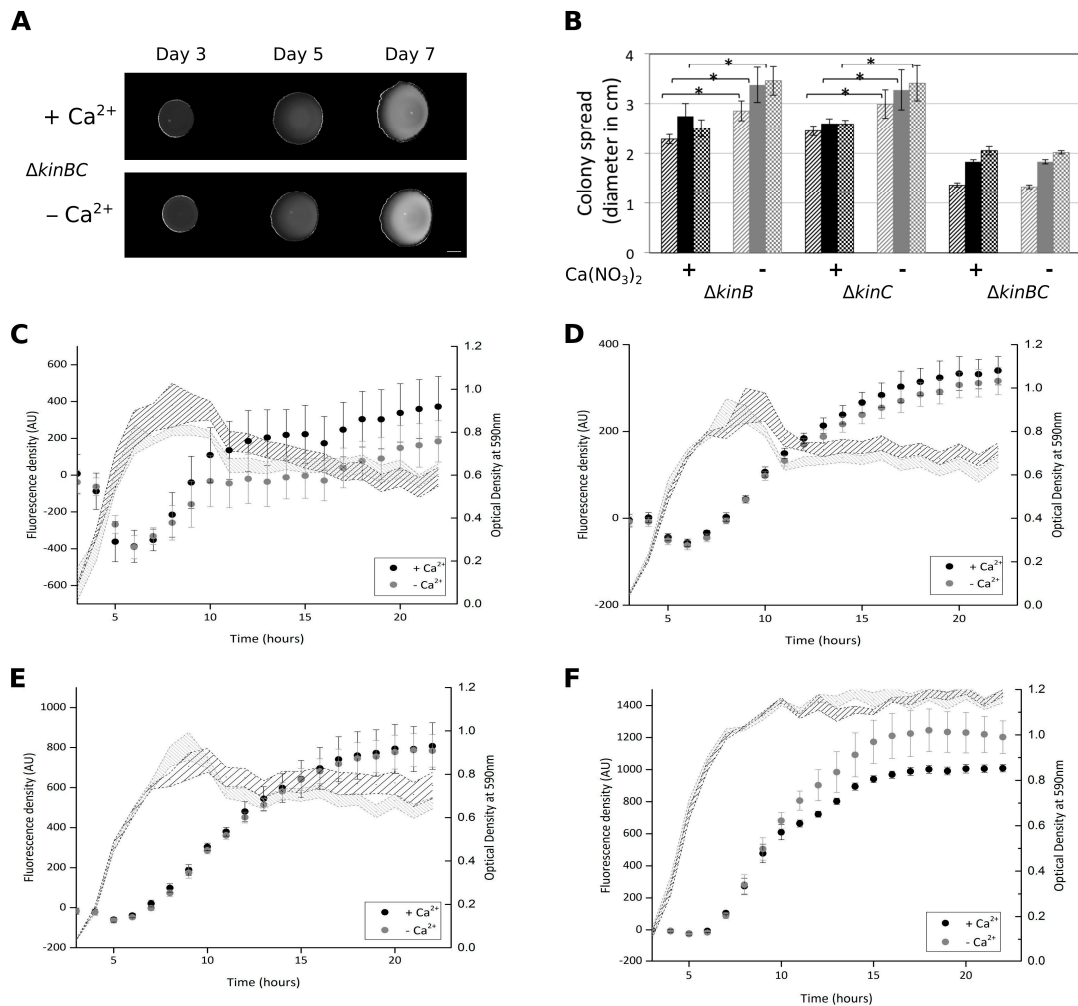


Figure 4. Colony expansion of histidine kinase mutant and expression of selected genes in the presence or absence of Ca^{2+} . (A) Colony expansion of the $\Delta kinB\Delta kinC$ double mutant after three, five, and seven days. Scale bar indicates 5 mm. (B) The colony expansion diameters of the $\Delta kinB$, $\Delta kinC$ single, and $\Delta kinB\Delta kinC$ double mutant are shown after three (striped), five (filled), and seven (checked) days. Black bars present data in the presence of Ca^{2+} , while grey bars indicate the absence of Ca^{2+} . The error bars indicate 95% confidence interval. * denotes significant differences ($p < 0.05$) analysed with paired t-test. Relative fluorescence and growth profile (optical density) of *B. subtilis* strains harbouring the P_{stfAA} -yfp (C), P_{epsA} -gfp (D), P_{tapA} -gfp (E), or P_{bslA} -gfp (F) constructs in the presence (indicated in black) or the absence (indicated in grey) of Ca^{2+} supplemented in the 2×SG medium.

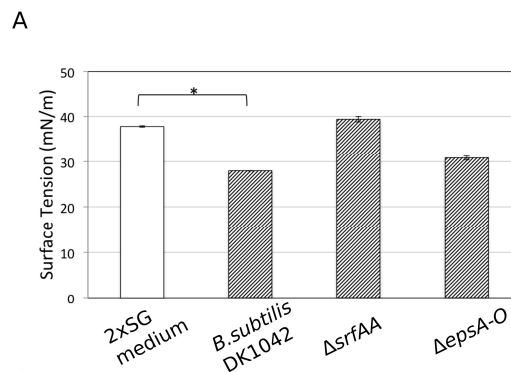


Figure 5. Cont.

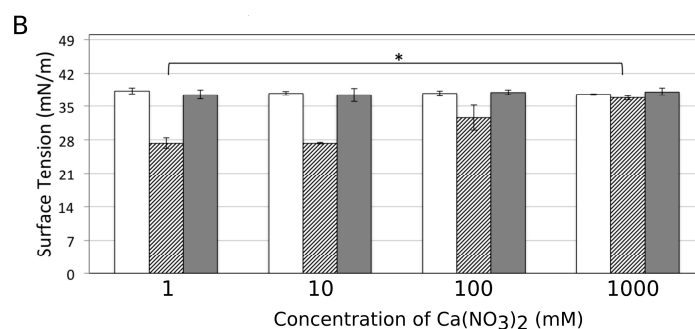


Figure 5. Surface tension measurement of the 2×SG medium and the supernatants of various *B. subtilis* mutants in the presence of different Ca²⁺ levels. (A) Surface tension of the 2×SG medium (white bar), wild type, $\Delta srfAA$, and $\Delta epsA-O$ mutant supernatants (black striped bars). (B) Surface tension of the 2×SG medium (white bars), the supernatants of WT (striped bars), and of $\Delta srfAA$ (filled bars) strains in the presence of different Ca²⁺ concentrations. The error bars indicate 95% confidence intervals. Data was analysed with paired t-test for significantly different samples (* = $p < 0.05$).

The absence or presence of 1 mM of Ca²⁺ had no significant impact on the surface tension of the 2×SG medium. However, when the Ca²⁺ concentration was gradually increased to 100–500 mM, the surface tension values of the medium elevated (Figure 5B). The amount of surplus Ca²⁺ was possibly high enough to form complexes with most of the surfactin molecules in the medium abolishing their surface tension reducing properties. When Ca²⁺ was added to the medium control or the $\Delta srfAA$ supernatant, the surface tension was not altered and stayed similar to the WT supernatant with high amounts of Ca²⁺.

4. Discussion

The quantity of ions in the environment influences various cellular pathways in *B. subtilis*, including biofilm development [15,40–43]. In our study, we highlighted the role of Ca²⁺ in maintaining the integrity and robust structure of biofilm colonies. In commonly used laboratory media that promote colony biofilm development of *B. subtilis*, cells attach to the agar surface and produce complex robust structures within three to four days. The biofilm matrix components such as EPS, TasA, and BslA play an essential role in colony wrinkleality as well as influence the indentation on the agar surface [44,45]. Interestingly, in the absence of Ca²⁺, peripheral cells in the complex colonies expand radially after four days, likely due to nutrient depletion. In the presence of Ca²⁺, however, the structure is maintained and colony size barely increases. Here, we demonstrated that extracellular polymeric substances and surfactants that are essential for expansion by sliding play an important role in the colony expansion. Mutants that do not produce either surfactin, EPS, the hydrophobin BslA, or the protein component TasA failed to expand from the matured biofilm colonies in medium with reduced Ca²⁺ levels, while the presence or the absence of Ca²⁺ had no major influence on the structural properties of the developing biofilm colonies.

Divalent cations, including Ca²⁺, are known to influence electrostatic interactions and bacterial attachment processes [46,47]. Ca²⁺ is also required for poly- γ -glutamate acid production in *B. subtilis* natto [48]. The influence of Ca²⁺ on surfactin has been extensively studied in X-ray diffraction experiments to demonstrate how the amphiphilic properties of surfactin are reduced during complex formation [38,49]. Moreover, Ca²⁺ also captures and localizes the ionized surfactin molecules in the phospholipid bilayers of the cell membrane. During colony development of *B. subtilis*, Ca²⁺-carbonate present in the agar medium plays an important role during bio-mineralization, establishing scaffold formation and nutrient channelling in the biofilms [33]. The ability of Ca²⁺ to establish complexes with surfactin molecules might explain the lack of colony expansion on an agar medium supplemented with Ca²⁺. Surface tension measurements with bacterial supernatant demonstrated that the high surplus of

Ca²⁺ could preclude surfactin dependent reduction of the surface tension. Notably, the amount of Ca²⁺ required for the in vitro inhibition of the surfactin activity was two magnitudes higher than used in the colony experiments. In addition, reduction of sliding and swarming also requires increased Ca²⁺ levels compared to the concentration used for colony biofilms. We hypothesize that this conflicting observation might be resolved by the possibility that the presence of Ca²⁺ ions impact the freshly secreted surfactin at the biofilm colony edge, while Ca²⁺-surfactin complex formation in fluids or in soft agars with increased diffusion is less stable. Colony expansion observed in our experiments on highly viscous medium (i.e., with 1.5% agar) might be more sensitive to alteration in surfactin properties compared to swarming/sliding conditions or liquid medium. Importantly, elevated Ca²⁺ levels in various media were able to reduce swarming and sliding of *B. subtilis*. As both swarming and sliding necessitates the reduction of surface tension by surfactin, these experiments further supported that interaction of Ca²⁺ and surfactin has great impact on surface spreading on soft agar medium.

This study adds to our understanding of rugose colony structure development in *B. subtilis* and the factors involved in maintaining these structures. The presence of Ca²⁺ in the medium not only prevented the expansion of the cells from the colonies but also restricted them in the nutritionally depleted environment, thus probably indirectly influencing late stationary processes such as sporulation. The cells in the biofilm colonies were previously described to form white rugose structures due to sporulation. Thus, Ca²⁺ has a substantial impact on the fate of colonies and the differentiation properties of these complex biofilm populations. In addition, our results might have implications towards surface engineering of various materials related to biofilm formation and bacterial colonization in general.

Supplementary Materials: The following are available online at www.mdpi.com/2076-2607/5/1/7/s1, Figure S1: Ca²⁺ specifically reduces colony expansion, Figure S2: Impact of Ca²⁺ on pellicle formation and colony spreading at different nutrient concentrations, Figure S3: Colony expansion of various strains on MSgg and 2×SG medium.

Acknowledgments: The laboratory of Á.T.K. was supported by a Marie Skłodowska Curie career integration grant (PheHetBacBiofilm), and grants KO4741/2-1 and KO4741/3-1 from the Deutsche Forschungsgemeinschaft (DFG). E.M. and T.H. were supported by Jena School for Microbial Communications (JSMC) and International Max Planck Research School (IMPRS) fellowships, respectively.

Author Contributions: E.M. and Á.T.K. conceived the study; E.M., A.S., and T.H. performed the experimental work and analysed the data; M.M. and B.J. contributed with reagents and analysis tools; E.M. and Á.T.K. wrote the paper. All authors reviewed the manuscript.

Conflicts of Interest: The authors have no conflict of interest to declare.

References

1. Branda, S.S.; González-Pastor, J.E.; Ben-Yehuda, S.; Losick, R.; Kolter, R. Fruiting body formation by *Bacillus subtilis*. *Proc. Natl. Acad. Sci. USA* **2001**, *98*, 11621–11626. [CrossRef] [PubMed]
2. Shapiro, J.A. Thinking about bacterial populations as multicellular organisms. *Annu. Rev. Microbiol.* **1998**, *52*, 81–104. [CrossRef] [PubMed]
3. Branda, S.S.; Chu, F.; Kearns, D.B.; Losick, R.; Kolter, R. A major protein component of the *Bacillus subtilis* biofilm matrix. *Mol. Microbiol.* **2006**, *59*, 1229–1238. [CrossRef] [PubMed]
4. Hogley, L.; Ostrowski, A.; Rao, F.V.; Bromley, K.M.; Porter, M.; Prescott, A.R.; MacPhee, C.E.; Van Aalten, D.M.; Stanley-Wall, N.R. BslA is a self-assembling bacterial hydrophobin that coats the *Bacillus subtilis* biofilm. *Proc. Natl. Acad. Sci. USA* **2013**, *110*, 13600–13605. [CrossRef] [PubMed]
5. Kobayashi, K.; Iwano, M. BslA (YuaB) forms a hydrophobic layer on the surface of *Bacillus subtilis* biofilms. *Mol. Microbiol.* **2012**, *85*, 51–66. [CrossRef] [PubMed]
6. Vlamakis, H.; Chai, Y.; Beaugard, P.; Losick, R.; Kolter, R. Sticking together: Building a biofilm the *Bacillus subtilis* way. *Nat. Rev. Microbiol.* **2013**, *11*, 157–168. [CrossRef] [PubMed]
7. Stein, T. *Bacillus subtilis* antibiotics: Structures, syntheses and specific functions. *Mol. Microbiol.* **2005**, *56*, 845–857. [CrossRef] [PubMed]
8. Dragoš, A.; Kovács, Á.T. The peculiar functions of bacterial extracellular matrix. *Trends Microbiol.* **2017**. [CrossRef] [PubMed]

9. Kovács, Á.T.; van Gestel, J.; Kuipers, O.P. The protective layer of biofilm: A repellent function for a new class of amphiphilic proteins. *Mol. Microbiol.* **2012**, *85*, 8–11. [CrossRef] [PubMed]
10. Seminara, A.; Angelini, T.E.; Wilking, J.N.; Vlamakis, H.; Ebrahim, S.; Kolter, R.; Weitz, D.A.; Brenner, M.P. Osmotic spreading of *Bacillus subtilis* biofilms driven by an extracellular matrix. *Proc. Natl. Acad. Sci. USA* **2012**, *109*, 1116–1121. [CrossRef] [PubMed]
11. Grau, R.R.; de Oña, P.; Kunert, M.; Leñini, C.; Gallegos-Monterrosa, R.; Mhatre, E.; Vileta, D.; Donato, V.; Hölscher, T.; Boland, W.; et al. A duo of potassium-responsive histidine kinases govern the multicellular destiny of *Bacillus subtilis*. *mBio* **2015**, *6*, e00581-15. [CrossRef] [PubMed]
12. Van Gestel, J.; Vlamakis, H.; Kolter, R. From cell differentiation to cell collectives: *Bacillus subtilis* uses division of labor to migrate. *PLoS Biol.* **2015**, *13*, e1002141. [CrossRef]
13. Kinsinger, R.F.; Shirk, M.C.; Fall, R. Rapid surface motility in *Bacillus subtilis* is dependent on extracellular surfactin and potassium ion. *J. Bacteriol.* **2003**, *185*, 5627–5631. [CrossRef] [PubMed]
14. Kovács, Á.T. Bacterial differentiation via gradual activation of global regulators. *Curr. Genet.* **2016**, *62*, 125–128. [CrossRef] [PubMed]
15. Mhatre, E.; Troszok, A.; Gallegos-Monterrosa, R.; Lindstädt, S.; Hölscher, T.; Kuipers, O.P.; Kovács, Á.T. The impact of manganese on biofilm development of *Bacillus subtilis*. *Microbiology* **2016**, *162*, 1468–1478. [CrossRef] [PubMed]
16. Grimshaw, C.E.; Huang, S.; Hanstein, C.G.; Strauch, M.A.; Burbulys, D.; Wang, L.; Hoch, J.A.; Whiteley, J.M. Synergistic kinetic interactions between components of the phosphorelay controlling sporulation in *Bacillus subtilis*. *Biochemistry* **1998**, *37*, 1365–1375. [CrossRef] [PubMed]
17. Jiang, M.; Shao, W.; Perego, M.; Hoch, J.A. Multiple histidine kinases regulate entry into stationary phase and sporulation in *Bacillus subtilis*. *Mol. Microbiol.* **2000**, *38*, 535–542. [CrossRef] [PubMed]
18. Liu, J.; Prindle, A.; Humphries, J.; Gabalda-Sagarra, M.; Asally, M.; Lee, D.Y.; Ly, S.; Garcia-Ojalvo, J.; Suel, G.M. Metabolic co-dependence gives rise to collective oscillations within biofilms. *Nature* **2015**, *523*, 550–554. [CrossRef] [PubMed]
19. Kobayashi, K. *Bacillus subtilis* pellicle formation proceeds through genetically defined morphological changes. *J. Bacteriol.* **2007**, *189*, 4920–4931. [CrossRef] [PubMed]
20. Konkol, M.A.; Blair, K.M.; Kearns, D.B. Plasmid-encoded ComI inhibits competence in the ancestral 3610 strain of *Bacillus subtilis*. *J. Bacteriol.* **2013**, *195*, 4085–4093. [CrossRef] [PubMed]
21. Veening, J.-W.; Murray, H.; Errington, J. A mechanism for cell cycle regulation of sporulation initiation in *Bacillus subtilis*. *Genes Dev.* **2009**, *23*, 1959–1970. [CrossRef] [PubMed]
22. Van Gestel, J.; Weissing, F.J.; Kuipers, O.P.; Kovács, A.T. Density of founder cells affects spatial pattern formation and cooperation in *Bacillus subtilis* biofilms. *ISME J.* **2014**, *8*, 2069–2079. [CrossRef] [PubMed]
23. Susanna, K.A.; Mironczuk, A.M.; Smits, W.K.; Hamoen, L.W.; Kuipers, O.P. A single, specific thymine mutation in the ComK-binding site severely decreases binding and transcription activation by the competence transcription factor ComK of *Bacillus subtilis*. *J. Bacteriol.* **2007**, *189*, 4718–4728. [CrossRef] [PubMed]
24. López, D.; Vlamakis, H.; Losick, R.; Kolter, R. Paracrine signaling in a bacterium. *Genes Dev.* **2009**, *23*, 1631–1638. [CrossRef] [PubMed]
25. Verhamme, D.T.; Murray, E.J.; Stanley-Wall, N.R. DegU and Spo0A jointly control transcription of two loci required for complex colony development by *Bacillus subtilis*. *J. Bacteriol.* **2009**, *191*, 100–108. [CrossRef] [PubMed]
26. Kovács, Á.T.; Kuipers, O.P. Rok regulates *yuaB* expression during architecturally complex colony development of *Bacillus subtilis* 168. *J. Bacteriol.* **2011**, *193*, 998–1002. [CrossRef] [PubMed]
27. Kraas, F.I.; Helmetag, V.; Wittmann, M.; Strieker, M.; Marahiel, M.A. Functional dissection of surfactin synthetase initiation module reveals insights into the mechanism of lipoinitiation. *Chem. Biol.* **2010**, *17*, 872–880. [CrossRef] [PubMed]
28. Gallegos-Monterrosa, R.; Mhatre, E.; Kovács, Á.T. Specific *Bacillus subtilis* 168 variants do form biofilms on nutrient rich medium. *Microbiology* **2016**, *162*, 1922–1932. [PubMed]
29. Oslizlo, A.; Stefanic, P.; Dogsa, I.; Mandic-Mulec, I. Private link between signal and response in *Bacillus subtilis* quorum sensing. *Proc. Natl. Acad. Sci. USA* **2014**, *111*, 1586–1591. [CrossRef] [PubMed]

30. Hölscher, T.; Dragoš, A.; Gallegos-Monterrosa, R.; Martin, M.; Mhatre, E.; Richter, A.; Kovács, Á.T. Monitoring spatial segregation in surface colonizing microbial populations. *J. Vis. Exp.* **2016**, *116*, e54752. [CrossRef] [PubMed]
31. McDougald, D.; Rice, S.A.; Barraud, N.; Steinberg, P.D.; Kjelleberg, S. Should we stay or should we go: Mechanisms and ecological consequences for biofilm dispersal. *Nat. Rev. Microbiol.* **2012**, *10*, 39–50. [CrossRef] [PubMed]
32. Kearns, D.B.; Losick, R. Swarming motility in undomesticated *Bacillus subtilis*. *Mol. Microbiol.* **2003**, *49*, 581–590. [CrossRef] [PubMed]
33. Oppenheimer-Shaanan, Y.; Sibony-Nevo, O.; Bloom-Ackermann, Z.; Suissa, R.; Steinberg, N.; Kartvelishvily, E.; Brumfeld, V.; Kolodkin-Gal, I. Spatio-temporal assembly of functional mineral scaffolds within microbial biofilms. *NPJ Biofilms Microbiomes* **2016**, *2*, 15031. [CrossRef]
34. Barabesi, C.; Galizzi, A.; Mastromei, G.; Rossi, M.; Tamburini, E.; Perito, B. *Bacillus subtilis* gene cluster involved in calcium carbonate biomineralization. *J. Bacteriol.* **2007**, *189*, 228–235. [CrossRef] [PubMed]
35. Kobayashi, K. Gradual activation of the response regulator DegU controls serial expression of genes for flagellum formation and biofilm formation in *Bacillus subtilis*. *Mol. Microbiol.* **2007**, *66*, 395–409. [CrossRef] [PubMed]
36. Marlow, V.L.; Porter, M.; Hogley, L.; Kiley, T.B.; Swedlow, J.R.; Davidson, F.A.; Stanley-Wall, N.R. Phosphorylated DegU manipulates cell fate differentiation in the *Bacillus subtilis* biofilm. *J. Bacteriol.* **2014**, *196*, 16–27. [CrossRef] [PubMed]
37. Gao, T.; Greenwich, J.; Li, Y.; Wang, Q.; Chai, Y. The bacterial tyrosine kinase activator TkmA contributes to biofilm formation largely independently of the cognate kinase PtkA in *Bacillus subtilis*. *J. Bacteriol.* **2015**, *197*, 3421–3432. [CrossRef] [PubMed]
38. Arutchelvi, J.; Sangeetha, J.; Philip, J.; Doble, M. Self-assembly of surfactin in aqueous solution: Role of divalent counterions. *Colloids Surf. B Biointerfaces* **2014**, *116*, 396–402. [CrossRef] [PubMed]
39. Wilhelmly, L. Über die abhängigkeit der capillaritäts—Constanten des alkohols von substanz und gestalt des benetzten festen körpers. *Ann. Phys. Chem.* **1863**, *119*, 177–217. [CrossRef]
40. López, D.; Gontang, E.A.; Kolter, R. Potassium sensing histidine kinase in *Bacillus subtilis*. *Methods Enzymol.* **2010**, *471*, 229–251. [PubMed]
41. Shemesh, M.; Chai, Y. A combination of glycerol and manganese promotes biofilm formation in *Bacillus subtilis* via histidine kinase kind signaling. *J. Bacteriol.* **2013**, *195*, 2747–2754. [CrossRef] [PubMed]
42. Oknin, H.; Steinberg, D.; Shemesh, M. Magnesium ions mitigate biofilm formation of *Bacillus* species via downregulation of matrix genes expression. *Front. Microbiol.* **2015**, *6*. [CrossRef] [PubMed]
43. Herbaud, M.-L.; Guiseppi, A.; Denizot, F.; Haiech, J.; Kilhoffer, M.-C. Calcium signalling in *Bacillus subtilis*. *Biochim. Biophys. Acta* **1998**, *1448*, 212–226. [CrossRef]
44. Zhang, W.; Dai, W.; Tsai, S.-M.; Zehnder, S.; Sarntinoranont, M.; Angelini, T. Surface indentation and fluid intake generated by the polymer matrix of *Bacillus subtilis* biofilms. *Soft Matter* **2015**, *11*, 3612–3617. [CrossRef] [PubMed]
45. Zhang, X.; Wang, X.; Nie, K.; Li, M.; Sun, Q. Simulation of *Bacillus subtilis* biofilm growth on agar plate by diffusion–reaction based continuum model. *Phys. Biol.* **2016**, *13*, 046002. [CrossRef] [PubMed]
46. Fletcher, M. Attachment of *Pseudomonas fluorescens* to glass and influence of electrolytes on bacterium-substratum separation distance. *J. Bacteriol.* **1988**, *170*, 2027–2030. [CrossRef] [PubMed]
47. Malik, A.; Kakii, K. Intergeneric coaggregations among *Oligotropha carboxidovorans* and *Acinetobacter* species present in activated sludge. *FEMS Microbiol. Lett.* **2003**, *224*, 23–28. [CrossRef]
48. Meng, Y.; Dong, G.; Zhang, C.; Ren, Y.; Qu, Y.; Chen, W. Calcium regulates glutamate dehydrogenase and poly- γ -glutamic acid synthesis in *Bacillus natto*. *Biotechnol. Lett.* **2016**, *38*, 673–679. [CrossRef] [PubMed]
49. Grau, A.; Fernandez, J.C.G.; Peypoux, F.; Ortiz, A. A study on the interactions of surfactin with phospholipid vesicles. *Biochim. Biophys. Acta* **1999**, *1418*, 307–319. [CrossRef]



© 2017 by the authors; licensee MDPI, Basel, Switzerland. This article is an open access article distributed under the terms and conditions of the Creative Commons Attribution (CC BY) license (<http://creativecommons.org/licenses/by/4.0/>).

Chapter 9

Monitoring spatial segregation in surface colonizing microbial populations

Published in: Journal of Visualized Experiments (2016)

Video Article

Monitoring Spatial Segregation in Surface Colonizing Microbial Populations

Theresa Hölscher¹, Anna Dragoš¹, Ramses Gallegos-Monterrosa¹, Marivic Martin¹, Eisha Mhatre¹, Anne Richter¹, Ákos T. Kovács¹¹Terrestrial Biofilms Group, Institute of Microbiology, Friedrich Schiller University, Jena

Correspondence to: Ákos T. Kovács at akos-tibor.kovacs@uni-jena.de

URL: <https://www.jove.com/video/54752>

DOI: doi:10.3791/54752

Keywords: Genetics, Issue 116, *Bacillus subtilis*, green-fluorescence protein, red-fluorescence protein, biofilm, swarming, sliding, assortment, imaging, surface spreading

Date Published: 10/29/2016

Citation: Hölscher, T., Dragoš, A., Gallegos-Monterrosa, R., Martin, M., Mhatre, E., Richter, A., Kovács, Á.T. Monitoring Spatial Segregation in Surface Colonizing Microbial Populations. *J. Vis. Exp.* (116), e54752, doi:10.3791/54752 (2016).

Abstract

Microbes provide an intriguing system to study social interaction among individuals within a population. The short generation times and relatively simple genetic modification procedures of microbes facilitate the development of the sociomicrobiology field. To assess the fitness of certain microbial species, selected strains or their genetically modified derivatives within one population, can be fluorescently labelled and tracked using microscopy adapted with appropriate fluorescence filters. Expanding colonies of diverse microbial species on agar media can be used to monitor the spatial distribution of cells producing distinctive fluorescent proteins.

Here, we present a detailed protocol for the use of green- and red-fluorescent protein producing bacterial strains to follow spatial arrangement during surface colonization, including flagellum-driven community movement (swarming), exopolysaccharide- and hydrophobin-dependent growth mediated spreading (sliding), and complex colony biofilm formation. Non-domesticated isolates of the Gram-positive bacterium, *Bacillus subtilis* can be utilized to scrutinize certain surface spreading traits and their effect on two-dimensional distribution on the agar-solidified medium. By altering the number of cells used to initiate colony biofilms, the assortment levels can be varied on a continuous scale. Time-lapse fluorescent microscopy can be used to witness the interaction between different phenotypes and genotypes at a certain assortment level and to determine the relative success of either.

Video Link

The video component of this article can be found at <https://www.jove.com/video/54752/>

Introduction

In the last decades, microbes have been recognized as social communities associated with various ecosystems on earth^{1,2}. In contrast to planktonic cultures used in general laboratory practice, microbes in the environment show a diverse range of spatial community structures depending on the ecological setting. Simple microbial systems can be utilized to understand the consequence of spatial structures on the evolution of social interactions^{3,4}. Publications in the last 2-3 years using both eukaryotic and prokaryotic model systems highlighted the impact of spatial structures on the stability of cooperation within microbial populations⁵⁻⁸. Additionally, obligate interactions among microbes, e.g. metabolic cross-feeding, might also alter the spatial distribution of interacting partners⁹⁻¹¹. The influence of spatial structure in these studies is mostly examined using surface attached sessile cells inhabiting the so-called biofilms or in colonies growing on the surface of an agar medium. Genetic drift resulting in high spatial assortment can be observed in microbial colonies where nutrient depletion at the edge of a cell division mediated expansion results in series of genetic bottlenecks that causes high local fixation probability for certain clonal lineages¹². Genetic drift can be therefore employed to examine the role of spatial segregation in microbial colonies.

In the environment, biofilms are multispecies communities surrounded by self-produced polymeric matrix¹³. Biofilm structure, function and stability depend on a complex network of social interactions where bacteria exchange signals, matrix components and resources, or compete for space and nutrients using toxins and antibiotics. *Bacillus subtilis* is a soil dwelling and root-colonizing bacterium that develops highly organized biofilm communities¹⁴. In analogy to social insects, *B. subtilis* cells employ a division of labor strategy, developing subpopulations of extracellular matrix producers and cannibals, motile cells, dormant spores and other cell types^{15,16}. The differentiation process is dynamic and can be altered by environmental conditions^{17,18}.

Strategies of surface colonization by bacteria can be easily manipulated under laboratory conditions by modifying the agar concentration in the growth media. At low agar levels (0.2-0.3%), bacteria harboring active flagella are able to swim, while semi-solid agar (0.7-1% agar) facilitates flagellum driven community spreading, called swarming¹⁹⁻²¹. In the absence of flagellum, certain bacterial strains are able to move over semi-solid medium via sliding, i.e. growth dependent population expansion facilitated by exopolysaccharide matrix and other secreted hydrophobin compounds²²⁻²⁴. Finally, bacteria which are capable of biofilm development form architecturally complex colonies on hard agar medium (1.2-2%)^{14,17,25}. While these traits are examined in the laboratory by precisely adjusting the conditions, in natural habitats these surface-spreading strategies might transit gradually from one to another depending on the environmental conditions²⁶. While single cell based motility is critical during initiation of biofilm development at the air-liquid interface in both Gram-positive and -negative bacteria²⁷, complex colony biofilms

of *B. subtilis* are not affected by deletion of flagellar motility²⁸. However, spatial organization during the development of *B. subtilis* colony biofilms depends on the density of the bacterial inoculum used to initiate the biofilm⁸.

Here, we use *B. subtilis* to show that spatial segregation during surface colonization depends on the mechanism of population level motility (*i.e.* swarming or sliding), and colony biofilm development depends on the founder cell density. We present a fluorescent microscopy tool that can be applied to continuously monitor microbial biofilm growth, surface colonization and assortment at the macro scale. Further, a quantification method is presented to determine the relative strain abundance in the population.

Protocol

1. Preparation of Culture Media, Semi-solid Agar and Biofilm plates, Pre-cultures

- Medium Preparation for Swarming and Sliding
 - Dissolve 2 g of Lenox Broth (LB) and 0.7 g of Agar-agar in 100 ml ion-exchanged water and autoclave for 20 min at 120 °C. Use small volumes (50-200 ml) to improve reproducibility between experiments.
 - Immediately after sterilization, close the cap of the medium bottle to reduce evaporation and place in a 55 °C incubator for at least 2 hr.
 - After the medium temperature has tempered to 55 °C, pour 20 ml agar LB medium into a 90 mm diameter polystyrene Petri dish under a laboratory sterile hood. For time-lapse experiments, pour 5 ml agar LB medium per 35 mm diameter polystyrene Petri dish.
 - Close the petri dish immediately after pouring, stack no more than 4 plates on top of each other and let the agar medium solidify for at least 1 hr.
- 2xSG Medium Preparation for Colony Biofilms
 - Dissolve 1.6 g of Nutrient Broth, 0.2 g of KCl, 0.05 g of MgSO₄·7H₂O, and 1.5 g of Agar-agar in 100 ml ion-exchanged water and autoclave for 20 min at 120 °C. Use small volumes (50-200 ml) to improve reproducibility between experiments.
 - Immediately after sterilization, close the cap of the medium bottle to reduce evaporation and place the bottle in a 55 °C incubator for at least 2 hr.
 - After the medium temperature has self-adjusted to 55 °C, add 0.1 ml filter sterilized 1M Ca(NO₃)₂ solution, 0.1 ml filter sterilized 100 mM MnCl₂ solution, 0.1 ml filter sterilized 1 mM FeSO₄ solution, and 0.5 ml sterile 20% glucose solution.
 - In a laboratory sterile hood, pour 20 ml agar 2x SG medium per 90 mm diameter polystyrene Petri dish. For time-lapse experiments, pour 5 ml agar LB medium per 35 mm diameter polystyrene Petri dish.
 - Close the petri dish immediately after pouring, stack the plate on top of each other, but not more than 4 plates, and let the agar medium to solidify for at least 1 hr.
- Preparation of Starter Cultures

NOTE: The *B. subtilis* 168, NCIB 3610 derivative strains used in the methods described below constitutively produce green- or red-fluorescence proteins and were described before^{8,27}. Strains are stored routinely in the -80 °C freezer.

 - Inoculate starter cultures from -80 °C stocks in 3 ml LB medium and incubate overnight (16-18 hr) at 37 °C with horizontal shaking (225 rpm). Do not incubate the culture longer than 18 hr as wild isolates of *B. subtilis* are mostly prone to aggregate and form a biofilm in the test tube.

2. Co-inoculation of Fluorescently Labeled Bacterial Strains for Surface Spreading

- Drying of Semi-solid Agar Plates for Swarming and Sliding of *B. subtilis*.
 - Dry agar plates for swarming and sliding for 20 min prior to inoculation. Dry plates uncovered in a laminar flow hood (see **Figure 1**). NOTE: Bacterial swarming and sliding depends on the dryness of the semi-solid agar medium. Insufficient drying allows water accumulation on the agar medium resulting in flagellum-mediated swimming. Prolonged drying time results in lack of swarming.

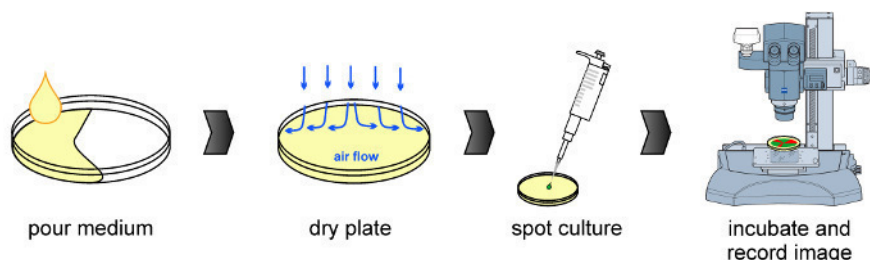


Figure 1: Experimental workflow. The common procedure is depicted in the figure, including preparation of the culturing medium, drying the plate, inoculation and fluorescence microscopy detection (from left to right). Please click here to view a larger version of this figure.

- Co-inoculation of Bacterial Cultures for Swarming and Sliding
 - Determine the optical densities of the overnight starter cultures at 600 nm and mix density normalized green- and red-fluorescent protein producing strains of *B. subtilis* NCIB 3610 or its Δhag derivative in a 1.5 ml reaction tube. For example, mix 100 μ l of strain 1 with (100*[OD₆₀₀ of overnight culture of strain 1]/[OD₆₀₀ of overnight culture of strain 2]) μ l of strain 2. Mildly vortex (3 sec at max speed) for homogenous distribution. NOTE: *B. subtilis* NCIB 3610 strains are inoculated to observe swarming, while their Δhag derivatives are used for sliding.

2. Spot 2 μ l of mixed culture on the middle of a pre-dried plate (see **Figure 1**) and further dry the plate for 10 min after inoculation.
3. Incubate plates at 37 °C upright to allow excess moisture to condense on the lid and not on the agar surface.
NOTE: Incubation time for *B. subtilis* swarming is typically between 8-16 hr. Generally, the edge of the swarm reaches the side of the 90 mm Petri dish in 8 hr. Sliding is a slower process and requires at least 16 to 42 hr of incubation. After 36 hr, the sliding front reaches the side of the 90 mm Petri dish.
4. For time-lapse experiments, place the 35 mm diameter Petri dishes in a preheated stage incubation chamber set at 37 °C. Ensure that the lid of the Petri dish remains removed throughout the duration of the experiment. Set the cover of the stage incubator to 40 °C to circumvent moisture formation on the top of the incubator.

3. Co-inoculation of Fluorescently Labelled Bacterial Strains with Different Initial Cell Densities

1. Drying of Agar Plates for Colony Biofilm Formation of *B. subtilis*.
 1. Dry the plates for colony biofilm development without cover in a laminar flow hood for 15 min prior to inoculation.
NOTE: Insufficient drying results in increased humidity and swimming or swarming may be possible²⁹. Drying too long results in small biofilm colonies.
2. Preparation of 10-fold Diluted Starter Cultures for Colony Biofilms
 1. Mix 100 μ l of green- and red-fluorescent protein producing overnight starter cultures of *B. subtilis* 168 in a 1.5 ml reaction tube and mildly vortex for homogenous distribution. Prepare 10-fold dilution series in LB medium.
 2. Spot 2 μ l of non-diluted or 10^1 , 10^2 , 10^3 , 10^4 diluted mixed cultures on the plate containing biofilm-inducing medium.
NOTE: 6 to 9 biofilm colonies can be initiated on a single 90 mm Petri dish taking into account that the colonies are separated at equal distance from each other.
 3. Incubate plates at 30 °C upright to allow excess moisture to condense on the lid and not on the agar surface.
NOTE: The incubation time for *B. subtilis* biofilm is between 1 to 3 days. Generally, the colony biofilm of *B. subtilis* reaches its average size and complex structure in 2 days.
 4. For time-lapse experiments, place a single inoculum in the middle of a 35 mm diameter Petri dish and place the dish in a preheated stage incubation chamber set at 30 °C. Ensure that the top of the Petri dish remains removed throughout the duration of the experiment. Set the cover of the stage incubator to 35 °C to circumvent moisture formation on the top of the incubator.

4. Fluorescent Microscopy Detection of Labelled Strains

1. Equipment Description for Imaging.
 1. To detect surface colonization and fluorescence signal, use a motorized fluorescence stereo zoom microscope (see detailed list in **Materials Table**) equipped with a 0.5X PlanApo Objective, two LED Cold-light sources (one for fluorescence detection and one for the visible light), filter sets for GFP (excitation at 470/40 nm and emission at 525/50 nm) and mRFP (excitation at 572/25 nm and emission at 629/62 nm), and a high resolution monochrome camera.
 2. Perform image acquisition and processing with appropriate software available for the stereo zoom microscope including multichannel and time-lapse modules. For time lapse experiment, use a standard heating stage incubator mounted to the stereo zoom microscope with an adapter.
2. Imaging of Swarming and Sliding Expansion
 1. Use the lowest magnification to capture the biggest possible area of the 90 mm plate. Set the origin of inoculation (middle of the 90 mm Petri dish) to the corner of the visible field for monitoring radial bacterial expansion and fluorescence.
 2. Adjust optimal exposure time depending on the strength of the fluorescence signal.
NOTE: For constitutively expressed fluorescence genes in *B. subtilis*, green- and red-fluorescence with 1.5 and 3 sec exposure times can be used, respectively. Additionally, 10 msec exposure time is appropriate for visible light.
3. Use the magnification that allows the detection of the whole biofilm colony and adjust the colony in the middle of the field of view.
NOTE: As for swarming and sliding expansions, the optimal exposure times to detect the fluorescence signals in the biofilm colonies depends on the expression level of the fluorescent protein coding genes. For the representative results below, green- and red-fluorescence was detected using 1 and 3 sec exposure intervals, respectively.
4. For time-lapse imaging, obtain images at certain intervals using constant exposure times.
5. Save the fluorescence stereomicroscope recorded images in a file format that is recognized by ImageJ software for quantitative data analysis.

5. Data Analysis

1. To analyze the area occupied by each differently labelled fluorescent strain, open the file of interest in ImageJ software expanded with a BioVoxel plugin.
 1. When a window called "Bio-Formats Import Options" appears where only the options "Open all series" and "Autoscale" are selected, open the file by clicking "OK".
NOTE: The files are displayed as a stack of three images, one for each channel used to record an image in the microscope (green-, red-fluorescence and bright-field images).
 2. Separate the stack into individual channel images by selecting "Image" - "Stacks" - "Stack to Images" in the ImageJ control panel.

NOTE: Images appear and are numbered as 1/3 (green channel), 2/3 (red channel) and 3/3 (bright-field). Here, the bright-field image is excluded from the analysis.

2. To analyze the images, transform each into an 8-bit image by selecting "Image" - "Type" - "8-bit".
3. To determine the occupied area in pixel², reset the scale of the images using "Analyze" - "Set Scale". When a window pops up with different scale options, reset the scale by selecting "Click to Remove Scale". Check the option "Global" to remove the scale for all open images.
4. To remove the background, draw an oval area (region of interest, ROI) outside the fluorescent area using the "Oval" tool in the ImageJ control panel.
 1. To ensure that the size of the background oval is the same for all analyzed images, add it to the ROI manager via the [t] character of the keyboard. A ROI Manager window comes up where the background oval ROI can be saved via "More" - "Save" options.
 2. If the background oval ROI is visible on the image, measure the intensity of the area by choosing "Analyze" - "Measure".
NOTE: A results window appears where amongst others the mean fluorescence intensity is displayed in the column labelled "Mean".
 3. Subtract the value of the mean background fluorescence intensity from the image by unselecting the background oval ROI, clicking "Process" - "Math" - "Subtract" and inserting the measured value.
5. Apply a threshold to the image via the "Image" - "Adjust" - "Threshold" option. Select the method Otsu and black & white (B&W). Check the "Dark background" option and employ the threshold by clicking "Apply".
NOTE: The image changes to a binary image where the area above the threshold is shown in white and that below the threshold is shown in black.
6. Select everything above the threshold via the "Analyze" - "Analyze Particles" option. In the window with the settings, keep the default options and keep the "Display results" and "Summarize" options checked. Click "OK" to display the summary in the results window and the display the occupied area in the column labelled "Total Area".

Representative Results

Laboratory systems of bacterial populations provide an appealing approach to explore ecological or evolutionary questions. Here, three surface colonization modes of *B. subtilis* were used to examine the appearance of population assortment, *i.e.* the segregation of genetically identical, but fluorescently different labelled strains. Swarming, which is a flagellum dependent collective surface movement of *B. subtilis*, results in a highly mixed population. In these swarming colonies, the green- and red-fluorescent bacteria colonized areas were overlapping (see **Figure 2A**). The rapid surface colonization can be followed in time (**Video Figure 1**). During swarming of *B. subtilis*, a thin layer of cells expands from the inoculation center after a few hours of incubation (see **Figure 2B**).

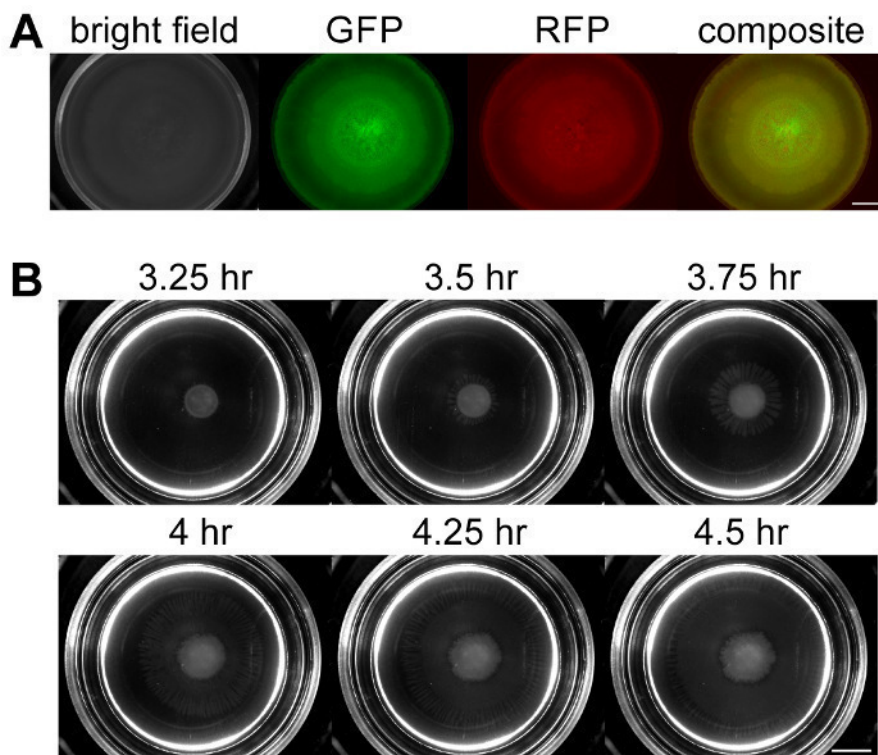


Figure 2: Swarming expansion of *B. subtilis*. The swarming colony contains green- and red-fluorescent strains that were mixed 1:1 before inoculation. **(A)** After 15 hr, the green- and red-fluorescence (GFP and RFP, respectively) were detected with appropriate fluorescence filters. **(B)** Images of thin layer of swarming *B. subtilis* are shown at selected time points extracted from Video Figure 1. Scale bar = 5 mm. Please click here to view a larger version of this figure.

However, when *B. subtilis* strains, that are lacking functional flagella but are able to spread with the help of produced exopolysaccharide, hydrophobin and surfactin, were spotted on semi-solid agar medium, the differently labelled strains were separated in certain defined sectors (see **Figure 3A**). The development of the sliding colony can be recorded in time (see **Figure 3B** or **Video Figure 2**).

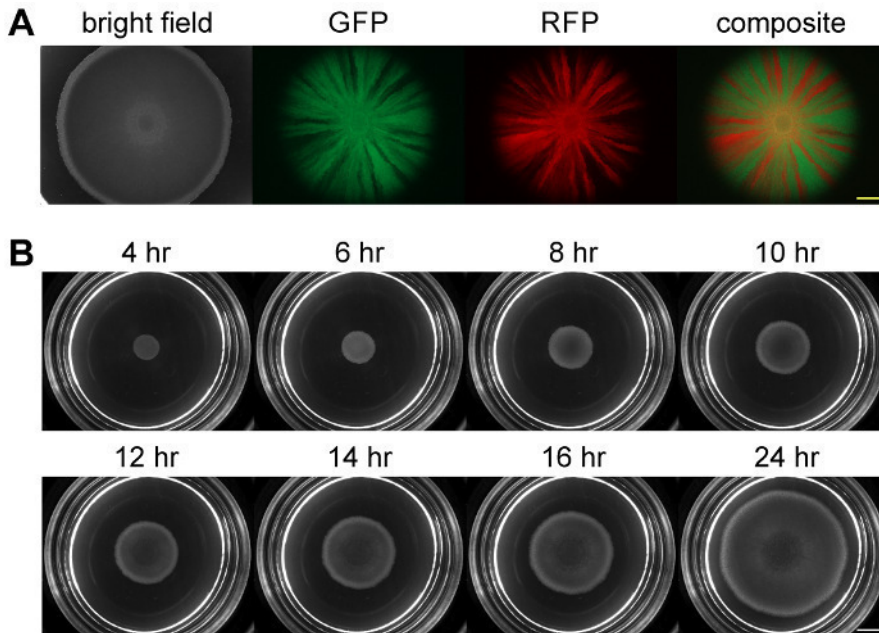


Figure 3: Sliding colony of *B. subtilis*. The colony contains green- and red-fluorescent strains that were mixed 1:1 before inoculation. **(A)** After 24 hr, the green- and red-fluorescence (GFP and RFP, respectively) were detected with appropriate fluorescence filters. **(B)** Images of the *B. subtilis* sliding disk are shown at selected time points extracted from Video Figure 2. Scale bar = 5 mm. Please click here to view a larger version of this figure.

While the assortment levels of swarming and sliding expanding colonies could not be modified, the spatial segregation of differently labelled fluorescent strains in the colony biofilm could be influenced by the starting cell densities. When a colony biofilm of *B. subtilis* was initiated with high cell density of the mixed populations, the green- and red-fluorescent strains showed minor or no spatial assortment (see **Figure 4**). On the contrary, when the cell density to initiate the biofilm was low, clear green- and red-fluorescence sectors could be detected by fluorescence microscopy. The assortment level was clearly dependent on the dilution level of the biofilm initiating population. **Video Figure 3** and **4** present the colony expansion for the lowest and highest dilution of the inoculated strains.

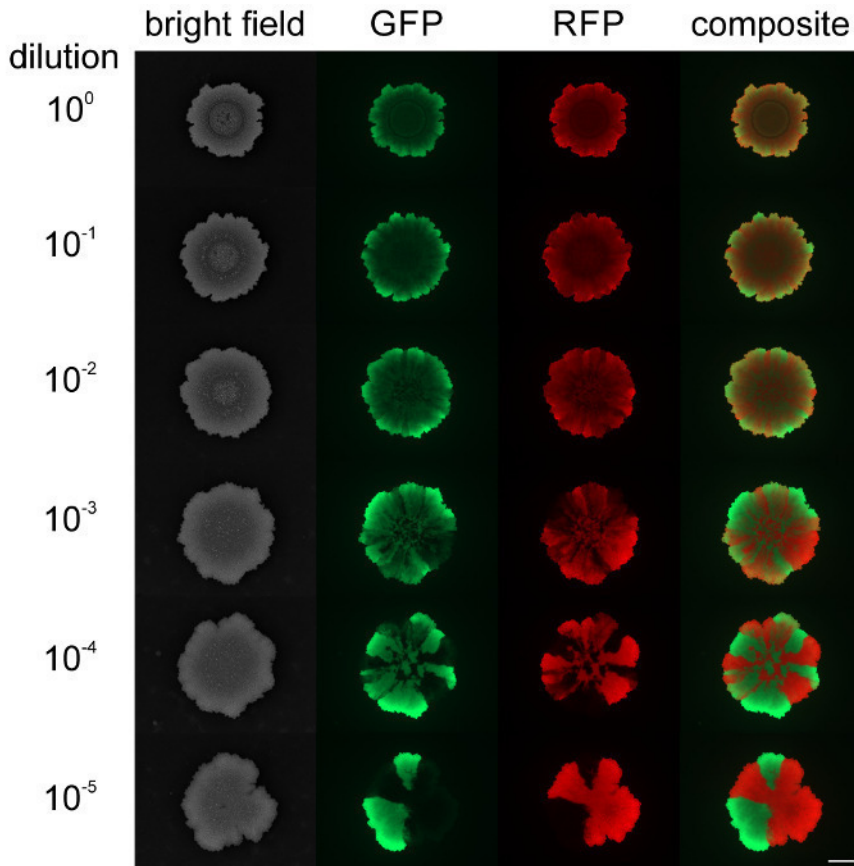
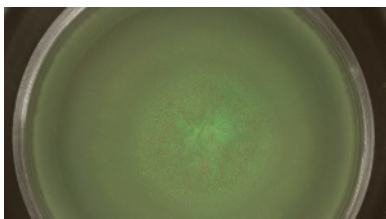
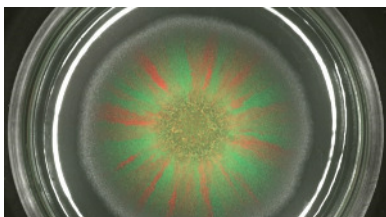


Figure 4: Assortment level in colony biofilms of *B. subtilis* at various initial cell densities. The colony biofilms of green- and red-fluorescence strains are shown after 2 days that were inoculated with different initial cell densities (from above to below: non-diluted to 10^5 times diluted initiating cultures, respectively). Scale bar = 5 mm. Please click here to view a larger version of this figure.

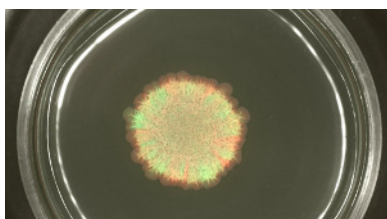
The ratio of green- and red-fluorescent strains can be further quantified using ImageJ software that allows the quantitative characterization of population structure and competitiveness of the strains used for the experiments.



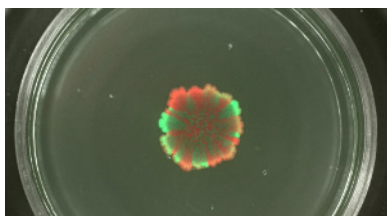
Video Figure 1: Time lapse images of swarming *B. subtilis* initiated with 1:1 mix of green- and red-fluorescent strains. (Right click to download.) The video shows a time course of 10 hr. Scale bar = 7 mm.



Video Figure 2: Time lapse images of sliding *B. subtilis* initiated with 1:1 mix of green- and red-fluorescent strains. (Right click to download.) The video shows a time course of 24 hr. Scale bar = 5 mm.



Video Figure 3: Time lapse images of *B. subtilis* colony biofilms initiated with 1:1 mix of green- and red-fluorescent strains at high cell densities. (Right click to download.) The video shows a time course of 48 hr. Scale bar = 5 mm.



Video Figure 4: Time lapse images of *B. subtilis* colony biofilms initiated with 1:1 mix of green- and red-fluorescent strains at low cell densities. (Right click to download.) The video shows a time course of 48 hr. Scale bar = 5 mm.

Discussion

The availability of a fluorescent toolbox for bacteria facilitates not only the study of heterogeneous gene expression^{30,31} and protein localization³², but also the analysis of spatial distribution of strains within a population⁸. Fluorescent markers with sufficiently different excitation and emission wavelengths allow to distinctly localize two strains that otherwise are indistinguishable from each other when mixed. The described protocol can be employed for observing the population dynamics in mixed cultures, e.g. competition experiments or synergism between strains or species. The ability to determine the relative abundances of fluorescently labelled strains in a mixed population is not restricted to surface attached swarming, sliding, or biofilm colonies, but can also be used for other multicellular biofilm systems, including submerged, flow cell or air-medium interface biofilms^{27,33-35}.

While the presented technique is a powerful tool to detect spatial distribution of strains and design competition experiments, it also allows following gene expression heterogeneity in expanding colonies. The culturing conditions described here apply for *B. subtilis* and the exact parameters for expansion on agar media might require optimization for other species or strains²⁰. Placing the samples in an incubation chamber while imaging permits the experimenter to follow the population dynamics in time, although attention should be given to the humidity level within the chamber during the incubation.

The techniques described here also require the genetic modification of the examined bacterial strains so that the strains express fluorescent markers which can be distinguished from each other. Moreover, besides having distinct excitation and emission spectra, it is recommended that the two chosen fluorescent markers have similar quantum yields (i.e. ratio of absorbed photons that are emitted) and are expressed in a comparable level. In addition, relative intensity changes in time can be measured and normalized to an early time-point of an experiment. The relative increase or decrease can be then compared between different fluorophores with different quantum efficiencies. For the presented experimental system, different green- and red-fluorescent proteins were tested previously^{36,37} to select for the most optimal fluorescent pairs that can be detected in *B. subtilis*. The optimal exposure time should be determined for each fluorescent protein and sample. Certain cell densities or multiple layers of cells might be required to detect the signal efficiently within the population. Certain fluorescent proteins might have low intensities in the bacterial cells due to inefficient expression and/or translation of the protein and thus low quantum yield. Such inefficient fluorescent markers could reduce the sensitivity of the system and extend the time needed to detect the bacterial strains possibly resulting in cytotoxicity by the excitation light. The fluorescent intensities can be accordingly modified by altering the promoter used to express the fluorescent reporter coding gene. An expression level that is too high could result in unnecessary overproduction of the fluorescent protein leading to detrimental fitness costs for the bacterium. When performing competition experiments, one should consider the cost of particular fluorescent protein production in the cells. Control experiments, where the fluorescent markers are swapped between competed strains or where two isogenic strains differing only in their fluorescent markers are competed against each other, are always required to determine any bias toward one marker. The lifetimes of the fluorescent proteins within the cells might also affect the measured intensity. In addition, the autofluorescence of certain bacterial species might require the use of different fluorescent markers other than described here.

To precisely determine the spatial distributions and abundances of the distinct bacterial strains, the background signal originating from the first fluorescent protein while using the fluorescence filter for the second fluorescent marker and vice versa should be individually tested on monoculture samples (containing bacteria producing only one marker). This allows the subtraction of overlapping fluorescent signal intensities. Importantly, as the stereomicroscope records the fluorescence signal from above the expanding colony, the presented protocol is convenient to determine the spatial arrangement in two dimensions. The architecture of the expanding bacterial population could result in varying fluorescence levels (i.e. wrinkle-like structures might contain more cells displaying higher local fluorescence intensities). Therefore, the described analysis of the images determines the spatial distribution, but not the abundance of the strains within a certain location. Previous protocols described the sample preparation for swarming²⁰ or fluorescence imaging of population dynamics in bacterial colonies³⁸, but our protocol combines these techniques. Other microscopy techniques that permit the observation of three dimensional resolution of the population structure (e.g. confocal laser scanning microscopy^{39,40} or structured illumination microscopy⁴¹) can be applied for samples with increased structural complexities. These additional techniques also support single cell based detection of the strains³¹ that is not available using stereomicroscopes.

Disclosures

Open Access for this video-article was paid for by Carl Zeiss Microscopy GmbH.

Acknowledgements

This work was funded by grant KO4741/3-1 from the Deutsche Forschungsgemeinschaft (DFG). Further, the laboratory of Á.T.K. was supported by a Marie Skłodowska Curie career integration grant (PheHetBacBiofilm) and grant KO4741/2-1 from DFG. T.H., A.D., R.G.-M., and E.M. were supported by International Max Planck Research School, Alexander von Humboldt foundation, Consejo Nacional de Ciencia y Tecnología-German Academic Exchange Service (CONACyT-DAAD), and JSMC fellowships, respectively.

References

- Nadell, C. D., Xavier, J. B., & Foster, K. R. The sociobiology of biofilms. *FEMS Microbiol Rev.* **33** (1), 206-224 (2009).
- West, S. A., Griffin, A. S., Gardner, A., & Diggle, S. P. Social evolution theory for microorganisms. *Nat Rev Microbiol.* **4** (8), 597-607 (2006).
- Kovács, Á. T. Impact of spatial distribution on the development of mutualism in microbes. *Front Microbiol.* **5** 649 (2014).
- Martin, M., Hölscher, T., Dragoš, A., Cooper, V. S., & Kovács, Á. T. Laboratory evolution of microbial interactions in bacterial biofilms. *J Bacteriol.* (2016).
- Drescher, K., Nadell, C. D., Stone, H. A., Wingreen, N. S., & Bassler, B. L. Solutions to the public goods dilemma in bacterial biofilms. *Curr Biol.* **24** (1), 50-55 (2014).
- Momeni, B., Waite, A. J., & Shou, W. Spatial self-organization favors heterotypic cooperation over cheating. *Elife.* **2** e00960 (2013).
- van Dyken, J. D., Müller, M. J., Mack, K. M., & Desai, M. M. Spatial population expansion promotes the evolution of cooperation in an experimental Prisoner's Dilemma. *Curr Biol.* **23** (10), 919-923 (2013).
- van Gestel, J., Weissing, F. J., Kuipers, O. P., & Kovács, Á. T. Density of founder cells affects spatial pattern formation and cooperation in *Bacillus subtilis* biofilms. *ISME J.* **8** (10), 2069-2079 (2014).
- Momeni, B., Brileya, K. A., Fields, M. W., & Shou, W. Strong inter-population cooperation leads to partner intermixing in microbial communities. *Elife.* **2** e00230 (2013).
- Müller, M. J., Neugeboren, B. I., Nelson, D. R., & Murray, A. W. Genetic drift opposes mutualism during spatial population expansion. *Proc Natl Acad Sci U S A.* **111** (3), 1037-1042 (2014).
- Pande, S. *et al.* Privatization of cooperative benefits stabilizes mutualistic cross-feeding interactions in spatially structured environments. *ISME J.* **10** 1413-1423 (2016).
- Hallatschek, O., Hersen, P., Ramanathan, S., & Nelson, D. R. Genetic drift at expanding frontiers promotes gene segregation. *Proc Natl Acad Sci U S A.* **104** (50), 19926-19930 (2007).
- Flemming, H. C., & Wingender, J. The biofilm matrix. *Nat Rev Microbiol.* **8** (9), 623-633 (2010).
- Vlamakis, H., Chai, Y., Beaugard, P., Losick, R., & Kolter, R. Sticking together: building a biofilm the *Bacillus subtilis* way. *Nat Rev Microbiol.* **11** (3), 157-168 (2013).
- Lopez, D., & Kolter, R. Extracellular signals that define distinct and coexisting cell fates in *Bacillus subtilis*. *FEMS Microbiol Rev.* **34** (2), 134-149 (2010).
- Lopez, D., Vlamakis, H., & Kolter, R. Generation of multiple cell types in *Bacillus subtilis*. *FEMS Microbiol Rev.* **33** (1), 152-163 (2009).
- Mhatre, E., Monterrosa, R. G., & Kovács, Á. T. From environmental signals to regulators: Modulation of biofilm development in Gram-positive bacteria. *J Basic Microbiol.* (2014).
- Zhang, W. *et al.* Nutrient depletion in *Bacillus subtilis* biofilms triggers matrix production. *New J Physics.* **16** 015028 (2014).
- Kearns, D. B. A field guide to bacterial swarming motility. *Nat Rev Microbiol.* **8** (9), 634-644 (2010).
- Morales-Soto, N. *et al.* Preparation, imaging, and quantification of bacterial surface motility assays. *J Vis Exp.* (98) (2015).
- Angelini, T. E., Roper, M., Kolter, R., Weitz, D. A., & Brenner, M. P. *Bacillus subtilis* spreads by surfing on waves of surfactant. *Proc Natl Acad Sci U S A.* **106** (43), 18109-18113 (2009).
- Grau, R. R. *et al.* A Duo of Potassium-Responsive Histidine Kinases Govern the Multicellular Destiny of *Bacillus subtilis*. *MBio.* **6** (4), e00581 (2015).
- Park, S. Y., Pontes, M. H., & Groisman, E. A. Flagella-independent surface motility in *Salmonella enterica* serovar Typhimurium. *Proc Natl Acad Sci U S A.* **112** (6), 1850-1855 (2015).
- van Gestel, J., Vlamakis, H., & Kolter, R. From cell differentiation to cell collectives: *Bacillus subtilis* uses division of labor to migrate. *PLoS Biol.* **13** (4), e1002141 (2015).
- Abee, T., Kovács, Á. T., Kuipers, O. P., & van der Veen, S. Biofilm formation and dispersal in Gram-positive bacteria. *Curr Opin Biotechnol.* **22** (2), 172-179 (2011).
- Kovács, Á. T. Bacterial differentiation via gradual activation of global regulators. *Curr Genet.* **62** (1), 125-128 (2016).
- Hölscher, T. *et al.* Motility, chemotaxis and aerotaxis contribute to competitiveness during bacterial pellicle biofilm development. *J Mol Biol.* **427** (23), 3695-3708 (2015).
- Seminara, A. *et al.* Osmotic spreading of *Bacillus subtilis* biofilms driven by an extracellular matrix. *Proc Natl Acad Sci U S A.* **109** (4), 1116-1121 (2012).
- Patrick, J. E., & Kearns, D. B. Laboratory strains of *Bacillus subtilis* do not exhibit swarming motility. *J Bacteriol.* **191** (22), 7129-7133 (2009).
- de Jong, I. G., Beilharz, K., Kuipers, O. P., & Veening, J. W. Live Cell Imaging of *Bacillus subtilis* and *Streptococcus pneumoniae* using Automated Time-lapse Microscopy. *J Vis Exp.* **53** 3145 (2011).
- García-Betancur, J. C., Yepes, A., Schneider, J., & Lopez, D. Single-cell analysis of *Bacillus subtilis* biofilms using fluorescence microscopy and flow cytometry. *J Vis Exp.* (60) (2012).
- Turnbull, L. *et al.* Super-resolution imaging of the cytokinetic Z ring in live bacteria using fast 3D-structured illumination microscopy (f3D-SIM). *J Vis Exp.* **91** 51469 (2014).

33. Barken, K. B. *et al.* Roles of type IV pili, flagellum-mediated motility and extracellular DNA in the formation of mature multicellular structures in *Pseudomonas aeruginosa* biofilms. *Environ Microbiol.* **10** (9), 2331-2343 (2008).
34. Oliveira, N. M. *et al.* Biofilm formation as a response to ecological competition. *PLoS Biol.* **13** (7), e1002191 (2015).
35. Wang, X. *et al.* Probing phenotypic growth in expanding *Bacillus subtilis* biofilms. *Appl Microbiol Biotechnol.* **100** 4607 - 4615 (2016).
36. Detert Oude Weme, R. G. *et al.* Single cell FRET analysis for the identification of optimal FRET-pairs in *Bacillus subtilis* using a prototype MEM-FLIM system. *PLoS One.* **10** (4), e0123239 (2015).
37. Overkamp, W. *et al.* Benchmarking various green fluorescent protein variants in *Bacillus subtilis*, *Streptococcus pneumoniae*, and *Lactococcus lactis* for live cell imaging. *Appl Environ Microbiol.* **79** (20), 6481-6490 (2013).
38. Stannek, L., Egelkamp, R., Gunka, K., & Commichau, F. M. Monitoring intraspecies competition in a bacterial cell population by cocultivation of fluorescently labelled strains. *J Vis Exp.* (83), e51196 (2014).
39. Bridier, A., & Briandet, R. Contribution of confocal laser scanning microscopy in deciphering biofilm tridimensional structure and reactivity. *Methods Mol Biol.* **1147** 255-266 (2014).
40. Khajotia, S. S., Smart, K. H., Pilula, M., & Thompson, D. M. Concurrent quantification of cellular and extracellular components of biofilms. *J Vis Exp.* (82), e50639 (2013).
41. Neu, T. R., & Lawrence, J. R. Innovative techniques, sensors, and approaches for imaging biofilms at different scales. *Trends Microbiol.* **23** (4), 233-242 (2015).

Chapter 10

Differential shareability of goods explains social exploitation during sliding

In preparation for future submission for publication.

Differential shareability of goods explains social exploitation during sliding

Theresa Hölscher¹, Jordi van Gestel², Ákos T. Kovács^{1,3#}

¹ Terrestrial Biofilms Group, Institute of Microbiology, Friedrich Schiller University Jena, 07743 Jena, Germany

² Department of Evolutionary Biology and Environmental Studies, University of Zürich, 8057 Zürich, Switzerland

³ Bacterial Interactions and Evolution Group, Department of Biotechnology and Biomedicine, Technical University of Denmark, 2800 Kgs Lyngby, Denmark

For correspondence. Email atkovacs@dtu.dk

Keywords: sliding, *Bacillus subtilis*, public goods, cooperation

Abstract

Sliding is a collective and cooperative type of motility where cells passively move over semi-solid surfaces powered by the force of cell division. In addition, sliding is usually promoted by a surfactant, extracellular polysaccharides or other secreted sliding facilitating compounds. Such secreted molecules are often assumed to be public goods since alongside the producer they should be available to the majority of cells in a population. Sliding of the Gram-positive model bacterium *Bacillus subtilis* is promoted by secretion of three potentially shareable goods: in addition to the surfactant surfactin, the bacterial hydrophobin protein BslA and exopolysaccharides (EPS) are required for sliding. Here, we investigated the cooperation promoting properties of these sliding facilitating goods, that is their shareability. Further, we analyzed the social interactions between producer and non-producer strains or among two non-producers of surfactin, BslA and EPS. We found that only surfactin is genuinely public whereas BslA and EPS are privatized to a certain extent i.e. shared less with neighboring cells. Therefore, surfactin production can be exploited by non-producers whereas BslA and EPS production is mostly protected from exploitation. The experimentally obtained results were confirmed by a simple mathematical model that examined the impact of diffusion properties of sliding facilitating compounds.

Introduction

In the field of sociomicrobiology, one of the major research interests is the development and maintenance of cooperative behaviors. Cooperation in bacteria can be achieved for example by the production of commonly available resources, so called public goods, by different species or differentiated cell types of the same species, to reach a common goal (Tarnita, 2017). Therefore, this kind of cooperation is often associated with division of labor. The common goal could be the formation of a biofilm (van Gestel *et al.*, 2014, Brockhurst *et al.*, 2010), migration (van Gestel *et al.*, 2015), access to nutrients (Griffin *et al.*, 2004; Drescher *et al.*, 2014) or dispersal (Velicer and Vos, 2009). However, an important problem arises while studying cooperation: If the cooperative behavior is costly to maintain and benefitting an interaction partner, it can in theory be exploited by cells that are not contributing to pay the cost but receiving the benefit. Therefore, it is a puzzling question, why we observe cooperative behaviors and how they are protected from exploitation by non-cooperators. This problem can be solved if, in one way or another, the benefit of the public good is predominantly directed towards the cooperators. Possible solutions for the maintenance of cooperation include limited diffusion or slow degradation of the public good (Allen *et al.*, 2013), kin discrimination (Stefanic *et al.*, 2015; Lyons and Kolter, 2017), or spatial structuring and, thus, spatial separation of cooperators and cheaters (Momeni *et al.*, 2013; Kovács, 2014).

Research has revealed cases of both exploitation and stability of the cooperative behavior in the presence on non-cooperative cells. For example, Drescher *et al.* (2014) showed that the public good chitinase (secreted chitin degrading enzyme) produced by *Vibrio cholerae* is exploitable by cheaters but certain population-level properties, e.g. the formation of a thick biofilm can prevent exploitation by limiting the diffusion of secreted enzymes from the producer and therefore the cheaters' access to the public good. In another study, a population of yeast (*Saccharomyces cerevisiae*) cooperatively degrading sucrose with the enzyme invertase was found to be susceptible to invasion by "cheaters" that do not produce invertase (Gore *et al.*, 2009). However, also the wildtype was able to invade "cheater" populations leading to coexistence of the two strains. Additionally, the wild type was shown to withhold a small part of the monosaccharides produced by the invertase, possibly providing enough benefit for the wildtype to maintain the cooperative behavior (Gore *et al.*, 2009).

Here, we investigated the cooperative traits of shareable goods in social populations of the Gram-positive model organism *Bacillus subtilis*. Cooperative communities of *B. subtilis* that have been investigated in detail mostly comprise different forms of biofilms or swarming cells. Another type of cooperative movement is the so called sliding motility. Sliding is a

passive bacterial motility form that facilitates movement of populations of cells across semi-solid surfaces powered by the pushing force of cell division (Henrichsen, 1972; Hölscher and Kovács, 2017). In general, sliding requires additional components but the nature of those varies between different bacterial species (Hölscher and Kovács, 2017). In this study, we investigate sliding of *B. subtilis* that is not only dependent on growth but also requires self-produced and excreted exopolysaccharides (EPS), the bacterial hydrophobin protein BslA and the lipopeptide surfactant surfactin (Kinsinger *et al.*, 2003, Grau *et al.*, 2015). The exopolysaccharides are believed to aid the movement of the cells by swelling via hydration causing an osmotic pressure similar to biofilm formation (Seminara *et al.*, 2012). As a surfactant, surfactin lowers the surface tension of water and thereby alleviates the movement of the cells across the surface. Through its hydrophobic properties, BslA is assumed to have a similar effect. Since these three compounds are excreted in the environment and are in theory available to all cells in the surrounding area, they can qualify as public goods.

It was previously demonstrated by van Gestel *et al.* (2015) that division of labor between matrix-producers and surfactin producers shapes the sliding colony structure of *B. subtilis*, albeit under conditions promoting the dendritic sliding form (van Gestel *et al.*, 2015; see also Hölscher and Kovács, 2017). Now, we investigated the possible public good and sharing properties of the sliding facilitating goods EPS, BslA and surfactin during continuous sliding of *B. subtilis*.

We present how population dynamics of a wild-type strain was modulated in the presence of a non-producer lacking one of the secreted components in addition to examining the interaction of two non-producers, and determine the success of each strain during surface colonization. We reveal the limited sharing properties of EPS and BslA, and show that surfactin qualifies as a genuine public good as it is freely available and costly to produce under sliding promoting conditions. Additionally, surfactin but not BslA or EPS was exploitable by non-producers.

Results

Assortment during sliding

Strains of *B. subtilis* lacking a functional flagellum are able to colonize an agar surface by expansion of the sliding disk. All strains used in this study lacked single cell motility (Δhag) to eliminate the influence of swarming motility. Therefore, “wild type” refers to a strain harboring only Δhag without additional mutations. Unlike swarming, the sliding expansion of *B. subtilis* shows a noticeable spatial segregation independently from the founder cell density (Hölscher *et al.*, 2016), however, the expanding front is uniform for both spreading types.

To assess the progress of wild-type sliding in the presence of non-producers and their influence on sliding colony structure, we mixed green and red fluorescently labeled strains of wild-type and non-producer strains lacking EPS, BslA or surfactin in a 1:1 ratio and let them expand for 24 h on semi-solid medium (see Experimental Procedures). Similarly, different non-producers were mixed with each other and the structure of the sliding colony was evaluated. Results are presented for green fluorescent strain 1 versus red fluorescent strain 2. As control, the same mixtures with swapped fluorescence markers were investigated and similar results were obtained (see Supplemental material, Fig S1).

Usually, after a certain lag-phase, the expansion of a wildtype sliding colony was continuous and the diameter of the colony reached around 3 cm after 24 h (Fig. 1; see also Hölscher *et al.*, 2016). As EPS, BslA and surfactin are crucial for sliding motility of *B. subtilis*, mutants lacking either one of these goods were not able to expand much beyond the inoculation point (Fig. 1). In the structure of the wild-type colony, a high degree of assortment was evident, visualized by fluorescence labeling. The two wildtype strains formed mostly evenly distributed sectors growing out from the middle of the colony which is caused by the passive nature of sliding (Fig. 2A; see also Hölscher *et al.*, 2016).

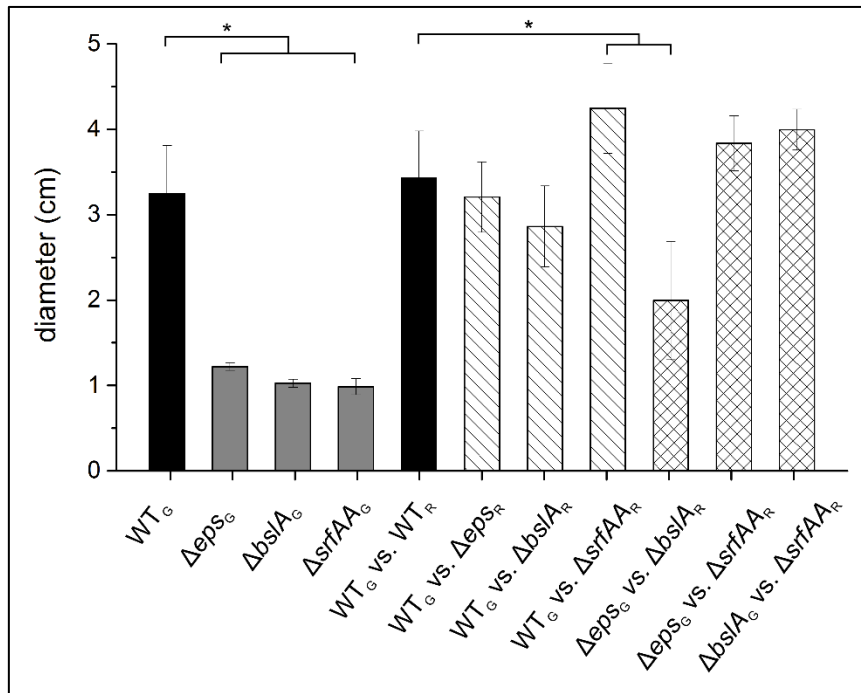


Figure 1. Competition of sliding good producers and non-producers affects sliding expansion. Diameter of sliding colonies were recorded after incubation on semi-solid medium at 37°C for 24 h. For competition assays, fluorescently labeled wildtype (WT) and EPS, BslA and surfactin non-producers (Δeps , $\Delta bslA$, $\Delta srfAA$ respectively) were mixed at 1:1 initial ratio (G – green fluorescent strain, R – red fluorescent strain). Asterisks indicate significant differences; error bars indicate the standard deviation.

Diminished expansion of EPS and BslA non-producers

When combined with EPS or BslA non-producers, the expansion of the mixed population was similar to the colonies of wild type only samples (Fig. 1). In contrast, the expansion of the wild type and surfactin non-producer mix after 24 h was significantly higher than the wildtype expansion (Fig. 1, unpaired two-sample t-test with Welch Correction: $P = 0.043$, $n = 5$). In addition, the expansion of the mix of EPS and BslA non-producers was also significantly different and considerably reduced in comparison to the wild type (Fig. 1 unpaired two-sample t-test with Welch Correction: $P = 0.007$, $n = 5$). The mixtures of the surfactin non-producer with both EPS and BslA non-producer showed comparable expansion to the wild type (Fig. 1). These results indicated that the BslA and EPS non-producers could not be fully complemented by another strain producing the respective good. The opposite seemed to be valid for surfactin: here, no reduction in expansion of the sliding colony could be observed, suggesting that the surfactin non-producer was able to utilize the surfactin produced by the partner strain in the mixture.

The spatial structure of the sliding colony was qualitatively evaluated using fluorescence stereomicroscopy (Fig. 2A). Interestingly, the consistent sector-assortment observed for wild type only samples was absent for all other strain mixtures. EPS and BslA non-producers were located mostly in the center of the sliding colony, albeit the BslA non-producer reached

the rim in few places. Thus, both strains seemed to lack the ability to expand properly even though the respective good they cannot produce, was provided by the wild type. This was important for their success as the location at the rim of the sliding colony can be considered as the preferable environment since the cells there have access to new nutrients.

When mixed with the surfactin non-producer, the wildtype seemed to have a disadvantage since it was underrepresented in the sliding colony (Fig. 2A). Likewise, in a mixture with the BslA and EPS non-producer, the surfactin non-producer seemed to be the dominant strain (Fig. 2A). Notably, the EPS non-producer was not confined to the center of the sliding colony like in the wild type + Δeps mixture, although it occupied less space than the surfactin non-producer (see below). The structure of the sliding colony of the EPS and BslA non-producers was most striking: Besides the above described reduced size, the colonies often had an undulate rim with mainly the BslA non-producer occupying the indentation (Fig. 2A). A similar pattern could be observed for the other mixtures with the BslA non-producer, although not as pronounced.

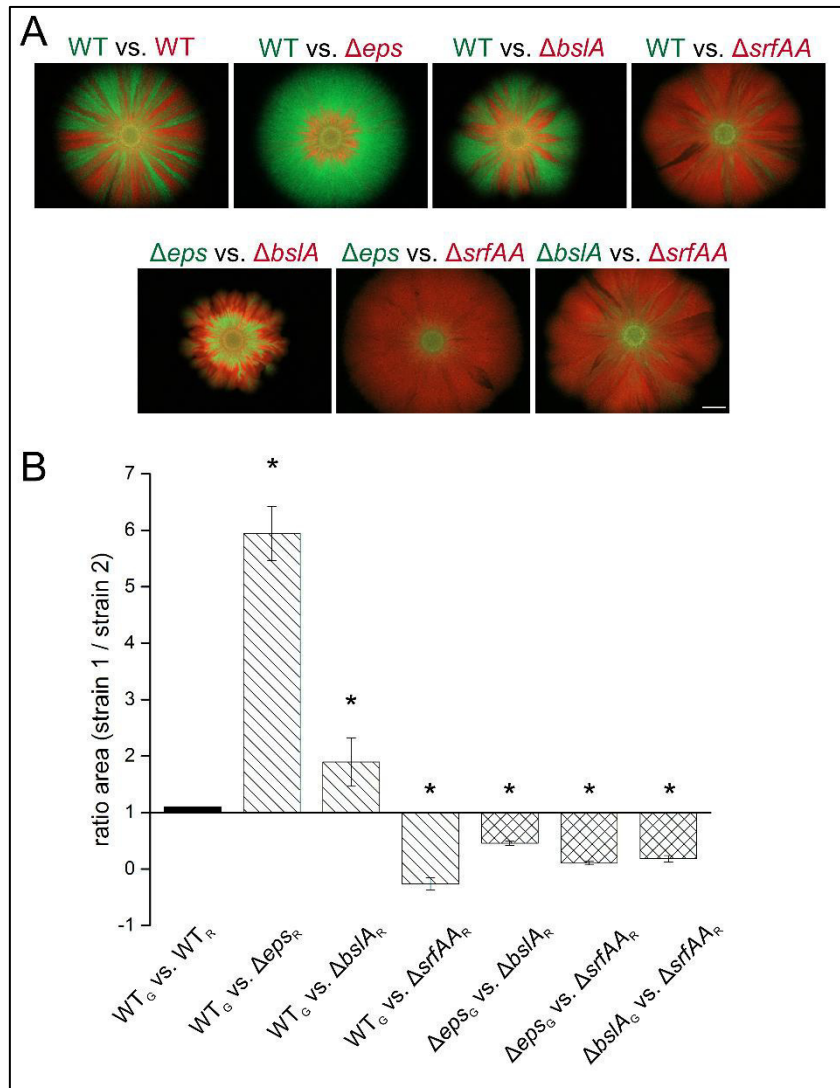


Figure 2. Structure and success of individual strains in competition assay sliding colonies. (A) Overlay of green and red fluorescent images from representative sliding colonies of competition assay from Figure 1, with 1:1 initial ratio. Green text indicates a green fluorescent strain; red text indicates a red fluorescent strain. The scale is equal for all images and the scale bar represents 5 mm. (B) Ratio of occupied area of strain 1 versus strain 2 (in pixel²) of the sliding colonies from (A) obtained by quantitative image analysis using ImageJ. G indicates a green fluorescent strain; R indicates a red fluorescent strain. Asterisks indicate significant differences to 1, error bars indicate the standard deviation.

Surfactin production is exploitable

To additionally estimate the success of each strain in the sliding colony in a quantitative manner, we determined the area each strain occupies using the different fluorescence labels (see Experimental Procedures). By calculating the ratio of the two strains' areas we could assess whether one strain had an advantage over the other. When analyzing the ratio of mixed wild-type strains with different fluorescence markers as a control, the ratio was around 1 as is expected (Fig. 2B, one-sample t-test, test mean = 1: P = 0.34, n = 5). However, as the fluorescence image already suggested, in the mixture of wildtype and EPS non-producer, the wildtype clearly dominated in the sliding colony with a wild type to Δeps ratio of

around 6 (Fig. 2B, one-sample t-test, test mean = 1: $P = 2 \cdot 10^{-5}$, $n = 5$). The wild type had a similar advantage over the BslA non-producer with a ratio of ca. 1.9, although the difference here was not as distinct (Fig. 2B, one-sample t-test, test mean = 1: $P = 0.01$, $n = 5$). These results suggested that BslA and especially EPS could only be shared partially so that insufficient good was available for the respective mutant to achieve a wild-type level of sliding. The area ratios of all mixtures containing the surfactin non-producer were below one, indicating that the surfactin mutant dominated each sliding colony (Fig. 2B, one-sample t-test, test mean = 1: $P < 0.05$, $n = 5$). This indicated a possible exploitation of surfactin production of the respective other strain by the surfactin non-producer.

To test the impact of an initial advantage of one strain, we investigated different starting ratios and the resulting structure of the sliding colony as well as each strain's success. Each combination of wild type and non-producers was tested with an initial ratio of 1:10 or 10:1. The resulting ratios of the area occupied by each strain in the sliding colony are depicted in Figure 3. In general, the same trends could be observed as in the assay with 1:1 initial ratio. As expected, the value of the wild type control mix ratio was below one for the 1:10 and above one for the 10:1 assay, however the advantage of the more abundant strain in the sliding colony was not linear. In the mixture of wild type and EPS non-producer, the established final ratio was scarcely affected by an initial higher abundance of cells of one strain, but the wildtype was always dominating the colony (Fig. 3A, B). The same was true for the mixture of EPS and BslA non-producer: the latter seemed to always have an advantage during sliding. Interestingly, when incubated together with a ten times higher number of surfactin non-producers, the resulting ratio of the occupied area was only slightly lower than 1 and just on the border of significant difference (Fig. 3A, one-sample t-test, test mean = 1: $P = 0.048$, $n = 5$). In the fluorescence image of the sliding colony, the surfactin non-producer seemed to be dominating, but a thin layer of EPS non-producer was spread almost over the complete area of the sliding colony (see Supplemental material, Fig. S2). This effect could be caused by the low amount of EPS non-producer strain and the therefore diminished abundance of surfactin. In the case of the reversed initial ratio, the EPS non-producer continued to be outcompeted by the surfactin non-producer even if initiated at a high relative frequency in the inoculum (Fig. 3B). In the case of the BslA non-producer, an initial high abundance had more impact on the final sliding colony structure: with a final area ratio of one, it was not outcompeted any more by the wildtype (Fig. 3A, one-sample t-test, test mean = 1: $P = 0.65$, $n = 5$). However, its high abundance was clearly restricting the wild type since the sliding colony was smaller and exhibited an undulate rim indicating an overall decrease in sliding (see Supplemental material, Fig. S2). Similarly, in the competition of BslA and surfactin non-producers, the presence of high amounts of BslA non-producer was

accompanied with a ratio of around 1 and thus a decreased advantage of the surfactin non-producer compared to the 1:1 assay (Fig. 3B, one-sample t-test, test mean = 1: P = 0.47, n = 5; Fig. 2). We suggest that the high abundance of the BslA non-producer dampened the expansion of the surfactin non-producer, since the sliding colony structure showed sliding expansion only in distinct positions where the surfactin non-producer reached the colony rim and was able to diverge from the BslA non-producer abundant sections (see Supplemental material, Fig. S2).

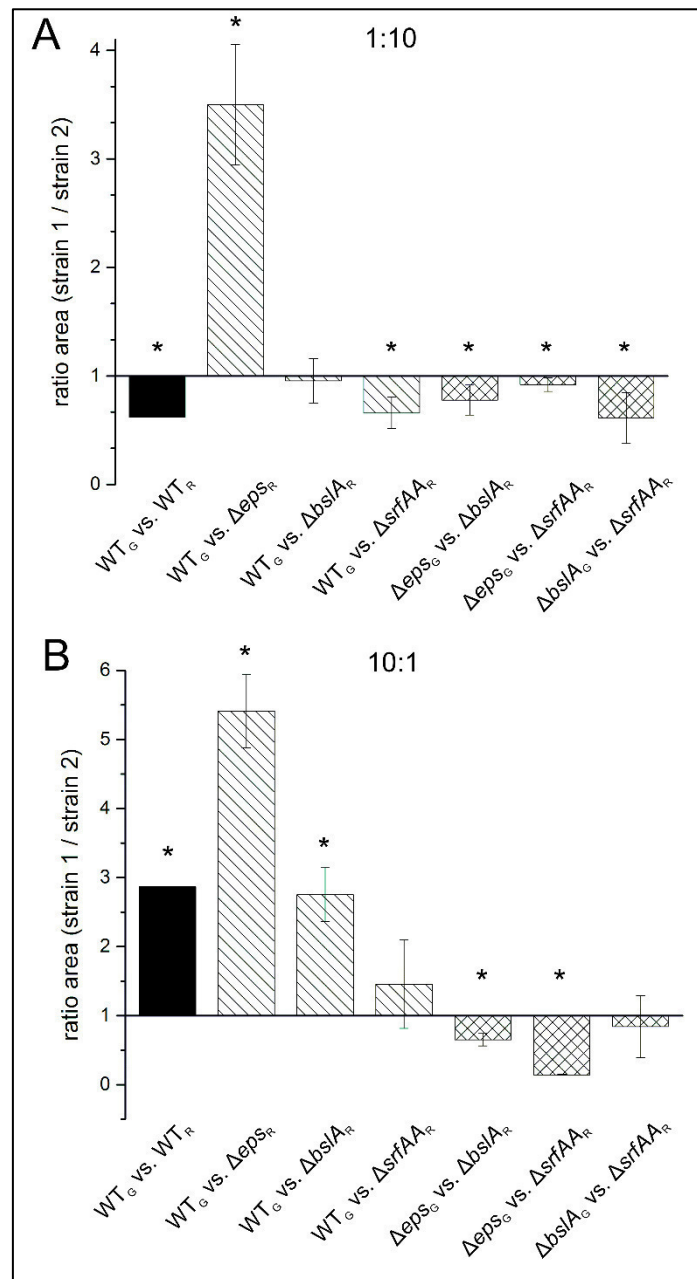


Figure 3. Sliding competition with initial advantage of one strain. Ratio of occupied area of strain 1 versus strain 2 (in pixel²) of sliding colonies from competition assays with 1:10 (A) or 10:1 (B) initial ratio obtained by quantitative image analysis using ImageJ. Strains were incubated on semi-solid medium at 37°C for 24 h. G indicates a green fluorescent strain; R indicates a red fluorescent strain. Asterisks indicate significant differences to 1, error bars indicate the standard deviation.

Privatization hypothesis

The above described results indicated that the availability of the investigated goods to their neighbors was different for each one of them. Based on the experimental results we hypothesized that the privatization level for EPS was the highest (Fig. 4), since the EPS non-producer seemed to be able to exploit only a small amount of EPS provided by another strain and was therefore not able to slide efficiently (see above). The sliding assay results suggested that BslA was also privatized partially but less than EPS (Fig. 4). The BslA non-producer could expand partly along with a producer strain at distinct sectors, yet expansion of this strain was restricted. In contrast, surfactin seemed freely available to the surrounding cells and was not privatized (Fig. 4).

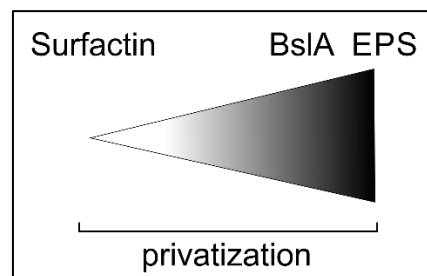


Figure 4. Privatization hypothesis. Schematic hypothesis based on the high privatization (black color) of BslA and especially EPS and high sharing (white color) of surfactin during sliding in consort with the obtained results.

Cost of sliding goods

Since public good production is usually accompanied by an energetic cost, we tested whether the three sliding facilitating goods are costly under sliding promoting conditions. Therefore, we created strains with an IPTG-inducible promoter in front of the gene or operon encoding the respective good (see Experimental Procedures). This step was necessary since the spatial structure of the sliding colony makes a direct cost determination impossible and mixed liquid cultures had to be employed. Using the inducible sliding gene constructs, we could mimic the level of the good production to be comparable with wild-type sliding. The strains were incubated under sliding promoting conditions with different IPTG concentrations and the expansion of the sliding colony was used as a measure to determine the induction necessary to reach wild-type level (see Supplemental material, Fig. S3). To determine the cost of good production, a mutant strain was competed against the respective inducible strain in medium with and without supplemented IPTG and the relative fitness of the inducible strain towards the mutant was calculated from the initial and final cfu. Figure 5 shows the relative fitness for each good production. Conspicuously, only surfactin production caused attenuation of the relative fitness, where the synthetic surfactin producer with supplemented IPTG, i.e. surfactin production similar to the wildtype, showed a significant difference to 1, indicating an energetic cost for surfactin production under these conditions (Fig. 5, one-sample t-test, test mean = 1: $P = 6.9 \cdot 10^{-4}$, $n = 6$). This also means that EPS and

BsIA did not have a measurable production cost in the medium used for sliding promoting conditions.

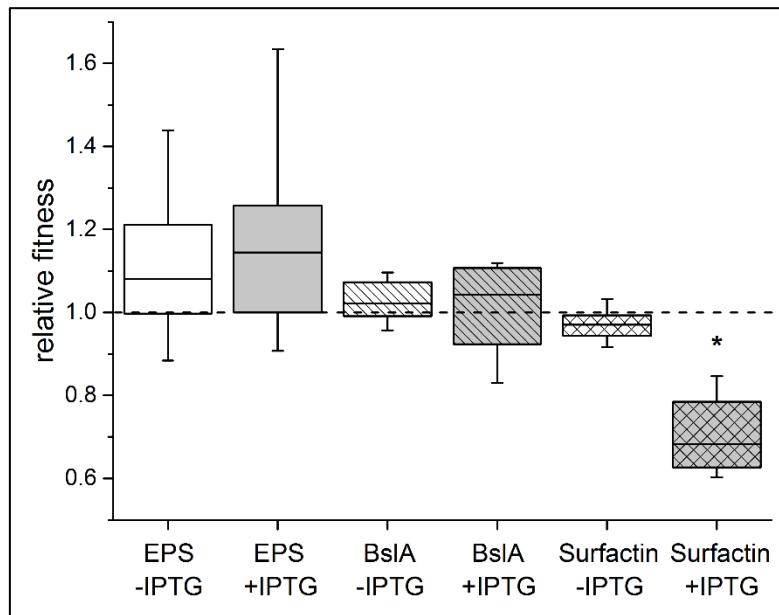


Figure 5. Surfactin is costly to produce under sliding promoting conditions. Relative fitness calculated from initial and final cfu of competitions between a good non-producer against the respective IPTG-inducible strain. The competition was conducted in IPTG containing medium (+IPTG) and as control in medium lacking IPTG (-IPTG). The box indicates the 25th-75th percentile; the line in the boxes represents the median. The dashed line indicates a relative fitness of 1. The asterisk indicates a significant difference to 1.

Complementation with externally supplied goods reflects privatization hypothesis

Based on our privatization hypothesis we wondered if sliding of the good non-producers can be complemented or if the privatization of some goods prevents successful sliding with externally supplied goods. Therefore, we isolated the goods in different forms or used the commercially available form in case of surfactin. We isolated EPS from biofilms of the wildtype and *tasA* mutant (encoding the main protein component of the *B. subtilis* matrix) as well as from the *eps* mutant as control. These were spotted prior to the culture on sliding plates and sliding was evaluated after 24 h (see Experimental procedures). As shown in Figure 6A, supplementation of EPS could not restore sliding of the EPS non-producer since there was no significant difference between the EPS non-producer with and without supplied EPS (unpaired two-sample t-test with Welch Correction: $P > 0.05$, $n = 6$). The quality of the purified EPS was tested in complementation experiments, where pellicle biofilm formation of the Δeps strain was restored by the purified EPS (Fig. S4). For BsIA, we used the supernatant of an *Escherichia coli* strain harbouring the BsIA overproduction plasmid in addition to the supernatant of a strain lacking the *bsIA* overexpressing plasmid as a control (see Experimental procedures). The non-diluted BsIA containing supernatant was able to increase sliding of the BsIA non-producer significantly in comparison to the mutant alone (Fig. 6B, unpaired two-sample t-test with Welch Correction: $P = 1.2 \cdot 10^{-6}$, $n = 6$) or the control

(Fig. 6B, unpaired two-sample t-test with Welch Correction: $P = 9.4 \cdot 10^{-7}$, $n = 6$), but incomparable to wild-type level (Fig. 6B, unpaired two-sample t-test with Welch Correction: $P = 7.6 \cdot 10^{-8}$, $n = 6$). This effect ceased using ten times diluted BslA containing supernatant (unpaired two-sample t-test with Welch Correction: $P = 0.21$, $n = 6$). Again, the overexpressed BslA was shown to restore genuine biofilm formation and hydrophobicity of biofilms when added to the $\Delta bsIA$ mutant strain (Fig. S5). Surfactin was also supplied in different concentrations and since it was dissolved in methanol, this solvent was used as control. With a low surfactin concentration of 0.01 mg/ml, sliding was not increased compared to the surfactin non-producer or the methanol control (Fig. 6C, unpaired two-sample t-test with Welch Correction: $P = 0.2$, $n = 6$). However higher surfactin concentrations resulted in increased sliding similar to the wildtype (1 mg/ml, unpaired two-sample t-test with Welch Correction: $P = 0.049$, $n = 6$) and in surprisingly fast sliding surpassing even the wildtype (10 mg/ml, unpaired two-sample t-test with Welch Correction: $P = 6 \cdot 10^{-5}$, $n = 6$). These results reflected very well the results from the competition assays and the derived privatization hypothesis since the supposedly well shared surfactin could complement a surfactin non-producer. In contrast, the less shared BslA can only partially complement a non-producer, whereas the EPS non-producer could not be complemented with externally supplied EPS at all since it was supposedly privatized.

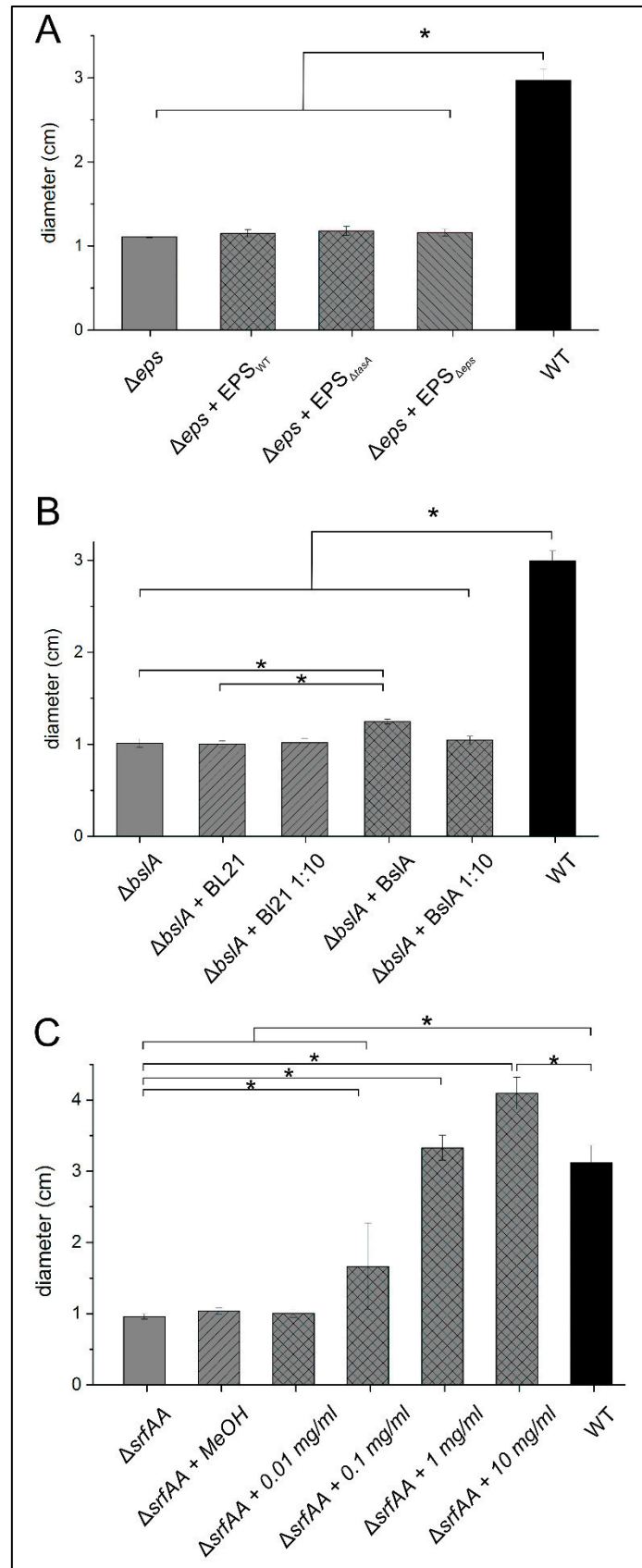


Figure 6. Complementation of non-producer sliding with supplied goods. Diameter of EPS (A), BslA (B) and surfactin (C) non-producers (Δeps , $\Delta bslA$, $\Delta srfAA$ respectively) incubated under sliding promoting conditions with supplied goods or a control substance as well as wildtype controls for 24 h. For EPS non-producer complementation (A), EPS isolated from wildtype, *tasA* mutant or *eps* mutant biofilms was used. For BslA non-

producer complementation (B), BslA containing supernatant from an *E. coli* strain harboring a BslA production plasmid was used (+BslA); supernatant from an *E. coli* strain without the plasmid served as control (+BL21). For surfactin non-producer complementation (C), commercially available surfactin was used in different concentrations (0.01, 0.1, 1, and 10 mg/ml) dissolved in methanol, which was used as control (+MeOH). Asterisks indicate significant differences; error bars indicate the standard deviation.

Model

To obtain a better understanding of the competition assays between the different strains, we constructed a simple agent-based model that approximates colony growth as seen in the experiments. Although our model incorporates some of the growth parameters obtained from the experiments, and estimates others based on existing literature, the primary goal of the model was not to accurately represent the biophysical processes underlying colony growth. Rather, we intended to use this model to improve our intuition of what happens in the laboratory experiments. Thus, like in the experiments, we modeled colony growth in which two strains are mixed. These strains competed, while the colony grew, thereby changing their relative abundance and spatial configuration.

The colonies resulting from the model are shown in Fig 7. It was evident that their structure closely resembled the structure of the experimental colonies (inset of Fig 7), although the EPS non-producer reached the edge of the sliding colony in few places in the model. Also, the success of each strain in the mixture was similar to the experimental data, with the wild type clearly dominating over the EPS non-producer and the surfactin non-producer having an advantage over the wild type as well as the EPS non-producer (Fig. 7). In total, our hypothesis of a different privatization extent of the goods based on the experimental results was confirmed by the outcome of a simple model that altered the shareability of secreted goods.

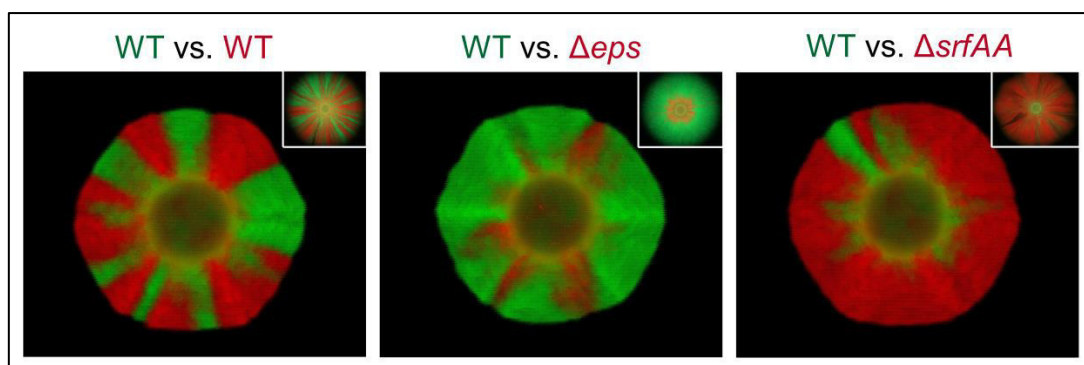


Figure 7. Model of sliding colony structure resulting from competition assays. Outcome of an agent-based model of competitions between fluorescently labelled wildtype strains (WT vs. WT), wildtype and EPS non-producer (WT vs. Δeps) as well as wildtype and surfactin non-producer (WT vs. $\Delta srfAA$). The inset shows a representative image of experimentally obtained results of the same competitions. For model description and parameters see Experimental procedures and Supplemental material.

Discussion

Cooperative interactions such as public good mediated cooperation can have a crucial influence on the ecology of microbial communities and collective behaviors like sliding. Here, we highlighted how the presence of cells not contributing to the cooperative behavior can influence the structure of a simple microbial population. The striking differences observed in a population consisting of only one species suggest that in more complex communities a vast amount of interactions is possible and the influence of non-cooperative subgroups or the dynamics of cooperative behaviors and therefore the community structure might be hard to analyze.

Additionally, we find that although secreted in the environment, not all shareable goods can be qualified as truly “public”. In this case, although EPS and BslA have been shown to be present outside of the cell (Branda *et al.*, 2006; Kobayashi and Iwano, 2012), during sliding these can be shared only to a limited extent with other cells in the population. This is interesting since especially EPS was already shown to be shared with non-producers during biofilm formation and mutants lacking either EPS or the protein components of the *B. subtilis* biofilm matrix were demonstrated to complement each other (Branda *et al.*, 2006, Martin *et al.*, 2017). However, the environmental differences of the two processes, biofilm formation and sliding motility have to be considered as well when comparing the sharing properties of EPS. The sharing properties of EPS were demonstrated in pellicles, i.e. biofilms at the air-liquid interface whereas sliding is analyzed on semi-solid medium. The restriction and almost two-dimensional scale of the sliding environment might therefore result in different diffusion properties of EPS, reducing its availability for other cells. A limited diffusion of EPS would also explain the consensus of experiments and model where the diffusion of EPS was also assumed lower compared to surfactin (see Supplemental material). Moreover, we cannot exclude the possibility of additional components present during sliding, but not biofilm formation, possibly anchoring the EPS to the producer cell. For example, the secreted matrix protein RbmA of *Vibrio cholerae* links cells to each other and to the matrix polysaccharides (Nadell *et al.*, 2015). It was also shown for the *Pseudomonas aeruginosa* Psl exopolysaccharide that it is anchored to the cell in early stages of biofilm formation (Ma *et al.*, 2009) that might also be a possible privatization mechanism for EPS during sliding. This demonstrates that the availability of a substance and therefore qualification as public good can vary depending on the environmental conditions or the developmental stage of the producer.

In contrast, we demonstrated that surfactin is publicly available and shared with other cells in the population, so that it is exploitable by non-producers. The latter have the advantage of not paying the production costs for surfactin that is therefore available for metabolism and growth. This could also explain an increased sliding observed in the competition experiment

of wild type and surfactin non-producer: after the quorum sensing controlled surfactin production starts in the wild type cells, the non-producer can simply out-grow the wildtype and utilize the secreted surfactin for sliding causing the observed dominance of the non-producer in the sliding colony.

The exploitation of the surfactin producers by the non-producer is also interesting with regard to the trend of enhanced sliding performance. Recent research has revealed that the presence of so called “cheaters” can be accompanied with an advantage for the whole population: For example, MacLean *et al.* (2010) demonstrated a maximized fitness of structured yeast populations consisting of cooperators and “cheaters” under certain conditions. Therefore, one might argue that the presence of non-producers in a sliding colony could be beneficial if it leads to enhanced sliding, i.e. faster access to new nutrient sources, especially since the wild type has to be present to allow sliding. However, additional investigations about long-term population dynamics of surfactin producers and non-producers might reveal if such a mixed population is stable or collapses when the non-producer becomes too dominant.

The amount of surfactin produced by *B. subtilis* ranges from ca 0.1 mg/ml to ca. 6 mg/ml depending on the strain and culturing conditions (Arima *et al.*, 1968, Chen *et al.*, 2015). Therefore, the amount of externally supplied surfactin necessary to complement sliding to wild-type level is with ca. 1 mg/ml in the naturally possible production range. Interestingly, faster sliding than observed in the wild type is possible with higher amounts of surfactin as shown by the complementation assay. Even though, it might be too costly for *B. subtilis* to invest in slightly faster sliding since we showed that surfactin production is accompanied with a substantial cost and the benefit gained by more surfactin might be too small. Additionally, our experiments suggest that a relatively small amount of surfactin producing cells in a population is sufficient to promote sliding. These might explain why we don't observe faster sliding naturally.

In general, compounds produced by bacteria should be defined as a public good only after analyses of the social properties and the possible production costs. It is also important to be aware of the investigated environment and the possibility that a substance that is publicly available in condition A, but might be privatized in condition B.

Experimental Procedures

Strains and cultivating conditions

All *B. subtilis* strains used in this study are derivatives of a competence enhanced NCBI3610 (DK1042, Konkol *et al.*, 2013). A Δhag mutant lacking flagellin was used as “sliding wild type” since motile strains would swarm and sliding could not be investigated under the used conditions. The strains used in this study are listed in Table S1. To obtain mutants, a *B. subtilis* receptor strain was transformed with genomic DNA from a donor strain (slightly modified after Konkol *et al.*, 2013) or with the respective plasmid. A detailed description of the strain construction can be found in the Supplemental material. The following antibiotic concentrations were used for respective resistant strains if appropriate: Ampicillin 100 $\mu\text{g/ml}$ (Amp), Spectinomycin 100 $\mu\text{g/ml}$ (Spec), Kanamycin 5 $\mu\text{g/ml}$ (Km), Chloramphenicol 5 $\mu\text{g/ml}$ (Cm), Tetracyclin 10 $\mu\text{g/ml}$ (Tet), MLS: Erythromycin 1 $\mu\text{g/ml}$ + Lincomycin 12.5 $\mu\text{g/ml}$.

Sliding competition assay

Sliding assays were performed as described previously (Hölscher *et al.*, 2016). Briefly, overnight cultures of *B. subtilis* were density normalized and if required, mixed in a 1:1, 1:10 or 10:1 ratio with a competitor strain. 2 μl of the strain or mixture were spotted on semi-solid LB (lysogeny broth, LB Lennox, Carl Roth) plates supplemented with 0.7 % Agar-agar which were dried 20 min prior and 10 min post inoculation. The plates were incubated at 37°C for 24 h if not stated otherwise and sliding was evaluated by assessing the diameter of the sliding colony. Additionally, sliding and strain distribution of mixtures of fluorescently labeled strains were evaluated by detecting the fluorescence signal with an AxioZoom V16 fluorescence stereomicroscope equipped with a Zeiss CL 9000 LED light source, HE eGFP filter set (excitation at 470/40 nm and emission at 525/50 nm), HE mRFP filter set (excitation at 572/25 nm and emission at 629/62 nm) and an AxioCam MRm monochrome camera (Carl Zeiss Microscopy GmbH; for details see Hölscher *et al.*, 2016). For image display, the brightness of all fluorescence images was adjusted in the same way and the background was subtracted using the program ImageJ with the rolling ball option (1100 pixels radius).

Determination of occupied area in the sliding colony

The area each strain occupies in the sliding colony was determined using fluorescence stereomicroscope images of the mixtures of different fluorescently labelled strains and the software ImageJ (detailed description in Hölscher *et al.*, 2016). Briefly, the images were opened in ImageJ, separated by channel and the scale was changed to pixel. After background removal, a defined threshold was applied to the image of the green and red channel to separate the fluorescence signal corresponding to the occupied area of the

respective strain. The total area above the threshold was selected and measured as number of pixels. To compare both strains in the sliding colony, the ratio of the two areas was calculated. A summary of the area and percentage calculation was not possible since there was often at least a small overlap between the areas of the different strains, especially in the center of the sliding colony. For this analysis, original images were used.

Complementation assay

To complement sliding of mutants with externally supplied goods, cultures and plates were prepared as described above (see Sliding competition assay). Additionally, 2 μ l of the respective compound was spotted 5 min before the mutant culture (TB532, TB534, TB536) on the same inoculation point. The respective mutant and wild-type cultures alone were used as controls. For surfactin complementation, 10, 1, 0.1 and 0.01 mg/ml of commercial surfactin (Merck KGaA, Darmstadt, Germany) dissolved in methanol was used and pure methanol was spotted as control.

For BslA complementation, the lysate of a BslA-producing *Escherichia coli* BL21 strain (NRS4110 containing plasmid pNW1128, Hopley *et al.*, 2013) and an *E. coli* BL21 strain without the BslA-production plasmid was used. To obtain the *E. coli* lysate, the strains were grown overnight in LB medium and were afterwards inoculated 1:100 in autoinduction medium (Morris *et al.*, 2016). The NRS4110 culture was always supplemented with 100 μ g/ml ampicillin. The cultures were grown for 7-8 h at 37°C with 225 rpm shaking and cells were collected by centrifugation at 4000 g for 15 min. The pellet was resuspended in 5ml PBS buffer supplemented with 1 mM EDTA and cooled on ice for 10 min. The suspension was then sonicated using an Ultrasonic Processor VCX-130 (Zinsser Analytics, Frankfurt am Main, Germany) with ten repeats of a 10 s pulse of 45 % amplitude. During sonication, the suspension was cooled on ice. To obtain the lysate, the suspension was centrifuged (5000 g, 15 min), the supernatant was collected, filter sterilized and stored at 4°C.

For exopolysaccharide complementation, EPS was isolated from pellicle biofilms of a *B. subtilis* 3610 wildtype strain, a Δ *tasA* and as control a Δ *eps* mutant with slight modifications after Dogsa *et al.*, (2013). Briefly, four wells of a 24-well plate containing 2 ml biofilm promoting liquid MSgg medium each (Branda *et al.*, 2001) were inoculated 1:100 with overnight culture of the respective strain and incubated at 30°C for 2-3 d. The pellicle formed at the air-liquid interface was collected together with the medium, diluted 1:1 with PBS buffer and vortexed. The pellicles were sonicated (Ultrasonic Processor VCX-130, Zinsser Analytics, Frankfurt am Main, Germany; 2 \times 12 pulses of 1 s with 30% amplitude), 0.2 M NaOH was added to a final concentration of 0.1 M and the samples were incubated at room temperature for 10 min with short periodic vortexing. Afterwards, the samples were chilled on ice for 5 min before adding cold 0.4 M HCl to a final concentration of 0.1 M. The samples

were centrifuged (7000 g for 15 min at 4°C), the supernatant was collected and transferred to a three-fold volume of cold 96% ethanol and incubated for ca. 20 h at 4°C. The precipitated EPS was collected by centrifugation (7000 g for 15 min at 4°C) and the pellet was dried overnight at 55°C. After drying, the EPS was re-dissolved with deionized water in a 1:10 ratio and NaCl was added to a final concentration of 0.5%. The precipitation, collection and dissolving step was repeated once and the isolated EPS was filter sterilized and stored at 4°C.

The functionality of the BslA-containing lysate and the isolated EPS was successfully verified by testing them for biofilm formation (see supplemental material, supplemental figures S4, S5).

Fitness assay

To determine the relative fitness under sliding conditions, strains with inducible gene constructs of *epsA*, *bslA* and *srfAA* (TB875, TB873, TB977, respectively) were competed against the respective mutants (TB893, TB922, TB895, respectively). Therefore, the strains were density normalized and mixed in a 1:1 ratio in a reaction tube. This mixture was used to a) determine the colony forming units (cfu) at the start by plating on antibiotic containing plates selective for each strain and b) to inoculate a 50 ml Schott bottle containing 5 ml LB medium in a 1:100 dilution. The cultures were incubated at 37°C and 225 rpm shaking for 6-6 ½ h after which they were diluted 1:100 and grown again for 6-6 ½ h under the same conditions. Following incubation, the final cfu of the two competing strains was determined as described above. Initial and final cfu were then used to calculate the relative fitness via the so called malthusian parameter after Lenski *et al.*, (1991) with $r = (m \text{ inducible strain}) / (m \text{ mutant})$ and $m = \ln [(final \text{ cfu}) / (initial \text{ cfu})]$.

Mathematical model

To investigate the competition between producers and non-producers, an agent-based model was constructed. The parameters and variables used for the model are listed in Table S3 and S4, respectively. In short, we represent the agar surface by a discrete hexagonal lattice, in which each lattice element contains a certain quantity of resources (R) – i.e. limiting resource component in the medium. The colony is placed on top of this surface and is modelled in discrete units of biomass (B). Each biomass unit represents a certain quantity of cells. These cells consume the resources for division. In order to simplify the model, cell division is modelled implicitly, by an increase in the number of biomass units. Given the availability of resources, each unit of biomass can double with a given probability. This probability differs between strains (as shown by the competition experiments, surfactin-producing strains have lower division rates as a surfactin mutants). Importantly, every unit of

biomass is assigned to a single strain only. Depending on the strain, cells inside the biomass also secrete molecules: surfactin (M_1) and / or EPS (M_2) (for now we do not consider BslA). These molecules are required for colony expansion, as will be described below. Biomass growth is modelled as a stochastic process, the diffusion of molecules (M_1 , M_2 and R) over the hexagonal surface is modelled as a deterministic process, using Euler's approximation. At the onset of colony growth, a number of biomass units of both strains (i.e. the particular strains that are part of the competition assay of interest) are evenly distributed within a small radius in the center of the surface. From that moment, cells can start consuming resources and producing molecules. These molecules diffuse through space and affect colony expansion. Upon a biomass doubling, every new unit can either accumulate on the same lattice element as the old unit, or move in space (e.g. cells might push each other out). We assume that the new unit moves away from the old grid element with a probability, m (which is the same for all strains), given that the concentrations of both surfactin (M_1) and EPS (M_2) are above a critical concentration, τ (i.e. it is known that both molecules are required for gliding). When there is colony expansion, we assume that new units of biomass always follow the path of least resistance, ending up in a neighbouring grid element with the lowest quantity of biomass.

Acknowledgement

We thank Nicola Stanley-Wall for providing strain NRS4110. We thank Christian Kost for his valuable suggestions during the project. This work was funded by the Deutsche Forschungsgemeinschaft (DFG) to Á.T.K. (KO4741/3.1). T.H. was supported by the International Max Planck Research School.

Conflict of interest. None declared

References

- Allen, B., Gore, J., and Nowak, M. (2013) Spatial dilemmas of diffusible public goods. *Elife* **2**: e01169.
- Arima, K., Kakinuma, A., and Tamura, G. (1968) Surfactin, a crystalline peptidolipid surfactant produced by *Bacillus subtilis*: isolation, characterization and its inhibition of fibrin clot formation. *Biochem Biophys Res Commun* **31**: 488–494.
- Branda, S.S., González-Pastor, J.E., Ben-Yehuda, S., Losick, R., and Kolter, R. (2001) Fruiting body formation by *Bacillus subtilis*. *Proc Natl Acad Sci U S A* **98**: 11621–6.
- Branda, S.S., Chu, F., Kearns, D.B., Losick, R., and Kolter, R. (2006) A major protein component of the *Bacillus subtilis* biofilm matrix. *Mol Microbiol* **59**: 1229–38.
- Brockhurst, M. a., Habets, M.G.J.L., Libberton, B., Buckling, A., and Gardner, A. (2010) Ecological drivers of the evolution of public-goods cooperation in bacteria. *Ecology* **91**: 334–340.
- Chen, W.C., Juang, R.S., and Wei, Y.H. (2015) Applications of a lipopeptide biosurfactant, surfactin, produced by microorganisms. *Biochem Eng J* **103**: 158–169.
- Dogsa, I., Brložnik, M., Stopar, D., and Mandić-Mulec, I. (2013) Exopolymer Diversity and the Role of Levan in *Bacillus subtilis* Biofilms. *PLoS One* **8**: 2–11.
- Drescher, K., Nadell, C.D., Stone, H. a, Wingreen, N.S., and Bassler, B.L. (2014) Solutions to the public goods dilemma in bacterial biofilms. *Curr Biol* **24**: 50–5.
- Gore, J., Youk, H., and Oudenaarden, A. van (2009) Snowdrift game dynamics and facultative cheating in yeast. *Nature* **459**: 253–256.
- Grau, R.R., Oña, P. De, Kunert, M., Leñini, C., Gallegos-monterrosa, R., Mhatre, E., and Vileta, D. (2015) A Duo of Potassium-Responsive Histidine Kinases Govern the Multicellular Destiny of *Bacillus subtilis*. **6**: 1–16.
- Griffin, A.S., West, S.A., and Buckling, A. (2004) Cooperation and competition in pathogenic bacteria. **430**: 2–5.
- Henrichsen, J. (1972) Bacterial surface translocation: a survey and a classification. *Bacteriol Rev* **36**: 478–503.
- Hobley, L., Ostrowski, A., Rao, F. V, Bromley, K.M., Porter, M., Prescott, A.R., *et al.* (2013) BslA is a self-assembling bacterial hydrophobin that coats the *Bacillus subtilis* biofilm. *Proc Natl Acad Sci U S A* **110**: 13600–5.
- Hölscher, T., Dragoš, A., Gallegos-Monterrosa, R., Martin, M., Mhatre, E., Richter, A., and Kovács, Á.T. (2016) Monitoring Spatial Segregation in Surface Colonizing Microbial Populations. *J Vis Exp* e54752.
- Hölscher, T., and Kovács, Á.T. (2017) Sliding on the surface: bacterial spreading without an active motor. *Environ Microbiol* **19**: 2537–2545.
- Kinsinger, R.F., Shirk, M.C., and Fall, R. (2003) Rapid surface motility in *Bacillus subtilis* is dependent on extracellular surfactin and potassium ion. *J Bacteriol* **185**: 5627–5631.
- Kobayashi, K., and Iwano, M. (2012) BslA(YuaB) forms a hydrophobic layer on the surface of *Bacillus subtilis* biofilms. *Mol Microbiol* **85**: 51–66.
- Konkol, M.A., Blair, K.M., and Kearns, D.B. (2013) Plasmid-encoded ComI inhibits competence in the ancestral 3610 strain of *Bacillus subtilis*. *J Bacteriol* **195**: 4085–4093.
- Kovács, Á.T. (2014) Impact of spatial distribution on the development of mutualism in microbes. **5**: 1–5.
- Lenski, R.E., Rose, M.R., Simpson, S.C., and Tadler, S.C. (1991) Long-Term Experimental Evolution in *Escherichia coli*. I. Adaptation and Divergence during 2,000 Generations. *Am Nat* **138**: 1315–1341.

- Lyons, N.A., and Kolter, R. (2017) *Bacillus subtilis* Protects Public Goods by Extending Kin Discrimination to Closely Related Species. *MBio* **8**: e00723-17.
- Ma, L., Conover, M., Lu, H., Parsek, M.R., Bayles, K., and Wozniak, D.J. (2009) Assembly and development of the *Pseudomonas aeruginosa* biofilm matrix. *PLoS Pathog* **5**.
- MacLean, R.C., Fuentes-Hernandez, A., Greig, D., Hurst, L.D., and Gudelj, I. (2010) A mixture of “cheats” and “co-operators” can enable maximal group benefit. *PLoS Biol* **8**.
- Martin, M., Dragoš, A., Hölscher, T., Maróti, G., Bálint, B., Westermann, M., and Kovács, Á.T. (2017) De novo evolved interference competition promotes the spread of biofilm defectors. *Nat Commun* **8**: 15127.
- Momeni, B., Waite, A.J., and Shou, W. (2013) Spatial self-organization favors heterotypic cooperation over cheating. *Elife* **2**: e00960.
- Morris, R.J., Schor, M., Gillespie, R.M.C., Ferreira, A.S., Baldauf, L., Earl, C., *et al.* (2017) Natural variations in the biofilm-associated protein BslA from the genus *Bacillus*. *Sci Rep* **7**: 6730.
- Nadell, C.D., Drescher, K., Wingreen, N.S., and Bassler, B.L. (2015) Extracellular matrix structure governs invasion resistance in bacterial biofilms. *ISME J* 1–10.
- Seminara, A., Angelini, T.E., Wilking, J.N., Vlamakis, H., Ebrahim, S., Kolter, R., *et al.* (2012) Osmotic spreading of *Bacillus subtilis* biofilms driven by an extracellular matrix. *Proc Natl Acad Sci U S A* **109**: 1116–21.
- Stefanic, P., Kraigher, B., Lyons, N.A., Kolter, R., and Mandic-Mulec, I. (2015) Kin discrimination between sympatric *Bacillus subtilis* isolates. *Proc Natl Acad Sci* 201512671.
- Tarnita, C.E. (2017) The ecology and evolution of social behavior in microbes. *J Exp Biol* 18–24.
- Gestel, J. van, Vlamakis, H., and Kolter, R. (2015) From Cell Differentiation to Cell Collectives: *Bacillus subtilis* Uses Division of Labor to Migrate. 1–29.
- Gestel, J. van, Weissing, F.J., Kuipers, O.P., and Kovács, A.T. (2014) Density of founder cells affects spatial pattern formation and cooperation in *Bacillus subtilis* biofilms. *ISME J* 1–11.
- Velicer, G.J., and Vos, M. (2009) Sociobiology of the myxobacteria. *Annu Rev Microbiol* **63**: 599–623.

General Discussion

As has been recognized in the last two decades, microbes engage in intra- and interspecific social interactions and social theory can be applied to them. Social interactions can be complex in higher organisms which is also true for microorganisms. However, they provide useful systems to study the relationships of these interactions since we know a lot about the genes responsible for social phenotypes as well as their regulation, and their short generation time facilitates dissection of population level effects. Microbes are capable of a vast number of different traits and phenotypes and engage in a variety of interactions from beneficial to detrimental ones. The in this dissertation mainly discussed phenomena of biofilm formation and flagellar as well as sliding motility represent only a small part of possible behaviors of microbes. And although *B. subtilis* is only one bacterium among a huge number of other species, as a Gram-positive model organism we can transfer at least some of the insight gained from studying it to other bacteria or use them as basis for further investigations.

1. Motility as social behavior

Motility is a common microbial trait that was among the first to be recognized in the early years of the discovery of microorganisms. The pioneer microbiologist Antonie van Leeuwenhoek, called the “father of microbiology”, described various microorganisms, their form and behavior in detail in a set of letters shortly after the first documentation of fungi by Robert Hooke¹. He also was probably the first person to observe and describe the motion of little “animalcules” as he called the examined small organisms^{223,224}. Motility is widespread among bacteria since it confers several advantages in many different environments. It represents not only a means to reach nutrient sources and thus a favorable habitat, but it can also be for example a crucial trait for pathogenic bacteria to survive inside their host²²⁵. Besides, it also allows the fast escape from overwhelming competitors, which can be the difference between life and death in nature. The latter is not only true for different species but can also reduce competition between members of the same species. In this regard, motility is also an important dispersal mechanism, permitting the colonization of new habitats if for example the nutrients are exhausted.

It could be naively assumed that motility is equal to swimming and only possible in liquid habitats. However, during the last century, various other forms of motile behavior have been recognized apart from flagellum-mediated swimming motility. Most of these types of movement mediate translocation over a surface^{121,123,220}. Swarming motility requires flagella like swimming, but is a collective form of motility instead of an individual one. The second

collective but passive type of surface translocation is sliding whose requirements are described in detail in Chapter 6 and analyzed for *B. subtilis* in Chapters 7 to 10. Another form of individual surface motility encompasses so called twitching which involves the extension and retraction of pili. Besides twitching, gliding is also a type of individual movement requiring focal adhesion complexes distributed over the cell body^{121,123,220}. An excellent example for the necessity of surface motility is *Myxococcus xanthus*, a bacterium that employs so called S-motility, a social type of twitching motility with the additional requirement of cell-cell contact³⁴. It is used by *M. xanthus* to hunt for prey in groups on the one hand and to promote tight packing of spores in fruiting bodies, i.e. completion of the life cycle on the other hand^{34,226}. Additional benefits of the collective types of motility like swarming include elevated resistance to antimicrobial substances^{227,228}, the (for the bacterium) beneficial expression of virulence factors²²⁸, transportation of non-motile bacteria²²⁹ or a mechanism to move during the attack of other microorganisms^{122,230}.

2. Phenotypic heterogeneity and bet-hedging

Motile behavior mediated by flagella is a process based on a complex machinery that composes many structural parts and individual proteins and as a result is energetically expensive. This leads to a large energy load for the cell during flagellar assembly, especially if many other behaviors are expressed by the same cell that also require a lot of energy. To save this cost, many genetically identical populations are phenotypically diverse so that one task is performed by only a subpopulation of cells, a different task by a second subpopulation etc²³¹. This way, the energetic of e.g. collective behaviors is not carried by all cells but divided between different, sometimes overlapping subpopulations, making the whole process more cost efficient. In consequence, phenotypic heterogeneity often creates trade-offs in processes like surface colonization and dispersal. The example of a study with evolving *Burkholderia cenocepacia* populations (also analyzed in Chapter 4) illustrates this possible trade-off well since it investigated the development of variants with effective colonization properties that had poor dispersal abilities²¹. In contrast, variants that could disperse well, showed weaker surface colonization.

In *B. subtilis*, phenotypic heterogeneity is characteristic for a number of processes such as motility, competence and biofilm formation^{115,116,211}. It is evident that a regulatory control is necessary to ensure phenotypic heterogeneity, although noise in e.g. transcription is also a possible mechanism to start the development into one phenotype. Therefore, positive as well as negative feedback loops are often ensuring the stability of a phenotype²³². An example for such a control is represented by the autostimulatory effect of the ComK master regulator for competence, which can bind to the promoter of its own gene and stimulate transcription. This results in a strong amplification of ComK establishing the activation of ComK dependent processes like the competence system^{232,233}. The regulatory control of different processes is

complex and intertwined in *B. subtilis* so that a disturbance of one mechanism has also consequences for other connected ones. This is evident from Chapter 1 where the disturbance of flagellar motility has a large impact on the success of *B. subtilis* to take up DNA. This connection is likely mediated by the global regulator DegU, possibly by elevated levels of its phosphorylated form that results in a decreased competence in mutants lacking structural components of the flagellum. Since we used selected mutants, we were not able to undeniably discern in our study whether the loss of function of the flagellum or the incomplete assembly is responsible for the observed effect on DegU and consequently on competence. The observed increase in competence in viscous medium points to a connection with flagellar rotation and therefore function, but as this is an indirect connection, other factors could also play a role here. Therefore, one approach for future experiments could be the overexpression of the flagellar clutch EpsE, which inhibits motility by interacting with the flagellar rotor and disabling rotation²⁰⁷, or a hybrid protein exhibiting only clutch function. This would cause a functional inhibition of the flagellum without disturbing its assembly. In addition, it would be interesting to investigate the competence in biofilms, since EpsE is also involved in matrix production and represents one mechanism to ensure that matrix-producing cells are non-motile¹¹⁶. Are matrix-producers more or less competent than non-producers in the biofilm? Especially the microscopic investigation of strains with different fluorescence reporters could give insight in whether there is a trade-off in competence between matrix-producers and non-producers in the biofilm.

The observation of phenotypic heterogeneity further resulted in the development of the evolutionary theory of bet-hedging. Bet-hedging describes the investment in different strategies at the same time (conferred by phenotypic heterogeneity) which allows the fast adaptation to changing environmental conditions^{234,235}. One strategy is likely to be advantageous in the adaptation to a new niche after a disturbance, facilitating the survival of the respective subpopulation and therefore the genotype without the potentially crucial time delay of establishing the respective strategy. This way, bet-hedging increases long-term fitness despite the risk of losing a part of the population which is not properly adapted^{234,235}. Although it might be a disadvantageous strategy in homogeneous environments, natural habitats have often fluctuating conditions, favoring bet-hedging (also see below). One bet-hedging strategy of *B. subtilis* is the development of motile cells with flagella and non-motile chains in planktonic cultures. If necessary, this allows the rapid development of a biofilm, for example on a submerged surface, but at the same time maintains the ability to reach possible new niches fast and distribute throughout the favorable habitat.

The important effect of a time delay in niche colonization is illustrated by Chapter 2. Here, a mixture of *B. subtilis* or *P. aeruginosa* wild type and non-motile mutant cells was allowed to colonize the niche of the air-liquid interface and form a pellicle. The non-motile cells displayed a severe competitive disadvantage, since they relied on chance or Brownian motion to reach the surface resulting in a time delay of surface colonization. This is also the

case for single strains. In the competition experiments this delay proved fatal since the motile cells could reach the medium surface and establish a pellicle there, while the non-motile cells were a minority at the air-liquid interface at this timepoint (also see below). In addition, Chapter 2 emphasizes the competitive advantage of sensing the favorable environment via chemotaxis. Again, competition experiments revealed how motile cells that are unable to translate the signal into directed motility (i.e. lacking the chemotaxis receptor-coupled kinase CheA or regulator CheY) are inferior to the chemotaxis proficient wild type in pellicle formation. Further, the competitive disadvantage of a mutant lacking *hemAT*, the gene encoding the potential oxygen sensor of *B. subtilis*, indicates that our model bacterium senses the favorable habitat of the air-liquid interface by the declining oxygen gradient throughout the medium. Interestingly, several components of the chemotaxis adaptation system were tested as well and found to be of slightly different importance for the competitiveness of *B. subtilis*. While the $\Delta cheD$ mutant is more severely outcompeted by the wild type, the $\Delta cheV$ mutant fares better although still exhibiting a slight disadvantage and the $\Delta cheB$ mutant is roughly equal to the wild type in competitiveness. As here the specific case of oxygen sensing is investigated, it is possible that specific adaptation systems are involved in sensing different signals or are at least more effective for specific receptors. The results suggest that during aerotaxis, the three chemotaxis adaptation systems (CheV, CheC-CheD, methylation including CheB) are not exchangeable or redundant but may have distinct operating processes or preferences and are not able to assume all tasks of one another. This is in accordance with conclusions reached by Rao and colleagues, who proposed that the different adaptation systems of *B. subtilis* result in a higher robustness of the system¹⁵⁴. Further, they argue that there are likely differences in the adaptation ability of the three systems to different attractant concentrations and gradients: It was suggested that the CheV and CheC-CheD system assist in chemotaxis adaptation to low attractant concentrations and small gradients whereas the methylation system facilitates adaptation to high attractant concentrations and large gradients¹⁵⁴. The possible difference in adaptation for aerotaxis might also be connected to the solubility of the oxygen sensor²³⁶ in contrast to membrane-bound receptors such as McpC.

3. The flexible strategy of *B. subtilis*

B. subtilis employs a flexible strategy of different motile states like sliding or flagella-based movement and the sessile state of biofilm formation. But is this an advantageous strategy or does it confer drawbacks in a competition with other bacteria specialized in one of those strategies? This question was analyzed using *V. cholerae* populations that lived as either the motile or sessile form or could engage in both lifestyles²³⁷. The authors found that in an environment with frequent fluctuations, the flexible lifestyle was indeed the most beneficial strategy although being subdued by a specialist in the biofilm habitat²³⁷. Since soil, as an

environment in which *B. subtilis* is commonly found, is often characterized by inconstant conditions, it is likely that the result of Yan and colleagues can also be applied to our model bacterium. In fact, the advantage over specialists and the ability to adapt to various conditions as well as to survive the most extreme ones by spore formation, may well be the reason of the environmental success and assumed ubiquity of *B. subtilis*.

The flexible strategy of *B. subtilis* confers the additional advantage of reaching favorable or escaping from unfavorable environments before or after establishing a sessile community. As Chapter 2 demonstrates, cells without flagellar motility are inferior to swimming proficient cells in the initial stages of biofilm formation at the air-liquid interface. The switch to biofilm formation, i.e. the sessile strategy allows then the extended utilization of the valuable resources and establishment of a persisting colony. The flagellum seems to play an important role at the onset of biofilm formation, not only in reaching the air-liquid interface to form pellicles but also as a so called mechanosensor in the identification and attachment to solid surfaces of many bacterial species²³⁸. This function of the flagellum in the initial stages of biofilm formation is not restricted to one specific group but is crucial in multiple biofilm forming bacterial species^{97,239}, as was also demonstrated in Chapter 2.

In the mature biofilm of *B. subtilis*, a small proportion of the cells is still motile²¹⁷ and may escape from the biofilm via swimming or swarming motility if required. However, escape is not only possible by flagella-mediated motility but also by means of passive sliding movement. Chapter 8 shows that in the absence of Ca^{2+} , colony biofilms on agar surfaces expand in late stages of biofilm formation via sliding motility whereas presence of Ca^{2+} restricts expansion due to complex formation with surfactin. The latter seems to alter the properties of surfactin so that it is unable to facilitate movement. This expansion is likely an escape mechanism from the biofilm that occurs when nutrient levels become low or depleted while the biofilm develops. Thus, sliding represents a means for the cells to reach a new and potentially more favourable environment. It is possible without many regulatory changes since many components necessary for biofilm formation are also important for sliding (see Chapter 6, 7 and below) and is therefore cost efficient. Besides, the sliding escape may also provide a way for *B. subtilis* populations to avoid intraspecific competition for nutrients, which likely increases with biofilm development, and therefore also a delay of the (after a critical point) irreversible differentiation into spores.

4. Experimental evolution as a tool to investigate microbial social interactions

As demonstrated by Chapter 4 and 5, laboratory evolution is a powerful tool to analyze possible evolutionary trajectories under certain selection pressure regimes. Especially the use of microorganisms facilitates testing of evolutionary theory which is difficult to examine in organisms with for example a long generation time or with uncontrollable habitat

conditions^{240–242}. As useful as microorganisms are for answering evolutionary questions, experimental evolution with microorganisms is not always a straightforward process. Genes can be acquired by horizontal gene transfer from other species which is sometimes hard to identify and can be hard to track to the originating species. In general, mobile genetic elements can play an important role in obtaining beneficial traits, genome rearrangements or ecological strain dynamics²⁴³ with transposable elements, plasmids or bacteriophages representing the transition vehicles.

In Chapter 5, we evolved *B. subtilis* matrix-producers and non-producers under pellicle formation promoting condition in the absence and presence of a sporulation bottleneck. In the bottleneck regime, the initially underrepresented non-producer was able to incorporate into the pellicle which was coupled to the appearance of hybrid prophages with higher lytic activity. A recent study examined *P. aeruginosa* public good producer and non-producer dynamics in the presence of a lytic phage²⁴⁴. Similar to Chapter 5, the authors found that the phage pressure benefited the non-producers. This was potentially due to an increased production of public goods by the producers and a thus increased cost for them²⁴⁴. This could also happen in case of *B. subtilis* in addition to the already discussed mechanisms and would also explain the stability of the pellicles despite high non-producer frequency (see below). However, if this hypothesis is true, the matrix production in the presence of non-producers and phages would probably be still lower than in wild type pellicles since the productivity of the evolved pellicles is lower in comparison to the ancestor.

Although the matrix components were demonstrated to be public goods and shared with neighboring cells of the pellicle also in other studies^{117,245}, the wild type seems to be somehow protected from “cheater” invasion since non-producers could not invade the pellicle without being evolved. In addition, traits to enhance incorporation did not evolve without heat treatment to select for spores, indicating a high robustness of *B. subtilis* cooperative pellicle formation. After long-term incubation with a sporulation bottleneck, the non-producer was not able to invade via improving evolution of a single or small set of altered genes, but the better pellicle incorporation was connected to a newly developed competitive strategy. It is possible that on account of the large number of mutations, we overlooked an evolved gene specifically contributing to pellicle incorporation of the non-producers. However, mutations contributing to increased incorporation could also be transferred via phage infection. At the end of the evolution experiment, the non-producer percentage of the pellicle population increased above 30%, and even to 80% in one population without collapsing. As the non-producer percentage was partly fluctuating during the experiment, it would be interesting to examine, if in an extended experiment the non-producer reaches an equilibrium state or continues to fluctuate. Since the total productivity of the pellicle was lower with invaded non-producers than with solely the wild type, a robustness of pellicle formation and minimum number of producers is necessary to maintain sufficient matrix production. A low relative level of producers should lead to a collapse of the pellicle as shown for other systems (e.g.⁴⁴)

and it is astonishing that this did not happen for *B. subtilis* despite one pellicle consisting of 80% non-producers. Nevertheless, this low percentage of producers might result in an architectural instability causing higher susceptibility to a predator attack or antimicrobials.

Chapter 2 showed that during competition of two different fluorescently labeled and non-motile, but otherwise matrix producing biofilm proficient strains, large patches of identical cells are formed in the pellicle in comparison to the at macroscale more uniform distribution of the wild type. This spatial organization leads to a more pronounced separation of two different cultures, which could affect interaction between different subpopulations or strains. Interestingly, it was shown in a recent study that the high spatial segregation in pellicles of non-motile strains has a negative effect on the genetic division of labor of different matrix non-producers²⁴⁵ (see also Chapter 5), demonstrating that sufficient exchange of matrix components is necessary.

Chapter 2 and Chapter 3 also highlight, that evolution can be observed already at a very short time scale, at least if sufficient selection pressure is present. It seems the pressure of reaching the air-liquid interface during pellicle formation of non-motile strains was high enough to promote evolution of an alternative way to reach the medium surface, in this case overproduction of the biofilm matrix. Here, the limiting factor could be oxygen availability, since it was also discovered to be the driving force leading to matrix overproducer evolution in other strains²⁴⁶. As matrix overproduction was achieved by probably one single mutation (per strain), other alternatives might exist that require several mutations or confer a smaller advantage and were thus not observed during the pellicle experiments. However, in previous studies different genetical alterations were discovered that lead to a similar effect or phenotype, like the different mutational routes to the wrinkly spreader phenotype of *P. fluorescens* which were discovered by removing the initial mutation targets of the regulatory pathway^{247,248}. Therefore, removal of one regulatory component or gene, i.e. the use of mutants facilitates the detection of new possible regulatory connections and solutions for better adaptation, as also demonstrated by Chapter 1 and 3. Further, more mutations leading to the same advantage might be discovered under conditions with a slightly relaxed selective pressure. Further, *sinR* seems to be a likely target for adjusting matrix production or rescuing defective biofilm formation in *B. subtilis*, which was confirmed by other studies^{23,249,103}. Probably because slight changes in the amino acid composition are sufficient to alter the DNA or dimerization properties and therefore its effectiveness as matrix gene repressor, SinR can facilitate fast adaptation.

5. The purpose of sliding motility

Sliding is a collective and cooperative type of movement over surfaces¹²³. As described in Chapter 6, sliding of different bacterial species often seems to require secreted substances which can be considered potential public goods. However, as the nature and type of the sliding facilitating goods varies in between species, it can be concluded that there are different functional solutions to overcome the friction between cell and substratum. The purpose of sliding movement appears to be the translocation over surfaces for bacteria that lack flagella and pili or the movement in conditions where other types of motility are impossible such as the movement of rhizobia through infection threads during nodule formation²⁵⁰. Although it is slower than e.g. swarming, sliding might be an efficient type of motility when the required substances are already produced, since it allows rapid reaction and the formation of new flagella is complex, costly and requires time^{139,141,142,149}. The exact difference in necessary energy needs to be investigated in detail, but sliding could be employed under conditions in which the cell has to move forward but save energy for other processes as well. However, I consider it very likely that in nature, the transition between different types of movement, for example swarming and sliding, is smooth and dependent on the micro-environmental conditions.

The experiments in Chapter 7 suggest that in *B. subtilis* one function of sliding motility could be to cover the distance towards plant roots in the soil and reaching the rhizosphere to eventually establish a biofilm in this favorable habitat (see Fig. 1). In combination with swimming motility along an oxygen gradient towards the air-liquid interface indicated by Chapter 2, this suggestion provides us with a possible model of *B. subtilis* movement through the soil. It can move by either sliding or swarming in moist but not liquid conditions and swim through water-filled areas to reach a favorable habitat such as the rhizosphere. Once on location, *B. subtilis* can form pellicles if a standing water surface is present or colonize plant roots and form surface attached biofilms (see Fig. 1).

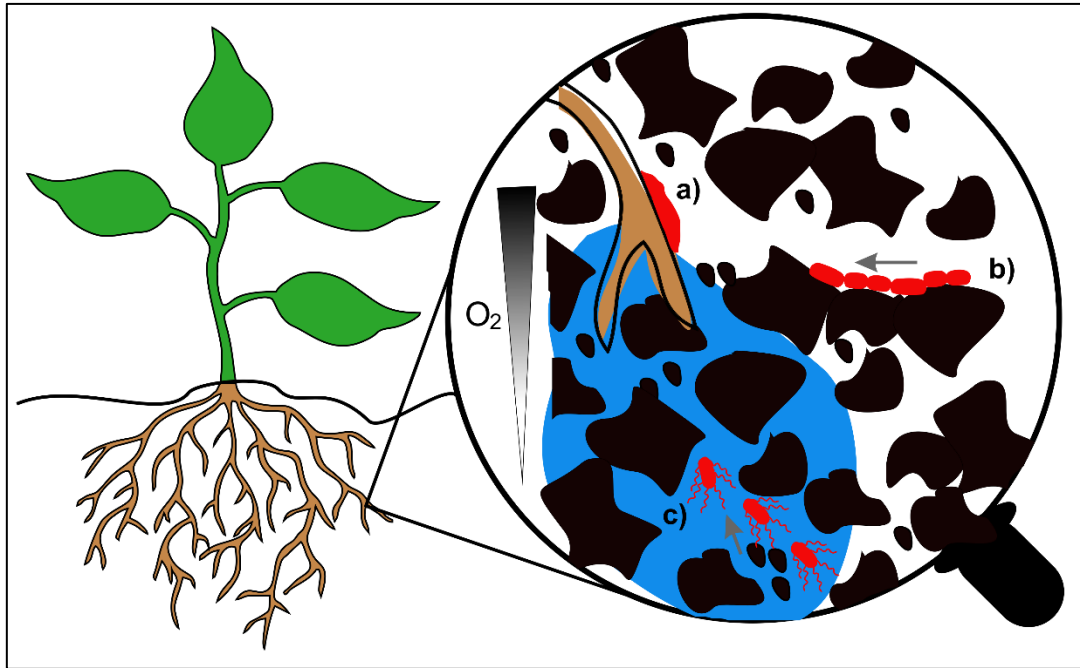


Figure 1. Model for *B. subtilis* soil ecology and mechanisms of plant root colonization. a) Biofilm formation on the surface of a plant root. *B. subtilis* reaches the rhizosphere by means of b) sliding or swarming and c) swimming motility.

6. Sliding as byproduct or distinct process?

Van Gestel *et al.* as well as Chapters 7 and 10 demonstrate that sliding motility is one of the social behaviors of *B. subtilis*¹²⁷. Nevertheless, it is not clear whether sliding of *B. subtilis* is just a side effect of biofilm formation or a distinct process that can be viewed irrespective of biofilms¹⁰⁴. At first glance, the former seems to be true, since *B. subtilis* sliding is regulated by the same pathways and regulatory components than biofilm formation and requires similar extracellular molecules (although the TasA requirement is debatable). Similar to biofilm formation the master regulator Spo0A controls sliding, the inducing signal potassium also is known to trigger biofilm formation and is transmitted by the same set of kinases. However, as established in Chapter 7, although the regulation is tightly linked, there are small differences like the level of Spo0A required for each process. The results suggest that a lower level of Spo0A is necessary for sliding compared to biofilm formation. This indicates sliding as a distinct process which allows movement prior to biofilm formation since it is already induced when biofilm formation is not yet possible. Further, the so far identified sliding inducing signal, potassium, is sensed by KinB at the intracellular level whereas potassium leakage as a biofilm inducer was shown to be sensed by KinC although the sensing mechanism is not clear¹⁹⁸. This differentiation suggests distinct processes, although it is possible that a potential link between them has not yet been discovered. In addition, it seems likely that sliding does not have to be inevitably followed by biofilm formation. This is indicated by experiments investigating planar as well as dendritic sliding, since the sliding colony usually

expands till the edge of the petri dish is reached and usually lacks wrinkles and the architectural complexity of biofilms even after three days of incubation^{127,127} (also see Chapters 7, 9, 10). After this time, a *B. subtilis* biofilm is matured and sufficient levels of Spo0A should be present to promote biofilm formation. Hence, a control mechanism or signal could exist that ensures maintenance of low Spo0A levels if expansion via sliding is possible.

I therefore suggest that sliding should be regarded as a distinct process, but it is nevertheless likely that it developed as a byproduct of biofilm formation. In general, it is evident from the close regulatory connections, that social behaviors in *B. subtilis*, especially the collective motilities swarming and sliding as well as biofilm formation, are not totally secluded phenomena. Rather, there is a flowing transition between these three processes depending on the environmental conditions and requirements. It is highly probable, that this transition also occurs in nature and *B. subtilis* employs these sessile and motile lifestyles to be able to adapt to as many conditions as possible. Soil as habitat reflects the necessity for such adaptations as it exhibits various and changing conditions like high to low nutrient levels, humidity, granularity, porosity, etc. The assumed ubiquity and success of *B. subtilis* is likely caused by its adaptation potential and endospore formation as the last option to survive a large number of stress conditions^{251,252}.

7. Public goods and the maintenance of cooperation during sliding

Fluorescent markers represent excellent tools to follow the spatial distribution of different strains throughout an experiment. This is not only possible at microscale with e.g. Confocal laser scanning microscopy as demonstrated in Chapter 5, but also at lower magnification so that the analysis of an entire surface colonizing colony is possible like explained in Chapter 9. Since spatial segregation is an important mechanism in social interactions, especially as a means to promote cooperation, this method can lead to discoveries about the impact of spatial dynamics on microbial sociality.

It was indeed demonstrated for different bacteria, *B. subtilis* among them⁷¹, that spatial structure is able to promote and maintain cooperation^{63,66}. However, exceptions exist, where this might not be the case. One such example was presented in Chapter 10 where we showed that surfactin production is exploitable by a non-producer. This is in contrast to microbial social theory which predicts that in spatially segregated environments, potential cheaters should not be favored since the benefit of a public good is preferentially directed to neighbors of the producer which are likely other cooperators. Therefore, the question arises, why exploitation is possible in the case of surfactin production.

In this regard, the inherent properties of sliding with its genetic drift and therefore high assortment may have some influence. Some studies demonstrate that a strong mutualistic interaction can have an anti-assorting effect and lead to mixing of the interaction partners

despite genetic drift^{253,254}. Yet, the dependence of for example BslA and surfactin non-producer on each other seems to be too weak to oppose the effect of genetic drift. This is connected to the proposed difference in diffusion properties or sharing of e.g. BslA and surfactin. Since surfactin seems to diffuse very well throughout the sliding colony, the surfactin non-producer can use the available surfactin without requiring to be very close to its producer. In contrast, the BslA and also the exopolysaccharide non-producers are dependent on their partner being in the vicinity, since BslA and exopolysaccharides seem to be privatized to some extent. However, this provides an advantage of a certain protection from exploitation as the results of Chapter 10 demonstrate, which verifies one social theory of possible maintenance of cooperation through public good privatization.

Hence, to achieve a genetic division of labor during sliding, the diffusion and sharing properties of the goods need to be similar. This seems to be possible in dendritic sliding, although the distribution of both strains in the resulting sliding colony was not tested in the study of van Gestel *et al.*¹²⁷. It would be interesting to investigate the distribution of e.g. surfactin and exopolysaccharide non-producers at macroscale in dendritic sliding.

8. Cooperative interactions in nature

So far, cooperative interactions have been mainly analyzed in laboratory settings and under defined conditions. But how robust is cooperation in nature and under ever changing conditions that are characteristic for many a natural habitat? Lately, it has become clear, that it is not enough to study social interactions in an isolated system, but in the ecological context in which they exist²⁵⁵. It is therefore necessary to set up experiments that include components reflecting natural habitats to investigate the microbial behavior there. Most studies regarding disturbance and natural settings have been conducted with focus on diversity, competitive interactions or metabolic pathways^{256,257}. Nevertheless, several studies already tried to at least partly include the influence of ecological fluctuations. For example, Connelly and colleagues investigated the impact of different levels of resource abundance on cooperation in a model system as well as laboratory experiments²⁵⁸. In the model, a resource level above a critical threshold was necessary for cooperation and the cooperating population reached higher cell densities. In contrast, a transition to lower resource levels decreased cooperation and resulted in lower proportion of cooperators in the population. This was confirmed by experiments with biofilm formation of the bacterium *V. cholerae* as cooperative behavior²⁵⁸.

As Chapter 5 and 10 show, the invasion of non-producers is possible under mostly stable conditions in the laboratory, the question arises whether fluctuating natural settings enhance or diminish this possibility. Brockhurst *et al.* examined different levels of disturbance in a mathematical model, which predicted that intermediate disturbance levels support

cooperation. Sparse disturbance promotes evolution of cheaters but high levels of disturbance cause inadequate cell density for cooperation²⁵⁹. Interestingly, the latter effect seems to be reduced if resource availability is higher, leading to the conclusion that indeed a variety of environmental conditions can promote cooperation²⁶⁰. Further, in a recent study, biofilm formation of *P. aeruginosa* in different flow conditions was examined with respect to matrix producer (i.e. cooperator) and non-producer dynamics²⁶¹. These experiments revealed that in the environment most resembling natural settings with irregular flow patterns, cooperators and non-cooperators could stably coexist²⁶¹.

This as well as the examples mentioned above, demonstrate that despite the presence of non-producers, the potential for maintenance of cooperation is also present under unstable environmental conditions. Thus, the mechanisms of preservation and evolution of cooperation revealed so far can possibly be applied to natural environments. Especially surface attached submerged biofilms are argued to be more resistant to environmental changes because of their architectural plasticity²⁶². However, this potential has to be regarded carefully, since it is clear from many studies, that the conditions of the experiments and also the number and identity of the interaction partners have a large influence. Hence, it is possible that if a third, fourth, etc. interaction partner of another species would be introduced in the flow system described above, cooperation might not be stable anymore.

The difficulty to translate results from laboratory experiments to natural environments leads to a requirement of experimental setups with a higher transferability, especially since the specific conditions seem to be important as discussed above. Numerous attempts have already been conducted to generate a laboratory system that can be manipulated and resembles the soil more closely than agar surfaces or liquid cultures. To name two examples, Downie *et al.* developed a substratum that possesses physical and chemical properties similar to soil and is suitable for plant growth²⁶³. Moreover, it is transparent so that fluorescently labelled root colonizing bacteria and plant roots can be imaged easily also in 3D and interactions in the rhizosphere can be studied in greater depth without the need for liquid media. In the second example study, the use of microfluidics systems as possible heterogeneous environment to answer questions in soil microbial ecology was investigated²⁶⁴ (see Fig. 2). The authors argued that spatio-temporal heterogeneity is, among others, an important feature of soil habitats and is being neglected by many artificial soil systems but is possible at the right scale utilizing the microfluidics technique. Further, the conditions are control- and changeable and can be set up with minimum amount of space and material, for example on microchips²⁶⁴. Undoubtedly, more sophisticated systems or possibly combinations will be developed in the future, allowing a detailed analysis of microbial interactions in complex systems.

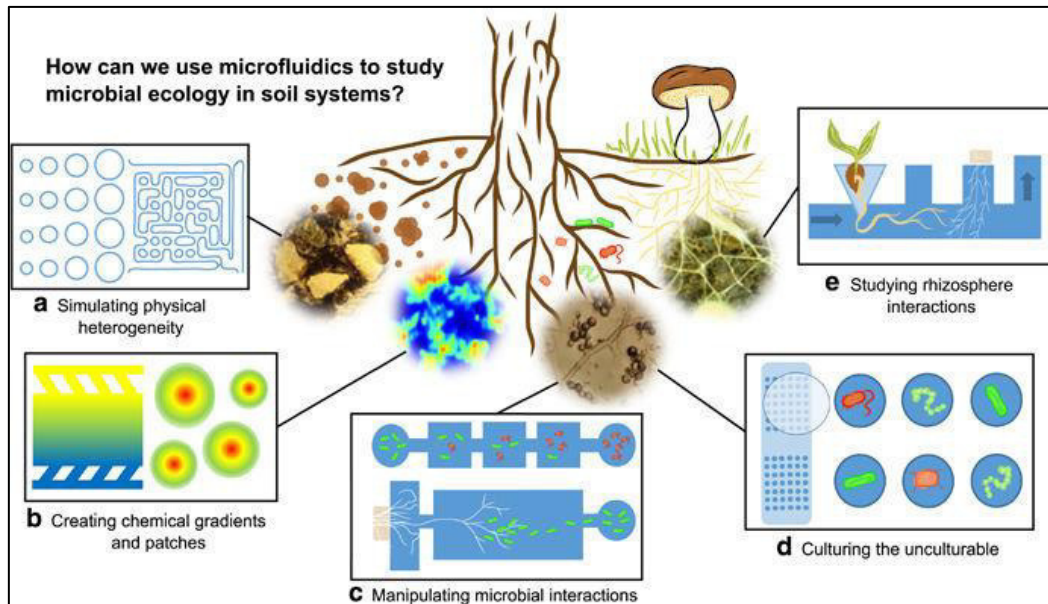


Figure 2. Possible applications of microfluidic devices for the investigation of microbial ecology in soil (adapted from Aleklett *et al.*, 2017²⁶⁴).

However, as important as it is to answer the questions about cooperative and social interactions in general and in natural settings, I believe that the understanding of cooperation principles, obtained by investigating defined conditions and strains in the laboratory, is the basis from where to start. This way, already understanding the underlying mechanics, complex ecological interactions and relationships in multispecies communities as occurring in a gut microbiome or the rhizosphere, are more likely and potentially easier to unravel.

Concluding remarks

The understanding of social interactions gained from the work presented in this dissertation expands the view on collective microbial behaviors with special emphasis on intraspecific interactions of *B. subtilis*. The social behaviors of biofilm formation and different motile behaviors, especially sliding motility analyzed and discussed here were shown to be connected not only by their regulatory elements, but also through their function governing different life styles of *B. subtilis*. Those processes are however not only characteristic for *B. subtilis* but occur in many other bacterial species, so hopefully parts of the knowledge gained in this dissertation can be transferred to other bacterial systems. Future work will also encompass transferring these findings mostly obtained in experimental laboratory settings into setups which mimic natural conditions and investigate specific social interactions in their relevant ecological context.

References

The following list comprises the references of Introduction and General Discussion.

1. Madigan, M. T., Martinko, J. M., Stahl, D. A. & Clark, D. P. *Brock biology of microorganisms*. 13th Edition (Pearson, 2012).
2. Costerton, J. W., Lewandowski, Z., Caldwell, D. E., Korber, D. R. & Lappin-Scott, H. M. Microbial biofilms. *Annu. Rev. Microbiol.* 711–745 (1995).
3. Crespi, B. J. The evolution of social behavior in microorganisms. *Trends Ecol. Evol.* **16**, 178–183 (2001).
4. West, S. A., Griffin, A. S., Gardner, A. & Diggle, S. P. Social evolution theory for microorganisms. *Nat. Rev. Microbiol.* **4**, 597–607 (2006).
5. West, S. A., Diggle, S. P., Buckling, A., Gardner, A. & Griffin, A. S. The Social Lives of Microbes. *Annu. Rev. Ecol. Evol. Syst.* **38**, 53–77 (2007).
6. Xavier, J. B. Social interaction in synthetic and natural microbial communities. *Mol. Syst. Biol.* **7**, 483 (2011).
7. Parsek, M. R. & Greenberg, E. P. Sociomicrobiology: The connections between quorum sensing and biofilms. *Trends Microbiol.* **13**, 27–33 (2005).
8. Greenberg, E. P. The new science of sociomicrobiology and the realm of synthetic and systems ecology in *The Science and Applications of Synthetic and Systems Biology* (ed. IOM Institute of Medicine) 213–222 (The National Academies Press, 2011).
9. Hall-Stoodley, L., Costerton, J. W. & Stoodley, P. Bacterial biofilms: from the natural environment to infectious diseases. *Nat. Rev. Microbiol.* **2**, 95–108 (2004).
10. Widder, S. *et al.* Challenges in microbial ecology: building predictive understanding of community function and dynamics. *ISME J.* **10**, 2557–2568 (2016).
11. Xavier, J. B. Sociomicrobiology and pathogenic bacteria. *Microbiol Spectr.* **4**, 1–10 (2016).
12. Gallegos-Monterrosa, R. *et al.* *Lysinibacillus fusiformis* M5 induces increased complexity in *Bacillus subtilis* 168 colony biofilms via hypoxanthine. *J. Bacteriol.* **199**, e00204-17 (2017).
13. Foster, K. R. & Bell, T. Competition, not cooperation, dominates interactions among culturable microbial species. *Curr. Biol.* **22**, 1845–1850 (2012).
14. Kreft, J.-U. Biofilms promote altruism. *Microbiology* **150**, 2751–60 (2004).
15. Capdevila, S., Martínez-Granero, F. M., Sánchez-Contreras, M., Rivilla, R. & Martín, M. Analysis of *Pseudomonas fluorescens* F113 genes implicated in flagellar filament synthesis and their role in competitive root colonization. *Microbiology* **150**, 3889–3897 (2004).
16. Alsohim, A. S. *et al.* The biosurfactant viscosin produced by *Pseudomonas fluorescens* SBW25 aids spreading motility and plant growth promotion. *Environ. Microbiol.* **16**, 2267–2281 (2014).
17. Pukatzki, S. *et al.* Identification of a conserved bacterial protein secretion system in *Vibrio cholerae* using the *Dictyostelium* host model system. *Proc. Natl. Acad. Sci. U. S. A.* **103**, 1528–1533 (2006).
18. Basler, M., Ho, B. T. & Mekalanos, J. J. Tit-for-tat: Type VI secretion system counterattack during bacterial cell-cell interactions. *Cell* **152**, 884–894 (2013).
19. Rainey, P. B. & Travisano, M. Adaptive radiation in a heterogeneous environment. *Nature* **394**, 69–72 (1998).
20. Spiers, A. J., Kahn, S. G., Bohannon, J., Travisano, M. & Rainey, P. B. Adaptive divergence in experimental populations of *Pseudomonas fluorescens*. I. Genetic and phenotypic bases of wrinkly spreader fitness. *Genetics* **161**, 33–46 (2002).
21. Poltak, S. R. & Cooper, V. S. Ecological succession in long-term experimentally evolved biofilms produces synergistic communities. *ISME J.* **5**, 369–78 (2011).
22. Cramer, N. *et al.* Microevolution of the major common *Pseudomonas aeruginosa*

- clones C and PA14 in cystic fibrosis lungs. *Environ. Microbiol.* **13**, 1690–1704 (2011).
23. Leiman, S. A., Arboleda, L. C., Spina, J. S. & Mcloon, A. L. SinR is a mutational target for fine-tuning biofilm formation in laboratory-evolved strains of *Bacillus subtilis*. *BMC Microbiol.* **14**, 301 (2014).
 24. Traverse, C. C., Mayo-smith, L. M., Poltak, S. R. & Cooper, V. S. Tangled bank of experimentally evolved *Burkholderia* biofilms reflects selection during chronic infections. *Proc. Natl. Acad. Sci. U. S. A.* **110**, E250-9 (2013).
 25. Cornelis, P. Iron uptake and metabolism in pseudomonads. *Appl. Microbiol. Biotechnol.* **86**, 1637–1645 (2010).
 26. Ghoul, M. & Mitri, S. The Ecology and Evolution of Microbial Competition. *Trends Microbiol.* **24**, 833–845 (2016).
 27. Mirleau, P. *et al.* Fitness in soil and rhizosphere of *Pseudomonas fluorescens* C7R12 compared with a C7R12 mutant affected in pyoverdine synthesis and uptake. *FEMS Microbiol. Ecol.* **34**, 35–44 (2000).
 28. Kümmerli, R. & Brown, S. P. Molecular and regulatory properties of a public good shape the evolution of cooperation. *Proc. Natl. Acad. Sci. U. S. A.* **107**, 18921–18926 (2010).
 29. Griffin, A. S., West, S. A. & Buckling, A. Cooperation and competition in pathogenic bacteria. *Nature* **430**, 2–5 (2004).
 30. Sachs, J. L., Mueller, U. G., Wilcox, T. P. & Bull, J. J. The evolution of cooperation. *Q. Rev. Biol.* **79**, 135–160 (2004).
 31. Darwin, C. *On the origin of species by means of natural selection, or the preservation of favoured races in the struggle for life.* (John Murray, 1859).
 32. Ghoul, M., Griffin, A. S. & West, S. A. Toward an evolutionary definition of cheating. *Evolution* **68**, 318–31 (2014).
 33. Hardin, G. The tragedy of the commons. *Science* **162**, 1243–1248 (1968).
 34. Velicer, G. J. & Vos, M. Sociobiology of the myxobacteria. *Annu. Rev. Microbiol.* **63**, 599–623 (2009).
 35. Pande, S. *et al.* Fitness and stability of obligate cross-feeding interactions that emerge upon gene loss in bacteria. *ISME J.* **8**, 953–962 (2014).
 36. Pande, S. *et al.* Metabolic cross-feeding via intercellular nanotubes among bacteria. *Nat. Commun.* **6**, 1–13 (2015).
 37. Morris, J. J. Black Queen evolution: The role of leakiness in structuring microbial communities. *Trends Genet.* **31**, 475–482 (2015).
 38. Morris, J. J., Lenski, R. E. & Zinser, E. R. The Black Queen hypothesis: Evolution of dependencies through adaptative gene loss. *MBio* **3**, 1–7 (2012).
 39. Sachs, J. L. & Hollowell, A. C. The origins of cooperative bacterial communities. *MBio* **3**, e00099-12 (2012).
 40. Greig, D. & Travisano, M. The Prisoner's Dilemma and polymorphism in yeast SUC genes. *Proc. R. Soc. B Biol. Sci.* **271**, S25–S26 (2004).
 41. Veening, J. W. *et al.* Transient heterogeneity in extracellular protease production by *Bacillus subtilis*. *Mol. Syst. Biol.* **4**, 184 (2008).
 42. Ross-Gillespie, A., Dumas, Z. & Kümmerli, R. Evolutionary dynamics of interlinked public goods traits: an experimental study of siderophore production in *Pseudomonas aeruginosa*. *J. Evol. Biol.* **28**, 29–39 (2015).
 43. Buckling, A. *et al.* Siderophore-mediated cooperation and virulence in *Pseudomonas aeruginosa*. *FEMS Microbiol. Ecol.* **62**, 135–141 (2007).
 44. Rainey, P. B. & Rainey, K. Evolution of cooperation and conflict in experimental bacterial populations. *Nature* **425**, 72–74 (2003).
 45. Branda, S. S., González-Pastor, J. E., Ben-Yehuda, S., Losick, R. & Kolter, R. Fruiting body formation by *Bacillus subtilis*. *Proc. Natl. Acad. Sci. U. S. A.* **98**, 11621–6 (2001).
 46. Kearns, D. B. & Losick, R. Swarming motility in undomesticated *Bacillus subtilis*. *Mol. Microbiol.* **49**, 581–590 (2003).
 47. Diggle, S. P., Crusz, S. A. & Cámara, M. Quorum sensing. *Curr. Biol.* **17**, 907–910 (2007).
 48. Whiteley, M., Diggle, S. P. & Greenberg, E. P. Progress in and promise of bacterial

- quorum sensing research. *Nature* **551**, 313–320 (2017).
49. Özkaya, Ö., Xavier, K. B., Dionisio, F. & Balbotín, R. Maintenance of microbial cooperation mediated by public goods in single- and multiple-trait scenarios. *J. Bacteriol.* **199**, e00297-17 (2017).
 50. Bruger, E. L. & Waters, C. M. Bacterial quorum sensing stabilizes cooperation by optimizing growth strategies. *Appl. Environ. Microbiol.* **82**, 6498–6506 (2016).
 51. Allen, R. C., McNally, L., Popat, R. & Brown, S. P. Quorum sensing protects bacterial co-operation from exploitation by cheats. *ISME J.* **10**, 1706-16 (2016).
 52. Xavier, J. B., Kim, W. & Foster, K. R. A molecular mechanism that stabilizes cooperative secretions in *Pseudomonas aeruginosa*. *Mol. Microbiol.* **79**, 166–179 (2011).
 53. Strassmann, J. E., Gilbert, O. M. & Queller, D. C. Kin discrimination and cooperation in microbes. *Annu. Rev. Microbiol.* **65**, 349–367 (2011).
 54. Diggle, S. P., Griffin, A. S., Campbell, G. S. & West, S. A. Cooperation and conflict in quorum-sensing bacterial populations. *Nature* **450**, 411-4 (2007).
 55. Hamilton, W. D. The genetical evolution of social behaviour. I. *J. Theor. Biol.* **7**, 1–16 (1964).
 56. Hamilton, W. D. The genetical evolution of social behaviour. II. *J. Theor. Biol.* **7**, 17–52 (1964).
 57. Gibbs, K. A. & Greenberg, E. P. Territoriality in *Proteus*: Advertisement and aggression. *Chem. Rev.* **111**, 188–194 (2011).
 58. Lyons, N. A., Kraigher, B., Stefanic, P., Mandic-Mulec, I. & Kolter, R. A combinatorial kin discrimination system in *Bacillus subtilis*. *Curr. Biol.* **26**, 733–742 (2016).
 59. Nadell, C. D., Foster, K. R. & Xavier, J. B. Emergence of spatial structure in cell groups and the evolution of cooperation. *PLoS Comput. Biol.* **6**, e1000716 (2010).
 60. Kümmerli, R., Griffin, A. S., West, S. A., Buckling, A. & Harrison, F. Viscous medium promotes cooperation in the pathogenic bacterium *Pseudomonas aeruginosa*. *Proc. R. Soc. B Biol. Sci.* **276**, 3531–3538 (2009).
 61. Allen, B., Gore, J. & Nowak, M. Spatial dilemmas of diffusible public goods. *Elife* **2**, e01169 (2013).
 62. Pande, S. *et al.* Privatization of cooperative benefits stabilizes mutualistic cross-feeding interactions in spatially structured environments. *ISME J.* **10**, 1413–1423 (2016).
 63. Drescher, K., Nadell, C. D., Stone, H. A., Wingreen, N. S. & Bassler, B. L. Solutions to the public goods dilemma in bacterial biofilms. *Curr. Biol.* **24**, 50–5 (2014).
 64. Nadell, C. D., Drescher, K. & Foster, K. R. Spatial structure, cooperation, and competition in biofilms. *Nat. Rev. Microbiol.* **14**, 589–600 (2016).
 65. Nadell, C. D., Drescher, K., Wingreen, N. S. & Bassler, B. L. Extracellular matrix structure governs invasion resistance in bacterial biofilms. *ISME J.* **9**, 1700–1709 (2015).
 66. Momeni, B., Waite, A. J. & Shou, W. Spatial self-organization favors heterotypic cooperation over cheating. *Elife* **2**, e00960 (2013).
 67. Ratzke, C. & Gore, J. Self-organized patchiness facilitates survival in a cooperatively growing *Bacillus subtilis* population. *Nat. Microbiol.* **1**, 16022 (2016).
 68. Tekwa, E., Nguyen, D., Loreau, M. & Gonzalez, A. Defector clustering is linked to cooperation in a pathogenic bacterium. *Proc. R. Soc. B* **284**, 20172001 (2017).
 69. Hallatschek, O., Hersen, P., Ramanathan, S. & Nelson, D. R. Genetic drift at expanding frontiers promotes gene segregation. *Proc. Natl. Acad. Sci. U. S. A.* **104**, 19926–19930 (2007).
 70. Kovács, Á. T. Impact of spatial distribution on the development of mutualism in microbes. *Front. Microbiol.* **5**, 649 (2014).
 71. van Gestel, J., Weissing, F. J., Kuipers, O. P. & Kovács, A. T. Density of founder cells affects spatial pattern formation and cooperation in *Bacillus subtilis* biofilms. *ISME J.* **8**, 2069–2079 (2014).
 72. Van Dyken, J. D., Müller, M. J. I., Mack, K. M. L. & Desai, M. M. Spatial population expansion promotes the evolution of cooperation in an experimental prisoner's

- dilemma. *Curr. Biol.* **23**, 919–923 (2013).
73. Mitri, S., Clarke, E. & Foster, K. R. Resource limitation drives spatial organization in microbial groups. *ISME J.* **10**, 1471–1482 (2016).
 74. Cremer, J., Melbinger, A. & Frey, E. Growth dynamics and the evolution of cooperation in microbial populations. *Sci. Rep.* **2**, 281 (2012).
 75. Pollak, S. *et al.* Facultative cheating supports the coexistence of diverse quorum-sensing alleles. *Proc. Natl. Acad. Sci. U. S. A.* **113**, 2152–2157 (2016).
 76. Gore, J., Youk, H. & van Oudenaarden, A. Snowdrift game dynamics and facultative cheating in yeast. *Nature* **459**, 253–256 (2009).
 77. MacLean, R. C., Fuentes-Hernandez, A., Greig, D., Hurst, L. D. & Gudelj, I. A mixture of ‘cheats’ and ‘co-operators’ can enable maximal group benefit. *PLoS Biol.* **8**, e1000486 (2010).
 78. Celiker, H. & Gore, J. Competition between species can stabilize public-goods cooperation within a species. *Mol. Syst. Biol.* **8**, 621 (2012).
 79. Earl, A. M., Losick, R. & Kolter, R. Ecology and genomics of *Bacillus subtilis*. *Trends Microbiol.* **16**, 269–275 (2008).
 80. van Gestel, J., Vlamakis, H. & Kolter, R. Division of labor in biofilms: the ecology of cell differentiation. *Microbiol. Spectr.* **3**, MB-0002-2014 (2015).
 81. Dubnau, D. & Mirouze, N. Chance and necessity in *Bacillus subtilis* development. *Microbiol. Spectr.* **1**, TBS-0004-2012 (2013).
 82. Dubnau, D. Genetic competence in *Bacillus subtilis*. *Microbiol. Rev.* **55**, 395–424 (1991).
 83. Higgins, D. & Dworkin, J. Recent progress in *Bacillus subtilis* sporulation. *FEMS Microbiol. Rev.* **36**, 131–48 (2012).
 84. Cairns, L. S., Hobley, L. & Stanley-Wall, N. R. Biofilm formation by *Bacillus subtilis*: New insights into regulatory strategies and assembly mechanisms. *Mol. Microbiol.* **93**, 587–598 (2014).
 85. Mhatre, E., Monterrosa, R. G. & Kovács, A. T. From environmental signals to regulators: modulation of biofilm development in Gram-positive bacteria. *J. Basic Microbiol.* **54**, 616–32 (2014).
 86. Romero, D. Bacterial determinants of the social behavior of *Bacillus subtilis*. *Res. Microbiol.* **164**, 788–98 (2013).
 87. Mielich-Süss, B. & Lopez, D. Molecular mechanisms involved in *Bacillus subtilis* biofilm formation. *Environ. Microbiol.* **17**, 555–565 (2015).
 88. Yan, S. & Wu, G. Bottleneck in secretion of α -amylase in *Bacillus subtilis*. *Microb. Cell Fact.* **16**, 124 (2017).
 89. Gupta, M. & Rao, K. K. Phosphorylation of DegU is essential for activation of *amyE* expression in *Bacillus subtilis*. *J. Biosci.* **39**, 747–752 (2014).
 90. Maget-Dana, R. & Ptak, M. Interfacial properties of surfactin. *J. Colloid Interface Sci.* **153**, 285–291 (1992).
 91. Heerklotz, H. & Seelig, J. Leakage and lysis of lipid membranes induced by the lipopeptide surfactin. *Eur. Biophys. J.* **36**, 305–314 (2007).
 92. Carrillo, C., Teruel, J. A., Aranda, F. J. & Ortiz, A. Molecular mechanism of membrane permeabilization by the peptide antibiotic surfactin. *Biochim. Biophys. Acta - Biomembr.* **1611**, 91–97 (2003).
 93. Gonzalez, D. J. *et al.* Microbial competition between *Bacillus subtilis* and *Staphylococcus aureus* monitored by imaging mass spectrometry. *Microbiology* **157**, 2485–2492 (2011).
 94. Zhao, H. *et al.* Biological activity of lipopeptides from *Bacillus*. *Appl. Microbiol. Biotechnol.* **101**, 5951–5960 (2017).
 95. Raaijmakers, J. M., de Bruijn, I., Nybroe, O. & Ongena, M. Natural functions of lipopeptides from *Bacillus* and *Pseudomonas*: More than surfactants and antibiotics. *FEMS Microbiol. Rev.* **34**, 1037–1062 (2010).
 96. Davey, M. E. & O’Toole, G. A. Microbial Biofilms: from Ecology to Molecular Genetics. *Microbiol. Mol. Biol. Rev.* **64**, 847–867 (2000).
 97. Flemming, H.-C. *et al.* Biofilms: an emergent form of bacterial life. *Nat. Rev. Microbiol.*

- 14**, 563–575 (2016).
98. Flemming, H.-C. & Wingender, J. The biofilm matrix. *Nat. Rev. Microbiol.* **8**, 623–33 (2010).
 99. Olsen, I. Biofilm-specific antibiotic tolerance and resistance. *Eur. J. Clin. Microbiol. Infect. Dis.* **34**, 877–886 (2015).
 100. Stewart, P. S. & Costerton, J. W. Antibiotic resistance of bacteria in biofilms. *Lancet* **358**, 135–8 (2001).
 101. Dragoš, A. & Kovács, Á. T. The peculiar functions of the bacterial extracellular matrix. *Trends Microbiol.* **25**, 257–266 (2017).
 102. Cornforth, D. M. & Foster, K. R. Competition sensing: the social side of bacterial stress responses. *Nat. Rev. Microbiol.* **11**, 285–293 (2013).
 103. Chai, Y., Beauregard, P. B., Vlamakis, H., Losick, R. & Kolter, R. Galactose metabolism plays a crucial role in biofilm formation by *Bacillus subtilis*. *MBio* **3**, e00184-12 (2012).
 104. Hughes, A. C. & Kearns, D. B. Swimming, swarming and sliding motility in *Bacillus subtilis* in *Bacillus: Cellular and molecular biology* (ed. Graumann, P. L.) 415–438 (Caister Academic Press, 2017).
 105. Stubbendieck, R. M. & Straight, P. D. Escape from lethal bacterial competition through coupled activation of antibiotic resistance and a mobilized subpopulation. *PLoS Genet.* **11**, e1005722 (2015).
 106. Rosenberg, G. *et al.* Not so simple, not so subtle: the interspecies competition between *Bacillus simplex* and *Bacillus subtilis* and its impact on the evolution of biofilms. *NPJ Biofilms Microbiomes* **2**, 15027 (2016).
 107. Veening, J.-W. *et al.* Bet-hedging and epigenetic inheritance in bacterial cell development. *Proc. Natl. Acad. Sci. U. S. A.* **105**, 4393–4398 (2008).
 108. González-Pastor, J. E. Cannibalism: a social behavior in sporulating *Bacillus subtilis*. *FEMS Microbiol. Rev.* **35**, 415–24 (2011).
 109. González-Pastor, J. E., Hobbs, E. C. & Losick, R. Cannibalism by sporulating bacteria. *Science* **301**, 510–513 (2003).
 110. Dragoš, A. *et al.* Evolution of exploitative interactions during diversification in *Bacillus subtilis* biofilms. *FEMS Microbiol. Ecol.* **93**, fix155 (2018).
 111. Augustine, N., Kumar, P. & Thomas, S. Inhibition of *Vibrio cholerae* biofilm by AiiA enzyme produced from *Bacillus* spp. *Arch. Microbiol.* **192**, 1019–1022 (2010).
 112. Dong, Y., Gusti, A. R., Zhang, Q., Xu, J. & Zhang, L. Identification of quorum-quenching N-acyl homoserine lactonases from *Bacillus* species. *Appl. Environ. Microbiol.* **68**, 1754–1759 (2002).
 113. Hammer, B. K. & Bassler, B. L. Quorum sensing controls biofilm formation in *Vibrio cholerae*. *Mol. Microbiol.* **50**, 101–104 (2003).
 114. Kamruzzaman, M. *et al.* Quorum-regulated biofilms enhance the development of conditionally viable, environmental *Vibrio cholerae*. *Proc. Natl. Acad. Sci. U. S. A.* **107**, 1588–1593 (2010).
 115. Lopez, D., Vlamakis, H. & Kolter, R. Generation of multiple cell types in *Bacillus subtilis*. *FEMS Microbiol. Rev.* **33**, 152–63 (2009).
 116. Vlamakis, H., Chai, Y., Beauregard, P., Losick, R. & Kolter, R. Sticking together: building a biofilm the *Bacillus subtilis* way. *Nat. Rev. Microbiol.* **11**, 157–68 (2013).
 117. Branda, S. S., Chu, F., Kearns, D. B., Losick, R. & Kolter, R. A major protein component of the *Bacillus subtilis* biofilm matrix. *Mol. Microbiol.* **59**, 1229–38 (2006).
 118. Marlow, V. L. *et al.* The prevalence and origin of exoprotease-producing cells in the *Bacillus subtilis* biofilm. *Microbiology* **160**, 56–66 (2014).
 119. Prindle, A. *et al.* Ion channels enable electrical communication in bacterial communities. *Nature* **527**, 59–63 (2015).
 120. Liu, J. *et al.* Coupling between distant biofilms and emergence of nutrient time-sharing. *Science* **356**, 638–642 (2017).
 121. Kearns, D. B. A field guide to bacterial swarming motility. *Nat. Rev. Microbiol.* **8**, 634–44 (2010).
 122. Harshey, R. M. & Partridge, J. D. Shelter in a Swarm. *J. Mol. Biol.* **427**, 3683–3694

- (2015).
123. Henrichsen, J. Bacterial surface translocation: a survey and a classification. *Bacteriol. Rev.* **36**, 478–503 (1972).
 124. Stefanic, P., Kraigher, B., Lyons, N. A., Kolter, R. & Mandic-Mulec, I. Kin discrimination between sympatric *Bacillus subtilis* isolates. *Proc. Natl. Acad. Sci. U. S. A.* **112**, 14042–14047 (2015).
 125. Lyons, N. A. & Kolter, R. *Bacillus subtilis* protects public goods by extending kin discrimination to closely related species. *MBio* **8**, e00723-17 (2017).
 126. Kinsinger, R. F., Shirk, M. C. & Fall, R. Rapid surface motility in *Bacillus subtilis* is dependent on extracellular surfactin and potassium ion. *J. Bacteriol.* **185**, 5627–5631 (2003).
 127. van Gestel, J., Vlamakis, H. & Kolter, R. From cell differentiation to cell collectives: *Bacillus subtilis* uses division of labor to migrate. *PLOS Biol.* **13**, e1002141 (2015).
 128. McLoon, A. L., Guttenplan, S. B., Kearns, D. B., Kolter, R. & Losick, R. Tracing the domestication of a biofilm-forming bacterium. *J. Bacteriol.* **193**, 2027–34 (2011).
 129. Zeigler, D. R. *et al.* The origins of 168, W23, and other *Bacillus subtilis* legacy strains. *J. Bacteriol.* **190**, 6983–6995 (2008).
 130. Burkholder, P. R. & Giles, N. H. Induced biochemical mutations in *Bacillus subtilis*. *Am. J. Bot.* **34**, 345–348 (1947).
 131. Konkol, M. A., Blair, K. M. & Kearns, D. B. Plasmid-encoded ComI inhibits competence in the ancestral 3610 strain of *Bacillus subtilis*. *J. Bacteriol.* **195**, 4085–4093 (2013).
 132. Veening, J. W., Kuipers, O. P., Brul, S., Hellingwerf, K. J. & Kort, R. Effects of phosphorelay perturbations on architecture, sporulation, and spore resistance in biofilms of *Bacillus subtilis*. *J. Bacteriol.* **188**, 3099–3109 (2006).
 133. Patrick, J. E. & Kearns, D. B. Laboratory strains of *Bacillus subtilis* do not exhibit swarming motility. *J. Bacteriol.* **191**, 7129–7133 (2009).
 134. Gallegos-Monterrosa, R., Mhatre, E. & Kovács, Á. T. Specific *Bacillus subtilis* 168 variants form biofilms on nutrient-rich medium. *Microbiol. (United Kingdom)* **162**, 1922–1932 (2016).
 135. Nishito, Y. *et al.* Whole genome assembly of a natto production strain *Bacillus subtilis* natto from very short read data. *BMC Genomics* **11**, 243 (2010).
 136. Itaya, M. & Matsui, K. Conversion of *Bacillus subtilis* 168: Natto producing *Bacillus subtilis* with mosaic genomes. *Biosci. Biotechnol. Biochem.* **63**, 2034–2037 (2014).
 137. Chan, J. M., Guttenplan, S. B. & Kearns, D. B. Defects in the flagellar motor increase synthesis of poly- γ -glutamate in *Bacillus subtilis*. *J. Bacteriol.* **196**, 740–53 (2014).
 138. Kamada, M. *et al.* Whole-genome sequencing and comparative genome analysis of *Bacillus subtilis* strains isolated from non-salted fermented soybean foods. *PLoS One* **10**, e0141369 (2015).
 139. Guttenplan, S. B., Shaw, S. & Kearns, D. B. The cell biology of peritrichous flagella in *Bacillus subtilis*. *Mol. Microbiol.* **87**, 211–229 (2013).
 140. Chevance, F. F. V & Hughes, K. T. Coordinating assembly of a bacterial macromolecular machine. *Nat. Rev. Microbiol.* **6**, 455–465 (2008).
 141. Macnab, R. M. How bacteria assemble flagella. *Annu. Rev. Microbiol.* **57**, 77–100 (2003).
 142. Mukherjee, S. & Kearns, D. B. The structure and regulation of flagella in *Bacillus subtilis*. *Annu. Rev. Genet.* **48**, 319–40 (2014).
 143. Zuberi, A. R., Ying, C., Bischoff, D. S. & Ordal, G. W. Gene-protein relationships in the flagellar hook-basal body complex of *Bacillus subtilis*: sequences of the *flgB*, *flgC*, *flgG*, *fliE* and *fliF* genes. *Gene* **101**, 23–31 (1991).
 144. Lee, L. K., Ginsburg, M. A., Crovace, C., Donohoe, M. & Stock, D. Structure of the torque ring of the flagellar motor and the molecular basis for rotational switching. *Nature* **466**, 996–1000 (2010).
 145. Zhou, J., Lloyd, S. A. & Blair, D. F. Electrostatic interactions between rotor and stator in the bacterial flagellar motor. *Proc. Natl. Acad. Sci. U. S. A.* **95**, 6436–41 (1998).
 146. Sircar, R., Greenswag, A. R., Bilwes, A. M., Gonzalez-Bonet, G. & Crane, B. R.

- Structure and activity of the flagellar rotor protein FliY: A member of the CheC phosphatase family. *J. Biol. Chem.* **288**, 13493–13502 (2013).
147. Bren, A. & Eisenbach, M. The N terminus of the flagellar switch protein, FliM, is the binding domain for the chemotactic response regulator, CheY. *J. Mol. Biol.* **278**, 507–514 (1998).
 148. Courtney, C. R., Cozy, L. M. & Kearns, D. B. Molecular characterization of the flagellar hook in *Bacillus subtilis*. *J. Bacteriol.* **194**, 4619–4629 (2012).
 149. Altegoer, F. & Bange, G. Undiscovered regions on the molecular landscape of flagellar assembly. *Curr. Opin. Microbiol.* **28**, 98–105 (2015).
 150. LaVallie, E. R. & Stahl, M. L. Cloning of the flagellin gene from *Bacillus subtilis* and complementation studies of an in vitro-derived deletion mutation. *J. Bacteriol.* **171**, 3085–3094 (1989).
 151. Bange, G. *et al.* FlhA provides the adaptor for coordinated delivery of late flagella building blocks to the type III secretion system. *Proc. Natl. Acad. Sci. U. S. A.* **107**, 11295–11300 (2010).
 152. Porter, S. L., Wadhams, G. H. & Armitage, J. P. Signal processing in complex chemotaxis pathways. *Nat. Rev. Microbiol.* **9**, 153–165 (2011).
 153. Szurmant, H., Muff, T. J. & Ordal, G. W. *Bacillus subtilis* CheC and FliY are members of a novel class of CheY-P-hydrolyzing proteins in the chemotactic signal transduction cascade. *J. Biol. Chem.* **279**, 21787–21792 (2004).
 154. Rao, C. V., Glekas, G. D. & Ordal, G. W. The three adaptation systems of *Bacillus subtilis* chemotaxis. *Trends Microbiol.* **16**, 480–487 (2008).
 155. Cozy, L. M. & Kearns, D. B. Gene position in a long operon governs motility development in *Bacillus subtilis*. *Mol. Microbiol.* **76**, 273–285 (2010).
 156. Mirel, D. B. & Chamberlin, M. J. The *Bacillus subtilis* flagellin gene (*hag*) is transcribed by the σ_{28} form of RNA polymerase. *J. Bacteriol.* **171**, 3095–3101 (1989).
 157. Marquez-Magana, L. M. & Chamberlin, M. J. Characterization of the sigD transcription unit of *Bacillus subtilis*. *J. Bacteriol.* **176**, 2427–2434 (1994).
 158. Mäder, U. *et al.* *Bacillus subtilis* functional genomics: Genome-wide analysis of the DegS-DegU regulon by transcriptomics and proteomics. *Mol. Genet. Genomics* **268**, 455–467 (2002).
 159. Amati, G., Bisicchia, P. & Galizzi, A. DegU-P represses expression of the motility flhA operon in *Bacillus subtilis*. *J. Bacteriol.* **186**, 6003–6014 (2004).
 160. Hsueh, Y. H. *et al.* DegU-phosphate activates expression of the anti-sigma factor FlgM in *Bacillus subtilis*. *Mol. Microbiol.* **81**, 1092–1108 (2011).
 161. Ogura, M. & Tsukahara, K. SwrA regulates assembly of *Bacillus subtilis* DegU via its interaction with N-terminal domain of DegU. *J. Biochem.* **151**, 643–655 (2012).
 162. Mordini, S. *et al.* The Role of SwrA, DegU and PD3 in *fla/che* Expression in *B. subtilis*. *PLoS One* **8**, e85065 (2013).
 163. Kearns, D. B. & Losick, R. Cell population heterogeneity during growth of *Bacillus subtilis*. *Genes Dev.* **19**, 3083–94 (2005).
 164. Chen, R., Guttenplan, S. B., Blair, K. M. & Kearns, D. B. Role of the σ_D -dependent autolysins in *Bacillus subtilis* population heterogeneity. *J. Bacteriol.* **191**, 5775–5784 (2009).
 165. Veening, J. W. & Kuipers, O. P. Gene position within a long transcript as a determinant for stochastic switching in bacteria. *Mol. Microbiol.* **76**, 269–272 (2010).
 166. Chai, Y., Norman, T., Kolter, R. & Losick, R. An epigenetic switch governing daughter cell separation in *Bacillus subtilis*. *Genes Dev.* **24**, 754–765 (2010).
 167. Chu, F., Kearns, D. B., Branda, S. S., Kolter, R. & Losick, R. Targets of the master regulator of biofilm formation in *Bacillus subtilis*. *Mol. Microbiol.* **59**, 1216–1228 (2006).
 168. Kearns, D. B., Chu, F., Branda, S. S., Kolter, R. & Losick, R. A master regulator for biofilm formation by *Bacillus subtilis*. *Mol. Microbiol.* **55**, 739–49 (2005).
 169. Kobayashi, K. *Bacillus subtilis* pellicle formation proceeds through genetically defined morphological changes. *J. Bacteriol.* **189**, 4920–31 (2007).
 170. Chu, F. *et al.* A novel regulatory protein governing biofilm formation in *Bacillus subtilis*. *Mol. Microbiol.* **68**, 1117–1127 (2008).

171. Norman, T. M., Lord, N. D., Paulsson, J. & Losick, R. Memory and modularity in cell-fate decision making. *Nature* **503**, 481–6 (2013).
172. Chai, Y., Kolter, R. & Losick, R. Reversal of an epigenetic switch governing cell chaining in *Bacillus subtilis* by protein instability. *Mol. Microbiol.* **78**, 218–229 (2010).
173. Jiang, M., Shao, W., Perego, M. & Hoch, J. A. Multiple histidine kinases regulate entry into stationary phase and sporulation in *Bacillus subtilis*. *Mol. Microbiol.* **38**, 535–542 (2000).
174. Hamon, M. A. & Lazazzera, B. A. The sporulation transcription factor Spo0A is required for biofilm development in *Bacillus subtilis*. *Mol. Microbiol.* **42**, 1199–1209 (2001).
175. Burbulys, D., Trach, K. A. & Hoch, J. A. Initiation of sporulation in *B. subtilis* is controlled by a multicomponent phosphorelay. *Cell* **64**, 545–552 (1991).
176. Shafikhani, S. H., Mandic-mulec, I., Strauch, M. A., Smith, I. & Leighton, T. Postexponential regulation of *sin* operon expression in *Bacillus subtilis*. *J. Bacteriol.* **184**, 564–571 (2002).
177. Verhamme, D. T., Murray, E. J. & Stanley-Wall, N. R. DegU and Spo0A jointly control transcription of two loci required for complex colony development by *Bacillus subtilis*. *J. Bacteriol.* **91**, 100–108 (2009).
178. Strauch, M., Webbt, V., Spiegelmant, G. & Hoch, J. A. The Spo0A protein of *Bacillus subtilis* is a repressor of the *abrB* gene. **87**, 1801–1805 (1990).
179. Branda, S. S. *et al.* Genes involved in formation of structured multicellular communities by *Bacillus subtilis*. *J. Bacteriol.* **186**, 3970–3979 (2004).
180. Roux, D. *et al.* Identification of poly-N-acetyl glucosamine as a major polysaccharide component of the *Bacillus subtilis* biofilm matrix. *J. Biol. Chem.* **290**, 19261–72 (2015).
181. Dogsa, I., Brložnik, M., Stopar, D. & Mandic-Mulec, I. Exopolymer diversity and the role of levan in *Bacillus subtilis* biofilms. *PLoS One* **8**, e62044 (2013).
182. Dragoš, A. & Kovács, Á. T. The role of functional amyloids in multicellular growth and development of Gram-positive bacteria. *Biomolecules* **7**, 60 (2017).
183. Romero, D., Aguilar, C., Losick, R. & Kolter, R. Amyloid fibers provide structural integrity to *Bacillus subtilis* biofilms. *Proc. Natl. Acad. Sci. U. S. A.* **107**, 2230–4 (2010).
184. Romero, D., Vlamakis, H., Losick, R. & Kolter, R. An accessory protein required for anchoring and assembly of amyloid fibres in *B. subtilis* biofilms. *Mol. Microbiol.* **80**, 1155–68 (2011).
185. Hamon, M. A., Stanley, N. R., Britton, R. A., Grossman, A. D. & Lazazzera, B. A. Identification of AbrB-regulated genes involved in biofilm formation by *Bacillus subtilis*. *Mol. Microbiol.* **52**, 847–860 (2004).
186. Hogley, L. *et al.* BslA is a self-assembling bacterial hydrophobin that coats the *Bacillus subtilis* biofilm. *Proc. Natl. Acad. Sci. U. S. A.* **110**, 13600–5 (2013).
187. Arnaouteli, S., MacPhee, C. E. & Stanley-Wall, N. R. Just in case it rains: building a hydrophobic biofilm the *Bacillus subtilis* way. *Curr. Opin. Microbiol.* **34**, 7–12 (2016).
188. Arnaouteli, S. *et al.* Bifunctionality of a biofilm matrix protein controlled by redox state. *Proc. Natl. Acad. Sci. U. S. A.* **114**, E6184–E6191 (2017).
189. Kobayashi, K. & Iwano, M. BslA(YuaB) forms a hydrophobic layer on the surface of *Bacillus subtilis* biofilms. *Mol. Microbiol.* **85**, 51–66 (2012).
190. Kovács, A. T., van Gestel, J. & Kuipers, O. P. The protective layer of biofilm: a repellent function for a new class of amphiphilic proteins. *Mol. Microbiol.* **85**, 8–11 (2012).
191. Shemesh, M. & Chai, Y. A combination of glycerol and manganese promotes biofilm formation in *Bacillus subtilis* via histidine kinase KinD signaling. *J. Bacteriol.* **195**, 2747–54 (2013).
192. Mhatre, E. *et al.* The impact of manganese on biofilm development of *Bacillus subtilis*. *Microbiology* **162**, 1468–1478 (2016).
193. Beauregard, P. B., Chai, Y., Vlamakis, H., Losick, R. & Kolter, R. *Bacillus subtilis* biofilm induction by plant polysaccharides. *Proc. Natl. Acad. Sci. U. S. A.* **110**, E1621–E1630 (2013).

194. Beaugregard, P. B. *Not Just Sweet Talkers: How Roots Stimulate Their Colonization by Beneficial Bacteria*. *Advances in Botanical Research* **75**, (Elsevier Ltd, 2015).
195. Kolodkin-Gal, I. *et al.* Respiration control of multicellularity in *Bacillus subtilis* by a complex of the cytochrome chain with a membrane-embedded histidine kinase. *Genes Dev.* **27**, 887–99 (2013).
196. McLoon, A. L., Kolodkin-Gal, I., Rubinstein, S. M., Kolter, R. & Losick, R. Spatial regulation of histidine kinases governing biofilm formation in *Bacillus subtilis*. *J. Bacteriol.* **193**, 679–685 (2011).
197. Kovács, Á. T. Bacterial differentiation via gradual activation of global regulators. *Curr. Genet.* **62**, 125–8 (2016).
198. López, D., Fischbach, M. A., Chu, F., Losick, R. & Kolter, R. Structurally diverse natural products that cause potassium leakage trigger multicellularity in *Bacillus subtilis*. *Proc. Natl. Acad. Sci. U. S. A.* **106**, 280–285 (2009).
199. López, D., Gontang, E. a & Kolter, R. *Potassium sensing histidine kinase in Bacillus subtilis*. *Methods in enzymology* **471**, (Elsevier Inc., 2010).
200. López, D., Vlamakis, H., Losick, R. & Kolter, R. Paracrine signaling in a bacterium. *Genes Dev.* **23**, 1631–8 (2009).
201. Cairns, L. S., Marlow, V. L., Bissett, E., Ostrowski, A. & Stanley-Wall, N. R. A mechanical signal transmitted by the flagellum controls signalling in *Bacillus subtilis*. *Mol. Microbiol.* **90**, 6–21 (2013).
202. Kobayashi, K. Gradual activation of the response regulator DegU controls serial expression of genes for flagellum formation and biofilm formation in *Bacillus subtilis*. *Mol. Microbiol.* **66**, 395–409 (2007).
203. Verhamme, D. T., Kiley, T. B. & Stanley-Wall, N. R. DegU co-ordinates multicellular behaviour exhibited by *Bacillus subtilis*. *Mol. Microbiol.* **65**, 554–68 (2007).
204. Murray, E. J., Kiley, T. B. & Stanley-Wall, N. R. A pivotal role for the response regulator DegU in controlling multicellular behaviour. *Microbiology* **155**, 1–8 (2009).
205. Ostrowski, A., Mehert, A., Prescott, A., Kiley, T. B. & Stanley-Wall, N. R. YuaB functions synergistically with the exopolysaccharide and TasA amyloid fibers to allow biofilm formation by *Bacillus subtilis*. *J. Bacteriol.* **193**, 4821–31 (2011).
206. Guttenplan, S. B., Blair, K. M. & Kearns, D. B. The EpsE flagellar clutch is bifunctional and synergizes with EPS biosynthesis to promote *Bacillus subtilis* biofilm formation. *PLoS Genet.* **6**, e1001243 (2010).
207. Blair, K. M., Turner, L., Winkelman, J. T., Berg, H. C. & Kearns, D. B. A molecular clutch disables flagella in the *Bacillus subtilis* biofilm. *Science* **320**, 1636–1638 (2008).
208. Guttenplan, S. B. & Kearns, D. B. Regulation of flagellar motility during biofilm formation. *FEMS Microbiol. Rev.* **37**, 849–871 (2013).
209. Chai, Y., Chu, F., Kolter, R. & Losick, R. Bistability and biofilm formation in *Bacillus subtilis*. *Mol. Microbiol.* **67**, 254–63 (2008).
210. Veening, J.-W., Hamoen, L. W. & Kuipers, O. P. Phosphatases modulate the bistable sporulation gene expression pattern in *Bacillus subtilis*. *Mol. Microbiol.* **56**, 1481–1494 (2005).
211. Dubnau, D. & Losick, R. Bistability in bacteria. *Mol. Microbiol.* **61**, 564–572 (2006).
212. de Jong, I. G., Veening, J. W. & Kuipers, O. P. Heterochronic phosphorelay gene expression as a source of heterogeneity in *Bacillus subtilis* spore formation. *J. Bacteriol.* **192**, 2053–2067 (2010).
213. Chastanet, A. *et al.* Broadly heterogeneous activation of the master regulator for sporulation in *Bacillus subtilis*. *Proc. Natl. Acad. Sci. U. S. A.* **107**, 8486–8491 (2010).
214. Russell, J. R., Cabeen, M. T., Wiggins, P. A., Paulsson, J. & Losick, R. Noise in a phosphorelay drives stochastic entry into sporulation in *Bacillus subtilis*. *EMBO J.* **36**, e201796988 (2017).
215. Fujita, M., González-Pastor, J. E. & Losick, R. High- and low-threshold genes in the Spo0A regulon of *Bacillus subtilis*. *J. Bacteriol.* **187**, 1357–1368 (2005).
216. Fujita, M. & Losick, R. Evidence that entry into sporulation in *Bacillus subtilis* is governed by a gradual increase in the level and activity of the master regulator Spo0A. *Genes Dev.* **19**, 2236–2244 (2005).

217. Vlamakis, H., Aguilar, C., Losick, R. & Kolter, R. Control of cell fate by the formation of an architecturally complex bacterial community. *Genes Dev.* **22**, 945–53 (2008).
218. Aguilar, C., Vlamakis, H. & Guzman, A. KinD is a checkpoint protein linking spore formation to extracellular-matrix production in *Bacillus subtilis* biofilms. *MBio* **1**, e00035-10 (2010).
219. Wilking, J. N. *et al.* Liquid transport facilitated by channels in *Bacillus subtilis* biofilms. *Proc. Natl. Acad. Sci. U. S. A.* **110**, 848–52 (2013).
220. Harshey, R. M. Bacterial motility on a surface: many ways to a common goal. *Annu. Rev. Microbiol.* **57**, 249–273 (2003).
221. Kinsinger, R. F., Kearns, D. B., Hale, M. & Fall, R. Genetic requirements for potassium ion-dependent colony spreading in *Bacillus subtilis*. *J. Bacteriol.* **187**, 8462–8469 (2005).
222. Fall, R., Kearns, D. B. & Nguyen, T. A defined medium to investigate sliding motility in a *Bacillus subtilis* flagella-less mutant. *BMC Microbiol.* **6**, 31 (2006).
223. van Leeuwenhoek, A. Part of a letter from Mr Antony Van Leeuwenhoek, F. R. S. concerning green weeds growing in water, and some animalcula found about them. *Philos. Trans. R. Soc. London* **23**, 1304–1311 (1703).
224. Lane, N. The unseen world: reflections on Leeuwenhoek (1677) ‘Concerning little animals’. *Philos. Trans. R. Soc. London B* **370**, 20140344 (2015).
225. Josenhans, C. & Suerbaum, S. The role of motility as a virulence factor in bacteria. *Int. J. Med. Microbiol.* **291**, 605–614 (2002).
226. Berleman, J. E. & Kirby, J. R. Deciphering the hunting strategy of a bacterial wolfpack. *FEMS Microbiol. Rev.* **33**, 942–957 (2009).
227. Butler, M. T., Wang, Q. & Harshey, R. M. Cell density and mobility protect swarming bacteria against antibiotics. *Proc. Natl. Acad. Sci. U. S. A.* **107**, 3776–3781 (2010).
228. Overhage, J., Bains, M., Brazas, M. D. & Hancock, R. E. W. Swarming of *Pseudomonas aeruginosa* is a complex adaptation leading to increased production of virulence factors and antibiotic resistance. *J. Bacteriol.* **190**, 2671–2679 (2008).
229. Hagai, E. *et al.* Surface-motility induction, attraction and hitchhiking between bacterial species promote dispersal on solid surfaces. *ISME J.* **8**, 1147–1151 (2014).
230. Alteri, C. J. *et al.* Multicellular bacteria deploy the type VI secretion system to preemptively strike neighboring cells. *PLoS Pathog.* **9**, e1003608 (2013).
231. Ackermann, M. A functional perspective on phenotypic heterogeneity in microorganisms. *Nat. Rev. Microbiol.* **13**, 497–508 (2015).
232. Smits, W. K., Kuipers, O. P. & Veening, J.-W. Phenotypic variation in bacteria: the role of feedback regulation. *Nat. Rev. Microbiol.* **4**, 259–271 (2006).
233. Van Sinderen, D. & Venema, G. comK Acts as an autoregulatory control switch in the signal transduction route to competence in *Bacillus subtilis*. *J. Bacteriol.* **176**, 5762–5770 (1994).
234. Grimbergen, A. J., Siebring, J., Solopova, A. & Kuipers, O. P. Microbial bet-hedging: the power of being different. *Curr. Opin. Microbiol.* **25**, 67–72 (2015).
235. Veening, J.-W., Smits, W. K. & Kuipers, O. P. Bistability, epigenetics, and bet-hedging in bacteria. *Annu. Rev. Microbiol.* **62**, 193–210 (2008).
236. Martínková, M., Kitanishi, K. & Shimizu, T. Heme-based globin-coupled oxygen sensors: Linking oxygen binding to functional regulation of diguanylate cyclase, histidine kinase, and methyl-accepting chemotaxis. *J. Biol. Chem.* **288**, 27702–27711 (2013).
237. Yan, J., Nadell, C. D. & Bassler, B. L. Environmental fluctuation governs selection for plasticity in biofilm production. *ISME J.* **11**, 1569–1577 (2017).
238. Belas, R. Biofilms, flagella, and mechanosensing of surfaces by bacteria. *Trends Microbiol.* **22**, 517–527 (2014).
239. O’Toole, G., Kaplan, H. B. & Kolter, R. Biofilm formation as microbial development. *Annu. Rev. Microbiol.* **54**, 49–79 (2000).
240. Bennett, A. F. & Hughes, B. S. Microbial experimental evolution. *Am. J. Physiol. Regul. Integr. Comp. Physiol.* **297**, R17-25 (2009).
241. Barrick, J. E. & Lenski, R. E. Genome dynamics during experimental evolution. *Nat.*

- Rev. Genet.* **14**, 827–39 (2013).
242. Steenackers, H. P., Parijs, I., Foster, K. R. & Vanderleyden, J. Experimental evolution in biofilm populations. *FEMS Microbiol. Rev.* **40**, 980 (2016).
 243. Howard-Varona, C., Hargreaves, K. R., Abedon, S. T. & Sullivan, M. B. Lysogeny in nature: mechanisms, impact and ecology of temperate phages. *ISME J.* **11**, 1511–1520 (2017).
 244. Vasse, M., Torres-Barcélo, C. & Hochberg, M. E. Phage selection for bacterial cheats leads to population decline. *Proc. R. Soc. B Biol. Sci.* **208**, 20152207 (2015).
 245. Dragoš, A. *et al.* Division of labor during biofilm matrix production. *bioRxiv* 237230 (2017). doi:<https://doi.org/10.1101/237230>
 246. Kusmierska, A. & Spiers, A. J. New insights into the effects of several environmental parameters on the relative fitness of a numerically dominant class of evolved niche specialist. **2016**, 4846565 (2016).
 247. Lind, P. A., Farr, A. D. & Rainey, P. B. Evolutionary convergence in experimental *Pseudomonas* populations. *ISME J.* **11**, 589-600 (2017).
 248. Lind, P. A., Farr, A. D. & Rainey, P. B. Experimental evolution reveals hidden diversity in evolutionary pathways. *Elife* **4**, e07074 (2015).
 249. Yan, F. *et al.* The *comER* gene plays an important role in biofilm formation and sporulation in both *Bacillus subtilis* and *Bacillus cereus*. *Front. Microbiol.* **7**, 1025 (2016).
 250. Fournier, J. *et al.* Mechanism of infection thread elongation in root hairs of *Medicago truncatula* and dynamic interplay with associated rhizobial colonization. *PLANT Physiol.* **148**, 1985–1995 (2008).
 251. Tan, I. S. & Ramamurthi, K. S. Spore formation in *Bacillus subtilis*. *Environ. Microbiol. Rep.* **6**, 212–225 (2014).
 252. Setlow, P. Spores of *Bacillus subtilis*: Their resistance to and killing by radiation, heat and chemicals. *J. Appl. Microbiol.* **101**, 514–525 (2006).
 253. Momeni, B., Brileya, K. a, Fields, M. W. & Shou, W. Strong inter-population cooperation leads to partner intermixing in microbial communities. *Elife* **2**, e00230 (2013).
 254. Müller, M. J. I., Neugeboren, B. I., Nelson, D. R. & Murray, A. W. Genetic drift opposes mutualism during spatial population expansion. *Proc. Natl. Acad. Sci. U. S. A.* **111**, 1037–42 (2014).
 255. Tarnita, C. E. The ecology and evolution of social behavior in microbes. *J. Exp. Biol.* **220**, 18–24 (2017).
 256. Yan, Y., Kuramae, E. E., De Hollander, M., Klinkhamer, P. G. & Van Veen, J. A. Functional traits dominate the diversity-related selection of bacterial communities in the rhizosphere. *ISME J.* **11**, 56–66 (2016).
 257. Buckling, A., Kassen, R., Bell, G. & Rainey, P. B. Disturbance and diversity in experimental microcosms. *Nature* **408**, 961–964 (2000).
 258. Connelly, B. D., Bruger, E. L., McKinley, P. K. & Waters, C. M. Resource abundance and the critical transition to cooperation. *J. Evol. Biol.* **30**, 750–761 (2017).
 259. Brockhurst, M. A., Buckling, A. & Gardner, A. Cooperation peaks at intermediate disturbance. *Curr. Biol.* **17**, 761–765 (2007).
 260. Brockhurst, M. A., Habets, M. G. J. L., Libberton, B., Buckling, A. & Gardner, A. Ecological drivers of the evolution of public-goods cooperation in bacteria. *Ecology* **91**, 334–340 (2010).
 261. Nadell, C. D., Ricaurte, D., Yan, J., Drescher, K. & Bassler, B. L. Flow environment and matrix structure interact to determine spatial competition in *Pseudomonas aeruginosa* biofilms. *Elife* **6**, e21855 (2017).
 262. Bridier, A. *et al.* Spatial organization plasticity as an adaptive driver of surface microbial communities. *Front. Microbiol.* **8**, 1364 (2017).
 263. Downie, H. *et al.* Transparent soil for imaging the rhizosphere. *PLoS One* **7**, e44276 (2012).
 264. Aleklett, K. *et al.* Build your own soil: exploring microfluidics to create microbial habitat structures. *ISME J.* **12**, 312-319 (2017).

Supporting information for Chapter 1

Impaired competence in flagellar mutants of *Bacillus subtilis* is connected to the regulatory network governed by DegU

Published in: Environmental Microbiology Reports (2018)

Supplementary materials for Höscher, Schiklang et al

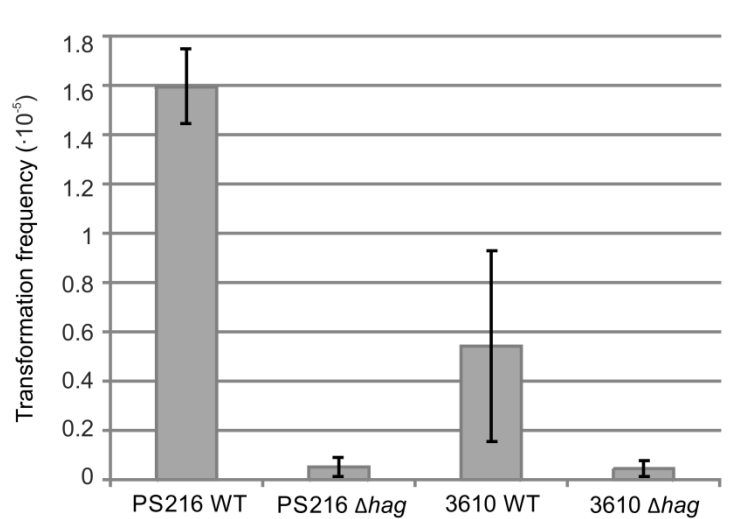


Figure S1. Reduced competence in different *B. subtilis* strains. Transformation frequency of *B. subtilis* wild-type and *hag*-mutant of strains PS216 and 3610 after incubation in competence medium for 6 h (n = 3). Error bars represent the standard deviation.

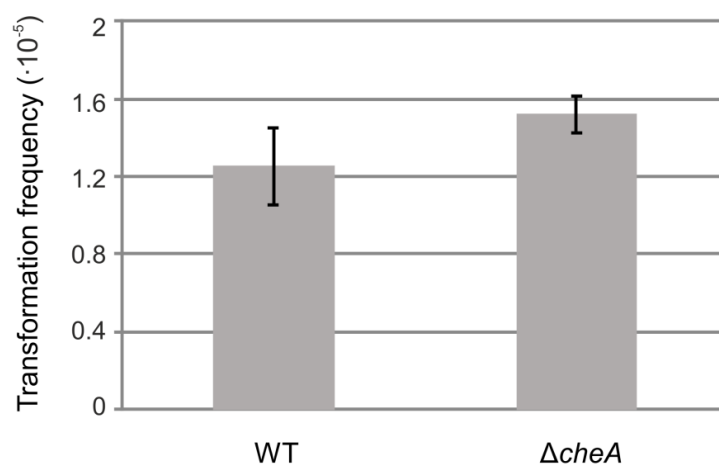


Figure S2. Chemotactic response is not connected to competence. Transformation frequency of *B. subtilis* wild-type and *cheA*-mutant, encoding the main sensor kinase of the chemotaxis system, after incubation in competence medium for 6 h (unpaired two-sample t-test with Welch Correction: P = 0.232, n = 3). Error bars represent the standard deviation.

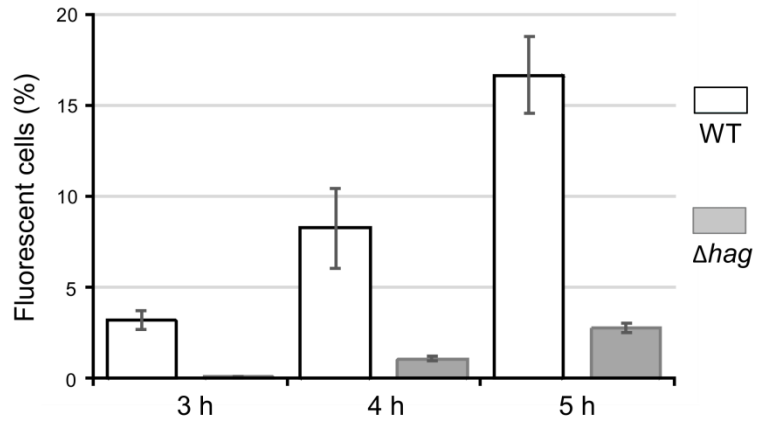


Figure S3. Fewer cells express competence genes in the *hag*-mutant over time. Percentage of fluorescent (i.e. competence gene expressing) cells determined from flow cytometric measurements of wild-type and *hag*-mutant harboring P_{comG} -*gfp* after 3 h, 4 h and 5 h incubation in competence medium (unpaired two-sample t-test with Welch Correction: $P < 0.05$, $n = 3$). A gate at fluorescence intensities above 3 A.U. was used to isolate the fluorescent population. Error bars represent the standard deviation.

Table S1. Strains used in this study. Antibiotics are abbreviated as follows: Kanamycin – Kan, Chloramphenicol – Chl, Tetracyclin – Tet.

Strain	Genotype	Reference
168	$\Delta trpC$	Gallegos-Monterrosa <i>et al.</i> , 2016
TB115	$\Delta trpC$; <i>hag</i> ::Kan	This study
TB710	$\Delta trpC$; $\Delta motA$	This study
TB689	$\Delta trpC$; $\Delta flgE$	This study
P_{comG} - <i>gfp</i>	$\Delta trpC$; P_{comG} - <i>gfp</i> Chl ^R	Veening <i>et al.</i> , 2006
P_{comG} - <i>gfp</i> $\Delta comK$	$\Delta trpC$; P_{comG} - <i>gfp</i> Chl ^R ; <i>comK</i> ::Kan	Veening <i>et al.</i> , 2006
TB831	$\Delta trpC$; P_{comG} - <i>gfp</i> Chl ^R ; <i>hag</i> ::Tet	This study
TB926	$\Delta trpC$; P_{comG} - <i>gfp</i> Chl ^R ; $\Delta motA$	This study
TB925	$\Delta trpC$; P_{comG} - <i>gfp</i> Chl ^R ; $\Delta flgE$	This study
168 P_{xyl} - <i>comK</i>	$\Delta trpC$; <i>amyE</i> :: P_{xyl} - <i>comK</i> <i>xylR</i> Chl ^R	van den Esker <i>et al.</i> , 2017
TB928	$\Delta trpC$; <i>amyE</i> :: P_{xyl} - <i>comK</i> Chl ^R <i>xylR</i> ; <i>hag</i> ::Kan	This study
TB935	$\Delta trpC$; <i>degU</i> (Hy)32::Kan	This study
TB936	$\Delta trpC$; <i>degU</i> 146::Kan	This study
TB923	$\Delta trpC$; <i>degU</i> (Hy)32::Kan; <i>hag</i> ::Chl	This study
TB924	$\Delta trpC$; <i>degU</i> 146::Kan; <i>hag</i> ::Chl	This study
TB779	$\Delta trpC$; $\Delta cheA$	This study
PE277	PY79 <i>safA</i> ::Tet	Eichenberger <i>et al.</i> , 2001

Table S2. Oligonucleotides used in this study

Oligo	Experimental purpose	Sequence (5' to 3')
oTB90	confirmation of <i>hag</i> deletion	ACAGGTTGTAAACGTAGTG
oTB91	confirmation of <i>hag</i> deletion	TCCAGCGATGTGATCTCC
oAR11	confirmation of <i>motA</i> deletion	GGAGTGACACTGGAGTAG
oAR12	confirmation of <i>motA</i> deletion	CCGCTTAGAAGAACCATC
oAR3	confirmation of <i>flgE</i> deletion	ATCCGCTTAACCCGATTG
oAR4	confirmation of <i>flgE</i> deletion	TTCCGGTTCCTCTATTCC
oAR7	confirmation of <i>cheA</i> deletion	GGCACTGCTGGACTAAAG
oAR8	confirmation of <i>cheA</i> deletion	CCAGCCGACTTCAATATC
oTH37	confirmation of <i>degU</i> 32 and <i>degU</i> 146 point mutations	GGTTCGGTTATCTCTTTGAC

Supporting information for Chapter 2

Motility, chemotaxis and aerotaxis contribute to competitiveness during bacterial pellicle biofilm development

Published in: Journal of Molecular Biology (2015)

Fig. S1 Growth curves of *B. subtilis* strains lacking certain genes involved in flagellum synthesis and regulation (A), chemotaxis (B), and aerotaxis (C) compared to the wild-type strain (black line). Growth in LB medium was followed by recording optical density at 595 nm in a microtiter-plate reader. Growth curves represent the average of 6 replicates and error bars indicate standard deviation.

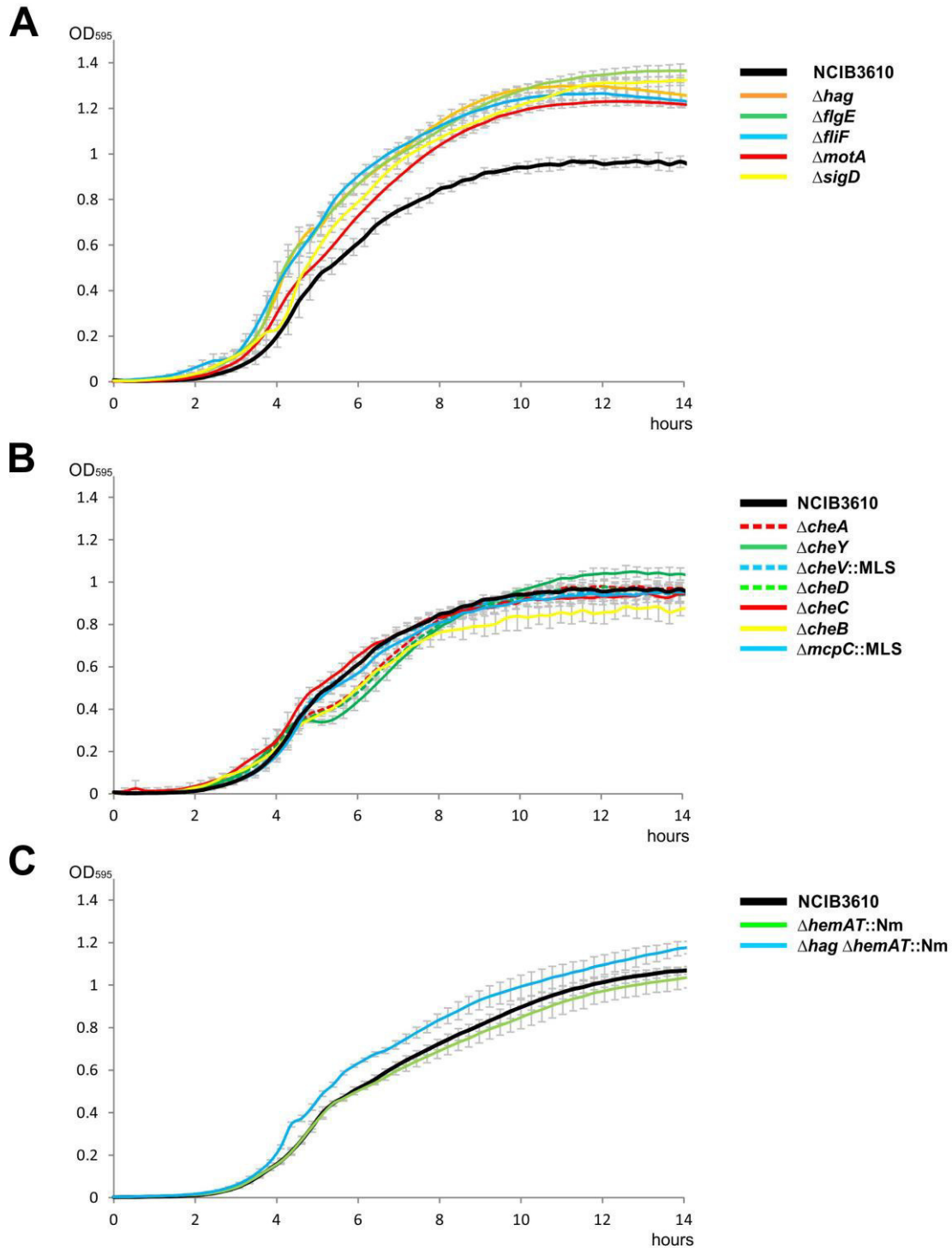


Fig. S2 Competition of GFP or mKATE2 labelled strains of *B. subtilis* strains during pellicle formation. Wells of a 24-well plate containing mixes of cells are shown in the green- or red-fluorescence channels (false coloured in green and red, respectively) together with its bright light images. The images in the right side of the figure show the pellicle pictures of the pure mutant cultures.

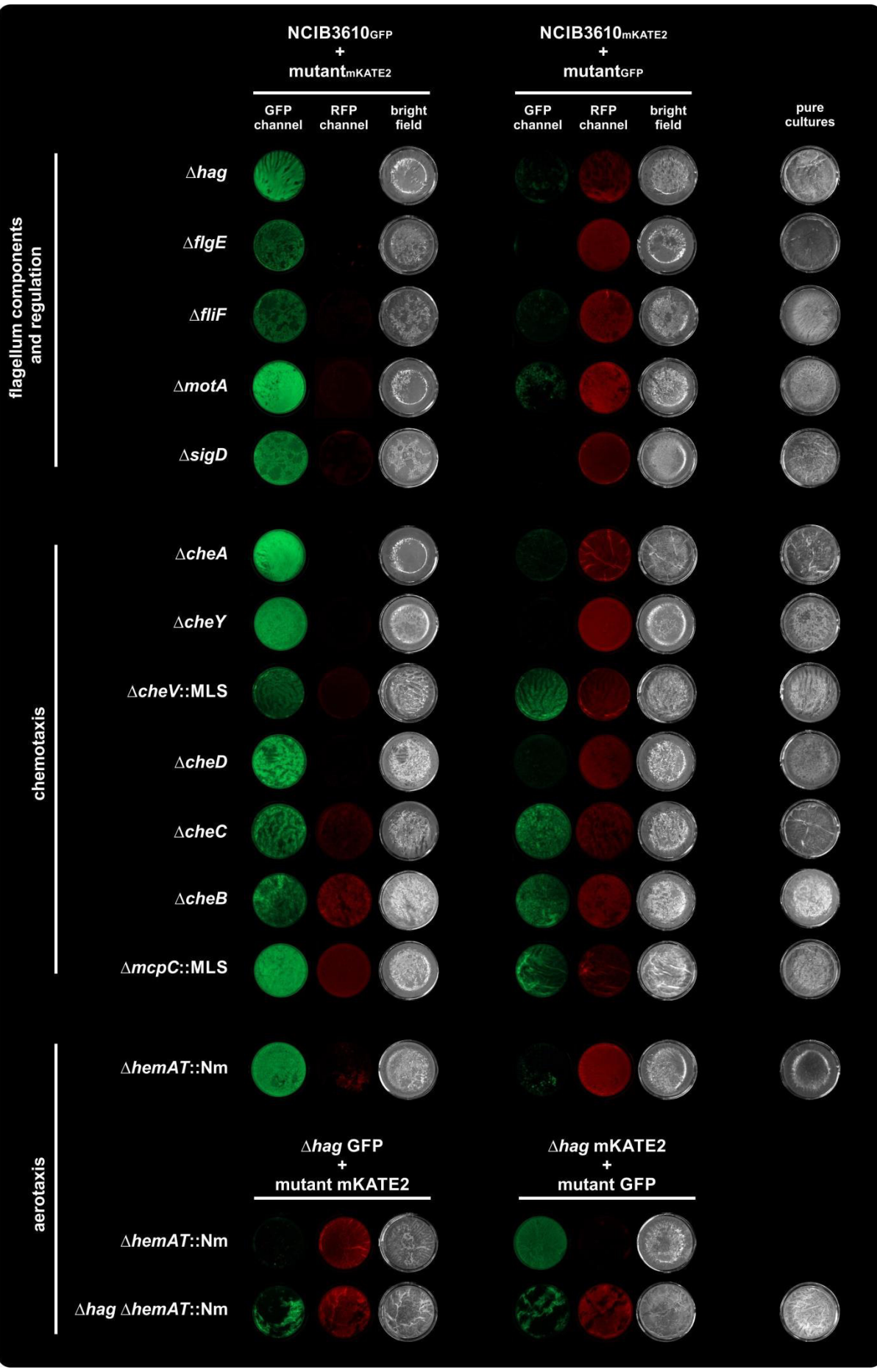
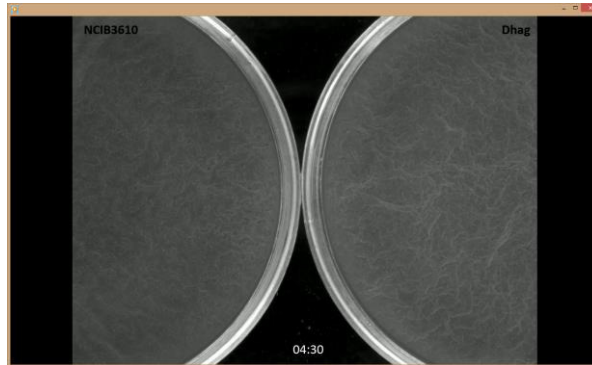


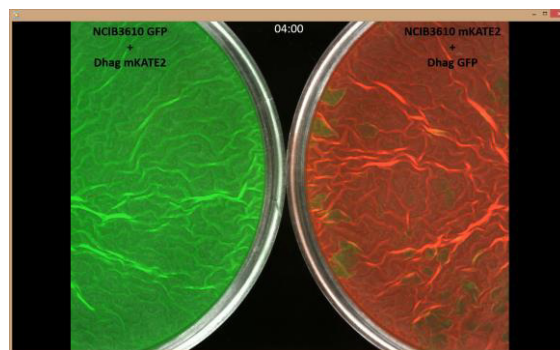
Table S1. Competition experiments of various *B. subtilis* mutant strains lacking motility, chemotaxis or oxygen sensing against wild-type strain (3610) during pellicle formation. Values are arbitrary units as described in the Materials and Methods.

Strains	Signal abundance		Strains	Signal abundance	
	GFP	mKATE2		GFP	mKATE2
<i>flagellum synthesis and function</i>					
3610 _{GFP} vs Δ <i>hag</i> _{mKATE2}	2.41±0.53	0.03±0.02	3610 _{mKATE2} vs Δ <i>hag</i> _{GFP}	0.08±0.05	2.51±0.29
3610 _{GFP} vs Δ <i>flgE</i> _{mKATE2}	1.67±0.37	0.16±0.08	3610 _{mKATE2} vs Δ <i>flgE</i> _{GFP}	0.16±0.11	5.24±2.69
3610 _{GFP} vs Δ <i>fliF</i> _{mKATE2}	1.43±0.25	0.11±0.02	3610 _{mKATE2} vs Δ <i>fliF</i> _{GFP}	0.59±0.21	2.20±0.35
3610 _{GFP} vs Δ <i>motA</i> _{mKATE2}	2.08±0.92	0.21±0.08	3610 _{mKATE2} vs Δ <i>motA</i> _{GFP}	0.33±0.17	3.38±0.98
3610 _{GFP} vs Δ <i>sigD</i> _{mKATE2}	1.41±0.42	0.04±0.01	3610 _{mKATE2} vs Δ <i>sigD</i> _{GFP}	0.38±0.29	2.29±0.24
<i>chemotaxis</i>					
3610 _{GFP} vs Δ <i>cheA</i> _{mKATE2}	2.35±0.57	0.03±0.01	3610 _{mKATE2} vs Δ <i>cheA</i> _{GFP}	0.26±0.18	3.18±0.56
3610 _{GFP} vs Δ <i>cheY</i> _{mKATE2}	1.82±0.25	0.05±0.03	3610 _{mKATE2} vs Δ <i>cheY</i> _{GFP}	0.11±0.02	2.32±0.34
3610 _{GFP} vs Δ <i>cheV</i> _{mKATE2}	1.31±0.41	0.48±0.15	3610 _{mKATE2} vs Δ <i>cheV</i> _{GFP}	0.63±0.12	1.54±0.24
3610 _{GFP} vs Δ <i>cheD</i> _{mKATE2}	2.11±0.27	0.09±0.04	3610 _{mKATE2} vs Δ <i>cheD</i> _{GFP}	0.09±0.03	2.66±0.44
3610 _{GFP} vs Δ <i>cheC</i> _{mKATE2}	0.60±0.18	1.61±0.35	3610 _{mKATE2} vs Δ <i>cheC</i> _{GFP}	1.27±0.15	0.76±0.47
3610 _{GFP} vs Δ <i>cheB</i> _{mKATE2}	0.75±0.23	1.02±0.28	3610 _{mKATE2} vs Δ <i>cheB</i> _{GFP}	1.33±0.46	1.39±0.65
3610 _{GFP} vs Δ <i>mcpC</i> _{mKATE2}	0.70±0.14	1.14±0.12	3610 _{mKATE2} vs Δ <i>mcpC</i> _{GFP}	1.11±0.11	0.7±0.17
<i>aerotaxis</i>					
3610 _{GFP} vs Δ <i>hemAT</i> _{mKATE2}	1.72±0.33	0.10±0.09	3610 _{mKATE2} vs Δ <i>hemAT</i> _{GFP}	0.55±0.33	2.20±0.46
Δ <i>hag</i> _{GFP} vs Δ <i>hemAT</i> _{mKATE2}	0.59±0.37	1.66±0.24	Δ <i>hag</i> _{mKATE2} vs Δ <i>hemAT</i> _{GFP}	1.56±0.26	0.05±0.05
Δ <i>hag</i> _{GFP} vs Δ <i>hemAT</i> _{mKATE2}	1.57±1.30	1.30±0.40	Δ <i>hag</i> _{mKATE2} vs Δ <i>hemAT</i> _{GFP}	1.87±0.86	0.69±0.35

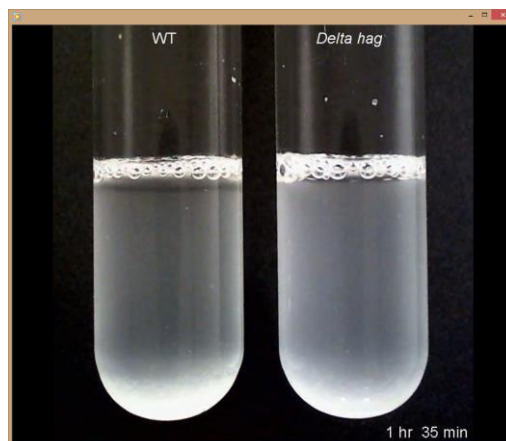
Video S1 Pellicle formation of *B. subtilis* wild-type (left petri-dish) and its Δhag derivative (right petri-dish) is shown in MSgg medium. Cultures were grown in 35 mm diameter Falcon petri dishes at 30 °C and images were recorded every 30 min.



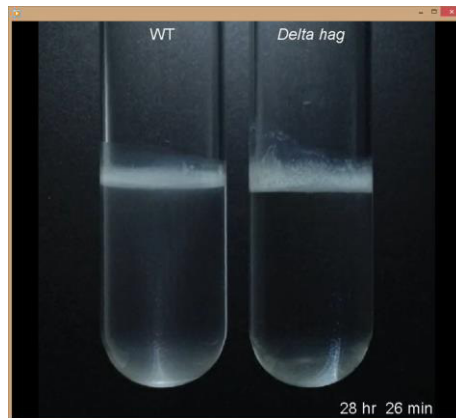
Video S2 Competition of GFP or mKATE2 labelled wild-type and Δhag strains of *B. subtilis* strains during pellicle formation (GFP and mKATE2 signals were false coloured in green and red, respectively). Cultures were grown in 35 mm diameter Falcon petri dishes at 30 °C and images were recorded every 15 min. Left: NCIB3610_{GFP} co-inoculated with Δhag _{mKATE2} strain. Right: NCIB3610_{mKATE2} co-inoculated with Δhag _{GFP} strain.



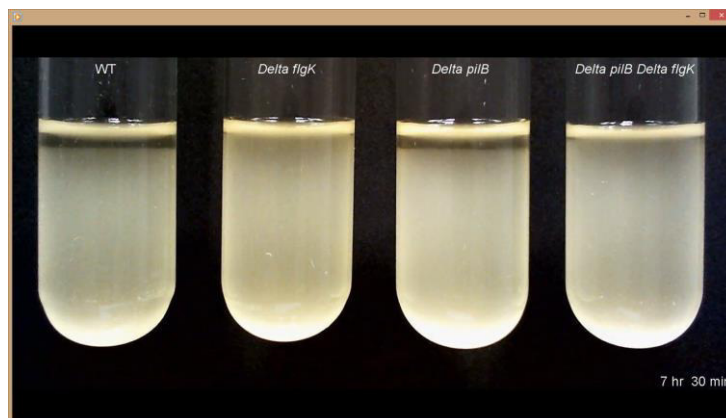
Video S3 Pellicle formation of *B. subtilis* cultures recorded from the side of the glass tubes. Cultures were inoculated in MSgg medium at high cell densities (OD_{500} of 1.2) and incubated at 30 °C.



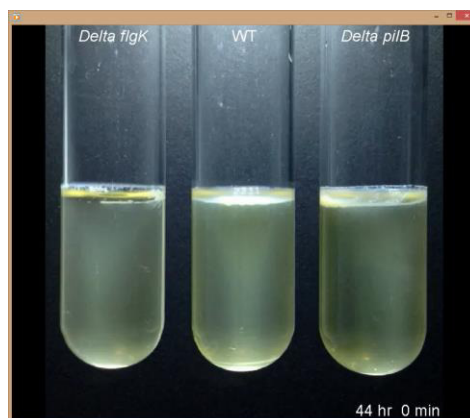
Video S4 Pellicle formation of *B. subtilis* cultures recorded from the side of the glass tubes. Cultures were inoculated in MSgg medium at low cell densities (OD₅₀₀ of 0.005) and incubated at 30 °C.



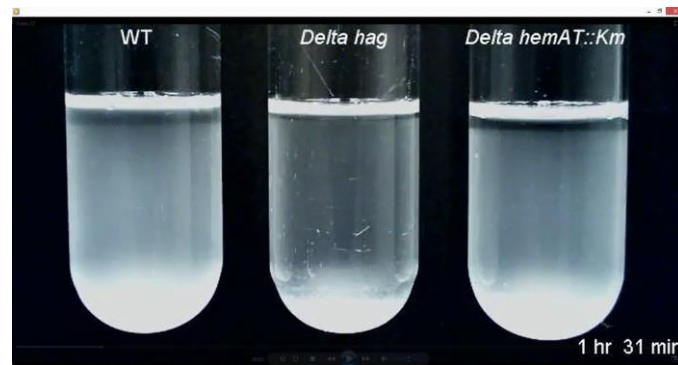
Video S5 Pellicle formation of *P. aeruginosa* cultures recorded from the side of the glass tubes. Cultures were inoculated in LB medium at high cell densities (OD₅₀₀ of 2.0) and incubated at 37 °C.



Video S6 Pellicle formation of *P. aeruginosa* cultures recorded from the side of the glass tubes. Cultures were inoculated in LB medium at low cell densities (OD₅₀₀ of 0.005) and incubated at 37 °C.



Video S7 Pellicle formation of *B. subtilis* cultures recorded from the side of the glass tubes. Wild type, Δhag and $\Delta hemAT$ cultures (from left to right) were inoculated in MSgg medium at high cell densities (OD_{500} of 1.0-1.2) and incubated at 30 °C.



Videos can be found at:

Video S1: <https://ars.els-cdn.com/content/image/1-s2.0-S002228361500354X-mmc2.mp4>

Video S2: <https://ars.els-cdn.com/content/image/1-s2.0-S002228361500354X-mmc3.mp4>

Video S3: <https://ars.els-cdn.com/content/image/1-s2.0-S002228361500354X-mmc4.mp4>

Video S4: <https://ars.els-cdn.com/content/image/1-s2.0-S002228361500354X-mmc5.mp4>

Video S5: <https://ars.els-cdn.com/content/image/1-s2.0-S002228361500354X-mmc6.mp4>

Video S6: <https://ars.els-cdn.com/content/image/1-s2.0-S002228361500354X-mmc7.mp4>

Video S7: <https://ars.els-cdn.com/content/image/1-s2.0-S002228361500354X-mmc8.mp4>

Supporting information for Chapter 3

Hampered motility promotes the evolution of wrinkly phenotype in
Bacillus subtilis

Submitted for publication to: Molecular Microbiology (2018)

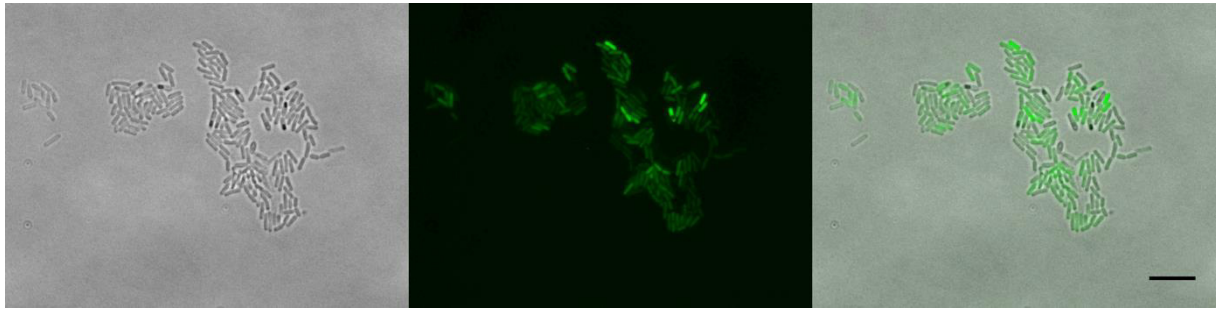


Figure S1: Prolonged incubation of wild-type *B. subtilis* in LB medium results in aggregation with increased, but heterogeneous *tapA* expression. Representative microscopy images of strains harboring the P_{tapA} -*yfp* reporter in wild type background. Images were recorded as in Fig. 2, but after longer (>12 h) incubation in LB medium. The presented aggregates were observed in addition to homogeneously dispersed cells similar to those observed in Fig. 2. The scale bar represents 10 μ m.

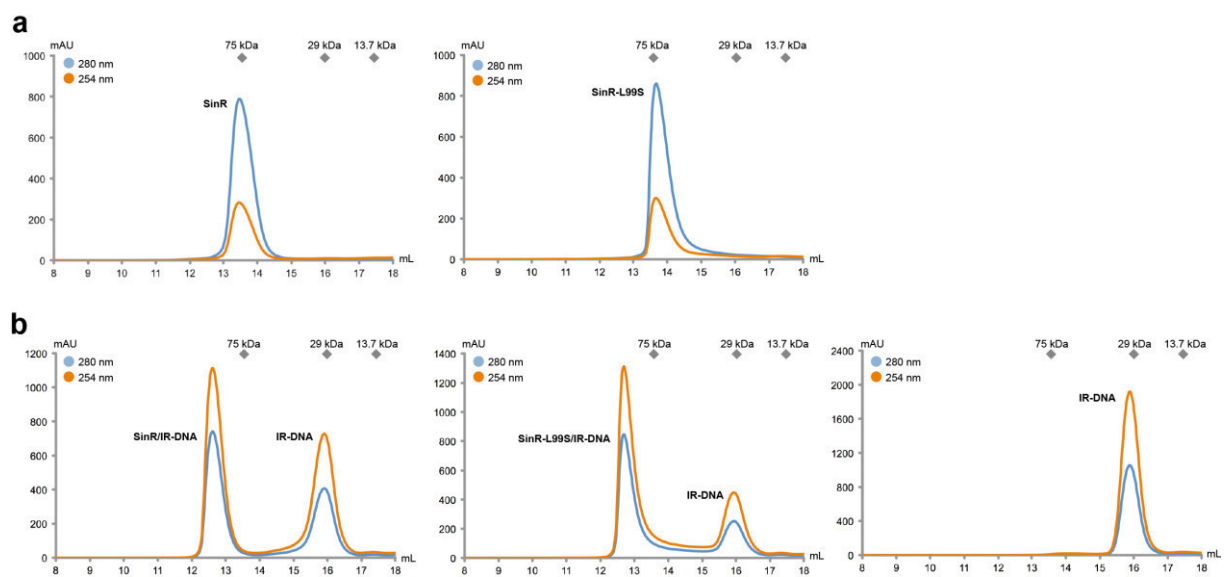


Figure S2: SinR and SinR-L99S function as tetramers. (a) Analytical size exclusion chromatograms of SinR (left) and SinR-L99S (right). Runs were performed on a Superdex 200 Increase 10/300 GL column. The absorbance was recorded at 254 nm (red curve) and 280 nm (blue curve) in mAU (arbitrary units). (b) Analytical size exclusion chromatograms of the reconstituted SinR/IR-DNA complex (left), the SinR-L99S/IR-DNA complex (middle) and the individual IR-DNA duplex. Runs were performed on a Superdex 200 Increase 10/300 GL column. The absorbance was recorded at 254 nm (red curve) and 280 nm (blue curve) in mAU (arbitrary units).

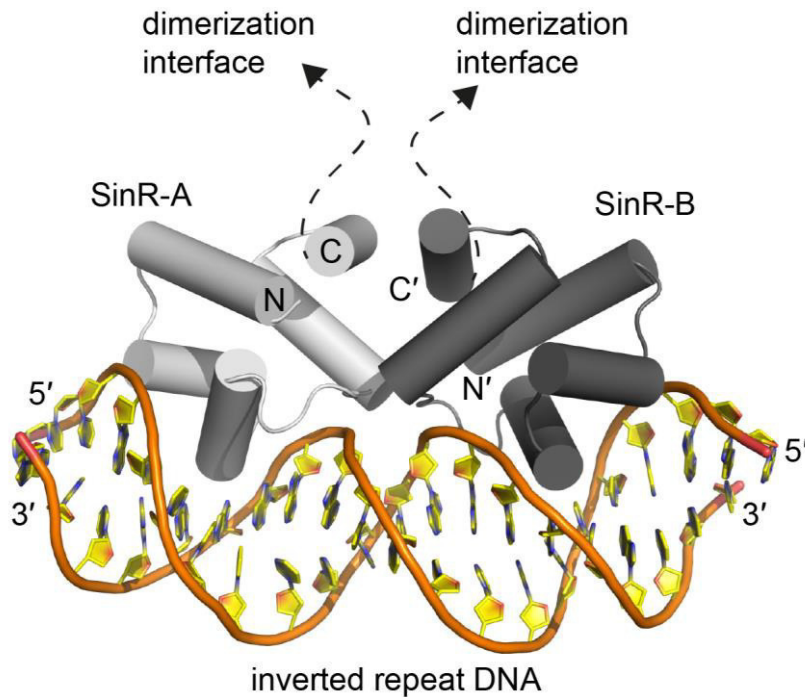


Figure S3: Crystal structure of the SinR/DNA complex. The crystal structure of the *B. subtilis* SinR/IR-DNA complex is shown in cartoon representation (PDB-ID: 3ZKC; (Newman *et al.*, 2013)). Two SinR proteins (SinR-A, colored in light grey and SinR-B, colored in dark grey) bind via their N-terminal DNA interaction domain to inverted repeat DNA. N and C indicate N-termini and C-termini, respectively.

Video S1: Timing of pellicle initiation in *B. subtilis* Δ hag and its WS derivative differs. Pellicle formation of *B. subtilis* Δ hag (mixture of TB36 (Δ hag^{GFP}) and TB37 (Δ hag^{mKATE}), left petri-dish) and its WS derivative (mixture of TB775 (Δ hagWS2^{GFP}) and TB776 (Δ hagWS2^{mKATE}), right petri-dish) is shown in MSgg medium. Cultures were grown in 35 mm diameter Falcon petri dishes at 30 °C and images were recorded every 30 min.

For Video S1 see <https://www.biorxiv.org/content/early/2018/03/27/288951>

Table S1. Strains and plasmids used in the current study.

Strains labeled with *might contain additional mutations

Name	Genotype and features	Source
<i>E. coli</i>		
BL21 (DE3)	<i>fhuA2 [lon] ompT gal (λDE3) [dcm] ΔhsdS</i>	Novagen
<i>B. subtilis</i>		
NCIB3610	prototroph	(Branda <i>et al.</i> , 2001)
DS1677	NCIB3610 <i>Δhag</i>	(Blair <i>et al.</i> , 2008)
DS4681	NCIB3610 <i>ΔflgE</i>	(Courtney <i>et al.</i> , 2012)
DS7080	NCIB3610 <i>ΔfliF</i>	(Chan <i>et al.</i> , 2014)
DS7498	NCIB3610 <i>ΔmotA</i>	(Chan <i>et al.</i> , 2014)
DS6420	NCIB3610 <i>ΔsigD</i>	(Cozy <i>et al.</i> , 2012)
DK1042	NCIB3610 <i>comI</i> ^{Q121}	(Konkol <i>et al.</i> , 2013)
GP901	<i>Δhag::Km^R</i>	Jörg Stülke, lab collection
TB406	NCIB3610 <i>comI</i> ^{Q121} <i>ΔsinR::Cm</i>	this work
168 hyGFP	168 <i>amyE::P_{hyperspank}-GFP; Cm^R</i>	(van Gestel <i>et al.</i> , 2014)
168 hymKATE2	168 <i>amyE::P_{hyperspank}-mKATE2; Cm^R</i>	(van Gestel <i>et al.</i> , 2014)
TB34	NCIB3610 <i>comI</i> ^{Q121} <i>amyE::P_{hyperspank}-GFP; Cm^R</i>	(Hölscher <i>et al.</i> , 2016)
TB35	NCIB3610 <i>comI</i> ^{Q121} <i>amyE::P_{hyperspank}-mKATE2; Cm^R</i>	(Hölscher <i>et al.</i> , 2016)
WTWS1*	<i>comI</i> ^{Q121} <i>sinR</i> ^{L99S}	this work
WTWS4*	<i>comI</i> ^{Q121} <i>sinR</i> ^{A85T}	this work
WTWS8*	<i>comI</i> ^{Q121} <i>sinR</i> ^{V26G}	this work
WTWS9*	<i>comI</i> ^{Q121} <i>sinR</i> ^{V26G}	this work
<i>ΔhagWS1*</i>	<i>comI</i> ^{Q121} <i>Δhag::Km^R sinR</i> ^{Q108stop}	this work
<i>ΔhagWS2*</i>	<i>comI</i> ^{Q121} <i>Δhag::Km^R sinR</i> ^{L99S}	this work
<i>ΔhagWS9*</i>	<i>comI</i> ^{Q121} <i>Δhag::Km^R sinR</i> ^{V26G}	this work
TB773	WTWS1 <i>comI</i> ^{Q121} <i>sinR</i> ^{L99S} <i>amyE::P_{hyperspank}-GFP; Cm^R</i>	this work
TB774	WTWS1 <i>comI</i> ^{Q121} <i>sinR</i> ^{L99S} <i>amyE::P_{hyperspank}-mKATE2; Cm^R</i>	this work
TB282	NCIB3610 <i>comI</i> ^{Q121} <i>Δhag::Km^R</i>	this work
TB36	NCIB3610 <i>comI</i> ^{Q121} <i>Δhag::Km^R amyE::P_{hyperspank}-GFP; Cm^R</i>	this work
TB37	NCIB3610 <i>comI</i> ^{Q121} <i>Δhag::Km^R amyE::P_{hyperspank}-mKATE2; Cm^R</i>	this work
TB775	<i>ΔhagWS2 comI</i> ^{Q121} <i>Δhag::Km^R sinR</i> ^{L99S} <i>amyE::P_{hyperspank}-GFP; Cm^R</i>	this work
TB776	<i>ΔhagWS2 comI</i> ^{Q121} <i>Δhag::Km^R sinR</i> ^{L99S} <i>amyE::P_{hyperspank}-mKATE2; Cm^R</i>	this work
TB697	NCIB3610 <i>comI</i> ^{Q121} <i>amyE::P_{hyperspank}-sinI lacI; Spec^R</i>	this work
TB698	NCIB3610 <i>comI</i> ^{Q121} <i>amyE::P_{hyperspank}-sinI⁹⁻³⁹ lacI; Spec^R</i>	this work
DL821	NCIB3610 <i>lacA::P_{tapA}-yfp; MLS^R</i>	(López <i>et al.</i> , 2009)
TB699	NCIB3610 <i>comI</i> ^{Q121} <i>lacA::P_{tapA}-yfp; MLS^R</i>	this work
TB778	NCIB3610 <i>comI</i> ^{Q121} <i>Δhag; lacA::P_{tapA}-yfp; MLS^R</i>	this work
TB777	NCIB3610 <i>comI</i> ^{Q121} <i>ΔsinR; lacA::P_{tapA}-yfp; MLS^R</i>	this work
TB700	WTWS1 <i>comI</i> ^{Q121} <i>sinR</i> ^{L99S} <i>lacA::P_{tapA}-yfp; MLS^R</i>	this work
TB701	WTWS8 <i>comI</i> ^{Q121} <i>sinR</i> ^{V26G} <i>lacA::P_{tapA}-yfp; MLS^R</i>	this work
TB702	<i>ΔhagWS2 comI</i> ^{Q121} <i>Δhag::Km^R sinR</i> ^{L99S} <i>lacA::P_{tapA}-yfp; MLS^R</i>	this work
TB703	<i>ΔhagWS9 comI</i> ^{Q121} <i>Δhag::Km^R sinR</i> ^{V26G} <i>lacA::P_{tapA}-yfp; MLS^R</i>	this work
plasmids		
pDR111	<i>amyE</i> integration vector; <i>P_{hyperspank}; lacI; Amp^R, Spec^R</i>	David Rudner, lab collection

pTB695	<i>sinI</i> cloned into pDR111; Amp ^R , Spec ^R	this work
pTB696	<i>sinI</i> ⁹⁻³⁹ cloned into pDR111; Amp ^R , Spec ^R	this work
pET24d	IPTG inducible overexpression vector; Km ^R	Novagen
pET24sinR ^{WT}	wild type <i>sinR</i> cloned into pET24d; Km ^R	this work
pET24sinR ^{V26G}	<i>sinR</i> ^{V26G} cloned into pET24d; Km ^R	this work
pET24sinR ^{A85D}	<i>sinR</i> ^{A85T} cloned into pET24d; Km ^R	this work
pET24sinR ^{L99S}	<i>sinR</i> ^{L99S} cloned into pET24d; Km ^R	this work

Table S2. Oligonucleotides used in the current study

Name	Sequence	Feature
oTB98	GGCCGTCTCGATGGTTATTG	<i>sinIR</i> locus sequencing
oTB99	GGCCGGACTGGCTGAAATAC	<i>sinIR</i> locus sequencing
oTB124	CTGAAGCTTAGGAGGAGAACTGCATGAAG	<i>sinI</i> cloning
oTB125	CATGGCATGCGCACATTCAGAAAGGATTTAC	<i>sinI</i> cloning
oTB126	CTGAAGCTTAGGAGGAGAACTGCATGTTTGAATTGGATCAAGAATGG	<i>sinI</i> cloning (shortened)
oTB127	CATGGCATGCGCACATTCAGTTTAAAGTAAATATTTTCGTATTTTC	<i>sinI</i> cloning (shortened)
SinR_NcoI_F	TATACCATGGGCATTGGCCAGCGTATTAAC	<i>sinR</i> overexpression
SinR_H6_BamHI_R	TAATGGATCCTTAGTGATGGTGATGGTGATGCTCCTCTTTTTGGGATTTTCTCC	<i>sinR</i> overexpression
SinR_V26G_F	GAAAAAGCTGGGGGCGCGAAGTCTTA	V26G mutagenesis
SinR_V26G_R	TAAGACTTCGCGCCCCAGCTTTTTTC	V26G mutagenesis
SinR_A85D_F	GGTTCGCGATGATATGACATCCGG	A85D mutagenesis
SinR_A85D_R	CCGGATGTCATATCATCGCGAACCC	A85D mutagenesis
SinR_L99S_F	CGTGAATTTAGCGATTATCAAAAATG	L99S mutagenesis
SinR_L99S_R	CATTTTTGATAATCGCTAAATTCACG	L99S mutagenesis
SinR_IR_F	TTTGTCTCTAAAGAGAACTTA	SinR binding site
SinR_IR_R	TAAGTTCTCTTAGAGAACAAA	SinR binding site

References

- Blair, K.M., Turner, L., Winkelman, J.T., Berg, H.C., and Kearns, D.B. (2008) A molecular clutch disables flagella in the *Bacillus subtilis* biofilm. *Science* **320**: 1636–1638.
- Branda, S.S., González-Pastor, J.E., Ben-Yehuda, S., Losick, R., and Kolter, R. (2001) Fruiting body formation by *Bacillus subtilis*. *Proc Natl Acad Sci U S A* **98**: 11621–11626.
- Chan, J.M., Guttenplan, S.B., and Kearns, D.B. (2014) Defects in the flagellar motor increase synthesis of poly- γ -glutamate in *Bacillus subtilis*. *J Bacteriol* **196**: 740–753.
- Courtney, C.R., Cozy, L.M., and Kearns, D.B. (2012) Molecular characterization of the flagellar hook in *Bacillus subtilis*. *J Bacteriol* **194**: 4619–4629.
- Cozy, L.M., Phillips, A.M., Calvo, R.A., Bate, A.R., Hsueh, Y.H., Bonneau, R., et al. (2012) SlrA/SinR/SlrR inhibits motility gene expression upstream of a hypersensitive and hysteretic switch at the level of σ^D in *Bacillus subtilis*. *Mol Microbiol* **83**: 1210–1228.
- Gestel, J. van, Weissing, F.J., Kuipers, O.P., and Kovács, Á.T. (2014) Density of founder cells affects spatial pattern formation and cooperation in *Bacillus subtilis* biofilms. *ISME J* **8**: 2069–2079.
- Hölscher, T., Dragoš, A., Gallegos-Monterrosa, R., Martin, M., Mhatre, E., Richter, A., and Kovács, Á.T. (2016) Monitoring spatial segregation in surface colonizing microbial populations. *J Vis Exp* **2016**: e54752.

Konkol, M.A., Blair, K.M., and Kearns, D.B. (2013) Plasmid-encoded comI inhibits competence in the ancestral 3610 strain of *Bacillus subtilis*. *J Bacteriol* **195**: 4085–4093.

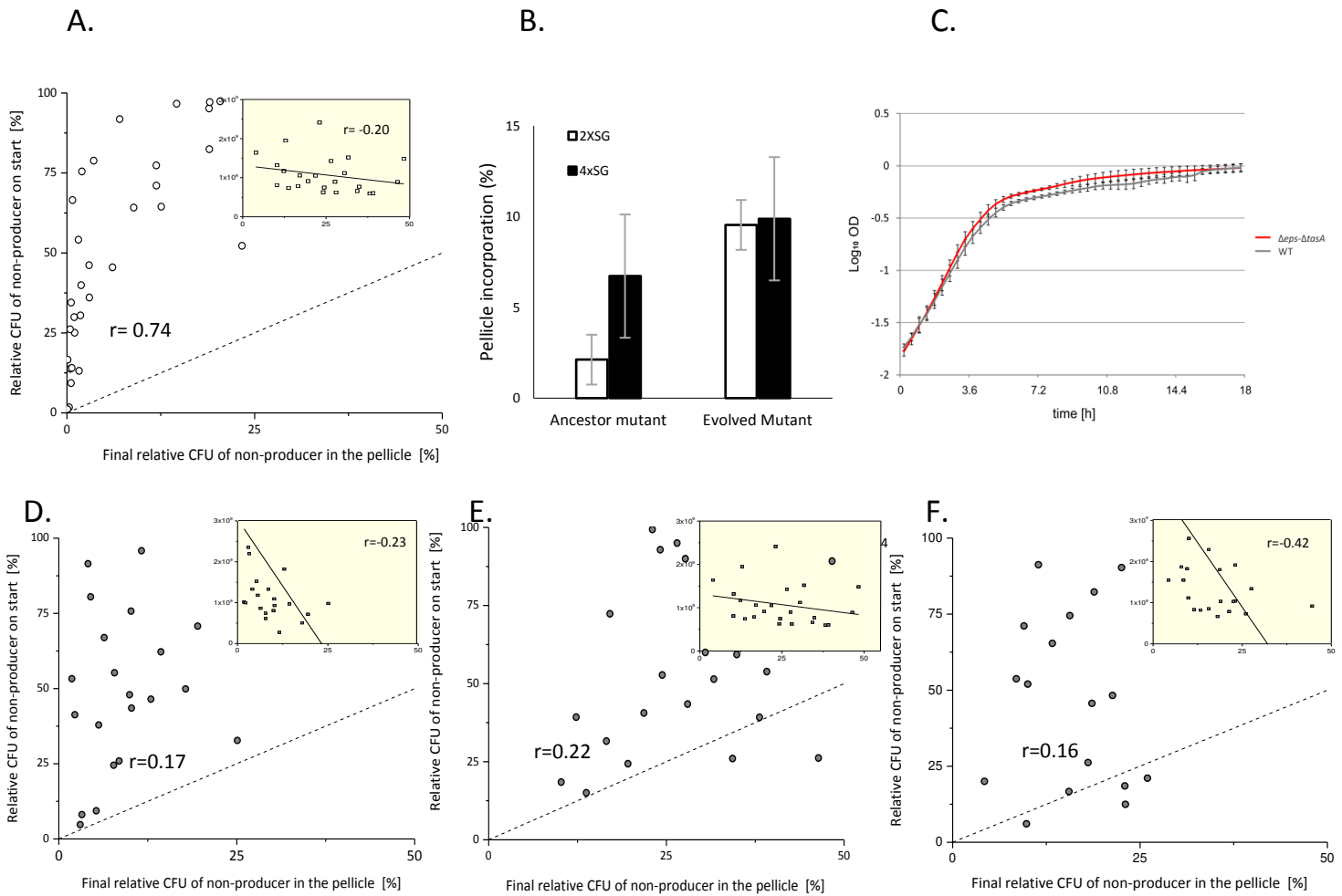
López, D., Vlamakis, H., Losick, R., and Kolter, R. (2009) Paracrine signaling in a bacterium. *Genes Dev* **23**: 1631–1638.

Newman, J.A., Rodrigues, C., and Lewis, R.J. (2013) Molecular basis of the activity of SinR Protein, the master regulator of biofilm formation in *Bacillus subtilis*. *J Biol Chem* **288**: 10766–10778.

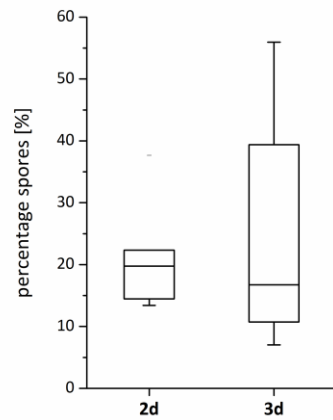
Supporting information for Chapter 5

De novo evolved interference competition promotes the spread of biofilm defectors

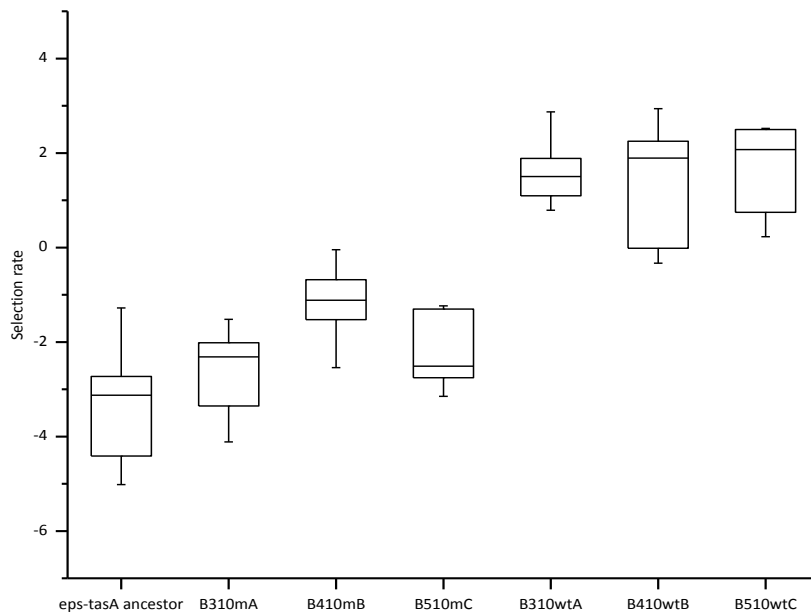
Published in: Nature Communications (2017)



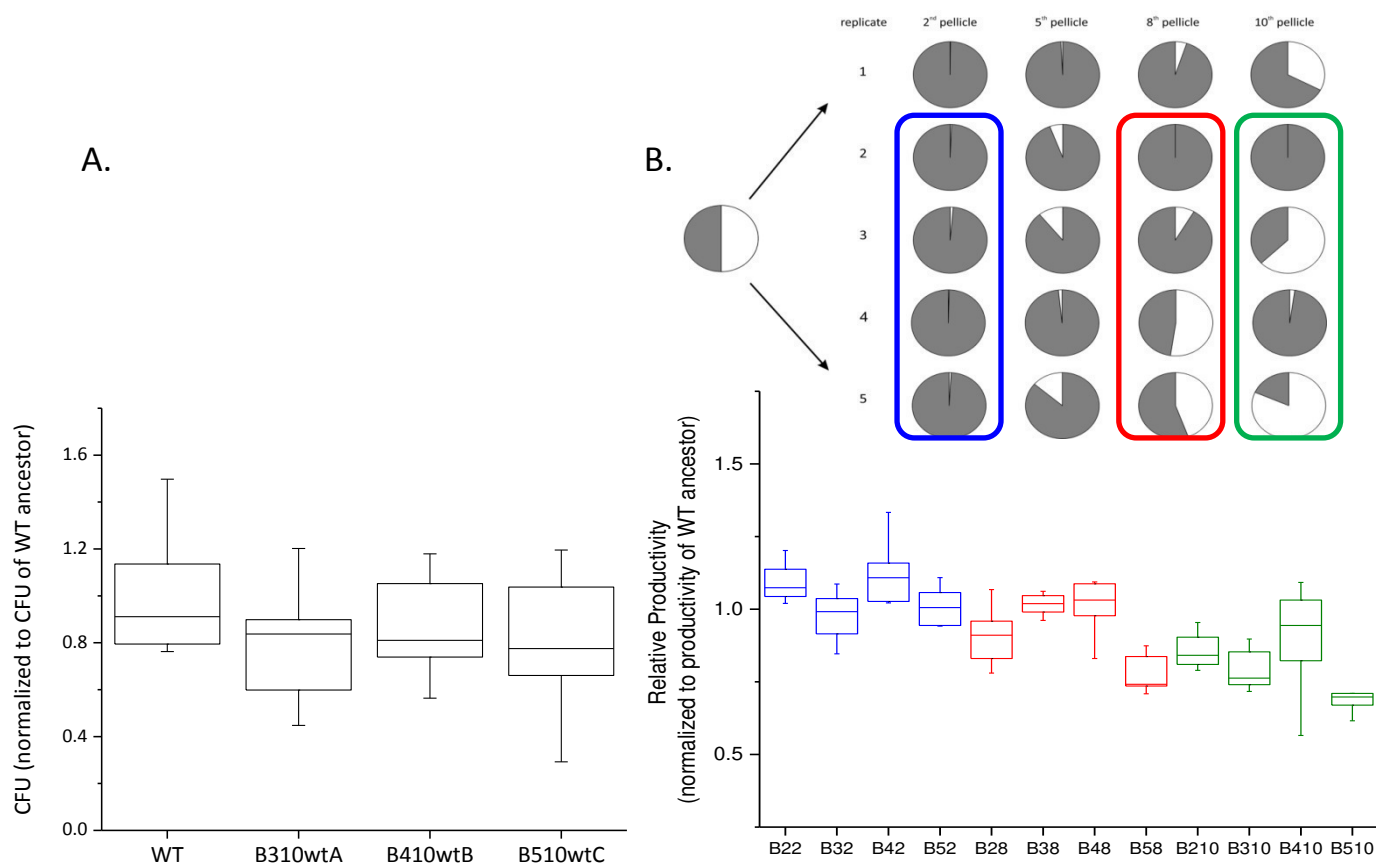
Supplementary Figure 1. Pellicle competition assays at different starting ratio of the producer and non-producer. **A.** Pellicle competition assay of *B. subtilis* wild type against the non-producer $\Delta eps-\Delta tasA$ at different starting (%) ratio ($n=28$; $r=0.74$). The incorporation of the non-producer $\Delta eps-\Delta tasA$ into the pellicle is dependent on its initial frequency. Dashed line represents 1.0 slope. Total CFU in the pellicle for each final relative CFU on the non-producer were plotted in the upper-right corner. **B.** Pellicle competition assay of *B. subtilis* wild type against the non-producer $\Delta eps-\Delta tasA$ (left: ancestor, right: evolved) at different nutrient concentrations ($n=5$): 2xSG medium (standard nutrient concentration) and 4xSG medium (doubled nutrient concentration). Starting ratios were set to 50%. Pellicle incorporation of the ancestor non-producer $\Delta eps-\Delta tasA$ escalates as the nutrient concentration increases. On the contrary, nutrient concentration has no effect on incorporation of the eNMP into the pellicle. Values represent the mean and error bars s.d.m. **C.** Growth curve of the *B. subtilis* 168 wild-type and $\Delta eps-\Delta tasA$ mutant. OD⁵⁹⁵ was measured every 15 min using a TECAN Infinite F200 PRO microplate reader. The experiment was conducted in 2xSG medium at 30°C ($n=9$). Central values represent the mean and error bars s.d.m. Calculated growth rates [OD/h] for the WT and $\Delta eps-\Delta tasA$ were $\mu=0.65$ and $\mu=0.71$, respectively, indicating a faster growth of the mutant strain; *t*-Student, two-tail $p < 0.05$. **D-F.** Pellicle incorporation of evolved non-producers at different starting (%) ratios. The incorporation success of the evolved non-producers B310mA ($n=21$; $r=0.17$) (**D**), B410mB ($n=21$; $r=0.22$) (**E**) and B510mC ($n=18$; $r=0.16$) (**F**) does not depend on their initial frequency. Dashed lines represent 1.0 slopes. Total CFU in the pellicle for each final relative CFU on the non-producer were plotted in the upper-right corner in each graph. Each experiment was performed at least twice.



Supplementary Figure 2. Sporulation frequency in *B. subtilis* 168 pellicle. Sporulation frequency in *B. subtilis* 168 pellicle was determined after 2 and 3 days by comparing the total CFU (vegetative cells+spores) with the CFU after 20 min of incubation at 80°C (where only the spores survive) (n=7). Boxes represent Q1-Q3, lines represent the median and bars span from max to min. The experiment performed twice.

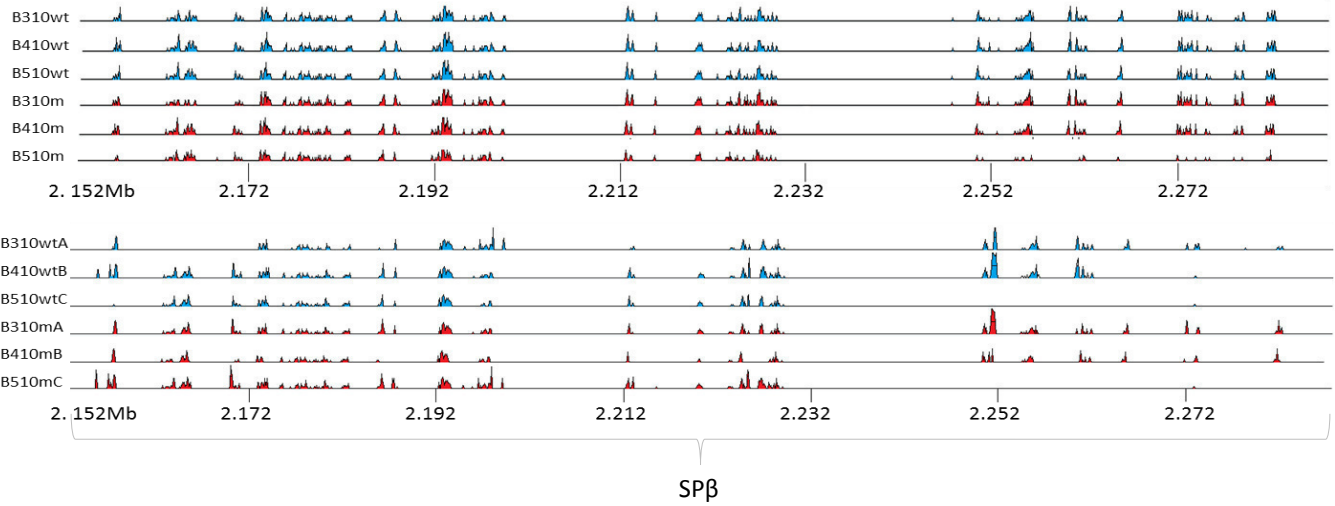


Supplementary Figure 3. Improved selection rate of evolved non-producers and producers against the wild type ancestor. Performance of selected strains against the wild type ancestor in pellicle competition assay was examined and the selection rate for each strain was calculated. The initial ratios of the strains in competition assays were in the range from 35% to 70% (n = 6-12). Boxes represent Q1-Q3, lines represent the median and bars span from max to min. Each $\Delta eps-\Delta tasA$ vs eMP/eNMP comparison was performed at least twice. The incorporation of the eMPs B310wtA, B410wtB and B510wtC into pellicles were $73.2 \pm 6.4(\%)$, $67.8 \pm 8.8(\%)$ and $82.0 \pm 2.9(\%)$, respectively.

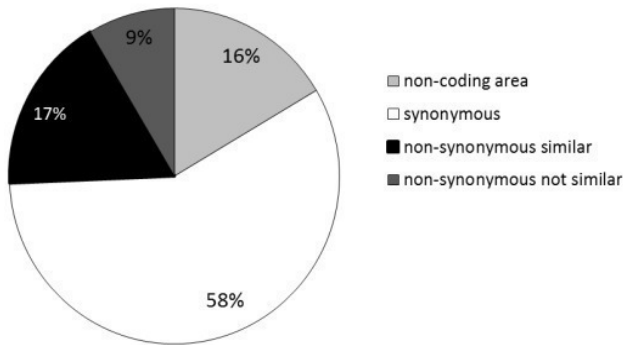


Supplementary Figure 4. Viable cell counts and productivity changes in the evolved pellicles. A. Total cell count of pellicles of evolved WT strains, B310wtA, B410wtB, B510wtC (n=10) normalized to the CFU of WT ancestor showing no significant difference compared to WT ancestor. We did not observe increased viable cell numbers in the eMP, as was the case for the overall biomass. We hypothesize that increased frequency of cell lysis, linked to spontaneous lytic induction in the eMP, may lead to release of various substances that contribute to the extracellular matrix and overall biomass. **B.** Productivity estimates of pellicle population mixes of WT and $\Delta eps-\Delta tsaA$ in replicates 2, 3, 4 and 5 at different time points (2nd, 8th, and 10th transfer) (n=10); Boxes represent Q1-Q3, lines represent the median and bars span from max to min. The experiments were performed twice.

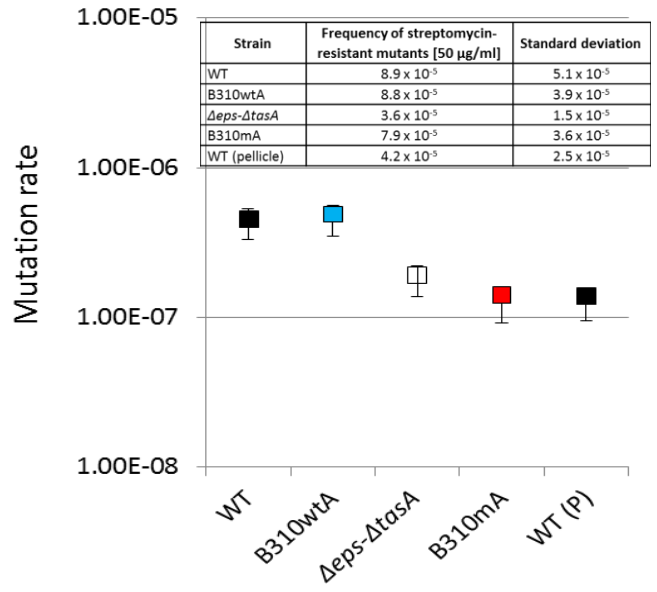
A.



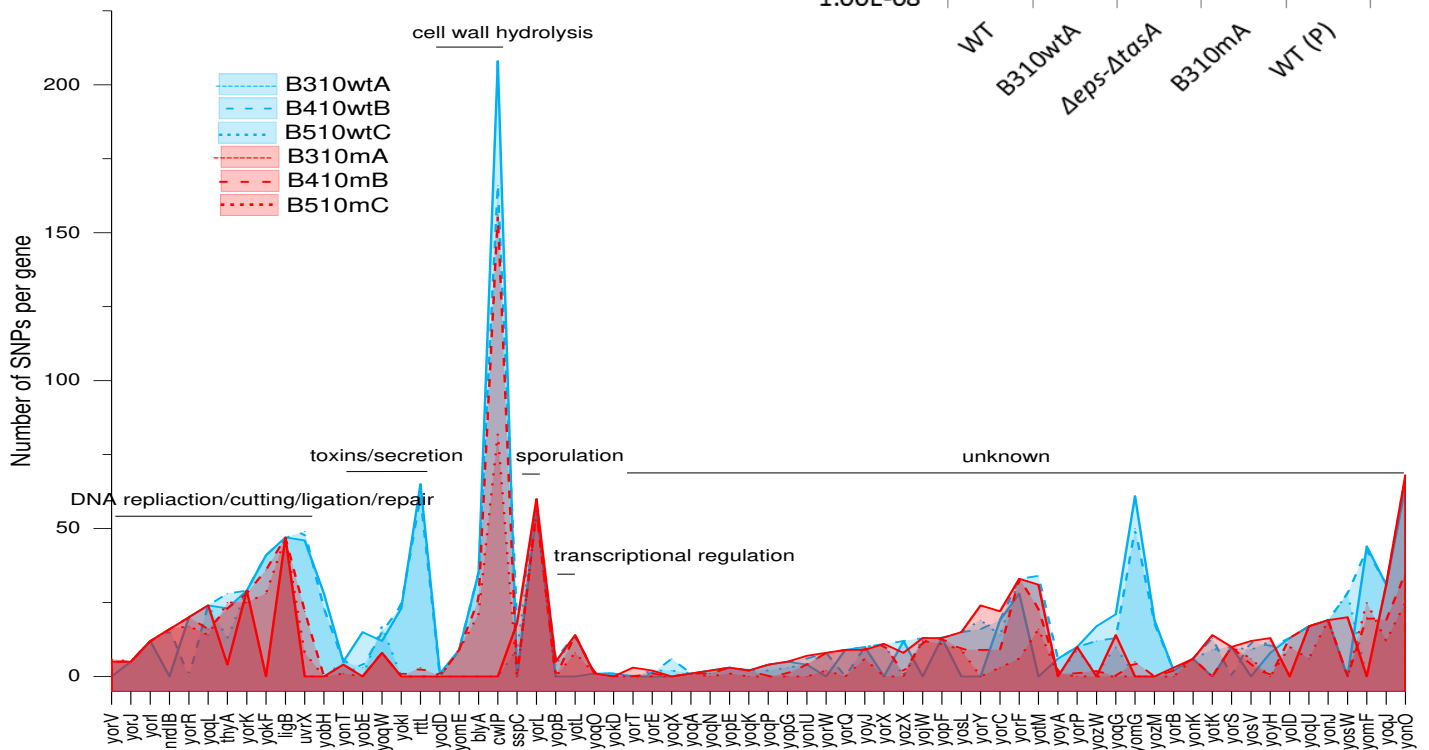
B.



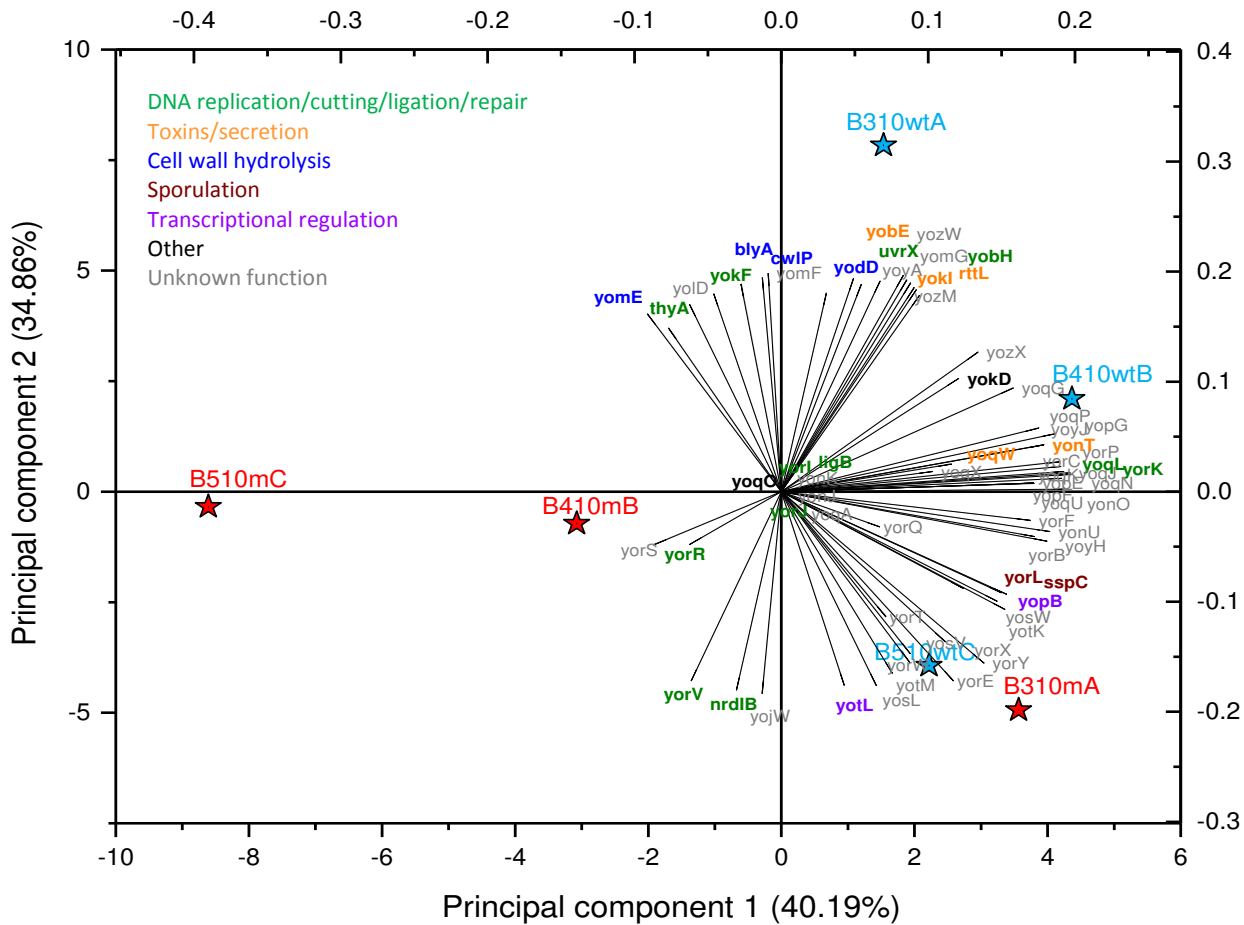
C.



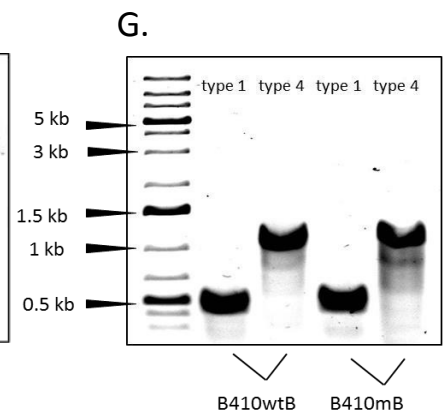
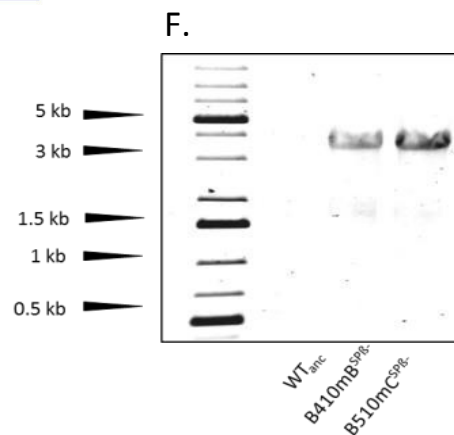
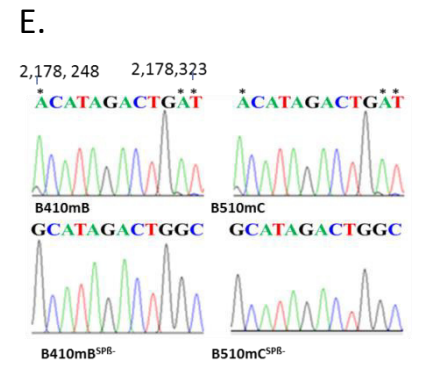
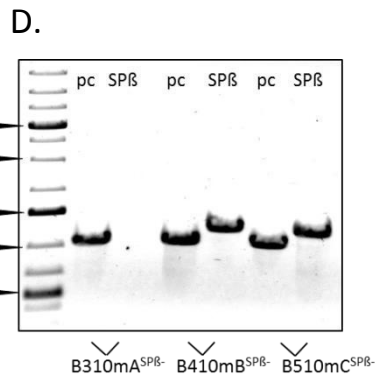
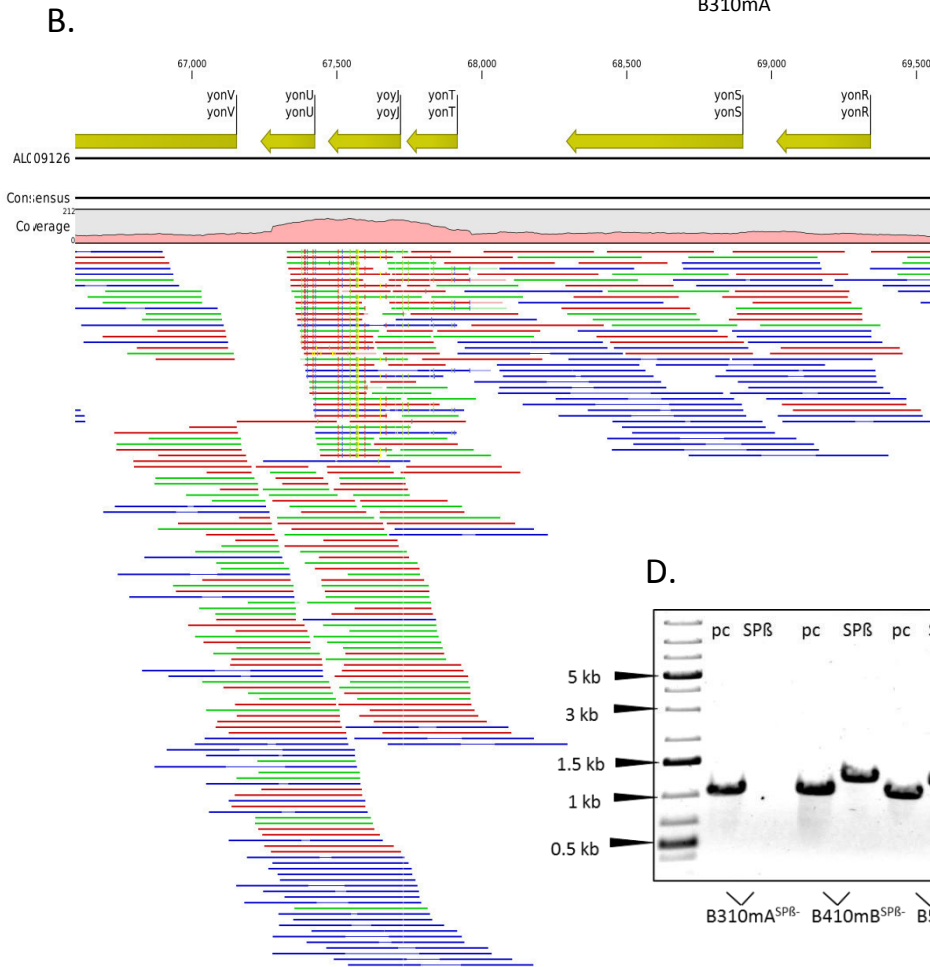
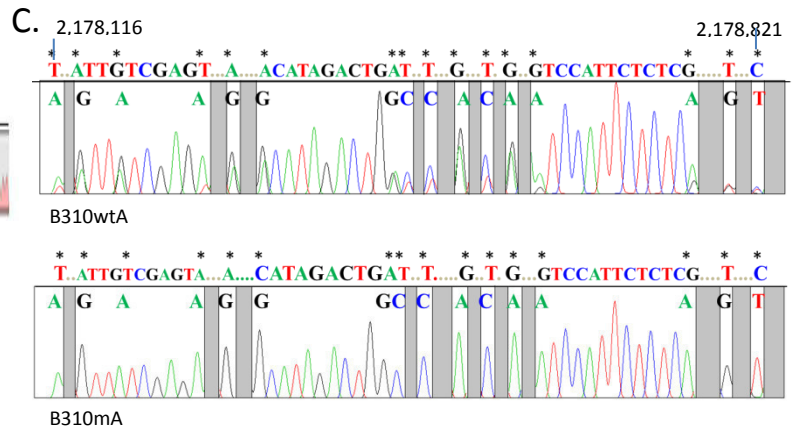
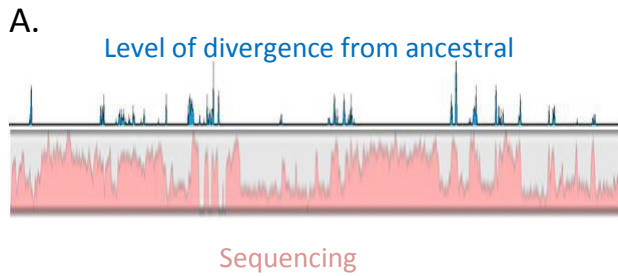
D.



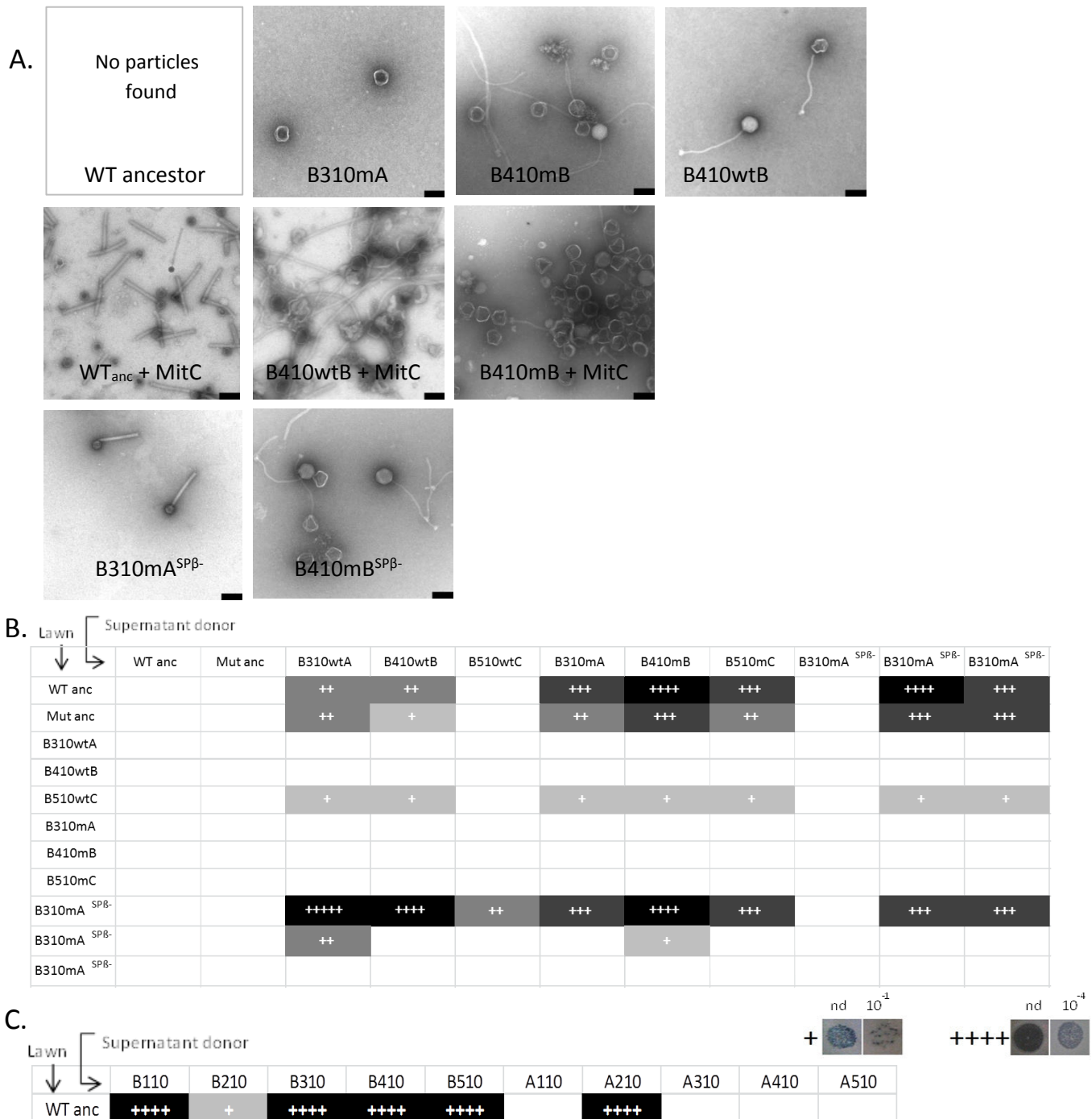
E.



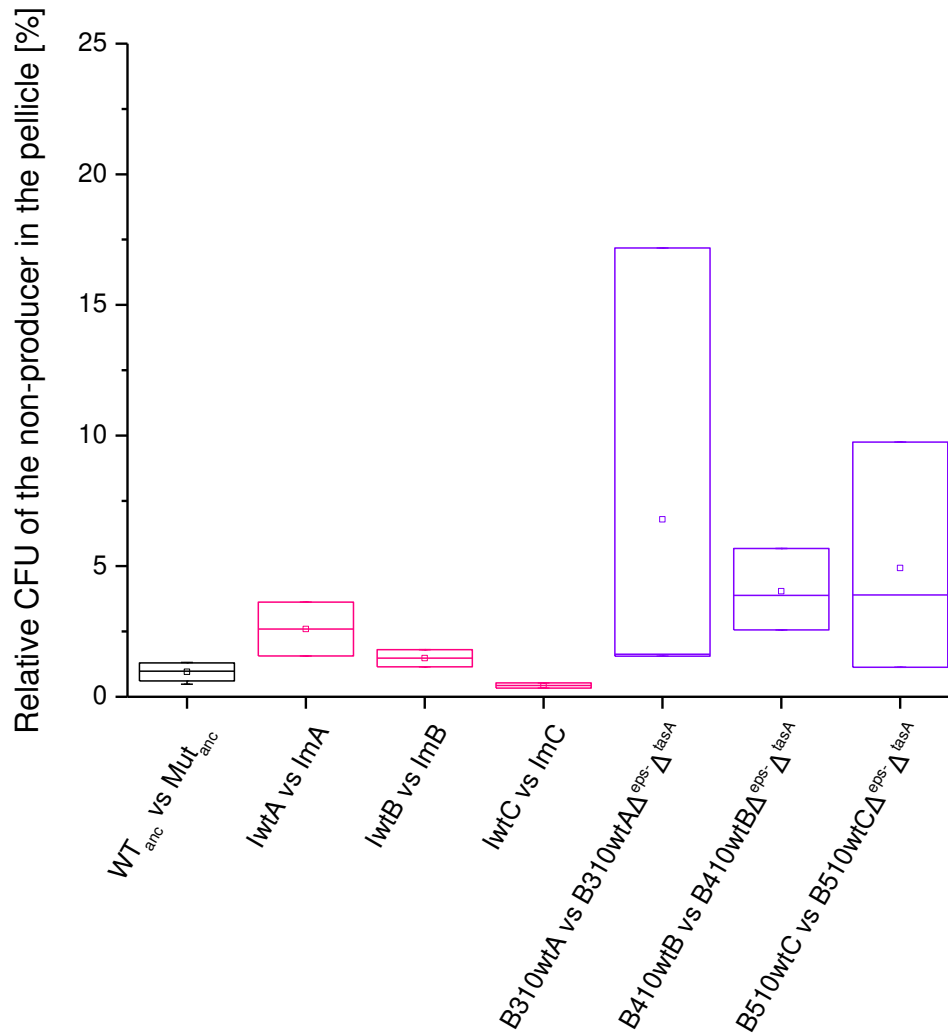
Supplementary Figure 5. Comparisons of SNPs patterns and mutation rates in the eMP and eNMP strains. A. The SP β prophage regions of 6 evolved populations (the above panel) and corresponding single isolates (the below panel) were aligned with the SP β sequence of the ancestor strain using VISTA tools (<http://genome.lbl.gov/vista/index.shtml>, 54). Peaks represent non-conserved regions based on scores for each base pair in the genomic interval of 100-bp and conservation identity 70%. A region is considered conserved if the conservation over this region is greater/equal to 70% and has minimum length of 100-bp. **B.** Percent distribution of different SNPs types detected in 6 evolved single isolates. Non-synonymous similar substitutions had Blosum62 matrix score ≥ 1 . Non-synonymous not similar substitutions had Blosum62 matrix score ≤ 0 . **C.** Fluctuation assay ($n=10$) was done to determine the frequency of streptomycin-resistant mutants in $\Delta ps\Delta tasA$ ancestor, evolved mutant B410mB, evolved WT B310wtA and WT ancestor strains in liquid and in pellicle (P). Analysis was conducted using LB agar medium without and with 50 μ g/ml streptomycin. Results show overlapping frequency rate of evolved strains with the ancestor wild type. Mutation rate estimates was determined using bz-rates web based tool (<http://www.lcqb.upmc.fr/bzrates>). Data points represent the mean and bars span from lower to upper CI (95%). **D.** Linear plots showing the number of SNPs per each mutated gene (genes are sorted according to their functional group) for eMPs (shown in blue) and eNMPs (shown in red). **E.** PCA biplot containing the mutated genes of eMPs (B310wtA, B410wtB and B510wtC) and eNMPs (B310mA, B410mB and B510mC) strains in two dimensions using their projections onto the first two principal components. All mutated genes are represented on the plot using their weights for the components. The genes are color-coded by functional category. The scales shown on x and y axis are for the strains; the scales shown above the plot and on the right are for genes.



Supplementary Figure 6. Detailed molecular analysis confirm presence of genome rearrangements in the evolved strains. **A.** Alignment of Vista curve (54) showing regions of SNPs accumulation within the evolved SP β sequence (see also S5A) (blue) and the sequencing coverage curve (pink) indicates duplications of mutated SP β fragments. **B.** Sequence reads obtained for the evolved *B. subtilis* strains that are mapped to reference genome. Color coding: green-reads mapped based on the FWD strand; red-reads mapped based on the REV strand; blue-paired reads. Mismatch SNPs are marked as vertical stripes. Two types of reads were identified: reference-matching reads without SNPs and reads with SNPs. **C.** Selected SP β fragment was amplified by PCR using B310wtA and B310mA gDNA and re-sequenced by Sanger method. Product obtained from B310wtA showed double peaks on the sequencing chromatogram at the positions of SNPs detected by high-throughput sequencing. The double peaks correlated with ~50% SNPs frequency in SP β region, confirming presence of two types of SP β fragments in the B310wtA, but not in the B310mA. **D.** Presence of a selected SP β fragment was confirmed by PCR using primer pair oTB86F/oTB87R (for oligo sequences, see Supplementary Table 3) in the strains B410mB Δ SP β and B510mC Δ SP β but not in the B310mA Δ SP β . Pc= positive control, amplified fragment outside SP β . **E.** Comparison of Sanger sequencing chromatograms obtained for selected SP β fragments before and after SP β deletion in B410mB and B510mC strains. After deletion of SP β PCR product could still be obtained (see Fig. S6D), but it produced clear sequencing result with single peaks at the SNPs positions containing solely the evolved sequence. **F.** Knockout of SP β prophage region in strains B410mB Δ SP β and B510mC Δ SP β was confirmed by PCR using primers oAD1F/oAD2R. **G.** Presence of predicted genome rearrangements (see Fig. 5CD) of type 1 and type 4 was confirmed in the evolved strains and not in the ancestor strains using primer pairs AD4F/oAD5R and oAD6F/oAD7R, respectively.



Supplementary Figure 7. Evolved strains spontaneously release SPbeta-like phage that is lytic towards the ancestral strains. A. Electron micrographs of phage particles purified from *B. subtilis* supernatants. No phage particles were spontaneously released by the WT ancestor strain. All evolved strains tested spontaneously released SPβ-like phage particles and treatment with Mitomycin C dramatically increased the number of those particles. WT ancestor incubated with Mitomycin C and the evolved B310mA ΔSPβ produced solely PBSX-like phage particles. Scale bar equals 100 nm. **B.** Results of the plaque assays performed with the ancestor WT, ancestor Δ*eps-DtasA* and all the evolved strains, where each strain served both as a supernatant donor and as a potential host. To better access lytic activity of the strains, their supernatants were diluted using saline solution and scored as shown on the scale below. Blank cell in the table translates into lack of lytic activity towards given host even if non-diluted supernatant was applied on the lawn. **C.** Lytic activity of all evolved populations (transfer method A and transfer method B) against the WT ancestor was tested. All populations that showed increase of Δ*eps-DtasA* ratio (see Fig. 2) through the evolutionary time showed lytic activity towards the WT ancestor.



Supplementary Figure 8. When producers and non-producers carry the same evolved genetic background, improved incorporation of non-producers is not observed. Pellicle competition assay performed for 3 randomly selected WT and $\Delta eps-\Delta tasA$ colonies after the infection assay (n=2) (columns 2-4). In addition, pellicle competition assays between WT evolved strains and their corresponding strains with $\Delta eps-\Delta tasA$ markers (n=3) were performed (columns 5-7). Boxes represent Q1-Q3 and lines represent median values. Results show that the infected mutant strains cannot increase their performance when competed against infected WT strains. The same is true for the evolved WT strains with deleted *eps* and *tasA* that behave comparably as the ancestor $\Delta eps-\Delta tasA$ mutant when competed with WT (first column). The experiments were performed twice.

Supplementary Table 1. Strains used in this study

Strain name	Genotype	Reference
168	$\Delta trpC$	1
DL821	NCIB 3610 <i>lacA::P_{tapA}:yfp</i> (Mls ^R)	2
DL1032	NCIB 3610 $\Delta epsA-O::Tet^R \Delta tasA::Km^R amyE::P_{srfAA}-lacZ$	2
168 hymKATE <i>P_{tapA}-yfp</i>	$\Delta trpC amyE::P_{hyperspank}-mKATE$ (Cm ^R) <i>lacA::P_{tapA}:yfp</i> (Mls ^R)	this work
$\Delta eps-\Delta tasA$	$\Delta trpC \Delta epsA-O::Tet^R \Delta tasA::Km^R$	this work
Δeps	$\Delta trpC \Delta epsA-O::Tet^R$	this work
$\Delta tasA$	$\Delta trpC \Delta tasA::Km^R$	this work
168 hyGFP	$\Delta trpC amyE::P_{hyperspank}-GFP$ (Cm ^R)	3
168 hymKate	$\Delta trpC amyE::P_{hyperspank}-mKATE2$ (Cm ^R)	3
$\Delta eps-\Delta tasA$ hyGFP	$\Delta trpC \Delta epsA-O::Tet^R \Delta tasA::Km^R amyE::P_{hyperspank}-GFP$ (Cm ^R)	this work
$\Delta eps-\Delta tasA$ hymKate	$\Delta trpC \Delta epsA-O::Tet^R \Delta tasA::Km^R amyE::P_{hyperspank}-mKATE$ (Cm ^R)	this work

Supplementary Table 2. Evolved populations and single isolates obtained in the study and used for further analyses.

Co-culture name	Population	Single isolate	Strains derived from single isolates
B310	B310wt	B310wtA	B310wtA GFP
			B310wtA mKate
			B310wtA $\Delta eps\Delta tasA$
		B310mB	
		B310mC	
	B310m	B310mA	B310mA
			B310mA mKate
			B310mA $\Delta SP\beta$
	B310mB		
	B310mC		
B410	B410wt	B410wtB	B410wtB GFP
			B410wtB mKate
			B410wtB $\Delta eps\Delta tasA$
		B410wtA	
		B410wtC	
	B410m	B410mB	B410mB
			B410mB mKate
			B410mB $\Delta SP\beta$
	B410mA		
	B410mC		
B510	B510wt	B510wtC	B510wtC GFP
			B510wtC mKate
			B510wtC $\Delta eps\Delta tasA$
		B510wtA	
		B510wtB	
	B510m	B510mC	B510mC
			B510mC mKate
			B510mC $\Delta SP\beta$
	B510mA		
	B510mB		

Supplementary Table 3. Primers used in this study

Primer	Experimental purpose	Sequence
oAD1F	confirm SPbeta deletion from the original position in the chromosome	ATCTGGACTGGCACCTTATGGATACC
oAD2R	confirm SPbeta deletion from the original positions in the chromosome	CTGCTCTGGAAAGGAAGGCAGAGTAA
oTB86F	check for additional copy of SPbeta, examine Sanger chromatogram	CACGCTTGTCTCCAAACC
oTB87R	check for additional copy of SPbeta, examine Sanger chromatogram	GATTGGCCATAACAGACC
oAD4F	confirm SPbeta rearrangement type 1	CTAAGGAGAGATAGGGCAT
oAD5R	confirm SPbeta rearrangement type 1	TGGTTTGAAGGCCATCACA
oAD6F	confirm SPbeta rearrangement type 4	CGATTCAGCTGCCAAATCC
oAD7R	confirm SPbeta rearrangement type 4	CAGGAAAACCTGGTCAGAAAC
oTB74	confirm <i>eps</i> deletion	GGGAAGTGCAGTAAATTAG
oTB75	confirm <i>eps</i> deletion	GAAACGGATTCAGCATTTAG
oTB73	confirm <i>tasA</i> deletion	GATCAGCAGCGCCATTAGAG
oTB72	confirm <i>tasA</i> deletion	CATGGCATGCGCCTGAGCAGAGGCACTAAC

Supplementary References:

- 1 Kovács, Á. T. & Kuipers, O. P. Rok regulates *yuaB* expression during architecturally complex colony development of *Bacillus subtilis* 168. *J Bacteriol* **193**, 998-1002 (2011).
- 2 López, D., Vlamakis, H., Losick, R. & Kolter, R. Paracrine signaling in a bacterium. *Genes Dev* **23**, 1631-1638 (2009).
- 3 van Gestel, J., Weissing, F. J., Kuipers, O. P. & Kovács, Á. T. Density of founder cells affects spatial pattern formation and cooperation in *Bacillus subtilis* biofilms. *ISME J* **8**, 2069-2079 (2014).

The list of detected SNPs of evolved strains and their functional analysis (Supplementary Data 1) can be found at:

<https://www.nature.com/articles/ncomms15127#supplementary-information>

Supporting information for Chapter 7

A duo of potassium-responsive histidine kinases govern the multicellular destiny of *Bacillus subtilis*

Published in: mBio (2015)

Grau_FigS1

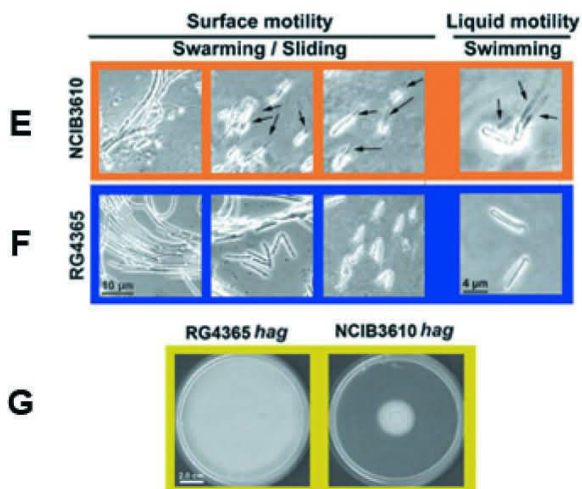
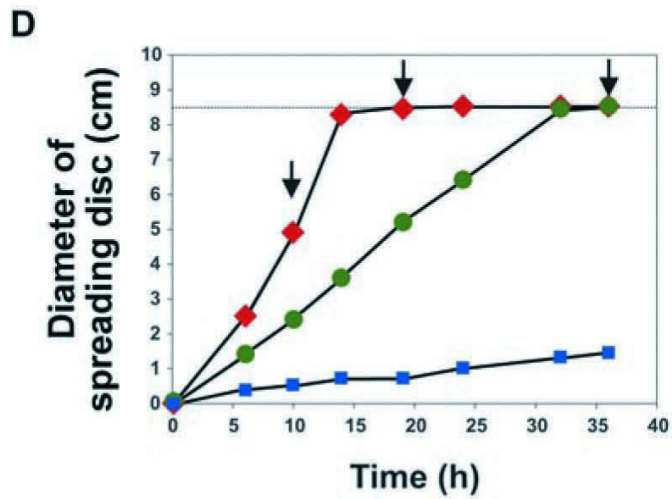
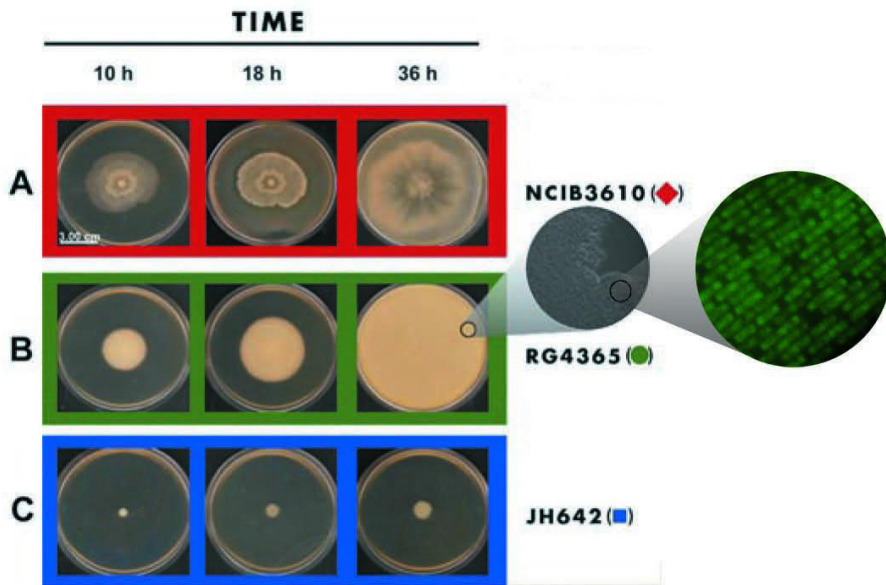


Figure S1

Spreading behavior of the undomesticated *B. subtilis* natto strain. Surface motility of undomesticated *B. subtilis* Marburg-related strain NCIB3610 (A), human-probiotic natto-related strain RG4365 (B), and domesticated laboratory strain JH642 (C) 10 h, 18 h, and 36 h after inoculation. Briefly, petri dishes containing LB medium fortified with 0.7% agar were centrally inoculated with any of the three *B. subtilis* strains and incubated at 37°C (see Materials and Methods for details). (A) In these pictures, it is possible to appreciate the rapid ability of the NCIB3610 strain to swarm on the agar surface. It was previously reported that robust swarming motility, a type of social motility that relies on groups of cells (rafts) that express numerous flagella and differentiate to migrate coordinately along a solid substrate, was present in the NCIB3610 strain (4, 12). (B) The strain RG4365 needed a longer incubation to start to move (as would be expected from a strain that is able only to slide), but after the first 5 h of incubation, it was possible to observe a uniform and highly hydrophobic monolayer of cells that cooperatively and uniformly advanced in large filaments made of close cell-to-cell contacts, predominantly along the longitudinal axis, across the agar plate; see amplified views (phase-contrast and fluorescence images) of RG4365 cells on the right. (C) As expected, the domesticated *B. subtilis* strain JH642 was unable to move because it harbors a mutation in a gene (*sfp*) needed for surfactin synthesis and a frameshift mutation in the regulatory gene *swrA* (24). In contrast, the undomesticated strains NCIB3610 and RG4365 do not harbor those mutations and therefore are able to spread on solid surfaces (12, 75). (D) Kinetics of motility diameter of the various strains: NCIB3610 (red diamonds), RG4365 (green circles), and JH642 (blue squares). Arrows in panel D indicate time points with representative pictures above, while a line at 8.5 cm shows the maximal size of motility related to the size of the plate used. The rate of surface motility was maximal ($0.75 \text{ cm} \cdot \text{h}^{-1}$) for the strain NCIB3610, followed by the natto strain RG4365 ($0.30 \text{ cm} \cdot \text{h}^{-1}$). (E and F) One essential factor for the swimming and swarming ability of the strain NCIB3610 is the flagellum, the proposed motor for those motilities (12). In contrast, the RG4365 strain grown in shaking liquid culture was completely nonmotile (data not shown). Cell samples for flagellum visualization were prepared as indicated previously (12) after 10 h (for NCIB3610 strain [E]) and 20 h (for RG4365 strain [F]) of inoculation on motility plates. These time points represent the stages of maximal surface motility for each wild-type strain (see panel D). Samples were taken from the borders of the surface motility discs, and cells were carefully separated and diluted (from left to right in panels E and F) in order to improve the visualization of flagella. Pictures on the right side of panels E and F are representative photographs of wild-type NCIB3610 cells (E) and RG4365 cells (F) taken from liquid cultures grown until late exponential phase (optical density at 525 nm [OD_{525}], 0.9) in LB medium with aeration (200 rpm). Under all the examined conditions (swarming and swimming), *B. subtilis* NCIB3610 cells harbored flagella and were motile (E). In contrast, wild-type *B. subtilis* RG4365 cells were motile only on soft agar plates but without harboring flagella (F). In liquid culture, the RG4365 cells also were devoid of flagella and completely nonmotile (right image in panel F). Cells were stained for flagella as described in Materials and Methods. Arrows indicate the positions of some flagella shown as examples. (G) To confirm the dispensability of flagellum production for the surface-associated motility (sliding) in RG4365, we proceeded to delete the *hag* gene (75), which is involved in the synthesis of the flagellin subunit of the flagellum (76). As shown (left photograph), the isogenic *hag* mutant strain RG4387 (see Table S1) was able to slide on the agar surface at the same rate as the wild-type parental strain RG4365 after 24 h of incubation at 37°C. Similarly, the *hag* inactivation in the NCIB3610 strain abolished its ability to swarm under similar incubation conditions (right photograph). Alignment of the Hag protein sequences based on the available genomes (75) showed that the sequence of the Hag protein in the *B. subtilis* natto strain contains a 6-amino-acid insertion and a 5-amino-acid deletion at different positions; however, the total sizes of the proteins are similar in various *Bacilli* (304 and 305 amino acids in strain 168 and the natto strain, respectively). The promoter regions of the *hag* genes on the genomes of strain 168 and the natto strain are highly similar (98% identical), and the σ^D binding sites are identical in the two strains.

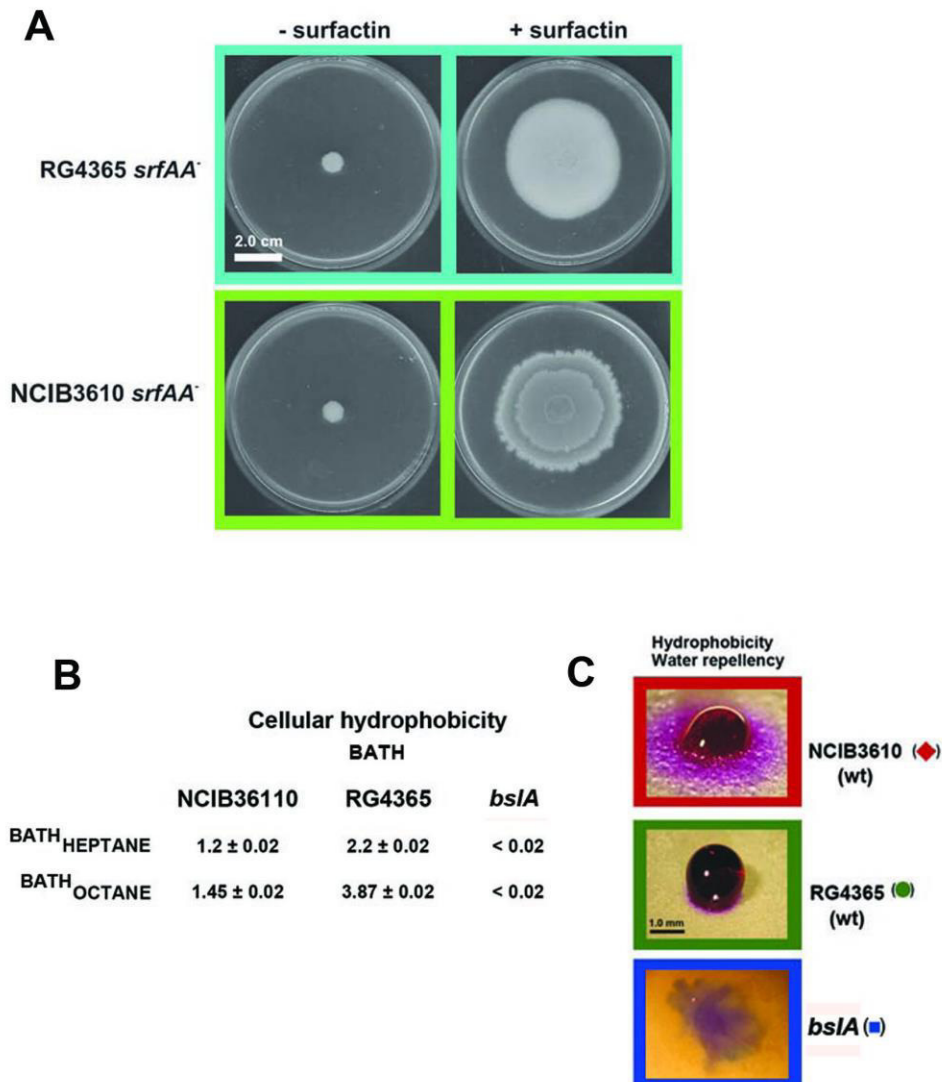


Figure S2

Surfactin production and the hydrophobin BslA are essential for sliding motility in *B. subtilis*. (A) After addition of synthetic surfactin to surfactin-deficient RG4365 and NCIB3610 cells, surface motilities were reestablished. The supplementation of the petri dishes with synthetic surfactin (Sigma-Aldrich; see Materials and Methods) restored the sliding and swarming ability of *B. subtilis* natto strain and Marburg-derived *srfAA* cells and confirmed that surfactin is the essential biosurfactant that allows the surface-associated translocation (sliding and swarming) of *B. subtilis*. (B) BslA contributes to the hydrophobicity of *B. subtilis* under surface motility conditions. Cellular hydrophobicity was calculated using the BATH assay (77) between a hydrocarbon (octane or heptane) and cultures of NCIB3610, RG4365, and *bslA* natto cells. (C) Surface water repellence of wild-type and *bslA* natto cells. After overnight incubation on soft LB agar plates at 37°C, 5.0 µl of a hydrophilic staining solution was carefully poured on the patch of motile cells and the colony of the *bslA* mutant. The swarming- and sliding-proficient cells (NCIB3610 and RG4365, respectively) prevented the water penetration into the cell matrix. In contrast, the *bslA*-deficient cells were unable to repel the water, which almost immediately and uniformly penetrated throughout them.

Grau_FigS3

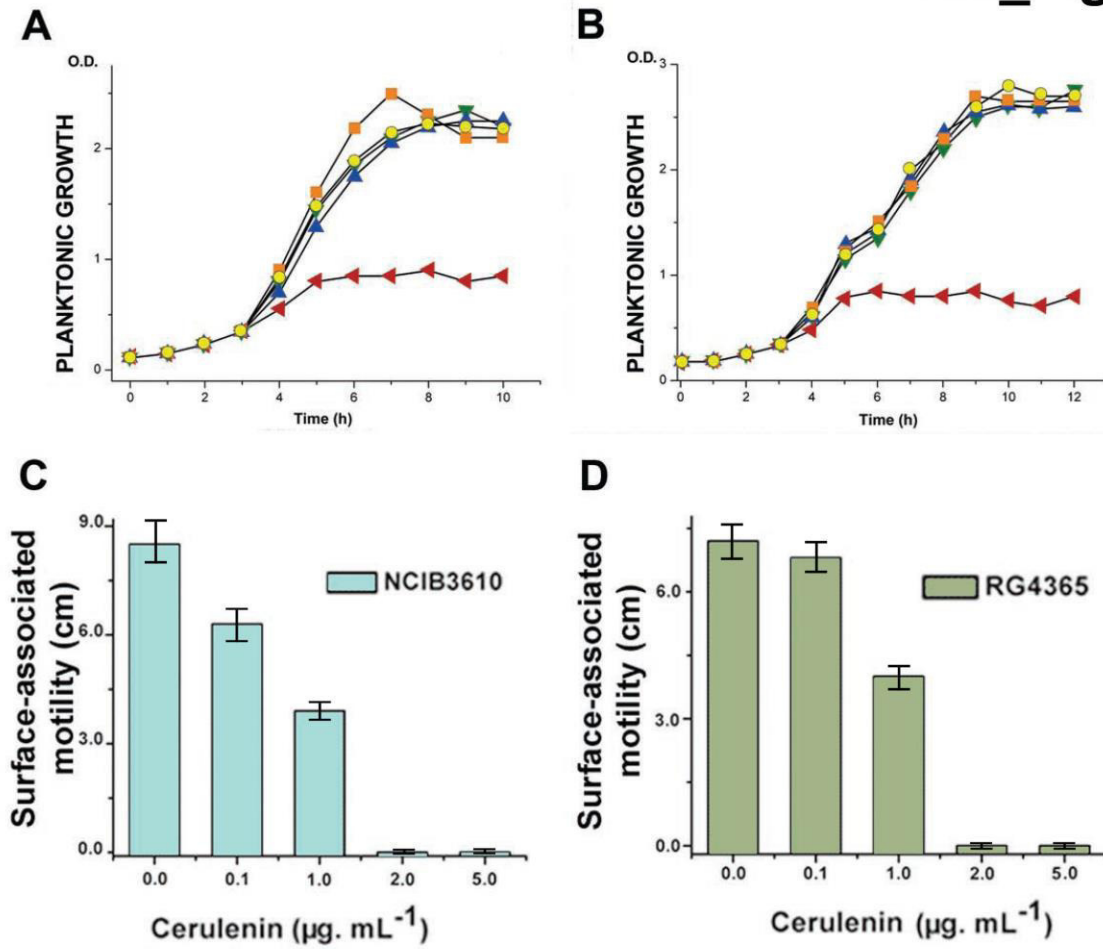
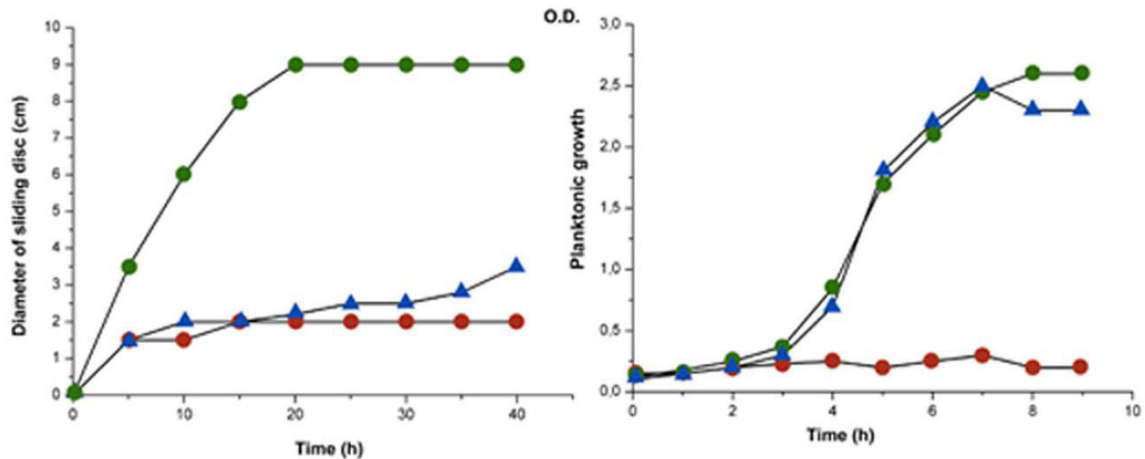


Figure S3

Sub-MICs of cerulenin do not affect planktonic growth of *B. subtilis* cells but impair social surface translocation. NCIB3610 (A) and RG4365 (B) wild-type cells were grown in LB broth at 200 rpm and 37°C in the absence or presence of different concentrations of cerulenin. The averages from three independent experiments are shown. Cerulenin concentrations were as follows: 5.0 $\mu\text{g} \cdot \text{mL}^{-1}$ (red triangles), 2.0 $\mu\text{g} \cdot \text{mL}^{-1}$ (blue triangles), 1.0 $\mu\text{g} \cdot \text{mL}^{-1}$ (green triangles), 0.1 $\mu\text{g} \cdot \text{mL}^{-1}$ (yellow circles), and 0 (orange squares). (C and D) Dose-dependent inhibitory effect of different cerulenin concentrations on swarming (C) and sliding (D) proficiencies of *B. subtilis* cells.

Grau_FigS4

A



B

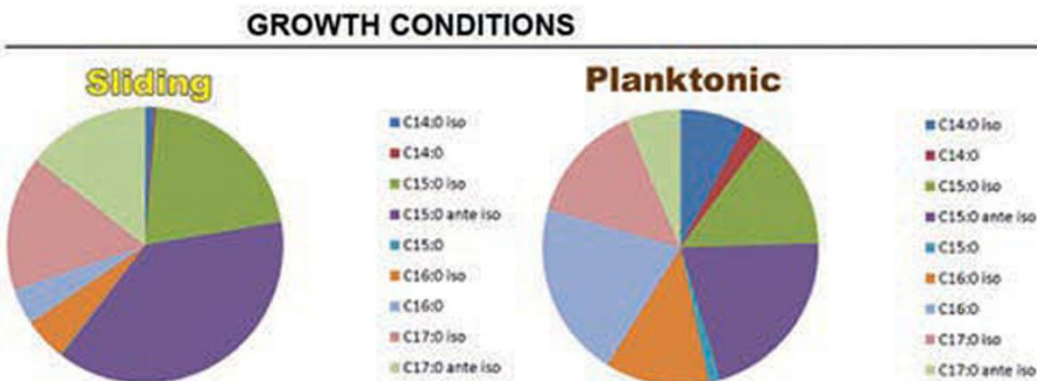


Figure S4

(A) Supplementation with straight fatty acids (palmitic [nC_{16:0}] and oleic [nC_{18:1}] fatty acids) does not restore the sliding proficiency of wild-type RG4365 cells treated with a sub-MIC of cerulenin (left) but allows restart of the growth of RG4365 cells in the presence of the antibiotic under planktonic conditions (right). The graphs are the results of one representative experiment repeated five times. Symbols are as follows: red circles, 2.0 µg · ml⁻¹ cerulenin (left graph) and 5.0 µg · ml⁻¹ cerulenin (right graph); blue triangles, 2.0 µg · ml⁻¹ cerulenin plus nC_{16:0} and nC_{18:1} and 5.0 µg · ml⁻¹ cerulenin plus nC_{16:0} and nC_{18:1} (left and right graphs, respectively); green circles, no cerulenin. (B) Profile of fatty acids (FAs) synthesized *de novo* by wild-type *B. subtilis* RG4365 cells under conditions of planktonic growth in LB broth (right circle) and active sliding on soft agar LB plates (left circle). The averages from eight biological replicates are presented.

Grau_FigS5

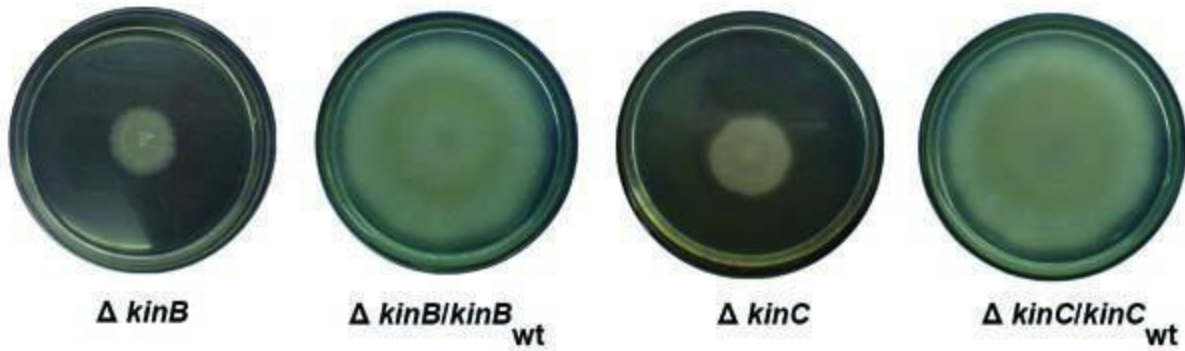


Figure S5

Transcomplementation of *kinB*-deficient and *kinC*-deficient *B. subtilis* strains. RG4365-derived *kinB* and *kinC* mutants were transcomplemented with wild-type *kinB* and *kinC* alleles (see [Table S1](#)), respectively, which were ectopically integrated into the nonessential locus *amyE*.

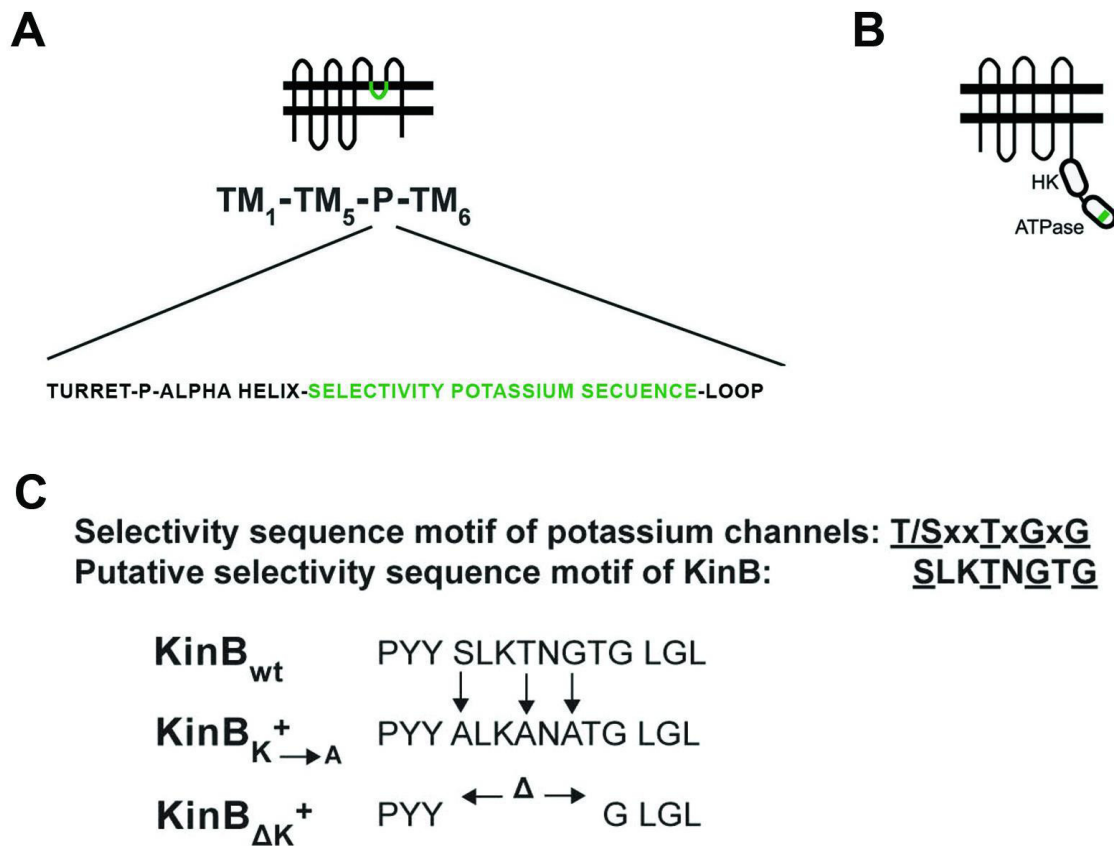


Figure S6

KinB harbors a potassium-sensing domain with homology to the selectivity filter of potassium channels. (A) Representative cartoon of the membrane topology of a typical prokaryotic potassium channel harboring six transmembrane domains. The region of the potassium pore (P) surrounded by two alpha helices that dips into the membrane is highlighted to indicate the components of the pore region: turret, pore helix, selectivity filter, and the loop that precedes the sixth transmembrane domain (TM6). The membrane-embedded selectivity filter for potassium is emphasized in green. (B) Representative drawing of the membrane topology of KinB. The known cytoplasmic domains (HK and ATPase) of the kinase are indicated. The position of the putative potassium-sensing domain harbored by the kinase is also highlighted in green (see text for details). (C) The 8-amino-acid sequence of KinB (S-L-K-T-N-G-T-G) with homology to the selectivity filter present in potassium channels (S/T-X-X-T-X-G-X-G) (56, 60, 78). Out of the 8 amino acids of the motif, position seven of potassium channels is generally assigned to an aromatic amino acid (mainly tyrosine [Y] but also phenylalanine can be present) (56, 57, 60, 79). In KinB, this position is occupied by a threonine (T). However, it has been shown that nonconservative substitutions of the Y residue in position 7 of the selectivity filter leave selectivity for potassium intact, and data show that an aromatic group at position 7 is not essential in determining potassium selectivity (56). More recently, it was found that other amino acids (i.e., leucine, aspartic acid, etc.) can be present in position 7 of the selectivity filter of functional potassium channels (57, 79).

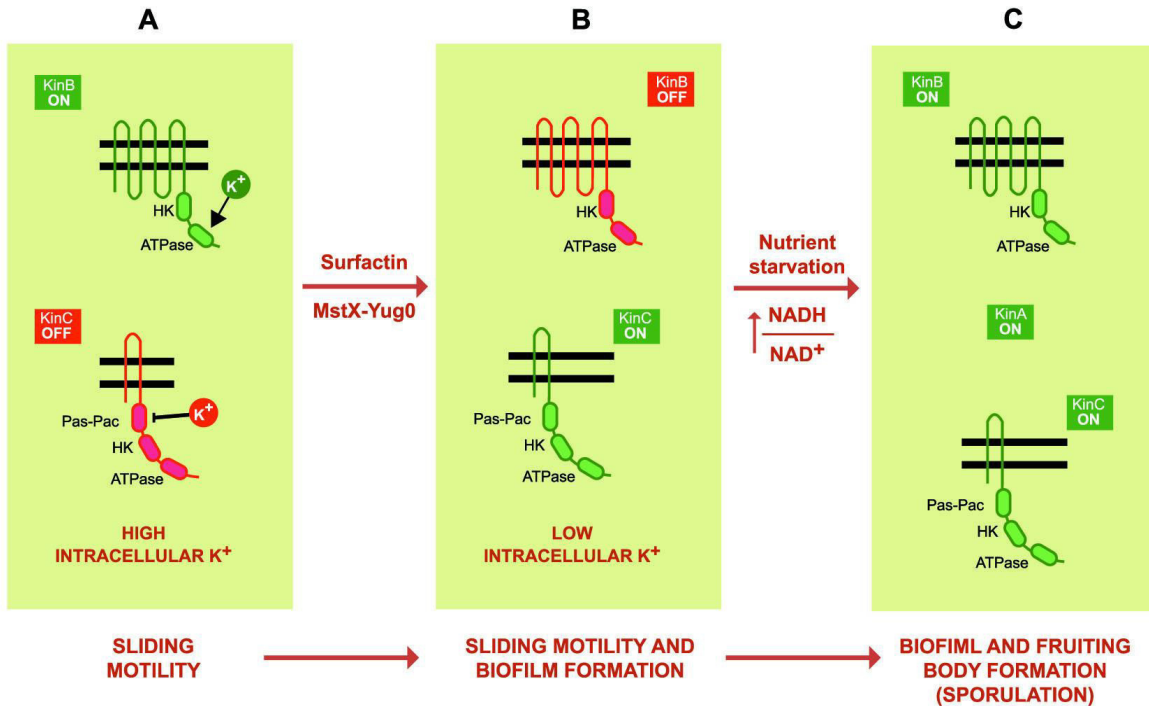


Figure S7

Working model for the spatiotemporal regulation of the different social behaviors in *B. subtilis*. (A) When *B. subtilis* is attached and committed to a surface (i.e., in soft LB agar plates), its social behaviors fall under the control of the master regulator Spo0A. Initially, KinB becomes autophosphorylated under the positive input of a high intracellular concentration of potassium ions. At the same time, the high level of potassium inhibits KinC activation (autophosphorylation). Not indicated in the cartoon is the possibility that KinB might inhibit KinC in its proficiency to trigger biofilm formation (see text for details). At this early time of development, the levels of formed KinB~P_i are enough to produce low levels of active Spo0A (Spo0A~P_i) that trigger expression of the sliding machinery. Because the two phenomena, sliding and biofilm formation, share essentially similar structural components, there is the possibility that the expression levels of these components under the initial input of KinB~P_i might be different during sliding and biofilm formation in order to allow one or the other behavior and/or that other essential components of the sliding and biofilm formation machineries are differently regulated and have not yet been identified (9, 31–33). (B) At middle times of sliding development, there should be a drop in the intracellular concentration of potassium ions in cells located at the inner part of the sliding disc that leads to the downregulation of KinB and activation of KinC, respectively. KinC~P_i feeds the phosphorelay to produce higher levels of Spo0A~P_i to maintain active sliding in soft LB agar plates. Under special conditions of cultivation (i.e., in soft LBY agar plates), KinC~P_i would also trigger biofilm formation at the inner part of the sliding disc. At the border of both sliding discs (in LB and LBY agar plates), KinB and KinC remain active and inactive, respectively, due to the high intracellular concentration of potassium ions in the cells (not shown in the cartoon). (C) At later times of development, KinC remains active and KinB and KinA become activated by nutrient deficiency as previously described (53). The three activated kinases (KinA~P_i, KinB~P_i, and KinC~P_i) produce high levels of Spo0A~P_i to allow fruiting body formation (filled with spores) at the tips of the biofilm.

Table S1. *B. subtilis* strains used in this study

Strains	Relevant phenotype	Reference and/or source
JH642	Prototroph, domesticated strain	(1)
RG4365	Natto, prototroph, undomesticated strain	(2)
NCIB3610	Prototroph, undomesticated strain	Bacillus Genetic Stock Center (BGSC)
GP901	168 <i>hag::aphA3</i>	Jörg Stülke, laboratory collection
RG4387	natto <i>hag::aphA3</i>	This work, GP901→RG4365 (DNA from donor strain → receptor strain)
TB24	3610 <i>hag::aphA3</i>	This work, GP901→NCIB3610
RG551	642 <i>srfAA::cat</i>	B. Lazazzera, laboratory collection
RG4390	natto <i>srfAA::cat</i>	This work, RG551→RG4365
RG4391	3610 <i>srfAA::cat</i>	This work, RG551→NCIB3610
SS995	$\Delta spo0A::ery^r$	(3)
RG4370	natto $\Delta spo0A::ery^r$	This work, SS995→RG4365
RG4399	3610 $\Delta spo0A::ery^r$	This work, SS995→NCIB3610
RG432	642 <i>sinR::pheo</i>	(4)
RG4373	natto <i>sinR::pheo</i>	This work, RG432→RG4365
RG4392	3610 <i>sinR::pheo</i>	This work, RG432→NCIB3610
RG19148	642 <i>spoIIAC::kan</i>	(3)
RG4372	natto <i>spoIIAC::kan</i>	This work, RG19148→RG4365
RG4380	natto $\Delta spo0A::ery$, <i>sinR::pheo</i>	This work, RG4370→RG4373
RG12607	642 <i>abrB::spc</i>	(3)
RG12617	Natto <i>abrB::spc</i>	This work, RG12607→RG4365
RG4381	natto $\Delta spo0A::ery$, <i>abrB::cat</i>	This work, RG4370→RG12607
SIK31	642 $\Delta spo0A::ery$ <i>P_{spac}-spo0A_{sad67}</i>	(1)
RG4382	natto $\Delta spo0A::ery$ / <i>P_{spac}-spo0A-sad67cat</i>	This work, SIK31→RG4365
RG4385	3610 <i>hag::aphA3</i> , $\Delta spo0A::ery$	This work, RG4399→TB24
AGS207	168 <i>tasA::spc</i>	(5)
NRS1502	3610 <i>epsG::pBL601</i> (spc)	(6)
NRS2097	3610 <i>bslA::cat</i>	(6)

TB21	natto <i>blsA</i> ::cat	This work, NRS2097→RG4365
TB22	natto <i>epsG</i> ::pBL601 (spc)	This work, NRS1502→RG4365
TB23	natto <i>tasA</i> ::spc	This work, AGS207→RG4365
TB25	3610 <i>blsA</i> ::cat, <i>hag</i> ::aphA3	This work, NRS2097→TB24
TB26	3610 <i>epsG</i> ::pBL601 (spc), <i>hag</i> ::aphA3	This work, NRS1502→TB24
TB163	3610 <i>tasA</i> ::spc	This work, AGS207→NCIB3610
TB228	3610 <i>hag</i> ::aphA3 <i>tasA</i> ::spc	This work, ADS207→TB24
JH12638	<i>kinA</i> ::ery	(7)
RG5000	natto <i>kinA</i> ::ery	This work, JH12638→RG4365
JH19980	<i>kinB</i> ::tet	(7)
RG5001	natto <i>kinB</i> ::tet	This work, JH19980→RG4365
BAL393	<i>kinC</i> ::spc	B. Lazazzera, laboratory collection
RG5002	natto <i>kinC</i> ::spc	This work, BAL393→RG4365
BAL691	<i>kinD</i> ::cat	B. Lazazzera, laboratory collection
RG5003	natto <i>kinD</i> ::cat	This work, BAL691→RG4365
BAL692	<i>kinE</i> ::cat	B. Lazazzera, laboratory collection
RG5004	natto <i>kinE</i> ::cat	This work, BAL692→RG4365
RG5005	natto <i>kinB</i> ::tet <i>kinC</i> ::spc	This work, RG5002→RG5001
BAL370	<i>spo0F</i> ::cat	B. Lazazzera, laboratory collection
RG4371	natto <i>spo0F</i> ::cat	This work, BAL370→RG4365
TB40	168 <i>amyE</i> :: <i>kinB</i> (wt) kan	This work
TB41	168 <i>amyE</i> :: <i>kinB</i> (ΔK^*) kan	This work
TB42	168 <i>amyE</i> :: <i>kinB</i> ($K^* \rightarrow A$) kan	This work
TB43	168 <i>amyE</i> :: <i>kinC</i> (wt)kan	This work
RG5011	natto <i>kinB</i> ::tet <i>amyE</i> :: <i>kinB</i> (wt) kan	This work, TB40→RG5001
RG5012	natto <i>kinB</i> ::tet <i>amyE</i> :: <i>kinB</i> ($K^* \rightarrow A$) kan	This work, TB42→RG5001
RG5013	natto <i>kinB</i> ::tet <i>amyE</i> :: <i>kinB</i> (ΔK^*) kan	This work, TB41→RG5001
RG5021	natto <i>kinC</i> ::spc <i>amyE</i> :: <i>kinC</i> (wt)kan	This work, TB43→RG5002
RG5051	natto <i>kinB</i> ::tet <i>kinC</i> ::spc <i>amyE</i> :: <i>kinB</i> (wt) kan	This work, TB40→RG5005
RG5052	natto <i>kinB</i> ::tet <i>kinC</i> ::spc <i>amyE</i> :: <i>kinB</i> ($K^* \rightarrow A$) kan	This work, TB42→RG5005
RG5053	natto <i>kinB</i> ::tet <i>kinC</i> ::spc <i>amyE</i> :: <i>kinB</i> (ΔK^*) kan	This work, TB41→RG5005
RG5006	natto <i>kinA</i> ::ery <i>kinB</i> ::tet	This work, RG5000→RG5001

RG5061	natto <i>kinA::ery kinB::tet amyE::kinB(wt)</i> kan	This work, TB40→RG5001
RG5062	natto <i>kinA::ery kinB::tet amyE::kinB(K*→A)</i> kan	This work, TB42→RG5001
RG5063	natto <i>kinA::ery kinB::tet amyE::kinB(ΔK*)</i> kan	This work, TB41→RG5001
RG12604	natto <i>amyE::abrB-lacZ</i> cat	(2)

References

1. **Arabolaza AL, Nakamura A, Pedrido ME, Martelotto L, Orsaria L, Grau RR.** 2003. Characterization of a novel inhibitory feedback of the anti-anti-sigma SpoIIAA on Spo0A activation during development in *Bacillus subtilis*. *Mol Microbiol* **47**:1251-1263.
2. **Lombardía E, Rovetto AJ, Arabolaza AL, Grau RR.** 2006. A LuxS-dependent cell-to-cell language regulates social behavior and development in *Bacillus subtilis*. *J Bacteriol* **188**:4442-4452.
3. **Méndez MB, Orsaria LM, Philippe V, Pedrido ME, Grau RR.** 2004. Novel roles of the master transcription factors Spo0A and sigmaB for survival and sporulation of *Bacillus subtilis* at low growth temperature. *J Bacteriol* **186**:989-1000.
4. **Gottig N, Pedrido ME, Méndez M, Lombardía E, Rovetto A, Philippe V, Orsaria L, Grau R.** 2005. The *Bacillus subtilis* SinR and RapA developmental regulators are responsible for inhibition of spore development by alcohol. *J Bacteriol* **187**:2662-2672.
5. **Stöver AG, Driks A.** 1999. Secretion, localization, and antibacterial activity of TasA, a *Bacillus subtilis* spore-associated protein. *J Bacteriol* **181**:1664-1672.
6. **Verhamme DT, Murray EJ, Stanley-Wall NR.** 2009. DegU and Spo0A jointly control transcription of two loci required for complex colony development by *Bacillus subtilis*. *J Bacteriol* **191**:100-108.
7. **Wang L, Grau R, Perego M, Hoch J.** 1997. A novel histidine kinase inhibitor regulating development in *Bacillus subtilis*. *Genes Dev* **11**:2569-2579.

Table S2.

(A) Array analysis of *spo0A* and wild-type cells under sliding permissive conditions. List of significantly (p value $<10^{-4}$) up or downregulated *B. subtilis* genes (fold > 3 or < -3) in the *spo0A* mutant compared to the sliding wild type cells.

(B) Array analysis of wild-type cells under sliding-permissive and sliding-restrictive conditions. List of significantly (p value $<10^{-4}$) up or downregulated *B. subtilis* genes (fold > 3 or < -3) in the samples from 1.5% agar plates compared to the sliding cells from plates with 0.7% agar.

Table S2 can be found at:

<http://mbio.asm.org/content/6/4/e00581-15.full#sec-23>

Table S3. Oligonucleotides used in this study. Introduced restriction sites (*Bam*HI and *Eco*RI) are underlined.

Name	Sequence	Target gene or vector
oTB56	5`-CAT <u>GGATCC</u> TGGCGGAGAAGGATTTATG-3`	<i>kinB</i>
oTB57	5`-CAC <u>GGAATTC</u> TGTCTCAAACGTGCTCATC-3`	<i>kinB</i>
oTB58	5`-ATAATAAGGTTGCGCCGAGTTTTTGC-3`	<i>kinB</i>
oTB59	5`-GCAAAA <u>ACTCGGCGAACCTT</u> ATTATGGACTCGGCCTCACCGTAACCTTTTCC-3`	<i>kinB</i>
oTB60	5`- GCAAAA <u>ACTCGGCGAACCTT</u> ATTATGCCTTAAAAGCGAACGCAACGGGACTCGGC CTCAC-3`	<i>kinB</i>
oTB61	5`-CAT <u>GGATCC</u> ATTACGCTAAGCCCTGAG-3`	<i>kinC</i>
oTB62	5`-CAC <u>GGAATTC</u> TTGTGCCAGCAAATGATG-3`	<i>kinC</i>
oDG1	5`-AGGCCTCGAGATCTATCGATA-3`	pDG782
oDG2	5`-GGATCCATATGACGTCGACGCG-3`	pDG782
oX1	5`- GGATCCGCTCAACGGCCTCAACCTACTACTG-3`	pX
oX2	5`- AGGCCTGCCGGTCGCTACCATTACCAG-3`	pX

Supporting information for Chapter 8

Presence of calcium lowers the expansion of *Bacillus subtilis* colony biofilms

Published in: Microorganisms (2017)

Presence of Calcium Lowers the Expansion of *Bacillus subtilis* Colony Biofilms

Eisha Mhatre ¹, Anandaroopan Sundaram ¹, Theresa Hölscher ¹, Mike Mühlstädt ², Jörg Bossert ², Ákos T. Kovács ^{1,*}

¹ Terrestrial Biofilms Group, Institute of Microbiology, Friedrich Schiller University Jena, 07743 Jena, Germany; eisha.r.mhatre@gmail.com (E.M.); sundar.sabitha@gmail.com (A.S.); thoelscher@ice.mpg.de (T.H.),

² Otto Schott Institute of Materials Research, Friedrich Schiller University Jena, 07743 Jena, Germany; mike.muehlstaedt@uni-jena.de (M.M.); Joerg.Bossert@uni-jena.de (J.B.)

* Correspondence: akos-tibor.kovacs@uni-jena.de

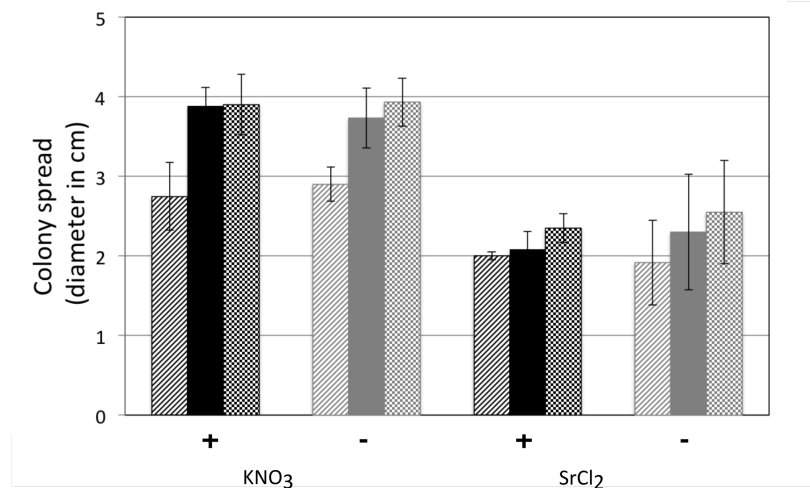


Figure S1. Ca²⁺ specifically reduce colony escape. The colony expansion diameters of *B. subtilis* DK1042 are shown after 3 (striped), 5 (filled), and 7 (checked) days. Black bars present data in presence, while grey bars indicate in absence of KNO₃ and SrCl₂ in the 2×SG medium. KNO₃ was used to observe the impact of NO₃⁻, while SrCl₂ was applied to assay the influence of another divalent cation. The error bars indicate 95% confidence intervals.

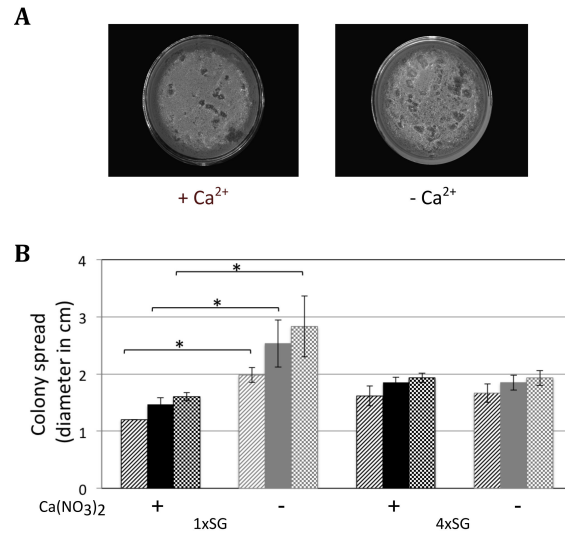


Figure S2. Impact of Ca²⁺ on pellicle formation and colony spreading at different nutrient concentrations. (A) Pellicle formation of *B. subtilis* DK1042 on 2×SG medium in the presence (left) and absence (right) of Ca²⁺ supplementation after 3 days. (B) The colony expansion diameters of the *B. subtilis* DK1042 are shown on 1×SG and 4×SG media with 1.5% agar after 3 (striped), 5 (filled), and 7 (checked) days. The black bars present data in presence, while grey bars indicate in absence of Ca²⁺ supplementation in the media. The error bars indicate 95% confidence intervals. * denotes significant differences (p<0.05) analyzed with paired t-test.

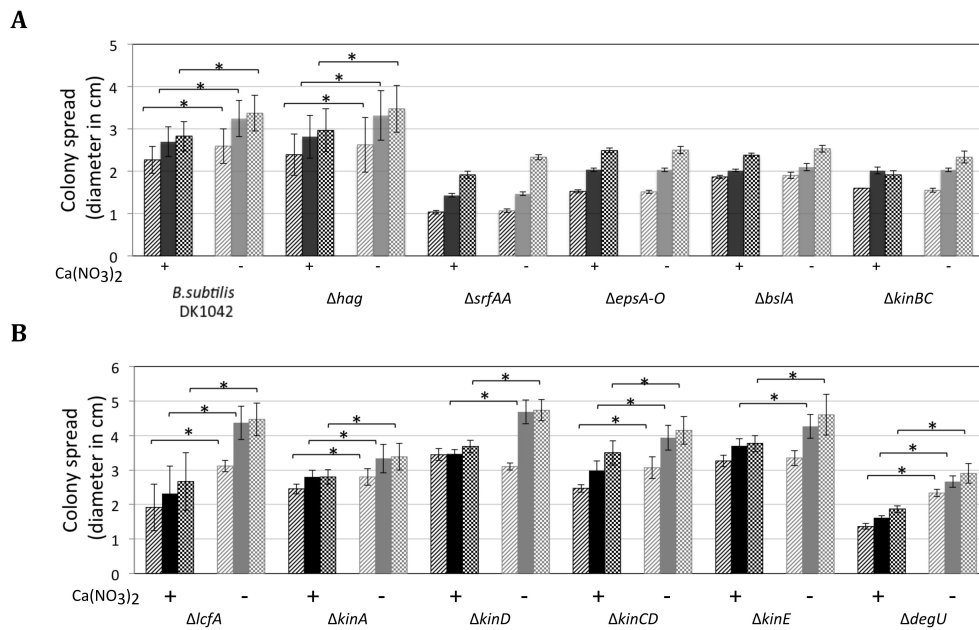


Figure S3. Colony escape of various strains on MSgg (A) and 2×SG (B) medium. (A) The colony expansion diameters of the *B. subtilis* DK1042 and its derivatives, Δ*hag*, Δ*srfAA*, Δ*epsA-O*, Δ*bslA*, and Δ*kinB*Δ*kinC* are shown on MSgg medium after 4 (striped), 6 (filled), and 8 (checked) days. (B) The colony expansion diameters of the *B. subtilis* Δ*lcfA*, Δ*kinA*, Δ*kinB*, Δ*kinC*, Δ*kinD*, Δ*kinE*, Δ*kinC*Δ*kinD*, and Δ*degU* are shown on 2×SG medium after 3 (striped), 5 (filled), and 7 (checked) days. Black bars present data in presence, while grey bars indicate in absence of Ca²⁺ supplementation in the respective media in both panels. The error bars indicate 95% confidence intervals. * denotes significant differences (p<0.05) analyzed with paired t-test.

Supporting information for Chapter 9

Monitoring spatial segregation in surface colonizing microbial populations

Published in: Journal of Visualized Experiments (2016)

Materials List for:

Monitoring Spatial Segregation in Surface Colonizing Microbial Populations

Theresa Hölscher¹, Anna Dragoš¹, Ramses Gallegos-Monterrosa¹, Marivic Martin¹, Eisha Mhatre¹, Anne Richter¹, Ákos T. Kovács¹

¹Terrestrial Biofilms Group, Institute of Microbiology, Friedrich Schiller University, Jena

Correspondence to: Ákos T. Kovács at akos-tibor.kovacs@uni-jena.de

URL: <https://www.jove.com/video/54752>

DOI: [doi:10.3791/54752](https://doi.org/10.3791/54752)

Materials

Name	Company	Catalog Number	Comments
Lennox Broth (LB)	Carl Roth GmbH	X964	
Agar-agar, Kobe I	Carl Roth GmbH	5210	
Petri dish (90 mm diameter)	any	NA	Use Petri dishes without ventilation cams
Petri dish (35 mm diameter)	any	NA	Use Petri dishes without ventilation cams
Difco Nutrient Broth	BD Europe	234000	
KCl	any	NA	
MgSO ₄ 7H ₂ O	any	NA	
Ca(NO ₃) ₂ 4H ₂ O	any	NA	
MnCl ₂ 4H ₂ O	any	NA	
FeSO ₄	any	NA	
D-Glucose	any	NA	
Fluorescence AxioZoom V16 time-lapse microscope	Carl Zeiss Microscopy GmbH		see below detailed description
AxioZoom V16 Microscope body	Carl Zeiss Microscopy GmbH	435080 9030 000	
Phototube Z 100:0 for Axio Zoom V16	Carl Zeiss Microscopy GmbH	435180 9020 000	without eyepieces
Fluar Illuminator Z mot Fluorescence intermediate tube for Axio Zoom.V16	Carl Zeiss Microscopy GmbH	435180 9060 000	
Controller EMS 3	Carl Zeiss Microscopy GmbH	435610 9010 000	
System Control Panel SYCOP 3	Carl Zeiss Microscopy GmbH	435611 9010 000	
Reflector module Z	Carl Zeiss Microscopy GmbH	435180 9160 000	For Fluar Illuminator Z mot on Axio Zoom.V16 and SYCOP 3
Filter set 38 HE eGFP shift free (E)	Carl Zeiss Microscopy GmbH	489038 9901 000	EX BP 470/40, BS FT 495, EM BP 525/50
Filter set 63 HE mRFP shift free (E)	Carl Zeiss Microscopy GmbH	489063 0000 000	EX BP 572/25, BS FT 590, EM BP 629/62
Mount S	Carl Zeiss Microscopy GmbH	435402 0000 000	
Objektive PlanApo Z 0,5x/0,125 FWD 114 mm	Carl Zeiss Microscopy GmbH	435280 9050 000	164 mm parfocal length; M62x0.75 thread at front
Coarse/fine drive with profile column	Carl Zeiss Microscopy GmbH	435400 0000 000	490 mm, 10 kg load capacity, compatible with stand bases 300/450
Stand base 450	Carl Zeiss Microscopy GmbH	435430 9902 000	
Cold-light source Zeiss CL 9000 LED CAN	Carl Zeiss Microscopy GmbH	435700 9000 000	
CAN-bus cable	Carl Zeiss Microscopy GmbH	457411 9011 000	2.5 m length

Slit-ring illuminator	Carl Zeiss Microscopy GmbH	417075 9010 000	d = 66 mm
Flexible light guide 1500	Carl Zeiss Microscopy GmbH	417063 9901 000	8/1,000 mm
Illumination Adapter for light guide	Carl Zeiss Microscopy GmbH	000000 1370 927	
Lightguide HXP with liquid fill	Carl Zeiss Microscopy GmbH	000000 0482 760	ø3 mm x 2,000 mm
Camera Adapter 60N-C	Carl Zeiss Microscopy GmbH	426113 0000 000	2/3" 0.63X
High Resolution Microscopy Camera AxioCam MRm Rev. 3 FireWire	Carl Zeiss Microscopy GmbH	426509 9901 000	
AxioCam FireWire Trigger Cable Set	Carl Zeiss Microscopy GmbH	426506 0002 000	for direct shutter synchronization
ZEN pro 2012	Carl Zeiss Microscopy GmbH	410135 1002 120	Blue edition, requires min. Windows 7 64-bit
ZEN Module Time Lapse	Carl Zeiss Microscopy GmbH	410136 1031 110	
Standard Heating Stage Top Incubator	Tokai Hit	INUL-MS1-F1	
Zeiss Stereo Microscope Base Adapter	Tokai Hit	MS-V12	
Softwares			
ImageJ	National Institute of Health, Bethesda, MD, USA	v 1.49m	
BioVoxel plugin	BioVoxel		http://www.biovoxxel.de/development/

Supporting information for Chapter 10

Differential shareability of goods explains social exploitation during sliding

In preparation for future submission for publication.

Supplemental material

Table S1. Strains used in this study

Strain	Genotype	Reference
<i>Bacillus subtilis</i> 3610		
TB530	<i>P_{hyperspank}</i> -GFP:Spec hag::Km	Mhatre <i>et al.</i> , 2017
TB531	<i>P_{hyperspank}</i> -mKATE2:Spec hag::Km	This study
TB532	<i>P_{hyperspank}</i> -GFP:Spec hag::Km eps::Tet	This study
TB533	<i>P_{hyperspank}</i> -mKATE2:Spec hag::Km eps::Tet	This study
TB534	<i>P_{hyperspank}</i> -GFP:Spec hag::Km bslA::Cm	This study
TB535	<i>P_{hyperspank}</i> -mKATE2:Spec hag::Km bslA::Cm	This study
TB536	<i>P_{hyperspank}</i> -GFP:Spec hag::Km srfAA::MLS	This study
TB537	<i>P_{hyperspank}</i> -mKATE2:Spec hag::Km srfAA::MLS	This study
TB873	<i>P_{spachy}</i> -bslA:Spec bslA::Cm hag::Km	This study
TB875	<i>P_{hyperspank}</i> -epsA-O:Spec hag::Km	This study
TB977	<i>P_{hyperspank}</i> -srfA:MLS hag::Tet	This study
TB893	<i>hag::Km eps::Tet</i>	This study
TB922	<i>hag::Tet bslA::Cm</i>	This study
TB895	<i>hag::Km srfAA::MLS</i>	This study
DK1042	<i>comI^{Q12L}</i>	Konkol <i>et al.</i> , 2013
TB601	<i>eps::Tet</i>	(Dragoš <i>et al.</i> , 2017)
TB602	<i>tasA::Km</i>	(Dragoš <i>et al.</i> , 2017)
<i>Escherichia coli</i>		
<i>E. coli</i> TB887	MC1061 pTB887 (pTB234:hxIR:lacl:Phy-srfA)	This study
<i>E. coli</i>	BL21	Novagen
<i>E. coli</i> NRS4110	BL21 pGEX_TEV_BslA ₄₂₋₁₈₂ ::Amp	Hobley <i>et al.</i> , 2013

Table S2. Primers

Primer	Sequence (5'-3')
oTH1 (Mhatre <i>et al.</i> , 2017)	GCATCTAGAGTTGCTCGCGGGTAAATGTG
oTH2 (Mhatre <i>et al.</i> , 2017)	CGAGAATTCATCCAGAAGCCTTGCATATC
oTH33	CTGAAGCTTAAGATTAGGGGAGGTATGAC
oTH34	GGAGCATGCAATGTTCCCGTCACAACATC
oTH35	GCAGGTACCGCAATGTTCCCGTCACAACATC
oTH36	CATCTCGAGGTAATGTGAGCACTCACAATTC

Table S3. Model parameters.

Symbol	Parameter	Value
T	Duration of the simulation	24h
x	Width hexagonal lattice	100mm
ΔT	Discretization of time	1 min ⁻¹
Δx	Discretization of space	0.25 mm ⁻¹
Δt	Discretization of time for Euler approximation	3 s ⁻¹
\emptyset	Diameter of inoculum	10 mm
μ_{ij}	Production rate molecule <i>i</i> by strain <i>j</i>	0.01 min ⁻¹ B ⁻¹
δ	Degradation rate of surfactin and eps	0.01 min ⁻¹
m	Probability of expansion upon biomass doubling	0.90
α_1	Diffusion coefficient of surfactin	10 ⁻³ mm ² /s ^{***}
α_2	Diffusion coefficient of eps	10 ⁻⁸ mm ² /s
α_R	Diffusion coefficient of resources	10 ⁻³ mm ² /s
T	Threshold concentration needed for expansion	0.01

*** Comparable to the diffusion of glycerol in water at a temperature of 25°C.

Table S4. Model variables.

Symbol	Variable
<i>B</i>	Biomass
<i>R</i>	Resource
<i>M</i> ₁	Secreted molecule 1, surfactin
<i>M</i> ₂	Secreted molecule 2, eps

Supplementary methods

Strain construction

To create fluorescently labelled strains, the gene of the respective fluorescence marker was coupled with a Spectinomycin resistance cassette in plasmid pWK-Sp (Susanna *et al.*, 2007), resulting in plasmids pTB498 (mKATE2) and pTB497 (GFP) as described in Mhatre *et al.* (2017). Similarly, for pTB498, the *Phyperspank-mKATE2* fragment was amplified using primers oTH1 and oTH2 (Mhatre *et al.*, 2017) from plasmid phy-mKATE2 (van Gestel *et al.*,

2014) and was after digestion with XbaI and EcoRI ligated into pWK-Sp (Susanna *et al.*, 2007). The plasmid was transformed into *E. coli* MC1061 and verified by sequencing. *B. subtilis* DK1042 was transformed with the plasmids and successful transformation was verified by PCR and fluorescence microscopy. Subsequently, *hag::Km* as well as *eps::Tet*, *bslA::Cm* and *srfAA::MLS* deletion constructs were inserted in each fluorescent strain using gDNA of GP901 (J. Stülke lab collection) as well as DL1032 (López *et al.*, 2009), NRS2097 (Verhamme *et al.*, 2009) and DL107 (López *et al.*, 2009) resulting in strains TB530 and 531, TB532 and 533 TB534 and 535 and TB536 and 537, respectively.

To create TB873, *B. subtilis* was transformed with plasmid pDRyuaB (Kovács and Kuipers, 2011) harbouring a copy of the *bslA* gene (formerly *yuaB*) under control of an IPTG inducible promoter. The insertion in *amyE* was confirmed by PCR and subsequently, deletion constructs *bslA::Cm* and *hag::Km* were inserted by transformation with gDNA of NRS2097 (Verhamme *et al.*, 2009) and GP901, respectively. To create TB875, *B. subtilis* DK1042 was transformed with gDNA of NRS1685 (Verhamme *et al.*, 2009) and GP901. To create TB977, the *srfA* gene was PCR amplified using primers oTH33 and oTH34, digested with HindIII and SphI and inserted into pDR111 (D. Rudner). The fragment *Phy-srfA* was then PCR amplified using primers oTH35 and oTH36, digested with XhoI and KpnI, inserted into pTB886 containing the *lacI* gene and the region upstream of *srfA* and transformed into *E. coli* resulting in pTB887. The plasmid pTB887 was then used to transform *B. subtilis*, successful integration was verified by sequencing and subsequent transformation with gDNA of GP902 (Diethmaier *et al.*, 2011) resulted in strain TB977. For TB893, *B. subtilis* DK1042 was transformed subsequently with gDNA of GP901 and DL1032 (López *et al.*, 2009). To create TB922, *B. subtilis* DK1042 was transformed subsequently with gDNA of NRS2097 and GP902 (Diethmaier *et al.*, 2011). For TB895, *B. subtilis* DK1042 was transformed subsequently with gDNA of GP901 and DL107 (López *et al.*, 2009).

Test of BslA containing lysate and isolated EPS for pellicle formation

To test functionality of the BslA containing lysate and the isolated EPS, both compounds were mixed in a 1:4 ratio with concentrated biofilm promoting MSgg medium (1.3x concentrated, Branda *et al.*, 2001). As controls for BslA and EPS, PBS buffer and deionized water were used, respectively. The compound supplemented medium was inoculated 1:100 with overnight cultures of the respective mutant (Δ *bslA* or Δ *eps*) in a 24- or 48-well plate and a control with only MSgg medium was inoculated with the wildtype (all strains in Δ *hag* background, TB532, TB534 and TB530, respectively). The cultures were incubated for 2-3 d to allow for pellicle formation and imaged using a Axio Zoom V16 stereomicroscope (Carl

Zeiss, Jena, Germany). Additionally, in the BslA test the hydrophobicity of the pellicles was determined by depositing a 5 μ l water droplet on the pellicle. The test was determined successful since the isolated EPS from wild-type and Δ *tasA* mutant could promote pellicle formation of the Δ *eps* mutant but not EPS isolated from this mutant (negative control) (see Fig. S4). Likewise, the BslA containing lysate promoted wild-type like wrinkle formation and robustness of the *bslA* mutant and restored its hydrophobic properties which was not the case for the control lysate (see Fig. S5).

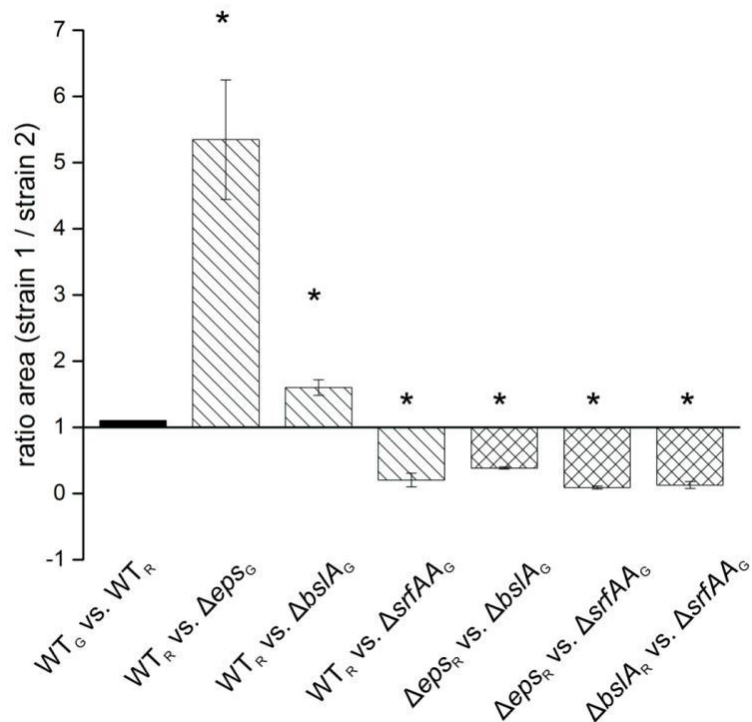


Figure S1. Sliding competition with swapped fluorescence markers. Ratio of occupied area of strain 1 versus strain 2 (in pixel²) of sliding colonies with initial ratios of 1:1 obtained by quantitative image analysis using ImageJ. G indicates a green fluorescent strain; R indicates a red fluorescent strain. Asterisks indicate significant differences to 1 (one-sample t-test, test mean = 1: P < 0.05, n = 5), error bars indicate the standard deviation.

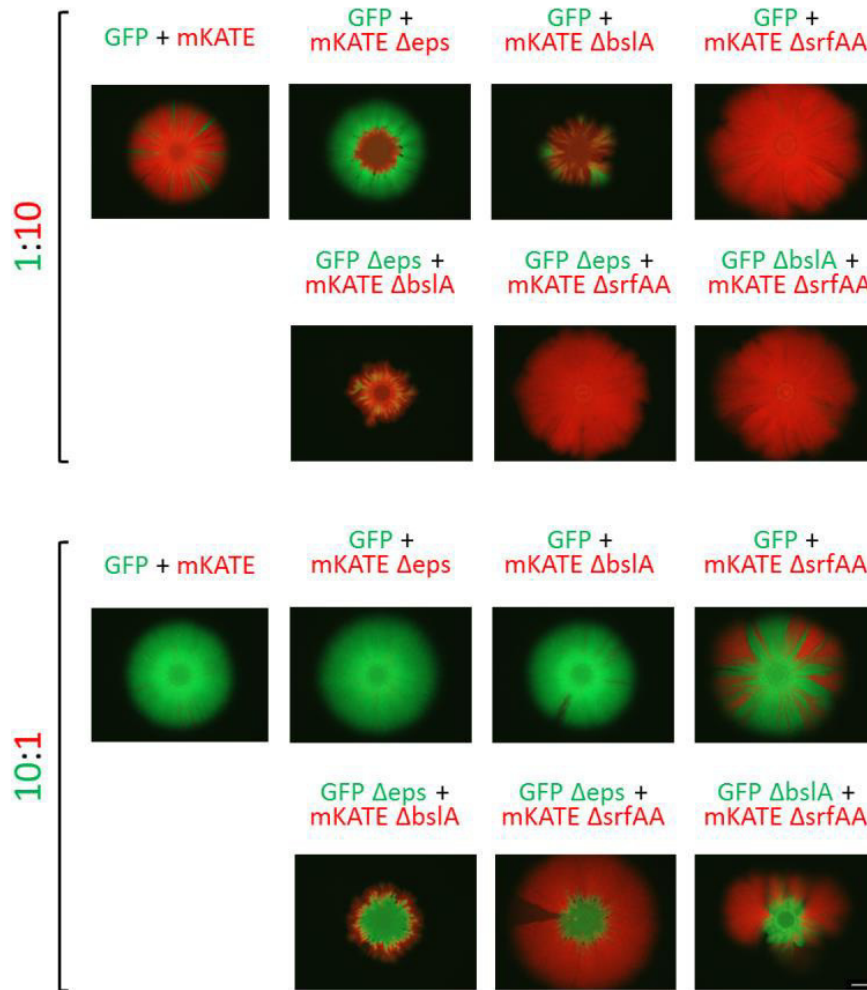


Figure S2. Structure of sliding colonies from competition assays with initial advantage of one strain. Representative overlays of green and red fluorescent images of competition assays with initial ratio of 1:10 (above) and 10:1 (below) are displayed. Green text indicates a green fluorescent strain; red text indicates a red fluorescent strain. The scale bar indicates 5 mm.

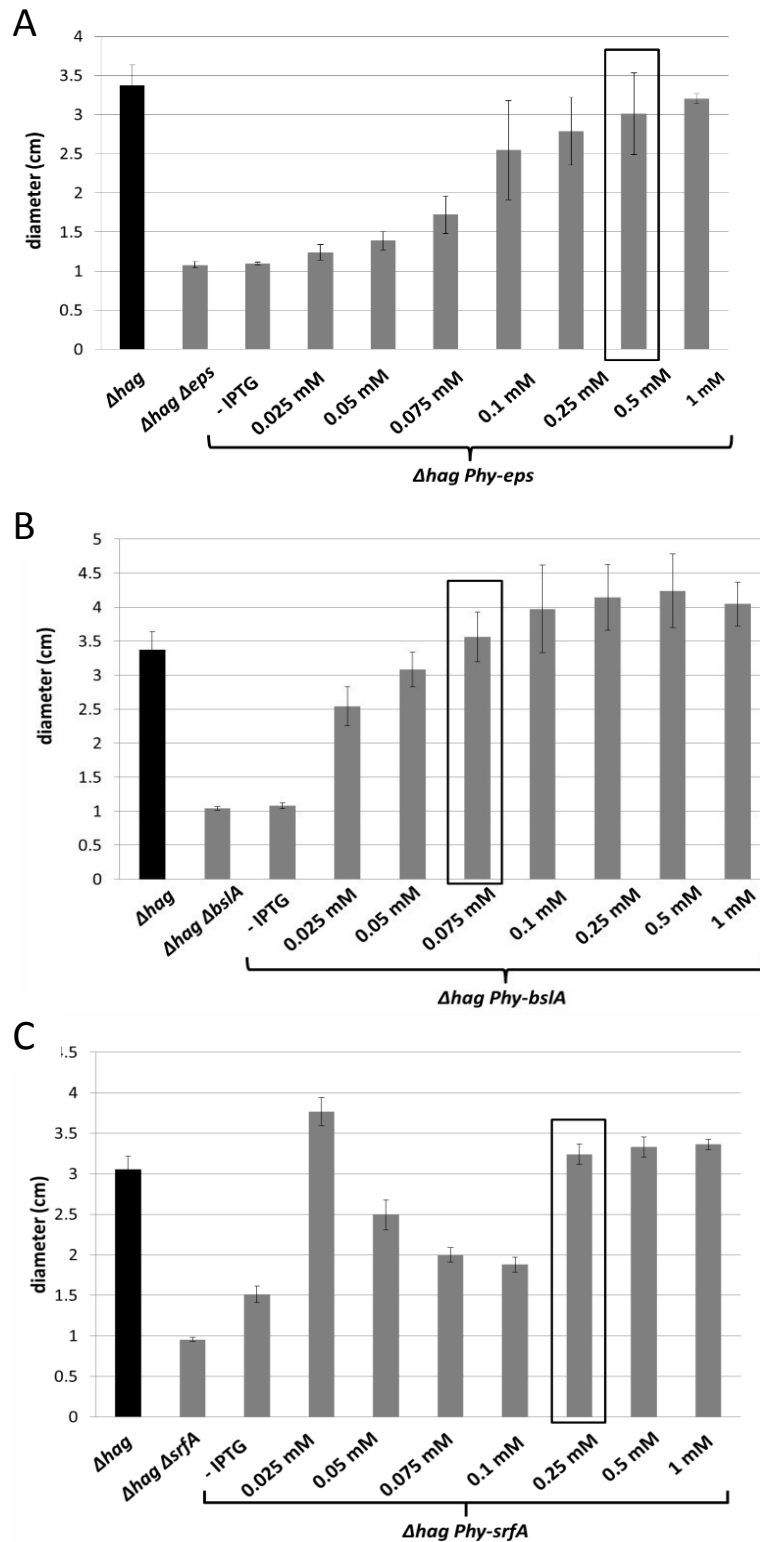


Figure S3. Determination of wild-type level of induction with IPTG. The strains with IPTG inducible (*Phy*) *epsA-O* (A), *bslA* (B) and *srfA-D* (C) genes were tested for wild-type level of sliding at different concentrations of IPTG. The sliding assay was conducted as described in Experimental procedures with IPTG supplemented medium and was evaluated after 24 h by measuring the diameter and was compared to wild-type (Δhag) and the respective mutant. The box indicates the selected IPTG concentration used in the fitness experiments. Note, that the sliding colonies of *Phy-srfA* without and with 0.025-0.075 mM IPTG were partly translucent and showed outgrowth of few denser sectors indicating additional mutations. Error bars indicate the standard deviation (n= 6).

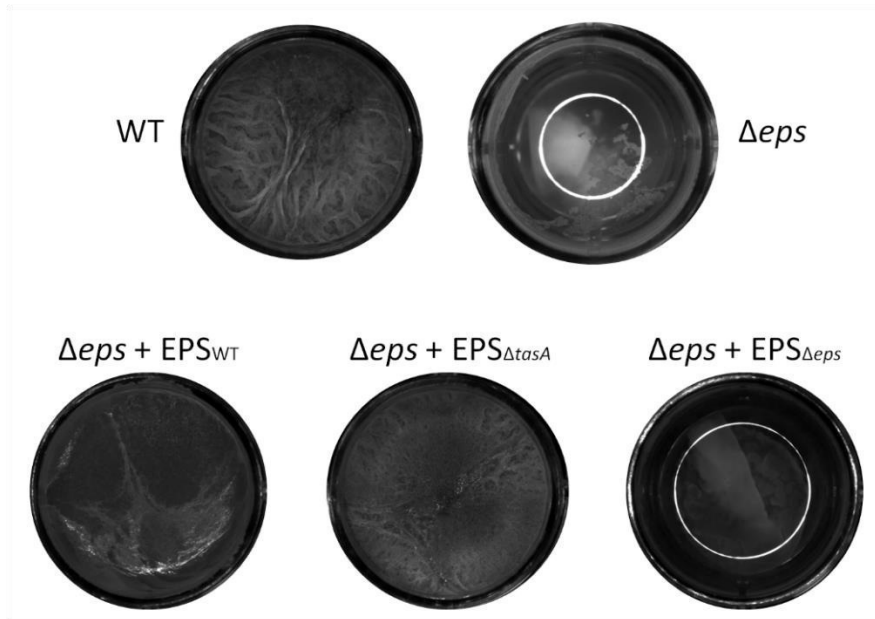


Figure S4. Test of isolated EPS. Strains were incubated statically in concentrated MSgg medium supplemented with deionized water (control WT and Δeps) or isolated EPS from wild-type, $\Delta tasA$ mutant or Δeps mutant (EPS_{WT}, EPS _{$\Delta tasA$} , and EPS _{Δeps} , respectively) for 2-3 d. The displayed pellicles are representative examples of three or more replicates. Pellicle images were recorded using a Zeiss Axio Zoom stereomicroscope equipped with a black and white camera.

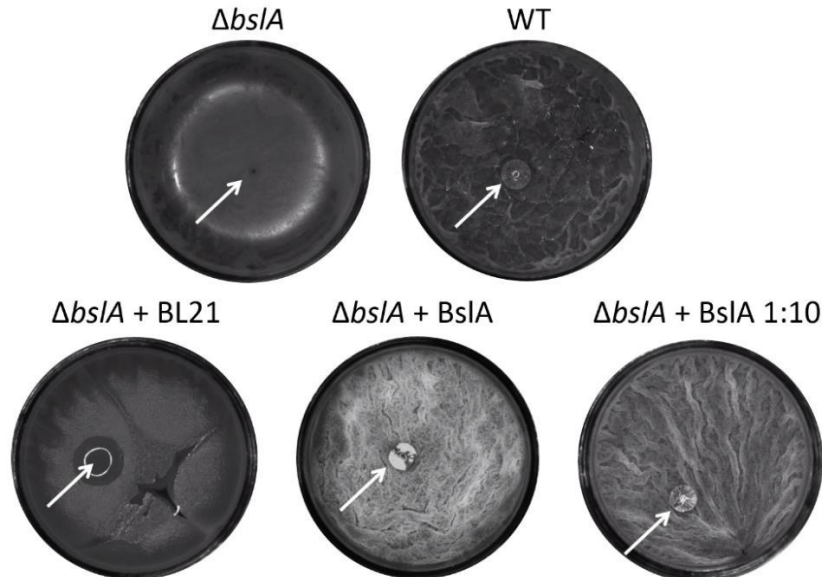


Figure S5. Test of BslA containing lysate. Strains were incubated statically in concentrated MSgg medium supplemented with PBS (control WT and $\Delta bslA$), BL21 lysate or BslA containing lysate for 2-3 d. The displayed pellicles are representative examples of three or more replicates and were recorded few seconds after application of a water droplet on the pellicle surface. Images were recorded using a Zeiss Axio Zoom stereomicroscope equipped with a black and white camera and the Camstudio onscreen video program.

Supplementary references

- Branda, S.S., González-Pastor, J.E., Ben-Yehuda, S., Losick, R., and Kolter, R. (2001) Fruiting body formation by *Bacillus subtilis*. *Proc. Natl. Acad. Sci. U. S. A.* **98**: 11621–6.
- Diethmaier, C., Pietack, N., Gunka, K., Wrede, C., Lehnik-Habrink, M., Herzberg, C., *et al.* (2011) A novel factor controlling bistability in *Bacillus subtilis*: the YmdB protein affects flagellin expression and biofilm formation. *J. Bacteriol.* **193**: 5997–6007.
- Dragoš, A., Kiesevalter, H., Martin, M., Hsu, C.-Y., Hartmann, R., Wechsler, T., *et al.* (2017) Division of labor during biofilm matrix production. *bioRxiv* 237230.
- van Gestel, J., Weissing, F.J., Kuipers, O.P., and Kovács, Á.T. (2014) Density of founder cells affects spatial pattern formation and cooperation in *Bacillus subtilis* biofilms. *ISME J.* 1–11.
- Hobley, L., Ostrowski, A., Rao, F. V, Bromley, K.M., Porter, M., Prescott, A.R., *et al.* (2013) BslA is a self-assembling bacterial hydrophobin that coats the *Bacillus subtilis* biofilm. *Proc. Natl. Acad. Sci. U. S. A.* **110**: 13600–5.
- Konkol, M.A., Blair, K.M., and Kearns, D.B. (2013) Plasmid-encoded ComI inhibits competence in the ancestral 3610 strain of *Bacillus subtilis*. *J. Bacteriol.* **195**: 4085–4093.
- Kovács, A.T. and Kuipers, O.P. (2011) Rok regulates *yuaB* expression during architecturally complex colony development of *Bacillus subtilis* 168. *J. Bacteriol.* **193**: 998–1002.
- López, D., Fischbach, M.A., Chu, F., Losick, R., and Kolter, R. (2009) Structurally diverse natural products that cause potassium leakage trigger multicellularity in *Bacillus subtilis*. *Proc. Natl. Acad. Sci.* **106**: 280–285.
- López, D., Vlamakis, H., Losick, R., and Kolter, R. (2009) Paracrine signaling in a bacterium. *Genes Dev.* **23**: 1631–8.
- Mhatre, E., Sundaram, A., Hölscher, T., Mühlstädt, M., Bossert, J., and Kovács, Á.T. (2017) Presence of calcium lowers the expansion of *Bacillus subtilis* colony biofilms. *Microorganisms* **5**: 7.
- Susanna, K.A., Mironczuk, A.M., Smits, W.K., Hamoen, L.W., and Kuipers, O.P. (2007) A single, specific thymine mutation in the ComK-binding site severely decreases binding and transcription activation by the competence transcription factor ComK of *Bacillus subtilis*. *J. Bacteriol.* **189**: 4718–4728.
- Verhamme, D.T., Murray, E.J., and Stanley-Wall, N.R. (2009) DegU and Spo0A jointly control transcription of two loci required for complex colony development by *Bacillus subtilis*. *J. Bacteriol.* **91**: 100–108.

Acknowledgements

Many wonderful people have enriched the time of my doctoral studies and helped me to reach this important step. Whether it was by scientific advice, philosophical discussions during coffee breaks, moral support, or simply motivation, all these people contributed to make the last years a great time – thank you!

I want to thank my supervisor Ákos, first for his encouragement to do a PhD, which proved to be the right decision. Thank you very much for your support, inspiration and countless discussions which pushed me to think critically and helped to expand my scientific understanding. Thank you for being a great mentor who always listened to concerns and whose door was (not only literally) always open.

I thank my family for always supporting me, celebrating with me during the ups and motivating me during the (only few) downs of the last years and especially for their love. Thank you, Nils, for being with me!

Thanks to the great people that were members of the TeBi group during the last years, I cannot imagine a better group or nicer people to work with! Thank you all for contributing to a great work atmosphere, for all the fun in and out of the lab, for exciting gaming nights, for lots of cakes and desserts, for terrific summer lab-trips, for great intercultural experiences like the various foods during the Christmas party or lessons in different languages and for the many (more or less) scientific debates. Special thanks to Eisha and Ramses who helped me since the start, to Ben, Mavic, Anne and Anna! Thank you for the motivation, advice, your friendship and lots of fun! Thanks to Stefi, Soumyajit and especially Tina for their patience, interest, great teamwork and improvement of the projects as well as my supervision.

Many thanks also go to my supervisor Christian for his valuable advice and constructive discussions of my project.

Thanks to Prof. Kothe, Katrin, Petra, Christin and the Microbial Communication group for their help, advice and discussions during the Monday seminars.

Many thanks for the support of the IMPRS & MPI-CE and for the opportunity to do my doctoral studies. Thanks to IMPRS and JSMC for providing an excellent framework of guidance, courses, lectures and scientific interactions as well as to fellow doctoral students for fruitful discussions. Many thanks also to the JSMC and IMPRS teams for their help with lots of questions and concerns.

Thanks to the fellow members of the Neugasse 23 building for relaxing coffee breaks and celebrating new papers with us!

Thanks to all of my collaborators, that helped me to greatly improve my research and dissertation.

And last but not least, thanks to all friends who helped me relax and enjoy my free time to create a healthy work-life balance.

Declaration of Independent Assignment

I declare in accordance with the conferral of the degree of doctor from the Faculty of Biology and Pharmacy of the Friedrich-Schiller-University of Jena that I wrote the submitted thesis only with the assistance of the literature cited in the text and in accordance with the Course of Examination for Doctoral Candidates of the aforementioned faculty.

People who assisted in experiments, data analysis and writing of the manuscripts are listed as co-authors of the respective manuscripts.

A doctoral consultant did not assist me and no third parties received either direct or indirect monetary benefits from me for work connected to the writing of this dissertation.

The thesis has not been previously submitted elsewhere, whether to the Friedrich-Schiller-University of Jena or to any other university.

Jena,

Theresa Hölscher